CORA Cork Open Research Archive
Cartlann Taighde Oscailte Chorcaí

Title	Bugs, breathing and blood pressure: the microbiota-gut-brain axis in cardiorespiratory control
Authors	O'Connor, Karen M.
Publication date	2019
Original Citation	O'Connor, K. M. 2019. Bugs, breathing and blood pressure: the microbiota-gut-brain axis in cardiorespiratory control. PhD Thesis, University College Cork.
Type of publication	Doctoral thesis
Rights	© 2019, Karen M. O'Connor. - http://creativecommons.org/licenses/by-nc-nd/3.0/
Download date	2026-11-15 04:24:35
Item downloaded from	https://hdl.handle.net/10468/9476

UCC
University College Cork, Ireland
Coláiste na hOllscoile Corcaigh



University College Cork, Ireland
Coláiste na hOllscoile Corcaigh

Bugs, breathing and blood pressure: The microbiota-gut-brain axis in cardiorespiratory control

Karen M. O'Connor, BSc (Hons)

Departments of Physiology, and Anatomy &

Neuroscience and APC Microbiome Ireland

Thesis submitted to National University of Ireland, Cork for the award of

Doctor of Philosophy

Under the supervision of:

Professor Ken D. O'Halloran, Head of Department of Physiology

Professor John F. Cryan, Head of Department of Anatomy & Neuroscience and Principal Investigator in the APC Microbiome Ireland

July 2019

Table of Contents

Declaration x

Acknowledgments xi

Abstract xiii

Chapter 1. Introduction - Microbiota-gut-brain axis signalling and cardiorespiratory control in health and disease 1

Abbreviations 2

1.1. The gut microbiota 3

1.1.1 Gut microbiota composition 3

1.1.2 Gut microbiota evolution 3

1.2. Microbiota-gut-brain axis communication pathways 5

1.2.1 Microbiota-gut-brain axis 5

1.2.2 Short-chain fatty acids (SCFAs) 7

1.2.3 Tryptophan metabolism and neurotransmitters 8

1.2.4 Immune system 9

1.2.5 Neuronal pathways 10

1.3. Microbiota modulation and analysis 12

1.3.1 Germ-free animals 12

1.3.2 Antibiotics 12

1.3.3 Diet 13

1.3.4 Faecal microbiota transplant 14

1.3.5 Analysis of the microbiome 15

1.4. Control of breathing and cardiovascular function 16

1.4.1 Overview of cardiorespiratory control 16

1.4.2 Neuronal networks 18

1.4.3 Central chemoreceptors 18

1.4.4 Peripheral sensors 19

1.4.5 Cardiorespiratory coupling 22

1.4.6 Plasticity 22

1.5. Autonomic dysfunction and aberrant gut microbiota 26

1.5.1 Stress and aberrant gut microbiota 26

1.6. Blood pressure, breathing and the gut microbiota 28

1.6.1 Blood pressure and gut microbiota composition and diversity 28

1.6.2 Respiratory control and gut microbiota 30

1.7. Cardiorespiratory and pulmonary disorders 31

1.7.1 Obstructive sleep apnoea (OSA) 31
1.7.2 Apnoea of prematurity and bradycardia 31
1.7.3 Asthma 32
1.7.4 Chronic Obstructive Pulmonary Disease 33
1.7.5 Cystic fibrosis 33
1.8. Knowledge gaps addressed in this thesis 35
1.9. Thesis structure and specific aims 38
1.10. References 40

Chapter 2. Manipulation of gut microbiota blunts the ventilatory response to hypercapnia in adult rats 68
Abbreviations 70
Abstract 71
Research in Context 72
2.1. Introduction 73
2.2. Methods 76
2.2.1 Ethical approval 76
2.2.2 Experiment animals 76
2.2.3 Antibiotic administration 76
2.2.4 Faecal microbiota transfer (FMT) protocol 78
2.2.5 Assessment of respiratory flow and metabolism in unrestrained, unanaesthetised rats 78
2.2.6 Assessment of cardiorespiratory parameters under urethane anaesthesia 80
2.2.7 Macromolecular permeability in small and large intestine ex vivo 82
2.2.8 Brainstem monoamine concentrations 82
2.2.9 16S rRNA sequence-based microbiota composition and diversity analysis in caecal content 83
2.2.10 Statistical analysis 83
2.3. Results 85
2.3.1 Body and tissue weights 85
2.3.2 Baseline ventilation and metabolism in behaving rats during quiet rest 87
2.3.3 Respiratory timing variability, apnoeas and sighs during normoxia in behaving rats during quiet rest 87
2.3.4 Ventilatory and metabolic responsiveness to chemostimulation in behaving rats during quiet rest 92
2.3.5 Respiratory timing variability, apnoeas and sighs during hypoxia and hypercapnia in behaving rats during quiet rest 93

2.3.6 Cardiorespiratory recordings in anaesthetised rats 98
2.3.7 Brainstem neurochemistry 103
2.3.8 Ex vivo intestinal macromolecular permeability 106
2.3.9 Alterations in the caecal microbiota 108
2.3.10 Correlation analysis between microbiota composition and brainstem neurochemistry and heart rate 112
2.4. Discussion 114
2.4.1 Animal model 114
2.4.2 Chronic antibiotic administration and faecal microbiota transfer blunt ventilatory responses to hypoxia and hypercapnia 115
2.4.3 Chronic antibiotic administration decreases systolic blood pressure 118
2.4.4 Cardiorespiratory responsiveness to vagal afferent nerve stimulation is unaffected by chronic antibiotic administration and faecal microbiota transfer 119
2.4.5 Chronic antibiotic administration and faecal microbiota transfer alter brainstem monoamine and monoamine metabolite concentrations 120
2.4.6 Chronic antibiotic administration and faecal microbiota transfer increase distal ileum permeability 122
2.4.7 Limitations 123
2.4.8 Summary and conclusions 124
2.5. Additional information 125
2.6. References 126

Chapter 3. Chronic intermittent hypoxia disrupts cardiorespiratory homeostasis and gut microbiota composition in adult male guinea-pigs 137
Abstract 139
Research in Context 140
3.1. Introduction 141
3.2. Materials and Methods 144
3.2.1 Ethical approval 144
3.2.2 Chronic intermittent hypoxia animal model 144
3.2.3 Assessment of respiratory flow in awake guinea-pigs 144
3.2.4 Assessment of cardiorespiratory parameters under urethane anaesthesia 145
3.2.5 Analysis of brainstem homogenates and urine 147
3.2.6 Microbiota composition analysis of faecal content 148
3.2.7 Statistical analysis 149
3.3. Results 151

3.3.1 Baseline ventilation and ventilatory responses to chemostimulation in sham and CIH-exposed awake guinea-pigs. 151

3.3.2 Cardiorespiratory parameters in sham and CIH-exposed anaesthetised guinea-pigs....158

3.3.3 Brainstem monoamine analysis.....165

3.3.4 Microbiota richness and composition....168

3.4. Discussion....172

3.5. Additional information....179

3.6. References....180

Chapter 4. Chronic intermittent hypoxia lowers *Lactobacillus rhamnosus* relative abundance and increases apnoea index and blood pressure: Effects of prebiotic supplementation....187

Abbreviations....188

Abstract....189

4.1. Introduction....190

4.2. Materials and Methods....193

4.2.1 Ethical approval....193

4.2.2 Experimental animals....193

4.2.3 Prebiotic administration....193

4.2.4 Chronic intermittent hypoxia rat model....193

4.2.5 Assessment of respiratory flow in rats during quiet rest....193

4.2.6 Assessment of cardiorespiratory parameters under urethane anaesthesia....195

4.2.7 Brainstem monoamine concentrations....197

4.2.8 Plasma and brainstem cytokine concentrations....197

4.2.9 Plasma corticosterone....198

4.2.10 Microbiota composition and diversity....198

4.2.11 Faecal short-chain fatty acid concentrations....199

4.2.12 Statistical analysis....199

4.3. Results....201

4.3.1 Body and tissue weight....201

4.3.2 Baseline ventilation and metabolism in rats during quiet rest....203

4.3.3 Respiratory timing variability, apnoeas and sighs during normoxia in rats during quiet rest....203

4.3.4 Ventilatory and metabolic responsiveness to chemostimulation in rats during quiet rest....207

4.3.5 Baseline cardiorespiratory and blood gas parameters in anaesthetised rats....212

4.3.6 Cardiorespiratory responses to 5-HT_3 receptor agonism evoking the cardiopulmonary reflex 218

4.3.7 Cardiovascular responses to pharmacological blockade of sympathetic activity in anaesthetised rats 220

4.3.8 Pons and medulla oblongata neurochemistry 222

4.3.9 Plasma cytokine and corticosterone concentrations 225

4.3.10 Caecal microbiota 228

4.3.11 Correlation analysis 232

4.3.12 Faecal short-chain fatty acid concentrations 232

4.4. Discussion 234

4.4.1 Summary and conclusion 242

4.5 Additional information 244

4.6 References 245

Chapter 5. Discussion - The microbiota-gut-brain axis in the control of breathing and cardiovascular function 259

Abstract 260

5.1. Gut microbiota 261

5.2. Cardiorespiratory control 262

5.3. The gut microbiota, cardiorespiratory and autonomic control 263

5.4. Respiratory control in animal models of manipulated gut microbiota 264

5.5. Cardiorespiratory and autonomic control in animal models sleep-disordered breathing 267

5.6. Potential mechanisms linking cardiorespiratory and autonomic dysfunction to the gut microbiota 271

5.7. Future studies 273

5.8. Conclusion 275

5.9. References 277

Presentations 286

Conference proceedings 287

Appendix A. Manipulation of gut microbiota blunts the ventilatory response to hypercapnia in adult rats 289

Appendix B. Chronic intermittent hypoxia disrupts cardiorespiratory homeostasis and gut microbiota composition in adult male guinea-pigs 330

Appendix C. Chronic intermittent hypoxia lowers *Lactobacillus rhamnosus* relative abundance and increases apnoea index and blood pressure: Effects of prebiotic supplementation 340

List of figures

Chapter 1.

Figure 1. 1 The microbiota-gut-brain axis..... 6
Figure 1. 2 Summary of the cardiorespiratory control network, which is composed of sensors, central control regions and effectors..... 17
Figure 1. 3 The microbiota-gut-brain axis, brain and behaviours 36

Chapter 2.

Figure 2. 1 Experimental design 77
Figure 2. 2 Chronic antibiotic administration and faecal microbial transfer do not alter respiratory timing variability, or the prevalence of apnoeas and sighs in behaving rats during quiet rest 88
Figure 2. 3 Chronic antibiotic administration and faecal microbial transfer blunts hypercapnic ventilation in behaving rats during quiet rest..... 94
Figure 2. 4 Chronic antibiotic administration and faecal microbial transfer do not alter cardiorespiratory responses to phenylbiguanide administration in anaesthetised rats 102
Figure 2. 5 Chronic antibiotic administration and faecal microbial transfer alter rat brainstem neurochemistry 104
Figure 2. 6 Chronic antibiotic administration increases the macromolecular permeability of rat distal ileum.....107
Figure 2. 7 Faecal microbiota transfer alters rat caecal microbiota composition.....110
Figure 2. 8 Brainstem neurochemistry and heart rate are associated with the abundance of specific genera.....113

Chapter 3.

Figure 3. 1 CIH does not significantly affect baseline, hypoxic or hypercapnic ventilation in guinea-pigs.....152
Figure 3. 2 Normoxic breathing variability is reduced in CIH-exposed awake guinea-pigs..155
Figure 3. 3 Sigh frequency is reduced in CIH-exposed awake guinea-pigs.....157
Figure 3. 4 Autonomic control of heart rate is altered in CIH-exposed anaesthetised guinea-pigs.....162
Figure 3. 5 Pontine and medulla oblongata noradrenaline concentrations are reduced in CIH-exposed guinea-pigs 166
Figure 3. 6 Significant correlations are evident between pontine noradrenaline concentrations and various cardiorespiratory parameters.....167
Figure 3. 7 Faecal microbiota richness is reduced CIH-exposed guinea-pigs 170
Figure 3. 8 CIH reduces Firmicutes and increases Bacteroidetes relative abundance in guinea-pig faecal samples.....171

Chapter 4.

Figure 4. 1 CIH increase apnoea index 204
Figure 4. 2 CIH causes hypertension and cardiac autonomic imbalance 213
Figure 4. 3 CIH did not alter cardiorespiratory responses to pulmonary vagal afferent C-fibre stimulation.....219
Figure 4. 4 Prebiotic administration alters brainstem neurochemistry.....223

Figure 4. 5 Corticosterone and inflammatory mediators were equivalent between groups 226
Figure 4. 6 Prebiotic administration alters rat caecal microbiota structure 230
Figure 4. 7 Caecal microbiota composition. 231
Figure 4. 8 Prebiotic administration increases faecal acetic and propanoic acid 233

Chapter 5.

Figure 5. 1 Potential mechanisms linking aberrant cardiorespiratory and autonomic control to the gut microbiota**.**.....272

List of tables

Chapter 2.

Table 2. 1 Body and organ weights 86
Table 2. 2 Baseline ventilation, respiratory timing variability and metabolism in behaving rats during quiet rest 90
Table 2. 3 Ventilatory and metabolic responsiveness during hypoxia in behaving rats during quiet rest 95
Table 2. 4 Respiratory timing variability, apnoeas and sighs during hypoxia in behaving rats during quiet rest 95
Table 2. 5 Ventilatory and metabolic responsiveness during hypercapnia in behaving rats during quiet rest 96
Table 2. 6 Respiratory timing variability, apnoeas and sighs during hypercapnia in behaving rats during quiet rest 97
Table 2. 7 Baseline ventilation, blood gases and cardiovascular measurements in anaesthetised rats 99

Chapter 3.

Table 3. 1 Baseline ventilation and metabolic parameters in sham and CIH-exposed awake guinea-pigs 153
Table 3. 2 Baseline arterial blood gas and electrolyte concentrations in sham and CIH-exposed guinea-pigs 159
Table 3. 3 CIH induces tachycardia and hyperventilation in anaesthetised guinea-pigs 159
Table 3. 4 Body organ weights and urinary stress profile of sham and CIH-exposed guinea-pigs 160
Table 3. 5 Respiratory responsiveness to chemostimulation in sham and CIH-exposed anaesthetised guinea-pigs 164

Chapter 4.

Table 4. 1 Body and tissue weights 202
Table 4. 2 Baseline ventilation, apnoea, sigh and metabolism in rats during quiet rest 206
Table 4. 3 Ventilatory and metabolic responsiveness to chemostimulation in rats during quiet rest 211
Table 4. 4 Baseline ventilation, blood gases and cardiovascular parameters in anaesthetised rats 215
Table 4. 5 Heart rate variability in the urethane anaesthetised rats 217
Table 4. 6 Cardiovascular responses to pharmacological blockade of sympathetic activity in urethane anaesthetised rats 221

Declaration

I hereby declare that this thesis is my own original work. It has not been submitted to another institution for an award. The contribution of others through collaborations has been acknowledged.

Chapter 2: Dr. Eric Lucking and I contributed equally to this manuscript, including experimental design, acquisition of data, data and statistical analysis, interpretation of data and drafting of the original manuscript. Dr. Anna Golubeva performed and statistically analysed Ussing chamber studies. Dr. Conall Strain and Dr. Fiona Fouhy conducted 16S rRNA sequencing and Dr. María Cenit performed DNA extractions. Mr. Pardeep Dhaliwal, Dr. David Burns and Mr. Thomaz Bastiaanssen contributed to data analysis. Alongside my supervisory team, Prof. Catherine Stanton and Dr. Gerard Clarke critically revised relevant sections of the manuscript for important intellectual content.

Chapter 3: Dr. Eric Lucking and I contributed equally to this manuscript, including experimental design, acquisition of data, data and statistical analysis, interpretation of data and drafting of the original manuscript. Dr. Conall Strain and Dr. Fiona Fouhy conducted 16S rRNA sequencing. Mr. Thomaz Bastiaanssen contributed to 16S rRNA sequencing data and statistical analysis and Dr. David Burns was involved in experimental design. Alongside my supervisory team, Dr. Anna Golubeva, Prof. Catherine Stanton and Dr. Gerard Clarke critically revised relevant sections of the manuscript for important intellectual content.

Chapter 4: Dr. Eric Lucking and I contributed equally to this manuscript, including experimental design, acquisition of data, data and statistical analysis, interpretation of data and drafting of the original manuscript. Mr. Thomaz Bastiaanssen contributed to whole-metagenome shotgun sequencing data interpretation and statistical analysis. Dr. Veronica Peterson conducted metagenomic bioinformatic analysis and Dr. Fiona Crispie performed DNA extractions and whole-metagenome shotgun sequencing. Dr. Anna Golubeva contributed to statistical analysis design of whole-metagenome shotgun sequencing. Dr. Paul Cotter and Dr. Gerard Clarke were involved in interpretation of whole-metagenome shotgun sequencing and HPLC studies, respectively.

Karen O'Connor

July 2019

Acknowledgments

Professor Ken O'Halloran and Professor John Cryan, thank you for your continuous support throughout my time as a PhD trainee. I am sincerely grateful for your guidance, which has contributed to my personal and professional development. It's been a privilege training as a PhD student under your supervision. Thank you for encouraging and supporting my training at national and international meetings. I am very fortunate to call you my mentors. Ken, thank you for the intellectual, supportive and encouraging chats throughout the journey. I look forward to continuing our collaborations in the coming year.

Dr. Eric Lucking, I'm truly grateful for your friendship, encouragement, collegiality and guidance. This research would not be complete without your continuous support throughout the duration of my PhD, which includes countless trips to Doughcloyne from pubs/airports/buses and many days of 'just the two of us' in the lab. You have sincerely been an excellent role-model. I look forward to continuing working together over the coming year. Finally, thank you for all the tea, flapjacks and scones!

Thank you to my thesis examiners and past and present academic, technical and administration staff in the Departments of Physiology and Anatomy & Neuroscience, APC Microbiome Ireland and the Biological Services Unit whom I've had the pleasure of working with over the past four years.

To the past and present postgraduate students within the Department of Physiology for your friendship, camaraderie and support. I am glad to have worked alongside you. I look forward to the many more trips to Toms and beyond!

I would like to say a tremendous thank you to the people I've lived with during my time as a PhD trainee, especially Hannah, Anna, Stacey and Jack. Thank you for the endless evening chats and LOLS, litres of tea and for keeping me sane. I truly appreciate your friendship and look forward to the laughs ahead. Roll on the celebrations!

To Peter, I am eternally grateful for your love, encouragement and support over the last three years. Thank you for the countless weekends commuting, the many days spent working/studying together and most importantly thank you for all the chats and laughs!

To my parents, Joan and Ger, I would like to say that I am forever grateful for the support received to advance my education. Aisling, thank you for paving the pathway which led me to undertake a PhD. I hope to see you next year 'down under'. To mam, dad and Aisling for

your love, encouragement and support not only over the last four years but the last twenty-six years; I dedicate this thesis to you.

Abstract

Dysregulated microbiota-gut-brain axis communication adversely influences neurocontrol systems, consequently affecting brain behaviours. It is plausible that microbiota-gut-brain axis signalling has a role in the control of breathing and cardiovascular function, as networks that govern cardiorespiratory control reside within the brainstem, a region innervated by the vagus nerve, a key signalling pathway of the microbiota-gut-brain axis. Cardiovascular and respiratory diseases are serious, potentially life-threatening conditions with limited treatment options. Thus, improved understanding of the underlying pathophysiology and novel therapeutic approaches are required.

We performed an assessment of cardiorespiratory physiology in animal models of modified gut microbiota [antibiotic-treated (ABX) and faecal microbiota transfer (FMT)], and sleep-disordered breathing [chronic intermittent hypoxia (CIH)-exposed guinea-pigs and rats]. We investigated if dietary prebiotic supplementation prevented CIH-induced cardiorespiratory dysfunction in rats. Whole-body plethysmography was used to record ventilation and metabolism in unanaesthetised animals during normoxia and chemostimulation. Under anaesthesia, cardiorespiratory assessments were performed during normoxia, chemosensory stimulation and drug administration. Brainstem neurochemistry was assessed by high-performance liquid chromatography. 16S rRNA and whole-metagenome shotgun sequencing was used to characterise the gut microbiota.

ABX and FMT disrupted the gut microbiota, brain neurochemistry and intestinal integrity, blunting chemoreflex control of breathing. Decreased brainstem noradrenaline and altered gut microbiota as well as impaired respiratory and autonomic control were evident in CIH-exposed guinea-pigs. CIH–exposed rats developed cardiorespiratory pathologies and decreased gut *Lactobacillus rhamnosus* relative abundance. Prebiotic administration increased short-chain fatty acid concentrations, measured by gas chromatography, but *Lactobacillus rhamnosus* and cardiorespiratory dysfunctions were not restored. Several commensal and pathogenic bacterial species correlated with blood pressure parameters.

Our findings add to emerging research exploring microbiota-gut-brain signalling in homeostatic systems, extending investigations to cardiorespiratory control. Our studies draw focus to the potential application of manipulation of the gut microbiota as an adjunctive therapy for cardiorespiratory disease.

Chapter 1. Introduction - Microbiota-gut-brain axis signalling and cardiorespiratory control in health and disease

Abbreviations: BBB, blood-brain barrier; CIH, Chronic intermittent hypoxia; COPD, chronic obstructive pulmonary disease; FFARs, free-fatty acid receptors; FMT, faecal microbiota transplant; GABA, gamma-aminobutyric acid; GLP-1, glucagon-like peptide 1; HFD, high-fat diet; HPA-axis, HFD+OSA, high-fat diet and obstructive sleep apnoea; hypothalamic pituitary adrenal axis; LPS, lipopolysaccharide; NTS, nucleus tractus solitarius; OSA, obstructive sleep apnoea; $PaCO_2$, partial pressure of arterial carbon dioxide; PaO_2, partial pressure of arterial oxygen; PCO_2, partial pressure of carbon dioxide; Reg3γ, regenerating family member 3 gamma; RTN, retrotrapezoid nucleus, SCFAs, short-chain fatty acids; SDB, sleep-disordered breathing.

1.1. The gut microbiota

1.1.1 Gut microbiota composition

The microbiota describes the substantial community of various commensal, symbiotic and pathogenic microbes that populate the skin, lungs, urogenital and gastrointestinal tract. This microbial community includes bacteria, viruses, fungi, archaea and parasites. The gastrointestinal tract possesses the most extensive and diverse ecosystem and is home to trillions of microorganisms. This community harbours 1000-1150 prevalent bacterial species, which combine to dominate the population of microorganisms (Qin *et al.*, 2010). Recently, the intestinal bacterial population alone is estimated to establish a ratio of host:bacterial cells 1:1 (Sender *et al.*, 2016).

1.1.2 Gut microbiota evolution

Gut microbiota modulation by perinatal factors: Microbiota colonisation of an infant commences during parturition, where perinatal factors such as mode of delivery, gestation age at birth and antibiotic exposure shape the maternal microbiota imprint (Penders *et al.*, 2006; Moya-Perez *et al.*, 2017; Fouhy *et al.*, 2019). Caesarean delivery leads to reduced microbiota richness and diversity compared with vaginally delivered infants (Azad *et al.*, 2013). Furthermore, premature babies have diminished microbiota diversity, decreased *Bifidobacterium* and *Bacteroides* abundance as well as increased proliferation of Proteobacteria phyla, due to insufficient gastric secretion, compared with full-term delivered infants (Sondheimer *et al.*, 1985; Barrett *et al.*, 2013; Dahl *et al.*, 2017; Korpela *et al.*, 2018). Breastfed infants are colonised with the mother's unique breast milk microbial pattern and increased levels of *Bifidobacterium* compared with formula-fed infants (Roger *et al.*, 2010; Azad *et al.*, 2013). Vaginally delivered, full-term babies that were breastfed, born to healthy non-antibiotic treated mothers have optimal progression of infant microbiota (Penders *et al.*, 2006). It has recently been shown that perinatal factors result in perpetual microbiota evolution up to four years after parturition (Fouhy *et al.*, 2019).

Gut microbiota adaptation: Remarkably, this diverse and highly complex gut microbiota community continuously evolves and adapts over an entire lifetime (Borre *et al.*, 2014; McVey Neufeld *et al.*, 2016; Kundu *et al.*, 2017). Distinctive functional and compositional hallmarks are evident across various life periods, including neonatal, early-life, puberty, adulthood and ageing, with large interpersonal differences (Kundu *et al.*, 2017). Notwithstanding the vast degree of interpersonal variation, the adult gut microbiota is primarily dominated by Firmicutes and Bacteroidetes (Kurokawa *et al.*, 2007; Arumugam *et*

al., 2011). More recently, the adult gut microbiota was classified into three different enterotypes, *Prevotella, Ruminococcus* and *Bacteroides* (Arumugam *et al.,* 2011). Furthermore, microbiota diversity and composition are influenced by nutrition, life-style, hormone and health status, ageing, environment, stress and medication, amongst other factors (Woodmansey, 2007; O'Mahony *et al.*, 2011; Albenberg & Wu, 2014; Panda *et al.*, 2014; Golubeva *et al.*, 2015; Kelly *et al.*, 2015; Foster *et al.*, 2017; Boehme *et al.*, 2019). A growing body of evidence now points to the gut microbiota as a potent contributor to whole-body homeostasis in both health and disease (Cryan & O'Mahony, 2011; Grenham *et al.*, 2011; Kelly *et al.*, 2016b; Sarkar *et al.*, 2016; Dinan & Cryan, 2017).

1.2. Microbiota-gut-brain axis communication pathways

1.2.1 Microbiota-gut-brain axis

The gut microbiota functions in a multimodal bidirectional communication pathway termed, microbiota-gut-brain axis, enabling microbes to share information with the brain and the brain to communicate with the gut (Rhee *et al.*, 2009). This bidirectional communication network includes the central, both brain and spinal cord, enteric and autonomic nervous systems and the hypothalamic pituitary adrenal axis (HPA-axis). There is compelling evidence to illustrate that dysregulated microbiota-gut-brain axis signalling affects homeostatic neurocontrol systems, with consequences for behaviours such as anxiety, depression, social interactions and learning and memory (Desbonnet *et al.*, 2014; Hoban *et al.*, 2016; Burokas *et al.*, 2017; Dinan & Cryan, 2017). Many of these maladies are associated with neurodegenerative, neurodevelopmental or biopsychosocial disorders such as Parkinson's disease, autism and irritable bowel syndrome (Cryan & O'Mahony, 2011; Dinan & Cryan, 2017).

The mechanisms of microbiota-gut-brain axis signalling are multifaceted and comprise afferent and efferent pathways (Burokas *et al.*, 2015). Despite the vast amount of experimental evidence from rodent and human studies, supporting the role of the gut microbiota in regulating physiological homeostasis and brain functions, signalling pathways have not been entirely elucidated. Currently, a number of afferent (neuronal, immune system, gut microbiota metabolites, tryptophan metabolism and neurotransmitters) and efferent (neuronal and HPA-axis) pathways have been proposed (Figure 1.1).

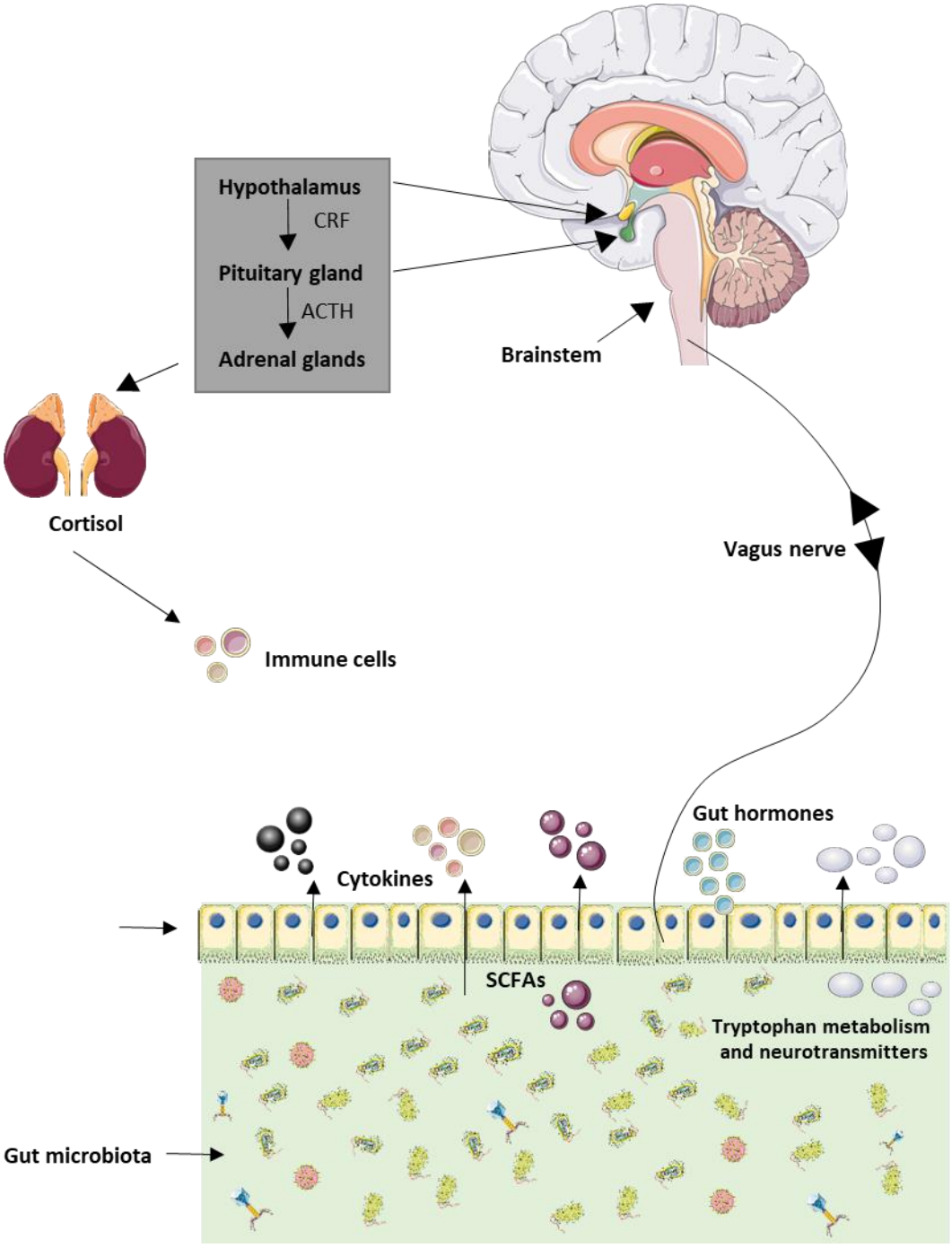


Figure 1. 1 The microbiota-gut-brain axis

The microbiota-gut-brain axis permits microbes to communicate with the brain and the brain to convey information to gut. A number of complex communication pathways are proposed. CRF, corticotropin-releasing factor; ACTH, adrenocorticotrophic hormone; SCFA, short-chain fatty acid. Cortisol and corticosterone are released from the adrenal medulla in humans and rodents, respectively.

1.2.2 Short-chain fatty acids (SCFAs)

Acetic, propionic and butyric acid are principal SCFAs, which are primary end-products produced by microbial fermentation of partially digestible and indigestible polysaccharides (Macfarlane & Macfarlane, 2012). They function as major signalling mediators of host-microbiome communication, playing a crucial role in the maintenance of physiological homeostasis and brain functions (Stilling *et al.*, 2014a; Canfora *et al.*, 2015). SCFAs are either utilised in colonocytes or transferred and circulated by diffusion and monocarboxylate transporters (Kekuda *et al.*, 2013; Vijay *et al.*, 2015).

It is widely accepted that free-fatty acid receptors (FFARs), especially FFAR 2 and 3, are located on an extensive range of cells throughout the body (Sina *et al.*, 2009; Tolhurst *et al.*, 2012; Nohr *et al.*, 2015; Lu *et al.*, 2018b). SCFAs can bind to FFARs expressed on enteroendocrine cells of the gastrointestinal tract, subsequently releasing gut hormones such as glucagon-like peptide 1 (GLP-1) (Tolhurst *et al.*, 2012). They can cause neuronal activation by binding to FFARs, specifically FFARs 3, which are located on neuronal ganglia throughout the body, including the superior cervical ganglion (Kimura *et al.*, 2011), sympathetic ganglia of the thoracic and lumbar sympathetic trunks and vagal ganglia (Nohr *et al.*, 2015). In addition, it is apparent that FFARs 2 are highly expressed in immune cells, suggesting immune system regulation by SCFAs (Sina *et al.*, 2009; Smith *et al.*, 2013b). Furthermore, SCFAs may directly influence neurotransmitters. For example, it has been shown that butyrate and propionate modify tyrosine hydroxylase gene expression in PC12 cell lines, which can affect dopamine and noradrenaline synthesis (DeCastro *et al.*, 2005; Nankova *et al.*, 2014; Stilling *et al.*, 2016).

Additionally, SCFAs affect microglia, the resident macrophages of the central nervous system (Erny *et al.*, 2015; Mosher & Wyss-Coray, 2015). Germ-free mice, born and raised in sterile environments, have advanced defects in microglia maturation, morphology and function (Erny *et al.*, 2015), increased blood-brain barrier (BBB) permeability and decreased expression of brain tight junction proteins (Braniste *et al.*, 2014). SCFA supplementation reversed these microglial defects (Erny *et al.*, 2015), up-regulated brain tight junction proteins and reduced BBB permeability (Braniste *et al.*, 2014). Of note, microglia may play a key role in regulating neural circuits within the brain (Bilimoria & Stevens, 2015). Not only have SCFAs been reported to modulate microglial activity and function in germ-free mice, but SCFA administration and microglia modulation has also been described in a rodent model of sleep-disordered breathing (SDB). Ganesh and colleagues reported reduced acetate and increased microglia activation in a rat model of obstructive sleep apnoea (OSA). Probiotic or

prebiotic supplementation prevented the decrease in acetate levels and the augmented microglial activity (Ganesh *et al.*, 2018).

Noteworthy, under healthy physiological conditions a limited amount of SCFAs may cross the BBB (Stilling *et al.*, 2014a). FFARs are sparsely distributed in the brain, thus it has been suggested that persistent secretion of SCFAs may result in epigenetic modulation through histone deacetylase (Stilling *et al.*, 2014b; Stilling *et al.*, 2016). For example, SCFAs particularly butyrate can inhibit the activity of histone deacetylases, resulting in hyper-acetylation of histones (Waldecker *et al.*, 2008; Kratsman *et al.*, 2016; Dalile *et al.*, 2019).

1.2.3 Tryptophan metabolism and neurotransmitters

The gut microbiota facilitates central neurotransmitter regulation by synthesising and releasing neurotransmitters from bacteria directly or by altering levels of neurotransmitter precursors (Desbonnet *et al.*, 2010; Lyte, 2013, 2014a; O'Mahony *et al.*, 2015). Several studies link the gut microbiota to the serotonergic system (Clarke *et al.*, 2013; O'Mahony *et al.*, 2015). Serotonin orchestrates modulation of complex physiological functions (O'Mahony *et al.*, 2015). Interestingly, 95% of serotonin synthesis predominantly occurs within the gastrointestinal tract, with only 5% produced in the brain (Spiller, 2008).

Tryptophan, which is a serotonin precursor, was increased in plasma of germ-free mice. Gut microbial colonisation normalised plasma tryptophan concentrations. Furthermore, the absence of microbiota in germ-free mice affected the central serotonergic system within the brain. Heightened tryptophan levels correlate with elevated hippocampus serotonin concentrations and turnover in a sex-dependent manner (Clarke *et al.*, 2013). Consistent observations were evident utilising a probiotic strain, *Bifidobacterium infantis*, which increased tryptophan concentrations in plasma, with subsequent effects on central 5-hydroxyindoleacetic acid, which is a serotonin precursor (Desbonnet *et al.*, 2008). Furthermore, within the gastrointestinal tract, microbes including *Candida*, *Escherichia, Streptococcus* and *Enterococcus* species produce serotonin (Lyte, 2013, 2014a).

Microbial species can also produce other neurotransmitters. *Bacillus* species produce dopamine. *Lactobacillus* species produce acetylcholine, *Bifidobacterium* and *Lactobacillus* species produce gamma-aminobutyric acid (GABA) and *Bacillus, Escherichia* and *Saccharomyces* species produce noradrenaline (Lyte, 2013, 2014a; Strandwitz, 2018).

Microbial-synthesised neurotransmitters transfer through the mucosal layer of the intestines. However, in healthy physiological states these neurotransmitters cannot cross the

BBB, even when circulating within the bloodstream. Noteworthy, tryptophan is more readily proficient in passing through BBB capillaries, which may sequentially initiate production of serotonin within the raphé nuclei of the brainstem (Le Floc'h *et al.*, 2011). It is plausible that neurotransmitters predominantly influence brain function through activation of the enteric nervous system; however, there is paucity of information regarding signalling mechanisms. Of interest, serotonin can bind to serotonin type 3 receptors on vagal afferents, prompting neuronal activation (Glatzle *et al.*, 2002; Raybould *et al.*, 2003).

1.2.4 Immune system

Immune cells within the gastrointestinal tract play a crucial regulatory role at the host-microbiome interface, influencing whole-body health (Macpherson & Uhr, 2004; Sonnenburg *et al.*, 2006; Belkaid & Hand, 2014). Commensal gut microbes frequently reside in regions enriched in immune cells, which produce mucus, antimicrobial peptides and immunoglobulin A (Belkaid & Hand, 2014). The immune system supports a symbiotic relationship between the gut microbiota and the host tissue. Mucus, produced by goblet cells, creates the first line of defence, limiting interactions between host tissue and gut microbiota, subsequently preventing microbial translocation (McGuckin *et al.*, 2011; Belkaid & Hand, 2014). Additionally, an antimicrobial peptide, regenerating family member 3 gamma (Reg3γ) has been shown to deplete gram-positive bacteria, whereas colonisation of germ-free mice with gram-negative bacteria augmented Reg3γ expression (Cash *et al.*, 2006; Sonnenburg *et al.*, 2006). Similarly, intestinal dendritic cells in concert with T and B cells of Peyer's patches mediate immunoglobulin A production, specifically for commensal-derived antigens (Macpherson & Uhr, 2004). Thus, when functioning optimally, an important regulatory interaction exists at the luminal surface between the gut microbiota and the host tissue, which is vital for integrative body systems.

The immune system functions as a principal communication pathway of the microbiota-gut-brain axis (El Aidy *et al.*, 2014b). Sensory vagal afferent fibres can detect cytokines and other inflammatory mediators and inform the brain of inflammation in the periphery (Goehler *et al.*, 2000; Johnston & Webster, 2009). However, the mechanism by which the vagus nerve detects the presence of inflammatory mediators remains unclear. In situations of dysregulated intestinal permeability, such as stress, bacterial components including lipopolysaccharide (LPS), found on the outer membrane of gram-negative bacteria, can translocate from the intestinal lumen into the circulatory system. Systemic LPS prompts peripheral immune system stimulation and HPA-axis activation (Kelly *et al.*, 2015; Araujo *et al.*, 2017). Intriguingly, it appears that microbes within the gut can also exert effects on

microglia (Erny *et al.*, 2015). As such, microglia of germ-free mice are immature; microbial colonisation normalised these deficits (Erny *et al.*, 2015). Under healthy physiological conditions, it is implausible that immune molecules, such as chemokines cross the BBB. Interestingly, recent studies suggest an increased potential for chemokines to cross a dysregulated BBB, suggesting microbiota-induced immune modulation may directly affect brain function (Banks & Erickson, 2010).

1.2.5 Neuronal pathways

The neuronal pathways of microbiota-gut-brain communication include central, enteric and autonomic nervous systems, such as spinal, vagal and sympathetic pathways (Houlden *et al.*, 2016; Kigerl *et al.*, 2016; Breit *et al.*, 2018; Fulling *et al.*, 2019). A growing body of animal and human studies suggest the vagus nerve is the leading and most direct communication pathway of the microbiota-gut-brain axis (Fulling *et al.*, 2019). The 10th cranial nerve is the principal nerve of the parasympathetic nervous system, consisting of 80% afferent and 20% efferent fibres. It emerges from the medulla oblongata of the brainstem and terminates within the colon (Berthoud & Neuhuber, 2000). Vagal efferent fibres of preganglionic neurones arise from the dorsal motor nucleus of the vagus nerve and supply muscular and mucosal layers in the lamina propria and in the muscularis externa of the gut wall (Berthoud & Neuhuber, 2000). The celiac branch of the vagus innervates the proximal duodenum to the distal descending colon (Wang & Powley, 2007; Mukudai *et al.*, 2016). Afferent cell bodies of the nodose ganglia convey sensory cues from the periphery to the nucleus tractus solitarius (NTS) in the dorsal medulla oblongata, which projects afferent signals to multiple regions within the central nervous system, such as the rostral ventrolateral medulla and locus coeruleus, which are involved in cardiovascular control and central chemosensitivity, respectively (Berthoud & Neuhuber, 2000).

Studies in mice report that administration of *Lactobacillus rhamnosus* modified GABA receptor expression in the brain and mitigated anxiety and depressive-related behaviours (Bravo *et al.*, 2011). These behavioural and neurochemical outcomes were abolished in vagotomised mice, suggesting vagal-mediated communication between the gut microbes and the brain (Bravo *et al.*, 2011). Furthermore, oral administration of *Campylobacter jejuni* in mice, elevated anxiogenic behaviour and induced neuronal activation in the NTS, parabrachial and paraventricular nuclei and amygdala, which are components of the respiratory control and/or central autonomic networks (Gaykema *et al.*, 2004; Goehler *et al.*, 2008). Additionally, anxiolytic benefits of probiotic, *Bifidobacterium longum* were eradicated after vagotomy in mice (Bercik *et al.*, 2011b). Furthermore, vagotomy in young patients

minimised the risk of developing neurodegenerative disorders (Svensson *et al.*, 2015). Indeed, it has been suggested that vagal afferents respond to many stimuli within the gut, including nutrients, cytokines, gut hormones and metabolites, and neurotransmitters (Goehler *et al.*, 2000; Raybould *et al.*, 2003; Johnston & Webster, 2009; Kimura *et al.*, 2011; Nohr *et al.*, 2015).

Intriguingly, the vagus nerve and the NTS, its chief projection site and central 'relay hub' translate visceral information from sensors in numerous peripheral sites, such as the gut, to several regions involved in the control of breathing and cardiovascular function. Considering this and the regulatory role of the microbiota-gut-brain axis in physiological behaviours and brain functions, microbiota-gut-brain axis signalling has potential relevance for cardiorespiratory control, both in health and disease.

1.3. Microbiota modulation and analysis

A variety of well-established methods are routinely utilised to alter the gut microbiota in rodent models and appropriately assess microbiota-gut-brain axis modulation in health and disease states. These methods include, but are not limited to germ-free animals, antibiotic administration, faecal microbiota transplant (FMT), diet and prebiotic and probiotic administration (Burokas *et al.*, 2015).

1.3.1 Germ-free animals

Germ-free animals are born and raised in gnotobiotic units, which are sterile environmental chambers. This approach eliminates the opportunity for postnatal colonisation of the gastrointestinal tract (Cryan & Dinan, 2012; Luczynski *et al.*, 2016). The primary advantage of germ-free animals in assessing the role of the gut microbiota in physiological behaviours and brain functions is in proof-of-principle studies. Furthermore, an additional benefit involves microbial colonisation of germ-free animals at various developmental time-points. Nonetheless, animals born and raised in sterile environments have various deficits, exhibiting permanent neurodevelopmental dysfunctions. For these various reasons germ-free animals are often unsuitable for investigations not involving early-life microbiota deficiencies (Luczynski *et al.*, 2016).

1.3.2 Antibiotics

There is compelling evidence that microbial patterns fluctuate in response to antibiotic administration (Panda *et al.*, 2014; Desbonnet *et al.*, 2015; Hoban *et al.*, 2016; Haak *et al.*, 2019). Indeed, the 'antibiotic revolution' was one of the greatest achievements of modern medicine saving millions of lives (Brown, 2005). Nevertheless, antibiotics are not only beneficial but also detrimental to the host (Sullivan *et al.*, 2001; Benoun *et al.*, 2016; Gasparrini *et al.*, 2016). The majority of antibiotics have a broad spectrum of action, affecting not only pathogenic bacteria but also perturbing resident gut microbes (Panda *et al.*, 2014; Hoban *et al.*, 2016; Haak *et al.*, 2019). Thus, antibiotic overexposure using broad spectrum antibiotics may overwhelm the microbiome, culminating in genotypic antibiotic resistance of resident microbes and pathogenic bacteria (Sullivan *et al.*, 2001). In humans, seven consecutive days of fluoroquinolone and β-lactam antibiotic administration disturbed gut microbiota assembly by decreasing core phylogenetic microbiota and microbial diversity by 25% (Panda *et al.*, 2014). However, antibiotics increased proportions of unknown species, with β-lactam enhancing microbial load by two-fold (Panda *et al.*, 2014). Humans receiving a cocktail of antibiotics for one week, including vancomycin, ciprofloxacin and metronidazole,

displayed a perturbed microbial structure, with diminished diversity and richness 9 and 49 days after completion of the antibiotic regime (Haak *et al.*, 2019); 8-31 months following antibiotic administration microbial diversity was normalised to baseline levels (Haak *et al.*, 2019). In rodents, exposure to broad-spectrum antibiotics reduced bacterial DNA load by 400-fold, altered microbial diversity and richness and the relative abundance of many residential microbes (Reikvam *et al.*, 2011; Desbonnet *et al.*, 2015; Hoban *et al.*, 2016). In rodents, many pathophysiological conditions relating to altered brain functions, such as deficits in memory and depressive-like behaviours, present following antibiotic-induced changes in the gut microbiota (Desbonnet *et al.*, 2015; Hoban *et al.*, 2016).

1.3.3 Diet

Diet directly shapes gut microbiota composition, structure and diversity, providing nutrients to gut microbes, *via* indigestible ingredients or by-products of digestion (Brown *et al.*, 2012; Albenberg & Wu, 2014). Dietary regimes provoke distinct microbial patterns within the gut (Brown *et al.*, 2012; Kallus & Brandt, 2012; Murphy *et al.*, 2015). Consumption of a western diet, containing copious amounts of salt, sugars and fats results in elevated Firmicutes:Bacteroidetes ratio, which is associated with hypertension and diet-induced obesity (Kallus & Brandt, 2012; Murphy *et al.*, 2015; Yang *et al.*, 2015). Mediterranean diet consisting of whole grains, vegetables, fruit and minimal consumption of animal products significantly increased SCFAs and reduced trimethylamine oxide in humans, a metabolite linked to atherosclerosis and cardiovascular disease (De Filippis *et al.*, 2016). Moreover, consumption of a Mediterranean diet reveals marked decreases in other chronic diseases resulting in reduced mortality (Del Chierico *et al.*, 2014). In essence, the gut microbiota plays a vital role in carbohydrate, protein and polyphenol fermentation and vitamin synthesis (vitamin B12, B6, B5, B3, D and K). In turn, diet orchestrates a unique microbial pattern within the gut (Sandhu *et al.*, 2017).

Dietary fibres: Carbohydrates represent a substantial component of the human diet. They are metabolised by the gut microbiota and subsequently absorbed as simple sugars in the intestines (Rajilić-Stojanović, 2013). Microbial fermentation of carbohydrates generates energy from undigested food by producing bacterial metabolites, including SCFAs. Dietary fibres are specific carbohydrates or carbohydrate-containing compounds that cannot be readily digested or absorbed in the small intestines but are fermented in the large intestines. These fibres are classified based on their specific function in the plant, fibre components, polysaccharide type, gastrointestinal solubility, digestion site and products and physiological properties (Staffolo *et al.*, 2012).

Prebiotics: Prebiotics are a type of dietary fibre which are resistant to gastric acid and enzymes and convey health benefits *via* upregulation of microbes associated with whole-body health (Gibson *et al.*, 2004; Slavin, 2013). Inulin, lactulose, fructooligosaccharides and galactooligossacharides are the most extensively studied prebiotics (Roberfroid *et al.*, 2010). Fructooligosaccharides and galactooligossacharides are oligosaccharides present in plants (e.g. asparagus, garlic, banana, tomato, artichoke and onions) and human milk, respectively. These oligosaccharides have direct and indirect effects on overall he alth, including decreased risk of obesity, reduced levels of cholesterol, immune regulation, ameliorated mineral absorption, anxiolytic and antidepressant effects and reduced colonic carcinogenic substances (Cani *et al.*, 2006; Sabater-Molina *et al.*, 2009; Kuo, 2013; Burokas *et al.*, 2017).

1.3.4 Faecal microbiota transplant

There is growing appreciation for the use of FMT in animal models and in modern medicine. FMT is the transfer of stool from a donor into the gastrointestinal tract of a recipient in order to directly change the microbial pattern of the recipient (Kelly *et al.*, 2016b; Pevsner-Fischer *et al.*, 2016; Zheng *et al.*, 2016).

Transplantation of faecal microbiota from depressed patients into antibiotic-treated rats, altered a number of microbial taxa and reduced gut microbiota richness and diversity compared with controls (Kelly *et al.*, 2016b). Depressive behaviours were evident in antibiotic-treated and germ-free rodents that received FMT from depressed individuals (Kelly *et al.*, 2016b; Zheng *et al.*, 2016). Moreover, blood pressure phenotypes in donor animals can be transferred to recipient animals *via* FMT (Li *et al.*, 2017; Toral *et al.*, 2019). Additionally, mice receiving faecal microbiota from patients with irritable bowel syndrome had an altered gut microbiota along with intestinal barrier dysfunction, innate immune activation and anxiety-like behaviours (De Palma *et al.*, 2015). Mice receiving faecal microbiota from autistic patients exhibited a perturbed gut microbiota and autistic-like social behaviours (Sharon *et al.*, 2019).

Intriguingly, autologous FMT following antibiotic administration resulted in rapid and near complete restoration of the gut microbiota in a human population (Suez *et al.*, 2018). Clinically, FMT has proven to benefit individuals with *Clostridium difficile* infection and to a lesser extent patients with biopsychosocial disorder, irritable bowel syndrome and individuals with a neurodegenerative and immune disorder-multiple sclerosis (Pevsner-Fischer *et al.*, 2016). These animal and human studies suggest that FMT may be a viable strategy to investigate brain functions in health and disease.

1.3.5 Analysis of the microbiome

Whole genome shotgun and 16S rRNA gene sequencing allow for advanced compositional analysis of the microbiome. 16S sequencing is a technique wherein highly conserved regions of the transcript (cDNA) or 16S rRNA (DNA) are used to identify metabolically active or present microbes, respectively. In contrast, whole-genome shotgun sequencing is a technique wherein all DNA in a sample is sequenced to classify microbes that are present and their functional (metagenomic) potential (Claesson *et al.*, 2017; Bastiaanssen *et al.*, 2019).

Beta and alpha diversity are terms used in ecology that represent between and within-sample variability, respectively. Multiple formulas define diversity differently, due to different weightings ascribed to aspects such as how rare/abundant the species are, binary abundance/presence, number of species and taxonomic distance between species (Bastiaanssen *et al.*, 2019).

1.4. Control of breathing and cardiovascular function

1.4.1 Overview of cardiorespiratory control

The cardiorespiratory control network is a highly complex homeostatic system. Exquisite cardiovascular and respiratory regulatory mechanisms are required to maintain sufficient blood oxygenation to meet metabolic demands, which is vital for whole-body health. Neuronal networks within the brain, particularly the brainstem, tightly regulate the cardiorespiratory system. They depend on critical feedback from the periphery (Guyenet, 2006; Garcia *et al.*, 2011). There is substantial sensory-guided modulation of autonomic and respiratory motor outputs from the periphery, which implement appropriate cardiorespiratory reflex control (Guyenet, 2014). Autonomic centres execute sympathetic and parasympathetic motor output to the heart and circulation (Guyenet, 2006). Respiratory centres transduce appropriate reflex responses through numerous efferent pathways, directly or indirectly *via* spinal nuclei to muscles of breathing, providing superb breath-by-breath ventilatory control (Garcia *et al.*, 2011) (Figure 1.2). There is considerable respiratory modulation of autonomic outflow (Guyenet, 2014). Notwithstanding the homeostatic capacity governing breathing and blood pressure control, there is an extensive degree of evidence supporting remarkable potential for adaptive and maladaptive plasticity, which can occur at multiple regions within the cardiorespiratory control system, including peripheral and central levels (Edge *et al.*, 2009; Peng *et al.*, 2009; Edge *et al.*, 2010; Kumar & Prabhakar, 2012; Edge & O'Halloran, 2015; O'Halloran, 2016; Burns *et al.*, 2017; Fuller & Mitchell, 2017; Hocker *et al.*, 2017; Laouafa *et al.*, 2017). Maladaptive plasticity may result in devastating consequences for integrative body systems (Bavis, 2005; Gulemetova & Kinkead, 2011; Fournier *et al.*, 2013a; Kinkead *et al.*, 2013; Golubeva *et al.*, 2015; Soliz *et al.*, 2016; Laouafa *et al.*, 2017).

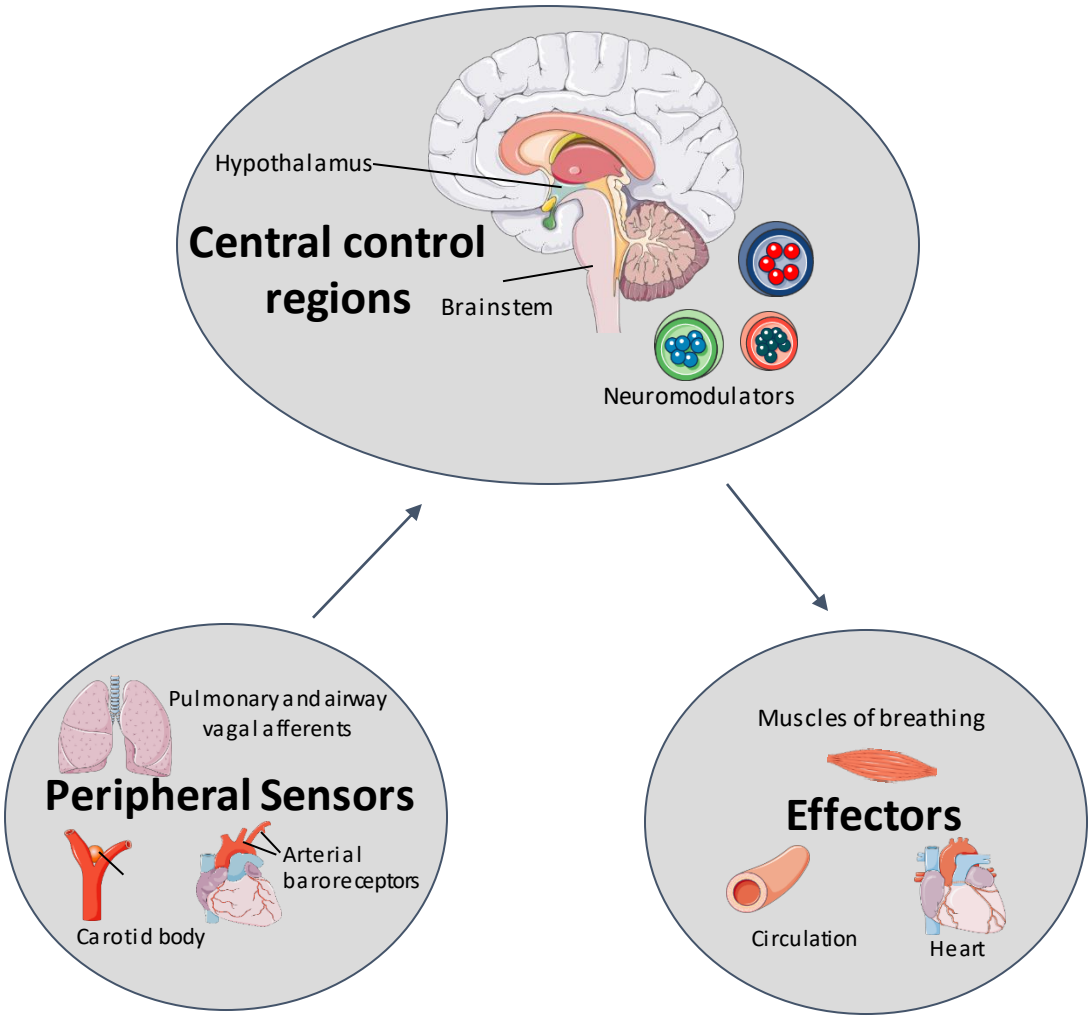


Figure 1. 2 Summary of the cardiorespiratory control network, which is composed of sensors, central control regions and effectors.

These components work in unison to maintain adequate blood oxygenation to meet metabolic demands of the body. Sensory afferent cues from the periphery, including peripheral chemoreceptors, pulmonary and airway vagal afferents and arterial baroreceptors project to the brainstem, where information is integrated and processed. Appropriate respiratory and autonomic responses are generated to maintain acid-base and blood pressure homeostasis.

1.4.2 Neuronal networks

The pontomedullary regions of the brainstem consists of interconnected neuronal networks that are vital for production of automatic breathing and for generation of autonomic outflow involved in cardiovascular homeostasis (Guyenet, 2014). The NTS, ventrolateral pons (A5 pons), dorsolateral pons (inter-trigeminal region, lateral parabrachial nuclei and Kolliker-Fuse nucleus) and ventral respiratory column (Bötzinger complex, pre-Bötzinger complex, rostral and caudal ventral respiratory group), which resides in the ventrolateral medulla are the principal building blocks of the respiratory pattern generator (Feldman *et al.*, 2003; Alheid & McCrimmon, 2008; Smith *et al.*, 2013a). Additionally, the ventrolateral medulla (rostral, intermediate and caudal), lateral parabrachial nuclei and NTS are recognised to contain the main components of the network that generates sympathetic and parasympathetic autonomic outflow to the cardiovascular system. Another principal component of cardiovascular control is the hypothalamus, particularly the paraventricular nucleus (Guyenet, 2006). The hypothalamus has extensive connections with brainstem circuitry and predominantly contributes to cardiorespiratory regulation in response to environmental stressors or threats (Guyenet, 2006; Behan & Kinkead, 2011).

Respiratory and autonomic outputs are further regulated by numerous neuromodulators, such as serotonin and noradrenaline, as well as excitatory (glutamatergic) and inhibitory (GABA and/or glycinergic) neurones (Doi & Ramirez, 2008; Ramirez *et al.*, 2012; Abbott *et al.*, 2013; Smith *et al.*, 2013a). Neuromodulators have multiple functions at various levels of the control network. Often the same modulator can exert differential effects on activity by acting on different G-protein receptors. Disturbances in neuromodulation can have significant impact on cardiorespiratory control (Doi & Ramirez, 2008; Harris-Warrick & Johnson, 2010).

This network in turn phasically activates respiratory motor neurones located in the phrenic nucleus of cervical spinal cord and elsewhere (hypoglossal and ambiguus nuclei of the medulla) and modulates sympathetic and parasympathetic preganglionic outflow, which contribute to cardiovascular control (Guyenet, 2006, 2014).

1.4.3 Central chemoreceptors

Some neuronal networks within the central nervous system detect changes in carbon dioxide (PCO_2) and hydrogen ion concentrations (pH) in brain extracellular fluid. These central chemoreceptors are essential in the maintenance of acid-base homeostasis. During eupnoea (normal unlaboured breathing at rest), the partial pressure of arterial carbon dioxide ($PaCO_2$) is maintained within the physiological set-point. However, $PaCO_2$ may increase as a result of

airway blockade, diving, bronchial disease and disordered breathing, among other factors such as disease states. Elevated $PaCO_{2,}$ sensed by chemoreceptors, initiates an increase in ventilation and arousal from sleep to maintain optimal pulmonary ventilation and gas exchange.

A substantial degree of evidence suggests that the putative principal chemosensitive region within the brain is the retrotrapezoid nucleus (RTN), which detects carbon dioxide (CO_2) *via* signals from astrocytes, synaptic input from peripheral chemoreceptors or intrinsic proton receptors (Guyenet & Bayliss, 2015). Phox2b mutation in mice (born without RTN neurones) and genetic elimination of RTN neurones significantly reduced the ventilatory responsiveness to hypercapnia (elevated CO_2) (Amiel *et al.*, 2003; Dubreuil *et al.*, 2008; Ramanantsoa *et al.*, 2011; Ruffault *et al.*, 2015).

Additionally, several studies suggest that a subset of serotonergic neurones residing in the raphé magnus may have central chemosensitive properties (Hodges *et al.*, 2008; Corcoran *et al.*, 2009; Brust *et al.*, 2014; Buchanan *et al.*, 2015). Impairment in serotonergic neurone development in mice results in reduced ventilation during hypercapnia (Hodges *et al.*, 2008; Hodges *et al.*, 2009; Buchanan & Richerson, 2010). Furthermore, pharmacological inhibition of serotonergic neurones (Di-expressing and Egr2-Pet1 subtype) in rodents diminished CO_2-induced ventilation (Ray *et al.*, 2011; Brust *et al.*, 2014).

Of further interest, partial lesions of catecholaminergic neurones (locus coeruleus and other brainstem noradrenergic neurones) reduced the hypercapnic ventilatory response in mice (Li & Nattie, 2006). Furthermore, oxidopamine-induced lesions of the locus coeruleus in rats attenuated ventilation in response to hypercapnia, but not hypoxia (Biancardi *et al.*, 2008; Biancardi *et al.*, 2010). Other neurones within the brain may also function as central chemoreceptors, however at present there are unmet knowledge gaps in this regard (Guyenet & Bayliss, 2015).

1.4.4 Peripheral sensors

Peripheral sensors are essential components of the cardiorespiratory control network. Sensory afferent cues from the periphery, including peripheral chemoreceptors, pulmonary and airway vagal afferents and arterial baroreceptors, project to the NTS within the brainstem. In turn, the NTS relays information to other cardiorespiratory regions where information is processed and appropriate respiratory and autonomic responses are generated to maintain acid-base and blood pressure homeostasis (Coleridge & Coleridge, 1984; Purves *et al.*, 2001; Widdicombe, 2003; Prabhakar & Peng, 2004).

Peripheral chemoreceptors: Peripheral chemoreceptors residing at the carotid body and aortic arch detect partial pressure of arterial oxygen (PaO_2)(Prabhakar & Peng, 2004; Teppema & Dahan, 2010; Kumar & Prabhakar, 2012). The carotid body is the dominant peripheral oxygen sensor, situated at the bifurcation of the common carotid arteries, bilaterally. It receives sensory innervation from the carotid sinus nerve, which is a branch of the glossopharyngeal nerve (9th cranial nerve). Type 1 (glomus) and type II sustentacular (glia) cells form the structure of the carotid body (Kumar & Prabhakar, 2012).

Chemoafferent sensory discharge from the carotid body is modest during normoxia (~100mg PaO_2) (Lipski *et al.*, 1977; Prabhakar, 2006) and within blood PaO_2 range of 100 to 60mmHg. However, the carotid body is extremely sensitive to reductions in PaO_2 below 60mmHg. Hypoxaemia (low blood oxygenation), which occurs for example during high altitude exposure and in pulmonary and respiratory disorders such as chronic obstructive pulmonary disease (COPD) and sleep apnoea, activates carotid body afferent discharge, through the glossopharyngeal nerve, to the NTS within the brainstem (Kumar & Prabhakar, 2012). Appropriate respiratory and autonomic outputs are evoked in response to hypoxaemia, such as enhanced ventilatory drive and altered sympathetic and parasympathetic activity. This ensures adequate oxygen supply to tissues throughout the body (Machado, 2001).

Pulmonary and lower airway vagal afferents: Sensory fibres within the lung and smooth muscle of the lower airway send signals to the NTS within the brainstem, *via* vagal afferent fibres. These afferent fibres are broadly divided into 3 types: slowly- and rapidly-adapting myelinated stretch receptors and unmyelinated bronchopulmonary C-fibres.

Slowly- and rapidly-adapting mechanoreceptors are sensitive to dynamic and static functions of transmural pressure and lung volume. Indeed, these receptors are primarily activated by lung inflation (Schelegle, 2003; Widdicombe, 2003). Furthermore, rapidly-adapting stretch receptors are also activated by irritants (Widdicombe, 2003). Bronchopulmonary C-fibres are polymodal, activated by a variety of stimuli, including chemicals (phenylbiguanide and capsaicin) and lung oedema, among other factors (Coleridge & Coleridge, 1984; Dutta & Deshpande, 2010; Lucking *et al.*, 2018a).

Each group of sensory afferent fibres has specific functions in cardiorespiratory reflex responses. For example, classic cardiorespiratory responses to slowly-adapting mechanoreceptor activation include inspiratory termination, expiratory facilitation (Bre uer-Hering reflex) and tachycardia; rapidly-adapting mechanoreceptor stimulation results in

generation of cough; and bronchopulmonary C-fibre activation leads to apnoea, post-apnoea induced tachypnoea and bradycardia (reduced heart rate) (Kubin *et al.*, 2006).

Arterial baroreceptors: Arterial baroreceptors are mechanosensitive nerve endings that function as arterial blood pressure sensors. They are situated primarily in the aortic arch and carotid sinuses near the bifurcation of the common carotid artery. The carotid sinus and the glossopharyngeal nerves transmit sensory afferent information from the carotid sinus baroreceptors to the NTS within the brainstem (Guyenet, 2006). Furthermore, extra-carotid arterial baroreceptors found in the aortic arch and stretch-sensitive receptors of the heart and pulmonary vessels transduce sensory afferent cues *via* vagal nerves to the NTS (Purves *et al.*, 2001; Guyenet, 2006). Regardless of their anatomical location, these arterial baroreceptors function by transducing afferent information in a negative feedback loop to maintain homeostatic control of blood pressure (Purves *et al.*, 2001).

In essence, increased blood pressure stimulates baroreceptors, inhibiting activation of spinal cord sympathetic preganglionic neurones. In tandem, the elevated blood pressure stimulates parasympathetic preganglionic neurones, which are located in the nucleus ambiguus and dorsal motor nucleus of the vagus. This shift from sympathetic to parasympathetic dominance results in decreased noradrenergic stimulation of cardiac musculature and pacemaker postganglionic sympathetic fibres (Salman, 2016). In parallel, stimulatory effects of acetylcholine released through cholinergic parasympathetic supply to the heart has negative dromotropic effects, reducing cardiac pacemaker discharge frequency in the sinoatrial node and slowing ventricular conductance. Furthermore, negative chronotropic and inotropic effects occur, reducing heart rate and atrial and ventricular contractions. Peripheral vasodilation occurs predominantly *via* withdrawal of sympathetic vasoconstriction. This negative feedback loop lowers blood pressure (Gordan *et al.*, 2015; Salman, 2016).

In contrast, a decrease in blood pressure inhibits parasympathetic activity while increasing sympathetic drive. Norepinephrine is released from sympathetic postganglionic terminals, increasing cardiac pacemaker activity, enhancing inotropic effects and elevating catecholamine release from the adrenal medulla. Moreover, norepinephrine increases smooth muscle tone of peripheral arterioles leading to vasoconstriction and increases cardiac output. As a result, blood pressure is normalised (Purves *et al.*, 2001; Gordan *et al.*, 2015; Salman, 2016). The baroreflex is essential for homeostatic control of blood pressure.

1.4.5 Cardiorespiratory coupling

Accumulating evidence supports the concept of cardiorespiratory coupling, establishing a unique and dynamic twinned system. Recording of sympathetic and parasympathetic nerves innervating the blood vessels and heart suggest that autonomic nervous system activity displays discharge patterns coordinated with respiratory rhythm and pattern (Adrian *et al.*, 1932; Barman & Gebber, 2000; Bouairi *et al.*, 2004; Gilbey, 2007; Grossman & Taylor, 2007). Respiratory-related modulation of autonomic activities depends on the acid-base balance within the control network (Dick *et al.*, 2004; Molkov *et al.*, 2011). Cardiorespiratory coupling generates appropriate reflex responses with rhythmical oscillations in blood pressure and heart rate (Moraes *et al.*, 2012).

There are knowledge gaps regarding neuronal sources contributing to cardiorespiratory coupling. However, studies suggest that respiratory neurones of the ventral respiratory column establish connections with pre-sympathetic neurones of the rostral ventrolateral medulla, either directly or indirectly, through the caudal ventrolateral medulla, producing respiratory oscillations in sympathetic activity (Miyawaki *et al.*, 1995; Zoccal *et al.*, 2008; Zoccal *et al.*, 2014). Additionally, the NTS has a vital role in the regulation of sympathetic and respiratory activity in response to peripheral chemoreceptor and mechanoreceptor activation. Specific NTS neurones may underpin the coupling of cardiovascular and respiratory activities due to the recruitment of both respiratory and autonomic pathways (Costa-Silva *et al.*, 2010; Zoccal *et al.*, 2014). There is interest in respiratory-sympathetic coupling as a potential contributor to elevated blood pressure observed in animal models of chronic intermittent hypoxia, modelling human OSA (Moraes *et al.*, 2014; Machado *et al.*, 2017).

1.4.6 Plasticity

Due to the considerable capacity for impressive plasticity at both central and peripheral levels of the cardiorespiratory control system, plasticity is now recognised as a fundamental property of the integrated cardiorespiratory network (Fuller & Mitchell, 2017). Neuroplasticity describes a persistent modification in a neural control network based on a prior experience, resulting in reorganisation of structure and/or function within the network (Mitchell & Johnson, 2003). During both development and adulthood, physiological and pathological factors can challenge the neuronal network's capacity to maintain cardiorespiratory homeostasis (Almado *et al.*, 2012; Kumar & Prabhakar, 2012; Golubeva *et al.*, 2015; O'Halloran, 2016; Fuller & Mitchell, 2017; Hocker *et al.*, 2017). Such challenges include exercise, development/ageing, inflammation, stress and chronic and intermittent

hypoxia, amongst other factors (Powell *et al.*, 2000; Mitchell & Johnson, 2003; Edge *et al.*, 2010; Golubeva *et al.*, 2015; Hocker *et al.*, 2017). Adaptive plasticity, which is vital in the maintenance of pH regulation and appropriate blood oxygenation, may occur in response to physiological challenges. However, maladaptive plasticity also presents, revealing long-lasting perturbations to cardiorespiratory control and deleterious consequences for whole-body health (Mitchell & Johnson, 2003; Peng *et al.*, 2003; Bavis, 2005; Gulemetova & Kinkead, 2011; Edge *et al.*, 2012; Fournier *et al.*, 2013a; Kinkead *et al.*, 2013; Golubeva *et al.*, 2015; Soliz *et al.*, 2016; O'Halloran & McDonald, 2018).

Chronic intermittent hypoxia (CIH): In rodents, exposure to CIH alters cardiorespiratory homeostasis at many levels of the control network, including motor pathways, central brain regions and peripheral chemoreceptors (Fuller *et al.*, 2000; Peng *et al.*, 2003; Kline *et al.*, 2007). Noteworthy, IH may induce adaptive responses in the control system. However, depending on pattern, duration, intensity and timing of IH exposure, maladaptive plasticity can also occur (Lane *et al.*, 2008; Gonzalez-Rothi *et al.*, 2015). Many classic adverse effects develop due to CIH exposure. These include but are not limited to, development of hypertension, elevated sympathetic nervous activity, augmented peripheral chemoreflex responses, alterations in respiratory pattern such as increased central apnoeas and enhanced respiratory timing variability as well as disrupted cardiorespiratory coupling (Peng *et al.*, 2003; Braga *et al.*, 2006; Zoccal *et al.*, 2008; Zoccal *et al.*, 2009; Edge *et al.*, 2012; Moraes *et al.*, 2013; Lucking *et al.*, 2014; O'Halloran, 2016; Laouafa *et al.*, 2017).

CIH can induce carotid body plasticity, which manifests as sensory long-term facilitation. This promotes sympathetic nervous system activation, culminating in the manifestation of CIH-induced hypertension (Peng *et al.*, 2003). CIH-induced plasticity of the carotid body is dependent upon reactive oxygen species production by NADPH oxidase, transcriptional regulation of hypoxia-inducible factors and serotonergic signalling (Peng *et al.*, 2003; Prabhakar *et al.*, 2007; Peng *et al.*, 2009; Peng *et al.*, 2011). More recently it has been shown that lactate, a metabolite that is increased during hypoxia activates olfactory receptor 78 on glomus cells of the carotid body with resultant increases in carotid sinus nerve activity (Chang *et al.*, 2015).

Notwithstanding the effects of CIH at the level of the carotid body, CIH can also induce central plasticity. The NTS, which is the integration site of chemoafferent information from the carotid chemoreceptors, is a site of central plasticity. CIH exposure results in altered glutamatergic neurotransmission and second-order neurone activity in the NTS. As a result

increased excitatory drive to respiratory motor neurones and sympathetic preganglionic neurones may occur, which at least in part, could lead to CIH-induced cardiorespiratory dysfunction (Kline *et al.*, 2007; Costa-Silva *et al.*, 2012). Central plasticity is also well-documented in several other locations within the brain, such as the pre-Bötzinger complex (the major respiratory rhythm-generating site of the brainstem), hypothalamic paraventricular nucleus and medullary network (Moraes *et al.*, 2013; Garcia *et al.*, 2016; Li *et al.*, 2018).

Additionally, CIH exposure induces enhanced long-term facilitation of motor pathways to the diaphragm, inspiratory intercostal, hypoglossal and laryngeal nerves (Fregosi & Mitchell, 1994; Fuller *et al.*, 2000; Bautista *et al.*, 2012; Wilkerson *et al.*, 2018). Motor facilitation of pathways may occur *via* spinal serotonin release, spinal receptor 2 activation, TrkB receptor activation, ERK MAPK activity, reactive oxygen species formation and synthesis of brain derived neurotrophic factor (Baker-Herman & Mitchell, 2002; Baker-Herman *et al.*, 2004; MacFarlane *et al.*, 2009; Wilkerson & Mitchell, 2009).

Stress: Acute and chronic stress, which disrupt programming of the HPA axis, an efferent pathway of the microbiota-gut-brain axis, have a significant impact on vital homeostatic behaviours and brain functions (O'Mahony *et al.*, 2009; Golubeva *et al.*, 2015; Kelly *et al.*, 2015; O'Halloran & McDonald, 2018). In rats, exposure to a single stress elevated c-fos activity in cardiorespiratory control regions including the NTS, locus coeruleus and parabrachial nucleus (Jaccoby *et al.*, 1999; Berquin *et al.*, 2000).

Early life stress has devastating effects on the cardiorespiratory control network at various life stages, which can persist into adulthood depending on duration, intensity and timing of the stressor. Perinatal stress augmented apnoea (respiratory pause) index, increased the coefficient of variation for respiratory frequency, elevated blood pressure and affected the hypoxic ventilatory response during early life and adulthood compared with control rats (Genest *et al.*, 2004; Gulemetova & Kinkead, 2011; Fournier *et al.*, 2013a; Golubeva *et al.*, 2015). Furthermore, maternal separation leads to more variable minute ventilation and tidal volume during non-rapid eye movement sleep and wakefulness compared with control animals (Kinkead *et al.*, 2009). Indeed, stress, particularly early life stress dampens the capacity to achieve adequate 'fine-tuning' of breath-to-breath ventilatory control and it alters blood pressure.

Stress has been shown to elevate sympathetic drive, which may contribute to the hypertensive phenotype evident in stressed animal models (Fontes *et al.*, 2014). Additionally,

it is conceivable that disturbed excitatory and inhibitory neurotransmission within the paraventricular nucleus and/or the NTS contributes to the altered hypoxic ventilatory response (Genest *et al.*, 2007; Kinkead *et al.*, 2008; Behan & Kinkead, 2011; Gulemetova *et al.*, 2013). Furthermore, decreased serotonin and noradrenaline concentrations were evident in the medulla oblongata of new born rats subjected to gestational stress, which may have contributed to variations in respiratory rhythm (Fournier *et al.*, 2013a).

1.5. Autonomic dysfunction and aberrant gut microbiota

1.5.1 Stress and aberrant gut microbiota

It is well known that stress and the HPA axis can influence the gut microbiota (Tannock & Savage, 1974; Kelly *et al.*, 2015). Chronic social defeat, crowding and perinatal stress result in perturbations to gut microbiota structure and composition, with increased susceptibility to enteric pathogens (O'Mahony *et al.*, 2009; Bailey *et al.*, 2010; Foster *et al.*, 2017; van de Wouw *et al.*, 2018b). Chronic sleep disruption, an indirect stress, which occurs during sleep-disordered breathing, disturbs gut microbial diversity and composition in mice and this remains altered for the duration of sleep fragmentation (Poroyko *et al.*, 2016). Chronic sleep disruption increased the Firmicutes:Bacteroidetes ratio, which is an index of gut microbial imbalance and is associated with various pathologies (Poroyko *et al.*, 2016). This increased ratio was due to growth of *Lachnospiraceae* and *Ruminococcaceae* families and a decrease in *Lactobacillaceae* and *Bifidobacteriaceae* families, which consists of many beneficial species (Poroyko *et al.*, 2016).

In a hypertensive model with heightened sympathetic activity, gut inflammation and decreased tight junction expression occurred, manifesting as increased intestinal permeability (Santisteban *et al.*, 2017; Kim *et al.*, 2018; Toral *et al.*, 2019). These changes in gut pathology were associated with perturbed microbiota, including changes in *Alistipes, Bacteroides* and *Bifidobacterium* (Santisteban *et al.*, 2017). Similarly, CIH exposure caused gut inflammation, oxidative stress and decreased tight junction expression, compromising intestinal barrier function (Wu *et al.*, 2016). These maladies have previously been associated with disrupted gut microbiota (Kelly *et al.*, 2015; Santisteban *et al.*, 2017). Furthermore, CIH-exposed mice had a *Prevotella* enterotype and altered bacterial genera, including proliferation of obligate anaerobes, increased Shannon index (a measure of microbiome evenness) and a distinct diversity cluster compared with control mice (Moreno-Indias *et al.*, 2015). Similarly, in mice, high-fat diet (HFD) and intermittent cycles of hypoxia and hypercapnia altered the gut microbiota and gut microbiota metabolites (Tripathi *et al.*, 2018). Additionally, in CIH-exposed mice, elevated levels of endogenous LPS were evident systemically (Moreno-Indias *et al.*, 2015). Increased LPS is indicative of increased intestinal permeability, which may be due to sympathetic hyperactivity driven by CIH exposure (Fletcher *et al.*, 1992c; Fletcher *et al.*, 1992d; Santisteban *et al.*, 2017). In a follow-up study, CIH-exposed mice were afforded 6-weeks of normoxia as a recovery strategy to mimic treatment for sleep-disordered breathing. However, after this recovery period, the presence

of endotoxins systemically and CIH-induced gut microbiota perturbations persisted (Moreno-Indias *et al.*, 2016).

Systemic stress and CIH provoke sympathetic nervous system hyperactivity. This over-activity appears to be a cause of disrupted gut microbiota composition and diversity (Wu *et al.*, 2016; Santisteban *et al.*, 2017). However, considering the vagus nerve is key in the microbiota-gut-brain axis and vagal activity is altered in animal models with sympathetic nervous system hyperactivity, it remains plausible that autonomic dysregulation influences the gut microbiota rather than hyperactivity of the sympathetic nervous system alone (Mancia & Grassi, 2014).

CIH may also have direct effects on the gut microbiome. Interestingly, hyperbaric air affects the composition of the gut microbiota; a decrease in obligate anaerobes and an increase in total aerobes and facultative anaerobes occurred in hyperoxic rodent faecal samples compared with controls (Maity *et al.*, 2012; Albenberg *et al.*, 2014).

CIH can affect the gut microbiome indirectly *via* autonomic dysregulation and/or by direct effects on the gut microbiota (Moreno-Indias *et al.*, 2015; Moreno-Indias *et al.*, 2016). Therefore, the gut microbiota is a potential source contributing to CIH-induced cardiorespiratory dysregulation *via* altered 'microbiota-gut brain axis' signalling initiated by changes in gut microbiota composition.

1.6. Blood pressure, breathing and the gut microbiota

1.6.1 Blood pressure and gut microbiota composition and diversity

Hypertension is a risk factor for cardiovascular disease and stroke. High blood pressure is an independent risk factor associated with sleep-disordered breathing (Parish & Somers, 2004). Several animal models and human studies have recently linked the development of hypertension to aberrant gut microbiota composition and diversity (Yang *et al.*, 2015; Durgan *et al.*, 2016; Adnan *et al.*, 2017; Li *et al.*, 2017; Santisteban *et al.*, 2017; Yan *et al.*, 2017; Toral *et al.*, 2019).

An increased Firmicutes:Bacteroidetes ratio occurs in hypertensive rodents, which was also evident when the hypertensive phenotype was transferred *via* oral gavage (Yang *et al.*, 2015; Adnan *et al.*, 2017). Intriguingly, this shift was not observed in pre-hypertensive rodents (Santisteban *et al.*, 2017) and an anti-hypertensive agent, minocycline, recovered the Firmicutes:Bacteroidetes ratio (Yang *et al.*, 2015).

Furthermore, hypertensive rodents have reduced bacterial diversity as evident by a decrease in microbial evenness and richness (Yang *et al.*, 2015). Similarly, decreased species richness and evenness and distinct diversity cluster occurred in hypertensive individuals compared with normotensive individuals (Yang *et al.*, 2015; Li *et al.*, 2017; Yan *et al.*, 2017). Of interest, in the gut of hypertensive patients there was lower metabolism of amino acids, cofactors, vitamins and short chain fatty acid producing enzymes and higher lipopolysaccharide biosynthesis, steroid degradation, trimethylamine producing enzymes and membrane transport compared with controls (Yan *et al.*, 2017). Faecal transplant from two hypertensive patients into recipient germ-free mice produced hypertension and tachycardia in the recipient animals (Li *et al.*, 2017). Remarkably, faecal microbial transfer from normotensive donor rats to hypertensive recipient rats decreased blood pressure in the hypertensive recipients (Toral *et al.*, 2019).

Blood pressure and short-chain fatty acids: In hypertensive rats, butyrate- and acetate-producing bacterial taxa, such as *Clostridiaceae* families and *Bifidobacterium* respectively, were significantly reduced with lactate-producing bacterial taxa, such as *Streptococcaceae and Coriobacteriaceae families* increased (Yang *et al.*, 2015; Durgan *et al.*, 2016; Santisteban *et al.*, 2017; Ganesh *et al.*, 2018; Kim *et al.*, 2018). The relative abundance of lactate-, butyrate- and acetate-producing bacterial taxa were associated with systolic blood pressure (Adnan *et al.*, 2017; Toral *et al.*, 2019). *Lactobacillus* a lactate-producing genus positively correlated with systolic blood pressure, whereas *Clostridiaceae* and *Odoribactereae*,

butyrate-producing families and *Holdemani* and *Coprobacillus,* acetate-producing genera, negatively correlated with systolic blood pressure (Adnan *et al.*, 2017; Toral *et al.*, 2019). Additionally, minocycline administration trended towards an increase in acetate- and butyrate-producing bacteria (Yang *et al.*, 2015), showing that an increase in these bacterial taxa are associated with lower blood pressure.

In rodent models, propionate, acetate and butyrate administration attenuated cardiac fibrosis, cardiac hypertrophy and hypertension in chronic angiotensin II-induced and mineralocorticoid excess-induced hypertension (Marques *et al.*, 2017; Kim *et al.*, 2018; Bartolomaeus *et al.*, 2019). Additionally, acetate supplementation decreased the Firmicutes:Bacteroidetes ratio (Marques *et al.*, 2017) and butyrate treatment normalised gut barrier dysfunction (Kim *et al.*, 2018), two pathologies of hypertensive models (Adnan *et al.*, 2017; Santisteban *et al.*, 2017). Remarkably, probiotic (*Clostridium butyricum*) or prebiotic (Hylon VII) administration prevented hypertension in a high-fat diet and obstructive sleep apnoea (HFD+OSA) rat model, increasing the abundance of several SCFA producing taxa and caecum acetate, which were decreased in the hypertensive model. Furthermore, probiotic or prebiotic administration prevented epithelial goblet cell loss, mucus barrier thinning and microglia activation, which were evident in the HFD+OSA hypertensive model. Impressively, chronic acetate administration into the caecum of rats during exposure to HFD+OSA restored caecal acetate concentrations and prevented the development of hypertension and gut inflammation (Ganesh *et al.*, 2018).

Blood pressure regulation by gut microbiota: The precise mechanism of how perturbed gut microbiota and microbiota metabolites contributes to hypertension has yet to be elucidated. At present, sympathetic neuronal communication between the hypothalamic paraventricular nucleus and the gut has been proposed to be involved in blood pressure regulation (Santisteban *et al.*, 2017). Remarkably, faecal microbiota transfer from donor normotensive to recipient hypertensive rats decreased blood pressure, gut inflammation, plasma LPS as well as NADPH oxidase-dependent reactive oxygen species production and neuroinflammation in the hypothalamic paraventricular nucleus. Additionally, decreased plasma noradrenaline concentrations and blunted pentolinium-induced hypotensive responses were evident in recipient rats indicative of reduced sympathetic nervous system excitation (Toral *et al.*, 2019). This proposed mechanism may have relevance in hypertensive CIH-exposed animals (Li *et al.*, 2018).

Furthermore, studies in the literature have recurrently identified altered lactate, butyrate and acetate-producing bacterial taxa in hypertensive animal models (Yang *et al.*, 2015; Durgan *et al.*, 2016; Santisteban *et al.*, 2017; Ganesh *et al.*, 2018). Interestingly, SCFAs have been shown to affect brain microglia, reduce BBB permeability, influence neurotransmitter production and immune system regulation (DeCastro *et al.*, 2005; Braniste *et al.*, 2014; Erny *et al.*, 2015; Stilling *et al.*, 2016). Moreover, SCFAs can cause neuronal activation (Lal *et al.*, 2001; Nohr *et al.*, 2015), influencing the autonomic nervous system. When considered together, these studies suggest that hypertension, at least in part, results from the influence of perturbed gut microbiota on central cardiovascular control regions. Notwithstanding the influence of the sympathetic nervous system, given the dominant role of the vagus nerve, not only in microbiota-gut brain axis communication but also in the cardiorespiratory control network, microbiota-mediated dysfunction of vago-vagal signalling may contribute to development of hypertension.

1.6.2 Respiratory control and gut microbiota

Not only has the gut microbiota been associated with blood pressure control, but emerging evidence also suggests that the gut microbiota plays a potential role in respiratory physiology. Stress models have revealed maladaptive plasticity resulting in long-lasting insults to the respiratory control network (Fournier *et al.*, 2013b; Kinkead *et al.*, 2013; Golubeva *et al.*, 2015; Tenorio-Lopes *et al.*, 2017). Pre-natal stress results in enhanced variability of breathing frequency during normoxia and alters ventilatory control during hypoxic and hypercapnic chemostimulation in rat offspring. Importantly, these changes correlated with microbiota genera (Golubeva *et al.*, 2015). Variability of breathing frequency during normoxia was associated with *Mucispirillum* and *Papillibacter;* respiratory frequency response to hypercapnia correlated with *Oscillibacter* and *Anaerotruncus* (Golubeva *et al.*, 2015). Notably, these observed associations may well be interdependent due to the effects of systemic stress on the microbiota (O'Mahony *et al.*, 2011; Foster *et al.*, 2017; van de Wouw *et al.*, 2018a).

Given the anatomical location of central respiratory control regions, the potential for cardiorespiratory coupling and the involvement of the dominant communication pathway of the microbiota-gut brain axis, the vagus nerve, in the control of breathing, it is plausible to consider that perturbations to the gut microbiota could influence respiratory control. Moreover, it is interesting to speculate that there may be a putative role for specific taxa in the control of respiratory homeostasis.

1.7. Cardiorespiratory and pulmonary disorders

1.7.1 Obstructive sleep apnoea (OSA)

Although gut microbiota composition and diversity is modified in rodent models of SDB, at present there is paucity of information regarding the gut microbiome and microbiota metabolites in SDB patients. OSA is the most common form of SDB and has overwhelming consequences for integrative body systems, emerging as a major health crisis worldwide (Garvey *et al.*, 2015). OSA is characterised by repetitive collapse of the pharyngeal airway exclusively during sleep, leading to the development of episodic oxygen fluctuations manifesting in exposure to CIH. Compelling evidence exists for an association between OSA and cardiorespiratory, metabolic and neurocognitive morbidities, with CIH well established as the primary driving pathogenic factor behind the host of well-characterised maladies associated with OSA (O'Halloran, 2016).

It has recently been shown that OSA patients fall into any of the three enterotypes, *Bacteroides, Ruminococcus* and *Prevotella* (Ko *et al.,* 2019). Using apnoea-hypopnea index greater than 15, it was established that sleep architecture including arousal time and index, non-rapid eye movement phase 1, and sleep latency were altered in Prevotella enterotype OSA patients compared with patients with *Bacteroides* and *Ruminococcus* (Ko *et al.*, 2019). It is interesting to note that CIH exposure in mice also resulted in development of a *Prevotella* enterotype (Moreno-Indias *et al.*, 2015). Moreover, in the urine of OSA patients a number of metabolites were different compared with controls; 5 of these metabolites related to the gut microbiota (Xu *et al.*, 2018).

Although much remains to be known about the gut microbiota in OSA patients, advances have shown that oral, nasal and lung microbiota are significantly altered in OSA patients (Lu *et al.*, 2018a; Wu *et al.*, 2018; Xu *et al.*, 2018). Firmicutes, Proteobacteria and Fusobacteria were significantly different in both lung and oral OSA samples compared with controls (Lu *et al.*, 2018a; Xu *et al.*, 2018). Interestingly, 7 genera of the nasal microbiota correlated with apnea-hypopnea index in OSA patients (Wu *et al.*, 2018). Continuous positive airway pressure, the gold standard for treatment of SDB did not alter nasal microbiome diversity in OSA patients (Wu *et al.*, 2018).

1.7.2 Apnoea of prematurity and bradycardia

It is interesting to note that premature babies, where the gut microbiota is significantly distinct to that of full-term infants, often develop apnoea of prematurity and bradycardia (Barrett *et al.*, 2013; Korpela *et al.*, 2018). Apnoea of prematurity and bradycardia occur due

to immature respiratory centres and an underdeveloped nervous system (Cohen & Katz-Salamon, 2005). Furthermore, there is early deprivation of neuroprotective hormones including progesterone, in preterm infants; the lack of progesterone may have implications for brain development (Berger & Soder, 2015; Bairam *et al.*, 2019). Moreover, the gut microbiota is involved in early programming of brain circuits (Sudo *et al.*, 2004; Diaz Heijtz *et al.*, 2011; Clarke *et al.*, 2013; Desbonnet *et al.*, 2014). Of interest, progesterone supplementation alters the gut microbiota and increases *Bifidobacterium* abundance during the 3rd trimester of pregnancy in humans and rodents (Nuriel-Ohayon *et al.*, 2019). Notably, decreased *Bifidobacterium* is evident in preterm infants (Dahl *et al.*, 2017; Korpela *et al.*, 2018), in tandem with reduced progesterone levels (Bairam *et al.*, 2019). Studies have established that progesterone has an important role in respiratory regulation during the postnatal period in animals (Lefter *et al.*, 2007; Bairam *et al.*, 2013; Joseph *et al.*, 2018). It is interesting to speculate that there may be interplay between the gut microbiota and progesterone in the control of breathing at least during neonatal life.

Furthermore, organisms such as *Staphylococcus Aureus* often colonise the infant's gastrointestinal and respiratory tract and may cause or aggravate cardiorespiratory dysfunctions (Hofstetter *et al.*, 2008). CIH is a dominant pathological feature of apnoea of prematurity and directly/indirectly influences the gut microbiota (Moreno-Indias *et al.*, 2015; Moreno-Indias *et al.*, 2016). Perhaps the gut microbiota may in part contribute to maturation of cardiorespiratory centres within the brain and have relevance for apnoea of prematurity and bradycardia.

1.7.3 Asthma

Several studies have linked alterations to the gut microbiota during early life with increased risk of asthma later in life (van Nimwegen *et al.*, 2011; Abrahamsson *et al.*, 2014; Arrieta *et al.*, 2015). Caesarean section delivery increased the risk of developing airway sensitivity up to 12 years of age (Keag *et al.*, 2018). Additionally, asthmatic children had reduced gut microbiota diversity at 1 week and 1 month of age compared with non-asthmatic children (Abrahamsson *et al.*, 2014). Furthermore, the relative abundance of faecal *Veillonella, Faecalibacterium, Rothia* and *Lachnospiracea* were reduced in children at high risk of asthma (wheezy and atopy). Interestingly, faecal acetate was also decreased in these children (Arrieta *et al.*, 2015). Reduced gut microbiota diversity was evident in asthmatic adults compared with healthy controls (Wang *et al.*, 2018).

Not only are microbiota alterations evident in the gut of asthmatic patients but changes are evident in the lung microbiota. Proteobacteria enrichment has been described in lungs of asthmatic patients (Hilty *et al.*, 2010; Huang *et al.*, 2015). In patients with moderate to severe asthma an abundance of *Haemophilus* was evident (Hilty *et al.*, 2010). *Klebsiella* or *Moraxella catarrhalis* species were present in patients with severe asthma (Huang *et al.*, 2015).

Of note, pregnant mice receiving acetate supplementation had suppressed expression of genes linked to human asthma and mouse allergic airways disease in offspring (Thorburn *et al.*, 2015). In asthmatic children, *Lactobacillus acidophilus* and *Bifidobacterium bifidum* improved lung function and reduced asthmatic exacerbations (Gutkowski *et al.*, 2011).

1.7.4 Chronic Obstructive Pulmonary Disease

COPD is a progressive inflammatory disease characterised by persistent airflow limitation, leading to the development of hypoxia. To date, there is a paucity of studies investigating the gut microbiome in COPD patients. Smoking, which is a leading cause of COPD, has significant impact on gut microbiota structure. Smoking increased Proteobacteria and Bacteroidetes phyla, as well as *Clostridium, Bacteroides* and *Prevotella* (Benjamin *et al.*, 2012; Wang *et al.*, 2012). Conversely, Actinobacteria and Firmicutes phyla, as well as *Bifidobacterium* and *Lactococcus* were reduced due to cigarette smoke (Tomoda *et al.*, 2011; Savin *et al.*, 2018).

Additionally, it is well-established that potentially pathogenic taxa, including *Pseudomonas aeruginosa, Haemophilus influenza* and *Streptococcus* colonise the lungs in COPD patients (Garcia-Vidal *et al.*, 2009; Simpson *et al.*, 2016; Wang *et al.*, 2016). Non-pathogenic *Bacillus* species were decreased in the lungs of COPD patients (Simpson *et al.*, 2016).

1.7.5 Cystic fibrosis

Cystic fibrosis is an autosomal recessive disease due to a mutation in the cystic fibrosis transmembrane conductance regulatory gene. Cystic fibrosis patients have decreased gut microbiota diversity and altered composition compared with healthy controls. These compositional changes include increased Firmicutes:Bacteroidetes ratio as well as S*taphylococcus, Propionibacterium acnes, Clostridium difficile* and *Clostridiaceae* in cystic fibrosis patients (Burke *et al.*, 2017; Vernocchi *et al.*, 2018). Decreased abundance of healthy gut taxa including *Roseburia, Bifidobacterium* and *Faecalibacterium* were also evident (Burke *et al.*, 2017). Moreover gut microbiota differences were reported between various stages of cystic fibrosis (mild, moderate, severe)(Burke *et al.*, 2017). Interestingly, *Lactobacillus GG*

administration to cystic fibrosis patients promoted beneficial gut microbiota and decreased pulmonary exacerbations and hospital admissions (Bruzzese *et al.*, 2007).

1.8. Knowledge gaps addressed in this thesis

This area of research is undoubtedly in its infancy and currently there is paucity of studies investigating the role of microbiota-gut-brain axis signalling in cardiorespiratory and autonomic control. There is tremendous potential for microbiota-gut-brain axis signalling to play a regulatory role in cardiorespiratory homeostasis and dysfunction. At present, it remains unclear if the gut microbiota contributes to respiratory control and reflex responsiveness. Although a picture is emerging to illustrate that the development of hypertension is in part related to aberrant gut microbiota, there is a scarcity of studies assessing the role of the microbiota-gut-brain axis in cardiorespiratory homeostasis (Figure 1.3).

Exposure to CIH has been shown to affect major homeostatic control systems, altering the gut microbiota, enhancing sympathetic nervous system activity and destabilising cardiorespiratory control. However, it is not known if CIH affects the gut microbiota, independent of sympathetic hyperactivity. Furthermore, there is a need to determine if aberrant microbiota-gut-brain axis signalling at least partly contributes to cardiorespiratory dysfunction evident in CIH animal models. In parallel, there is a dearth of studies examining if beneficial modulation of the gut microbiota can improve or prevent cardiorespiratory dysfunctions that present in animal models associated with perturbed microbiota. These specific knowledge gaps amongst others are unravelled in this thesis.

Cardiovascular and respiratory diseases are serious and potentially life-threatening conditions (Benziger *et al.*, 2016). These illnesses are leading causes of mortality and disability worldwide, with cardiovascular disease being the number one cause of death (Thomas *et al.*, 2018). Globally more than 100 million people suffer from SDB alone (Organization, 2007). Untreated cardiorespiratory conditions/diseases result in exacerbation of symptoms, culminating in a portfolio of pathologies. Prolonged SDB may result in the development of cardiovascular disease, hypertension, stroke and cognitive deficits, to the name but a few maladies. Currently, there are multiple and often successful efforts to treat cardiovascular and respiratory diseases, including but not limited to beta blockers, lipid-lowering therapies and continuous positive airway pressure (Thomas *et al.*, 2018). However, treatments are not always favourable due to ineffectiveness or lack of compliance (Van Ryswyk *et al.*, 2019). It is of immense interest to further investigate the role of microbiota-gut-brain axis signalling in cardiorespiratory homeostasis and dysfunction in order to enhance therapeutic strategies to treat chronic cardiorespiratory diseases.

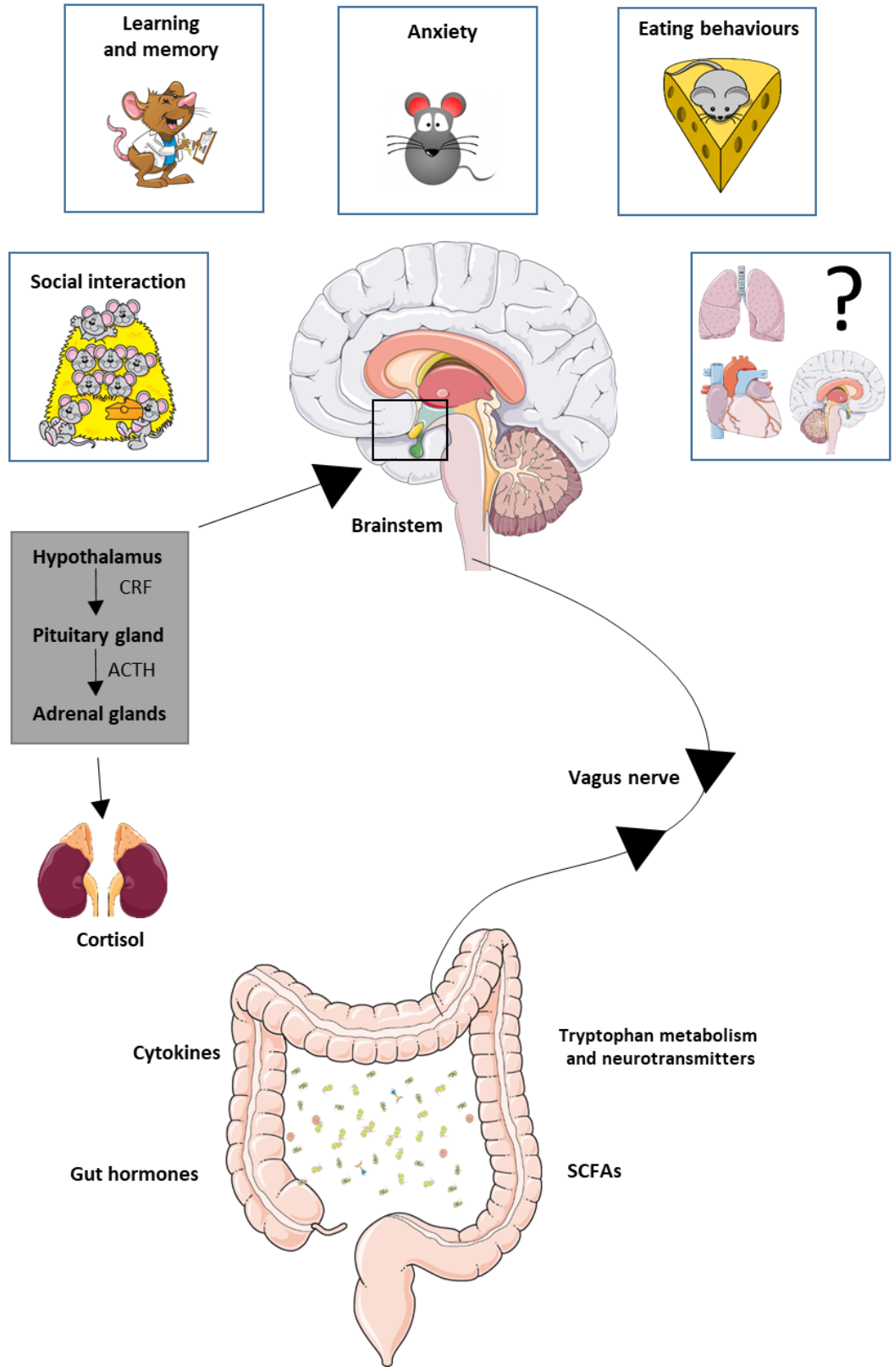


Figure 1. 3 The microbiota-gut-brain axis, brain and behaviours

A number of communication pathways are proposed as potential mechanisms of microbiota-gut-brain axis signalling. A growing body of evidence suggests vagal-mediated communication is the primary signalling pathway between the gut microbiota and the

brainstem (Fulling *et al.*, 2019). SCFAs, metabolites of the gut microbiota, can bind freely to free-fatty acid receptors located throughout the body, including vagal ganglia (Sina *et al.*, 2009; Tolhurst *et al.*, 2012; Nohr *et al.*, 2015; Lu *et al.*, 2018b). Gut hormones are released as a consequence of SCFAs binding to free-fatty acid receptors on enteroendocrine cells (Tolhurst *et al.*, 2012). SCFAs also have the capacity to affect microglia within the brain (Erny *et al.*, 2015). The gut microbiota can facilitate central neurotransmitter regulation by synthesising and releasing neurotransmitters from bacteria directly or by altering levels of neurotransmitter precursors i.e. tryptophan (Desbonnet *et al.*, 2010; Lyte, 2013, 2014a; O'Mahony *et al.*, 2015). The immune system also functions as a communication pathway of the microbiota-gut-brain axis (El Aidy *et al.*, 2014b). Cytokines signal to the brain via numerous pathways, including detection by vagal afferent fibres (Goehler *et al.*, 2000; Johnston & Webster, 2009). There is evidence to demonstrate that altered microbiota-gut-brain axis signalling affects neurocontrol systems, with consequences for behaviours such as social interactions, learning and memory, stress, eating behaviour and anxiety. Currently, there is a dearth of studies investigating the regulatory role of the gut microbiota in cardiorespiratory control. ACTH, adrenocorticotrophic hormone; CRF, corticotropin-releasing factor; SCFA, short-chain fatty acid. Cortisol and corticosterone are released from the adrenal medulla in humans and rodents, respectively.

1.9. Thesis structure and specific aims

The primary aim of this thesis was to investigate if microbiota-gut-brain axis signalling plays a regulatory role in cardiorespiratory and autonomic control. We sought to explore cardiorespiratory and reflex responsiveness in animal models of manipulated gut microbiota and of SDB, to uncover if altered microbiota, in the form of dysbiosis, manifests in cardiorespiratory impairments. Additionally, we aimed to unravel some of the mechanisms by which homeostatic functions are maintained or disrupted as a result of microbiota disturbances. Moreover, we explored whether manipulation of the gut microbiota *via* various methods, routinely deemed beneficial, could ameliorate or prevent cardiorespiratory dysfunctions evident in animal models.

Chapter 2: Manipulation of gut microbiota blunts the ventilatory response to hypercapnia in adult rats.

- We aimed to perform a comprehensive assessment of cardiorespiratory control and reflex responsiveness to chemostimulation and drug administration in adult rats following antibiotic administration or vehicle.
- We hypothesised that there would be evidence of aberrant plasticity in cardiorespiratory control in antibiotic-treated rats.
- We sought to examine monoamine concentrations in brain regions and *ex vivo* intestinal permeability in adult rats following antibiotic administration or vehicle.
- Thereafter, in a subset of animals, we aimed to explore if manipulation of the microbiota *via* faecal microbiota transfer could normalise the gut microbiota and reverse or ameliorate effects of antibiotic administration on cardiorespiratory control.
- We sought to assess monoamine concentrations in brain regions and *ex vivo* intestinal permeability in adult rats following faecal microbiota transfer.

Chapter 3: Chronic intermittent hypoxia disrupts cardiorespiratory homeostasis and gut microbiota composition in adult male guinea-pigs.

- We aimed to explore the effects of exposure to CIH on cardiorespiratory physiology and reflex responsiveness to chemostimulation and drug administration in guinea-pigs, mammals with hypoxia-insensitive carotid bodies.

- We hypothesised that CIH exposure would not lead to the development of hypertension in guinea-pigs, supporting the obligatory role for carotid body sensitisation in manifestation of CIH-induced hypertension.
- We sought to examine monoamine concentrations in brainstem regions and urine catecholamine and corticosterone concentrations in sham and CIH guinea-pigs.
- We aimed to assess the effects of CIH on the gut microbiota, independent of carotid body sensitisation, to consider if altered gut microbiota might have consequences for putative residual cardiorespiratory dysfunctions in CIH-exposed guinea-pigs.

Chapter 4: Chronic intermittent hypoxia lowers *Lactobacillus rhamnosus* relative abundance and increases apnoea index and blood pressure: Effects of prebiotic supplementation

- We aimed to perform an assessment of gut microbiota structure, cardiorespiratory control and reflex responsiveness in adult rats following CIH exposure.
- We sought to examine monoamine concentrations in brainstem regions and plasma corticosterone and inflammatory markers in CIH-exposed rats.
- We hypothesised that there would be evidence of cardiorespiratory dysfunction, altered brainstem neurochemistry and modified gut microbiota in CIH-exposed rats.
- We aimed to investigate if manipulation of the microbiota *via* prebiotic administration could prevent or ameliorate the deleterious effects of CIH exposure on cardiorespiratory control and brainstem neurochemistry.

1.10. References

Abbott SB, DePuy SD, Nguyen T, Coates MB, Stornetta RL & Guyenet PG. (2013). Selective optogenetic activation of rostral ventrolateral medullary catecholaminergic neurons produces cardiorespiratory stimulation in conscious mice. *The Journal of neuroscience : the official journal of the Society for Neuroscience* **33,** 3164-3177.

Abrahamsson TR, Jakobsson HE, Andersson AF, Bjorksten B, Engstrand L & Jenmalm MC. (2014). Low gut microbiota diversity in early infancy precedes asthma at school age. *Clinical and experimental allergy : journal of the British Society for Allergy and Clinical Immunology* **44,** 842-850.

Adnan S, Nelson JW, Ajami NJ, Venna VR, Petrosino JF, Bryan RM, Jr. & Durgan DJ. (2017). Alterations in the gut microbiota can elicit hypertension in rats. *Physiological genomics* **49,** 96-104.

Adrian ED, Bronk DW & Phillips G. (1932). Discharges in mammalian sympathetic nerves. *The Journal of physiology* **74,** 115-133.

Albenberg L, Esipova TV, Judge CP, Bittinger K, Chen J, Laughlin A, Grunberg S, Baldassano RN, Lewis JD, Li H, Thom SR, Bushman FD, Vinogradov SA & Wu GD. (2014). Correlation between intraluminal oxygen gradient and radial partitioning of intestinal microbiota. *Gastroenterology* **147,** 1055-1063 e1058.

Albenberg LG & Wu GD. (2014). Diet and the intestinal microbiome: associations, functions, and implications for health and disease. *Gastroenterology* **146,** 1564-1572.

Alheid GF & McCrimmon DR. (2008). The chemical neuroanatomy of breathing. *Respiratory physiology & neurobiology* **164,** 3-11.

Almado CE, Machado BH & Leao RM. (2012). Chronic intermittent hypoxia depresses afferent neurotransmission in NTS neurons by a reduction in the number of active synapses. *The Journal of neuroscience : the official journal of the Society for Neuroscience* **32,** 16736-16746.

Amiel J, Laudier B, Attie-Bitach T, Trang H, de Pontual L, Gener B, Trochet D, Etchevers H, Ray P, Simonneau M, Vekemans M, Munnich A, Gaultier C & Lyonnet S. (2003). Polyalanine expansion and frameshift mutations of the paired-like homeobox gene PHOX2B in congenital central hypoventilation syndrome. *Nature genetics* **33,** 459-461.

Araujo JR, Tomas J, Brenner C & Sansonetti PJ. (2017). Impact of high-fat diet on the intestinal microbiota and small intestinal physiology before and after the onset of obesity. *Biochimie* **141,** 97-106.

Arrieta MC, Stiemsma LT, Dimitriu PA, Thorson L, Russell S, Yurist-Doutsch S, Kuzeljevic B, Gold MJ, Britton HM, Lefebvre DL, Subbarao P, Mandhane P, Becker A, McNagny KM, Sears MR, Kollmann T, Investigators CS, Mohn WW, Turvey SE & Finlay BB. (2015). Early infancy microbial and metabolic alterations affect risk of childhood asthma. *Science translational medicine* **7,** 307ra152.

Arumugam M, Raes J, Pelletier E, Le Paslier D, Yamada T, Mende DR, Fernandes GR, Tap J, Bruls T, Batto JM, Bertalan M, Borruel N, Casellas F, Fernandez L, Gautier L, Hansen T, Hattori M, Hayashi T, Kleerebezem M, Kurokawa K, Leclerc M, Levenez F, Manichanh C, Nielsen HB, Nielsen T, Pons N, Poulain J, Qin J, Sicheritz-Ponten T, Tims S, Torrents D, Ugarte E, Zoetendal EG, Wang J, Guarner F, Pedersen O, de Vos WM, Brunak S, Dore J, Antolin M, Artiguenave F, Blottiere HM, Almeida M, Brechot C, Cara C, Chervaux C, Cultrone A, Delorme C, Denariaz G, Dervyn R, Foerstner KU, Friss C, van de Guchte M, Guedon E, Haimet F, Huber W, van Hylckama-Vlieg J, Jamet A, Juste C, Kaci G, Knol J, Lakhdari O, Layec S, Le Roux K, Maguin E, Merieux A, Melo Minardi R, M'Rini C, Muller J, Oozeer R, Parkhill J, Renault P, Rescigno M, Sanchez N, Sunagawa S, Torrejon A, Turner K, Vandemeulebrouck G, Varela E, Winogradsky Y, Zeller G, Weissenbach J, Ehrlich SD & Bork P. (2011). Enterotypes of the human gut microbiome. *Nature* **473,** 174-180.

Azad MB, Konya T, Maughan H, Guttman DS, Field CJ, Chari RS, Sears MR, Becker AB, Scott JA & Kozyrskyj AL. (2013). Gut microbiota of healthy Canadian infants: profiles by mode of delivery and infant diet at 4 months. *CMAJ : Canadian Medical Association journal = journal de l'Association medicale canadienne* **185,** 385-394.

Bailey MT, Dowd SE, Parry NM, Galley JD, Schauer DB & Lyte M. (2010). Stressor exposure disrupts commensal microbial populations in the intestines and leads to increased colonization by Citrobacter rodentium. *Infection and immunity* **78,** 1509-1519.

Bairam A, Boukari R & Joseph V. (2019). Targeting progesterone receptors in newborn males and females: From the animal model to a new perspective for the treatment of apnea of prematurity? *Respiratory physiology & neurobiology* **263,** 55-61.

Bairam A, Lumbroso D & Joseph V. (2013). Effect of progesterone on respiratory response to moderate hypoxia and apnea frequency in developing rats. *Respiratory physiology & neurobiology* **185,** 515-525.

Baker-Herman TL, Fuller DD, Bavis RW, Zabka AG, Golder FJ, Doperalski NJ, Johnson RA, Watters JJ & Mitchell GS. (2004). BDNF is necessary and sufficient for spinal respiratory plasticity following intermittent hypoxia. *Nature neuroscience* **7,** 48-55.

Baker-Herman TL & Mitchell GS. (2002). Phrenic long-term facilitation requires spinal serotonin receptor activation and protein synthesis. *The Journal of neuroscience : the official journal of the Society for Neuroscience* **22,** 6239-6246.

Banks WA & Erickson MA. (2010). The blood-brain barrier and immune function and dysfunction. *Neurobiology of disease* **37,** 26-32.

Barman SM & Gebber GL. (2000). "Rapid" rhythmic discharges of sympathetic nerves: sources, mechanisms of generation, and physiological relevance. *Journal of biological rhythms* **15,** 365-379.

Barrett E, Kerr C, Murphy K, O'Sullivan O, Ryan CA, Dempsey EM, Murphy BP, O'Toole PW, Cotter PD, Fitzgerald GF, Ross RP & Stanton C. (2013). The individual-specific and diverse nature of the preterm infant microbiota. *Archives of disease in childhood Fetal and neonatal edition* **98,** F334-340.

Bartolomaeus H, Balogh A, Yakoub M, Homann S, Marko L, Hoges S, Tsvetkov D, Krannich A, Wundersitz S, Avery EG, Haase N, Kraker K, Hering L, Maase M, Kusche-Vihrog K, Grandoch M, Fielitz J, Kempa S, Gollasch M, Zhumadilov Z, Kozhakhmetov S, Kushugulova A, Eckardt KU, Dechend R, Rump LC, Forslund SK, Muller DN, Stegbauer J & Wilck N. (2019). Short-Chain Fatty Acid Propionate Protects From Hypertensive Cardiovascular Damage. *Circulation* **139,** 1407-1421.

Bastiaanssen TFS, Cowan CSM, Claesson MJ, Dinan TG & Cryan JF. (2019). Making Sense of ... the Microbiome in Psychiatry. *The international journal of neuropsychopharmacology / official scientific journal of the Collegium Internationale Neuropsychopharmacologicum (CINP)* **22,** 37-52.

Bautista TG, Xing T, Fong AY & Pilowsky PM. (2012). Recurrent laryngeal nerve activity exhibits a 5-HT-mediated long-term facilitation and enhanced response to hypoxia following acute intermittent hypoxia in rat. *Journal of applied physiology (Bethesda, Md : 1985)* **112,** 1144-1156.

Bavis RW. (2005). Developmental plasticity of the hypoxic ventilatory response after perinatal hyperoxia and hypoxia. *Respiratory physiology & neurobiology* **149,** 287-299.

Behan M & Kinkead R. (2011). Neuronal control of breathing: sex and stress hormones. *Comprehensive Physiology* **1,** 2101-2139.

Belkaid Y & Hand TW. (2014). Role of the microbiota in immunity and inflammation. *Cell* **157,** 121-141.

Benjamin JL, Hedin CR, Koutsoumpas A, Ng SC, McCarthy NE, Prescott NJ, Pessoa-Lopes P, Mathew CG, Sanderson J, Hart AL, Kamm MA, Knight SC, Forbes A, Stagg AJ, Lindsay JO & Whelan K. (2012). Smokers with active Crohn's disease have a clinically relevant dysbiosis of the gastrointestinal microbiota. *Inflammatory bowel diseases* **18,** 1092-1100.

Benoun JM, Labuda JC & McSorley SJ. (2016). Collateral Damage: Detrimental Effect of Antibiotics on the Development of Protective Immune Memory. *mBio* **7**.

Benziger CP, Roth GA & Moran AE. (2016). The global burden of disease study and the preventable burden of NCD. *Global heart* **11,** 393-397.

Bercik P, Park AJ, Sinclair D, Khoshdel A, Lu J, Huang X, Deng Y, Blennerhassett PA, Fahnestock M, Moine D, Berger B, Huizinga JD, Kunze W, McLean PG, Bergonzelli GE, Collins SM & Verdu EF. (2011). The anxiolytic effect of Bifidobacterium longum NCC3001 involves vagal pathways for gut-brain communication. *Neurogastroenterology and motility : the official journal of the European Gastrointestinal Motility Society* **23,** 1132-1139.

Berger R & Soder S. (2015). Neuroprotection in preterm infants. *BioMed research international* **2015,** 257139.

Berquin P, Bodineau L, Gros F & Larnicol N. (2000). Brainstem and hypothalamic areas involved in respiratory chemoreflexes: a Fos study in adult rats. *Brain research* **857,** 30-40.

Berthoud HR & Neuhuber WL. (2000). Functional and chemical anatomy of the afferent vagal system. *Autonomic neuroscience : basic & clinical* **85,** 1-17.

Biancardi V, Bicego KC, Almeida MC & Gargaglioni LH. (2008). Locus coeruleus noradrenergic neurons and CO2 drive to breathing. *Pflugers Archiv : European journal of physiology* **455,** 1119-1128.

Biancardi V, da Silva LT, Bicego KC & Gargaglioni LH. (2010). Role of locus coeruleus noradrenergic neurons in cardiorespiratory and thermal control during hypoxia. *Respiratory physiology & neurobiology* **170,** 150-156.

Bilimoria PM & Stevens B. (2015). Microglia function during brain development: New insights from animal models. *Brain research* **1617,** 7-17.

Boehme M, van de Wouw M, Bastiaanssen TFS, Olavarria-Ramirez L, Lyons K, Fouhy F, Golubeva AV, Moloney GM, Minuto C, Sandhu KV, Scott KA, Clarke G, Stanton C, Dinan TG, Schellekens H & Cryan JF. (2019). Mid-life microbiota crises: middle age is associated with pervasive neuroimmune alterations that are reversed by targeting the gut microbiome. *Molecular psychiatry*.

Borre YE, O'Keeffe GW, Clarke G, Stanton C, Dinan TG & Cryan JF. (2014). Microbiota and neurodevelopmental windows: implications for brain disorders. *Trends in molecular medicine* **20,** 509-518.

Bouairi E, Neff R, Evans C, Gold A, Andresen MC & Mendelowitz D. (2004). Respiratory sinus arrhythmia in freely moving and anesthetized rats. *Journal of applied physiology (Bethesda, Md : 1985)* **97,** 1431-1436.

Braga VA, Soriano RN & Machado BH. (2006). Sympathoexcitatory response to peripheral chemoreflex activation is enhanced in juvenile rats exposed to chronic intermittent hypoxia. *Experimental physiology* **91,** 1025-1031.

Braniste V, Al-Asmakh M, Kowal C, Anuar F, Abbaspour A, Toth M, Korecka A, Bakocevic N, Ng LG, Kundu P, Gulyas B, Halldin C, Hultenby K, Nilsson H, Hebert H, Volpe BT, Diamond B & Pettersson S. (2014). The gut microbiota influences blood-brain barrier permeability in mice. *Science translational medicine* **6,** 263ra158.

Bravo JA, Forsythe P, Chew MV, Escaravage E, Savignac HM, Dinan TG, Bienenstock J & Cryan JF. (2011). Ingestion of Lactobacillus strain regulates emotional behavior and central GABA receptor expression in a mouse via the vagus nerve. *Proceedings of the National Academy of Sciences of the United States of America* **108,** 16050-16055.

Breit S, Kupferberg A, Rogler G & Hasler G. (2018). Vagus Nerve as Modulator of the Brain-Gut Axis in Psychiatric and Inflammatory Disorders. *Frontiers in psychiatry* **9,** 44.

Brown K. (2005). *Penicillin man: Alexander Fleming and the antibiotic revolution*. The History Press.

Brown K, DeCoffe D, Molcan E & Gibson DL. (2012). Diet-induced dysbiosis of the intestinal microbiota and the effects on immunity and disease. *Nutrients* **4,** 1095-1119.

Brust RD, Corcoran AE, Richerson GB, Nattie E & Dymecki SM. (2014). Functional and developmental identification of a molecular subtype of brain serotonergic neuron specialized to regulate breathing dynamics. *Cell reports* **9,** 2152-2165.

Bruzzese E, Raia V, Spagnuolo MI, Volpicelli M, De Marco G, Maiuri L & Guarino A. (2007). Effect of Lactobacillus GG supplementation on pulmonary exacerbations in patients with cystic fibrosis: a pilot study. *Clinical nutrition (Edinburgh, Scotland)* **26,** 322-328.

Buchanan GF & Richerson GB. (2010). Central serotonin neurons are required for arousal to CO2. *Proceedings of the National Academy of Sciences of the United States of America* **107,** 16354-16359.

Buchanan GF, Smith HR, MacAskill A & Richerson GB. (2015). 5-HT2A receptor activation is necessary for CO2-induced arousal. *Journal of neurophysiology* **114,** 233-243.

Burke DG, Fouhy F, Harrison MJ, Rea MC, Cotter PD, O'Sullivan O, Stanton C, Hill C, Shanahan F, Plant BJ & Ross RP. (2017). The altered gut microbiota in adults with cystic fibrosis. *BMC microbiology* **17,** 58.

Burns DP, Roy A, Lucking EF, McDonald FB, Gray S, Wilson RJ, Edge D & O'Halloran KD. (2017). Sensorimotor control of breathing in the mdx mouse model of Duchenne muscular dystrophy. *The Journal of physiology* **595,** 6653-6672.

Burokas A, Arboleya S, Moloney RD, Peterson VL, Murphy K, Clarke G, Stanton C, Dinan TG & Cryan JF. (2017). Targeting the Microbiota-Gut-Brain Axis: Prebiotics Have Anxiolytic and Antidepressant-like Effects and Reverse the Impact of Chronic Stress in Mice. *Biological psychiatry* **82,** 472-487.

Burokas A, Moloney RD, Dinan TG & Cryan JF. (2015). Microbiota regulation of the Mammalian gut-brain axis. *Advances in applied microbiology* **91,** 1-62.

Canfora EE, Jocken JW & Blaak EE. (2015). Short-chain fatty acids in control of body weight and insulin sensitivity. *Nature reviews Endocrinology* **11,** 577-591.

Cani PD, Joly E, Horsmans Y & Delzenne NM. (2006). Oligofructose promotes satiety in healthy human: a pilot study. *European journal of clinical nutrition* **60,** 567-572.

Cash HL, Whitham CV, Behrendt CL & Hooper LV. (2006). Symbiotic bacteria direct expression of an intestinal bactericidal lectin. *Science (New York, NY)* **313,** 1126-1130.

Chang AJ, Ortega FE, Riegler J, Madison DV & Krasnow MA. (2015). Oxygen regulation of breathing through an olfactory receptor activated by lactate. *Nature* **527,** 240-244.

Claesson MJ, Clooney AG & O'Toole PW. (2017). A clinician's guide to microbiome analysis. *Nature reviews Gastroenterology & hepatology* **14,** 585-595.

Clarke G, Grenham S, Scully P, Fitzgerald P, Moloney RD, Shanahan F, Dinan TG & Cryan JF. (2013). The microbiome-gut-brain axis during early life regulates the hippocampal serotonergic system in a sex-dependent manner. *Molecular psychiatry* **18,** 666-673.

Cohen G & Katz-Salamon M. (2005). Development of chemoreceptor responses in infants. *Respiratory physiology & neurobiology* **149,** 233-242.

Coleridge JC & Coleridge HM. (1984). Afferent vagal C fibre innervation of the lungs and airways and its functional significance. *Reviews of physiology, biochemistry and pharmacology* **99,** 1-110.

Corcoran AE, Hodges MR, Wu Y, Wang W, Wylie CJ, Deneris ES & Richerson GB. (2009). Medullary serotonin neurons and central CO2 chemoreception. *Respiratory physiology & neurobiology* **168,** 49-58.

Costa-Silva JH, Zoccal DB & Machado BH. (2010). Glutamatergic antagonism in the NTS decreases post-inspiratory drive and changes phrenic and sympathetic coupling during chemoreflex activation. *Journal of neurophysiology* **103,** 2095-2106.

Costa-Silva JH, Zoccal DB & Machado BH. (2012). Chronic intermittent hypoxia alters glutamatergic control of sympathetic and respiratory activities in the commissural NTS of rats. *American journal of physiology Regulatory, integrative and comparative physiology* **302,** R785-793.

Cryan JF & Dinan TG. (2012). Mind-altering microorganisms: the impact of the gut microbiota on brain and behaviour. *Nature reviews Neuroscience* **13,** 701-712.

Cryan JF & O'Mahony SM. (2011). The microbiome-gut-brain axis: from bowel to behavior. *Neurogastroenterology and motility : the official journal of the European Gastrointestinal Motility Society* **23,** 187-192.

Dahl C, Stanislawski M, Iszatt N, Mandal S, Lozupone C, Clemente JC, Knight R, Stigum H & Eggesbo M. (2017). Gut microbiome of mothers delivering prematurely shows reduced diversity and lower relative abundance of Bifidobacterium and Streptococcus. *PloS one* **12,** e0184336.

Dalile B, Van Oudenhove L, Vervliet B & Verbeke K. (2019). The role of short-chain fatty acids in microbiota-gut-brain communication. *Nature reviews Gastroenterology & hepatology*.

De Filippis F, Pellegrini N, Vannini L, Jeffery IB, La Storia A, Laghi L, Serrazanetti DI, Di Cagno R, Ferrocino I, Lazzi C, Turroni S, Cocolin L, Brigidi P, Neviani E, Gobbetti M, O'Toole PW & Ercolini D. (2016). High-level adherence to a Mediterranean diet beneficially impacts the gut microbiota and associated metabolome. *Gut* **65,** 1812-1821.

De Palma G, Blennerhassett P, Lu J, Deng Y, Park AJ, Green W, Denou E, Silva MA, Santacruz A, Sanz Y, Surette MG, Verdu EF, Collins SM & Bercik P. (2015). Microbiota and host determinants of behavioural phenotype in maternally separated mice. *Nature communications* **6,** 7735.

DeCastro M, Nankova BB, Shah P, Patel P, Mally PV, Mishra R & La Gamma EF. (2005). Short chain fatty acids regulate tyrosine hydroxylase gene expression through a cAMP-dependent signaling pathway. *Brain research Molecular brain research* **142,** 28-38.

Del Chierico F, Vernocchi P, Dallapiccola B & Putignani L. (2014). Mediterranean diet and health: food effects on gut microbiota and disease control. *International journal of molecular sciences* **15,** 11678-11699.

Desbonnet L, Clarke G, Shanahan F, Dinan TG & Cryan JF. (2014). Microbiota is essential for social development in the mouse. In *Molecular psychiatry*, pp. 146-148. England.

Desbonnet L, Clarke G, Traplin A, O'Sullivan O, Crispie F, Moloney RD, Cotter PD, Dinan TG & Cryan JF. (2015). Gut microbiota depletion from early adolescence in mice: Implications for brain and behaviour. *Brain, behavior, and immunity* **48,** 165-173.

Desbonnet L, Garrett L, Clarke G, Bienenstock J & Dinan TG. (2008). The probiotic Bifidobacteria infantis: An assessment of potential antidepressant properties in the rat. *Journal of psychiatric research* **43,** 164-174.

Desbonnet L, Garrett L, Clarke G, Kiely B, Cryan JF & Dinan TG. (2010). Effects of the probiotic Bifidobacterium infantis in the maternal separation model of depression. *Neuroscience* **170,** 1179-1188.

Diaz Heijtz R, Wang S, Anuar F, Qian Y, Bjorkholm B, Samuelsson A, Hibberd ML, Forssberg H & Pettersson S. (2011). Normal gut microbiota modulates brain development and behavior. *Proceedings of the National Academy of Sciences of the United States of America* **108,** 3047-3052.

Dick TE, Hsieh YH, Morrison S, Coles SK & Prabhakar N. (2004). Entrainment pattern between sympathetic and phrenic nerve activities in the Sprague-Dawley rat: hypoxia-evoked sympathetic activity during expiration. *American journal of physiology Regulatory, integrative and comparative physiology* **286,** R1121-1128.

Dinan TG & Cryan JF. (2017). The Microbiome-Gut-Brain Axis in Health and Disease. *Gastroenterology clinics of North America* **46,** 77-89.

Doi A & Ramirez JM. (2008). Neuromodulation and the orchestration of the respiratory rhythm. *Respiratory physiology & neurobiology* **164,** 96-104.

Dubreuil V, Ramanantsoa N, Trochet D, Vaubourg V, Amiel J, Gallego J, Brunet JF & Goridis C. (2008). A human mutation in Phox2b causes lack of CO2 chemosensitivity, fatal central apnea, and specific loss of parafacial neurons. *Proceedings of the National Academy of Sciences of the United States of America* **105,** 1067-1072.

Durgan DJ, Ganesh BP, Cope JL, Ajami NJ, Phillips SC, Petrosino JF, Hollister EB & Bryan RM, Jr. (2016). Role of the Gut Microbiome in Obstructive Sleep Apnea-Induced Hypertension. *Hypertension* **67,** 469-474.

Dutta A & Deshpande SB. (2010). Cardio-respiratory reflexes evoked by phenylbiguanide in rats involve vagal afferents which are not sensitive to capsaicin. *Acta physiologica (Oxford, England)* **200,** 87-95.

Edge D, Bradford A & O'Halloran KD. (2012). Chronic intermittent hypoxia increases apnoea index in sleeping rats. *Advances in experimental medicine and biology* **758,** 359-363.

Edge D & O'Halloran KD. (2015). Chronic Intermittent Hypoxia Blunts the Expression of Ventilatory Long Term Facilitation in Sleeping Rats. *Advances in experimental medicine and biology* **860,** 335-342.

Edge D, Skelly JR, Bradford A & O'Halloran KD. (2009). Ventilatory drive is enhanced in male and female rats following chronic intermittent hypoxia. *Advances in experimental medicine and biology* **648,** 337-344.

Edge D, Skelly JR, Bradford A & O'Halloran KD. (2010). Respiratory plasticity in the behaving rat following chronic intermittent hypoxia. *Advances in experimental medicine and biology* **669,** 267-270.

El Aidy S, Dinan TG & Cryan JF. (2014). Immune modulation of the brain-gut-microbe axis. *Frontiers in microbiology* **5,** 146.

Erny D, Hrabe de Angelis AL, Jaitin D, Wieghofer P, Staszewski O, David E, Keren-Shaul H, Mahlakoiv T, Jakobshagen K, Buch T, Schwierzeck V, Utermohlen O, Chun E, Garrett WS, McCoy KD, Diefenbach A, Staeheli P, Stecher B, Amit I & Prinz M. (2015). Host microbiota constantly control maturation and function of microglia in the CNS. *Nature neuroscience* **18,** 965-977.

Feldman JL, Mitchell GS & Nattie EE. (2003). Breathing: rhythmicity, plasticity, chemosensitivity. *Annual review of neuroscience* **26,** 239-266.

Fletcher EC, Lesske J, Culman J, Miller CC & Unger T. (1992a). Sympathetic denervation blocks blood pressure elevation in episodic hypoxia. *Hypertension (Dallas, Tex : 1979)* **20,** 612-619.

Fletcher EC, Lesske J, Qian W, Miller CC, 3rd & Unger T. (1992b). Repetitive, episodic hypoxia causes diurnal elevation of blood pressure in rats. *Hypertension (Dallas, Tex : 1979)* **19,** 555-561.

Fontes MA, Xavier CH, Marins FR, Limborco-Filho M, Vaz GC, Muller-Ribeiro FC & Nalivaiko E. (2014). Emotional stress and sympathetic activity: contribution of dorsomedial hypothalamus to cardiac arrhythmias. *Brain research* **1554,** 49-58.

Foster JA, Rinaman L & Cryan JF. (2017). Stress & the gut-brain axis: Regulation by the microbiome. *Neurobiology of stress* **7,** 124-136.

Fouhy F, Watkins C, Hill CJ, O'Shea CA, Nagle B, Dempsey EM, O'Toole PW, Ross RP, Ryan CA & Stanton C. (2019). Perinatal factors affect the gut microbiota up to four years after birth. *Nature communications* **10,** 1517.

Fournier S, Steele S, Julien C, Fournier S, Gulemetova R, Caravagna C, Soliz J, Bairam A & Kinkead R. (2013a). Gestational stress promotes pathological apneas and sex-specific disruption of respiratory control development in newborn rat. *The Journal of neuroscience : the official journal of the Society for Neuroscience* **33,** 563-573.

Fournier S, Steele S, Julien C, Gulemetova R, Caravagna C, Soliz J, Bairam A & Kinkead R. (2013b). Gestational stress promotes pathological apneas and sex-specific disruption of respiratory control development in newborn rat. *J Neurosci* **33,** 563-573.

Fregosi RF & Mitchell GS. (1994). Long-term facilitation of inspiratory intercostal nerve activity following carotid sinus nerve stimulation in cats. *The Journal of physiology* **477 (Pt 3),** 469-479.

Fuller DD, Bach KB, Baker TL, Kinkead R & Mitchell GS. (2000). Long term facilitation of phrenic motor output. *Respiration physiology* **121,** 135-146.

Fuller DD & Mitchell GS. (2017). Respiratory neuroplasticity - Overview, significance and future directions. *Experimental neurology* **287,** 144-152.

Fulling C, Dinan TG & Cryan JF. (2019). Gut Microbe to Brain Signaling: What Happens in Vagus. *Neuron* **101,** 998-1002.

Ganesh BP, Nelson JW, Eskew JR, Ganesan A, Ajami NJ, Petrosino JF, Bryan RM, Jr. & Durgan DJ. (2018). Prebiotics, Probiotics, and Acetate Supplementation Prevent Hypertension in a Model of Obstructive Sleep Apnea. *Hypertension (Dallas, Tex : 1979)* **72,** 1141-1150.

Garcia-Vidal C, Almagro P, Romani V, Rodriguez-Carballeira M, Cuchi E, Canales L, Blasco D, Heredia JL & Garau J. (2009). Pseudomonas aeruginosa in patients hospitalised for COPD exacerbation: a prospective study. *The European respiratory journal* **34,** 1072-1078.

Garcia AJ, 3rd, Zanella S, Dashevskiy T, Khan SA, Khuu MA, Prabhakar NR & Ramirez JM. (2016). Chronic Intermittent Hypoxia Alters Local Respiratory Circuit Function at the Level of the preBotzinger Complex. *Frontiers in neuroscience* **10,** 4.

Garcia AJ, 3rd, Zanella S, Koch H, Doi A & Ramirez JM. (2011). Chapter 3--networks within networks: the neuronal control of breathing. *Progress in brain research* **188,** 31-50.

Garvey JF, Pengo MF, Drakatos P & Kent BD. (2015). Epidemiological aspects of obstructive sleep apnea. *Journal of thoracic disease* **7,** 920-929.

Gasparrini AJ, Crofts TS, Gibson MK, Tarr PI, Warner BB & Dantas G. (2016). Antibiotic perturbation of the preterm infant gut microbiome and resistome. *Gut microbes* **7,** 443-449.

Gaykema RP, Goehler LE & Lyte M. (2004). Brain response to cecal infection with Campylobacter jejuni: analysis with Fos immunohistochemistry. *Brain, behavior, and immunity* **18,** 238-245.

Genest SE, Gulemetova R, Laforest S, Drolet G & Kinkead R. (2004). Neonatal maternal separation and sex-specific plasticity of the hypoxic ventilatory response in awake rat. *The Journal of physiology* **554,** 543-557.

Genest SE, Gulemetova R, Laforest S, Drolet G & Kinkead R. (2007). Neonatal maternal separation induces sex-specific augmentation of the hypercapnic ventilatory response in awake rat. *Journal of applied physiology (Bethesda, Md : 1985)* **102,** 1416-1421.

Gibson GR, Probert HM, Loo JV, Rastall RA & Roberfroid MB. (2004). Dietary modulation of the human colonic microbiota: updating the concept of prebiotics. *Nutrition research reviews* **17,** 259-275.

Gilbey MP. (2007). Sympathetic rhythms and nervous integration. *Clinical and experimental pharmacology & physiology* **34,** 356-361.

Glatzle J, Sternini C, Robin C, Zittel TT, Wong H, Reeve JR, Jr. & Raybould HE. (2002). Expression of 5-HT3 receptors in the rat gastrointestinal tract. *Gastroenterology* **123,** 217-226.

Goehler LE, Gaykema RP, Hansen MK, Anderson K, Maier SF & Watkins LR. (2000). Vagal immune-to-brain communication: a visceral chemosensory pathway. *Autonomic neuroscience : basic & clinical* **85,** 49-59.

Goehler LE, Park SM, Opitz N, Lyte M & Gaykema RP. (2008). Campylobacter jejuni infection increases anxiety-like behavior in the holeboard: possible anatomical substrates for viscerosensory modulation of exploratory behavior. *Brain, behavior, and immunity* **22,** 354-366.

Golubeva AV, Crampton S, Desbonnet L, Edge D, O'Sullivan O, Lomasney KW, Zhdanov AV, Crispie F, Moloney RD, Borre YE, Cotter PD, Hyland NP, O'Halloran KD, Dinan TG, O'Keeffe GW & Cryan JF. (2015). Prenatal stress-induced alterations in major physiological systems correlate with gut microbiota composition in adulthood. *Psychoneuroendocrinology* **60,** 58-74.

Gonzalez-Rothi EJ, Lee KZ, Dale EA, Reier PJ, Mitchell GS & Fuller DD. (2015). Intermittent hypoxia and neurorehabilitation. *Journal of applied physiology (Bethesda, Md : 1985)* **119,** 1455-1465.

Gordan R, Gwathmey JK & Xie LH. (2015). Autonomic and endocrine control of cardiovascular function. *World journal of cardiology* **7,** 204-214.

Grenham S, Clarke G, Cryan JF & Dinan TG. (2011). Brain-gut-microbe communication in health and disease. *Frontiers in physiology* **2,** 94.

Grossman P & Taylor EW. (2007). Toward understanding respiratory sinus arrhythmia: relations to cardiac vagal tone, evolution and biobehavioral functions. *Biological psychology* **74,** 263-285.

Gulemetova R, Drolet G & Kinkead R. (2013). Neonatal stress augments the hypoxic chemoreflex of adult male rats by increasing AMPA receptor-mediated modulation. *Experimental physiology* **98,** 1312-1324.

Gulemetova R & Kinkead R. (2011). Neonatal stress increases respiratory instability in rat pups. *Respiratory physiology & neurobiology* **176,** 103-109.

Gutkowski P, Madaliński K, Grek M, Dmeńska H, Syczewska M & Michałkiewicz J. (2011). Clinical immunology Effect of orally administered probiotic strains Lactobacillus and Bifidobacterium in children with atopic asthma. *Central European Journal of Immunology* **35**.

Guyenet PG. (2006). The sympathetic control of blood pressure. *Nature reviews Neuroscience* **7,** 335-346.

Guyenet PG. (2014). Regulation of breathing and autonomic outflows by chemoreceptors. *Comprehensive Physiology* **4,** 1511-1562.

Guyenet PG & Bayliss DA. (2015). Neural Control of Breathing and CO2 Homeostasis. *Neuron* **87,** 946-961.

Haak BW, Lankelma JM, Hugenholtz F, Belzer C, de Vos WM & Wiersinga WJ. (2019). Long-term impact of oral vancomycin, ciprofloxacin and metronidazole on the gut microbiota in healthy humans. *The Journal of antimicrobial chemotherapy* **74,** 782-786.

Harris-Warrick RM & Johnson BR. (2010). Checks and balances in neuromodulation. *Frontiers in behavioral neuroscience* **4**.

Hilty M, Burke C, Pedro H, Cardenas P, Bush A, Bossley C, Davies J, Ervine A, Poulter L, Pachter L, Moffatt MF & Cookson WO. (2010). Disordered microbial communities in asthmatic airways. *PloS one* **5,** e8578.

Hoban AE, Moloney RD, Golubeva AV, McVey Neufeld KA, O'Sullivan O, Patterson E, Stanton C, Dinan TG, Clarke G & Cryan JF. (2016). Behavioural and neurochemical consequences of chronic gut microbiota depletion during adulthood in the rat. *Neuroscience* **339,** 463-477.

Hocker AD, Stokes JA, Powell FL & Huxtable AG. (2017). The impact of inflammation on respiratory plasticity. *Experimental neurology* **287,** 243-253.

Hodges MR, Tattersall GJ, Harris MB, McEvoy SD, Richerson DN, Deneris ES, Johnson RL, Chen ZF & Richerson GB. (2008). Defects in breathing and thermoregulation in mice with near-complete absence of central serotonin neurons. *The Journal of neuroscience : the official journal of the Society for Neuroscience* **28,** 2495-2505.

Hodges MR, Wehner M, Aungst J, Smith JC & Richerson GB. (2009). Transgenic mice lacking serotonin neurons have severe apnea and high mortality during development. *The Journal of neuroscience : the official journal of the Society for Neuroscience* **29,** 10341-10349.

Hofstetter AO, Legnevall L, Herlenius E & Katz-Salamon M. (2008). Cardiorespiratory development in extremely preterm infants: vulnerability to infection and persistence of events beyond term-equivalent age. *Acta paediatrica (Oslo, Norway : 1992)* **97,** 285-292.

Houlden A, Goldrick M, Brough D, Vizi ES, Lenart N, Martinecz B, Roberts IS & Denes A. (2016). Brain injury induces specific changes in the caecal microbiota of mice via altered autonomic activity and mucoprotein production. *Brain, behavior, and immunity* **57,** 10-20.

Huang YJ, Nariya S, Harris JM, Lynch SV, Choy DF, Arron JR & Boushey H. (2015). The airway microbiome in patients with severe asthma: Associations with disease features and severity. *The Journal of allergy and clinical immunology* **136,** 874-884.

Jaccoby S, Koike TI & Cornett LE. (1999). c-fos expression in the forebrain and brainstem of White Leghorn hens following osmotic and cardiovascular challenges. *Cell and tissue research* **297,** 229-239.

Johnston GR & Webster NR. (2009). Cytokines and the immunomodulatory function of the vagus nerve. *British journal of anaesthesia* **102,** 453-462.

Joseph V, Uppari N, Kouchi H, De Bruyn C, Boukari R & Bairam A. (2018). Respiratory regulation by steroids in newborn rats: a sex-specific balance between allopregnanolone and progesterone receptors. *Experimental physiology* **103,** 276-290.

Kallus SJ & Brandt LJ. (2012). The intestinal microbiota and obesity. *Journal of clinical gastroenterology* **46,** 16-24.

Keag OE, Norman JE & Stock SJ. (2018). Long-term risks and benefits associated with cesarean delivery for mother, baby, and subsequent pregnancies: Systematic review and meta-analysis. *PLoS medicine* **15,** e1002494.

Kekuda R, Manoharan P, Baseler W & Sundaram U. (2013). Monocarboxylate 4 mediated butyrate transport in a rat intestinal epithelial cell line. *Digestive diseases and sciences* **58,** 660-667.

Kelly JR, Borre Y, C OB, Patterson E, El Aidy S, Deane J, Kennedy PJ, Beers S, Scott K, Moloney G, Hoban AE, Scott L, Fitzgerald P, Ross P, Stanton C, Clarke G, Cryan JF & Dinan TG. (2016). Transferring the blues: Depression-associated gut microbiota induces neurobehavioural changes in the rat. *Journal of psychiatric research* **82,** 109-118.

Kelly JR, Kennedy PJ, Cryan JF, Dinan TG, Clarke G & Hyland NP. (2015). Breaking down the barriers: the gut microbiome, intestinal permeability and stress-related psychiatric disorders. *Frontiers in cellular neuroscience* **9,** 392.

Kigerl KA, Hall JC, Wang L, Mo X, Yu Z & Popovich PG. (2016). Gut dysbiosis impairs recovery after spinal cord injury. *The Journal of experimental medicine* **213,** 2603-2620.

Kim S, Goel R, Kumar A, Qi Y, Lobaton G, Hosaka K, Mohammed M, Handberg EM, Richards EM, Pepine CJ & Raizada MK. (2018). Imbalance of gut microbiome and intestinal epithelial barrier dysfunction in patients with high blood pressure. *Clinical science (London, England : 1979)* **132,** 701-718.

Kimura I, Inoue D, Maeda T, Hara T, Ichimura A, Miyauchi S, Kobayashi M, Hirasawa A & Tsujimoto G. (2011). Short-chain fatty acids and ketones directly regulate sympathetic nervous system via G protein-coupled receptor 41 (GPR41). *Proceedings of the National Academy of Sciences of the United States of America* **108,** 8030-8035.

Kinkead R, Balon N, Genest SE, Gulemetova R, Laforest S & Drolet G. (2008). Neonatal maternal separation and enhancement of the inspiratory (phrenic) response to hypoxia in adult rats: disruption of GABAergic neurotransmission in the nucleus tractus solitarius. *The European journal of neuroscience* **27,** 1174-1188.

Kinkead R, Guertin PA & Gulemetova R. (2013). Sex, stress and their influence on respiratory regulation. *Current pharmaceutical design* **19,** 4471-4484.

Kinkead R, Montandon G, Bairam A, Lajeunesse Y & Horner R. (2009). Neonatal maternal separation disrupts regulation of sleep and breathing in adult male rats. *Sleep* **32,** 1611-1620.

Kline DD, Ramirez-Navarro A & Kunze DL. (2007). Adaptive depression in synaptic transmission in the nucleus of the solitary tract after in vivo chronic intermittent hypoxia: evidence for homeostatic plasticity. *The Journal of neuroscience : the official journal of the Society for Neuroscience* **27,** 4663-4673.

Ko CY, Fan JM, Hu AK, Su HZ, Yang JH, Huang LM, Yan FR, Zhang HP & Zeng YM. (2019). Disruption of sleep architecture in Prevotella enterotype of patients with obstructive sleep apnea-hypopnea syndrome. *Brain and behavior***,** e01287.

Korpela K, Blakstad EW, Moltu SJ, Strommen K, Nakstad B, Ronnestad AE, Braekke K, Iversen PO, Drevon CA & de Vos W. (2018). Intestinal microbiota development and gestational age in preterm neonates. *Scientific reports* **8,** 2453.

Kratsman N, Getselter D & Elliott E. (2016). Sodium butyrate attenuates social behavior deficits and modifies the transcription of inhibitory/excitatory genes in the frontal cortex of an autism model. *Neuropharmacology* **102,** 136-145.

Kubin L, Alheid GF, Zuperku EJ & McCrimmon DR. (2006). Central pathways of pulmonary and lower airway vagal afferents. *Journal of applied physiology (Bethesda, Md : 1985)* **101,** 618-627.

Kumar P & Prabhakar NR. (2012). Peripheral chemoreceptors: function and plasticity of the carotid body. *Comprehensive Physiology* **2,** 141-219.

Kundu P, Blacher E, Elinav E & Pettersson S. (2017). Our Gut Microbiome: The Evolving Inner Self. *Cell* **171,** 1481-1493.

Kuo SM. (2013). The interplay between fiber and the intestinal microbiome in the inflammatory response. *Advances in nutrition (Bethesda, Md)* **4,** 16-28.

Kurokawa K, Itoh T, Kuwahara T, Oshima K, Toh H, Toyoda A, Takami H, Morita H, Sharma VK, Srivastava TP, Taylor TD, Noguchi H, Mori H, Ogura Y, Ehrlich DS, Itoh K, Takagi T, Sakaki Y, Hayashi T & Hattori M. (2007). Comparative metagenomics revealed commonly enriched gene sets in human gut microbiomes. *DNA research : an international journal for rapid publication of reports on genes and genomes* **14,** 169-181.

Lal S, Kirkup AJ, Brunsden AM, Thompson DG & Grundy D. (2001). Vagal afferent responses to fatty acids of different chain length in the rat. *American journal of physiology Gastrointestinal and liver physiology* **281,** G907-915.

Lane MA, Fuller DD, White TE & Reier PJ. (2008). Respiratory neuroplasticity and cervical spinal cord injury: translational perspectives. *Trends in neurosciences* **31,** 538-547.

Laouafa S, Ribon-Demars A, Marcouiller F, Roussel D, Bairam A, Pialoux V & Joseph V. (2017). Estradiol Protects Against Cardiorespiratory Dysfunctions and Oxidative Stress in Intermittent Hypoxia. *Sleep* **40**.

Le Floc'h N, Otten W & Merlot E. (2011). Tryptophan metabolism, from nutrition to potential therapeutic applications. *Amino acids* **41,** 1195-1205.

Lefter R, Morency CE & Joseph V. (2007). Progesterone increases hypoxic ventilatory response and reduces apneas in newborn rats. *Respiratory physiology & neurobiology* **156,** 9-16.

Li A & Nattie E. (2006). Catecholamine neurones in rats modulate sleep, breathing, central chemoreception and breathing variability. *The Journal of physiology* **570,** 385-396.

Li J, Zhao F, Wang Y, Chen J, Tao J, Tian G, Wu S, Liu W, Cui Q, Geng B, Zhang W, Weldon R, Auguste K, Yang L, Liu X, Chen L, Yang X, Zhu B & Cai J. (2017). Gut microbiota dysbiosis contributes to the development of hypertension. *Microbiome* **5,** 14.

Li T, Chen Y, Gua C & Wu B. (2018). Elevated Oxidative Stress and Inflammation in Hypothalamic Paraventricular Nucleus Are Associated With Sympathetic Excitation and Hypertension in Rats Exposed to Chronic Intermittent Hypoxia. *Frontiers in physiology* **9,** 840.

Lipski J, McAllen RM & Spyer KM. (1977). The carotid chemoreceptor input to the respiratory neurones of the nucleus of tractus solitarus. *The Journal of physiology* **269,** 797-810.

Lu D, Yao X, Abulimiti A, Cai L, Zhou L, Hong J & Li N. (2018a). Profiling of lung microbiota in the patients with obstructive sleep apnea. *Medicine* **97,** e11175.

Lu VB, Gribble FM & Reimann F. (2018b). Free Fatty Acid Receptors in Enteroendocrine Cells. *Endocrinology* **159,** 2826-2835.

Lucking EF, Murphy KH, Burns DP, Jaisimha AV, Barry-Murphy KJ, Dhaliwal P, Boland B, Rae MG & O'Halloran KD. (2018). No evidence in support of a prodromal respiratory control signature in the TgF344-AD rat model of Alzheimer's disease. *Respiratory physiology & neurobiology*.

Lucking EF, O'Halloran KD & Jones JF. (2014). Increased cardiac output contributes to the development of chronic intermittent hypoxia-induced hypertension. *Experimental physiology* **99,** 1312-1324.

Luczynski P, McVey Neufeld KA, Oriach CS, Clarke G, Dinan TG & Cryan JF. (2016). Growing up in a Bubble: Using Germ-Free Animals to Assess the Influence of the Gut Microbiota on Brain and Behavior. *The international journal of*

neuropsychopharmacology / official scientific journal of the Collegium Internationale Neuropsychopharmacologicum (CINP) **19**.

Lyte M. (2013). Microbial endocrinology in the microbiome-gut-brain axis: how bacterial production and utilization of neurochemicals influence behavior. *PLoS pathogens* **9,** e1003726.

Lyte M. (2014). Microbial endocrinology and the microbiota-gut-brain axis. *Advances in experimental medicine and biology* **817,** 3-24.

Macfarlane GT & Macfarlane S. (2012). Bacteria, colonic fermentation, and gastrointestinal health. *Journal of AOAC International* **95,** 50-60.

MacFarlane PM, Satriotomo I, Windelborn JA & Mitchell GS. (2009). NADPH oxidase activity is necessary for acute intermittent hypoxia-induced phrenic long-term facilitation. *The Journal of physiology* **587,** 1931-1942.

Machado BH. (2001). Neurotransmission of the cardiovascular reflexes in the nucleus tractus solitarii of awake rats. *Annals of the New York Academy of Sciences* **940,** 179-196.

Machado BH, Zoccal DB & Moraes DJA. (2017). Neurogenic hypertension and the secrets of respiration. *American journal of physiology Regulatory, integrative and comparative physiology* **312,** R864-R872.

Macpherson AJ & Uhr T. (2004). Induction of protective IgA by intestinal dendritic cells carrying commensal bacteria. *Science (New York, NY)* **303,** 1662-1665.

Maity C, Adak A, Pathak TK, Pati BR & Chandra Mondal K. (2012). Study of the cultivable microflora of the large intestine of the rat under varied environmental hyperbaric pressures. *Journal of microbiology, immunology, and infection = Wei mian yu gan ran za zhi* **45,** 281-286.

Mancia G & Grassi G. (2014). The autonomic nervous system and hypertension. *Circulation research* **114,** 1804-1814.

Marques FZ, Nelson E, Chu PY, Horlock D, Fiedler A, Ziemann M, Tan JK, Kuruppu S, Rajapakse NW, El-Osta A, Mackay CR & Kaye DM. (2017). High-Fiber Diet and Acetate Supplementation Change the Gut Microbiota and Prevent the Development of Hypertension and Heart Failure in Hypertensive Mice. *Circulation* **135,** 964-977.

McGuckin MA, Linden SK, Sutton P & Florin TH. (2011). Mucin dynamics and enteric pathogens. *Nature reviews Microbiology* **9,** 265-278.

McVey Neufeld KA, Luczynski P, Seira Oriach C, Dinan TG & Cryan JF. (2016). What's bugging your teen?-The microbiota and adolescent mental health. *Neuroscience and biobehavioral reviews* **70,** 300-312.

Mitchell GS & Johnson SM. (2003). Neuroplasticity in respiratory motor control. *Journal of applied physiology (Bethesda, Md : 1985)* **94,** 358-374.

Miyawaki T, Pilowsky P, Sun QJ, Minson J, Suzuki S, Arnolda L, Llewellyn-Smith I & Chalmers J. (1995). Central inspiration increases barosensitivity of neurons in rat rostral ventrolateral medulla. *The American journal of physiology* **268,** R909-918.

Molkov YI, Zoccal DB, Moraes DJ, Paton JF, Machado BH & Rybak IA. (2011). Intermittent hypoxia-induced sensitization of central chemoreceptors contributes to sympathetic nerve activity during late expiration in rats. *Journal of neurophysiology* **105,** 3080-3091.

Moraes DJ, da Silva MP, Bonagamba LG, Mecawi AS, Zoccal DB, Antunes-Rodrigues J, Varanda WA & Machado BH. (2013). Electrophysiological properties of rostral ventrolateral medulla presympathetic neurons modulated by the respiratory network in rats. *The Journal of neuroscience : the official journal of the Society for Neuroscience* **33,** 19223-19237.

Moraes DJ, Machado BH & Zoccal DB. (2014). Coupling of respiratory and sympathetic activities in rats submitted to chronic intermittent hypoxia. *Progress in brain research* **212,** 25-38.

Moraes DJ, Zoccal DB & Machado BH. (2012). Medullary respiratory network drives sympathetic overactivity and hypertension in rats submitted to chronic intermittent hypoxia. *Hypertension (Dallas, Tex : 1979)* **60,** 1374-1380.

Moreno-Indias I, Torres M, Montserrat JM, Sanchez-Alcoholado L, Cardona F, Tinahones FJ, Gozal D, Poroyko VA, Navajas D, Queipo-Ortuno MI & Farre R. (2015). Intermittent hypoxia alters gut microbiota diversity in a mouse model of sleep apnoea. *The European respiratory journal* **45,** 1055-1065.

Moreno-Indias I, Torres M, Sanchez-Alcoholado L, Cardona F, Almendros I, Gozal D, Montserrat JM, Queipo-Ortuno MI & Farre R. (2016). Normoxic Recovery Mimicking Treatment of Sleep Apnea Does Not Reverse Intermittent Hypoxia-Induced Bacterial Dysbiosis and Low-Grade Endotoxemia in Mice. *Sleep* **39,** 1891-1897.

Mosher KI & Wyss-Coray T. (2015). Go with your gut: microbiota meet microglia. *Nature neuroscience* **18,** 930-931.

Moya-Perez A, Luczynski P, Renes IB, Wang S, Borre Y, Anthony Ryan C, Knol J, Stanton C, Dinan TG & Cryan JF. (2017). Intervention strategies for cesarean section-induced alterations in the microbiota-gut-brain axis. *Nutrition reviews* **75,** 225-240.

Mukudai S, Sugiyama Y & Hisa Y. (2016). Dorsal motor nucleus of the vagus. In *Neuroanatomy and Neurophysiology of the Larynx*, pp. 97-102. Springer.

Murphy EA, Velazquez KT & Herbert KM. (2015). Influence of high-fat diet on gut microbiota: a driving force for chronic disease risk. *Current opinion in clinical nutrition and metabolic care* **18,** 515-520.

Nankova BB, Agarwal R, MacFabe DF & La Gamma EF. (2014). Enteric bacterial metabolites propionic and butyric acid modulate gene expression, including CREB-dependent catecholaminergic neurotransmission, in PC12 cells--possible relevance to autism spectrum disorders. *PloS one* **9,** e103740.

Nohr MK, Egerod KL, Christiansen SH, Gille A, Offermanns S, Schwartz TW & Moller M. (2015). Expression of the short chain fatty acid receptor GPR41/FFAR3 in autonomic and somatic sensory ganglia. *Neuroscience* **290,** 126-137.

Nuriel-Ohayon M, Neuman H, Ziv O, Belogolovski A, Barsheshet Y, Bloch N, Uzan A, Lahav R, Peretz A, Frishman S, Hod M, Hadar E, Louzoun Y, Avni O & Koren O. (2019). Progesterone Increases Bifidobacterium Relative Abundance during Late Pregnancy. *Cell reports* **27,** 730-736.e733.

O'Halloran KD. (2016). Chronic intermittent hypoxia creates the perfect storm with calamitous consequences for respiratory control. *Respiratory physiology & neurobiology* **226,** 63-67.

O'Halloran KD & McDonald FB. (2018). The shape of things to come: Early life stress stunts brainstem microglia, with lasting implications for cardiorespiratory control and plasticity. *Experimental physiology* **103,** 1183-1184.

O'Mahony SM, Clarke G, Borre YE, Dinan TG & Cryan JF. (2015). Serotonin, tryptophan metabolism and the brain-gut-microbiome axis. *Behavioural brain research* **277,** 32-48.

O'Mahony SM, Hyland NP, Dinan TG & Cryan JF. (2011). Maternal separation as a model of brain-gut axis dysfunction. *Psychopharmacology* **214,** 71-88.

O'Mahony SM, Marchesi JR, Scully P, Codling C, Ceolho AM, Quigley EM, Cryan JF & Dinan TG. (2009). Early life stress alters behavior, immunity, and microbiota in rats: implications for irritable bowel syndrome and psychiatric illnesses. *Biological psychiatry* **65,** 263-267.

Organization WH. (2007). Global surveillance, prevention and control of chronic respiratory diseases: a comprehensive approach. In *Global surveillance, prevention and control of chronic respiratory diseases: a comprehensive approach*.

Panda S, El khader I, Casellas F, Lopez Vivancos J, Garcia Cors M, Santiago A, Cuenca S, Guarner F & Manichanh C. (2014). Short-term effect of antibiotics on human gut microbiota. *PloS one* **9,** e95476.

Parish JM & Somers VK. (2004). Obstructive sleep apnea and cardiovascular disease. *Mayo Clinic proceedings* **79,** 1036-1046.

Penders J, Thijs C, Vink C, Stelma FF, Snijders B, Kummeling I, van den Brandt PA & Stobberingh EE. (2006). Factors influencing the composition of the intestinal microbiota in early infancy. *Pediatrics* **118,** 511-521.

Peng YJ, Nanduri J, Khan SA, Yuan G, Wang N, Kinsman B, Vaddi DR, Kumar GK, Garcia JA, Semenza GL & Prabhakar NR. (2011). Hypoxia-inducible factor 2alpha (HIF-2alpha) heterozygous-null mice exhibit exaggerated carotid body sensitivity to hypoxia, breathing instability, and hypertension. *Proceedings of the National Academy of Sciences of the United States of America* **108,** 3065-3070.

Peng YJ, Nanduri J, Yuan G, Wang N, Deneris E, Pendyala S, Natarajan V, Kumar GK & Prabhakar NR. (2009). NADPH oxidase is required for the sensory plasticity of the carotid body by chronic intermittent hypoxia. *The Journal of neuroscience : the official journal of the Society for Neuroscience* **29,** 4903-4910.

Peng YJ, Overholt JL, Kline D, Kumar GK & Prabhakar NR. (2003). Induction of sensory long-term facilitation in the carotid body by intermittent hypoxia: implications for recurrent apneas. *Proceedings of the National Academy of Sciences of the United States of America* **100,** 10073-10078.

Pevsner-Fischer M, Rot C, Tuganbaev T & Elinav E. (2016). The Microbiota and Its Modulation in Immune-Mediated Disorders. In *Immune Rebalancing*, pp. 191-227. Elsevier.

Poroyko VA, Carreras A, Khalyfa A, Khalyfa AA, Leone V, Peris E, Almendros I, Gileles-Hillel A, Qiao Z, Hubert N, Farre R, Chang EB & Gozal D. (2016). Chronic Sleep Disruption Alters Gut Microbiota, Induces Systemic and Adipose Tissue Inflammation and Insulin Resistance in Mice. *Scientific reports* **6,** 35405.

Powell FL, Dwinell MR & Aaron EA. (2000). Measuring ventilatory acclimatization to hypoxia: comparative aspects. *Respiration physiology* **122,** 271-284.

Prabhakar NR. (2006). O2 sensing at the mammalian carotid body: why multiple O2 sensors and multiple transmitters? *Experimental physiology* **91,** 17-23.

Prabhakar NR & Peng YJ. (2004). Peripheral chemoreceptors in health and disease. *Journal of applied physiology (Bethesda, Md : 1985)* **96,** 359-366.

Prabhakar NR, Peng YJ, Kumar GK & Pawar A. (2007). Altered carotid body function by intermittent hypoxia in neonates and adults: relevance to recurrent apneas. *Respiratory physiology & neurobiology* **157,** 148-153.

Purves D, Augustine GJ, Fitzpatrick D, LaMantia A, McNamara J & Williams S. (2001). Autonomic regulation of cardiovascular function. *Neuroscience*.

Qin J, Li R, Raes J, Arumugam M, Burgdorf KS, Manichanh C, Nielsen T, Pons N, Levenez F, Yamada T, Mende DR, Li J, Xu J, Li S, Li D, Cao J, Wang B, Liang H, Zheng H, Xie Y, Tap J, Lepage P, Bertalan M, Batto JM, Hansen T, Le Paslier D, Linneberg A, Nielsen HB, Pelletier E, Renault P, Sicheritz-Ponten T, Turner K, Zhu H, Yu C, Li S, Jian M, Zhou Y, Li Y, Zhang X, Li S, Qin N, Yang H, Wang J, Brunak S, Dore J, Guarner F, Kristiansen K, Pedersen O, Parkhill J, Weissenbach J, Meta HITC, Bork P, Ehrlich SD & Wang J. (2010). A human gut microbial gene catalogue established by metagenomic sequencing. *Nature* **464,** 59-65.

Rajilić-Stojanović M. (2013). Function of the microbiota. *Best practice & research Clinical gastroenterology* **27,** 5-16.

Ramanantsoa N, Hirsch MR, Thoby-Brisson M, Dubreuil V, Bouvier J, Ruffault PL, Matrot B, Fortin G, Brunet JF, Gallego J & Goridis C. (2011). Breathing without CO(2) chemosensitivity in conditional Phox2b mutants. *The Journal of neuroscience : the official journal of the Society for Neuroscience* **31,** 12880-12888.

Ramirez JM, Doi A, Garcia AJ, 3rd, Elsen FP, Koch H & Wei AD. (2012). The cellular building blocks of breathing. *Comprehensive Physiology* **2,** 2683-2731.

Ray RS, Corcoran AE, Brust RD, Kim JC, Richerson GB, Nattie E & Dymecki SM. (2011). Impaired respiratory and body temperature control upon acute serotonergic neuron inhibition. *Science (New York, NY)* **333,** 637-642.

Raybould HE, Glatzle J, Robin C, Meyer JH, Phan T, Wong H & Sternini C. (2003). Expression of 5-HT3 receptors by extrinsic duodenal afferents contribute to intestinal inhibition of gastric emptying. *American journal of physiology Gastrointestinal and liver physiology* **284,** G367-372.

Reikvam DH, Erofeev A, Sandvik A, Grcic V, Jahnsen FL, Gaustad P, McCoy KD, Macpherson AJ, Meza-Zepeda LA & Johansen FE. (2011). Depletion of murine intestinal microbiota: effects on gut mucosa and epithelial gene expression. *PloS one* **6,** e17996.

Rhee SH, Pothoulakis C & Mayer EA. (2009). Principles and clinical implications of the brain-gut-enteric microbiota axis. *Nature reviews Gastroenterology & hepatology* **6,** 306-314.

Roberfroid M, Gibson GR, Hoyles L, McCartney AL, Rastall R, Rowland I, Wolvers D, Watzl B, Szajewska H, Stahl B, Guarner F, Respondek F, Whelan K, Coxam V, Davicco MJ, Leotoing L, Wittrant Y, Delzenne NM, Cani PD, Neyrinck AM & Meheust A. (2010). Prebiotic effects: metabolic and health benefits. *The British journal of nutrition* **104 Suppl 2,** S1-63.

Roger LC, Costabile A, Holland DT, Hoyles L & McCartney AL. (2010). Examination of faecal Bifidobacterium populations in breast- and formula-fed infants during the first 18 months of life. *Microbiology (Reading, England)* **156,** 3329-3341.

Ruffault PL, D'Autreaux F, Hayes JA, Nomaksteinsky M, Autran S, Fujiyama T, Hoshino M, Hagglund M, Kiehn O, Brunet JF, Fortin G & Goridis C. (2015). The retrotrapezoid nucleus neurons expressing Atoh1 and Phox2b are essential for the respiratory response to CO(2). *eLife* **4**.

Sabater-Molina M, Larque E, Torrella F & Zamora S. (2009). Dietary fructooligosaccharides and potential benefits on health. *Journal of physiology and biochemistry* **65,** 315-328.

Salman IM. (2016). Major Autonomic Neuroregulatory Pathways Underlying Short- and Long-Term Control of Cardiovascular Function. *Current hypertension reports* **18,** 18.

Sandhu KV, Sherwin E, Schellekens H, Stanton C, Dinan TG & Cryan JF. (2017). Feeding the microbiota-gut-brain axis: diet, microbiome, and neuropsychiatry. *Translational research : the journal of laboratory and clinical medicine* **179,** 223-244.

Santisteban MM, Qi Y, Zubcevic J, Kim S, Yang T, Shenoy V, Cole-Jeffrey CT, Lobaton GO, Stewart DC, Rubiano A, Simmons CS, Garcia-Pereira F, Johnson RD, Pepine CJ & Raizada MK. (2017). Hypertension-Linked Pathophysiological Alterations in the Gut. *Circulation research* **120,** 312-323.

Sarkar A, Lehto SM, Harty S, Dinan TG, Cryan JF & Burnet PWJ. (2016). Psychobiotics and the Manipulation of Bacteria-Gut-Brain Signals. *Trends in neurosciences* **39,** 763-781.

Savin Z, Kivity S, Yonath H & Yehuda S. (2018). Smoking and the intestinal microbiome. *Archives of microbiology* **200,** 677-684.

Schelegle ES. (2003). Functional morphology and physiology of slowly adapting pulmonary stretch receptors. *The Anatomical Record Part A: Discoveries in Molecular, Cellular, and Evolutionary Biology: An Official Publication of the American Association of Anatomists* **270,** 11-16.

Sender R, Fuchs S & Milo R. (2016). Are We Really Vastly Outnumbered? Revisiting the Ratio of Bacterial to Host Cells in Humans. *Cell* **164,** 337-340.

Sharon G, Cruz NJ, Kang DW, Gandal MJ, Wang B, Kim YM, Zink EM, Casey CP, Taylor BC, Lane CJ, Bramer LM, Isern NG, Hoyt DW, Noecker C, Sweredoski MJ, Moradian A, Borenstein E, Jansson JK, Knight R, Metz TO, Lois C, Geschwind DH, Krajmalnik-Brown R & Mazmanian SK. (2019). Human Gut Microbiota from Autism Spectrum Disorder Promote Behavioral Symptoms in Mice. *Cell* **177,** 1600-1618.e1617.

Simpson JL, Baines KJ, Horvat JC, Essilfie AT, Brown AC, Tooze M, McDonald VM, Gibson PG & Hansbro PM. (2016). COPD is characterized by increased detection of Haemophilus influenzae, Streptococcus pneumoniae and a deficiency of Bacillus species. *Respirology (Carlton, Vic)* **21,** 697-704.

Sina C, Gavrilova O, Forster M, Till A, Derer S, Hildebrand F, Raabe B, Chalaris A, Scheller J, Rehmann A, Franke A, Ott S, Hasler R, Nikolaus S, Folsch UR, Rose-John S, Jiang HP, Li J, Schreiber S & Rosenstiel P. (2009). G protein-coupled receptor 43 is essential for neutrophil recruitment during intestinal inflammation. *Journal of immunology (Baltimore, Md : 1950)* **183,** 7514-7522.

Slavin J. (2013). Fiber and prebiotics: mechanisms and health benefits. *Nutrients* **5,** 1417-1435.

Smith JC, Abdala AP, Borgmann A, Rybak IA & Paton JF. (2013a). Brainstem respiratory networks: building blocks and microcircuits. *Trends in neurosciences* **36,** 152-162.

Smith PM, Howitt MR, Panikov N, Michaud M, Gallini CA, Bohlooly YM, Glickman JN & Garrett WS. (2013b). The microbial metabolites, short-chain fatty acids, regulate colonic Treg cell homeostasis. *Science (New York, NY)* **341,** 569-573.

Soliz J, Tam R & Kinkead R. (2016). Neonatal Maternal Separation Augments Carotid Body Response to Hypoxia in Adult Males but Not Female Rats. *Frontiers in physiology* **7,** 432.

Sondheimer JM, Clark DA & Gervaise EP. (1985). Continuous gastric pH measurement in young and older healthy preterm infants receiving formula and clear liquid feedings. *Journal of pediatric gastroenterology and nutrition* **4,** 352-355.

Sonnenburg JL, Chen CT & Gordon JI. (2006). Genomic and metabolic studies of the impact of probiotics on a model gut symbiont and host. *PLoS biology* **4,** e413.

Spiller R. (2008). Serotonin and GI clinical disorders. *Neuropharmacology* **55,** 1072-1080.

Staffolo MD, Bevilacqua AE, Rodríguez MS & Albertengo L. (2012). Dietary fiber and availability of nutrients: a case study on yoghurt as a food model. In *The complex world of polysaccharides*. IntechOpen.

Stilling RM, Bordenstein SR, Dinan TG & Cryan JF. (2014a). Friends with social benefits: host-microbe interactions as a driver of brain evolution and development? *Frontiers in cellular and infection microbiology* **4,** 147.

Stilling RM, Dinan TG & Cryan JF. (2014b). Microbial genes, brain & behaviour - epigenetic regulation of the gut-brain axis. *Genes, brain, and behavior* **13,** 69-86.

Stilling RM, van de Wouw M, Clarke G, Stanton C, Dinan TG & Cryan JF. (2016). The neuropharmacology of butyrate: The bread and butter of the microbiota-gut-brain axis? *Neurochemistry international* **99,** 110-132.

Strandwitz P. (2018). Neurotransmitter modulation by the gut microbiota. *Brain research* **1693,** 128-133.

Sudo N, Chida Y, Aiba Y, Sonoda J, Oyama N, Yu XN, Kubo C & Koga Y. (2004). Postnatal microbial colonization programs the hypothalamic-pituitary-adrenal system for stress response in mice. *The Journal of physiology* **558,** 263-275.

Suez J, Zmora N, Zilberman-Schapira G, Mor U, Dori-Bachash M, Bashiardes S, Zur M, Regev-Lehavi D, Ben-Zeev Brik R, Federici S, Horn M, Cohen Y, Moor AE, Zeevi D, Korem T, Kotler E, Harmelin A, Itzkovitz S, Maharshak N, Shibolet O, Pevsner-Fischer M, Shapiro H, Sharon I, Halpern Z, Segal E & Elinav E. (2018). Post-Antibiotic Gut Mucosal Microbiome Reconstitution Is Impaired by Probiotics and Improved by Autologous FMT. *Cell* **174,** 1406-1423.e1416.

Sullivan A, Edlund C & Nord CE. (2001). Effect of antimicrobial agents on the ecological balance of human microflora. *The Lancet Infectious diseases* **1,** 101-114.

Svensson E, Horvath-Puho E, Thomsen RW, Djurhuus JC, Pedersen L, Borghammer P & Sorensen HT. (2015). Vagotomy and subsequent risk of Parkinson's disease. *Annals of neurology* **78,** 522-529.

Tannock GW & Savage DC. (1974). Influences of dietary and environmental stress on microbial populations in the murine gastrointestinal tract. *Infection and immunity* **9,** 591-598.

Tenorio-Lopes L, Henry MS, Marques D, Tremblay ME, Drolet G, Bretzner F & Kinkead R. (2017). Neonatal maternal separation opposes the facilitatory effect of castration on the respiratory response to hypercapnia of the adult male rat: evidence for the involvement of the medial amygdala. *Journal of neuroendocrinology*.

Teppema LJ & Dahan A. (2010). The ventilatory response to hypoxia in mammals: mechanisms, measurement, and analysis. *Physiological reviews* **90,** 675-754.

Thomas H, Diamond J, Vieco A, Chaudhuri S, Shinnar E, Cromer S, Perel P, Mensah GA, Narula J, Johnson CO, Roth GA & Moran AE. (2018). Global Atlas of Cardiovascular Disease 2000-2016: The Path to Prevention and Control. *Global heart* **13,** 143-163.

Thorburn AN, McKenzie CI, Shen S, Stanley D, Macia L, Mason LJ, Roberts LK, Wong CH, Shim R, Robert R, Chevalier N, Tan JK, Marino E, Moore RJ, Wong L, McConville MJ, Tull DL, Wood LG, Murphy VE, Mattes J, Gibson PG & Mackay CR. (2015). Evidence that asthma is a developmental origin disease influenced by maternal diet and bacterial metabolites. *Nature communications* **6,** 7320.

Tolhurst G, Heffron H, Lam YS, Parker HE, Habib AM, Diakogiannaki E, Cameron J, Grosse J, Reimann F & Gribble FM. (2012). Short-chain fatty acids stimulate glucagon-like peptide-1 secretion via the G-protein-coupled receptor FFAR2. *Diabetes* **61,** 364-371.

Tomoda K, Kubo K, Asahara T, Andoh A, Nomoto K, Nishii Y, Yamamoto Y, Yoshikawa M & Kimura H. (2011). Cigarette smoke decreases organic acids levels and population of bifidobacterium in the caecum of rats. *The Journal of toxicological sciences* **36,** 261-266.

Toral M, Robles-Vera I, de la Visitacion N, Romero M, Yang T, Sanchez M, Gomez-Guzman M, Jimenez R, Raizada MK & Duarte J. (2019). Critical Role of the Interaction Gut Microbiota - Sympathetic Nervous System in the Regulation of Blood Pressure. *Frontiers in physiology* **10,** 231.

Tripathi A, Melnik AV, Xue J, Poulsen O, Meehan MJ, Humphrey G, Jiang L, Ackermann G, McDonald D, Zhou D, Knight R, Dorrestein PC & Haddad GG. (2018). Intermittent Hypoxia and Hypercapnia, a Hallmark of Obstructive Sleep Apnea, Alters the Gut Microbiome and Metabolome. *mSystems* **3**.

van de Wouw M, Boehme M, Lyte JM, Wiley N, Strain C, O'Sullivan O, Clarke G, Stanton C, Dinan TG & Cryan JF. (2018a). Short-chain fatty acids: microbial metabolites that alleviate stress-induced brain-gut axis alterations. *The Journal of physiology*.

van de Wouw M, Boehme M, Lyte JM, Wiley N, Strain C, O'Sullivan O, Clarke G, Stanton C, Dinan TG & Cryan JF. (2018b). Short-chain fatty acids: microbial metabolites that alleviate stress-induced brain-gut axis alterations. *The Journal of physiology* **596,** 4923-4944.

van Nimwegen FA, Penders J, Stobberingh EE, Postma DS, Koppelman GH, Kerkhof M, Reijmerink NE, Dompeling E, van den Brandt PA, Ferreira I, Mommers M & Thijs C. (2011). Mode and place of delivery, gastrointestinal microbiota, and their influence

on asthma and atopy. *The Journal of allergy and clinical immunology* **128,** 948-955 e941-943.

Van Ryswyk E, Anderson CS, Antic NA, Barbe F, Bittencourt L, Freed R, Heeley E, Liu Z, Loffler KA, Lorenzi-Filho G, Luo Y, Margalef MJM, McEvoy RD, Mediano O, Mukherjee S, Ou Q, Woodman R, Zhang X & Chai-Coetzer CL. (2019). Predictors of long-term adherence to continuous positive airway pressure in patients with obstructive sleep apnea and cardiovascular disease. *Sleep*.

Vernocchi P, Del Chierico F, Russo A, Majo F, Rossitto M, Valerio M, Casadei L, La Storia A, De Filippis F, Rizzo C, Manetti C, Paci P, Ercolini D, Marini F, Fiscarelli EV, Dallapiccola B, Lucidi V, Miccheli A & Putignani L. (2018). Gut microbiota signatures in cystic fibrosis: Loss of host CFTR function drives the microbiota enterophenotype. *PloS one* **13,** e0208171.

Vijay N, Morse BL & Morris ME. (2015). A Novel Monocarboxylate Transporter Inhibitor as a Potential Treatment Strategy for gamma-Hydroxybutyric Acid Overdose. *Pharmaceutical research* **32,** 1894-1906.

Waldecker M, Kautenburger T, Daumann H, Busch C & Schrenk D. (2008). Inhibition of histone-deacetylase activity by short-chain fatty acids and some polyphenol metabolites formed in the colon. *The Journal of nutritional biochemistry* **19,** 587-593.

Wang FB & Powley TL. (2007). Vagal innervation of intestines: afferent pathways mapped with new en bloc horseradish peroxidase adaptation. *Cell and tissue research* **329,** 221-230.

Wang H, Zhao JX, Hu N, Ren J, Du M & Zhu MJ. (2012). Side-stream smoking reduces intestinal inflammation and increases expression of tight junction proteins. *World journal of gastroenterology* **18,** 2180-2187.

Wang Q, Li F, Liang B, Liang Y, Chen S, Mo X, Ju Y, Zhao H, Jia H, Spector TD, Xie H & Guo R. (2018). A metagenome-wide association study of gut microbiota in asthma in UK adults. *BMC microbiology* **18,** 114.

Wang Z, Bafadhel M, Haldar K, Spivak A, Mayhew D, Miller BE, Tal-Singer R, Johnston SL, Ramsheh MY, Barer MR, Brightling CE & Brown JR. (2016). Lung microbiome dynamics in COPD exacerbations. *The European respiratory journal* **47,** 1082-1092.

Widdicombe J. (2003). Functional morphology and physiology of pulmonary rapidly adapting receptors (RARs). *The Anatomical Record Part A: Discoveries in Molecular, Cellular, and Evolutionary Biology: An Official Publication of the American Association of Anatomists* **270,** 2-10.

Wilkerson JE & Mitchell GS. (2009). Daily intermittent hypoxia augments spinal BDNF levels, ERK phosphorylation and respiratory long-term facilitation. *Experimental neurology* **217,** 116-123.

Wilkerson JER, Devinney M & Mitchell GS. (2018). Intermittent but not sustained moderate hypoxia elicits long-term facilitation of hypoglossal motor output. *Respiratory physiology & neurobiology* **256,** 15-20.

Woodmansey EJ. (2007). Intestinal bacteria and ageing. *Journal of applied microbiology* **102,** 1178-1186.

Wu BG, Sulaiman I, Wang J, Shen N, Clemente JC, Li Y, Laumbach RJ, Lu SE, Udasin I, Le-Hoang O, Perez A, Alimokhtari S, Black K, Plietz M, Twumasi A, Sanders H, Malecha P, Kapoor B, Scaglione BD, Wang A, Blazoski C, Weiden MD, Rapoport DM, Harrison D, Chitkara N, Vicente E, Marin JM, Sunderram J, Ayappa I & Segal LN. (2018). Severe Obstructive Sleep Apnea is Associated with Alterations in the Nasal Microbiome and Increase in Inflammation. *American journal of respiratory and critical care medicine*.

Wu J, Sun X, Wu Q, Li H, Li L, Feng J, Zhang S, Xu L, Li K, Li X, Wang X & Chen H. (2016). Disrupted intestinal structure in a rat model of intermittent hypoxia. *Molecular medicine reports* **13,** 4407-4413.

Xu H, Li X, Zheng X, Xia Y, Fu Y, Li X, Qian Y, Zou J, Zhao A, Guan J, Gu M, Yi H, Jia W & Yin S. (2018). Pediatric Obstructive Sleep Apnea is Associated With Changes in the Oral Microbiome and Urinary Metabolomics Profile: A Pilot Study. *Journal of clinical sleep medicine : JCSM : official publication of the American Academy of Sleep Medicine* **14,** 1559-1567.

Yan Q, Gu Y, Li X, Yang W, Jia L, Chen C, Han X, Huang Y, Zhao L, Li P, Fang Z, Zhou J, Guan X, Ding Y, Wang S, Khan M, Xin Y, Li S & Ma Y. (2017). Alterations of the Gut Microbiome in Hypertension. *Frontiers in cellular and infection microbiology* **7,** 381.

Yang T, Santisteban MM, Rodriguez V, Li E, Ahmari N, Carvajal JM, Zadeh M, Gong M, Qi Y, Zubcevic J, Sahay B, Pepine CJ, Raizada MK & Mohamadzadeh M. (2015). Gut dysbiosis is linked to hypertension. *Hypertension (Dallas, Tex : 1979)* **65,** 1331-1340.

Zheng P, Zeng B, Zhou C, Liu M, Fang Z, Xu X, Zeng L, Chen J, Fan S, Du X, Zhang X, Yang D, Yang Y, Meng H, Li W, Melgiri ND, Licinio J, Wei H & Xie P. (2016). Gut microbiome remodeling induces depressive-like behaviors through a pathway mediated by the host's metabolism. *Molecular psychiatry* **21,** 786-796.

Zoccal DB, Bonagamba LG, Paton JF & Machado BH. (2009). Sympathetic-mediated hypertension of awake juvenile rats submitted to chronic intermittent hypoxia is not linked to baroreflex dysfunction. *Experimental physiology* **94,** 972-983.

Zoccal DB, Furuya WI, Bassi M, Colombari DS & Colombari E. (2014). The nucleus of the solitary tract and the coordination of respiratory and sympathetic activities. *Frontiers in physiology* **5,** 238.

Zoccal DB, Simms AE, Bonagamba LG, Braga VA, Pickering AE, Paton JF & Machado BH. (2008). Increased sympathetic outflow in juvenile rats submitted to chronic intermittent hypoxia correlates with enhanced expiratory activity. *The Journal of physiology* **586,** 3253-3265.

Chapter 2. Manipulation of gut microbiota blunts the ventilatory response to hypercapnia in adult rats

Karen M. O'Connor[a,b,c], Eric F. Lucking[a], Anna V. Golubeva[c], Conall R. Strain[d], Fiona Fouhy[c,d], María C. Cenit[b,e], Pardeep Dhaliwal[a], Thomaz F.S. Bastiaanssen[b,c], David P. Burns[a], Catherine Stanton[c,d], Gerard Clarke[c,f], John F. Cryan[b,c], Ken D. O'Halloran[a,c].

[a]*Department of Physiology, School of Medicine, College of Medicine & Health, University College Cork, Cork, Ireland*

[b]*Department of Anatomy & Neuroscience, School of Medicine, College of Medicine & Health, University College Cork, Cork, Ireland*

[c]*APC Microbiome Ireland, University College Cork, Cork, Ireland*

[d]*Teagasc Food Research Centre, Moorepark, Fermoy, County Cork, Ireland*

[e]*Institute of Agrochemistry and Food Technology (IATA), National Council for Scientific Research (CSIC), Valencia, Spain*

[f]*Department of Psychiatry and Neurobehavioural Science, School of Medicine, College of Medicine & Health, University College Cork, Cork, Ireland*

Published in EbioMedicine

Volume 44, June 2019, Pages 618-638, doi: 10.1016/j.ebiom.2019.03.029.



This image was generated by Natalia Komissarova. It is now on the EbioMedicine website.

Abbreviations: ABX, antibiotic-treated; AIH, acute intermittent hypoxia; BH, Benjamini-Hochberg; DA, dopamine; Dia, diaphragm; EMG, electromyogram; $ETCO_2$, end-tidal carbon dioxide; FDR, false discovery rate; FLASH, fast length adjustment of short reads to improve genome assemblies; FMT, faecal microbiota transfer; f_R, respiratory frequency; $FiCO_2$, fractional inspired carbon dioxide concentration; F_iO_2, fractional inspired oxygen concentration; Hb, haemoglobin; HVA, homovanillic acid; $_L$-DOPA, $_L$-3,4-dihydroxyphenylalanine; NA, noradrenaline; OTUs, operational taxonomic units; PBG, phenylbiguanide; PBS, phosphate buffered saline; PCoA, Principal coordinates analysis; $PaCO_2$, partial pressure of arterial carbon dioxide; PD whole tree, phylogenetic whole tree diversity; PaO_2, partial pressure of arterial oxygen; QIIME, quantitative insights into microbial ecology; SaO_2, arterial oxygen saturation; SD1, short-term respiratory timing variability; SD2, long-term respiratory timing variability; T_e, expiratory time; T_i, inspiratory time; T_{tot}, total breath duration; $V\dot{c}o_2$, carbon dioxide; V_E, minute ventilation; production; VEH, vehicle, autoclaved deionised water; $V_E/V\dot{c}o_2$, ventilatory equivalent for CO_2; $V\dot{o}_2$, oxygen consumption; V_T, tidal volume; V_T/T_i, mean inspiratory flow; 5-HIAA, 5-hydroindoleacetic acid; 5-HT, 5-hydroxytryptamine (serotonin); 5-HT_3, 5-hydroxytryptamine type 3.

Abstract

Background: It is increasingly evident that perturbations to the diversity and composition of the gut microbiota have significant consequences for the regulation of integrative physiological systems. There is growing interest in the potential contribution of microbiota-gut-brain signalling to cardiorespiratory control in health and disease.

Methods: In adult male rats, we sought to determine the cardiorespiratory effects of manipulation of the gut microbiota following a 4-week administration of a cocktail of antibiotics. We subsequently explored the effects of administration of faecal microbiota from pooled control (vehicle) rat faeces, given by gavage to vehicle- and antibiotic-treated rats.

Findings: Antibiotic intervention depressed the ventilatory response to hypercapnic stress in conscious animals, owing to a reduction in the respiratory frequency response to carbon dioxide. Baseline frequency, respiratory timing variability, and the expression of apnoeas and sighs were normal. Microbiota-depleted rats had decreased systolic blood pressure. Faecal microbiota transfer to vehicle- and antibiotic-treated animals also disrupted the gut microbiota composition, associated with depressed ventilatory responsiveness to hypercapnia. Chronic antibiotic intervention or faecal microbiota transfer both caused significant disruptions to brainstem monoamine neurochemistry, with increased homovanillic acid:dopamine ratio indicative of increased dopamine turnover, which correlated with the abundance of several bacteria of six different phyla.

Interpretation: Chronic antibiotic administration and faecal microbiota transfer disrupt gut microbiota, brainstem monoamine concentrations and the ventilatory response to hypercapnia. We suggest that aberrant microbiota-gut-brain axis signalling has a modulatory influence on respiratory behaviour during hypercapnic stress.

Funding: Department of Physiology and APC Microbiome Ireland, University College Cork, Ireland.

Keywords: Antibiotics; faecal microbiota transfer; breathing; hypercapnia; cardiovascular; vagus; neurochemistry; intestinal permeability; microbiota

Research in Context

Evidence before this study: The microbiota-gut-brain axis is implicated in the homeostatic control of physiological systems; however, its potential influence on the control of breathing is unclear.

Added value of this study: Chronic antibiotic administration in rats depleted gut microbiota, increased gut permeability, altered brainstem neurochemistry and depressed the ventilatory response to hypercapnic stress. Faecal microbiota transfer in vehicle- and antibiotic-treated rats significantly disrupted the microbiota composition, with associated disruptions to brainstem neurochemistry and depressed ventilation during hypercapnia. Brainstem monoamine neurochemistry correlated with the relative abundance of several bacteria, primarily of the Firmicutes phylum.

Implications of all the available evidence: Manipulation of the gut microbiota disrupts respiratory behaviour suggesting that the microbiota-gut-brain axis has the capacity to alter respiratory control through aberrant neuromodulation of breathing.

2.1. Introduction

There is a growing understanding of the significance of the gastrointestinal microbiome and its modulatory capacity in the homeostatic regulation of multiple physiological systems (Dinan & Cryan, 2017). Trillions of gut microbiota form a co-dependent, mutualistic relationship with the host, contributing to whole-body health (Bordenstein & Theis, 2015), through an extensive multimodal communication pathway termed the 'microbiota-gut-brain axis' (Sudo *et al.*, 2004). Dysregulated microbiota-gut-brain axis signalling disrupts major neurocontrol systems affecting anxiety, pain, depression and social behaviours (Neufeld *et al.*, 2011; O'Mahony *et al.*, 2014; De Palma *et al.*, 2015; Kelly *et al.*, 2016b; Burokas *et al.*, 2017; Golubeva *et al.*, 2017; Stilling *et al.*, 2018). Multiple contributors to microbiota-gut-brain axis communication have been identified, including neural pathways, immune mediators, bacterial metabolites, serotonin and tryptophan metabolism, host genetics and gut hormones (Burokas *et al.*, 2015). There is a wide appreciation of the potential contribution of microbiota-gut-brain signalling to cardiorespiratory control in health and disease (Golubeva *et al.*, 2015; Durgan *et al.*, 2016; Adnan *et al.*, 2017; Santisteban *et al.*, 2017; Ganesh *et al.*, 2018; Lucking *et al.*, 2018b).

The cardiorespiratory system is tightly regulated by neuronal networks residing within the brainstem. Respiratory rhythm and pattern, generated by complex brainstem networks is transduced via multiple efferent pathways, directly or indirectly via the spinal nuclei to the striated muscles of breathing, which provides for exquisite breath-by-breath control of pulmonary ventilation (Alheid & McCrimmon, 2008; Garcia *et al.*, 2011). Autonomic centres within the medulla oblongata (dorsal motor nucleus of the vagus, nucleus ambiguus and rostral ventrolateral medulla) transduce parasympathetic and sympathetic motor outflow to the heart and circulation. Of interest, there is considerable respiratory-related modulation of autonomic efferent signalling. The vagus nerve, a key bi-directional communication pathway of the microbiota-gut-brain axis (Bonaz *et al.*, 2018), provides visceral information from sensors in multiple peripheral sites to the nucleus of the solitary tract within the brainstem. There is considerable sensory-cued modulation of respiratory motor and autonomic outputs, from the periphery, which execute efficient cardiorespiratory control. Notwithstanding the primary homeostatic function of the neural networks governing breathing and blood pressure regulation, there is ample evidence in support of a remarkable capacity for plasticity at multiple sites within the control network, both at a central and

peripheral level, which underpin adaptive and maladaptive outcomes (Peng *et al.*, 2009; Almado *et al.*, 2012; Kumar & Prabhakar, 2012; Fuller & Mitchell, 2017; Hocker *et al.*, 2017).

Maladaptive plasticity expressed in several stress models have revealed considerable long-lasting perturbations to respiratory control, with deleterious consequences for whole-body health (Bavis, 2005; Gulemetova & Kinkead, 2011; Fournier *et al.*, 2013b; Kinkead *et al.*, 2013; Soliz *et al.*, 2016). Prenatal stress results in enhanced respiratory variability and alters ventilatory control during hypoxic and hypercapnic chemostimulation in rat offspring during adulthood (Golubeva *et al.*, 2015). Interestingly, respiratory frequency responses to hypercapnia correlated with alterations in the gut microbiota (Golubeva *et al.*, 2015). Recently, exposure to chronic intermittent hypoxia, modelling human sleep apnoea, was shown to disrupt cardiorespiratory homeostasis, with evidence of decreased prevalence of protective sigh behaviours, altered autonomic control of heart rate, decreased brainstem noradrenaline concentration, and altered gut microbiota composition (Lucking *et al.*, 2018b). To our knowledge, there are no other studies of the effects of manipulation of the microbiota on the control of breathing. Yet importantly, animal models of sleep-disordered breathing show evidence of altered microbiota composition and diversity, driven by altered diet and/or exposure to intermittent hypoxia (Moreno-Indias *et al.*, 2015; Durgan *et al.*, 2016; Moreno-Indias *et al.*, 2016; Tripathi *et al.*, 2018). Thus, it appears that respiratory dysregulation has the capacity to alter the microbiota. It is important to determine if disruption to the microbiota affects respiratory homeostasis.

Of relevance, the gut microbiota are important modulators of cardiovascular control. The transfer of faeces from hypertensive donors (spontaneously hypertensive rats, a hypertensive model of sleep-disordered breathing fed a high-fat diet, and hypertensive human donors) into normotensive recipient or germ-free animals leads to the development of hypertension in the recipient animal (Yang *et al.*, 2015; Durgan *et al.*, 2016; Adnan *et al.*, 2017; Li *et al.*, 2017). A decrease in butyrate-producing and an increase in lactate-producing bacteria are associated with a hypertensive phenotype (Yang *et al.*, 2015; Durgan *et al.*, 2016; Adnan *et al.*, 2017). More recently, it was established in an animal model of obstructive sleep apnoea that acetate is a key player in blood pressure regulation (Ganesh *et al.*, 2018). Collectively, these findings suggest an influential role for the microbiota-gut brain axis in cardiovascular homeostasis.

It is established that chronic administration of a cocktail of broad-spectrum antibiotics significantly depletes the gut microbiota (Desbonnet *et al.*, 2015; Hoban *et al.*, 2016). It is

also recognised that alterations to the gut microbiota can influence brain behaviours at a functional level (Hoban *et al.*, 2016; Kelly *et al.*, 2016b; Burokas *et al.*, 2017; Stilling *et al.*, 2018). Thus, we sought to perform a comprehensive assessment of cardiorespiratory physiology in the context of a manipulated gut microbiota. We examined cardiorespiratory control and reflex responsiveness in adult rats following a 4-week antibiotic intervention period. We hypothesised that there would be evidence of aberrant plasticity in cardiorespiratory control in antibiotic-treated rats. Thereafter, in a subset of animals, we explored if manipulation of the microbiota via faecal microbiota transfer could reverse or ameliorate the putative deleterious effects of antibiotic intervention on cardiorespiratory control.

2.2. Methods

2.2.1 Ethical approval

All procedures on live animals were performed under licence from the Government of Ireland Department of Health (B100/4498) in accordance with National and European Union directive 2010/63/EU, with prior ethical approval by University College Cork (AEEC #2013/035). Experiments were conducted in accordance with guidelines established by University College Cork's Animal Welfare Body.

2.2.2 Experiment animals

Ten-week old adult male Sprague Dawley rats (n=40; purchased from Envigo, UK) were housed as age-matched pairs in standard rat cages. All animals were housed under a 12-hour light: 12-hour dark cycle with standard rodent chow available *ad libitum*.

2.2.3 Antibiotic administration

Rats were randomly allocated to receive autoclaved deionised water (vehicle, VEH; n = 20) or broad-spectrum antibiotics (ABX; n=20) in autoclaved deionised water for 4-weeks. To deplete the microbiota, we used an antibiotic cocktail consisting of ampicillin (1g/l), vancomycin (500mg/l), ciprofloxacin (20mg/l), imipenem (250mg/l) and metronidazole (1g/l) (Hoban *et al.*, 2016; Kelly *et al.*, 2016b). Water bottles were replenished every second day and water consumption recorded per cage. Animal body weights were monitored daily (Appendix Fig. A.1 a). Weight loss in the beginning of ABX intervention is a commonly reported side effect related to the aversive taste of the ABX cocktail. Fresh bedding was given to ABX and VEH groups every other day to decrease the risk of microbiota re-establishment in ABX animals.

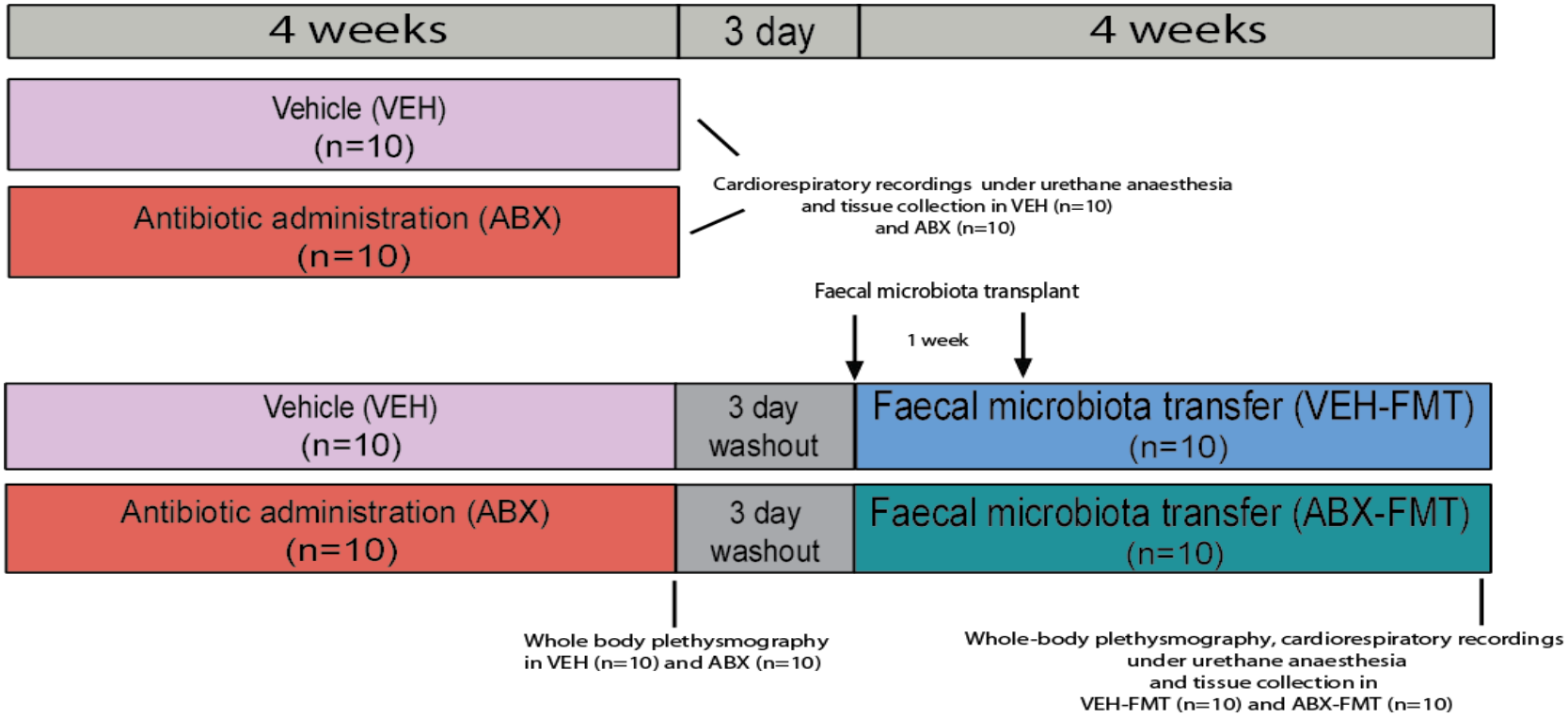


Figure 2. 1 Experimental design

Schematic representation of the experimental design employed in the study.

2.2.4 Faecal microbiota transfer (FMT) protocol

Collection and processing of donor microbiota for faecal microbiota transplantation: Donor faecal microbiota was acquired from the pooled faeces of 10 VEH rats, collected fresh from individual animals by massaging the lower abdomen and promoting the passage of faeces from the rats. Both the collection and the transportation and processing of faeces occurred under anaerobic conditions to prevent loss of anaerobic microbiota. Sterile reduced phosphate-buffered saline (PBS; 10ml) containing 20% glycerol (v/v) was added to each 1g of pooled faeces. The faecal material was thoroughly re-suspended. Samples were centrifuged at 2000rpm for 5 minutes at 4˚C (MIKRO 22R refrigerated centrifuge) to generate a sediment of undigested dietary fibres. Supernatants were aliquoted, frozen and stored at -80°C until use in oral gavage.

Administration of FMT: ABX rats (n=10) received a washout period of autoclaved deionised water for three days and VEH rats (n=10) remained on autoclaved deionised water. Two inoculations of donor microbiota (300µl) were administered via oral gavage to ABX and VEH rats, on day 1 and day 7 following the washout period. To reinforce the donor microbiota phenotype, the ABX rats were transferred to bedding previously occupied by VEH rats on inoculation day 1 and thereafter on a weekly basis (ABX-FMT group). VEH rats were transferred to fresh bedding adhering to the pattern described above (VEH-FMT group). All animals received autoclaved deionised water for the duration of the 4-week period (Fig. 2.1).

2.2.5 Assessment of respiratory flow and metabolism in unrestrained, unanaesthetised rats

Whole-body plethysmography: Whole-body plethysmography (DSI, St. Paul, Minnesota, USA) was used to record respiratory flow during quiet rest in unrestrained, unanaesthetised rats. This was performed at the animal housing facility of University College Cork as this subset of animals subsequently remained in the facility for faecal microbiota transfer and housing for a further period of 4 weeks. Animals were introduced into custom chambers (601-1427-001 PN, DSI) with room air pumped through the chambers (3l/min) ensuring the maintenance of oxygen (O_2) and carbon dioxide (CO_2). Animals were allowed to acclimate for 30-90 minutes to allow habituation to the surroundings. Contemporaneous observations were performed in ABX (n=10) *versus* VEH (n=10) and subsequently ABX-FMT (n=10) *versus* VEH-FMT (n=10) using a pair of plethysmograph chambers.

Metabolic measurements: CO_2 production (VCO_2) and O_2 consumption (VO_2) were measured in animals throughout the whole-body plethysmography protocol (O_2 and CO_2 analyser; AD

Instruments, Colorado Springs, CO, USA) as previously described (Haouzi *et al.*, 2009; Bavis *et al.*, 2014; Burns *et al.*, 2017; Burns *et al.*, 2018).

Experimental protocol: Once the acclimation period was complete, a 10-15-minute steady-state normoxia period allowed for the assessment of baseline parameters (FiO_2=0.21; balance N_2). Thereafter, rats were exposed to a 10-minute poikilocapnic hypoxia challenge (FiO_2=0.10; balance N_2). Each animal was then allowed to recover during normoxia (FiO_2=0.21; balance N_2) to re-establish stable breathing. Subsequently, another baseline period was recorded and rats were then exposed to a hypercapnic challenge ($FiCO_2$=0.05; balance O_2) for 10 minutes followed by a recovery period. A new baseline period was determined and animals were then exposed to 10 successive cycles of acute intermittent hypoxia (AIH), consisting of alternating periods of normoxia (FiO_2=0.21; balance N_2) for 6 minutes and hypoxia (FiO_2=0.10, balance N_2) for 6 minutes. Following the AIH protocol, a normoxia period was established (FiO_2=0.21; balance N_2) for 1 hour. On completion of the experimental protocol, faecal pellets in the plethysmograph chambers were counted per unit time.

Data analysis for whole-body plethysmography and metabolism: Respiratory parameters including respiratory frequency (f_R), tidal volume (V_T), minute ventilation (V_E), inspiratory time (T_i) and expiratory time (T_e) were recorded on a breath-by-breath basis for analysis (Finepoint software Buxco Research Systems, Wilmington, NC, USA). Artefacts in the signals due to movement and sniffing were excluded from analysis. A steady-state baseline period was averaged during normoxia to assess ventilatory and metabolic parameters at quiet rest. For acute hypoxic and hypercapnic challenges, respiratory and metabolic data were averaged for the last 5 minutes of these exposures to ensure adequate time for gas mixing in the chambers and assessment of steady-state ventilatory and metabolic responses. Data are expressed as a change in the absolute values from baseline values. Furthermore, to determine the peak hypoxic ventilatory response, respiratory frequency was averaged every 10 seconds for the first 120 seconds of the acute hypoxic gas challenge. Similarly, for the acute hypercapnic challenge, the respiratory frequency response was averaged for each minute of the 10-minute challenge. For AIH challenges, respiratory data were compared between groups for the last hypoxia challenge and expressed as a percentage change from the preceding baseline normoxia exposure. Data from the post-AIH normoxic period was collected at 5 minute intervals. The last 5-minute epoch of the 1-hour period of normoxia following exposure to AIH was compared with the normoxic baseline period preceding AIH and expressed as percentage change from baseline as a measure of AIH-induced respiratory

plasticity. Comparisons were made between the experimental groups. Respiratory flow signals were also analysed to quantify the occurrence of apnoeas (post-sigh apnoeas and spontaneous apnoeas) and augmented breaths (sighs) during normoxic baseline and hypoxic and hypercapnic breathing as previously described (Edge *et al.*, 2012). An apnoea was defined as two consecutive missed breaths and data are expressed as apnoea index (number of apnoeas per hour). Sighs (augmented breaths) were distinguished as breaths with double the amplitude of the average V_T. Poincaré plots were constructed showing breath-to-breath (BB*n*) versus the subsequent breath-to-breath interval (BB*n+1*) allowing determination of short-term (SD1) and long-term (SD2) respiratory timing variability during stable baseline as well as hypoxia and hypercapnia breathing. V_T, V_E, V_T/T_i, $\dot{V}O_2$ and $\dot{V}CO_2$ were normalised per 100g body mass.

2.2.6 Assessment of cardiorespiratory parameters under urethane anaesthesia

Surgical protocol and cardiorespiratory measures: Cardiorespiratory parameters were assessed in rats under urethane anaesthesia (1.5g/kg i.p.; 20% w/v) following isoflurane induction (5% by inhalation in room air). Depth of anaesthesia was assessed throughout the surgical and experimental protocol by carefully monitoring reflex responses to tail/paw pinch and the corneal reflex. If required, supplemental doses of anaesthetic were given. Rats were placed in the supine position and core body temperature was maintained at 37˚C using a homeothermic blanket system (Harvard Apparatus, Holliston, MA, USA) and a rectal temperature probe.

A mid-cervical tracheotomy was performed. The right jugular vein was then cannulated for intravenous (i.v.) infusion of supplemental anaesthetic and drugs. Next, the right carotid artery was cannulated and a pressure catheter inserted into the left ventricle to record left ventricular contractility (dP/dt max); artefacts were observed in the pressure signals in some animals and data acquired from these animals was excluded. The femoral artery was cannulated for the recording of arterial blood pressure and the withdrawal of arterial blood samples for blood gas, pH and electrolyte analysis (i-STAT; Abbott Laboratoies Ltd). All rats were maintained with a bias flow of supplemental O_2 to preserve arterial oxygen saturation above 95% during basal conditions (SaO_2; Starr Life Sciences, PA, USA). A pneumotachometer and a CO_2 analyser (microCapStar End-Tidal CO_2 analyser; CWE Inc., USA) were connected to a tracheal cannula to determine tracheal flow and end-tidal CO_2 ($ETCO_2$), respectively. A concentric needle electrode (26G; Natus Manufacturing Ltd, Ireland) was inserted into the costal diaphragm for the continuous measurement of diaphragm electromyogram (EMG) activity. Signals were amplified (x5,000), filtered (band pass; 500-5,000Hz) and integrated

(50ms time constant; Neurolog system, Digitimer Ltd, UK). LabChart v7 (ADInstruments) was used to display data in real-time.

Experimental protocol: An arterial blood gas sample was attained following a 30-minute period of stabilisation. Following the stabilisation period, baseline parameters were assessed for 10 minutes. An electronic gas mixer (GSM-3 Gas Mixer; CWE Inc.) was used to manipulate the gas composition of the bias flow to administer chemostimulation challenges to the rat. The rats were exposed to a graded hypercapnic challenge: $FiCO_2$=0.05 and 0.10 (supplemental O_2; balance N_2) consecutively for 5 minutes each. Following a recovery period, animals were challenged with poikilocapnic hypoxia (FiO_2=0.10, balance N_2) for 5 minutes, followed by a 5 minute hypoxic hypercapnic challenge (FiO_2=0.10, $FiCO_2$=0.05, balance N_2). After the chemostimulation challenges and a sufficient recovery period, the serotonin type 3 (5-HT_3) receptor agonist phenylbiguanide was administered in incremental doses (PBG; 2, 4, 8, 16, 32 µg/kg; i.v.) to stimulate pulmonary vagal afferent C-fibres (Dutta & Deshpande, 2010; Lucking *et al.*, 2018a). Then animals underwent bilateral cervical vagotomy. After a 20-minute recovery period, another blood gas sample was acquired and post-vagotomy baseline parameters were determined. The chemostimulation challenges described above were repeated under vagotomised conditions. Finally, a single bolus of 32 µg/kg PBG was administered to confirm that PBG-induced pulmonary chemoreflex responses were entirely dependent upon vagal nerve transmission.

Animals were euthanised by urethane overdose i.v. and whole brains were immediately harvested and frozen in -80°C isopentane and stored at -80°C until required. The caecum was removed, weighed and caecal contents were removed rapidly and snap frozen in liquid nitrogen. The distal ileum and proximal colon were removed. The heart was removed and the right ventricle and left ventricle + septum were separated and weighed. The lungs were removed and weighed and then were allowed to air dry at 37°C for at least 48 hours and re-weighed.

Data analysis of cardiorespiratory parameters in anaesthetised rats: 10 minutes of stable recording were averaged (baseline data) and are presented as absolute values. For cardiorespiratory and EMG responses during graded hypercapnia, hypoxia, hypoxic hypercapnia, vagotomy and chemostimulation challenges post-vagotomy, for each reported parameter, the average of the last minute of recordings was determined and data were compared with the 1-minute pre-challenge baseline. To assess the dynamic response to PBG administration, data were averaged in 3-second bins and the maximal response for each

concentration was determined for each cardiorespiratory parameter reported. Cardiovascular responses to PBG were expressed as absolute change from the preceding baseline value. Maximum apnoea and post-apnoea tachypnoea data from PBG stimulation were expressed as the duration of the apnoea or tachypnoea period normalised to the average cycle duration determined during the baseline period preceding PBG challenges i.e. fold change. Cardiorespiratory responses to vagotomy and chemostimulation before and after vagotomy were expressed as absolute change from the preceding baseline. EMG responses to vagotomy and chemostimulation before and after vagotomy were expressed as percent change from the preceding baseline value.

2.2.7 Macromolecular permeability in small and large intestine ex vivo

Epithelial permeability: Ussing chambers: In a subset of animals, distal ileum and proximal colon were removed and examined *ex vivo*. Distal ileum (a 2.0 cm segment adjacent to the caecum) and proximal colon (2.0 cm most distal segment of proximal colon) were gently flushed, cut open along the mesenteric line and mounted in Ussing chambers with an exposed tissue area of 0.12cm^2. Tissue was bathed with Krebs solution (in mM: 1.2 NaH_2PO_4; 117 NaCl; 4.8 KCl; 1.2 $MgCl_2$; 25 $NaHCO_3$; 11 $CaCl_2$ and 10 glucose) at 37°C with continuous carbogen (95% O_2, 5% CO_2) supply. 4-kDa FITC-dextran (4kDa, FD4, Sigma, Ireland) was added to the mucosal (luminal) chamber at a final concentration of 2.5mg/ml. To assess FITC flux through the epithelial barrier, samples (200µl) were collected from the serosal chamber at 0 (baseline), 60 and 120 minutes after the addition of FITC. At each time-point, the volume removed was replenished with Krebs buffer. To exclude the potential contribution of ileac Na^+-glucose co-transporter (Slc5a1) to paracellular permeability, glucose in the mucosal chamber buffer was substituted with 10mM mannitol in ileac tissue samples (Turner *et al.*, 1997).

Data analysis: FITC was measured on VICTOR-1 plate reader (PerkinElmer) at 485nm excitation/535nm emission wavelengths. FITC mucosal-to-serosal flux was calculated as an increment in fluorescence intensity *versus* baseline fluorescence over time and presented as ng/ml.

2.2.8 Brainstem monoamine concentrations

High-performance liquid chromatography (HPLC) coupled to electrochemical detection for the measurement of brainstem monoamine concentrations: After euthanasia, whole brains were immediately removed from the rats and snap frozen in isopentane cooled in liquid nitrogen. Whole brains were transferred to -80˚C for long-term storage. The frozen

brainstem was dissected from the brain at -20˚C and subsequently sonicated in 1ml of chilled mobile phase spiked with 2ng/20µl of N-methyl 5-HT (internal standard) (Bandelin Sonolus HD 2070). High-performance liquid chromatography was performed as previously described (Lucking *et al.*, 2018b). The monoamines noradrenaline (NA), dopamine (DA), serotonin (5-HT), monoamine precursor $_{L}$-3,4-dihydroxyphenylalanine ($_{L}$-DOPA) and metabolites 5-hydroxyindoleacetic acid (5-HIAA) and homovanillic acid (HVA) were assessed. Each monoamine and metabolite were identified by their respective characteristic retention times. This was determined by standard injections, which were run at regular intervals during the sample analysis.

Data analysis: Class-VP5 software processed chromatographs that identified specific monoamines. Analyte:internal standard peak response ratios were used to calculate concentrations. Data are expressed as nanograms of neurotransmitter per gram of tissue weight (ng/g).

2.2.9 16S rRNA sequence-based microbiota composition and diversity analysis in caecal content

Caecal microbiota DNA extraction and 16S rRNA gene sequencing: DNA extraction and 16S rRNA gene sequencing was performed as previously described (Lucking *et al.*, 2018b).

Bioinformatic sequence analysis: FLASH (fast length adjustment of short reads to improve genome assemblies) was used to assemble 300 base paired-end reads. Thereafter, QIIME suite of tools (Quantitative Insights Into Microbial Ecology) version 1.9.0 was used to further process paired-end reads. This processing included quality filtering based on a quality score > 25 and removal of mismatched barcodes and sequences below length thresholds. Denoising, chimera detection and operational taxonomic units (OTUs) clustering were performed using USEARCH v7 (64-bit)(Edgar, 2010). PyNAST (a flexible tool for aligning sequence to a template alignment) was used to align OTUs. BLAST against the SILVA SSURef database release 123 was used to assign taxonomy. Alpha diversity was generated in QIIME (Caporaso *et al.*, 2010).

2.2.10 Statistical analysis

For data sets with confirmed normal distribution, a one-way ANOVA with Bonferroni *post hoc* where appropriate or parametric two-tailed Student's unpaired *t* tests with Welch's correction where appropriate were used to test for statistically significant between-group differences. When the assumption of normal distribution was violated, a non-parametric Kruskal-Wallis with Dunn's *post hoc* where appropriate or non-parametric Mann-Whitney *U*

tests where appropriate were used. Two-way ANOVA or repeated measures two-way ANOVA with Bonferroni *post hoc* where appropriate were used for relevant data sets. Microbiota data are expressed as median (IQR). All other data sets are expressed as means ± SD or are displayed graphically as box and whisker plots (median, IQR and minimum to maximum values). Microbiota analysis was performed in SPSS and R software environment. The OTUs detected only in ≤ two animals in each group were excluded from the analysis. Bacterial genera that were significantly different at least in one comparison were used to construct the Log_2 fold change ratio heatmap. The 2D principal coordinates analysis (PCoA) plot based on Bray-Curtis distance matrices was constructed using R (version 3.4.4), R Studio (version 1.1.453), and the "vegan" package (version 2.5.1) using the vegdist function and recommended parameters. For the correlation analysis between the microbiota composition and a large array of parameters including cardiorespiratory, neuromodulators and intestinal permeability, Hierarchical All-against-All association-testing (HAllA) was used (version 0.8.7) with Spearman correlation as correlation metric and medoid as clustering method. Spearman correlation coefficients were determined for a subset of associations and data are graphically illustrated showing individual data points. GraphPad Prism Software v6 (GraphPad Software, San Diego, CA, USA) was used for all other statistical analysis. Statistical significance was set at $p<0.05$. Benjamini-Hochberg (BH) adjustment procedure was applied with the false discovery rate (FDR) set at 10% and 20% to correct for multiple testing in the relative abundance and correlation analyses, respectively. Adobe Illustrator CS5 (v15) was used to edit figures.

2.3. Results

2.3.1 Body and tissue weights

Compared with VEH controls, ABX rats tended to be underweight (Appendix Fig. A.1a), coincident with significantly reduced fluid intake during the first week of the experimental protocol (p=0.001, two-way ANOVA with Bonferroni *post hoc*, Appendix Fig. A.1b). During respiratory assessment in the plethysmograph chambers, manipulation of the gut microbiota altered faecal output per hour (p=0.04, Kruskal-Wallis, Appendix Fig. A.1c). Microbiota manipulation also significantly altered tissue weights (Table 2.1).

	VEH (n=10)	ABX (n=9)	VEH-FMT (n=10)	ABX-FMT (n=10)	One-way ANOVA	VEH vs ABX	VEH-FMT vs ABX-FMT	VEH vs VEH-FMT	ABX vs ABX-FMT	VEH vs ABX-FMT	ABX vs VEH-FMT
Body mass (g)	380 ± 23	369 ± 22	436 ± 27	420 ± 24	**<0.0001**	0.999	0.888	**0.0001**	**0.0002**	**0.004**	**0.0001**
RV (mg/100g)	58 ± 6	51 ± 3	55 ± 7	61 ± 6	**0.009**	0.133	0.196	0.999	**0.008**	0.999	0.999
LV (mg/100g)	219 ± 14	207 ± 10	206 ± 14	208 ± 9	0.053	-	-	-	-	-	-
LV+RV (mg/100g)	277 ± 16	258 ± 10	260 ± 14	269 ± 11	**0.011**	**0.018**	0.982	**0.043**	0.483	0.967	0.999
Lung dry weight (mg/100g)	100 ± 12	90 ± 11	98 ± 9	85 ± 10	**0.01**	0.217	0.067	0.999	0.999	**0.015**	0.723
Lung wet weight (mg/100g)	495 ± 104	404 ± 44	427 ± 43	406 ± 83	**0.03**	0.064	0.999	0.288	0.999	0.061	0.999
Oedema index (% wet weight)	79 ± 3	78 ± 1	77 ± 1	79 ± 3	**0.017**	0.999	0.196	0.112	0.999	0.999	**0.016**

Table 2. 1 Body and organ weights

BW, body weight; RV, right ventricle; LV, left ventricle; VEH, autoclaved deionised water; ABX, antibiotic-treated; VEH-FMT, VEH followed by faecal microbiota transfer; ABX-FMT, antibiotic-treated followed by faecal microbiota transfer. Data are shown as mean ± SD and were statistically compared using one-way ANOVA with Bonferroni *post hoc* where appropriate, or non-parametric Kruskal-Wallis test with Dunn's *post hoc*, where appropriate. Each *p*-value is adjusted to account for multiple comparisons. *p*-values shown in bold highlight significant differences.

2.3.2 Baseline ventilation and metabolism in behaving rats during quiet rest

During baseline breathing, V_T, f_R, and V_E and VCO_2 were all equivalent between groups (Table 2.2). However, manipulation of the gut microbiota had a significant effect on the ventilatory equivalent for carbon dioxide (V_E/VCO_2) (p=0.042, one-way ANOVA, Table 2.2). V_E/VCO_2 was significantly reduced in VEH-FMT rats compared with VEH rats (one-way ANOVA with Bonferroni *post hoc*, Table 2.2).

2.3.3 Respiratory timing variability, apnoeas and sighs during normoxia in behaving rats during quiet rest

Assessments of both short-term (SD1) and long-term (SD2) respiratory timing variability during normoxia were equivalent between groups: T_i (Table 2.2), T_e (p>0.05, one-way ANOVA, Fig. 2.2e, f) and total breath duration (T_{tot}, p>0.05, Fig. 2.2g, h). Sigh frequency was affected by manipulation of the gut microbiota (Fig. 2.2n). There was no difference in apnoea index (Fig. 2.2l) during normoxia between groups (p>0.05). The apnoea index combines spontaneous and post-sigh apnoeas, both of which were equivalent in their respective prevalences between groups (p>0.05). Furthermore, the average duration of apnoeas was equivalent between groups (Fig. 2.2m).

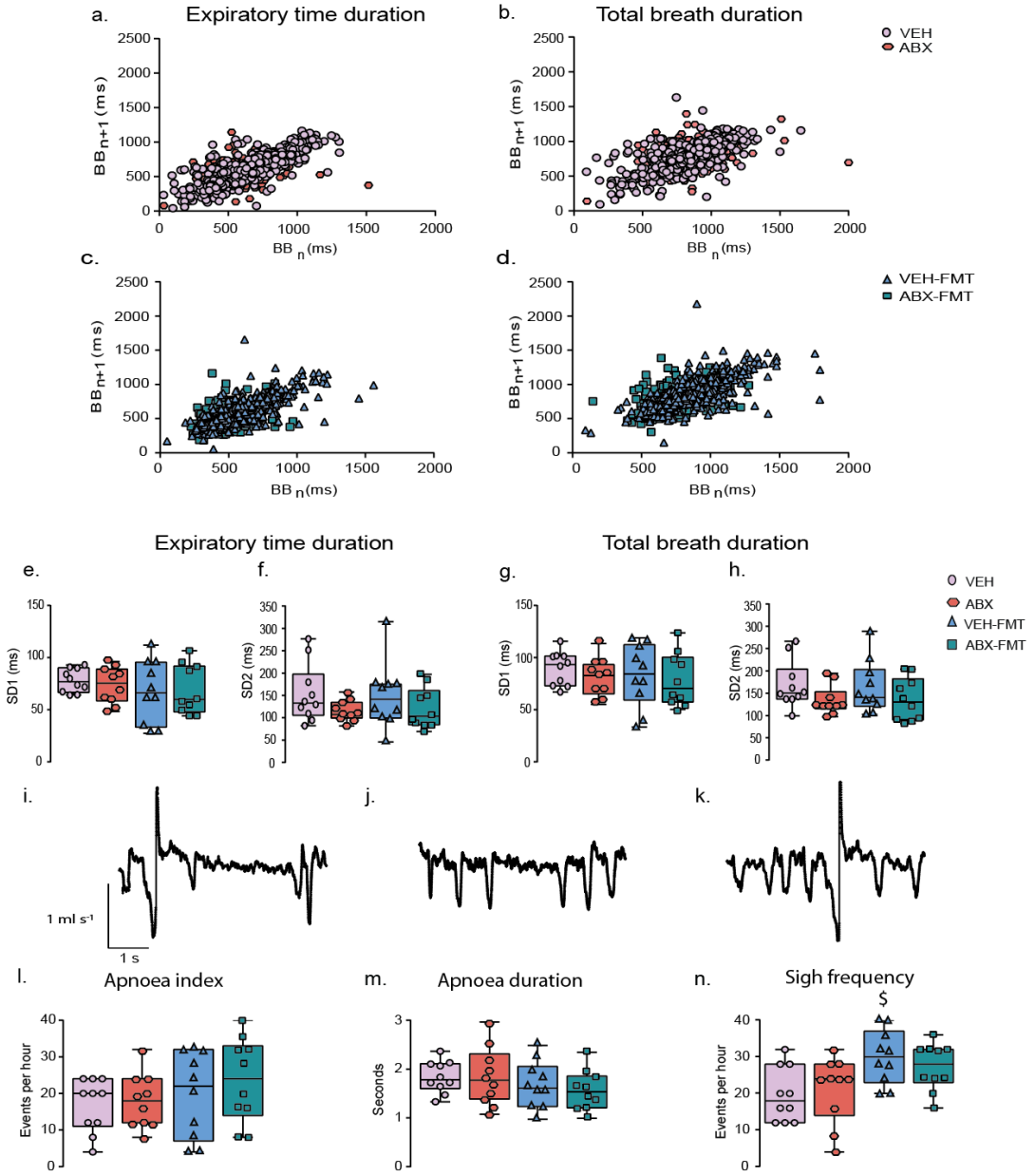


Figure 2. 2 Chronic antibiotic administration and faecal microbial transfer do not alter respiratory timing variability, or the prevalence of apnoeas and sighs in behaving rats during quiet rest

Poincaré plots of breath-to-breath (BB*n*) and subsequent breath-to-breath (BB*n+1*) interval of expiratory duration (T_e; a, c) and total breath duration (T_{tot}; b, d) for 200 consecutive breaths for VEH and ABX (a, b) and VEH-FMT and ABX-FMT rats (c, d). Group data for T_e short-term variability (SD1; e) and long-term variability (SD2; f) and T_{tot} SD1 (g) and SD2 (h) in VEH, ABX, VEH-FMT and ABX-FMT rats during normoxia. Representative respiratory flow traces (downward deflections represent inspiration) illustrating a spontaneous sigh followed by an apnoea (i), a spontaneous apnoea (j) and a spontaneous sigh (k). Group data of apnoea index (l), apnoea duration (m) and sigh frequency (n). VEH, autoclaved deionised water; ABX,

antibiotic-treated; VEH-FMT, VEH followed by faecal microbiota transfer; ABX-FMT, antibiotic-treated followed by faecal microbiota transfer. Groups (e-h, l-n) are expressed as box and whisker plots (median, IQR and minimum to maximum values); n=10 for all groups. Groups were statistically compared by one-way ANOVA or non-parametric Kruskal-Wallis with Dunn's *post hoc*, where appropriate. $ $p<0.05$, VEH-FMT *versus* VEH, Dunn's *post hoc* test.

	VEH (n=10)	ABX (n=10)	VEH-FMT (n=10)	ABX-FMT (n=10)	One-way ANOVA	VEH vs ABX	VEH-FMT vs ABX-FMT	VEH vs VEH-FMT	ABX vs ABX-FMT	VEH vs ABX-FMT	ABX vs VEH-FMT
f_R (brpm)	83 ± 13	79 ± 11	79 ± 11	79 ± 14	0.845	-	-	-	-	-	-
V_E (ml/min/ 100g)	50 ± 6	51 ± 8	48 ± 6	49 ± 7	0.855	-	-	-	-	-	-
V_T (ml/100g)	0.63±0.07	0.64±0.12	0.61±0.07	0.65±0.06	0.763	-	-	-	-	-	-
V_T/T_i (ml/s/ 100g)	2.5 ± 0.4	2.5 ± 0.6	2.5 ± 0.5	2.6 ± 0.4	0.936	-	-	-	-	-	-
T_i (ms)	252 ± 23	264 ± 36	261 ± 26	259 ± 33	0.813	-	-	-	-	-	-
T_e (ms)	537 ± 96	557 ± 86	527 ± 101	565 ± 132	0.844	-	-	-	-	-	-
T_i SD1 (ms)	29 ± 9	24 ± 7	28 ± 11	24 ± 6	0.484	-	-	-	-	-	-
T_i SD2 (ms)	47 ± 20	43 ± 14	50 ± 20	37 ± 11	0.415	-	-	-	-	-	-
VO_2 (ml/min/ 100g)	2.7 ± 0.6	3.3 ± 1.0	3.2 ± 0.7	3.0 ± 0.9	0.414	-	-	-	-	-	-
VCO_2 (ml/ min/100g)	1.6 ± 0.3	1.8 ± 0.2	1.8 ± 0.2	1.7 ± 0.3	0.093	-	-	-	-	-	-
V_E/VCO_2	33 ± 6	30 ± 7	27 ± 2	29 ± 3	**0.042**	0.999	0.999	**0.032**	0.999	0.437	0.700

Table 2. 2 Baseline ventilation, respiratory timing variability and metabolism in behaving rats during quiet rest

f_R, respiratory frequency (brpm, breaths per min); V_E, minute ventilation; V_T, tidal volume; V_T/T_i, mean inspiratory flow; T_i, inspiratory time; T_e, expiratory time; SD1, short-term respiratory timing variability; SD2, long-term respiratory timing variability VO_2, oxygen consumption; VCO_2, carbon dioxide production; V_E/VCO_2, ventilatory equivalent; VEH, autoclaved deionised water; ABX, antibiotic-treated; VEH-FMT, VEH followed by faecal microbiota transfer; ABX-FMT, antibiotic-treated followed by faecal microbiota transfer. Data are shown as mean ± SD and were statistically

compared using one-way ANOVA with Bonferroni *post hoc* where appropriate, or non-parametric Kruskal-Wallis test, where appropriate. Each *p*-value is adjusted to account for multiple comparisons. *p*-values shown in bold highlight significant differences.

2.3.4 Ventilatory and metabolic responsiveness to chemostimulation in behaving rats during quiet rest

Ventilatory and metabolic responsiveness to hypoxia: No significant differences were observed between respective groups in ventilatory and metabolic responsiveness to hypoxia determined under steady-state conditions during the last 5 minutes of exposure (two-way ANOVA, Fig. 2.3b, c, f, g, j, k, repeated measures two-way ANOVA; Appendix Fig. A.2a, b, e, f, i, j; and Table 2.3). However, analysis during the first 120 seconds of hypoxia, when the peak hypoxic ventilatory response was observed, revealed that manipulation of the gut microbiota had a significant effect on minute ventilation due to a decrease in the respiratory frequency response in ABX rats compared with VEH rats ($V_{E,}$ time, p=0.0001; ABX, p=0.045; time x ABX, p=0.459, two-way ANOVA; *fR*, time, p=0.0001; ABX, p=0.022; time x ABX, p=0.486, two-way ANOVA, Appendix Fig. A.3a) and in VEH-FMT rats compared with VEH rats ($V_{E,}$ time, p=0.0001; FMT, p=0.001; time x FMT, p=0.0009, two-way ANOVA*;* f_R, time, p=0.0001; FMT, p=0.002; time x FMT, p=0.039, two-way ANOVA, Appendix Fig. A.3c). Ventilatory responses to the AIH protocol were equivalent between respective groups (p>0.05; Appendix Fig. A.4, Appendix Table A.1).

Ventilatory and metabolic responsiveness to hypercapnia: One of the major findings of this study is that manipulation of the gut microbiota has a significant effect on the ventilatory response to hypercapnia (p=0.02, Kruskal-Wallis, Table 2.5). V_E was significantly blunted in ABX rats compared with VEH rats (p=0.038, two-way ANOVA, Fig. 2.3h; and p=0.045; Kruskal-Wallis with Dunn's *post hoc,* Table 2.5), a consequence of reduced f_R response to CO_2 challenge (p=0.044, two-way ANOVA, Fig. 2.3d; and p=0.043, one-way ANOVA with Bonferroni *post hoc,* Table 2.5). Further analysis of the f_R response during each minute of the hypercapnic exposure revealed a significant difference in the f_R response to CO_2 challenge in ABX rats compared with VEH rats (time, p<0.0001; ABX, p=0.047; time x ABX, p=0.638, Appendix Fig. A.5a). The hypoventilation was evident as a blunted V_E/VCO_2 response in ABX rats compared with VEH rats, however this was not statistically significant (p=0.093, two-way ANOVA, Fig. 2.3l), with values for VCO_2 during hypercapnia equivalent between groups (data not shown). Manipulation of the gut microbiota had a significant depressant effect on ventilatory drive to breathe (V_T/T_i) in response to hypercapnic challenge (Table 2.5). No other ventilatory differences were noted between groups (Appendix Fig. A.5b-d and Table 2.5). Repeated measures two-way ANOVA was performed for ventilatory and metabolic responsiveness to hypercapnia revealing that FMT significantly decreased V_E (gas, p<0.0001; FMT, p=0.014; gas x FMT, p=0.043; repeated measures two-way ANOVA, Appendix Fig. A.2g),

f_R (gas, p<0.0001; FMT, p=0.046; gas x FMT, p=0.103; repeated measures two-way ANOVA, Appendix Fig. A.2c) and V_E/VCO_2 (gas, p<0.0001; FMT, p=0.003; gas x FMT, p=0.048; repeated measures two-way ANOVA, Appendix Fig. A.2k) in VEH-FMT rats compared with VEH rats. Repeated measures two-way ANOVA revealed no difference for V_E, f_R, and V_E/VCO_2 in ABX rats compared with ABX-FMT (Appendix Fig. A.2d, h, i). Similarly, no differences were observed for values in ABX-FMT rats compared with VEH-FMT rats (Fig 2.3e, I, m; p>0.05; two-way ANOVA).

2.3.5 Respiratory timing variability, apnoeas and sighs during hypoxia and hypercapnia in behaving rats during quiet rest

Assessments of short-term (SD1) and long-term (SD2) respiratory timing variability for T_i, T_e and T_{tot} in response to hypoxia (Table 2.4) and for T_e and T_{tot} in response to hypercapnia (Table 2.6) were equivalent between groups. T_i SD2 in hypercapnia was altered by microbiota manipulation (Table 2.6). There was no difference in apnoea index or sigh frequency (Table 2.4 and 2.6) between groups. Furthermore, the average duration of apnoeas during hypercapnia (Table 2.6) was equivalent between groups.

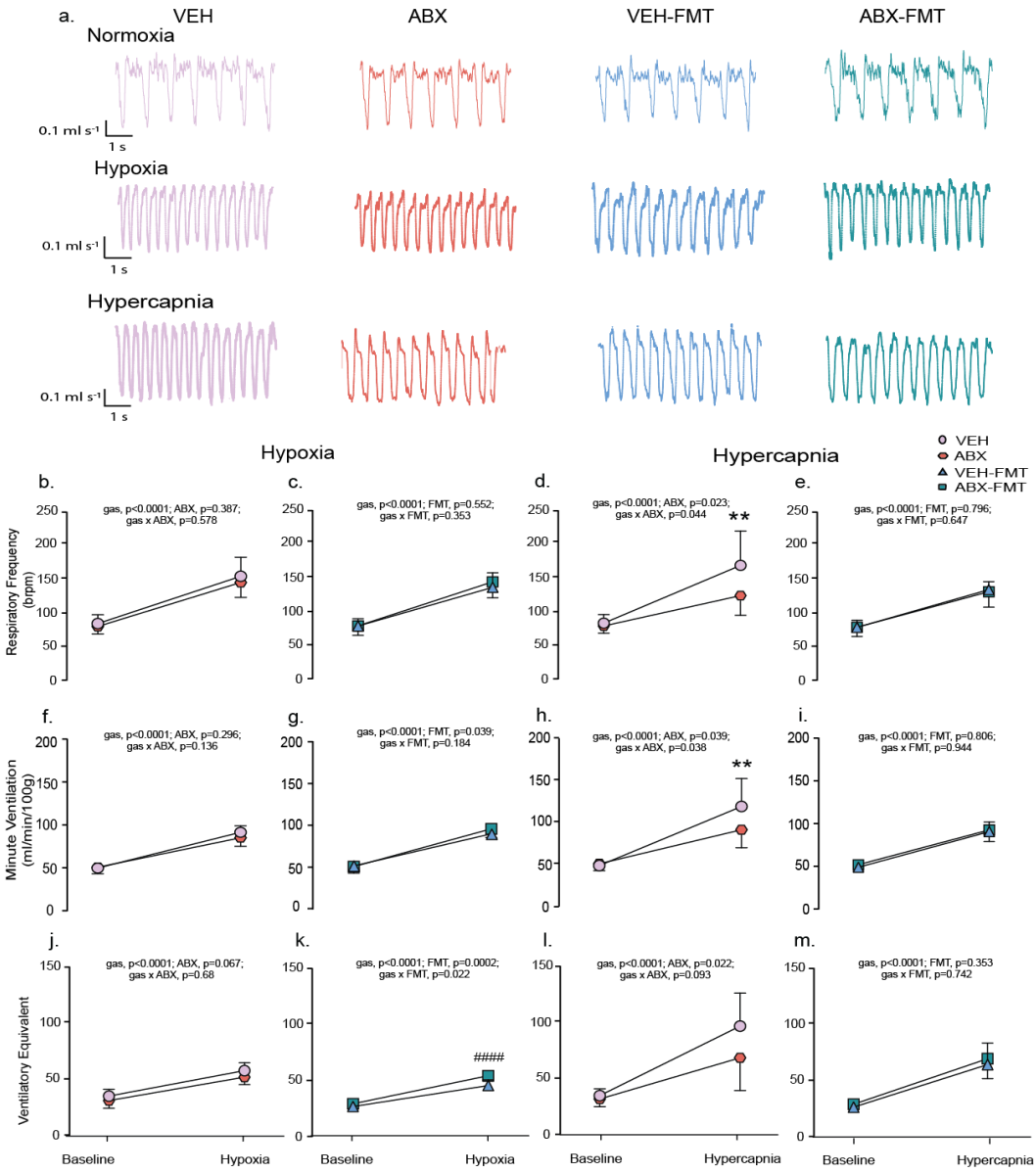


Figure 2. 3 Chronic antibiotic administration and faecal microbial transfer blunts hypercapnic ventilation in behaving rats during quiet rest

a) Representative traces of typical respiratory flow during normoxic, hypoxic and hypercapnic ventilation in VEH, ABX, VEH-FMT and ABX-FMT rats; downward deflections represent inspiration. Group data for respiratory frequency (b, c, d, e), minute ventilation (f, g, h, i) and ventilatory equivalent (j, k, l, m) during normoxia and in response to hypoxia (b, c, f, g, j, k) and hypercapnia (d, e, h, i, l, m) for VEH and ABX (b, f, j, d, h, l) and VEH-FMT and ABX-FMT (c, g, k, e, i, m). VEH, autoclaved deionised water; ABX, antibiotic-treated; VEH-FMT, VEH followed by faecal microbiota transfer; ABX-FMT, antibiotic-treated followed by faecal microbiota transfer. Data (b-m) are expressed as mean ± SD during baseline, hypoxia and hypercapnia; n=10 for all groups. Groups were statistically compared by two-way ANOVA with Bonferroni *post hoc* where appropriate. *p*-values are shown. ** $p<0.01$, ABX *versus* VEH, Bonferroni *post hoc* test.

	VEH (n=10)	ABX (n=10)	VEH-FMT (n=10)	ABX-FMT (n=10)	One-way ANOVA
Δ f_R (brpm)	68 ± 20	63 ± 20	57 ± 21	65 ± 17	0.585
Δ V_E (ml/min/ 100g)	43 ± 8	36 ± 14	36 ± 9	43 ± 13	0.244
Δ V_T (ml/100g)	0.07 ± 0.08	0.06 ± 0.08	0.08 ± 0.06	0.02 ± 0.08	0.35
Δ V_T/T_i (ml/s/100g)	4.4 ± 0.7	4.1 ± 1.1	3.6 ± 0.7	4.1 ± 0.6	0.168
Δ T_i (ms)	-87 ± 28	-95 ± 41	-87 ± 32	-92 ± 34	0.933
Δ T_e (ms)	-236 ± 62	-239 ± 78	-208 ± 72	-263 ± 106	0.153
Δ VO_2 (ml/min/ 100g)	-1.0 ± 0.7	-1.4 ± 1.1	-0.9 ± 0.8	-0.86 ± 0.9	0.522
Δ VCO_2 (ml/min/ 100g)	0.2 ± 0.5	-0.005 ± 0.3	0.09 ± 0.2	0.02 ± 0.2	0.444
Δ V_E/VCO_2	22 ± 10	20 ± 9	18 ± 6	24 ± 5	0.335

Table 2. 3 Ventilatory and metabolic responsiveness during hypoxia in behaving rats during quiet rest

f_R, respiratory frequency (brpm, breaths per min); V_E, minute ventilation; V_T, tidal volume; V_T/T_i, mean inspiratory flow; T_i, inspiratory time; T_e, expiratory time; SD1, short-term respiratory timing variability; SD2, long-term respiratory timing variability VO_2, oxygen consumption; VCO_2, carbon dioxide production; V_E/VCO_2, ventilatory equivalent; VEH, autoclaved deionised water; ABX, antibiotic-treated; VEH-FMT, VEH followed by faecal microbiota transfer; ABX-FMT, antibiotic-treated followed by faecal microbiota transfer. Data are shown as mean ± SD and were statistically compared using one-way ANOVA with Bonferroni *post hoc* where appropriate. Each *p*-value is adjusted to account for multiple comparisons. Data are expressed as absolute change from baseline (Δ parameter).

	VEH (n=10)	ABX (n=10)	VEH-FMT (n=10)	ABX-FMT (n=10)	One-way ANOVA
T_i SD1 (ms)	28 ± 5	30 ± 6	30 ± 6	29 ± 7	0.744
T_i SD2 (ms)	57 ± 10	67 ± 19	59 ± 9	57 ± 16	0.272
T_e SD1 (ms)	79 ± 28	89 ± 35	77 ± 15	80 ± 31	0.804
T_e SD2 (ms)	140 ± 27	147 ± 32	132 ± 37	130 ± 42	0.699
T_{tot} SD1 (ms)	102 ± 31	112 ± 38	99 ± 15	102 ± 33	0.803
T_{tot} SD2 (ms)	217 ± 30	237 ± 35	217 ± 32	203 ± 64	0.405
Apnoea index (events/hr)	0.6 ± 1.9	3.0 ± 4.2	1.2 ± 2.5	1.2 ± 2.5	0.398
Sigh frequency (events/hr)	148 ± 35	166 ± 71	172 ± 46	160 ± 29	0.715

Table 2. 4 Respiratory timing variability, apnoeas and sighs during hypoxia in behaving rats during quiet rest

T_i, inspiratory time; T_e, expiratory time; T_{tot}, total breath duration; SD1, short-term respiratory timing variability; SD2, long-term respiratory timing variability; VEH, autoclaved deionised water; ABX, antibiotic-treated; VEH-FMT, VEH followed by faecal microbiota transfer; ABX-FMT, antibiotic-treated followed by faecal microbiota transfer. Data are shown as mean ± SD and were statistically compared using one-way ANOVA or non-parametric Kruskal-Wallis test where appropriate.

	VEH (n=10)	ABX (n=10)	VEH-FMT (n=10)	ABX-FMT (n=10)	One-way ANOVA	VEH vs ABX	VEH-FMT vs ABX-FMT	VEH vs VEH-FMT	ABX vs ABX-FMT	VEH vs ABX-FMT	ABX vs VEH-FMT
Δ f_R (brpm)	86 ± 52	45 ± 29	56 ± 15	53 ± 18	**0.038**	**0.043**	0.999	0.281	0.999	0.164	0.999
Δ V_E (ml/min/ 100g)	67 ± 33	39 ± 23	42 ± 15	42 ± 14	**0.02**	**0.045**	0.999	0.091	0.999	0.066	0.999
Δ V_T (ml/100g)	0.15 ± 0.12	0.11 ± 0.16	0.08 ± 0.07	0.07 ± 0.06	0.33	-	-	-	-	-	-
Δ V_T/T_i (ml/s/100g)	4.7 ± 1.6	3.1 ± 1.3	2.9 ± 1.0	3.0 ± 0.8	**0.028**	0.131	0.999	0.059	0.999	0.082	0.999
Δ T_i (ms)	-75 ± 42	- 46 ± 33	-58 ± 35	-49 ± 30	0.253	-	-	-	-	-	-
Δ T_e (ms)	-273 ± 133	-250 ± 116	-261 ± 97	-281 ± 103	0.961	-	-	-	-	-	-
Δ VO_2 (ml/min/ 100g)	-1.4 ± 0.8	-1.9 ± 1	-1.5 ± 1.1	-1.5 ± 0.9	0.69	-	-	-	-	-	-
Δ VCO_2 (ml/min/ 100g)	- 0.2 ± 0.4	- 0.3 ± 0.5	- 0.2 ± 0.6	- 0.2 ± 0.5	0.886	-	-	-	-	-	-
Δ V_E/VCO_2	59 ± 30	35 ± 31	36 ± 18	38 ± 18	0.115	-	-	-	-	-	-

Table 2. 5 Ventilatory and metabolic responsiveness during hypercapnia in behaving rats during quiet rest

f_R, respiratory frequency (brpm, breaths per min); V_E, minute ventilation; V_T, tidal volume; V_T/T_i, mean inspiratory flow; T_i, inspiratory time; T_e, expiratory time; SD1, short-term respiratory timing variability; SD2, long-term respiratory timing variability VO_2, oxygen consumption; VCO_2, carbon dioxide production; V_E/VCO_2, ventilatory equivalent; VEH, autoclaved deionised water; ABX, antibiotic-administration; VEH-FMT, VEH followed by faecal microbiota transfer; ABX-FMT, antibiotic administration followed by faecal microbiota transfer. Data are shown as mean ± SD and were statistically compared using one-way ANOVA with Bonferroni *post hoc* where appropriate, or non-parametric Kruskal-Wallis test with Dunn's *post hoc*, where appropriate. Each *p*-value is adjusted to account for multiple comparisons. *p*-values shown in bold highlight significant differences. Responses are expressed as absolute change from baseline (Δ parameter).

	VEH (n=10)	ABX (n=10)	VEH-FMT (n=10)	ABX-FMT (n=10)	One-way ANOVA	VEH vs ABX	VEH-FMT vs ABX-FMT	VEH vs VEH-FMT	ABX vs ABX-FMT	VEH vs ABX-FMT	ABX vs VEH-FMT
T_i SD1 (ms)	24 ± 6	18 ± 8	17 ± 5	17 ± 4	**0.042**	0.232	0.999	0.091	0.999	0.083	0.999
T_i SD2 (ms)	55 ± 27	29 ± 14	30 ± 11	36 ± 10	**0.004**	**0.006**	0.999	**0.019**	0.701	0.511	0.999
T_e SD1 (ms)	28 ± 46	54 ± 27	53 ± 29	51 ± 22	0.697	-	-	-	-	-	-
T_e SD2 (ms)	109 ± 55	73 ± 32	78 ± 34	76 ± 28	0.329	-	-	-	-	-	-
T_{tot} SD1 (ms)	80 ± 29	64 ± 31	62 ± 26	61 ± 24	0.375	-	-	-	-	-	-
T_{tot} SD2 (ms)	161 ± 88	108 ± 51	103 ± 36	94 ± 41	0.170	-	-	-	-	-	-
Apnoea index (events/hr)	5.5 ± 5.5	9.5 ± 5.5	11.0 ± 6.1	12.0 ± 8.6	0.159	-	-	-	-	-	-
Apnoea duration (s)	2.3 ± 1.0	2.5 ± 0.8	2.2 ± 0.5	2.2 ± 0.7	0.689	-	-	-	-	-	-
Sigh frequency (events/hr)	14 ± 6	14 ± 5	15 ± 7	19 ± 11	0.87	-	-	-	-	-	-

Table 2. 6 Respiratory timing variability, apnoeas and sighs during hypercapnia in behaving rats during quiet rest

$T_{i,}$ inspiratory time; $T_{e,}$ expiratory time; T_{tot}, total breath duration; SD1, short-term respiratory timing variability; SD2, long-term respiratory timing variability; VEH, autoclaved deionised water; ABX, antibiotic-treated; VEH-FMT, VEH followed by faecal microbiota transfer; ABX-FMT, antibiotic-treated followed by faecal microbiota transfer. Data are shown as mean ± SD and were statistically compared using one-way ANOVA with Bonferroni *post hoc* where appropriate, or non-parametric Kruskal-Wallis test with Dunn's *post hoc*, where appropriate. Each *p*-value is adjusted to account for multiple comparisons. *p*-values shown in bold highlight significant differences.

2.3.6 Cardiorespiratory recordings in anaesthetised rats

Baseline cardiorespiratory and blood gas parameters: Baseline cardiorespiratory and blood gas measurements in anaesthetised rats are shown in Table 2.7. There were no significant differences for baseline respiratory parameters between groups. Arterial blood oxygenation, pH and carbon dioxide and bicarbonate concentration were equivalent across groups. Haematocrit and haemoglobin concentrations were significantly lower in ABX rats compared with VEH rats. Manipulation of the gut microbiota lowered systolic blood pressure (Table 2.7). *Post hoc* analysis revealed that systolic blood pressure was significantly lower in ABX rats compared with VEH, VEH-FMT and ABX-FMT rats but no difference in mean arterial blood pressure was observed between groups (Table 2.7).

	VEH (n=8-10)	ABX (n=8)	VEH-FMT (n=9)	ABX-FMT (n=10)	One-way ANOVA	VEH vs ABX	VEH-FMT vs ABX-FMT	VEH vs VEH-FMT	ABX vs ABX-FMT	VEH vs ABX-FMT	ABX vs VEH-FMT
f_R *(brpm)*	99 ± 13	103 ± 9	92 ± 14	88 ± 12	0.066	-	-	-	-	-	-
V_E (ml/ min/ 100g)	35.9 ± 3.7	36.3 ± 4.6	31.6 ± 6.7	30.2 ± 12	0.071	-	-	-	-	-	-
V_T (ml/ 100g)	0.36 ± 0.03	0.35 ± 0.04	0.34 ± 0.05	0.38 ± 0.06	0.312	-	-	-	-	-	-
$ETCO_2$	5.9 ± 0.6	5.9 ± 0.9	5.6 ± 0.6	5.6 ± 0.6	0.536	-	-	-	-	-	-
pH	7.34 ± 0.02	7.36 ± 0.06	7.36 ± 0.03	7.37 ± 0.03	0.272	-	-	-	-	-	-
$PaCO_2$ (mmHg)	48.2 ± 3.9	47.2 ± 7.9	48.6 ± 5.2	45.2 ± 4.3	0.272	-	-	-	-	-	-
PaO_2 (mmHg)	107 ± 16	100 ± 8	106 ± 10	104 ± 6	0.712	-	-	-	-	-	-
$[HCO_3^-]$ (mmol/ l)	26.3 ± 1.2	26.4 ± 2.0	27.1 ± 1.4	26.1 ± 0.9	0.106	-	-	-	-	-	-
TCO_2 (mmol/l)	27.7 ± 1.3	27.8 ± 2.4	28.3 ± 1.5	27.5 ± 1.0	0.303	-	-	-	-	-	-
S_aO_2 (%)	97.5 ± 1.1	97.3 ± 0.9	97.7 ± 0.7	97.6 ± 0.7	0.987	-	-	-	-	-	-
$[Na^+]$ (mmol /l)	136.6 ± 2.6	137.0 ± 1.8	135.4 ± 1.4	135.1 ±1.4	0.078	-	-	-	-	-	-
$[K^+]$ (mmol/l)	4.2 ± 0.1	4.0 ± 0.2	4.2 ± 0.1	4.2 ± 0.2	0.149	-	-	-	-	-	-
Haematocrit (%)	51.7 ± 2.9	47.9 ± 2.0	48.3 ± 2.9	49.7 ± 2.3	**0.016**	**0.024**	0.999	0.062	0.665	0.792	0.999
[Hb] (g/dl)	17.5 ± 0.9	16.3 ± 0.7	16.1 ± 1.4	16.1 ± 2.9	**0.021**	**0.028**	0.999	0.082	0.999	0.596	0.999
MAP (mmHg)	96 ± 9	93 ± 12	90 ± 10	94 ± 13	0.712	-	-	-	-	-	-
DBP (mmHg)	73 ± 9	74 ± 13	66 ± 7	70 ± 12	0.463	-	-	-	-	-	-
SBP (mmHg)	148 ± 15	119 ± 12	140 ± 15	147 ± 15	**0.0005**	**0.0007**	0.999	0.999	**0.001**	0.999	**0.024**
HR (bpm)	410 ± 29	407 ± 40	389 ± 27	410 ± 28	0.438	-	-	-	-	-	-

Table 2. 7 **Baseline ventilation, blood gases and cardiovascular measurements in anaesthetised rats**

f_R, respiratory frequency (brpm, breaths per min); V_E, minute ventilation; V_T, tidal volume; $ETCO_2$, end-tidal carbon dioxide production; Pco_2, partial pressure of arterial carbon dioxide, Pao_2, partial pressure of arterial oxygen; $[HCO_3^-]$, bicarbonate concentration; TCO_2, total carbon dioxide; S_aO_2, arterial oxygen saturation; $[Na^+]$, sodium concentration; $[K^+]$, potassium concentration; [Hb], haemoglobin concentration; MAP, mean arterial blood pressure; SBP, systolic blood pressure; DBP, diastolic blood pressure; HR, heart rate (bpm, beat per min); VEH, autoclaved de ionised water; ABX,

antibiotic-treated; VEH-FMT, VEH followed by faecal microbiota transfer; ABX-FMT, antibiotic-treated followed by faecal microbiota transfer. Data are shown as mean ± SD and were statistically compared using one-way ANOVA with Bonferroni *post hoc* where appropriate, or non-parametric Kruskal-Wallis test with Dunn's *post hoc,* where appropriate. Each *p*-value is adjusted to account for multiple comparisons. *p*-values shown in bold highlight significant differences.

Cardiorespiratory responses to 5-HT_3 receptor agonism evoking the cardiopulmonary reflex: Stimulation, using PBG, of 5-HT_3 receptors found on pulmonary vagal afferent nerves evoked the integrated cardiopulmonary reflex with no significant difference in apnoea duration in ABX rats compared with VEH rats (p>0.05, two-way ANOVA, Fig. 2.4b), or in ABX-FMT rats compared with VEH-FMT rats (p>0.05, two-way ANOVA, Fig. 2.4f). A similar outcome was determined for post-apnoea induced tachypnoeic episodes in ABX rats compared with VEH rats (p>0.05, two-way ANOVA, Fig. 2.4c), and ABX-FMT rats compared with VEH-FMT rats (p>0.05, two-way ANOVA, Fig. 2.4g). The depressor response to PBG administration (hypotension) and bradycardia were also equivalent between ABX rats and VEH rats (p>0.05, two-way ANOVA, Fig. 2.4d, e) and in ABX-FMT rats compared with VEH-FMT rats (p>0.05, two-way ANOVA, Fig. 2.4h, i). The cardiorespiratory responses to high-dose PBG were abolished following bilateral cervical vagotomy.

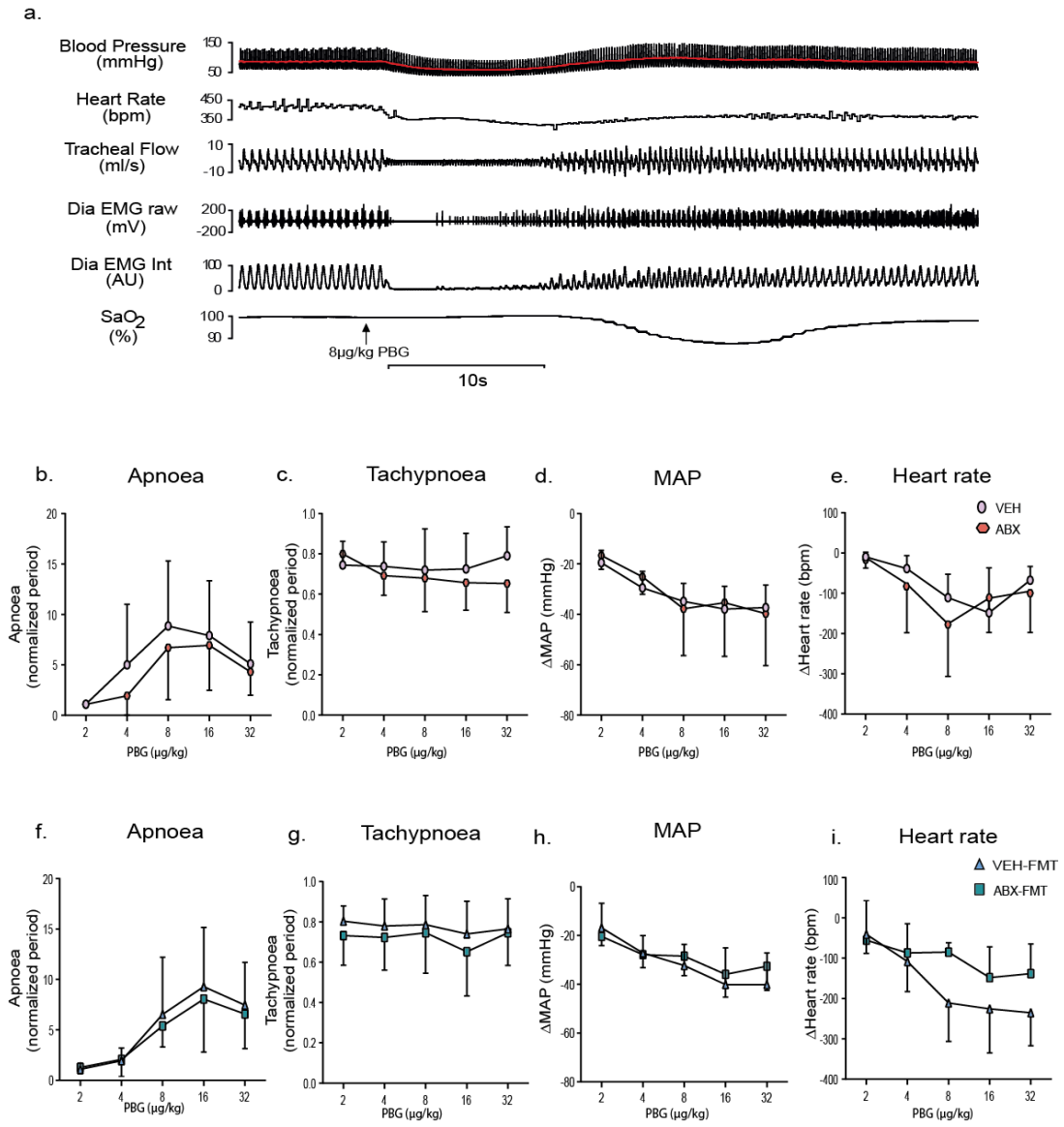


Figure 2. 4 Chronic antibiotic administration and faecal microbial transfer do not alter cardiorespiratory responses to phenylbiguanide administration in anaesthetised rats

a) Representative traces of blood pressure (red indicates mean value), heart rate, tracheal airflow, raw and integrated diaphragm (Dia) electromyogram (EMG) activity and arterial oxygen saturation (SaO_2) during intravenous administration of 5-HT_3 agonist phenylbiguanide (PBG; 8µg/kg) indicated by the upwards arrow. Group data for maximum apnoea duration (b, f) and tachypnoea (c, g) normalised to baseline respiratory period in response to 2 ,4, 8, 16 and 32µg/kg of PBG for VEH and ABX (b, c) and for VEH-FMT and ABX-FMT rats (f, g). Absolute change in mean arterial blood pressure (MAP; d, h) and heart rate (e, i) in response to 2 ,4, 8, 16 and 32µg/kg of PBG for VEH and ABX (d, e) and for VEH-FMT and ABX-FMT rats (h, i). VEH, autoclaved deionised water; ABX, antibiotic-treated; VEH-FMT, VEH followed by faecal microbiota transfer; ABX-FMT, antibiotic-treated followed by faecal microbiota transfer. Data (b-i) are expressed mean ± SD; VEH (n=8), ABX (n=8), VEH-FMT (n=9) and ABX-FMT (n=10). Groups were statistically compared by two-way ANOVA for VEH and ABX and separately for VEH-FMT and ABX-FMT.

2.3.7 Brainstem neurochemistry

$_{L}$-DOPA, DA, HVA, HVA/DA ratio, 5-HT and 5-HIAA concentrations in the brainstem were significantly affected by manipulation of the gut microbiota ($p<0.05$; one-way ANOVA or Kruskal-Wallis, Fig. 2.5). Additionally, *post hoc* analysis revealed that compared with VEH, ABX brainstem homogenates contained elevated concentrations of $_{L}$-DOPA ($p=0.009$; Kruskal-Wallis with Dunn's *post hoc,* Fig. 2.5a) and an increased HVA/DA ratio ($p=0.0001$; one-way ANOVA with Bonferroni *post hoc,* Fig. 2.5d), a consequence of augmented HVA concentrations ($p<0.0001$, one-way ANOVA with Bonferroni *post hoc,* Fig. 2.5c) and decreased DA concentrations ($p=0.025$; one-way ANOVA with Bonferroni *post hoc,* Fig. 2.5b). ABX-FMT samples compared with VEH, ABX and VEH-FMT brainstem homogenates had significant increases in HVA/DA ratio ($p<0.0001$; $p=0.001$; $p=0.0001$, respectively; one-way ANOVA with Bonferroni *post hoc*, Fig. 2.5d) due to elevated HVA concentrations ($p<0.0001$; $p=0.003$; $p=0.0002$, respectively; one-way ANOVA with Bonferroni *post hoc,* Fig. 2.5c). $_{L}$-DOPA was elevated in ABX-FMT rats compared with VEH and VEH-FMT brainstem homogenates ($p=0.001$; $p=0.038$, respectively, Kruskal-Wallis with Dunn's *post hoc,* Fig. 2.5a). Furthermore, ABX-FMT contained increased concentrations compared with VEH of 5-HT ($p=0.021$; one-way ANOVA with Bonferroni *post hoc,* Fig. 2.5f) and 5-HIAA ($p=0.01$; one-way ANOVA with Bonferroni *post hoc,* Fig. 2.5g) along with a decrease in DA concentration ($p=0.0009$; one-way ANOVA with Bonferroni *post hoc,* Fig. 2.5b). VEH-FMT brainstem homogenates compared with VEH had elevated HVA/DA ratio ($p=0.0005$; one-way ANOVA with Bonferroni *post hoc,* Fig. 2.5d) due to an increase in HVA ($p=0.0004$; one-way ANOVA with Bonferroni *post hoc,* Fig. 2.5c).

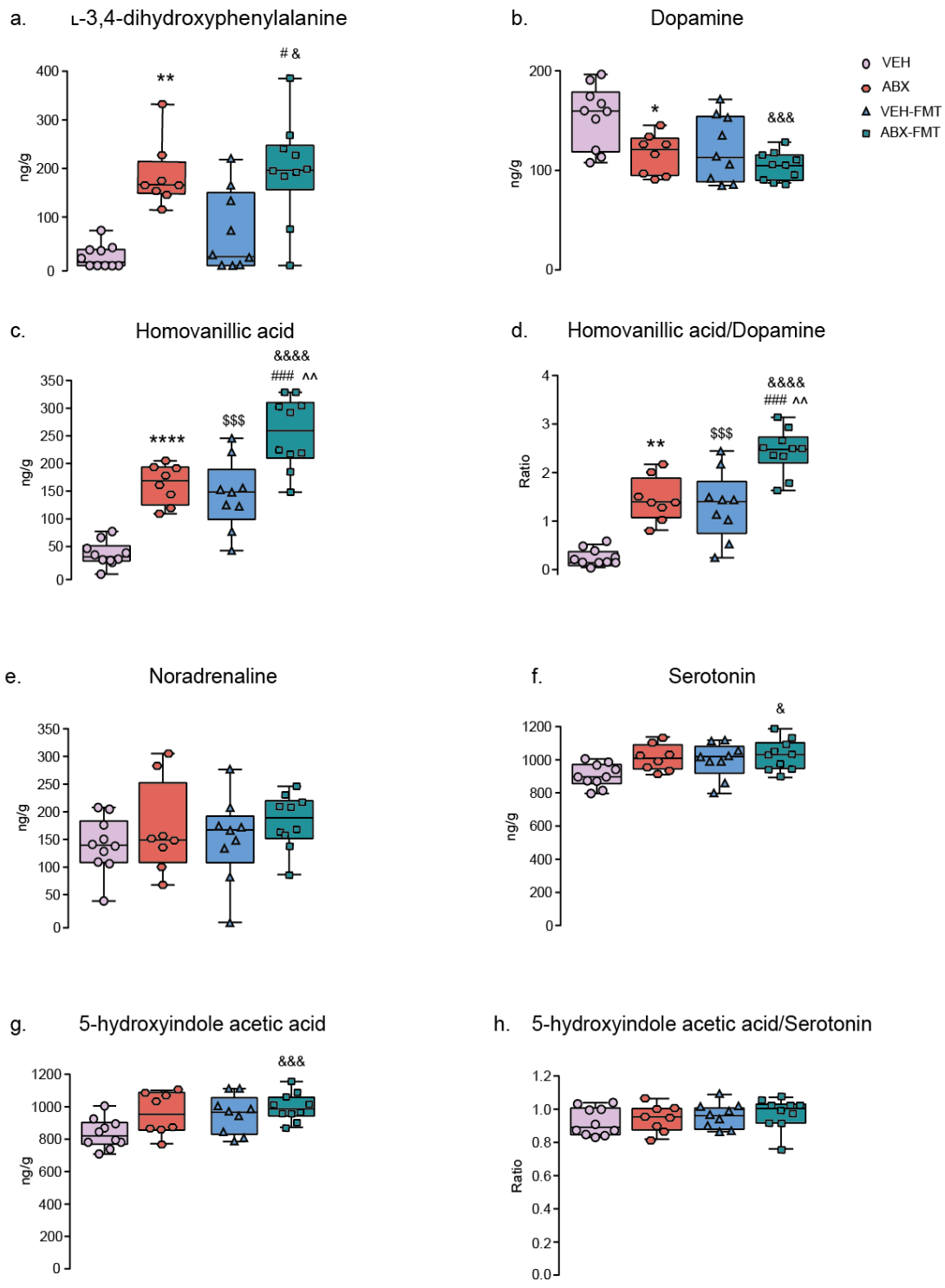


Figure 2. 5 Chronic antibiotic administration and faecal microbial transfer alter rat brainstem neurochemistry

Group data for L-3,4-dihydroxyphenylalanine (a), dopamine (b), homovanillic acid (c), homovanillic acid/dopamine ratio (d), noradrenaline (e), serotonin (f), 5-hydroxyindole acetic acid (g) and 5-hydroxyindole acetic acid/serotonin ratio (h) in VEH, ABX, VEH-FMT and ABX-FMT rats. VEH, autoclaved deionised water; ABX, antibiotic-treated; VEH-FMT, VEH followed by faecal microbiota transfer; ABX-FMT, antibiotic-treated followed by faecal

microbiota transfer. Data (a-h) are expressed as box and whisker plots (median, IQR and minimum to maximum values). VEH (n=10), ABX (n=8), VEH-FMT (n=9) and ABX-FMT (n=10). Groups were statistically compared by one-way ANOVA with Bonferroni *post hoc* or non-parametric Kruskal-Wallis with Dunn's *post hoc*, where appropriate. * $p<0.05$, ** $p<0.01$, **** $p<0.0001$, ABX *versus* VEH; $ $p<0.05$, $$$ $p<0.001$, VEH *versus* VEH-FMT; &$p<0.01$, &&& $p<0.001$, &&&& $p<0.0001$, VEH *versus* ABX-FMT; # $p<0.05$, ### $p<0.001$, VEH-FMT *versus* ABX-FMT; ^^ $p<0.01$, ABX *versus* ABX-FMT; all *post hoc* tests.

2.3.8 Ex vivo intestinal macromolecular permeability

The distal ileum from ABX rats was significantly more permeable compared with VEH rats: FITC flux was enhanced in ABX tissue compared with VEH at the 120-minute time point (p=0.025, two-way ANOVA with Bonferroni post-hoc, Fig. 2.6a). However, no statistically significant difference was detected in the permeability of the proximal colon of ABX rats compared with VEH rats (p>0.05; Fig. 2.6c). Permeability was equivalent in both the distal ileum and proximal colon of ABX-FMT rats compared with VEH-FMT rats (p>0.05; Fig. 2.6b, d). Permeability of the distal ileum, but not proximal colon, was increased in VEH-FMT compared with VEH (Appendix Fig. A.6).

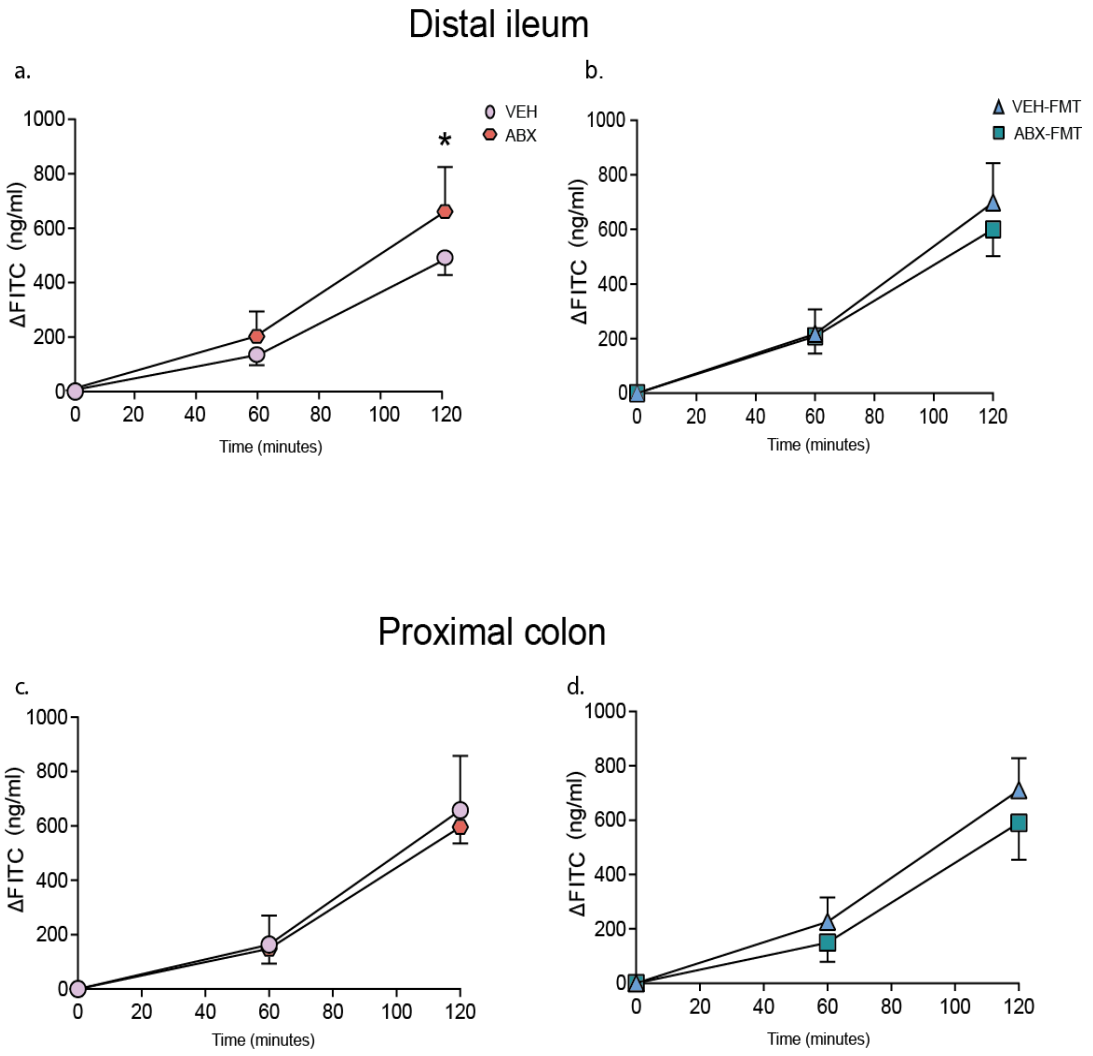


Figure 2. 6 Chronic antibiotic administration increases the macromolecular permeability of rat distal ileum

Group data for FITC flux in distal ileum (a, b) and proximal colon (c, d) in VEH and ABX (a, c) and in VEH-FMT and ABX-FMT rats (b, d). VEH, autoclaved deionised water; ABX, antibiotic-treated; VEH-FMT, VEH followed by faecal microbiota transfer; ABX-FMT, antibiotic-treated followed by faecal microbiota transfer. Groups (a-d) showing baseline (0 minutes), 60 minutes and 120 minutes FITC flux for VEH (n=4-5), ABX (n=6), VEH-FMT (n=5) and ABX-FMT (n=4). Groups were statistically compared by two-way ANOVA with Bonferroni *post hoc*, where appropriate. * $p<0.05$, ABX *versus* VEH.

2.3.9 Alterations in the caecal microbiota

As expected, ABX rats had a significantly heavier caecum compared with VEH rats (p=0.002; Kruskal-Wallis with Dunn's *post hoc,* Fig. 2.7d). Faecal microbiota transfer attenuated the effects of antibiotics on caecum weight; ABX-FMT and VEH-FMT rat caecum weights were lighter compared with ABX (p=0.0001 and p=0.03, respectively; Kruskal-Wallis with Dunn's *post hoc,* Fig. 2.7d). DNA concentrations in caecal samples from ABX rats were critically low, likely a result of depletion of bacteria by the broad-spectrum antibiotic cocktail and thus below the level of detection. This prevented a comparative analysis of microbiota composition and diversity as 16S rRNA sequencing was not possible in this group. In the remaining groups, 16S rRNA sequencing identified around 130 bacterial genera from 46 families of 9 different phyla (Appendix Tables A.14-22). The majority of the bacterial genera belonged to two major phyla (Bacteroidetes and Firmicutes), which together comprise 95% (VEH), 90% (VEH-FMT) and 85 % (ABX-FMT) of intestinal microbiota. The analysis of alpha and beta diversities revealed that FMT procedure significantly altered the microbiota composition in both VEH-FMT and ABX-FMT rats as compared with VEH rats. There was a clear trend towards enhanced species richness of caecal microbiota in VEH-FMT and ABX-FMT samples: number of observed species, Chao1 (an estimate of total richness in a sample (Chao, 1984)) and phylogenetic whole tree diversity (PD whole tree, an estimate of diversity based on structure and branch length of the phylogenetic tree in each sample (Faith, 1992)) indices were all increased in these groups (Fig. 2.7a, p=0.035, p=0.043 and p=0.004 between VEH-FMT *versus* VEH; p=0.052 for parameters in ABX-FMT *versus* VEH). However, only an increase in PD whole tree diversity in VEH-FMT vs. VEH rats remained significant after adjustment for multiple comparisons. Shannon and Simpson metrics of alpha diversity, which take into account the evenness of species abundance, were less affected by FMT. Further, PCoA analysis identified structural differences across all three groups, with VEH-FMT and ABX-FMT rats clearly separating from VEH rats (Fig. 2.7b, p=0.001, PERMANOVA).

At the phyla level, VEH-FMT and ABX-FMT rat caecal contents displayed a distinct shift towards an increase in Proteobacteria and Cyanobacteria with a decrease in Bacteroidetes and Deferribacteres compared with VEH rats (Appendix Tables A.14 and 15). Five minor phyla remained unchanged between VEH-FMT and ABX-FMT rats compared with VEH rats (Appendix Tables A.14 and 15). The minor phyla Verrucomicrobia and Saccharibacteria were significantly altered in ABX-FMT rats compared with VEH-FMT rats (Appendix Tables A.16).

An increase in the relative abundance of Proteobacteria in VEH-FMT and ABX-FMT rats was primarily caused by a shift in *Helicobacter* bacteria, a genus of *Helicobacteraceae* family (Fig. 2.7c). Increased abundance of *Helicobacter* in VEH-FMT rats compared with VEH rats appeared to be at the expense of *Parasutterella* (*Alcaligenaceae*) and *Enterobacter (Enterobacteriaceae)*, which both displayed a reduced relative abundance. The Cyanobacteria shifts evident in VEH-FMT and ABX-FMT rats were attributed to an increase in *Gastranaerophilales* uncultured species. *Bacteroidales S24-7* uncultured bacteria, a dominant genus of *S24-7* family, was the main source of Bacteroidetes reduction in VEH-FMT rat caecal samples compared with VEH rats; nonetheless, an increase in minor Bacteroidetes *V2.1 Bac22* uncultured species was noted (Fig. 2.7c). The decrease in Bacteroidetes in the ABX-FMT rats was not related to a compelling decrease in any one genus but rather small shifts in the relative abundance of multiple genera. Similar to the VEH-FMT group, a minor increase in Bacteroidetes *V2.1 Bac22* uncultured bacterium was detected in ABX-FMT rats. The decrease in Deferribacteres in VEH-FMT and ABX-FMT rats compared with VEH rats was a consequence of a decrease in *Mucispirillum* (*Deferribacteraceae* family). Although there was no significant difference at the Firmicutes phylum level, VEH-FMT rats showed an increase in uncultured bacterium and unidentified genera from *Clostridiales vadin BB60* family, *Lachnoclostridium-10*, *Lachnospiraceae* uncultured, *Flavonifractor, Ruminococcaceae UCG-013* compared with VEH. A decrease occurred in *Bacillus, Lachnospiraceae UCG-008*, *Tyzzerella* and *Ruminoclostridium-9* (Fig. 2.7c). In ABX-FMT rats there was an increase in *Lachnoclostridium-10* and *Ruminococcaceae UCG-011* and a decrease in *Bacillus, Streptococcus and Lachnospiraceae UCG-008* compared with VEH rats. Furthermore, uncultured *Coriobacteriaceae* bacteria from the Actinobacteria phylum was reduced in the VEH-FMT and ABX-FMT rats compared with VEH rats. The alterations evident at phyla level in ABX-FMT rats compared with VEH-FMT rats were not related to changes in highly abundant genera. Nonetheless, there was a decrease in *Streptococcus (Streptococcaceae*), *Peptoclostridium* (*Peptococcaceae*), *Ruminococcaceae UCG-005* (*Ruminococcaceae*) compared with VEH-FMT rats. ABX-FMT rats displayed an increase in *Allobaculum (Erysipelotrichaceae*) and *Parasutterella (Alcaligenaceae)* from the phyla Firmicutes and Proteobacteria, respectively (Fig. 2.7c).

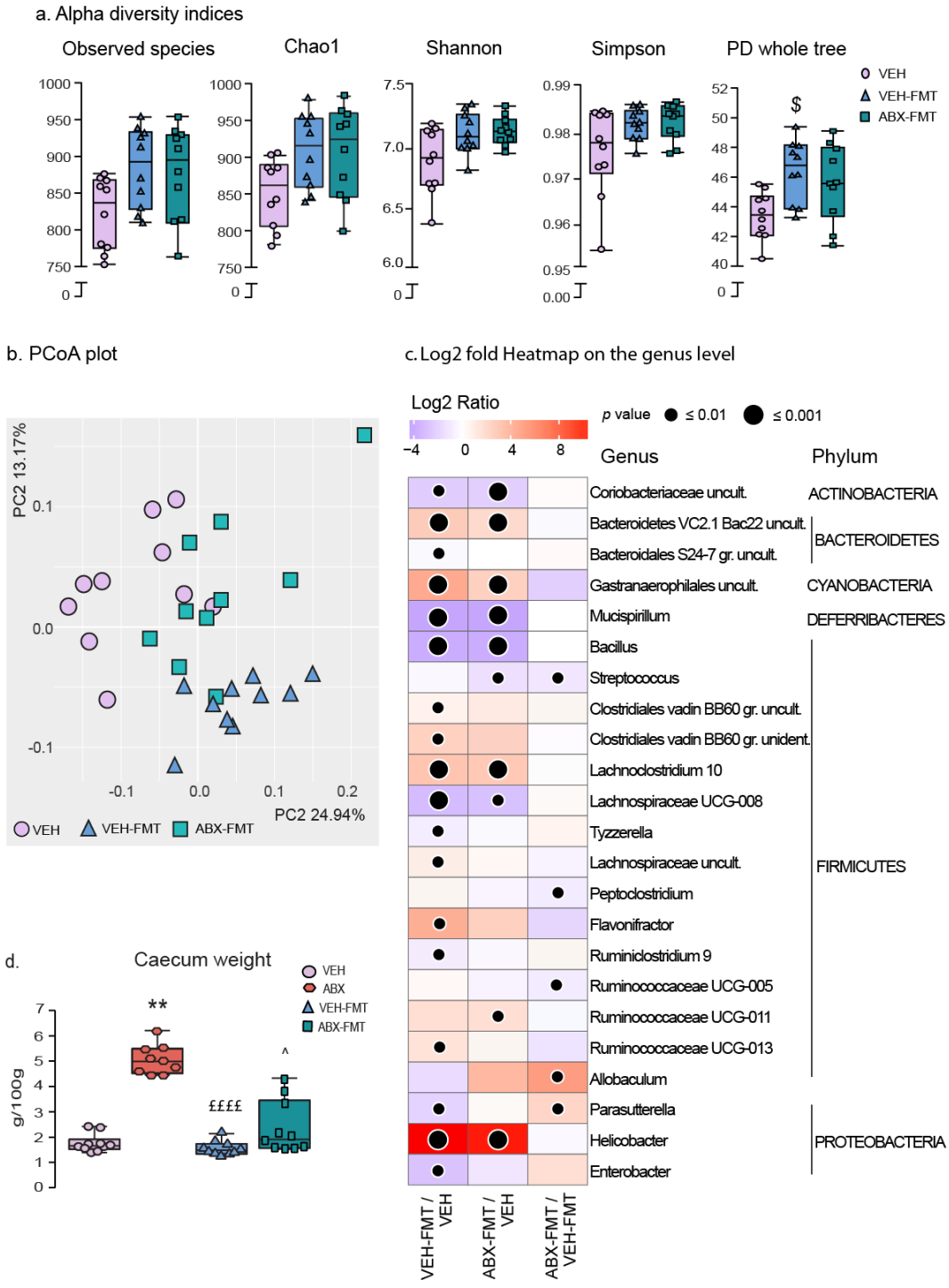


Figure 2. 7 Faecal microbiota transfer alters rat caecal microbiota composition

Group data for alpha diversity (a) and principal coordinate analysis (PCoA; b) in 2-dimensinal representations for VEH, VEH-FMT and ABX-FMT. Heatmap of Log2 fold change ratios on genus level (c) showing increases (red) and decreases (purple) in the relative abundance of bacterial genera in VEH-FMT (left column) and ABX-FMT (middle column) compared with VEH, as well as differences between ABX-FMT and VEH-FMT (right column). Group (d) data for caecum weight in VEH, ABX, VEH-FMT and ABX-FMT. VEH, autoclaved deionised water; VEH-FMT, VEH followed by faecal microbiota transfer; ABX-FMT, antibiotic-treated followed

by faecal microbiota transfer. Data (a and d) are expressed as box and whisker plots (median, IQR and minimum to maximum values). Data (a) were statistically compared by non-parametric Mann-Whitney *U* test. Group (d) were statistically compared by Kruskal-Wallis with Dunn's *post hoc*. ***p*<0.01, ABX *versus* VEH; ££££ *p*<0.0001, VEH-FMT vs ABX; ^ *p*<0.05, ABX-FMT vs. ABX. c) ● *p*<0.05, ● *p*<0.01, ● *p*<0.001 compared with VEH or VEH-FMT values. Benjamini-Hochberg adjustment with Q = 0.1 was used to correct *p* values for multiple testing; VEH (n=10), VEH-FMT (n=10) and ABX-FMT (n=10).

2.3.10 Correlation analysis between microbiota composition and brainstem neurochemistry and heart rate

Associations between genera and brainstem neurochemistry as well as basal heart rate in VEH, VEH-FMT and ABX-FMT rats were identified utilising Hierarchical All-against-All (HAllA) correlation analysis. Identified associations are presented as a correlogram in Figure 2.8. Individual data points for the most significant correlations for homovanillic, homovanillic/dopamine and dopamine are presented as scatter plots in Appendix Figure A.7. *Anaerovorax*, a member of Firmicutes phylum positively associated with basal heart rate. Further to this, several genera from different phyla correlated with brainstem neurochemistry. *Peptoclostridium* and *Ruminococcaceae UCG-005* of Firmicutes phylum negatively associated with L-DOPA. *Lachnspiraceae (Eubacterium) ventriosum* group and *Erysipelotrichaceae UCG-004* of Firmicutes positively associated with NA, while *Coriobacteriaceae* uncultured, a genus of Actinobacteria negatively associated with NA. *Helicobacter,* a member of Proteobacteria phylum as well as *Bacteroidetes VC2.1 Bac22* uncultured, a member of Bacteroidetes phylum negatively correlated with DA. *Bacillus*, of Firmicutes phylum and *Coriobacteriaceae* uncultured positively correlated with DA. *Bacteroidetes VC2.1 Bac22* uncultured *Gastranaerophilales* uncultured organism as well as 3 genera from Firmicutes phylum, *Ruminococcaceae UCG-011*, *Lachnoclostridium 10* and *Clostridiales vadin BB60* group uncultured bacterium positively associated with HVA, whereas *Bacillus* and *Mucispirillum*, a member of Deferribacteres phylum negatively associated with HVA. *Ruminococcaceae UCG-009*, *Lachnoclostrdium 10*, *Bacteroidetes VC2.1 Bac22* uncultured and *Burkholderia*, a member of phylum Proteobacteria positively associated with HVA/DA turnover. *Bacillus, Mucispirillum* and *Coriobacteriaceae* uncultured negatively associated with this ratio. *Lachnoclostridium 10* positively correlated with 5-HT. *Ruminococcaceae V9D2013* group, *Clostridiales vadinBB60* group uncultured bacterium, *Gastranaerophilales* uncultured bacterium and *Bacteroidetes VC2.1 Bac22* uncultured, positively correlated with 5-HIAA. *Natranaerovirga* negatively associated with 5-HIAA. *Clostridiales Family XII UCG-001* negatively associated with 5HIAA/5-HT.

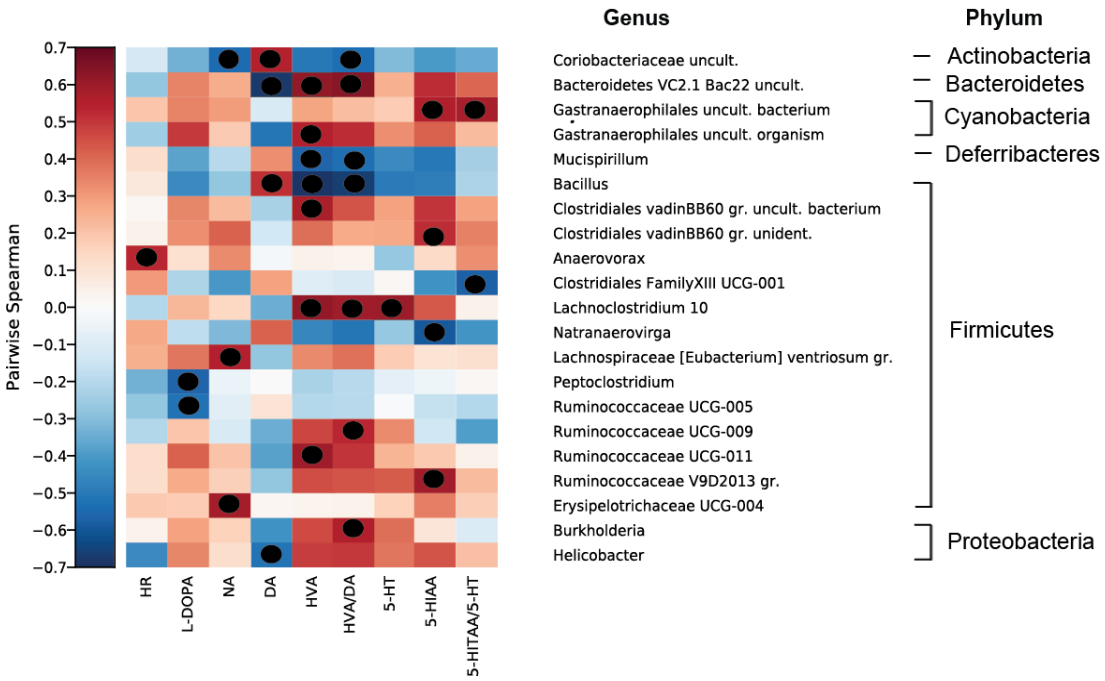


Figure 2. 8 Brainstem neurochemistry and heart rate are associated with the abundance of specific genera

Hallagram depicting spearman correlations between the relative abundance of bacterial genera and brainstem neurochemistry as well as basal heart rate (VEH, VEH-FMT and ABX-FMT). Genera are ordered taxonomically. HR, heart rate; $_{L}$-DOPA, $_{L}$-3,4-dihydroxyphenylalanine; NA, noradrenaline; DA, dopamine; HVA, homovanillic acid; HVA/DA, homovanillic acid/dopamine; 5-HT, serotonin; 5-HIAA, 5-hydroindole acetic acid; 5-HIAA/5-HT, 5-hydroindole acetic acid/serotonin. Significant correlations are represented by black dots (●). Benjamini-Hochberg adjustment *p*-value with Q = 0.2 was used to correct *p* values for multiple testing.

2.4. Discussion

There is considerable interest in the role of the gut microbiota in health and disease. This interest stems from established associations between the gut microbiota and brain behaviours (Bercik *et al.*, 2011a; Bravo *et al.*, 2011; Collins *et al.*, 2012; Cryan & Dinan, 2012; Kelly *et al.*, 2016b; Burokas *et al.*, 2017). Our interests relate to the potential influence of the microbiota on the cardiorespiratory system. We sought to assess the effects of manipulation of the gut microbiota by chronic antibiotic administration on cardiorespiratory physiology in adult male rats, and to investigate if faecal microbiota transfer of pooled control faeces could reverse or ameliorate putative deleterious effects induced by chronic antibiotic administration (microbiota disruption). The principal findings of this study are: 1) ABX and FMT blunt the ventilatory response to hypercapnia due to decreased respiratory frequency; 2) ABX and FMT blunt respiratory frequency during the peak hypoxic ventilatory response; 3) neither ABX nor FMT interventions alter respiratory timing variability; 4) ABX decreases systolic blood pressure; 5) cardiorespiratory responsiveness to vagal afferent nerve stimulation is unaffected by ABX or FMT; 6) ABX and FMT alter brainstem monoamine and monoamine metabolite concentrations; 7) ABX and FMT increase distal ileum permeability; 8) FMT significantly altered gut microbiota composition and diversity; 9) Genera from 6 phyla, predominantly Firmicutes, correlate with brainstem neurochemistry.

2.4.1 Animal model

Microbiota manipulation by chronic antibiotic administration: Two different approaches were used in this study to manipulate the microbiota. First, we used an antibiotic cocktail, informed by previous studies where microbiota depletion was successful (Hoban *et al.*, 2016; Kelly *et al.*, 2016b). Failure to determine the caecal microbiota composition of ABX rats in the current study was likely the result of severe microbiota depletion and substantially diminished available bacterial DNA for detection. This was further supported by the dramatic enlargement of the caecum in ABX rats; an increase in caecum mass results from the loss of bacterial fermentation, consistent with previous observations both in germ-free and antibiotic-treated animals (Grasa *et al.*, 2015; Luczynski *et al.*, 2016). Faecal output in ABX rats was qualitatively determined as having an increased water composition, a frequent complication of antibiotic administration (Grasa *et al.*, 2015). We postulate that altered defaecation may have resulted from antibiotic-induced microbiota depletion and potential expansion of opportunistic bacteria (Wurm *et al.*, 2017).

Faecal microbiota transfer significantly altered gut microbiota composition and diversity : In addition to ABX, we utilised a FMT strategy to manipulate microbiota. It has been shown that behavioural phenotypes can be transferred via FMT in rodents (Le Roy *et al.*, 2013; Li *et al.*, 2015; Kelly *et al.*, 2016a; Kelly *et al.*, 2016b). The FMT strategy used in our study did not recover or normalise the microbiota composition. VEH-FMT and ABX-FMT groups both displayed profound changes in microbiota structure and species diversity compared with the VEH group. Caecal samples from VEH-FMT and ABX-FMT animals had the relative abundance of 18 and 10 genera altered, respectively, compared with VEH animals. Only 5 genera were significantly different between VEH-FMT and ABX-FMT. Our findings are consistent with recent clinical data where FMT to persons with irritable bowel syndrome led to the establishment of unique taxonomy as well as increased diversity with no improvement in symptoms (Halkjaer *et al.*, 2018). Pooled exogenous bacteria has been shown to increase microbiota diversity in recipient rats, resembling that of the donor (Manichanh *et al.*, 2010). However, pre-treatment with antibiotics does not facilitate establishment of the donor microbiota (Manichanh *et al.*, 2010). Interestingly, autologous FMT had no effect on insulin sensitivity in obese metabolic syndrome, however allogenic FMT had transient benefits on insulin sensitivity which was driven by baseline faecal microbiota composition (Kootte *et al.*, 2017).

Caecum weights of ABX-FMT rats were lighter than that of ABX rats, but did not recover completely to VEH values. After discontinuing antibiotic exposure, gastrointestinal responses of ABX-FMT rats, assessed qualitatively by faecal output, returned to levels equivalent to VEH rats. Similar results were observed both in rodent and clinical studies where FMT was used to treat *Clostridium difficile* infection and sepsis (Li *et al.*, 2015; Jiang *et al.*, 2017). Thus, ABX-induced alterations to the microbiota were not reversed by FMT intervention in our study. Indeed, FMT itself led to significant modification of the microbiota, establishing a separate model of microbiota disruption in our study (VEH-FMT and ABX-FMT groups), with distinct microbiota signatures compared with that of VEH animals.

2.4.2 Chronic antibiotic administration and faecal microbiota transfer blunt ventilatory responses to hypoxia and hypercapnia

To date few studies have examined the consequences of manipulation of the gut microbiota on the control of breathing. We previously revealed enhanced variability of breathing frequency during normoxic breathing, and altered ventilation during hypoxic and hypercapnic chemostimulation in adult rats exposed to antecedent pre-natal stress

(Golubeva *et al.*, 2015). Significant correlations were found between respiratory frequency during hypercapnia and bacterial genera of the Firmicutes phylum (Golubeva *et al.*, 2015), suggesting a potential influence of alterations in the gut microbiota on the control of respiratory rhythm during CO_2 exposure.

We reasoned that perturbation of the gut microbiota by ABX would elicit a distinctive respiratory control signature. In conscious behaving rats during quiet rest, no apparent aberrant respiratory control phenotype was evident in ABX rats during normoxia such that we observed normal values for ventilation and metabolism equivalent to VEH. Moreover, VEH-FMT and ABX-FMT rats were similar to VEH revealing the remarkable capacity of the neural network to maintain homeostasis in the light of major disruption to brainstem monoamine concentrations (discussed below). V_E/VCO_2 was decreased in VEH-FMT rats compared with VEH during normoxia, revealing a relatively depressed level of ventilation *per se* in VEH-FMT rats.

Compared with VEH, ABX depressed the peak hypoxic ventilatory response and respiratory frequency component of the response during the first 2 minutes of exposure to hypoxia. A similar blunted minute ventilation and frequency response was observed in VEH-FMT rats compared with VEH revealing a consistent outcome in response to manipulation of the gut microbiota. Interestingly, respiratory timing variability was unaffected by ABX or FMT. Moreover, analysis of steady-state responses during the last 5 minutes of hypoxic exposure revealed that there was no aberrant respiratory phenotype evident in ABX or FMT rats. Our findings in ABX and FMT rats of a blunted minute ventilation and respiratory frequency response in phase 1 of the hypoxic ventilatory response is similar to the depressed hypoxic ventilatory response evident in adult rats exposed to pre-natal stress, where a significantly depressed respiratory frequency response to hypoxia was also observed (Golubeva *et al.*, 2015). It is plausible that manipulation of the gut microbiota resulted in altered integration of chemosensory inputs from the carotid bodies (the primary peripheral oxygen sensors) at the level of the nucleus tractus solitarius, leading to the development of a blunted frequency response to hypoxia. It is intriguing to consider that microbiota disruption may have resulted in re-programming of the carotid bodies, resulting in modified chemosensory afferent discharge to the brain, but this remains to be tested in future work. Although the peak hypoxic ventilatory response was blunted, the steady-state response (phase 2) was intact, again highlighting the robust capacity of the chemoreflex pathway in maintaining respiratory homeostasis in our models.

Chemoactivation of ventilation in response to hypercapnic stress (elevated inspired CO_2) revealed a robust blunted V_E response to CO_2 challenge in ABX rats compared with VEH, a ventilatory depression manifest as a reduced f_R response to hypercapnia (bradypnoea), which was maintained throughout the hypercapnic challenge. Manipulation of the gut microbiota had no effect on metabolic responses ($\dot{V}CO_2$) to hypercapnia. Thus, the ventilatory equivalent for carbon dioxide ($V_E/\dot{V}CO_2$), which relates ventilation to the prevailing metabolism, was depressed in ABX rats compared with VEH rats, highlighting inadequate ventilation to meet metabolic demand (hypoventilation). Microbiota disruption by FMT resulted in decreased ventilation in hypercapnia in FMT groups to levels similar to that seen in ABX animals, and significantly below that of VEH rats. Therefore, two modes of disrupted microbiota in our study were associated with depressed ventilatory response to hypercapnia. Respiratory timing variability and associated respiratory behaviours such as apnoeas and sighs were essentially unaffected by microbiota manipulation.

The disruptions to ventilation in response to hypoxic or hypercapnic stress observed in behaving animals using whole-body plethysmography, were not evident in urethane-anaesthetised animals, suggesting that the changes in respiratory control may be state-dependent (Doi & Ramirez, 2010). Indeed anaesthesia depresses respiratory drive and chemoresponsiveness (Teppema & Baby, 2011), and this may have masked the otherwise blunted ventilatory responsiveness to hypercapnic stress and the blunted peak ventilatory response to hypoxia in animals with manipulations to the microbiota. Alternatively, it may be that chemoreflex-driven homeostatic control of breathing is unaffected in ABX and FMT rats, but that the composite behavioural response to hypoxic and hypercapnic stress---manifest in the integrated respiratory behavioural response to challenges---is blunted.

The hypercapnic stimulus used in our study was modest, sufficient to evoke a ventilatory response through the activation of central nervous system CO_2 chemoreceptors, but not intended as an overt behavioural stressor. Nevertheless, hypercapnia can provoke fear-associated responses and there are strong links between emotion and respiratory behaviour. Indeed, ventilatory hypersensitivity to CO_2 is a hallmark of panic disorder in susceptible individuals. Thus, it is possible in our study that manipulation of the microbiota altered neurochemistry in brain regions such as the amygdala (Hoban *et al.*, 2016), which is known to modulate ventilatory responsiveness to CO_2 (Tenorio-Lopes *et al.*, 2017). Dopamine is a candidate neurotransmitter in emotion-associated respiratory control, with evidence that breathing is modulated by dopaminergic signalling in the basolateral amygdala (Sugita *et al.*, 2015). The data from behaving rats demonstrate a capacity for aberrant respiratory plasticity

in animals with altered gut microbiota, supporting the concept that the microbiota-gut-brainstem axis may function as an important modulator of the respiratory control network, either directly or indirectly. Blunted CO_2 chemoreflex ventilatory responses are physiologically significant as they increase the risk of the development of systemic acidosis in circumstances of elevated CO_2 (e.g. sleep, pulmonary and respiratory control diseases, respiratory depression by drugs) (Brinkman & Sharma, 2018; Patel & Majmundar, 2018). Hypercapnic acidosis can compromise the function of neural networks and systemic tissues due to pH imbalance. As such, disruptions to the microbiota could via aberrant respiratory control, exert deleterious effects on whole body homeostasis.

2.4.3 Chronic antibiotic administration decreases systolic blood pressure

Cardiovascular control is complex and multifaceted with recent studies in animal models and humans demonstrating the contribution of the gut microbiome to the regulation of blood pressure (Yang *et al.*, 2015; Adnan *et al.*, 2017; Li *et al.*, 2017). In spontaneously hypertensive rat and angiotensin-II hypertensive rat models, shifts in microbiota richness and increases in the Firmicutes:Bacteroidetes ratio are evident (Yang *et al.*, 2015). Of note, FMT from hypertensive human donors to germ-free mice elevates blood pressure in the recipient mice, which was observed to be transferrable through the microbiota (Li *et al.*, 2017). Similarly, it has been demonstrated that antibiotic-treated normotensive rats that received a FMT of donor faeces from hypertensive rats subsequently developed hypertension (Adnan *et al.*, 2017). Bacterial metabolites are associated with the development of high blood pressure; specifically, a decrease in butyrate-producing and acetate-producing bacteria, which promote intestinal barrier integrity, and an increase in lactate-producing bacteria are each associated with hypertension (Yang *et al.*, 2015; Durgan *et al.*, 2016; Adnan *et al.*, 2017). Oral administration of a probiotic (*Clostridium butyricum*) or a prebiotic (Hylon VII) prevented microbiota disruption, increased acetate levels and prevented the development of hypertension in a rat model of obstructive sleep apnoea (Ganesh *et al.*, 2018). Additionally, caecal acetate administration prevented obstructive sleep apnoea induced hypertension (Ganesh *et al.*, 2018). The anti-inflammatory antibiotic minocycline was shown to ameliorate hypertension and reduce the Firmicutes:Bacteroidetes ratio in an angiotensin II hypertensive rat model (Yang *et al.*, 2015). The absence of gut microbiota in germ free mice appears to be protective against angiotensin II induced hypertension and vascular dysfunction (Karbach *et al.*, 2016). Our study revealed that chronic broad-spectrum ABX intervention results in lower systolic blood pressure and pulse pressure, although no difference was evident in mean arterial blood pressure.

Evidence is accruing in support of a microbial influence over cardiovascular control although a defined microbiota signature essential to the maintenance of normal blood pressure has yet to be determined. An enrichment in *Lactobacillus, Bifidobacterium* and *Allobaculum* along with a reduction in *Lachnospiraceae, Lactococcus, Blautia, Coprobacillus* and *Erysipelotrichaceae* species occurred in a rat model of obstructive sleep apnoea compared with sham. In sham animals, prebiotic (Hylon VII) treatment increased the abundance of acetate-producing genera, including *Blautia, Collinsella, Bifidobacterium* and *Ruminococcus,* preventing the development of hypertension (Ganesh *et al.*, 2018). Intriguingly, a dramatic proliferation of certain genera such as *Prevotella* and *Klebsiella* has been shown both in pre-hypertensive and hypertensive individuals compared with normotensive controls. In this clinical population, Firmicutes including *Oscillibacter, Roseburia* and *Blautia*, *Bifidobacterium* from Actinobacteria phylum and *Akkermansia* from Verrucomicrobiaceae phylum were 5 out of 11 genera enriched in healthy normotensive controls compared with pre-hypertensive and hypertensive individuals (Li *et al.*, 2017). Indeed, these genera were in the top 45% of highly abundant genera in VEH, VEH-FMT and ABX-FMT groups. Genera which were highly abundant in pre-hypertensive and hypertensive humans were not abundant in this study, but comparisons between species may not be appropriate. Of interest, *Blautia* and *Bifidobacterium* were highly abundant in prebiotic-treated normotensive rodents and healthy normotensive controls. These acetate-producing bacterial taxa may have a role in the regulation of normal blood pressure (Li *et al.*, 2017; Ganesh *et al.*, 2018). Correlation analysis in our study revealed no associations between genera and blood pressure parameters. However, *Anaerovorax,* of Firmicutes phylum positively correlated with basal heart rate.

2.4.4 Cardiorespiratory responsiveness to vagal afferent nerve stimulation is unaffected by chronic antibiotic administration and faecal microbiota transfer

The afferent vagal pathway provides crucial signalling between the gut microbiota and the central nervous system (Forsythe *et al.*, 2014). Alterations in gut microbiota composition or diversity, resulting in differential production of bacterial metabolites, have been shown to influence afferent vagal traffic (Lal *et al.*, 2001; Bonaz *et al.*, 2018). Vagal afferents innervate the nucleus tractus solitarius, a critical relay hub in the integration of cardiorespiratory control (Foster *et al.*, 2017). The 5-HT_3 receptor agonist, PBG, stimulates pulmonary vagal afferent C-fibres manifesting the classical chemoreflex characterised by apnoea and post-apnoea tachypnoea, bradycardia and a fall in blood pressure (Dutta & Deshpande, 2010; Lucking *et al.*, 2018a). Manipulation of the gut microbiota could conceivably manifest

abnormal vagal afferent signalling and aberrant central processing of sensory inputs. However, in our study, there was no difference in the cardiorespiratory efferent responses to PBG challenge. We conclude that manipulation of the microbiota by ABX and FMT interventions does not alter the cardiorespiratory response to the vagal afferent pulmonary C-fibre stimulation, notwithstanding evidence of significant disruptions in brainstem monoamine concentrations. Whereas PBG can also induce neurotransmitter release centrally in the nucleus accumbens (Chen *et al.*, 1991) and the nucleus tractus solitarius (Hosford *et al.*, 2014), we confirmed in our study that cardiorespiratory effects were mediated exclusively by vagal afferent feedback since responses were abolished following bilateral cervical vagotomy. Examination of vagal afferent activation from other peripheral sites, notably the gut, was not performed in this study, but would be interesting to determine in future work.

2.4.5 Chronic antibiotic administration and faecal microbiota transfer alter brainstem monoamine and monoamine metabolite concentrations

We examined the concentrations of brainstem monoamines important in the neuromodulation of cardiorespiratory control with a particular interest in monoamines and metabolites that play a role in central chemoreception. Significant disruptions to monoamine, monoamine precursor and metabolite concentrations were determined in the brainstem of ABX and FMT rats, an outcome that coincides with depressed hypercapnic ventilation.

Noradrenaline is a potent modulator of breathing (Doi & Ramirez, 2008). We found no change in brainstem noradrenaline concentration between groups. 5-HT is a pivotal neuromodulator of the respiratory motor network and primarily has an excitatory effect on breathing (Richerson, 2004). It is well established that pharmacological manipulation of serotonergic signalling affects respiratory motor output (Fenik & Veasey, 2003; de Souza Moreno *et al.*, 2010). Transgenic mice lacking central 5-HT neurons show a significant reduction in the hypercapnic ventilatory response (Hodges & Richerson, 2008; Hodges *et al.*, 2008; Li & Nattie, 2008) and lesions of raphé serotonergic neurons decrease the respiratory response to hypercapnia (Dias *et al.*, 2007). Pharmacological manipulation of 5-HT affects ventilation and arousal during hypercapnia (Messier *et al.*, 2004; Buchanan *et al.*, 2015). Our data revealed a blunted ventilatory response to hypercapnia in ABX rats. However, 5-HT concentrations were not changed in ABX rats, thus, it is not likely that 5-HT is implicated in the depressed ventilatory responsiveness observed in ABX rats. 5-HT concentrations were

significantly increased in ABX-FMT compared with VEH with no change evident in VEH-FMT rats. This suggests that changes in brainstem 5-HT were not pivotal to hypercapnic ventilatory depression. Interestingly, an increase in 5-HT turnover was observed in the hippocampus and pre-frontal cortex following ABX treatment in rats (Hoban *et al.*, 2016), germ free mice (Clarke *et al.*, 2013) and acutely stressed mice (Desbonnet *et al.*, 2015).

Dopamine significantly contributes to the central control of breathing (Lalley, 2009). Transgenic mice lacking dopaminergic neurons or dopamine transport proteins exhibit severe breathing disturbances such as hypoventilation, apnoea and altered hypoxic ventilatory response (Nsegbe *et al.*, 2004; Vincent *et al.*, 2007). Similarly, blunted respiratory frequency during hypercapnic breathing was observed in rat models of Parkinson's disease with confirmed degeneration of tyrosine hydroxylase expressing neurons in the substantia nigra and a reduction in chemosensitive neurons (Phox2b-expressing and fos-activated) in the retrotrapezoid nucleus (Tuppy *et al.*, 2015; Oliveira *et al.*, 2017), a key brainstem site for CO_2 chemosensitivity (Guyenet & Bayliss, 2015). The modulatory influence of dopamine on respiratory physiology is complex and depends on target receptor sub-families (Kline *et al.*, 2002). There are 2 classes of dopamine receptors, D_1-like (D_1 and D_5) and D_2-like (D_2, D_3 and D_4) receptors (Beaulieu & Gainetdinov, 2011), with D_1, D_2 and D_4 receptors having a significant neuromodulatory role in respiration (Fujii *et al.*, 2004; Lalley, 2004, 2009). Dopaminergic neurons within the brainstem reinforce CO_2-dependent respiratory drive and increase minute ventilation, predominantly through the D_1 receptor (Lalley, 2004, 2008). Thus, it appears that D_1 receptor activation increases respiratory neuron excitability, whereas D_2 and D_4 receptor stimulation depresses respiratory rhythm (Fujii *et al.*, 2004; Lalley, 2004; Fujii *et al.*, 2006). Our data reveal an increase in brainstem dopamine turnover in ABX rats and depressed ventilation during hypercapnia compared with VEH rats. Similar findings are reported in Parkinson's disease models (Tuppy *et al.*, 2015; Blesa *et al.*, 2017; Oliveira *et al.*, 2017). An increase in the dopamine metabolite HVA was also evident in the cerebellum of ABX rats compared with VEH rats in our study (Appendix Table A.10). Increased concentrations of HVA were observed in the prefrontal cortex and amygdala of ABX-treated rodents (Desbonnet *et al.*, 2015; Hoban *et al.*, 2016). We observed depressed respiratory frequency responses to hypercapnic stress in ABX and FMT groups, which may have related to increased dopaminergic signalling via D_2 and D_4 receptors (Fujii *et al.*, 2004; Lalley, 2004; Fujii *et al.*, 2006).

Our findings demonstrate that disruption to the gut microbiota results in altered neurochemistry at the level of the brainstem and cerebellum, with striking effects on dopamine concentrations and dopamine turnover. Correlation analysis revealed significant associations between brainstem neurochemistry and genera from 6 phyla, suggesting a potential link. Of particular interest correlations were found between L-DOPA, DA, HVA and HVA/DA and genera predominantly of Firmicutes phylum; *Ruminococcaceae UCG-005*, *Peptoclostridium, Bacillus, Erysipelotrichaceae UCG-004, Ruminococcaceae UCG-011, Lachnoclostridium 10, Clostridiales vadinBB60* group uncultured bacterium and *Ruminococcaceae UCG-009*. Brainstem monoamines and metabolites also correlate with *Coriobacteriaceae* uncultured (Actinobacteria) *Bacteroidetes VC2.1 Bac22* uncultured (Bacteroidetes), *Gastranaerophilales* uncultured organism (Cyanobacteria), *Helicobacter* (Proteobacteria) and *Mucispirillum* (Deferribacteres). We acknowledge that correlations were often weak and in any event do not provide evidence of a mechanistic link. Disrupted brainstem neurochemistry is also evident in other models of microbiota perturbation. Germ free mice have increased 5-HT in hippocampal regions and acutely stressed and non-stressed ABX-treated animals have an increase in HVA in prefrontal cortex and amygdala (Clarke *et al.*, 2013; Desbonnet *et al.*, 2015; Hoban *et al.*, 2016). To assess if altered afferent vagal nerve communication (gut-brain axis) contributed to the altered brainstem neurochemistry and respiratory behaviour, future studies exploring manipulation of the gut microbiota in vagotomised animals are required. However, vagal axotomy may itself evoke plasticity within the brainstem neural circuits controlling cardiorespiratory control, which may be a confounding factor in such studies.

2.4.6 Chronic antibiotic administration and faecal microbiota transfer increase distal ileum permeability

Altered intestinal permeability has been described in various models of disrupted microbiota including a mouse model of autism (Golubeva *et al.*, 2017), spontaneously hypertensive rat (Santisteban *et al.*, 2017), and rat models of maternal separation stress (Gareau *et al.*, 2007) and pre-natal stress (Golubeva *et al.*, 2015). The dysfunctional barrier of the distal ileum in ABX rats in our study is consistent with reports of disrupted intestinal permeability in response to specific antibiotics, which also perturb the microbiota (Wlodarska *et al.*, 2011; Tulstrup *et al.*, 2015). An impaired epithelial barrier can induce low-grade inflammation and facilitate the passage of bacterial constituents, such as lipopolysaccharide across the epithelium into systemic tissues (Araujo *et al.*, 2017). It is conceivable that the 'leaky' distal ileum could have, at least partially, contributed to modulation of brainstem neurochemistry

and depressed ventilatory responsiveness to CO_2. However, ABX rats may have limited maladies associated with intestinal barrier breach due to reduced bacterial components and/or the direct effects of antibiotics on other inflammatory mediators.

The shifts evident in *Helicobacter* and *Mucispirillum* genera are of particular interest with respect to gastrointestinal health. Of critical importance, the highest log-fold change occurred in *Helicobacter*, which was significantly increased both in VEH-FMT and ABX-FMT rats compared with VEH rats. Guo *et al*. 2009 found that *Helicobacter pylori* was increased in the stomach of Balb/c mice in response to stress. A similar stress could have been evoked by the use of oral gavage, resulting in increased abundance of *Helicobacter*. The dominance of various species from *Helicobacter* genera in the gut microbiota coincides with gastrointestinal disorders in humans and rodents, often triggering intestinal inflammatory pathogenesis (Flahou *et al.*, 2013). A mucin degrading bacterium *Mucispirillum* was decreased in VEH-FMT and ABX-FMT rats compared with VEH. Increased abundance of *Mucispirillum* coincides with inflammatory response in germ-free mice (El Aidy *et al.*, 2014a), in a model of colitis (Rooks *et al.*, 2014), and in age-related inflammation in rodents (Conley *et al.*, 2016). It is plausible that *Helicobacter* proliferated at the expense of *Mucispirillum.* Intestinal pathogenesis could have occurred as a result of insults to the microbiota associated with our interventions.

2.4.7 Limitations

Our FMT strategy was designed to replenish the microbiota of ABX rats. To control for the FMT intervention, VEH rats also received FMT and were studied in parallel. However, FMT *per se* caused major disruption to the microbiota composition and diversity compared with VEH rats. As such, our study did not allow us to determine if restoration of normal (control) gut microbiota was associated with restoration of normal (control) brainstem neurochemistry and ventilatory responsiveness to hypercapnia. Whereas this is a limitation of the study, it nevertheless provided unexpected additional test groups (FMT groups), wherein gut microbiota disruptions were shown to be related to altered brainstem neurochemistry and blunted ventilatory responsiveness to CO_2, in essence confirming the observations made in ABX rats compared with VEH rats. Future studies could explore the capacity to transfer the phenotypes described in the present study from ABX donor to naïve recipient animals. Moreover, it would be interesting to explore FMT strategies designed to recover brainstem neurochemistry and ventilator responsiveness to hypercapnia in ABX-treated rats.

DNA concentrations in caecal samples from ABX rats were critically low, likely a result of the broad-spectrum antibiotic cocktail depleting bacteria and thus detectable bacterial DNA. This prevented the analysis of microbiota composition and diversity analysis as 16S rRNA sequencing was not possible in this group. Thus, correlation analysis was performed with metadata and microbiota composition from three groups (VEH, VEH-FMT and ABX-FMT).

Our study design was such that we were unable to perform correlations between breathing parameters and microbiota in ABX-treated rats, since ABX rats studied in the plethysmograph proceeded to FMT intervention.

2.4.8 Summary and conclusions

Using two modes to manipulate the gut microbiota (ABX and FMT), our study suggests that perturbation to the gut microbiota has consequences for brainstem neurochemistry and respiratory control. Our study reveals the capacity for chronic antibiotic administration and faecal microbiota transfer to affect respiratory behaviour, blunting a critical homeostatic reflex defence or integrated behavioural response to acute hypercapnic stress, with resultant consequences for acid-base status. Our results may have relevance to human respiratory disorders of the lungs or neural control networks, such as chronic obstructive pulmonary diseases and sleep disordered breathing, where there is evidence of altered gut microbiota composition. Blunted chemoreflex control of breathing, wherein arterial blood CO_2 levels can rise due to inadequate ventilatory drive, is a risk for the development of significant respiratory acidosis, with whole-body consequences. Our study adds to emerging evidence providing a rationale for manipulation of the gut microbiota as an adjunctive therapy in cardiorespiratory diseases.

2.5. Additional information

Competing interests: JFC is in receipt of research funding from 4D-Pharma, Mead Johnson, Nutricia, Dupont and Cremo and has been an invited speaker at meetings organised by Mead Johnson, Alkermes, Abbott Nutrition, Danone Nutricia and Janssen. All other authors report no financial, professional or personal conflicts of interest relating to this publication.

Funding: This project was funded by the Department of Physiology, and the APC Microbiome Ireland (funded by Science Foundation Ireland (SFI/12/RC/2273)), University College Cork, Ireland. The institution had no role in the study design, data collection, data analysis, interpretation or writing of the manuscript.

Acknowledgments: The authors wish to acknowledge the technical expertise of Dr. Paul Cotter, Dr. Fiona Crispie and Dr. Laura Finnegan from Teagasc Sequencing Facility at Moorepark and we thank them for their assistance with MiSeq sequencing. The authors are grateful to staff of the Biological Services Unit, University College Cork for their support with animal housing and welfare. We are grateful to Prof. Thomas Walther, Department of Pharmacology & Therapeutics, University College Cork for the use of equipment to measure cardiac contractility.

2.6. References

Adnan S, Nelson JW, Ajami NJ, Venna VR, Petrosino JF, Bryan RM, Jr. & Durgan DJ. (2017). Alterations in the gut microbiota can elicit hypertension in rats. *Physiological genomics* **49,** 96-104.

Alheid GF & McCrimmon DR. (2008). The chemical neuroanatomy of breathing. *Respiratory physiology & neurobiology* **164,** 3-11.

Almado CE, Machado BH & Leao RM. (2012). Chronic intermittent hypoxia depresses afferent neurotransmission in NTS neurons by a reduction in the number of active synapses. *The Journal of neuroscience : the official journal of the Society for Neuroscience* **32,** 16736-16746.

Araujo JR, Tomas J, Brenner C & Sansonetti PJ. (2017). Impact of high-fat diet on the intestinal microbiota and small intestinal physiology before and after the onset of obesity. *Biochimie* **141,** 97-106.

Bavis RW. (2005). Developmental plasticity of the hypoxic ventilatory response after perinatal hyperoxia and hypoxia. *Respir Physiol Neurobiol* **149,** 287-299.

Bavis RW, van Heerden ES, Brackett DG, Harmeling LH, Johnson SM, Blegen HJ, Logan S, Nguyen GN & Fallon SC. (2014). Postnatal development of eupneic ventilation and metabolism in rats chronically exposed to moderate hyperoxia. *Respiratory physiology & neurobiology* **198,** 1-12.

Beaulieu JM & Gainetdinov RR. (2011). The physiology, signaling, and pharmacology of dopamine receptors. *Pharmacological reviews* **63,** 182-217.

Bercik P, Denou E, Collins J, Jackson W, Lu J, Jury J, Deng Y, Blennerhassett P, Macri J, McCoy KD, Verdu EF & Collins SM. (2011). The intestinal microbiota affect central levels of brain-derived neurotropic factor and behavior in mice. *Gastroenterology* **141,** 599-609, 609 e591-593.

Blesa J, Trigo-Damas I, Dileone M, Del Rey NL, Hernandez LF & Obeso JA. (2017). Compensatory mechanisms in Parkinson's disease: Circuits adaptations and role in disease modification. *Experimental neurology* **298,** 148-161.

Bonaz B, Bazin T & Pellissier S. (2018). The Vagus Nerve at the Interface of the Microbiota-Gut-Brain Axis. *Front Neurosci* **12,** 49.

Bordenstein SR & Theis KR. (2015). Host Biology in Light of the Microbiome: Ten Principles of Holobionts and Hologenomes. *PLoS biology* **13,** e1002226.

Bravo JA, Forsythe P, Chew MV, Escaravage E, Savignac HM, Dinan TG, Bienenstock J & Cryan JF. (2011). Ingestion of Lactobacillus strain regulates emotional behavior and central GABA receptor expression in a mouse via the vagus nerve. *Proceedings of the National Academy of Sciences of the United States of America* **108,** 16050-16055.

Brinkman JE & Sharma S. (2018). Physiology, Respiratory Drive.

Buchanan GF, Smith HR, MacAskill A & Richerson GB. (2015). 5-HT2A receptor activation is necessary for CO2-induced arousal. *Journal of neurophysiology* **114,** 233-243.

Burns DP, Canavan L, Rowland J, O'Flaherty R, Brannock M, Drummond SE, O'Malley D, Edge D & O'Halloran KD. (2018). Recovery of respiratory function in mdx mice co-treated with neutralizing interleukin-6 receptor antibodies and urocortin-2. *The Journal of physiology* **596,** 5175-5197.

Burns DP, Roy A, Lucking EF, McDonald FB, Gray S, Wilson RJ, Edge D & O'Halloran KD. (2017). Sensorimotor control of breathing in the mdx mouse model of Duchenne muscular dystrophy. *The Journal of physiology* **595,** 6653-6672.

Burokas A, Arboleya S, Moloney RD, Peterson VL, Murphy K, Clarke G, Stanton C, Dinan TG & Cryan JF. (2017). Targeting the Microbiota-Gut-Brain Axis: Prebiotics Have Anxiolytic and Antidepressant-like Effects and Reverse the Impact of Chronic Stress in Mice. *Biological psychiatry* **82,** 472-487.

Burokas A, Moloney RD, Dinan TG & Cryan JF. (2015). Microbiota regulation of the Mammalian gut-brain axis. *Advances in applied microbiology* **91,** 1-62.

Caporaso JG, Kuczynski J, Stombaugh J, Bittinger K, Bushman FD, Costello EK, Fierer N, Pena AG, Goodrich JK, Gordon JI, Huttley GA, Kelley ST, Knights D, Koenig JE, Ley RE, Lozupone CA, McDonald D, Muegge BD, Pirrung M, Reeder J, Sevinsky JR, Turnbaugh PJ, Walters WA, Widmann J, Yatsunenko T, Zaneveld J & Knight R. (2010). QIIME allows analysis of high-throughput community sequencing data. In *Nature methods*, pp. 335-336. United States.

Chao A. (1984). Nonparametric estimation of the number of classes in a population. *Scandinavian Journal of statistics*, 265-270.

Chen JP, van Praag HM & Gardner EL. (1991). Activation of 5-HT3 receptor by 1-phenylbiguanide increases dopamine release in the rat nucleus accumbens. *Brain research* **543,** 354-357.

Clarke G, Grenham S, Scully P, Fitzgerald P, Moloney RD, Shanahan F, Dinan TG & Cryan JF. (2013). The microbiome-gut-brain axis during early life regulates the hippocampal serotonergic system in a sex-dependent manner. *Molecular psychiatry* **18,** 666-673.

Collins SM, Surette M & Bercik P. (2012). The interplay between the intestinal microbiota and the brain. *Nature reviews Microbiology* **10,** 735-742.

Conley MN, Wong CP, Duyck KM, Hord N, Ho E & Sharpton TJ. (2016). Aging and serum MCP-1 are associated with gut microbiome composition in a murine model. *PeerJ* **4,** e1854.

Cryan JF & Dinan TG. (2012). Mind-altering microorganisms: the impact of the gut microbiota on brain and behaviour. *Nature reviews Neuroscience* **13,** 701-712.

De Palma G, Blennerhassett P, Lu J, Deng Y, Park AJ, Green W, Denou E, Silva MA, Santacruz A, Sanz Y, Surette MG, Verdu EF, Collins SM & Bercik P. (2015). Microbiota and host determinants of behavioural phenotype in maternally separated mice. *Nature communications* **6,** 7735.

de Souza Moreno V, Bicego KC, Szawka RE, Anselmo-Franci JA & Gargaglioni LH. (2010). Serotonergic mechanisms on breathing modulation in the rat locus coeruleus. *Pflugers Archiv : European journal of physiology* **459,** 357-368.

Desbonnet L, Clarke G, Traplin A, O'Sullivan O, Crispie F, Moloney RD, Cotter PD, Dinan TG & Cryan JF. (2015). Gut microbiota depletion from early adolescence in mice: Implications for brain and behaviour. *Brain, behavior, and immunity* **48,** 165-173.

Dias MB, Nucci TB, Margatho LO, Antunes-Rodrigues J, Gargaglioni LH & Branco LG. (2007). Raphe magnus nucleus is involved in ventilatory but not hypothermic response to CO2. *Journal of applied physiology (Bethesda, Md : 1985)* **103,** 1780-1788.

Dinan TG & Cryan JF. (2017). The Microbiome-Gut-Brain Axis in Health and Disease. *Gastroenterology clinics of North America* **46,** 77-89.

Doi A & Ramirez JM. (2008). Neuromodulation and the orchestration of the respiratory rhythm. *Respiratory physiology & neurobiology* **164,** 96-104.

Doi A & Ramirez JM. (2010). State-dependent interactions between excitatory neuromodulators in the neuronal control of breathing. *The Journal of neuroscience : the official journal of the Society for Neuroscience* **30,** 8251-8262.

Durgan DJ, Ganesh BP, Cope JL, Ajami NJ, Phillips SC, Petrosino JF, Hollister EB & Bryan RM, Jr. (2016). Role of the Gut Microbiome in Obstructive Sleep Apnea-Induced Hypertension. *Hypertension* **67,** 469-474.

Dutta A & Deshpande SB. (2010). Cardio-respiratory reflexes evoked by phenylbiguanide in rats involve vagal afferents which are not sensitive to capsaicin. *Acta physiologica (Oxford, England)* **200,** 87-95.

Edgar RC. (2010). Search and clustering orders of magnitude faster than BLAST. *Bioinformatics (Oxford, England)* **26,** 2460-2461.

Edge D, Bradford A & O'Halloran KD. (2012). Chronic intermittent hypoxia increases apnoea index in sleeping rats. *Adv Exp Med Biol* **758,** 359-363.

El Aidy S, Derrien M, Aardema R, Hooiveld G, Richards SE, Dane A, Dekker J, Vreeken R, Levenez F, Dore J, Zoetendal EG, van Baarlen P & Kleerebezem M. (2014). Transient inflammatory-like state and microbial dysbiosis are pivotal in establishment of mucosal homeostasis during colonisation of germ-free mice. *Beneficial microbes* **5,** 67-77.

Faith DP. (1992). Conservation evaluation and phylogenetic diversity. *Biological conservation* **61,** 1-10.

Fenik P & Veasey SC. (2003). Pharmacological characterization of serotonergic receptor activity in the hypoglossal nucleus. *American journal of respiratory and critical care medicine* **167,** 563-569.

Flahou B, Haesebrouck F, Smet A, Yonezawa H, Osaki T & Kamiya S. (2013). Gastric and enterohepatic non-Helicobacter pylori Helicobacters. *Helicobacter* **18 Suppl 1,** 66-72.

Forsythe P, Bienenstock J & Kunze WA. (2014). Vagal pathways for microbiome-brain-gut axis communication. *Advances in experimental medicine and biology* **817,** 115-133.

Foster JA, Rinaman L & Cryan JF. (2017). Stress & the gut-brain axis: Regulation by the microbiome. *Neurobiology of stress* **7,** 124-136.

Fournier S, Steele S, Julien C, Gulemetova R, Caravagna C, Soliz J, Bairam A & Kinkead R. (2013). Gestational stress promotes pathological apneas and sex-specific disruption of respiratory control development in newborn rat. *J Neurosci* **33,** 563-573.

Fujii M, Umezawa K & Arata A. (2004). Dopaminergic modulation on respiratory rhythm in rat brainstem-spinal cord preparation. *Neuroscience research* **50,** 355-359.

Fujii M, Umezawa K & Arata A. (2006). Dopamine desynchronizes the pace-making neuronal activity of rat respiratory rhythm generation. *The European journal of neuroscience* **23,** 1015-1027.

Fuller DD & Mitchell GS. (2017). Respiratory neuroplasticity - Overview, significance and future directions. *Experimental neurology* **287,** 144-152.

Ganesh BP, Nelson JW, Eskew JR, Ganesan A, Ajami NJ, Petrosino JF, Bryan RM, Jr. & Durgan DJ. (2018). Prebiotics, Probiotics, and Acetate Supplementation Prevent Hypertension in a Model of Obstructive Sleep Apnea. *Hypertension (Dallas, Tex : 1979)* **72,** 1141-1150.

Garcia AJ, 3rd, Zanella S, Koch H, Doi A & Ramirez JM. (2011). Chapter 3--networks within networks: the neuronal control of breathing. *Progress in brain research* **188,** 31-50.

Gareau MG, Jury J, MacQueen G, Sherman PM & Perdue MH. (2007). Probiotic treatment of rat pups normalises corticosterone release and ameliorates colonic dysfunction induced by maternal separation. *Gut* **56,** 1522-1528.

Golubeva AV, Crampton S, Desbonnet L, Edge D, O'Sullivan O, Lomasney KW, Zhdanov AV, Crispie F, Moloney RD, Borre YE, Cotter PD, Hyland NP, O'Halloran KD, Dinan TG, O'Keeffe GW & Cryan JF. (2015). Prenatal stress-induced alterations in major physiological systems correlate with gut microbiota composition in adulthood. *Psychoneuroendocrinology* **60,** 58-74.

Golubeva AV, Joyce SA, Moloney G, Burokas A, Sherwin E, Arboleya S, Flynn I, Khochanskiy D, Moya-Perez A, Peterson V, Rea K, Murphy K, Makarova O, Buravkov S, Hyland NP, Stanton C, Clarke G, Gahan CGM, Dinan TG & Cryan JF. (2017). Microbiota-related Changes in Bile Acid & Tryptophan Metabolism are Associated with Gastrointestinal Dysfunction in a Mouse Model of Autism. *EBioMedicine* **24,** 166-178.

Grasa L, Abecia L, Forcen R, Castro M, de Jalon JA, Latorre E, Alcalde AI & Murillo MD. (2015). Antibiotic-Induced Depletion of Murine Microbiota Induces Mild Inflammation and Changes in Toll-Like Receptor Patterns and Intestinal Motility. *Microbial ecology* **70,** 835-848.

Gulemetova R & Kinkead R. (2011). Neonatal stress increases respiratory instability in rat pups. *Respiratory physiology & neurobiology* **176,** 103-109.

Guo G, Jia KR, Shi Y, Liu XF, Liu KY, Qi W, Guo Y, Zhang WJ, Wang T, Xiao B & Zou QM. (2009). Psychological stress enhances the colonization of the stomach by Helicobacter pylori in the BALB/c mouse. *Stress (Amsterdam, Netherlands)* **12,** 478-485.

Guyenet PG & Bayliss DA. (2015). Neural Control of Breathing and CO2 Homeostasis. *Neuron* **87,** 946-961.

Halkjaer SI, Christensen AH, Lo BZS, Browne PD, Gunther S, Hansen LH & Petersen AM. (2018). Faecal microbiota transplantation alters gut microbiota in patients with irritable bowel syndrome: results from a randomised, double-blind placebo-controlled study. *Gut* **67,** 2107-2115.

Haouzi P, Bell HJ, Notet V & Bihain B. (2009). Comparison of the metabolic and ventilatory response to hypoxia and H2S in unsedated mice and rats. *Respiratory physiology & neurobiology* **167,** 316-322.

Hoban AE, Moloney RD, Golubeva AV, McVey Neufeld KA, O'Sullivan O, Patterson E, Stanton C, Dinan TG, Clarke G & Cryan JF. (2016). Behavioural and neurochemical consequences of chronic gut microbiota depletion during adulthood in the rat. *Neuroscience* **339,** 463-477.

Hocker AD, Stokes JA, Powell FL & Huxtable AG. (2017). The impact of inflammation on respiratory plasticity. *Experimental neurology* **287,** 243-253.

Hodges MR & Richerson GB. (2008). Interaction between defects in ventilatory and thermoregulatory control in mice lacking 5-HT neurons. *Respiratory physiology & neurobiology* **164,** 350-357.

Hodges MR, Tattersall GJ, Harris MB, McEvoy SD, Richerson DN, Deneris ES, Johnson RL, Chen ZF & Richerson GB. (2008). Defects in breathing and thermoregulation in mice with near-complete absence of central serotonin neurons. *The Journal of neuroscience : the official journal of the Society for Neuroscience* **28,** 2495-2505.

Hosford PS, Mifflin SW & Ramage AG. (2014). 5-hydroxytryptamine-mediated neurotransmission modulates spontaneous and vagal-evoked glutamate release in the nucleus of the solitary tract effect of uptake blockade. *The Journal of pharmacology and experimental therapeutics* **349,** 288-296.

Jiang ZD, Alexander A, Ke S, Valilis EM, Hu S, Li B & DuPont HL. (2017). Stability and efficacy of frozen and lyophilized fecal microbiota transplant (FMT) product in a mouse model of Clostridium difficile infection (CDI). *Anaerobe* **48,** 110-114.

Karbach SH, Schonfelder T, Brandao I, Wilms E, Hormann N, Jackel S, Schuler R, Finger S, Knorr M, Lagrange J, Brandt M, Waisman A, Kossmann S, Schafer K, Munzel T, Reinhardt C & Wenzel P. (2016). Gut Microbiota Promote Angiotensin II-Induced Arterial Hypertension and Vascular Dysfunction. *Journal of the American Heart Association* **5**.

Kelly CR, Khoruts A, Staley C, Sadowsky MJ, Abd M, Alani M, Bakow B, Curran P, McKenney J, Tisch A, Reinert SE, Machan JT & Brandt LJ. (2016a). Effect of Fecal Microbiota Transplantation on Recurrence in Multiply Recurrent Clostridium difficile Infection: A Randomized Trial. *Annals of internal medicine* **165,** 609-616.

Kelly JR, Borre Y, C OB, Patterson E, El Aidy S, Deane J, Kennedy PJ, Beers S, Scott K, Moloney G, Hoban AE, Scott L, Fitzgerald P, Ross P, Stanton C, Clarke G, Cryan JF & Dinan TG. (2016b). Transferring the blues: Depression-associated gut microbiota induces neurobehavioural changes in the rat. *Journal of psychiatric research* **82,** 109-118.

Kinkead R, Guertin PA & Gulemetova R. (2013). Sex, stress and their influence on respiratory regulation. *Current pharmaceutical design* **19,** 4471-4484.

Kline DD, Takacs KN, Ficker E & Kunze DL. (2002). Dopamine modulates synaptic transmission in the nucleus of the solitary tract. *Journal of neurophysiology* **88,** 2736-2744.

Kootte RS, Levin E, Salojarvi J, Smits LP, Hartstra AV, Udayappan SD, Hermes G, Bouter KE, Koopen AM, Holst JJ, Knop FK, Blaak EE, Zhao J, Smidt H, Harms AC, Hankemeijer T, Bergman J, Romijn HA, Schaap FG, Olde Damink SWM, Ackermans MT, Dallinga-Thie GM, Zoetendal E, de Vos WM, Serlie MJ, Stroes ESG, Groen AK & Nieuwdorp M. (2017). Improvement of Insulin Sensitivity after Lean Donor Feces in Metabolic Syndrome Is Driven by Baseline Intestinal Microbiota Composition. *Cell metabolism* **26,** 611-619 e616.

Kumar P & Prabhakar NR. (2012). Peripheral chemoreceptors: function and plasticity of the carotid body. *Comprehensive Physiology* **2,** 141-219.

Lal S, Kirkup AJ, Brunsden AM, Thompson DG & Grundy D. (2001). Vagal afferent responses to fatty acids of different chain length in the rat. *American journal of physiology Gastrointestinal and liver physiology* **281,** G907-915.

Lalley PM. (2004). Dopamine1 receptor agonists reverse opioid respiratory network depression, increase CO2 reactivity. *Respiratory physiology & neurobiology* **139,** 247-262.

Lalley PM. (2008). Opioidergic and dopaminergic modulation of respiration. *Respiratory physiology & neurobiology* **164,** 160-167.

Lalley PM. (2009). D1/D2-dopamine receptor agonist dihydrexidine stimulates inspiratory motor output and depresses medullary expiratory neurons. *American journal of physiology Regulatory, integrative and comparative physiology* **296,** R1829-1836.

Le Roy T, Llopis M, Lepage P, Bruneau A, Rabot S, Bevilacqua C, Martin P, Philippe C, Walker F, Bado A, Perlemuter G, Cassard-Doulcier AM & Gerard P. (2013). Intestinal microbiota determines development of non-alcoholic fatty liver disease in mice. *Gut* **62,** 1787-1794.

Li A & Nattie E. (2008). Serotonin transporter knockout mice have a reduced ventilatory response to hypercapnia (predominantly in males) but not to hypoxia. *The Journal of physiology* **586,** 2321-2329.

Li J, Zhao F, Wang Y, Chen J, Tao J, Tian G, Wu S, Liu W, Cui Q, Geng B, Zhang W, Weldon R, Auguste K, Yang L, Liu X, Chen L, Yang X, Zhu B & Cai J. (2017). Gut microbiota dysbiosis contributes to the development of hypertension. *Microbiome* **5,** 14.

Li Q, Wang C, Tang C, He Q, Zhao X, Li N & Li J. (2015). Successful treatment of severe sepsis and diarrhea after vagotomy utilizing fecal microbiota transplantation: a case report. *Critical care (London, England)* **19,** 37.

Lucking EF, Murphy KH, Burns DP, Jaisimha AV, Barry-Murphy KJ, Dhaliwal P, Boland B, Rae MG & O'Halloran KD. (2018a). No evidence in support of a prodromal respiratory control signature in the TgF344-AD rat model of Alzheimer's disease. *Respiratory physiology & neurobiology*.

Lucking EF, O'Connor KM, Strain CR, Fouhy F, Bastiaanssen TFS, Burns DP, Golubeva AV, Stanton C, Clarke G, Cryan JF & O'Halloran KD. (2018b). Chronic intermittent hypoxia disrupts cardiorespiratory homeostasis and gut microbiota composition in adult male guinea-pigs. *EBioMedicine*.

Luczynski P, McVey Neufeld KA, Oriach CS, Clarke G, Dinan TG & Cryan JF. (2016). Growing up in a Bubble: Using Germ-Free Animals to Assess the Influence of the Gut Microbiota on Brain and Behavior. *The international journal of neuropsychopharmacology / official scientific journal of the Collegium Internationale Neuropsychopharmacologicum (CINP)* **19**.

Manichanh C, Reeder J, Gibert P, Varela E, Llopis M, Antolin M, Guigo R, Knight R & Guarner F. (2010). Reshaping the gut microbiome with bacterial transplantation and antibiotic intake. *Genome research* **20,** 1411-1419.

Messier ML, Li A & Nattie EE. (2004). Inhibition of medullary raphe serotonergic neurons has age-dependent effects on the CO2 response in newborn piglets. *Journal of applied physiology (Bethesda, Md : 1985)* **96,** 1909-1919.

Moreno-Indias I, Torres M, Montserrat JM, Sanchez-Alcoholado L, Cardona F, Tinahones FJ, Gozal D, Poroyko VA, Navajas D, Queipo-Ortuno MI & Farre R. (2015). Intermittent hypoxia alters gut microbiota diversity in a mouse model of sleep apnoea. *The European respiratory journal* **45,** 1055-1065.

Moreno-Indias I, Torres M, Sanchez-Alcoholado L, Cardona F, Almendros I, Gozal D, Montserrat JM, Queipo-Ortuno MI & Farre R. (2016). Normoxic Recovery Mimicking Treatment of Sleep Apnea Does Not Reverse Intermittent Hypoxia-Induced Bacterial Dysbiosis and Low-Grade Endotoxemia in Mice. *Sleep* **39,** 1891-1897.

Neufeld KM, Kang N, Bienenstock J & Foster JA. (2011). Reduced anxiety-like behavior and central neurochemical change in germ-free mice. *Neurogastroenterology and motility : the official journal of the European Gastrointestinal Motility Society* **23,** 255-264, e119.

Nsegbe E, Wallen-Mackenzie A, Dauger S, Roux JC, Shvarev Y, Lagercrantz H, Perlmann T & Herlenius E. (2004). Congenital hypoventilation and impaired hypoxic response in Nurr1 mutant mice. *The Journal of physiology* **556,** 43-59.

O'Mahony SM, Felice VD, Nally K, Savignac HM, Claesson MJ, Scully P, Woznicki J, Hyland NP, Shanahan F, Quigley EM, Marchesi JR, O'Toole PW, Dinan TG & Cryan JF. (2014). Disturbance of the gut microbiota in early-life selectively affects visceral pain in adulthood without impacting cognitive or anxiety-related behaviors in male rats. *Neuroscience* **277,** 885-901.

Oliveira LM, Moreira TS, Kuo FS, Mulkey DK & Takakura AC. (2016). alpha1- and alpha2-adrenergic receptors in the retrotrapezoid nucleus differentially regulate breathing in anesthetized adult rats. *Journal of neurophysiology* **116,** 1036-1048.

Oliveira LM, Tuppy M, Moreira TS & Takakura AC. (2017). Role of the locus coeruleus catecholaminergic neurons in the chemosensory control of breathing in a Parkinson's disease model. *Experimental neurology* **293,** 172-180.

Patel S & Majmundar SH. (2018). Physiology, Carbon Dioxide Absorption And Retention.

Peng YJ, Nanduri J, Yuan G, Wang N, Deneris E, Pendyala S, Natarajan V, Kumar GK & Prabhakar NR. (2009). NADPH oxidase is required for the sensory plasticity of the carotid body by chronic intermittent hypoxia. *The Journal of neuroscience : the official journal of the Society for Neuroscience* **29,** 4903-4910.

Richerson GB. (2004). Serotonergic neurons as carbon dioxide sensors that maintain pH homeostasis. *Nature reviews Neuroscience* **5,** 449-461.

Rooks MG, Veiga P, Wardwell-Scott LH, Tickle T, Segata N, Michaud M, Gallini CA, Beal C, van Hylckama-Vlieg JE, Ballal SA, Morgan XC, Glickman JN, Gevers D, Huttenhower C & Garrett WS. (2014). Gut microbiome composition and function in experimental colitis during active disease and treatment-induced remission. *The ISME journal* **8,** 1403-1417.

Santisteban MM, Qi Y, Zubcevic J, Kim S, Yang T, Shenoy V, Cole-Jeffrey CT, Lobaton GO, Stewart DC, Rubiano A, Simmons CS, Garcia-Pereira F, Johnson RD, Pepine CJ & Raizada MK. (2017). Hypertension-Linked Pathophysiological Alterations in the Gut. *Circulation research* **120,** 312-323.

Soliz J, Tam R & Kinkead R. (2016). Neonatal Maternal Separation Augments Carotid Body Response to Hypoxia in Adult Males but Not Female Rats. *Frontiers in physiology* **7,** 432.

Stilling RM, Moloney GM, Ryan FJ, Hoban AE, Bastiaanssen TF, Shanahan F, Clarke G, Claesson MJ, Dinan TG & Cryan JF. (2018). Social interaction-induced activation of RNA splicing in the amygdala of microbiome-deficient mice. *eLife* **7**.

Sudo N, Chida Y, Aiba Y, Sonoda J, Oyama N, Yu XN, Kubo C & Koga Y. (2004). Postnatal microbial colonization programs the hypothalamic-pituitary-adrenal system for stress response in mice. *The Journal of physiology* **558,** 263-275.

Sugita T, Kanamaru M, Iizuka M, Sato K, Tsukada S, Kawamura M, Homma I & Izumizaki M. (2015). Breathing is affected by dopamine D2-like receptors in the basolateral amygdala. *Respiratory physiology & neurobiology* **209,** 23-27.

Tenorio-Lopes L, Henry MS, Marques D, Tremblay ME, Drolet G, Bretzner F & Kinkead R. (2017). Neonatal maternal separation opposes the facilitatory effect of castration on the respiratory response to hypercapnia of the adult male rat: evidence for the involvement of the medial amygdala. *Journal of neuroendocrinology*.

Teppema LJ & Baby S. (2011). Anesthetics and control of breathing. *Respiratory physiology & neurobiology* **177,** 80-92.

Tripathi A, Melnik AV, Xue J, Poulsen O, Meehan MJ, Humphrey G, Jiang L, Ackermann G, McDonald D, Zhou D, Knight R, Dorrestein PC & Haddad GG. (2018). Intermittent Hypoxia and Hypercapnia, a Hallmark of Obstructive Sleep Apnea, Alters the Gut Microbiome and Metabolome. *mSystems* **3**.

Tulstrup MV, Christensen EG, Carvalho V, Linninge C, Ahrne S, Hojberg O, Licht TR & Bahl MI. (2015). Antibiotic Treatment Affects Intestinal Permeability and Gut Microbial Composition in Wistar Rats Dependent on Antibiotic Class. *PloS one* **10,** e0144854.

Tuppy M, Barna BF, Alves-Dos-Santos L, Britto LR, Chiavegatto S, Moreira TS & Takakura AC. (2015). Respiratory deficits in a rat model of Parkinson's disease. *Neuroscience* **297,** 194-204.

Turner JR, Rill BK, Carlson SL, Carnes D, Kerner R, Mrsny RJ & Madara JL. (1997). Physiological regulation of epithelial tight junctions is associated with myosin light-chain phosphorylation. *The American journal of physiology* **273,** C1378-1385.

Vincent SG, Waddell AE, Caron MG, Walker JK & Fisher JT. (2007). A murine model of hyperdopaminergic state displays altered respiratory control. *FASEB journal : official publication of the Federation of American Societies for Experimental Biology* **21,** 1463-1471.

Wlodarska M, Willing B, Keeney KM, Menendez A, Bergstrom KS, Gill N, Russell SL, Vallance BA & Finlay BB. (2011). Antibiotic treatment alters the colonic mucus layer and predisposes the host to exacerbated Citrobacter rodentium-induced colitis. *Infection and immunity* **79,** 1536-1545.

Wurm P, Spindelboeck W, Krause R, Plank J, Fuchs G, Bashir M, Petritsch W, Halwachs B, Langner C, Hogenauer C & Gorkiewicz G. (2017). Antibiotic-Associated Apoptotic

Enterocolitis in the Absence of a Defined Pathogen: The Role of Intestinal Microbiota Depletion. *Critical care medicine* **45,** e600-e606.

Yang T, Santisteban MM, Rodriguez V, Li E, Ahmari N, Carvajal JM, Zadeh M, Gong M, Qi Y, Zubcevic J, Sahay B, Pepine CJ, Raizada MK & Mohamadzadeh M. (2015). Gut dysbiosis is linked to hypertension. *Hypertension (Dallas, Tex : 1979)* **65,** 1331-1340.

Chapter 3. Chronic intermittent hypoxia disrupts cardiorespiratory homeostasis and gut microbiota composition in adult male guinea-pigs

Eric F. Lucking[a *], Karen M. O'Connor[a,b,c *], Conall R. Strain[d], Fiona Fouhy[c,d,], Thomaz F. S. Bastiaanssen[b,c], David P. Burns[a], Anna V. Golubeva[c], Catherine Stanton[c,d], Gerard Clarke[c,f], John F. Cryan[b,c], Ken D. O'Halloran[a,c]

[a]*Department of Physiology, School of Medicine, College of Medicine & Health, University College Cork, Cork, Ireland*

[b]*Department of Anatomy & Neuroscience, School of Medicine, College of Medicine & Health, University College Cork, Cork, Ireland*

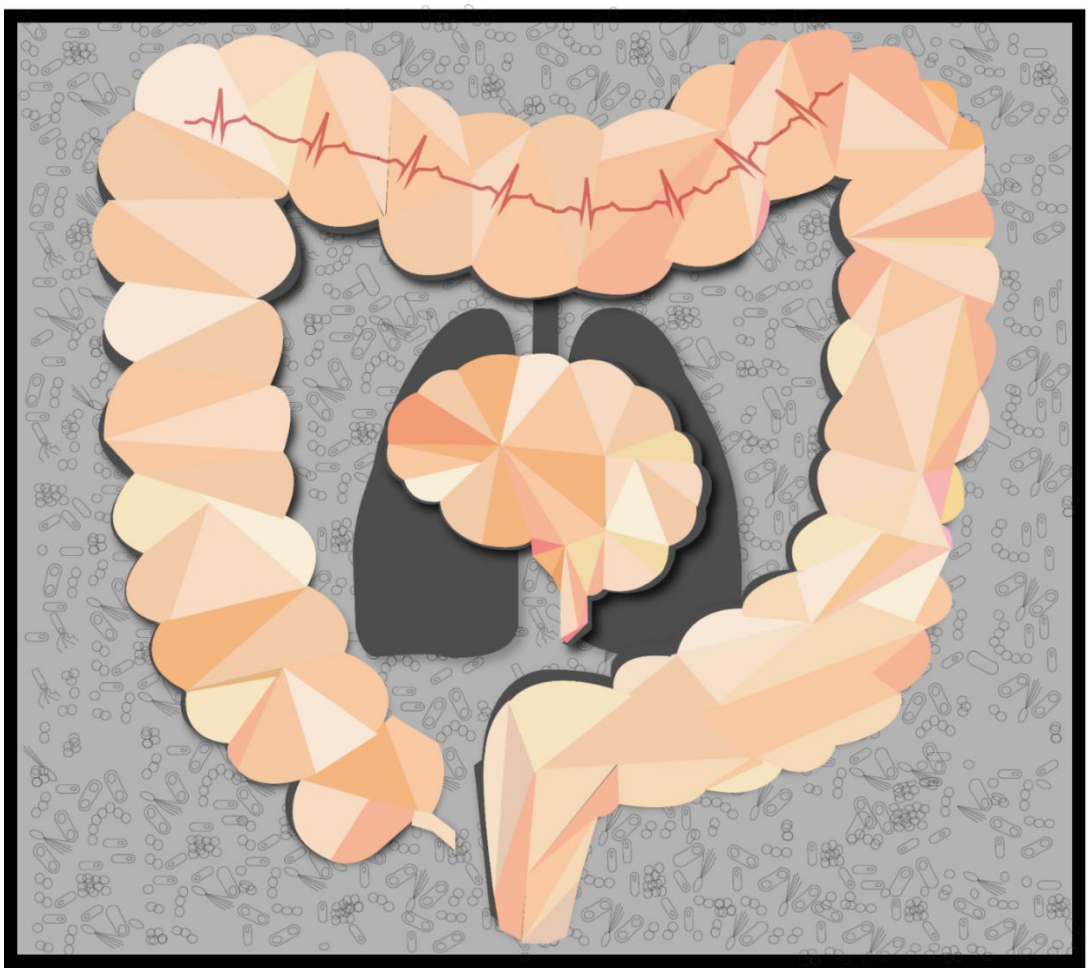
[c]*APC Microbiome Ireland, University College Cork, Cork, Ireland*

[d]*Teagasc Food Research Centre, Moorepark, Fermoy, County Cork, Ireland*

[f]*Department of Psychiatry and Neurobehavioural Science, School of Medicine, College of Medicine & Health, University College Cork, Cork, Ireland*

Published in EbioMedicine

Volume 38, December 2018, Pages 191-205, doi: 10.1016/j.ebiom.2018.11.010.



This image was generated by Kiran Sandhu. It is now on the EbioMedicine website.

Abstract

Background: Carotid body (peripheral oxygen sensor) sensitisation is pivotal in the development of chronic intermittent hypoxia (CIH)-induced hypertension. We sought to determine if exposure to CIH, modelling human sleep apnoea, adversely affects cardiorespiratory control in guinea-pigs, a species with hypoxia-insensitive carotid bodies. We reasoned that CIH-induced disruption of gut microbiota would evoke cardiorespiratory morbidity.

Methods: Adult male guinea-pigs were exposed to CIH (6.5% O_2 at nadir, 6 cycles.hour^{-1}) for 8h.day^{-1} for 12 consecutive days.

Findings: CIH-exposed animals established reduced faecal microbiota species richness, with increased relative abundance of Bacteroidetes and reduced relative abundance of Firmicutes bacteria. Urinary corticosterone and noradrenaline levels were unchanged in CIH-exposed animals, but brainstem noradrenaline concentrations were lower compared with sham. Baseline ventilation was equivalent in CIH-exposed and sham animals; however, respiratory timing variability, sigh frequency and ventilation during hypoxic breathing were all lower in CIH-exposed animals. Baseline arterial pressure was unaffected by exposure to CIH, but β-adrenoceptor-dependent tachycardia and blunted bradycardia during phenylephrine-induced pressor responses was evident compared with sham controls.

Interpretation: Increased carotid body chemo-afferent signalling appears obligatory for the development of CIH-induced hypertension and elevated chemoreflex control of breathing commonly reported in mammals, with hypoxia-sensitive carotid bodies. However, we reveal that exposure to modest CIH alters gut microbiota richness and composition, brainstem neurochemistry, and autonomic control of heart rate, independent of carotid body sensitisation, suggesting modulation of breathing and autonomic homeostasis via the microbiota-gut-brainstem axis. The findings have relevance to human sleep-disordered breathing.

Funding: The Department of Physiology, and APC Microbiome Ireland, UCC.

Keywords: Chronic intermittent hypoxia; hypertension; cardiorespiratory control; microbiome; guinea-pig

Research in Context

Evidence before this study: Chronic intermittent hypoxia (CIH) is the primary pathogenic factor associated with obstructive sleep apnoea. Carotid body (CB) sensitisation is widely implicated in the development of CIH-induced cardiorespiratory morbidity, including hypertension.

Added value of this study: We provide evidence of residual cardiorespiratory dysfunction in CIH-exposed guinea-pigs, a mammalian species with hypoxia-insensitive CBs, with a potential interplay via the microbiota-gut-brainstem axis. CIH alters microbiota richness and composition, brainstem neurochemistry and cardiorespiratory control, independent of CB sensitisation, suggesting modulation of brainstem control via the microbiota-gut-brainstem axis.

Implications of all the available evidence: Our findings have implications for human sleep-disordered breathing and contribute to an emerging interest in manipulation of the microbiota as an adjunctive therapy in human disease.

3.1. Introduction

Exposure to chronic intermittent hypoxia (CIH) mimicking the recurring episodic oxygen fluctuations that are characteristic of human sleep apnoea causes sympathetic nervous system hyperactivity and systemic hypertension (Lesske *et al.*, 1997; Dick *et al.*, 2007; Moraes *et al.*, 2012; Prabhakar *et al.*, 2015; Del Rio *et al.*, 2016). There is considerable evidence that exposure to CIH sensitises the carotid bodies---the dominant peripheral oxygen sensors---increasing chemo-afferent traffic to the brainstem, with consequential changes in autonomic outflow that serve to increase blood pressure (Peng *et al.*, 2014a; Moya *et al.*, 2016; Nanduri *et al.*, 2017). Fletcher and colleagues were the first to describe CIH-induced hypertension, highlighting the pivotal roles of carotid body chemoreceptors and sympatho-excitation in driving the hypertensive phenotype (Fletcher *et al.*, 1992b; Lesske *et al.*, 1997). The hypoxic sensitivity of the carotid body is elevated after exposure to CIH, which manifests increased hypoxic ventilatory and sympathetic responsiveness to chemo-stimulation (Peng *et al.*, 2003; Huang *et al.*, 2009). Hypertension is a consistent feature of various models of CIH in several mammalian species (Brooks *et al.*, 1997; Iturriaga & Alcayaga, 2007; Lucking *et al.*, 2014; Moreno-Indias *et al.*, 2015), including human subjects (Tamisier *et al.*, 2009). The significance of these findings is that enhanced peripheral sensory facilitation may serve to destabilise cardiorespiratory control, with resultant sympathetic nervous over-activity, leading to diurnal hypertension. Moreover, respiratory stability decreases in rats exposed to CIH, with evidence of increased propensity for central apnoea (Edge *et al.*, 2012; Donovan *et al.*, 2014; Souza *et al.*, 2015b), which disrupts respiratory-sympathetic coupling (Machado *et al.*, 2017) potentially establishing a vicious cycle of disrupted breathing and blood pressure in people with sleep apnoea.

Carotid body denervation or ablation blocks CIH-induced persistent elevations in blood pressure, with studies revealing that an intact peripheral chemosensory network appears essential for the development of respiratory plasticity, sympathetic nervous system hyperactivity and systemic hypertension after exposure to CIH (Fletcher *et al.*, 1992b; Lesske *et al.*, 1997; Edge *et al.*, 2012; Moraes & Machado, 2015; Del Rio *et al.*, 2016; Prabhakar, 2016). However, interruption of peripheral sensory input can give rise to central respiratory network reconfiguration and can establish a persistent hypoventilation (Mouradian *et al.*, 2012). Thus, whereas carotid bodies are implicated in the development and maintenance of CIH-induced cardiorespiratory morbidity, it is not clear if they are obligatory. There is clear evidence of CIH-induced plasticity in other key sites of the cardiorespiratory control network,

including cells of the nucleus tractus solitarius (Costa-Silva *et al.*, 2012), respiratory-related cells of the medullary network (Moraes *et al.*, 2012) and rhythmogenic cells of the pre-Bötzinger complex (Garcia *et al.*, 2017). Prabhakar and colleagues have revealed that epigenetic changes in the medulla oblongata dependent on increased chemoafferent input arising from exposure to CIH result in redox-dependent persistently elevated sympathetic outflow to target tissues implicated in the control of blood pressure (Nanduri *et al.*, 2017). However, neurons of the rostral ventrolateral medulla that govern spinal vasomotor neurons are excited by systemic hypoxia in carotid body denervated rats demonstrating that the carotid body is not obligatory to the hypoxic recruitment of sympathetic neurons *per se* (Sun & Reis, 1994). There is also evidence of direct effects of CIH on respiratory-related neurons within the medulla, and altered respiratory-autonomic coupling with implications for cardiovascular control (Garcia *et al.*, 2017; Machado *et al.*, 2017). Indeed, it is well recognised that exposure to CIH evokes adverse effects in various tissues, including end-effector organs of the cardio-respiratory system i.e. respiratory muscles (Skelly *et al.*, 2012; McDonald *et al.*, 2014) and cardiomyocytes (Chen *et al.*, 2008), which predisposes to cardiorespiratory morbidity. Moreover, there is the possibility that exposure to CIH indirectly affects host physiology. Intriguingly, exposure to CIH alters the gut microbiome (Moreno-Indias *et al.*, 2015; Tripathi *et al.*, 2018) and metabolome (Tripathi *et al.*, 2018) and CIH-induced alterations in microbiota composition remains perturbed even during extended normoxic recovery periods (Moreno-Indias *et al.*, 2016).

The microbiota are increasingly recognised as orchestrators of host physiology, brain and behaviour extending to cardiovascular homeostasis (Bravo *et al.*, 2011; Golubeva *et al.*, 2015; Durgan, 2017). Transplant of gut microbiota from spontaneously hypertensive rats into normotensive, microbiome-compromised control rats triggers the development of a hypertensive phenotype with evidence of a positive correlation between systolic blood pressure and *Lactobacillus* bacteria (Adnan *et al.*, 2017). Similarly, gut microbiota samples transferred from hypertensive donors (animal model of sleep apnoea fed a high-fat diet) to normotensive recipient rats caused gut microbiome disruption and hypertension (Durgan *et al.*, 2016). Reduced microbiota diversity and richness is established in hypertensive patients compared with normotensive controls (Li *et al.*, 2017). Furthermore, faecal transplant from hypertensive human donors into germ-free mice establishes higher blood pressures than faecal transplants from normotensive human donors (Li *et al.*, 2017). Collectively, these findings provided the rationale for our hypothesis that CIH-induced alterations in gut

microbiota modulate cardiorespiratory control via altered microbe-gut-brainstem signalling, independent of carotid body plasticity.

For a large number of problems there will be some animal of choice or a few such animals on which it can be most conveniently studied.

August Krogh ---The Progress of Physiology, 1929.

Examination of the putative effects of CIH-induced alterations to the microbiome and resultant influences on cardiorespiratory control in mammals are complicated by the dominant effect of exposure to CIH on carotid body function. Ablation of the carotid bodies to remove their contribution to CIH-induced cardiorespiratory morbidity (Del Rio *et al.*, 2016) is confounded by the potential for redundancy in hypoxia-sensing and central reconfiguration of the respiratory network in the absence of a major afferent drive to breathe. However, the carotid bodies of the guinea-pig are structurally and biochemically 'normal' (Kummer *et al.*, 1989) and yet the guinea-pig carotid body is generally insensitive to hypoxia (Schwenke *et al.*, 2007). Of interest, the carotid body of the guinea-pig is responsive to cyanide, severe hypoxia and to hypercapnia and as such is 'functional' but lacks the inherent capacity to respond to moderate hypoxaemia; moreover, it appears that the contribution of the carotid body to eupnoeic drive to breathe in the guinea-pig is negligible (Schwenke *et al.*, 2007). Because of these unique characteristics, we reasoned that guinea-pigs serve as a useful experimental model to explore the effects of exposure to CIH on cardiorespiratory control, as all afferent and efferent pathways maintain their physiological connections, therefore putative CIH-induced effects on cardiorespiratory control can be explored without a dominant influence of the carotid bodies.

Our major aim was to explore the effects of exposure to CIH on blood pressure in guinea-pigs, mammals with hypoxia-insensitive carotid bodies. We reasoned that exposure to CIH, utilising a paradigm that causes hypertension in rats (Ray *et al.*, 2015), would not evoke hypertension supporting suggestions of an obligatory role for carotid body sensitisation in the manifestation of CIH-induced hypertension. We also explored the potential for residual cardiorespiratory effects of exposure to CIH with a focus on the gut microbiota as a potential protagonist in CIH-related cardiorespiratory dysfunction.

3.2. Materials and Methods

3.2.1 Ethical approval

All procedures on live animals were performed under licence from the Government of Ireland Department of Health (B100/4498) in accordance with National and European Union legislation, with prior ethical approval by University College Cork (AEEC #2013/035). Experiments were carried out in accordance with guidelines laid down by University College Cork Animal Welfare Body, and conform to the principles and regulations described by Grundy (2015).

3.2.2 Chronic intermittent hypoxia animal model

Adult male Duncan Hartley guinea pigs (n=16; purchased from Envigo, UK) were randomly assigned to one of two groups: sham (810 ± 66g; mean ± SD; n=8) and CIH exposed (816 ± 60g; n=8). Animals were housed in standard cages in a temperature (20.4±0.6°C) and humidity-controlled (46.8±6.6%) environment on a 12h light:12h dark cycle, with *ad libitum* access to standard guinea-pig chow and water. The CIH group was placed in environmental chambers wherein ambient oxygen concentration was tightly-controlled using a dynamic oxygen/nitrogen controller (Oxycycler™; Biospherix, New York, NY, USA). Animals assigned to the CIH group were exposed to repeated 10-minute cycles consisting of 5 minutes of exposure to hypoxia (nadir, $FiO_2 = 0.065$, balance N_2) and 5 minutes of normoxia ($FiO_2 = 0.21$; balance N_2) for eight hours.day^{-1} for twelve consecutive days during the light phase. Contemporaneously, sham animals were exposed to room air in the same room with similar environmental cues for the duration of the study. Cardiorespiratory parameters were assessed on day 13, the day subsequent to the final episodes of CIH or sham exposure.

3.2.3 Assessment of respiratory flow in awake guinea-pigs

Whole-body plethysmography: Respiratory flow recordings were recorded in unrestrained, unanaesthetised awake guinea-pigs during quiet rest using the technique of whole-body plethysmography (Buxco Ltd., St. Paul, Minneapolis, USA). CIH-exposed and sham guinea-pigs were introduced into custom plethysmograph chambers with room air flushed through each chamber (4L/min) ensuring the maintenance of O_2 and CO_2 environmental conditions. Animals were allowed to settle during an acclimation period of 40 minutes to ensure the animals were habituated to the new environment.

Following the acclimation period, baseline respiratory parameters were assessed during a 10 to 15 minute steady-state normoxia period ($FiO_2 = 0.21$; balance N_2). This was followed by a

10 minute poikilocapnic hypoxia challenge (FiO_2=0.10; balance N_2). Following hypoxia, each animal was re-exposed to normoxia and after an adequate recovery period of at least 10 minutes a second baseline period was established. Animals were subsequently exposed to a 10 minute hypercapnia challenge ($FiCO_2$ = 0.05; balance O_2). Respiratory variables including respiratory frequency (f_R), minute ventilation (V_E), tidal volume (V_T), inspiratory time (T_i), expiratory time (T_e) and mean inspiratory flow (V_T/T_i) were recorded on a breath-by-breath basis for offline analysis. Concentrations of O_2 and CO_2 in gas entering and exiting the plethysmograph chambers were constantly measured (O_2 and CO_2 analyser; ADInstruments, Colorado Springs, CO, USA). O_2 consumption (VO_2) and CO_2 production (VCO_2) in sham and CIH-exposed animals were determined.

Data analysis for whole-body plethysmography: FinePointe software (Buxco Research Systems, Wilmington, NC, USA) generated breath-by-breath analysis of respiratory flow signals. Artefacts related to movement, exploratory behaviour and sniffing were excluded from analysis by software algorithm and by visual inspection of the recording sessions designated for analyses. Baseline breathing and metabolic analyses were averaged from the 10-15 minute period of stable normoxia. Data are reported for the final 5 minutes of each of the hypoxic and hypercapnic challenges allowing for steady-state assessment of respiratory and metabolic parameters. V_T, V_E, V_T/Ti, VO_2 and VCO_2 were normalised for body mass (per 100g). Additionally, respiratory flow signals were analysed for the occurrence of apnoeas and augmented breaths (sighs) during normoxic breathing. The criterion for apnoea was a pause in breathing greater than two missed breaths, expressed as either a spontaneous or post-sigh apnoea as previously described (Edge *et al.*, 2012). Sighs were defined as an augmented breath twice the amplitude of the average V_T. Poincaré plots expressing breath-to-breath (BBn) versus next breath-to-breath interval (BBn+1) for 200 consecutive breaths were extrapolated for sham and CIH-exposed guinea-pigs. Respiratory timing variability in total breath duration and expiratory time were analysed for short-term (SD1) and long-term (SD2) variability.

3.2.4 Assessment of cardiorespiratory parameters under urethane anaesthesia

Surgical protocol: Subsequent to plethysmography challenges, animals were anaesthetised via an intraperitoneal injection of 20% w/v urethane (1.5 $g.kg^{-1}$), placed in the supine body position and core body temperature was maintained at 38.5°C using a rectal temperature probe and homeothermic blanket system (Harvard Apparatus, Holliston, MA, USA). Depth of anaesthesia was regularly monitored by absence of the pedal withdrawal to noxious pinch;

supplemental doses of anaesthetic were administered as required. A mid-cervical tracheotomy was performed and the right jugular vein was cannulated for intravenous (i.v.) infusion of supplemental anaesthetic and drugs. The left femoral artery was cannulated for the recording of arterial blood pressure as well as withdrawal of arterial blood gas samples. Arterial blood gas, pH and electrolyte assessment was performed using specialised cartridges (EG6+; Abbott Laboratories Ltd, Dublin Ireland) and a portable blood gas analyser (I-STAT; Abbot Laboratories Ltd). All animals were maintained with a bias flow of supplemental O_2 to maintain an arterial oxygen saturation (SaO_2; Starr Life Sciences, PA, USA) above 95% during basal conditions. A pneumotachometer was connected to a tracheal cannula to determine tracheal flow (Hans Rudolph Inc., KS, USA). A side arm of the tracheal cannula was connected to a CO_2 analyser (microCapStar End-Tidal CO_2 analyser; CWE Inc., USA), which provided measurement of tracheal end-tidal CO_2. All data were digitised and displayed using LabChart v7 (ADInstruments).

Experimental protocol: Following a 30-minute period of stabilisation following surgical procedures, an arterial blood gas sample was acquired and baseline parameters were assessed. The bias flow was manipulated using an electronic gas mixer (GSM-3 Gas Mixer; CWE Inc.) to administer chemostimulation challenges to the animals. A graded hypercapnic challenge was performed in which animals were exposed to increasing levels of inspired carbon dioxide: $FiCO_2$=0.05 and 0.10 (supplemental O_2; balance N_2) consecutively for 5 minutes each with no recovery period between hypercapnic stimuli. A minimum of 10 minutes was allowed for the recovery of stable parameter recordings between all challenges. Animals were subsequently challenged with a 5 minute hypoxia challenge (FiO_2=0.1; balance N_2), followed by a 5 minute asphyxic challenge (FiO_2=0.1, $FiCO_2$=0.05, balance N_2). Subsequent to the inspired gas challenges and after recovery, sodium cyanide (NaCN; 200µg/kg) was administered i.v. to stimulate the type 1 glomus cell of the carotid body. Some guinea-pigs presented with an apnoea upon NaCN infusion and were excluded from data analysis as no hypoxic ventilatory response was elicited. Successively, intravenous administrations of phenylephrine (PE; 50µg.kg^{-1}), propranolol (PROP; 1mg.kg^{-1}) and hexamethonium (25mg.kg^{-1}) were used to assess cardiovascular responses to pharmacological manipulation. Due to the intrinsic hypotensive phenotype of guinea-pigs (Table 3.3), some animals failed to recover from the otherwise transient hypotensive state induced pharmacologically by propranolol (sham, n=2; CIH, n=3) and hexamethonium (sham, n=1; CIH, n=1). Animals were euthanised by i.v. anaesthetic overdose and various organs

were collected, weighed and frozen at -80°C for subsequent analysis. Lungs were weighed wet, dried at 37°C for a minimum of 48 hours and reweighed.

Data analysis of cardiorespiratory parameters in anaesthetised guinea-pigs: Baseline parameters were averaged over 10 minutes of stable recording and data are presented as absolute units. Cardiorespiratory responses during graded hypercapnic, hypoxic and asphyxic challenges were averaged in 10 second time bins and were compared with the respective 1-minute pre-challenge baseline. To assess dynamic responses to drug administration (NaCN, PE, PROP and hexamethonium), cardiorespiratory responses were averaged into 1-second time bins and were compared with the respective 1-minute pre-challenge baseline. Cardiorespiratory responses to chemostimulation and drug administration are expressed as a percent change from the preceding baseline value.

3.2.5 Analysis of brainstem homogenates and urine

Brainstem monoamine concentrations determined by high-performance liquid chromatography (HPLC) coupled to electrochemical detection: Brainstems were removed from the guinea-pigs immediately after euthanasia, snap frozen in isopentane cooled in liquid nitrogen and transferred to -80˚C for long-term storage. Each brainstem was separated into two distinct regions, pons and medulla oblongata at -20˚C. The dissected pons and medulla oblongata tissues were sonicated in 1 ml of chilled mobile phase, spiked with 2ng/20µl of a N-methyl 5-HT (internal standard) (Bandelin Sonolus HD 2070) for six by six second bursts. The mobile phase contained 0.1 M citric acid (Alkem/Reagecon), 0.01 mM ethylenediaminetetraacetic acid (EDTA), 0.1 M sodium dihydrogen phosphate (Alkem/Reagecon), 5.6 mM octane-1-sulphonic acid (Alkem/Reagecon) and 9% (v/v) methanol, adjusted to pH 2.8 using 4N sodium hydroxide. Samples were centrifuged at 14,000 *g* for 20 min at 4˚C (MIKRO 22R refrigerated centrifuge). Cell pellets were stored at -80 ˚C. The supernatant (20µl) was injected onto the HPLC system coupled to electrochemical detection. The HPLC system consisted of a SCL 10-Avp system controller, LC-10AS pump, SIL-10A autoinjector (with sample cooler maintained at 4˚C), CTO-10A oven, LECD 6A electrochemical detector and an online Gastorr Degasser. A reverse-phase column (kinetex 2.6u C18 100Amm X 4.6mm), maintained at 30˚C, was employed in the separation (flow rate 0.9 ml/min). The monoamines, dopamine, noradrenaline (NA), serotonin (5-HT), and monoamine metabolite 5-hydroxyindoleacetic acid (5-HIAA), $_{L}$-3,4-dihydroxyphenylalanine ($_{L}$-DOPA) and homovanillic acid (HVA) were assessed. The monoamines were identified by their characteristic retention times, which were determined by standard injections run at regular intervals during the sample analysis. Chromatographs were processed using Class-

VP5 software and allowed the identification of the desired monoamines. Concentrations were calculated using analyte:internal standard peak response ratios.

Urine immunoassays: Urine samples collected from anaesthetised animals were stored at -80 ˚C until use. After storage, samples were thawed and concentrations of corticosterone (ENZO Life Sciences, UK), noradrenaline (Abnova) and creatinine (Sigma-Aldrich, Ireland.) were determined (sham n=6; CIH n=6) using commercially available enzyme-linked immunosorbent assay kits according to the manufacturers' instructions. A spectrophotometer (SpectraMax M3, Molecular devices) was used in reading absorbance for each assay. Urine samples were diluted 50-fold to determine corticosterone concentrations and 100-fold to determine creatinine and catecholamine concentrations. Urinary catecholamine and corticosterone concentrations were normalised to creatinine concentration of the urine, which provided a biomarker of urine production.

3.2.6 Microbiota composition analysis of faecal content

Faecal content DNA extraction: Faecal content was removed from the guinea-pig rectum and snap frozen in liquid nitrogen for long-term storage. DNA was extracted from the faecal material using the QIAamp DNA Stool Mini Kit (Qiagen, Venlo, Netherlands) according to the manufacturer's instructions, but including an additional bead-beating step at the beginning of the procedure for mechanical lysis. 200mg of each faecal sample was homogenised in the extraction buffer and transferred to 2ml screw cap tubes containing 2 x 2.3mm, 0.2g of 1.0mm and 0.2g of 0.1mm zirconia/silica beads before being subjected to a 3-minute bead-beating step using a Mini-Beadbeater-16 (Bispec, Bartlesville, USA). The following steps were in accordance with the manufacturer's instructions. The obtained faecal genomic DNA was quantified using the Qubit broad range DNA kit (Qubit, London, UK), measured on a Qubit 3.0 fluorometer (Qubit, London, UK), normalised to 5ng/µl before following the Illumina 16S rRNA Metagenomic Sequencing Library protocol.

16S rRNA Gene sequence-based microbiota analysis: The V3-V4 hypervariable region of the 16S rRNA gene was amplified and prepared for sequencing, the amplicon products were purified with Agencourt AMPure XP kit (Backman Coulter, Pasadena, USA). Amplicon PCR negative controls were utilised and verified through a 1.5% agarose gel made up with a tris base, acetic acid and EDTA buffer with Midori green stain (100V for 30 mins; Nippon genetics, 52351 Dueren, Germany). In the next step the purified product underwent an index PCR step using the Nextere XT index primer kit (Illumina, San Diego, USA). Following this a second purification step occurred with Agencourt AMPure XP. The index PCR products were

quantified using the Qubit high sensitivity DNA kit (Qubit, London, UK) and measured on Qubit 3.0. The PCR products were normalised and pooled before being sequenced on the MiSeq sequencing platform (Illumina, San Diego, USA) using a 2 x 250bp cycle kit, according to standard Illumina sequencing protocols at the Teagasc sequencing facility, Teagasc Food Research Centre, Fermoy, County Cork, Ireland.

Bioinformatic sequence analysis: Briefly, 250 base paired-end sequences were assembled using FLASH (FLASH: fast length adjustment of short reads to improve genome assemblies). Further processing of paired-end reads including quality filtering based on a quality score > 25 and removal of mismatched barcodes and sequences below length thresholds was completed using QIIME version 1.9.0 (Quantitative Insights Into Microbial Ecology). Sequences were quality checked (denoising, chimera detection) and the remaining sequences were clustered into operational taxonomic units (OTUs) using USEARCH v7 (64-bit). OTUs were aligned using PyNAST (PyNAST; a flexible tool for aligning sequence to a template alignment) and taxonomy was assigned using BLAST against the SILVA SSURef database release 123. Data was rarefied to 60,000 reads. Alpha diversity indices were generated in QIIME and the beta diversity Bray Curtis index was calculated in R software package. Relative abundance of bacterial taxa was expressed as % of identified sequences.

3.2.7 Statistical analysis

Statistical analysis on microbiota data was carried out in SPSS version 24 and R statistical environment (R version 3.4.4). GraphPad Prism Software (GraphPad Software, San Diego, CA, USA) was used for all other statistical analysis and for the generation of graphs. Data are presented as mean ± SD, median (IQR) or box and whisker plots (median, IQR, minimum and maximum values). Data were checked for a normal distribution with a Shapiro-Wilk test and for homogeneity of variances with Levene's test. Two-tailed Student's unpaired *t* test and non-parametric Mann-Whitney *U* test were used, where appropriate, unless otherwise stated. Brainstem monoamine concentrations were assessed using two-way ANOVA (treatment and brainstem region as two independent factors) with Bonferroni post-hoc tests. Pearson correlation coefficients were used to assess associations between brainstem monoamines and physiological parameters.

Bacterial taxa that were detected in fewer than three samples in each group were omitted from the subsequent analysis. Principal coordinate analysis (PCoA) plots were generated from Bray-Curtis dissimilarity matrices using the Vegan and Car packages in R. Differences in Bray-Curtis dissimilarity on the PCoA were assessed by PERMANOVA with the vegan package

in R. The most substantially changed bacterial genera (p<0.053) were chosen for the construction of the Z-score heatmap with the ggplot2 package in R. LEfSe analysis (43) was carried out using Calypso (v8.72) (44) with Chloroplast and Cyanobacteria counts removed. Hierarchical All Against All (HAllA) was used to detect correlations between microbiota data and the physiological measurements. Statistical significance was accepted at p<0.05. The Benjamini-Hochberg adjustment procedure was applied with the false discovery rate (FDR) set at 20% to correct for multiple testing.

3.3. Results

3.3.1 Baseline ventilation and ventilatory responses to chemostimulation in sham and CIH-exposed awake guinea-pigs.

Baseline ventilation and metabolism in sham and CIH-exposed awake guinea-pigs: Baseline minute ventilation (Fig. 3.1e; p=0.545) and the ventilatory equivalent ($V_E/V\mathrm{CO_2}$) during normoxia (Fig. 3.1h; p=0.201) were equivalent in sham and CIH-exposed guinea-pigs. Basal O_2 consumption and CO_2 production (Table 3.1) were similar in sham and CIH-exposed guinea-pigs. Exposure to acute hypoxia (FiO_2=0.10) failed to evoke an excitatory ventilatory response (Fig. 3.1f; p=0.798); CO_2 production during exposure to hypoxia was higher in CIH-exposed guinea-pigs (1.00 ± 0.09 vs 1.15 ± 0.19 $ml.min^{-1}.100g^{-1}$; p= 0.067), such that ($V_E/V\mathrm{CO_2}$) during hypoxia was lower in CIH-exposed guinea-pigs compared with sham guinea-pigs (Fig. 3.1i; p<0.001). Minute ventilation during hypercapnia (Fig. 3.1g; p=0.180) and $V_E/V\mathrm{CO_2}$ during exposure to CO_2 (Fig. 3.1j; p=0.613) were equivalent in sham and CIH-exposed guinea-pigs.

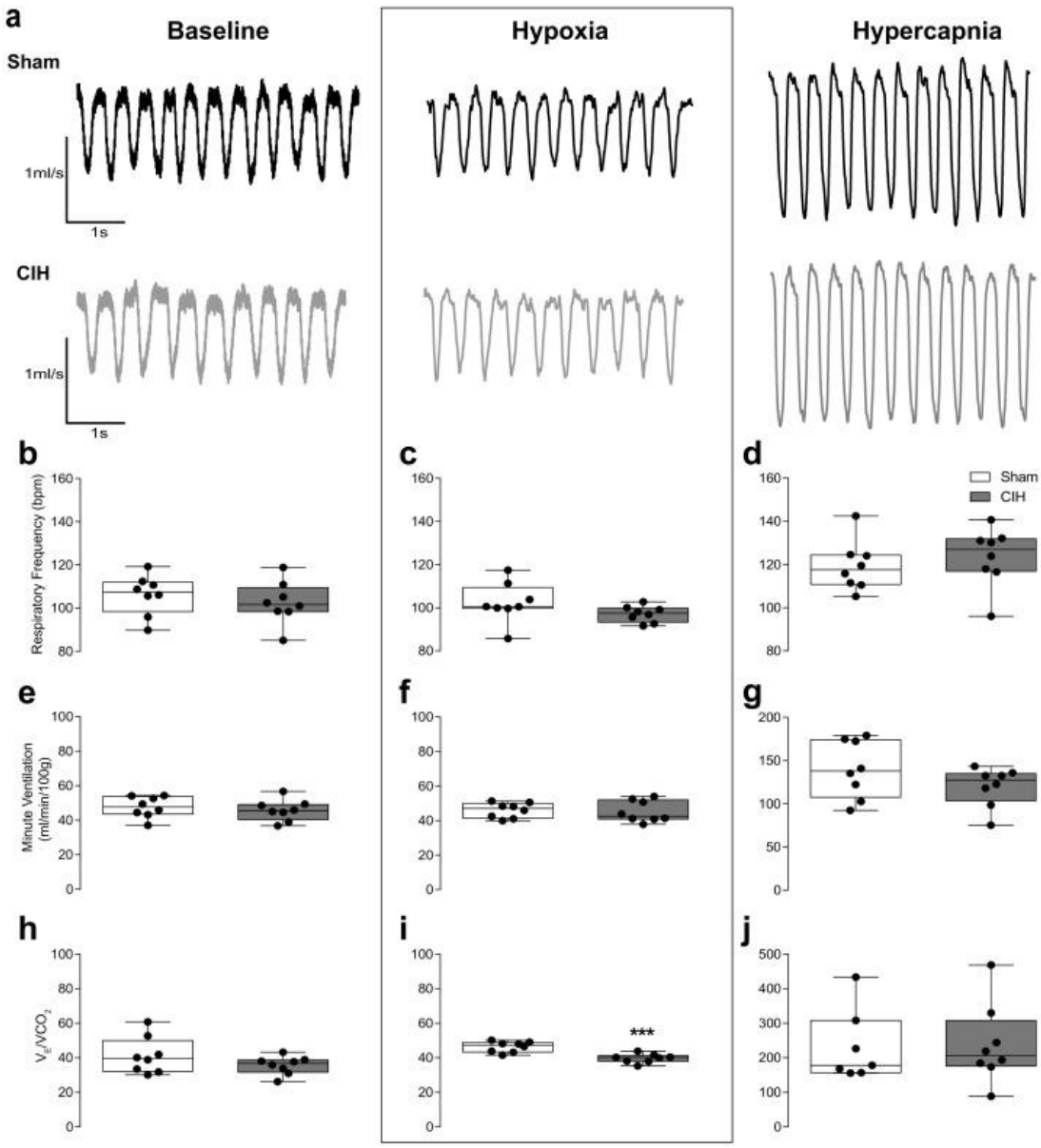


Figure 3. 1 CIH does not significantly affect baseline, hypoxic or hypercapnic ventilation in guinea-pigs.

(a) Representative respiratory airflow traces during normoxic, hypoxic and hypercapnic ventilation in Sham (black) and CIH-exposed (grey) guinea-pigs; inspiration represented by downward deflections. b-j) Group data for respiratory frequency (b-d) minute ventilation (e-g) and the ventilatory coefficient (h-j) in sham and CIH-exposed guinea-pigs during normoxic (b, e, h), hypoxic (c, f, i) and hypercapnic (d, g, j) ventilation. Values are expressed as box and whisker plots (median, 25–75 percentiles and minimum and maximum values). Groups were statistically compared by unpaired Student's t tests. ***p<0.001 compared with sham.

	Sham (n=8)	CIH (n=8)	p-value
V_T (ml/100g)	0.462 ± 0.502	0.454 ± 0.066	0.781
T_i (ms)	227 ± 23	239 ± 25	0.351
T_e (ms)	341 ± 57	363 ± 38	0.384
V_T/T_i (ml/s/100g)	2.03 ± 0.23	1.91 ± 0.28	0.341
VO_2 (ml/min/100g)	1.33 ± 0.61	1.75 ± 0.31	0.103
VCO_2 (ml/min/100g)	1.25 ± 0.27	1.32 ± 0.20	0. 603
VCO_2/VO_2	1.15 ± 0.57	0.76 ± 0.11	**0.038**

Table 3. 1 Baseline ventilation and metabolic parameters in sham and CIH-exposed awake guinea-pigs.

V_T, tidal volume; T_i, Inspiratory time; T_e, expiratory time; V_T/T_i, inspiratory flow; VO_2, oxygen consumption; VCO_2, carbon dioxide production. Data are shown as mean ± SD and were statistically compared using unpaired two-tailed Student's *t* tests.

Respiratory timing indices in sham and CIH-exposed awake guinea-pigs: Fig. 3.2 displays Poincaré plots of breath-to-breath period (BBn) and subsequent interval (BBn+1) during baseline breathing both for expiratory duration (T_e; Fig. 3.2a) and total breath duration (T_{tot}; Fig. 3.2b). Assessment of the short-term (SD1) and long-term (SD2) variability of respiratory timing revealed lower values in CIH-exposed guinea-pigs compared with sham guinea-pigs. Long-term variability for T_e (Fig. 3.2d; p=0.026), and both short-term (Fig. 3.2e; p=0.007) and long-term T_{tot} (Fig. 3.2f; p=0.048) were each lower in CIH-exposed guinea-pigs compared with sham animals.

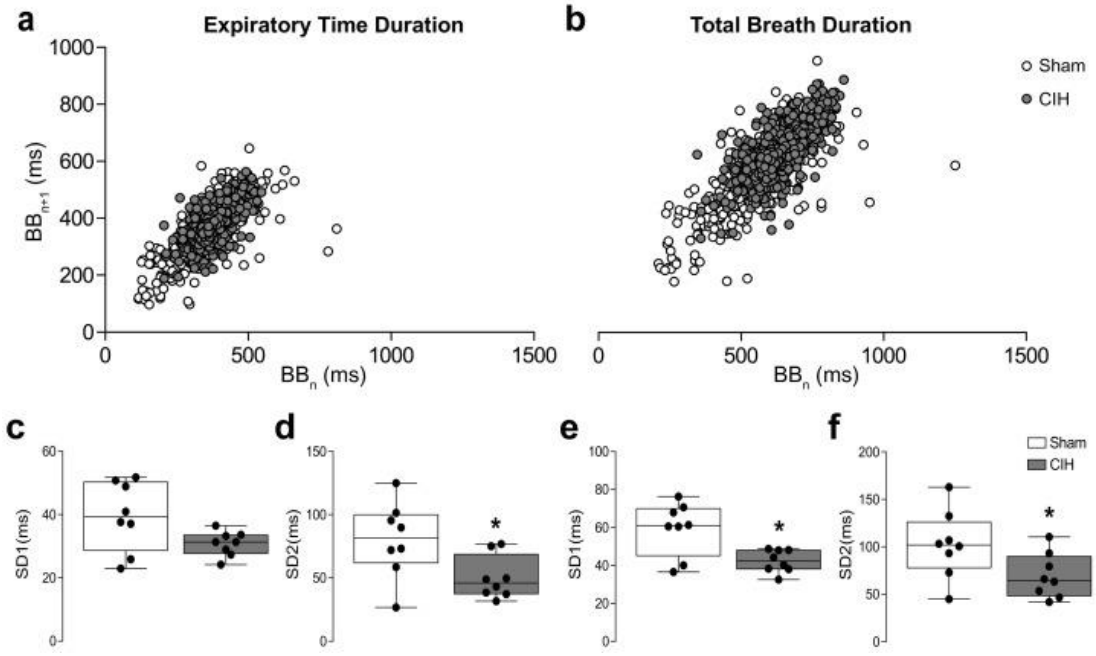


Figure 3. 2 Normoxic breathing variability is reduced in CIH-exposed awake guinea-pigs.

Poincaré plots of breath-to-breath (BBn) and next breath-to-breath interval (BBn+1) of time to expire (a) and total breath duration (b) during normoxic breathing in Sham (n = 8) and CIH-exposed (n = 8) guinea-pigs. Group data for average expiratory time short-term (c) and long-term (d) variability of breathing in sham and CIH-exposed guinea-pigs. Average total breath duration short-term (e) and long-term (f) variability of breathing in sham and CIH-exposed guinea-pigs. Values (c-f) are expressed as box and whisker plots (median, 25–75 percentiles and minimum and maximum values). Groups were statistically compared by unpaired Student's t tests. *p<0.05 compared with sham.

Expression of sighs and apnoeas in sham and CIH-exposed awake guinea-pigs: Sigh frequency was lower in CIH-exposed animals compared with sham animals (Fig. 3.3b; p=0.015). Lower sigh frequency was also observed during hypoxic (Fig. 3.3c; p=0.016) and hypercapnic ventilation (Fig. 3.3d; p=0.026) in CIH-exposed guinea-pigs compared with sham guinea-pigs. Sigh amplitude was equivalent in both groups during normoxia, hypoxia and hypercapnia (p>0.05). Spontaneous apnoeas were absent in sham and CIH-exposed guinea pigs. Post-sigh apnoeas were infrequent, however they were more prevalent in sham guinea-pigs (n=5) compared with CIH-exposed (n=2) guinea-pigs. Owing to the low apnoea count, statistical analysis was not performed on post-sigh apnoea data.

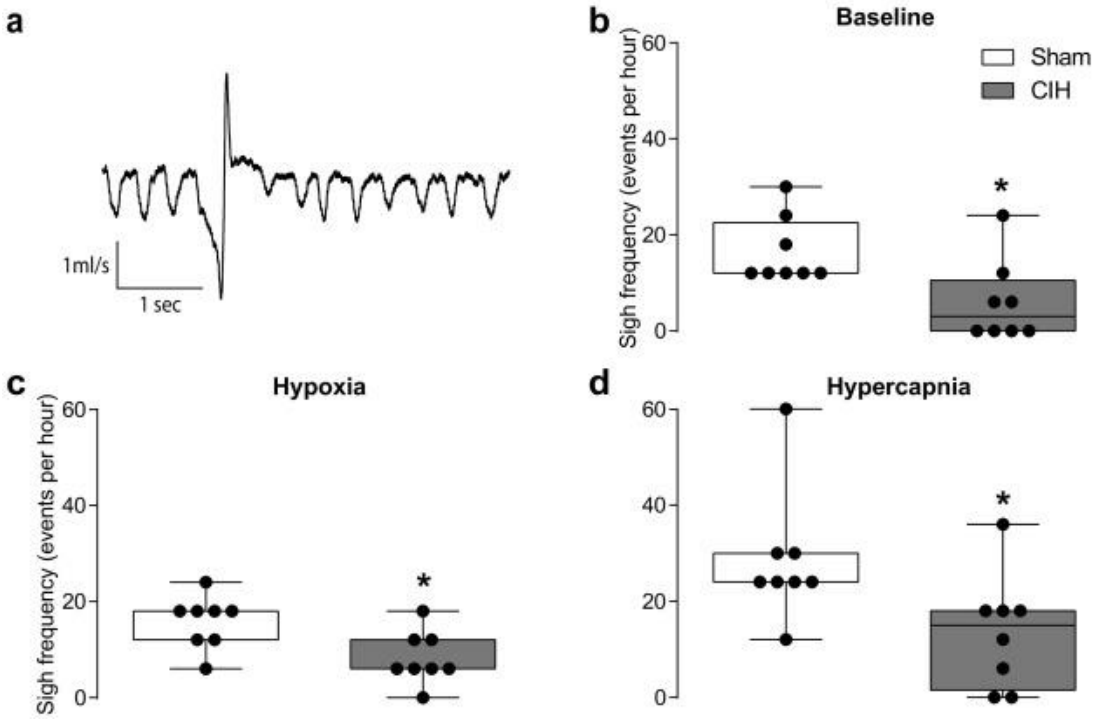


Figure 3. 3 Sigh frequency is reduced in CIH-exposed awake guinea-pigs.

(a) Representative trace of respiratory airflow demonstrating an augmented breath (sigh); inspiration represented by downward deflections. Group data for sigh frequency during normoxic (b), hypoxic (c) and hypercapnic ventilation (d) in Sham (n=8) and CIH-exposed (n=8) guinea pigs. Values (b-d) are expressed as box and whisker plots (median, 25–75 percentiles and minimum and maximum values). Groups were statistically compared by unpaired Student's t tests or non-parametric Mann-Whitney *U* test where appropriate. **p*<0.05 compared with sham.

3.3.2 Cardiorespiratory parameters in sham and CIH-exposed anaesthetised guinea-pigs.

Baseline respiratory parameters in sham and CIH-exposed anaesthetised guinea-pigs: Baseline arterial blood gases were similar in both groups (Table 3.2). Arterial blood bicarbonate concentration was lower (p=0.023) in CIH-exposed guinea-pigs compared with sham animals, consistent with a trend towards lower values for $PaCO_2$ (Table 3.2). Higher f_R and V_E was evident in CIH-exposed guinea-pigs compared with sham guinea-pigs (Table 3.3), but $ETCO_2$ values were similar in CIH-exposed and sham animals (Table 3.3).

Cardiovascular responsiveness in sham and CIH-exposed anaesthetised guinea-pigs: Guinea pigs exposed to 12 consecutive days of CIH did not develop systemic hypertension (Table 3.3); however, a significant tachycardia was evident in CIH-exposed guinea-pigs compared with sham animals. Left ventricular weights tended to be heavier in CIH-exposed guinea-pigs compared with sham guinea-pigs suggesting the onset of development of left ventricular hypertrophy (Table 3.4) in the absence of hypertension (no increase in afterload). There was a trend towards an increased haemoglobin concentration in CIH-exposed animals compared with sham animals (Table 3.2). Urinary concentrations of noradrenaline and corticosterone were not different in CIH-exposed animals compared with sham animals (Table 3.4).

	Sham (n=8)	CIH (n=8)	p-value
pH	7.36 ± 0.04	7.36 ± 0.06	0.820
$PaCO_2$ (mmHg)	46.1 ± 5.4	42.3 ± 3.7	0.137
PaO_2 (mmHg)	110 ± 15	111 ± 14	0.896
$[HCO_3^-]$ (mmol/L)	26.2 ± 2.3	24.1 ± 2.4	**0.041**
$[TCO_2]$ (mmol/L)	27.1 ± 2.9	25.3 ± 2.2	0.293
SaO_2 (%)	97.8 ± 0.9	98 ± 1	0.681
$[Na^+]$ (mmol/L)	143 ± 3	143 ± 4	0.745
$[K^+]$ (mmol/L)	3.43 ± 0.47	3.53 ± 0.34	0.338
Hct (%)	42.9 ± 4.8	45.4 ± 2.5	0.104
[Hb] (g/dl)	14.6 ± 1.6	15.5 ± 0.9	0.088

Table 3. 2 Baseline arterial blood gas and electrolyte concentrations in sham and CIH-exposed guinea-pigs

$PaCO_2$, arterial blood partial pressure of CO_2; PaO_2, arterial blood partial pressure of O_2; $[HCO_3^-]$, bicarbonate concentration; $[TCO_2]$, total CO_2 concentration; SaO_2, arterial oxygen saturation; $[Na^+]$, sodium concentration; $[K^+]$, potassium concentration; Hct, haematocrit; [Hb], haemoglobin concentration. Data are shown as mean ± SD. Haematocrit and haemoglobin parameters were statistically compared using one-tailed unpaired Student's *t* tests. All other parameters were statistically compared using two-tailed unpaired Student's *t* tests.

	Sham (n=8)	CIH (n=8)	p-value
MAP (mmHg)	37.3 ± 9.4	35.6 ± 6.9	0.346
SBP (mmHg)	51.0 ± 18.3	48.3 ± 11.1	0.362
DBP (mmHg)	27.9 ± 5.2	27.8 ± 4.7	0.483
HR (bpm)	279 ± 27	307 ± 36	**0.048**
f_R (brpm)	50.4 ± 12.1	62.4 ± 12.4	0.071
V_T (ml/100g)	0.184 ± 0.024	0.177 ± 0.014	0.515
V_E (ml/min/100g)	9.1 ± 1.4	11.0 ± 1.9	**0.036**
$ETCO_2$ (%)	6.26 ± 0.78	6.16 ± 0.92	0.818

Table 3. 3 CIH induces tachycardia and hyperventilation in anaesthetised guinea-pigs

MAP, mean arterial blood pressure; SBP, systolic blood pressure; DBP, diastolic blood pressure; HR, heart rate (bpm, beats.min^{-1}); f_R, respiratory frequency (brpm, breaths.min^{-1}); V_T, tidal volume; V_E, minute ventilation; $ETCO_2$, end-tidal carbon dioxide; CIH, chronic intermittent hypoxia. Data are shown as mean ± SD. Blood pressure and heart rate parameters were statistically compared using one-tailed unpaired Student's *t* tests. All other parameters were statistically compared using two-tailed unpaired Student's *t* tests.

	Sham (n=8)	**CIH (n=8)**	**p-value**
LV (mg/100g)	170 ± 12	179 ± 13	0.075
RV (mg/100g)	54.9 ± 4.0	57.5 ± 5.4	0.144
RV+LV (mg/100g)	225 ± 15	237 ± 17	0.074
RV:LV	0.324 ± 0.018	0.322 ± 0.027	0.409
Lung wet weight (mg/100g)	427 ± 26	487 ± 67	**0.032**
Lung dry weight (mg/100g)	95 ± 5	111 ± 13	**0.006**
Lung fluid content (%)	77.8 ± 1.4	77.2 ± 0.9	0.353
Spleen (mg/100g)	0.804 ± 0.163	0.678 ± 0.124	0.102
	(n=6)	(n=6)	
Urinary noradrenaline (ng/mg creatinine)	215 ± 156	190 ± 196	0.404
Urinary corticosterone (ng/mg creatinine)	2.56 ± 2.40	1.38 ± 0.34	0.410

Table 3. 4 Body organ weights and urinary stress profile of sham and CIH-exposed guinea-pigs

LV, left ventricle; RV right ventricle; CIH, chronic intermittent hypoxia. Data are shown as mean ± SD. Ventricular, noradrenaline and corticosterone parameters were statistically compared using one-tailed unpaired Student's *t* tests. All other parameters were statistically compared using two-tailed unpaired Student's *t* tests.

IV injection of phenylephrine produced a pressor response equivalent in CIH-exposed and sham guinea-pigs (Fig. 3.4a; p=0.327), however the associated reflex bradycardia was significantly blunted in CIH-exposed guinea-pigs compared with sham guinea-pigs (Fig. 3.4b p=0.032). β-adrenoceptor blockade with iv propranolol evoked a greater bradycardia in CIH-exposed guinea-pigs compared with sham guinea pigs (Fig. 3.4d; p=0.023). Interestingly, the propranolol-induced hypotensive response was blunted in CIH-exposed animals compared with sham controls (Fig. 3.4c; p=0.047). IV administration of hexamethonium produced similar hypotensive responses in CIH-exposed and sham guinea-pigs (-38 ± 7% vs. -35 ± 9%, % change from baseline MAP; sham, n= 5; CIH, n=5; p=0.582).

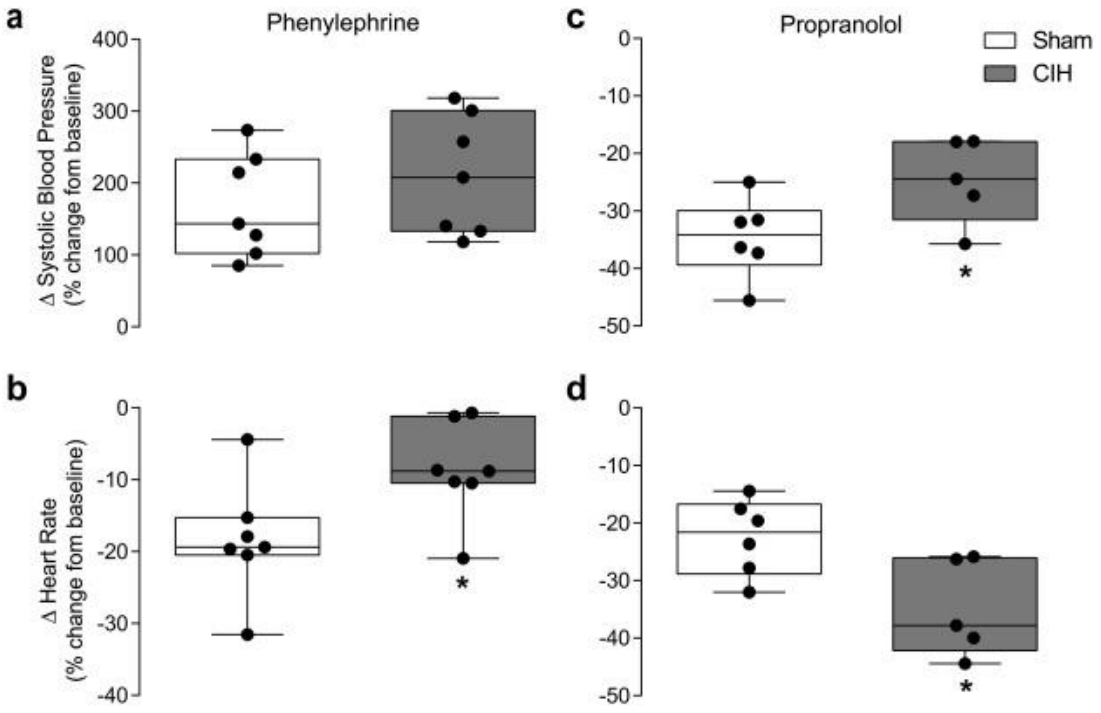


Figure 3. 4 Autonomic control of heart rate is altered in CIH-exposed anaesthetised guinea-pigs

Group data for systolic blood pressure (a, c), heart rate (b, d) in response to intravenous infusion of the β-adrenoceptor blocker propranolol (a-b) and α-adrenoceptor agonist phenylephrine (c-d). Values (a-d) are expressed as box and whisker plots (median, 25–75 percentiles and minimum and maximum values). Groups were statistically compared by unpaired Student's t tests. *p<0.05 compared with sham.

Cardiorespiratory responses to chemostimulation in sham and CIH-exposed anaesthetised guinea-pigs: Blood pressure and heart rate reflex responses to chemostimulation challenges were equivalent in CIH-exposed and sham animals in all instances (p>0.05). The hypercapnic ventilatory response in anaesthetised CIH-exposed guinea-pigs was significantly blunted compared with sham guinea-pigs (Table 3.5), particularly during the 10% inspired CO_2 challenge. Respiratory parameters were unaffected by exposure to acute hypoxia, however there was a trend for a blunted ventilatory response to asphyxia in CIH-exposed guinea-pigs (Table 3.5). There was a trend towards a blunted ventilatory response to iv NaCN administration in CIH-exposed guinea-pigs, arising predominantly due to a significantly reduced respiratory frequency response compared with sham guinea-pigs (Table 3.5).

	Sham (n=8)	CIH (n=8)	p-value
% change from baseline	**Hypercapnia ($FiCO_2$ = 0.05)**		
f_R	20 ± 13	3 ± 14	**0.027**
V_T	70 ± 14	74 ± 20	0.643
V_E	104 ± 30	79 ± 29	0.124
	Hypercapnia ($FiCO_2$ = 0.10)		
f_R	13 ± 26	-14 ± 18	**0.034**
V_T	171 ± 40	113 ± 71	0.064
V_E	206 ± 92	82 ± 69	**0.009**
	Hypoxia (FiO_2 = 0.10)		
	(n=8)	(n=7)	
f_R	1 ± 12	5 ± 18	0.286
V_T	5 ± 6	2 ± 13	0.298
V_E	6 ± 17	7 ± 20	0.451
	Asphyxia ($FiCO_2$ = 0.05 & FiO_2 = 0.10)		
	(n=8)	(n=8)	
f_R	25 ± 21	9 ± 19	0.064
V_T	71 ± 17	69 ± 17	0.413
V_E	114 ± 34	85 ± 42	0.086
	Sodium cyanide (200µg/kg i.v.)		
	(n=7)	(n=5)	
f_R	41 ± 19	22 ± 6	**0.043**
V_T	63 ± 25	63 ± 47	0.9922
V_E	101 ± 46	89 ± 36	0.086

Table 3. 5 Respiratory responsiveness to chemostimulation in sham and CIH-exposed anaesthetised guinea-pigs

f_R, respiratory frequency; V_T, tidal volume; V_E, minute ventilation; CIH, chronic intermittent hypoxia. Data are shown as mean ± SD and were statistically compared using unpaired Student's *t* tests.

3.3.3 Brainstem monoamine analysis.

Pontine and medulla oblongata noradrenaline concentrations were significantly lower in CIH-exposed guinea-pigs compared with sham guinea-pigs (Fig. 3.5a). Brainstem dopamine, 5-HIAA and 5-HT concentrations were equivalent in CIH-exposed and sham samples (Fig. 3.5c d). Correlation analysis was performed for pontine and medullary noradrenaline concentrations and breathing variability, sigh frequency, heart rate and heart rate responsiveness to drug administration. No significant correlations were evident between medullary noradrenaline concentrations and all physiological parameters (p>0.05; see supplementary data; Appendix Fig. B.1). However, there were positive correlations between pontine noradrenaline concentrations and T_e SD2 (p=0.032; Fig. 3.6b), T_{total} SD1 (p=0.047; Fig. 3.6d), T_{total} SD2 (p=0.049; Fig. 3.6d e) and respiratory frequency under urethane anaesthesia (p=0.017; Fig. 3.6f).

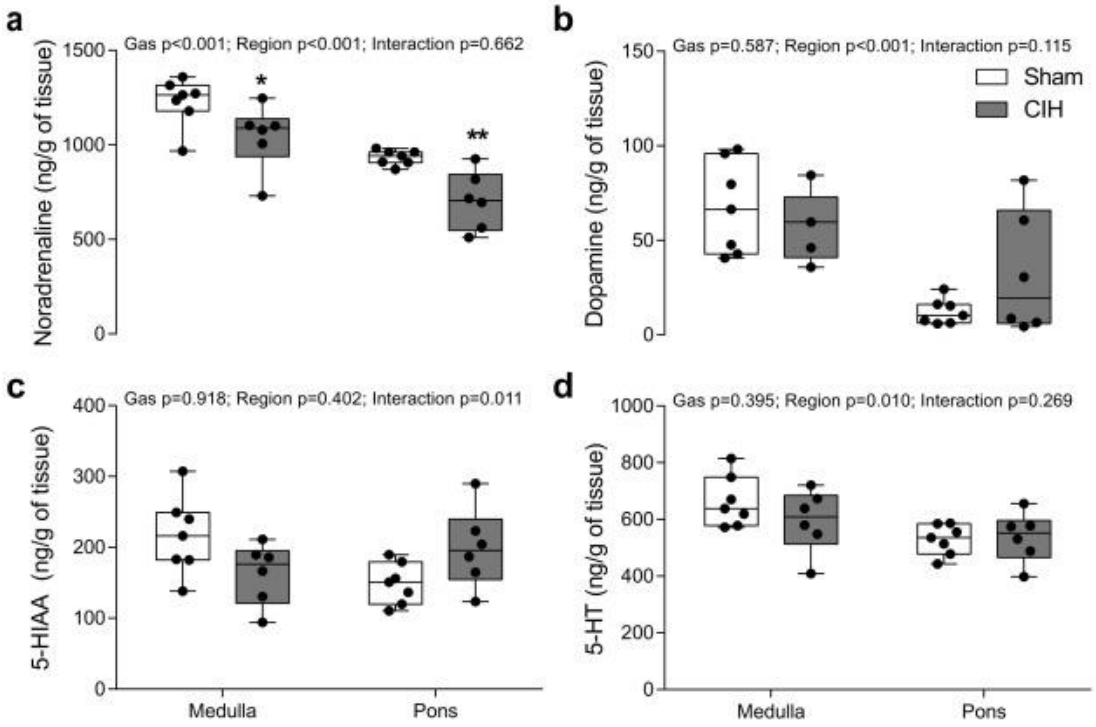


Figure 3. 5 Pontine and medulla oblongata noradrenaline concentrations are reduced in CIH-exposed guinea-pigs

Group data for noradrenaline (a), dopamine (b), 5-HIAA (c) and 5-HT (d) in pontine and medulla oblongata tissue homogenates from sham (n=7) and CIH-exposed (n=6) guinea-pigs. Values (a-d) are expressed as box and whisker plots (median, 25–75 percentiles and minimum and maximum values). 5-HIAA, 5-Hydroxyindole acetic acid; 5-HT, serotonin. Groups were statistically compared by two-way ANOVA with Bonferroni post hoc test. *sham pons vs. CIH pons, $p<0.05$; **sham medulla vs. CIH medulla, $p<0.01$.

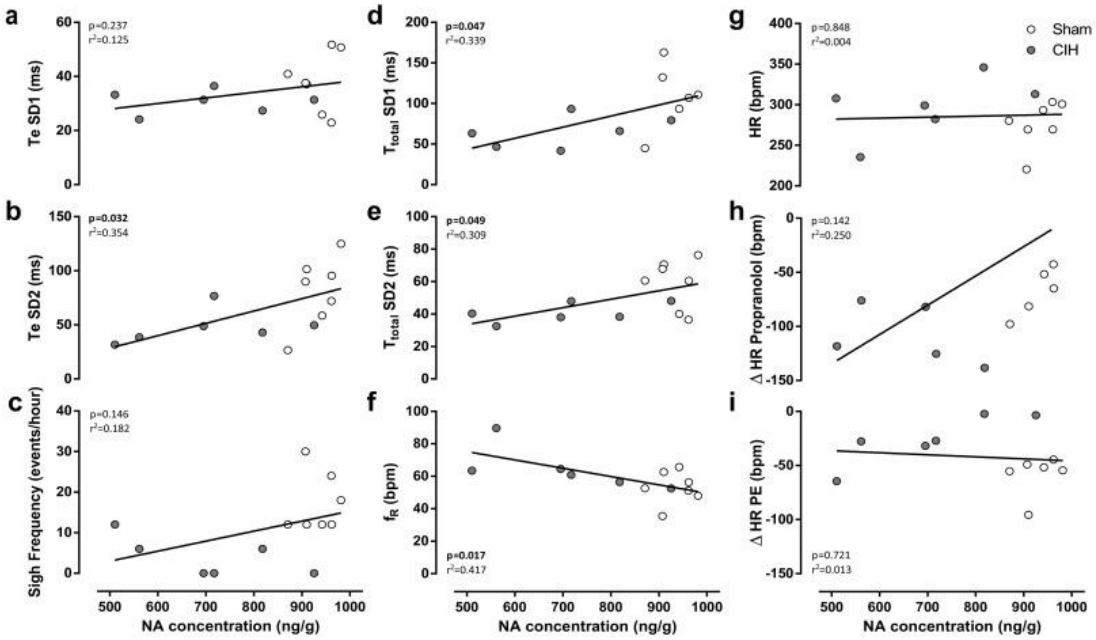


Figure 3. 6 Significant correlations are evident between pontine noradrenaline concentrations and various cardiorespiratory parameters.

Individual data points for correlations between pontine noradrenaline (NA) concentrations and time to expire (T_e) short-term variability (SD1; a), T_e long-term variability (SD2; b), sigh frequency (c), total breath duration (T_{total}) SD1 (d), T_{total} SD2 (e) in sham and CIH-exposed awake guinea-pigs, and respiratory frequency (f_R; f), heart rate (HR; g), change in HR in response to propranolol administration (h) and change in HR in response to phenylephrine (PE) administration (i) in sham and CIH-exposed anaesthetised guinea-pigs. Solid black lines represent linear regression analysis for each parameter.

3.3.4 Microbiota richness and composition

The species richness of faecal microbiota was reduced in CIH-exposed guinea-pigs (Chao1 index, p=0.011; total number of species observed, p=0.053; Fig. 3.7a-b). However, the difference in other metrics of alpha-diversity, which take into account the evenness of species abundance (Simpson and Shannon), was modest between groups (Fig. 3.7c-e). Principal coordinate analysis revealed a strong trend towards separation of microbiota communities between sham and CIH-exposed animals (p=0.059; Fig. 3.7f). To address in more detail the structural changes of faecal microbiota, we compared the relative abundance of individual bacterial taxa at the phylum, family and genus level. Significant differences between CIH-exposed and sham guinea-pigs were uncommon at the family and genus level (see supplementary data; Appendix Fig. B.2). However, at the phylum level, the relative abundance of Firmicutes bacteria was significantly lower (p=0.007), whereas Bacteroidetes phylum was significantly more abundant in CIH-exposed animals compared with sham animals (p=0.038; Fig. 3.8a and Appendix Table B.1). As a result, there was a trend for the Firmicutes:Bacteroidetes ratio to be lower in CIH-exposed guinea-pigs compared with sham guinea-pigs (p=0.068). The increase in Bacteroidetes in CIH-exposed samples was mainly driven by dominant *Bacteroidales S24-7 family* (Fig. 3.8b and Appendix Table B.2). These increases occurred at the expense of some Firmicutes taxa, such that bacterial genera from the *Lachnospiraceae* and *Ruminococcaceae* families were decreased in CIH-exposed faecal samples compared with sham faecal samples (Fig. 3.8b and Appendix Table B.2), although the changes in the relative abundance of bacterial genera were no longer significant after the Benjamini-Hochberg adjustment ((i/m)*Q<p; Appendix Table B.3).

The linear discriminant analysis (LDA) effect size method (LEfSe) was employed to identify bacterial genera associated with exposure to CIH, which might explain the underlying differences in the microbiota between sham and CIH-exposed animals (Appendix Fig. B.3). At the genus level, LEfSe analysis identified 7 genera associated with exposure to CIH and thus over-represented in the CIH-exposed group were: an uncultured bacterium belonging to the *Bacteroidales S24-7* family and *Butyricimonas* (both from the Bacteroidetes phylum), *Bifidobacterium* and *Coriobacteriaceae UCG002* (Actinobacteria), *Coprococcus 2* and *Flavonifractor* (Firmicutes), *Methanobrevibacter* (Eurvarchaeota). In contrast, 6 genera were associated with sham guinea-pigs and were therefore under-represented in CIH-exposed guinea-pigs. These genera were: *Blautia*, *Anaerotruncus*, *Lachnospiraceae UCG005*, *Intestinimonas, Ruminiclostridium 5* and *Lachnoclostridium 10* (all from the Firmicutes

phylum). Fig. 3.8c represents significant correlations identified between various physiological parameters and identified bacterial genera.

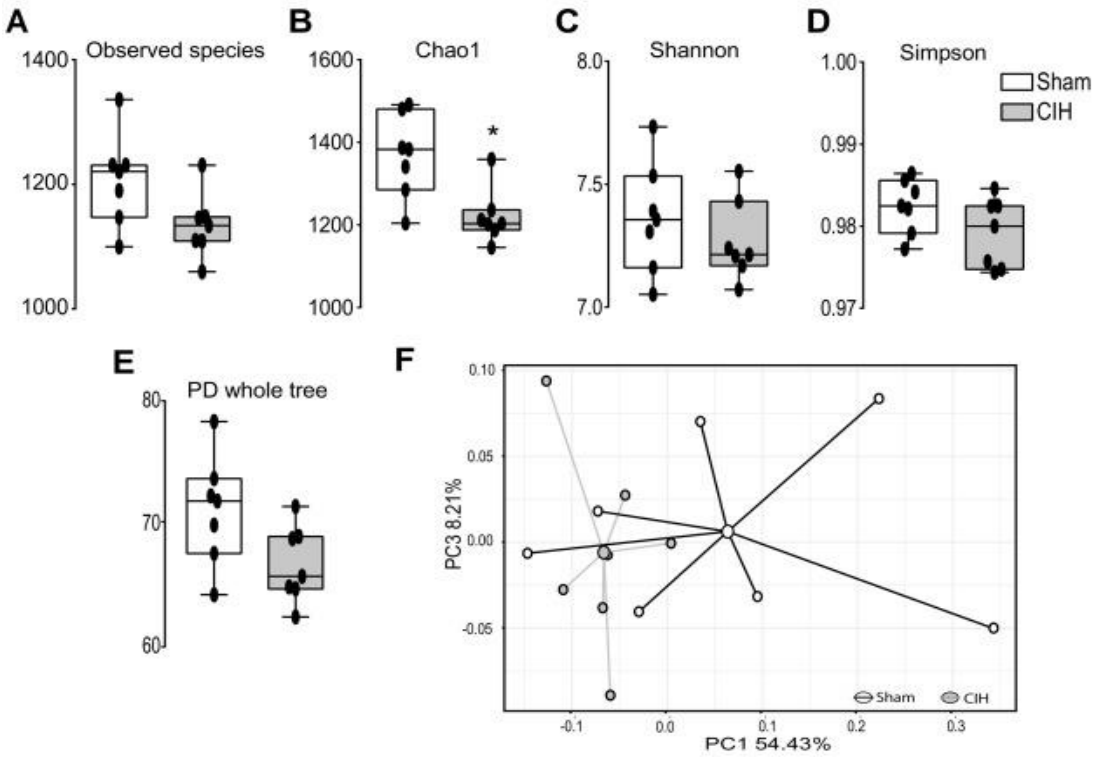


Figure 3. 7 Faecal microbiota richness is reduced CIH-exposed guinea-pigs

Group data for alpha-diversity indices (a-e) and principal coordinate analysis (PCoA) plot based on Bray-Curtis dissimilarity matrices (f) for Sham and CIH-exposed animals. Values (a-e) are expressed as box and whisker plots (median, 25-75 percentiles and minimum to maximum values) and were statistically compared by non-parametric Mann-Whitney *U* test. Benjamini-Hochberg adjustment with Q=0.2 was used to correct *p*-values for multiple testing (f). PD, phylogenetic diversity. Sham (n=7), CIH (n=7). **p*<0.05 compared with sham.

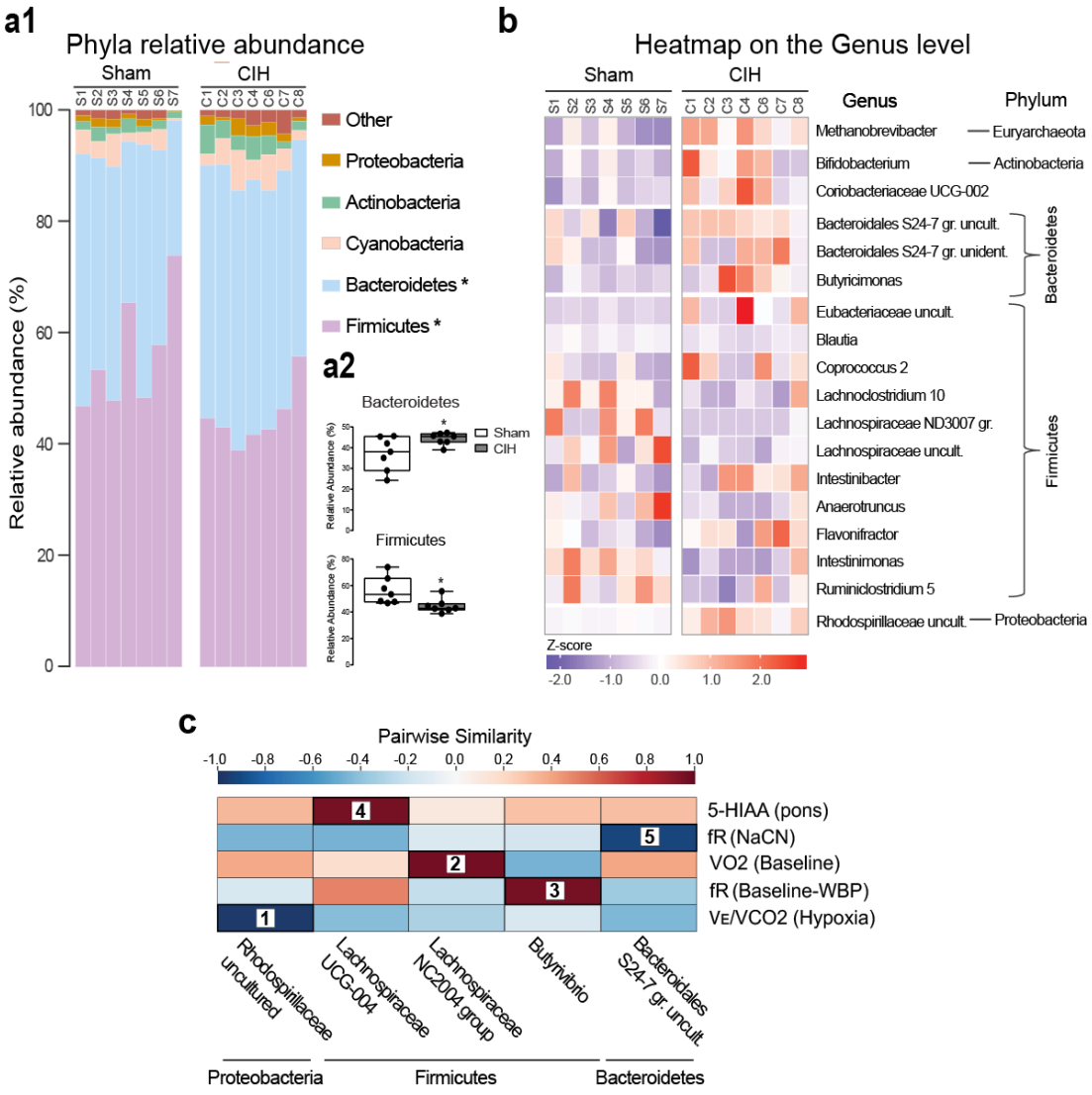


Figure 3. 8 CIH reduces Firmicutes and increases Bacteroidetes relative abundance in guinea-pig faecal samples

Stacked barplot (a1) at the phylum level of faecal samples taken from each guinea-pig with group data (a2) showing significant changes in the relative abundance of Bacteroidetes and Firmicutes phyla in CIH-exposed microbiota. Heatmap of Z-scores at the genus level (b) showing increases (red) and decreases (purple) in the relative abundance of bacterial genera in each guinea-pig; sham (left-side columns) and CIH (right-side columns). (c) Hallagram depicting Spearman correlations between the relative abundance of bacterial genera and physiological readouts. Genera are ordered taxonomically. Significant correlations are ranked 1-5 (strongest-weakest): positive associations are shown in red, negative – in blue. Benjamini-Hochberg adjustment p-value with Q=0.2 was used to correct p-values for multiple testing. 5-HIAA, 5-hydroindole acetic acid; f_R. respiratory frequency; NaCN, sodium cyanide; V_E/VCO_2, ventilatory equivalent; VO_2, oxygen consumption; WBP, whole-body plethysmography. Sham (n=7), CIH (n=7). *p<0.05, CIH compared with sham.

3.4. Discussion

There is considerable interest in the mechanisms driving CIH-induced respiratory plasticity and hypertension. This interest stems from the potential clinical relevance of the findings to an understanding of cardiorespiratory and autonomic function in persons with sleep-disordered breathing, a disorder characterised by recurrent apnoeic episodes during sleep manifesting in exposure to CIH. We sought to explore the putative obligatory role of carotid body sensitisation in the expression of aberrant cardiorespiratory control following exposure to CIH by use of a unique rodent model---the guinea-pig. If carotid body sensitisation is essential for aberrant respiratory plasticity and the development of hypertension following exposure to CIH, then little change should be expected in cardiorespiratory control in guinea-pigs exposed to CIH, based on the premise that the guinea-pig carotid body is essentially insensitive to hypoxia (Schwenke *et al.*, 2007; Gonzalez-Obeso *et al.*, 2017; Docio *et al.*, 2018). Conversely, if exposure to CIH disrupts cardiorespiratory control in guinea-pigs, this would provide evidence of sites beyond the carotid body that are sufficient to drive aberrant cardiorespiratory control in rodents, and perhaps humans. Our findings are generally supportive of the hypothesis that the carotid body is essential for the expression of CIH-induced aberrant control of breathing. In rodents with hypoxia-sensitive carotid bodies, CIH has been shown to cause hyperventilation and augmented responsiveness to hypoxic chemostimulation (Morgan *et al.*, 2016). Whereas elevated ventilatory responses to hypoxia have not been universally observed in studies of rodents exposed to CIH (Edge *et al.*, 2009), Morgan *et al.* 2016 provided the definitive study by measurement of breathing and metabolism (which are both affected by hypoxia in rodents), and careful consideration of the stimulus-response relationship by way of concurrent assessment of oxygen saturation during hypoxic challenge. Assessing the relationship of all three parameters reveals that exposure to CIH increases the ventilatory response to hypoxia in rats (Morgan *et al.*, 2016). Additionally, several groups have reported increased ventilatory drive in rats exposed to CIH (Skelly *et al.*, 2012; Morgan *et al.*, 2016).

Exposure to CIH in guinea-pigs did not affect baseline ventilation or metabolism or ventilatory responses to hypoxia and hypercapnia in awake animals. Indeed, the ventilatory equivalent ($V_E/V\dot{C}O_2$) during hypoxic ventilation was depressed, not augmented, in CIH-exposed guinea-pigs. Unaltered ventilation and ventilatory responsiveness to chemo-stimulation in CIH-exposed guinea-pigs supports the contention that carotid body sensory facilitation is wholly necessary for CIH-mediated enhancement of hypoxic ventilatory

responses. Likewise, in CIH-exposed anaesthetised guinea-pigs, there was no evidence of potentiated chemoreceptor responsiveness. Indeed, responses were generally less in CIH-exposed animals, with a significant blunting of the ventilatory response to 10% inspired CO_2. Of interest, in a recent study in guinea-pigs, utilising a more severe CIH protocol, consisting of 30 cycles.hour^{-1} (5% O_2 at nadir), 8h.day^{-1}, for 30 days, V_E/VO_2 during severe hypoxia (FiO_2 = 0.07) and hypercapnia ($FiCO_2$ = 0.05) was blunted compared with sham, principally owing to CIH-induced increases in oxygen consumption (Docio *et al.*, 2018). Whereas a modest hyperventilation can be evoked by severe hypoxia in sham guinea-pigs, these effects are not potentiated, but instead are diminished, following exposure to CIH (Docio *et al.*, 2018). Moreover, exposure to CIH failed to potentiate intracellular calcium or catecholamine release from carotid body type 1 cells during acute activation by hypoxia or high K^+, revealing convincingly that exposure to CIH fails to sensitise carotid bodies of the guinea-pig (Docio *et al.*, 2018). Carotid bodies of the guinea-pig lack O_2-sensitive K^+ channels (Gonzalez-Obeso *et al.*, 2017) and exposure to CIH does not evoke a capacity for hypoxia-dependent type 1 cell depolarisation and neurosecretory response (Docio *et al.*, 2018), which is essential to chemo-afferent signalling from the carotid body. However, the type 1 cells retain the ability to excite sensory nerve endings as evidenced by cyanide mitochondrial poisoning. These elegant data provide evidence that exposure to CIH does not potentiate carotid body activity in guinea-pigs (unlike rats), and confirm the characteristic quiescent nature of the guinea-pig carotid body in normoxia and hypoxia. In our study, exposure to CIH did not evoke alterations to breathing in normoxia or hypoxia, whereas similar paradigms disrupt respiratory control in rats (Edge *et al.*, 2012; Skelly *et al.*, 2012; Morgan *et al.*, 2016).

In rodents with hypoxia-sensitive carotid bodies, CIH increases the propensity for central apnoeas and respiratory instability (Edge *et al.*, 2012; Donovan *et al.*, 2014; Souza *et al.*, 2015b). Interestingly, CIH-exposed guinea-pigs exhibited reduced respiratory variability concurrent with decreased sigh frequency and qualitative observations of fewer central apnoeas. We observed altered brainstem neurochemistry evidenced by lower noradrenaline concentrations in CIH-exposed pons and medulla. Noradrenaline drives breathing irregularities in IH-exposed anaesthetised mice (Zanella *et al.*, 2014). Thus, lower sigh/apnoea frequency and lower brainstem noradrenaline concentrations in CIH-exposed guinea-pigs are congruent observations, especially when one considers that CIH-exposed rats show evidence of increased central noradrenergic terminals (Mody *et al.*, 2011) and elevated apnoea index (Edge *et al.*, 2012). Whereas, we observed no evidence of a significant correlation between sigh frequency and medullary or pontine noradrenaline concentrations,

significant correlations between respiratory timing variability and pontine noradrenaline concentrations were evident.

CIH impairs baroreflex control (Yan *et al.*, 2008) and drives the development of hypertension in rodents with hypoxia-sensitive carotid bodies (Marcus *et al.*, 2009; Ray *et al.*, 2015). Hypertension did not manifest in our guinea-pig model of CIH, which seemingly supports the hypothesis that carotid body sensitisation is essential for cardiovascular maladaptation, as previously suggested by carotid body denervation studies (Lesske *et al.*, 1997; Prabhakar, 2016). Exposure to CIH, using a profile similar to the present study evokes hypertension in rats (Ray *et al.*, 2015). Indeed, hypertension can manifest after as few as two days of exposure to CIH (Marcus *et al.*, 2009). Thus, we are confident that the CIH protocol utilised in this study would be sufficient to induce hypertension in a rodent model with hypoxia-sensitive carotid bodies. Remarkably, exposure to CIH (30 cycles.hour^{-1} for 8h.day^{-1} for 30 days) caused hypertension in guinea-pigs (Docio *et al.*, 2018), with tachycardia and increased concentrations of circulating noradrenaline, indicative of sympathetic nervous hyperactivity, the hallmark of carotid body-dependent sympatho-excitation in rat models of CIH. It is therefore apparent that exposure to CIH has the capacity to evoke cardiovascular morbidity in guinea-pigs, through a carotid body-independent mechanism. We posit that our modest paradigm (6 cycles.hour^{-1} for 8.hours day^{-1} for 12 days), sufficient to evoke hypertension in rats (Ray *et al.*, 2015), was most likely insufficient to provoke sensory facilitation of carotid chemoafferent input to the brainstem, but was also insufficient to evoke sympathetic overactivity, by whatever means, and hence hypertension. This is supported by urinary measures of noradrenaline and corticosterone in our study, which were unchanged in CIH-exposed guinea-pigs.

Of interest, we observed a CIH-induced tachycardia, which is also reported in some studies in CIH-exposed rats (Zoccal *et al.*, 2007b; Lucking *et al.*, 2014), and consistent with observations in the rat that CIH-induced tachycardia was amenable to β-adrenoceptor blockade with propranolol (Lucking *et al.*, 2014). Of note, enhanced heart rate responses to sympathetic nervous stimulation was observed in an isolated atria/right stellate ganglion preparation in CIH-exposed guinea-pigs (Mohan *et al.*, 2001). Tachycardia was also evident in guinea-pigs exposed to CIH for 30 days (Docio *et al.*, 2018), accompanied by evidence of sympathetic over-activity and hypertension. Our finding of a β-adrenoceptor-mediated tachycardia suggests activation of the cardiac sympathetic branch with resultant chronotropic effects without elevation in blood pressure. Blunted bradycardia responses to phenylephrine-induced elevations in blood pressure (which were equivalent in magnitude

between groups), suggests impaired baroreflex responsiveness in CIH-exposed guinea-pigs, perhaps secondary to CIH-induced central remodelling at the level of the nucleus tractus solitarius and paraventricular nucleus (Mifflin *et al.*, 2015) or related to increased inhibitory neurotransmission to cardiac vagal neurons of the nucleus ambiguous and dorsal motor nucleus of the vagus resulting in blunted heart rate responsiveness, which has been reported following exposure to CIH (Dyavanapalli *et al.*, 2014). We conclude that these effects are independent of carotid body sensitisation, or at least are not dependent upon it, revealing a capacity for CIH to alter autonomic control of the heart through actions at one or more extra-carotid sites. Whereas our modest paradigm of CIH was insufficient to evoke hypertension in guinea-pigs, at least over the timeframe of our study, Docio *et al*. 2018 have clearly demonstrated a capacity for more severe exposures to CIH to elicit sympathetic over-activity and hypertension in guinea-pigs, without carotid body sensitisation.

Regulation of blood pressure is complex with multiple contributory mechanisms over varying time domains. Increasing evidence supports the symbiotic gut microbiota as a major contributor to long-term blood pressure regulation (Durgan *et al.*, 2016; Adnan *et al.*, 2017). New evidence implicates sympathetic neuronal communication between the hypothalamic paraventricular nucleus and the gut in the regulation of blood pressure (Marques *et al.*, 2018). In recent years, it has become apparent that various hypertensive animal models develop gut dysbiosis, including spontaneously hypertensive rats (Adnan *et al.*, 2017; Santisteban *et al.*, 2017) and animal models of sleep apnoea (Everard & Cani, 2013; Moreno-Indias *et al.*, 2015; Durgan *et al.*, 2016). A variety of systemic stressors are capable of inducing alterations in the gut microbiota, including prenatal stress (Golubeva *et al.*, 2015), maternal separation (O'Mahony *et al.*, 2011), social disruption (Bailey *et al.*, 2011; van de Wouw *et al.*, 2018a) and sleep fragmentation (Bailey *et al.*, 2011). Hyper-activation of the sympathetic nervous system appears to be fundamental to this process. As such, exposure to CIH could conceivably disrupt gut microbiota through autonomic dysregulation. In addition, CIH is a systemic insult that may directly influence microbiota function and microbiota/host interaction. Repeated bouts of hypoxia may favour the proliferation of obligate anaerobes. Moreover, exposure to CIH induces oxidative stress and inflammation and decreases the expression of tight junction proteins (Wu *et al.*, 2016), all of which contribute to altered microbiota composition and diversity. Spontaneously hypertensive rats have decreased expression of several tight junction proteins in the gut, which increases intestinal permeability (Santisteban *et al.*, 2017). We did not examine the effects of exposure to CIH on intestinal permeability in this study, but others have reported that exposure to CIH results

in a late-onset persistent low-grade endotoxaemia in mice, with positive correlations between plasma LPS and the abundance of *Mucispirillum* and *Desulfovibrio* (Moreno-Indias *et al.*, 2016). Also, bacteria-derived metabolites such as short-chain fatty acids are influenced by CIH exposure (Adnan *et al.*, 2017; Marques *et al.*, 2018) and these bacterial metabolites, in addition to others such as hydrogen sulphide (Tomasova *et al.*, 2016) and indole (Huc *et al.*, 2018), are associated with blood pressure control.

A pivotal role for microbiota in blood pressure regulation is revealed by demonstration that faecal transplant from spontaneously hypertensive rats into normotensive, microbiome-compromised control rats induces hypertension and gut dysbiosis (Adnan *et al.*, 2017). Alterations in the composition of the gut microbiota coincide with increases in blood pressure, since changes in the microbiota are not evident in pre-hypertensive rats, whereas expansion of Bacteroidetes and a reduction in Firmicutes, as well as increased gut barrier permeability are evident once hypertension is established (Santisteban *et al.*, 2017). Changes in the relative proportions of Firmicutes and Bacteroidetes bacteria have been reported in animal models of hypertension and sleep apnoea, although the results are inconsistent across the studies (Everard & Cani, 2013; Moreno-Indias *et al.*, 2015; Durgan *et al.*, 2016). Indeed, six weeks of recovery in normoxia following exposure to CIH is insufficient for recovery of the microbiota (Moreno-Indias *et al.*, 2016), a potential mechanism underlying failed interventional therapy for hypertension despite prevention of CIH in persons with sleep apnoea, in addition to suggestions of persistent epigenetic redox changes driving sympathetic over-activity (Nanduri *et al.*, 2017).

In the present study, the relative abundance of Firmicutes was significantly reduced and the relative abundance of Bacteroidetes was significantly increased. As a consequence, the Firmicutes:Bacteroidetes ratio tended to decrease, as did the alpha diversity indices following exposure to CIH. Post-hoc analysis revealed that this comparison was underpowered to detect a significant difference, based upon the effect size determined in our study and sample size, which we acknowledge is a limitation of our study. LEfSe analysis detected statistically significant over-representation of Actinobacteria (*Bifidobacterium* and *Coriobacteriaceae UCG-002*) and Bacteroidetes species (*Butyricimonas* and *Bacteroidales S24-7* group) in the CIH-exposed group, while Firmicutes bacteria (*Blautia*, *Anaerotruncus*, *Ruminoclostridium*, *Lachnoclostridium*) were largely under-represented in CIH-exposed guinea pigs. The LEfSe results largely overlap with the differential abundance data presented on the heatmap (Fig. 3.8b), thus supporting the observed shift towards an increase in the relative abundance of Bacteroidetes and a reduction in Firmicutes bacteria in CIH-exposed

microbiota. Similar to our findings, an increase in the abundance of Bacteroidetes bacterial species was observed in deoxycorticosterone acetate (DOCA)-salt mice fed with a high fibre diet. This shift in the microbiota was accompanied by reduced systolic and diastolic blood pressures, as well as reduced cardiac weight index, cardiac fibrosis and improved cardiac function (Marques *et al.*, 2017), suggesting beneficial effects of increased abundance of Bacteroidetes on cardiovascular function in the DOCA model. An additional common feature of disrupted microbiota is reduced microbial diversity. Hypertensive animals have reduced Shannon diversity and Chao1 richness (Yang *et al.*, 2015; Durgan, 2017; Li *et al.*, 2017). We observed a decrease in Chao1 richness in CIH-exposed animals in our study, with trends towards decreases in other measures of microbiota diversity.

We posit that CIH-induced reduction in microbiota richness, in tandem with changes in microbiota composition demonstrate the physiologically significant influence of exposure to CIH on microbiota populations. These likely direct effects of exposure to CIH, independent of sympathetic nervous activation, notwithstanding that putative links between CIH-induced hypertension and alterations to the gut microbiome are dependent upon hyper-activation of the sympathetic nervous system, which in turn serves to perpetuate cardiorespiratory dysregulation. CIH in rodents with hypoxia-sensitive carotid bodies is associated with increased catecholamine secretions from the adrenal glands (Kumar *et al.*, 2006), hormones which act to promote epithelial barrier dysfunction (Lyte *et al.*, 2011; Santisteban *et al.*, 2017) as well as the proliferation of specific bacteria (Lyte, 2014b). It is plausible to suggest that exposure to CIH characterised by more frequent and/or severe and/or longer durations than those used in the present study, which have been shown to cause hypertension in guinea-pigs (Docio *et al.*, 2018), could cause severe disruption to gut microbiota, and indeed may be the basis for the observations of CIH-induced hypertension and sympathetic hyper-activity in guinea-pigs (Docio *et al.*, 2018).

Our study reveals the capacity for CIH to alter microbiota composition, richness and beta-diversity which may have contributed to altered autonomic control of the heart, effects independent both of carotid body sensitisation and sympathetic over-activity, therefore purportedly a result of direct actions of CIH on the microbiota. It is also possible that direct actions of CIH on the microbiota, in the absence of sympathetic over-activity, may have conferred cardiovascular protection in respect of blood pressure responses to exposure to CIH.

The afferent vagal nerve pathway is proposed as an essential link between the gut microbiota and the central nervous system (Bravo *et al.*, 2011; Foster *et al.*, 2017; Bonaz *et al.*, 2018). Alterations in microbiota diversity/populations and their production of metabolites could influence vagal afferent traffic directed towards the cardiorespiratory centres of the brainstem. Positive correlations between disruption of the microbiota and respiratory timing variability have been described in adult rats exposed to pre-natal stress (Golubeva *et al.*, 2015). Exposure to CIH in adult guinea-pigs caused a reduction in the frequency of sighs, a critical component of the normal respiratory control repertoire, important in the control of respiratory timing variability. Moreover, as a result of the mechanical consequences of augmented breaths, sighs defend the respiratory gas exchange units against collapse (atelectasis). CIH-associated alterations to the microbiota and/or direct effects on the central neural circuitry within the brainstem demonstrably interfered with the protective sigh reflex, revealing a CIH-induced respiratory-related morbidity unrelated to carotid body sensitisation.

In conclusion, hallmark features of cardiorespiratory morbidity evoked by exposure to CIH in rats, principally apnoea and high blood pressure, were not evident in guinea-pigs. There were nevertheless residual aberrant phenotypes including decreased respiratory timing variability and frequency of sighs as well as tachycardia and decreased heart rate responsiveness. Exposure to CIH altered brainstem neurochemistry, revealed as a significant reduction in the concentration of noradrenaline in the pons and medulla oblongata. In the absence of sympathetic over-activity, exposure to CIH decreased gut microbiota species richness, and altered microbiota composition, decreasing the relative abundance of Firmicutes and increasing the relative abundance of Bacteroidetes.

Our study reveals obligatory roles for the carotid body in CIH-induced cardiorespiratory morbidity. Moreover, the gut microbiota are potential players contributing to central remodelling during exposure to CIH through potential alterations in microbiota-gut-brain axis signalling. Our findings have implications for human sleep-disordered breathing and contribute to an emerging interest in the potential of manipulation of the microbiota as an adjunctive therapy in human disease (Durgan *et al.*, 2016; Farre *et al.*, 2018).

3.5. Additional information

Competing interests: The authors have no professional, personal or financial conflicts of interests relating to this publication.

Author contributions: EFL: experimental design; acquisition of data; data and statistical analysis; interpretation of data; drafting of the original manuscript; KMO'C: acquisition of data; data and statistical analysis and interpretation of data; drafting of the original manuscript; EFL and KMO'C contributed equally to this manuscript; CRS: 16S rRNA sequencing: acquisition of data; data and statistical analysis; FF: 16S rRNA sequencing: acquisition of data; data and statistical analysis; TFSB: Interpretation of data; Data analysis; Statistical analysis; DPB: experimental design; AVG: interpretation of data; statistical analysis; critical revision of the manuscript; CS: critical revision of the manuscript; GC: HPLC studies: experimental design; interpretation of data; critical revision of the manuscript; JFC: critical revision of the manuscript; KDO'H: experimental design; interpretation of physiological data; drafting and critical revision of the manuscript.

Funding sources: This project was funded by the Department of Physiology, and the APC Microbiome Ireland, University College Cork, Ireland. The institution had no role in the study design, data collection, data analysis, interpretation or writing of the manuscript.

Acknowledgements: We are grateful to staff of the Biological Services Unit, University College Cork for their support with animal housing and welfare. We thank Dr. Paul Cotter, Dr. Fiona Crispie and Dr. Laura Finnegan from the Teagasc Sequencing Facility for their assistance with MiSeq sequencing. We thank Dr. Grzegorz Jasionek for his assistance with urinary assays.

3.6. References

Adnan S, Nelson JW, Ajami NJ, Venna VR, Petrosino JF, Bryan RM, Jr. & Durgan DJ. (2017). Alterations in the gut microbiota can elicit hypertension in rats. *Physiological genomics* **49,** 96-104.

Bailey MT, Dowd SE, Galley JD, Hufnagle AR, Allen RG & Lyte M. (2011). Exposure to a social stressor alters the structure of the intestinal microbiota: implications for stressor-induced immunomodulation. *Brain Behav Immun* **25,** 397-407.

Bonaz B, Bazin T & Pellissier S. (2018). The Vagus Nerve at the Interface of the Microbiota-Gut-Brain Axis. *Front Neurosci* **12,** 49.

Bravo JA, Forsythe P, Chew MV, Escaravage E, Savignac HM, Dinan TG, Bienenstock J & Cryan JF. (2011). Ingestion of Lactobacillus strain regulates emotional behavior and central GABA receptor expression in a mouse via the vagus nerve. *Proceedings of the National Academy of Sciences of the United States of America* **108,** 16050-16055.

Brooks D, Horner RL, Kozar LF, Render-Teixeira CL & Phillipson EA. (1997). Obstructive sleep apnea as a cause of systemic hypertension. Evidence from a canine model. *J Clin Invest* **99,** 106-109.

Chen L, Zhang J, Gan TX, Chen-Izu Y, Hasday JD, Karmazyn M, Balke CW & Scharf SM. (2008). Left ventricular dysfunction and associated cellular injury in rats exposed to chronic intermittent hypoxia. *Journal of applied physiology (Bethesda, Md : 1985)* **104,** 218-223.

Costa-Silva JH, Zoccal DB & Machado BH. (2012). Chronic intermittent hypoxia alters glutamatergic control of sympathetic and respiratory activities in the commissural NTS of rats. *American journal of physiology Regulatory, integrative and comparative physiology* **302,** R785-793.

Del Rio R, Andrade DC, Lucero C, Arias P & Iturriaga R. (2016). Carotid Body Ablation Abrogates Hypertension and Autonomic Alterations Induced by Intermittent Hypoxia in Rats. *Hypertension (Dallas, Tex : 1979)* **68,** 436-445.

Dick TE, Hsieh YH, Wang N & Prabhakar N. (2007). Acute intermittent hypoxia increases both phrenic and sympathetic nerve activities in the rat. *Experimental physiology* **92,** 87-97.

Docio I, Olea E, Prieto LJ, Gallego-Martin T, Obeso A, Gomez-Nino A & Rocher A. (2018). Guinea Pig as a Model to Study the Carotid Body Mediated Chronic Intermittent Hypoxia Effects. *Frontiers in physiology* **9,** 694.

Donovan LM, Liu Y & Weiss JW. (2014). Effect of endothelin antagonism on apnea frequency following chronic intermittent hypoxia. *Respiratory physiology & neurobiology* **194,** 6-8.

Durgan DJ. (2017). Obstructive Sleep Apnea-Induced Hypertension: Role of the Gut Microbiota. *Curr Hypertens Rep* **19,** 35.

Durgan DJ, Ganesh BP, Cope JL, Ajami NJ, Phillips SC, Petrosino JF, Hollister EB & Bryan RM, Jr. (2016). Role of the Gut Microbiome in Obstructive Sleep Apnea-Induced Hypertension. *Hypertension* **67,** 469-474.

Dyavanapalli J, Jameson H, Dergacheva O, Jain V, Alhusayyen M & Mendelowitz D. (2014). Chronic intermittent hypoxia-hypercapnia blunts heart rate responses and alters neurotransmission to cardiac vagal neurons. *J Physiol* **592,** 2799-2811.

Edge D, Bradford A & O'Halloran KD. (2012). Chronic intermittent hypoxia increases apnoea index in sleeping rats. *Advances in experimental medicine and biology* **758,** 359-363.

Edge D, Skelly JR, Bradford A & O'Halloran KD. (2009). Ventilatory drive is enhanced in male and female rats following chronic intermittent hypoxia. *Advances in experimental medicine and biology* **648,** 337-344.

Everard A & Cani PD. (2013). Diabetes, obesity and gut microbiota. *Best Pract Res Clin Gastroenterol* **27,** 73-83.

Farre N, Farre R & Gozal D. (2018). Sleep Apnea Morbidity: A Consequence of Microbial-Immune Cross-Talk? *Chest*.

Fletcher EC, Lesske J, Behm R, Miller CC, 3rd, Stauss H & Unger T. (1992). Carotid chemoreceptors, systemic blood pressure, and chronic episodic hypoxia mimicking sleep apnea. *J Appl Physiol* **72,** 1978-1984.

Foster JA, Rinaman L & Cryan JF. (2017). Stress & the gut-brain axis: Regulation by the microbiome. *Neurobiology of stress* **7,** 124-136.

Garcia AJ, 3rd, Dashevskiy T, Khuu MA & Ramirez JM. (2017). Chronic Intermittent Hypoxia Differentially Impacts Different States of Inspiratory Activity at the Level of the preBotzinger Complex. *Front Physiol* **8,** 571.

Golubeva AV, Crampton S, Desbonnet L, Edge D, O'Sullivan O, Lomasney KW, Zhdanov AV, Crispie F, Moloney RD, Borre YE, Cotter PD, Hyland NP, O'Halloran KD, Dinan TG, O'Keeffe GW & Cryan JF. (2015). Prenatal stress-induced alterations in major physiological systems correlate with gut microbiota composition in adulthood. *Psychoneuroendocrinology* **60,** 58-74.

Gonzalez-Obeso E, Docio I, Olea E, Cogolludo A, Obeso A, Rocher A & Gomez-Nino A. (2017). Guinea Pig Oxygen-Sensing and Carotid Body Functional Properties. *Front Physiol* **8,** 285.

Grundy D. (2015). Principles and standards for reporting animal experiments in The Journal of Physiology and Experimental Physiology. *J Physiol* **593,** 2547-2549.

Huang J, Lusina S, Xie T, Ji E, Xiang S, Liu Y & Weiss JW. (2009). Sympathetic response to chemostimulation in conscious rats exposed to chronic intermittent hypoxia. *Respiratory physiology & neurobiology* **166,** 102-106.

Huc T, Konop M, Onyszkiewicz M, Podsadni P, Szczepanska A, Turlo J & Ufnal M. (2018). Colonic indole, gut bacteria metabolite of tryptophan, increases portal blood pressure in rats. *Am J Physiol Regul Integr Comp Physiol* **315,** R646-R655.

Iturriaga R & Alcayaga J. (2007). Effects of intermittent hypoxia on cat petrosal ganglion responses induced by acetylcholine, adenosine 5'-triphosphate and NaCN. *Brain Res* **1128,** 86-90.

Krogh A. (1929). THE PROGRESS OF PHYSIOLOGY. *Science* **70,** 200-204.

Kumar GK, Rai V, Sharma SD, Ramakrishnan DP, Peng YJ, Souvannakitti D & Prabhakar NR. (2006). Chronic intermittent hypoxia induces hypoxia-evoked catecholamine efflux in adult rat adrenal medulla via oxidative stress. *J Physiol* **575,** 229-239.

Kummer W, Fischer A & Heym C. (1989). Ultrastructure of calcitonin gene-related peptide- and substance P-like immunoreactive nerve fibres in the carotid body and carotid sinus of the guinea pig. *Histochemistry* **92,** 433-439.

Lesske J, Fletcher EC, Bao G & Unger T. (1997). Hypertension caused by chronic intermittent hypoxia--influence of chemoreceptors and sympathetic nervous system. *J Hypertens* **15,** 1593-1603.

Li J, Zhao F, Wang Y, Chen J, Tao J, Tian G, Wu S, Liu W, Cui Q, Geng B, Zhang W, Weldon R, Auguste K, Yang L, Liu X, Chen L, Yang X, Zhu B & Cai J. (2017). Gut microbiota dysbiosis contributes to the development of hypertension. *Microbiome* **5,** 14.

Lucking EF, O'Halloran KD & Jones JF. (2014). Increased cardiac output contributes to the development of chronic intermittent hypoxia-induced hypertension. *Experimental physiology* **99,** 1312-1324.

Lyte M. (2014). Microbial endocrinology: Host-microbiota neuroendocrine interactions influencing brain and behavior. *Gut Microbes* **5,** 381-389.

Lyte M, Vulchanova L & Brown DR. (2011). Stress at the intestinal surface: catecholamines and mucosa-bacteria interactions. *Cell and tissue research* **343,** 23-32.

Machado BH, Zoccal DB & Moraes DJA. (2017). Neurogenic hypertension and the secrets of respiration. *American journal of physiology Regulatory, integrative and comparative physiology* **312,** R864-R872.

Marcus N, Olsonjr E, Bird C, Philippi N & Morgan B. (2009). Time-dependent adaptation in the hemodynamic response to hypoxia. *Respiratory Physiology & Neurobiology* **165,** 90-96.

Marques FZ, Mackay CR & Kaye DM. (2018). Beyond gut feelings: how the gut microbiota regulates blood pressure. *Nature reviews Cardiology* **15,** 20-32.

Marques FZ, Nelson E, Chu PY, Horlock D, Fiedler A, Ziemann M, Tan JK, Kuruppu S, Rajapakse NW, El-Osta A, Mackay CR & Kaye DM. (2017). High-Fiber Diet and Acetate Supplementation Change the Gut Microbiota and Prevent the Development of Hypertension and Heart Failure in Hypertensive Mice. *Circulation* **135,** 964-977.

McDonald FB, Edge D & O'Halloran KD. (2014). Chronic nitric oxide synthase inhibition does not impair upper airway muscle adaptation to chronic intermittent hypoxia in the rat. *Prog Brain Res* **212,** 237-251.

Mifflin S, Cunningham JT & Toney GM. (2015). Neurogenic mechanisms underlying the rapid onset of sympathetic responses to intermittent hypoxia. *J Appl Physiol (1985)* **119,** 1441-1448.

Mody P, Rukhadze I & Kubin L. (2011). Rats subjected to chronic-intermittent hypoxia have increased density of noradrenergic terminals in the trigeminal sensory and motor nuclei. *Neuroscience letters* **505,** 176-179.

Mohan RM, Golding S & Paterson DJ. (2001). Intermittent hypoxia modulates nNOS expression and heart rate response to sympathetic nerve stimulation. *Am J Physiol Heart Circ Physiol* **281,** H132-138.

Moraes DJ & Machado BH. (2015). Electrophysiological properties of laryngeal motoneurones in rats submitted to chronic intermittent hypoxia. *The Journal of physiology* **593,** 619-634.

Moraes DJ, Zoccal DB & Machado BH. (2012). Medullary respiratory network drives sympathetic overactivity and hypertension in rats submitted to chronic intermittent hypoxia. *Hypertension (Dallas, Tex : 1979)* **60,** 1374-1380.

Moreno-Indias I, Torres M, Montserrat JM, Sanchez-Alcoholado L, Cardona F, Tinahones FJ, Gozal D, Poroyko VA, Navajas D, Queipo-Ortuno MI & Farre R. (2015). Intermittent hypoxia alters gut microbiota diversity in a mouse model of sleep apnoea. *The European respiratory journal* **45,** 1055-1065.

Moreno-Indias I, Torres M, Sanchez-Alcoholado L, Cardona F, Almendros I, Gozal D, Montserrat JM, Queipo-Ortuno MI & Farre R. (2016). Normoxic Recovery Mimicking Treatment of Sleep Apnea Does Not Reverse Intermittent Hypoxia-Induced Bacterial Dysbiosis and Low-Grade Endotoxemia in Mice. *Sleep* **39,** 1891-1897.

Morgan BJ, Adrian R, Wang ZY, Bates ML & Dopp JM. (2016). Chronic intermittent hypoxia alters ventilatory and metabolic responses to acute hypoxia in rats. *Journal of applied physiology (Bethesda, Md : 1985)* **120,** 1186-1195.

Mouradian GC, Forster HV & Hodges MR. (2012). Acute and chronic effects of carotid body denervation on ventilation and chemoreflexes in three rat strains. *J Physiol* **590,** 3335-3347.

Moya EA, Arias P, Varela C, Oyarce MP, Del Rio R & Iturriaga R. (2016). Intermittent Hypoxia-Induced Carotid Body Chemosensory Potentiation and Hypertension Are Critically Dependent on Peroxynitrite Formation. *Oxid Med Cell Longev* **2016,** 9802136.

Nanduri J, Peng YJ, Wang N, Khan SA, Semenza GL, Kumar GK & Prabhakar NR. (2017). Epigenetic regulation of redox state mediates persistent cardiorespiratory abnormalities after long-term intermittent hypoxia. *J Physiol* **595,** 63-77.

O'Mahony SM, Hyland NP, Dinan TG & Cryan JF. (2011). Maternal separation as a model of brain-gut axis dysfunction. *Psychopharmacology* **214,** 71-88.

Peng Y-J, Yuan G, Khan S, Nanduri J, Makarenko VV, Reddy VD, Vasavda C, Kumar GK, Semenza GL & Prabhakar NR. (2014). Regulation of hypoxia-inducible factor-α isoforms and redox state by carotid body neural activity in rats. *The Journal of Physiology* **592,** 3841-3858.

Peng YJ, Overholt JL, Kline D, Kumar GK & Prabhakar NR. (2003). Induction of sensory long-term facilitation in the carotid body by intermittent hypoxia: implications for recurrent apneas. *Proceedings of the National Academy of Sciences of the United States of America* **100,** 10073-10078.

Prabhakar NR. (2016). Carotid body chemoreflex: a driver of autonomic abnormalities in sleep apnoea. *Exp Physiol* **101,** 975-985.

Prabhakar NR, Peng YJ, Kumar GK & Nanduri J. (2015). Peripheral chemoreception and arterial pressure responses to intermittent hypoxia. *Compr Physiol* **5,** 561-577.

Ray CJ, Dow B, Kumar P & Coney AM. (2015). Mild Chronic Intermittent Hypoxia in Wistar Rats Evokes Significant Cardiovascular Pathophysiology but No Overt Changes in Carotid Body-Mediated Respiratory Responses. *Advances in experimental medicine and biology* **860,** 245-254.

Santisteban MM, Qi Y, Zubcevic J, Kim S, Yang T, Shenoy V, Cole-Jeffrey CT, Lobaton GO, Stewart DC, Rubiano A, Simmons CS, Garcia-Pereira F, Johnson RD, Pepine CJ & Raizada MK. (2017). Hypertension-Linked Pathophysiological Alterations in the Gut. *Circulation research* **120,** 312-323.

Schwenke DO, Bolter CP & Cragg PA. (2007). Are the carotid bodies of the guinea-pig functional? *Comparative biochemistry and physiology Part A, Molecular & integrative physiology* **146,** 180-188.

Skelly JR, Edge D, Shortt CM, Jones JF, Bradford A & O'Halloran KD. (2012). Tempol ameliorates pharyngeal dilator muscle dysfunction in a rodent model of chronic intermittent hypoxia. *American journal of respiratory cell and molecular biology* **46,** 139-148.

Souza GMPR, Bonagamba LGH, Amorim MR, Moraes DJA & Machado BH. (2015). Cardiovascular and respiratory responses to chronic intermittent hypoxia in adult female rats. *Experimental Physiology* **100,** 249-258.

Sun MK & Reis DJ. (1994). Hypoxia selectively excites vasomotor neurons of rostral ventrolateral medulla in rats. *Am J Physiol* **266,** R245-256.

Tamisier R, Gilmartin GS, Launois SH, Pepin JL, Nespoulet H, Thomas R, Levy P & Weiss JW. (2009). A new model of chronic intermittent hypoxia in humans: effect on ventilation, sleep, and blood pressure. *J Appl Physiol (1985)* **107,** 17-24.

Tomasova L, Konopelski P & Ufnal M. (2016). Gut Bacteria and Hydrogen Sulfide: The New Old Players in Circulatory System Homeostasis. *Molecules* **21**.

Tripathi A, Melnik AV, Xue J, Poulsen O, Meehan MJ, Humphrey G, Jiang L, Ackermann G, McDonald D, Zhou D, Knight R, Dorrestein PC & Haddad GG. (2018). Intermittent Hypoxia and Hypercapnia, a Hallmark of Obstructive Sleep Apnea, Alters the Gut Microbiome and Metabolome. *mSystems* **3**.

van de Wouw M, Boehme M, Lyte JM, Wiley N, Strain C, O'Sullivan O, Clarke G, Stanton C, Dinan TG & Cryan JF. (2018). Short-chain fatty acids: microbial metabolites that alleviate stress-induced brain-gut axis alterations. *J Physiol*.

Wu J, Sun X, Wu Q, Li H, Li L, Feng J, Zhang S, Xu L, Li K, Li X, Wang X & Chen H. (2016). Disrupted intestinal structure in a rat model of intermittent hypoxia. *Molecular medicine reports* **13,** 4407-4413.

Yan B, Soukhova-O'Hare GK, Li L, Lin Y, Gozal D, Wead WB, Wurster RD & Cheng ZJ. (2008). Attenuation of heart rate control and neural degeneration in nucleus ambiguus following chronic intermittent hypoxia in young adult Fischer 344 rats. *Neuroscience* **153,** 709-720.

Yang T, Santisteban MM, Rodriguez V, Li E, Ahmari N, Carvajal JM, Zadeh M, Gong M, Qi Y, Zubcevic J, Sahay B, Pepine CJ, Raizada MK & Mohamadzadeh M. (2015). Gut dysbiosis is linked to hypertension. *Hypertension (Dallas, Tex : 1979)* **65,** 1331-1340.

Zanella S, Doi A, Garcia AJ, 3rd, Elsen F, Kirsch S, Wei AD & Ramirez JM. (2014). When norepinephrine becomes a driver of breathing irregularities: how intermittent hypoxia fundamentally alters the modulatory response of the respiratory network. *The Journal of neuroscience : the official journal of the Society for Neuroscience* **34,** 36-50.

Zoccal DB, Bonagamba LG, Oliveira FR, Antunes-Rodrigues J & Machado BH. (2007). Increased sympathetic activity in rats submitted to chronic intermittent hypoxia. *Experimental physiology* **92,** 79-85.

Chapter 4. Chronic intermittent hypoxia lowers *Lactobacillus rhamnosus* relative abundance and increases apnoea index and blood pressure: Effects of prebiotic supplementation

Karen M. O'Connor[a,b,c] Eric F. Lucking[a], Thomaz F.S. Bastiaanssen[b,c], Veronica L. Peterson[d], Fiona Crispie[c,d], Anna V. Golubeva[c], Paul Cotter[c,d], Gerard Clarke[c,e], John F. Cryan[b,c], Ken D. O'Halloran[a,c]

[a]*Department of Physiology, School of Medicine, College of Medicine & Health, University College Cork, Cork, Ireland*

[b]*Department of Anatomy & Neuroscience, School of Medicine, College of Medicine & Health, University College Cork, Cork, Ireland*

[c]*APC Microbiome Ireland, University College Cork, Cork, Ireland*

[d]*Teagasc Food Research Centre, Moorepark, Fermoy, County Cork, Ireland*

[e]*Department of Psychiatry and Neurobehavioural Science, School of Medicine, College of Medicine & Health, University College Cork, Cork, Ireland*

Abbreviations: AUC, area under the curve; BH, Benjamini-Hochberg; CIH, chronic intermittent hypoxia; DA, dopamine; DOPAC, 3,4-Dihydroxyphenylacetic acid; Dia, diaphragm; EMG, electromyogram; $ETCO_2$, end-tidal carbon dioxide; FDR, false discovery rate; f_R, respiratory frequency; $FiCO_2$, fractional inspired carbon dioxide concentration; F_iO_2, fractional inspired oxygen concentration; GABA, gamma-Aminobutyric acid; HFD, high-fat diet; HSD, high-salt diet; HVA, homovanillic acid; IFN, interferon; IL, interleukin; KC/GRO, keratinocytechemoattractant/growth-related oncogene; LSD, least significant difference; $_L$-DOPA, $_L$-3,4-dihydroxyphenylalanine; NA, noradrenaline; NaCN, sodium cyanide; NTS, nucleus tractus solitarius; OSA, Obstructive sleep apnoea; PBG, phenylbiguanide; PCA, principal component analysis; PCoA, Principal coordinates analysis; $PaCO_2$, partial pressure of arterial carbon dioxide; PaO_2, partial pressure of arterial oxygen; PREB, prebiotic; SaO_2, arterial oxygen saturation; SDB, sleep-disordered breathing; SD1, short-term respiratory timing variability; SD2, long-term respiratory timing variability; T_e, expiratory time; T_i, inspiratory time; TMAO; trimethylamine N-oxide; TNF-α, tumor necrosis factor-α; T_{tot}, total breath duration; $\dot{V}co_2$, carbon dioxide production; V_E, minute ventilation; $V_E/\dot{V}co_2$, ventilatory equivalent for CO_2; $\dot{V}o_2$, oxygen consumption; V_T, tidal volume; V_T/T_i, mean inspiratory flow; 5-HIAA, 5-hydroindoleacetic acid; 5-HT, 5-hydroxytryptamine (serotonin); $5\text{-}HT_3$, 5-hydroxytryptamine type 3.

Abstract

Background: Evidence is accruing to suggest that microbiota-gut-brain signalling plays a regulatory role in cardiorespiratory physiology. Chronic intermittent hypoxia (CIH), modelling human sleep apnoea, affects gut microbiota composition and elicits cardiorespiratory morbidity. We determined if treatment with prebiotic fibres, promoting the expansion of beneficial microbes, ameliorates cardiorespiratory dysfunction in CIH-exposed rats.

Methods: Adult male rats were exposed to CIH (96 cycles/day, 6.0% O_2 at nadir) for 14 consecutive days with and without prebiotic supplementation (fructo- and galacto-oligosaccharides) beginning two weeks prior to gas exposures.

Findings: CIH increased apnoea index, and caused cardiac autonomic imbalance and hypertension. CIH exposure altered the gut microbiota, predominantly decreasing the relative abundance of *Lactobacillus rhamnosus* and increasing the relative abundance of pathogenic species. Faecal short-chain fatty acid (SCFA) concentrations, plasma and brainstem pro-inflammatory cytokine concentrations as well as brainstem neurochemistry were unaffected by exposure to CIH. Prebiotic administration modulated gut microbiota composition and diversity, increasing faecal acetic and propionic acid concentrations, but did not recover CIH-induced reductions in *Lactobacillus rhamnosus* or prevent adverse CIH-induced cardiorespiratory phenotypes.

Interpretation: CIH-induced cardiorespiratory dysfunction is not critically dependent upon decreased gut SCFA concentrations. Prebiotic-related boosting of SCFAs was not sufficient to prevent CIH-induced apnoea and hypertension in our model. We identified associations between multiple gut bacterial species and blood pressure. CIH-induced cardiorespiratory and autonomic dysfunction may relate to an aberrant gut microbiota signature contributing to maladaptive plasticity in the neural circuitry controlling respiratory and autonomic homeostasis. Our findings have relevance for human sleep-disordered breathing and contribute to an emerging interest in the manipulation of the gut microbiota as an adjunctive therapy for human cardiorespiratory disease.

Funding: Department of Physiology and APC Microbiome Ireland, University College Cork, Ireland.

Keywords: Chronic intermittent hypoxia; prebiotics; apnoea; hypertension; autonomic dysfunction; neurochemistry; short-chain fatty acids; vagus; microbiota

4.1. Introduction

Obstructive sleep apnoea (OSA), the most common form of sleep-disordered breathing (SDB), is recognised as a major worldwide health crisis with devastating consequences for integrative body systems (Garvey *et al.*, 2015). OSA is characterised by repetitive collapse of the pharyngeal airway during sleep, with episodic oxygen fluctuations culminating in recurrent exposure to chronic intermittent hypoxia (CIH). It is now apparent that exposure to CIH has adverse effects on the cardiorespiratory control network and is recognised as a major driver of OSA-related morbidities (Prabhakar *et al.*, 2007; Julien *et al.*, 2008; Edge & O'Halloran, 2015; O'Halloran, 2016; Iturriaga *et al.*, 2017; Laouafa *et al.*, 2017; Elliot-Portal *et al.*, 2018).

Studies have recurrently implicated the carotid bodies, the dominant peripheral oxygen sensors, in the manifestation of CIH-induced cardiorespiratory dysfunction (Prabhakar *et al.*, 2007; Peng *et al.*, 2011; Iturriaga *et al.*, 2015; Del Rio *et al.*, 2016; Iturriaga *et al.*, 2017). However, exposure to CIH elicits cardiorespiratory and autonomic disturbances in guinea-pigs with hypoxia-insensitive carotid bodies (Docio *et al.*, 2018; Lucking *et al.*, 2018b), revealing that sites beyond the carotid bodies can contribute to the manifestation of CIH-induced cardiorespiratory and autonomic disturbances. It is known that CIH-induced plasticity also occurs at other key sites of the cardiorespiratory control circuit, including the nucleus tractus solitarius (NTS), pre-Bötzinger complex, ponto-medullary network and paraventricular nucleus of the hypothalamus (Veasey *et al.*, 2004; Almado *et al.*, 2012; Moraes *et al.*, 2013; Garcia *et al.*, 2016; Garcia *et al.*, 2017; Li *et al.*, 2018). More recently, studies have described effects of CIH on other peripheral sites including the gut microbiota (Moreno-Indias *et al.*, 2015; Moreno-Indias *et al.*, 2016; Lucking *et al.*, 2018b; AlMarabeh *et al.*, 2019; O'Neill *et al.*, 2019).

The microbiota-gut-brain axis plays a critical regulatory role in physiological systems. Dysregulated microbiota-gut-brain axis signalling affects homeostatic neurocontrol networks manifesting in pathophysiological behaviours and brain functions (Golubeva *et al.*, 2015; Kelly *et al.*, 2016b; Dinan & Cryan, 2017). Recent studies extend this concept to cardiorespiratory control (Lucking *et al.*, 2018b; O'Connor *et al.*, 2019a). There is considerable interest in the modulatory role of the gut microbiota and the gut microbiota metabolites, short-chain fatty acids (SCFAs), in cardiovascular and autonomic function (Durgan *et al.*, 2016; Ganesh *et al.*, 2018; Kim *et al.*, 2018; Meng *et al.*, 2019). Proliferation of lactate-producing, as well as diminished butyrate- and acetate-producing taxa is evident

in hypertensive models (Yang *et al.*, 2015; Durgan *et al.*, 2016; Adnan *et al.*, 2017; Kim *et al.*, 2018). Hypertensive donor faeces transferred to normotensive animals leads to the development of hypertension in recipient animals (Durgan *et al.*, 2016; Adnan *et al.*, 2017; Toral *et al.*, 2019). Moreover, in a rat model of SDB, prebiotic administration (Hylon VII) stimulates the expansion of beneficial commensal microbiota, augmenting several SCFA-producing taxa including *Bifidobacterium, Ruminococcus, Blautia* and *Collinsella,* restoring caecal acetate concentrations and preventing the establishment of hypertension (Ganesh *et al.*, 2018). Chronic acetate administration into the caecum of OSA + high-fat diet (OSA+ HFD) rats prevents the development of high blood pressure (Ganesh *et al.*, 2018). Additionally, butyrate treatment in angiotensin-II-induced hypertensive mice prevented establishment of hypertension, decreased baroreceptor reflex gain, cardiac autonomic dysfunction and cardiac hypertrophy (Kim *et al.*, 2018).

In rat models, disruption of the gut microbiota using antibiotic administration, faecal microbiota transfer or pre-natal stress results in altered ventilatory responses to hypoxic and hypercapnic chemostimulation (Golubeva *et al.*, 2015; O'Connor *et al.*, 2019a). Respiratory frequency response to hypercapnic chemostimulation correlated with altered bacterial genera in adult rats with antecedent pre-natal stress (Golubeva *et al.*, 2015). Several genera, predominantly of Firmicutes phylum correlated with brainstem neuromodulators crucial in the control of breathing (O'Connor *et al.*, 2019a). Exposure to CIH dysregulates cardiorespiratory control in guinea pigs resulting in aberrant phenotypes including altered autonomic control of heart rate, decreased respiratory variability and prevalence of protective sighs and brainstem noradrenaline concentrations, as well as disturbed gut microbiota indicating that aberrant gut microbiota may at least partly contribute to cardiorespiratory and autonomic malaise in CIH-exposed guinea pigs (Lucking *et al.*, 2018b).

Collectively, these studies highlight a contributory role of perturbations to microbiota-gut-brain axis signalling in the manifestation of CIH-induced cardiorespiratory dysfunction, of relevance to OSA. There is a growing interest in developing strategies to manipulate the microbiota as a potential therapeutic intervention in the treatment of cardiorespiratory disease. Rodent and human studies have revealed that prebiotic administration has positive impacts on brain neurochemistry and functions (Savignac *et al.*, 2013; Burokas *et al.*, 2017; Dinan & Cryan, 2017; Mika *et al.*, 2017). Moreover, prebiotic feeding prevented the development of hypertension in a rat model of OSA (Ganesh *et al.*, 2018). Therefore, we assessed cardiorespiratory physiology and gut microbiota composition and diversity in adult rats following exposure to normoxia (Sham) or CIH. We hypothesised that there would be

evidence of cardiorespiratory and autonomic dysfunction and altered gut microbiota in CIH-exposed rats. We examined the effects of prebiotic fibre supplementation to test the hypothesis that manipulation of the gut microbiota ameliorates or prevents the deleterious effects of exposure to CIH on cardiorespiratory physiology. We performed whole-genome shotgun sequencing with a view to identifying microbial signatures that underscore cardiorespiratory homeostasis and dysfunction.

4.2. Materials and Methods

4.2.1 Ethical approval

Procedures on live animals were performed in accordance with European directive 2010/63/EU under authorisation from the Government of Ireland Department of Health (B100/4498) and Health Products Regulatory Authority (AE19130/P070). Ethical approval was obtained from University College Cork (AEEC #2013/035; #2017/023) and procedures were carried out in accordance with guidelines laid down by University College Cork's Animal Welfare Body.

4.2.2 Experimental animals

Eight- to ten-week old adult male Sprague Dawley rats (n=72; purchased from Envigo, UK) were housed as age-matched pairs in standard rat cages. Rodents had *ad libitum* access to standard rat chow and were housed under a 12-hr light: 12-hr dark cycle.

4.2.3 Prebiotic administration

Eight-week old rats (n=24) were randomly allocated to receive prebiotic fibres in water (PREB; galactooligossaccharides and fructooligosaccharides) with *ad libitum* access for 4-weeks to promote the growth of beneficial host microbiota (Savignac *et al.*, 2013; Alves *et al.*, 2017). After 2 weeks of PREB treatment, a subset of rats was exposed to CIH (see section 4.2.4) for the final 2 weeks creating two groups: Sham+PREB (n=12) and CIH+PREB (n=12).

4.2.4 Chronic intermittent hypoxia rat model

Ten-week old rats (n=48) were randomly assigned to one of two groups, each receiving vehicle (VEH): Sham+VEH (n=24) and CIH+VEH (n=24). CIH exposed rats were placed in chambers wherein ambient oxygen concentration was tightly regulated using a dynamic oxygen/nitrogen controller (Oxycycler™; Biospherix, New York, NY, USA). CIH exposure was comprised of 96 cycles of 90 secs of exposure to hypoxia (nadir, FiO_2 = 0.06, balance N_2) and 180 secs of exposure to normoxia (FiO_2 =0.21; balance N_2), over 8 hours during the light phase for 14 consecutive days. Animals were studied on the day subsequent to the last day of CIH exposure. Concurrently, rats assigned to the Sham group were exposed to room air (normoxia) in the same room with similar environmental cues for the duration of the study.

4.2.5 Assessment of respiratory flow in rats during quiet rest

Whole-body plethysmography: During quiet rest, whole-body plethysmography (DSI, St. Paul, Minnesota, USA) was used to record respiratory flow signals during quiet rest. Animals were placed into custom plethysmograph chambers (601-1427-001 PN, DSI) with a room air flow

rate maintained at 3l/min. Animals were allowed to acclimate for 30-90 minutes to encourage habituation to the new surroundings. Paired contemporaneous observations were performed during light hours in Sham+VEH (n=12) *versus* CIH+VEH (n=12) and subsequently Sham+PREB (n=12) *versus* CIH+PREB (n=12) using a pair of plethysmograph chambers.

Metabolic measurements: O_2 consumption (VO_2) and CO_2 production (VCO_2) were measured in rodents throughout the experimental protocol (O_2 and CO_2 analyser; AD Instruments, Colorado Springs, CO, USA) as previously described (Haouzi *et al.*, 2009; Bavis *et al.*, 2014; Lucking *et al.*, 2018b; O'Connor *et al.*, 2019a).

Experimental protocol: Once the acclimation period was complete and animals were confirmed to be at quiet rest, baseline parameters were recorded during a 10-15 minute steady-state normoxia period (FiO_2 = 0.21; balance N_2). This was followed by a 10 minute poikilocapnic hypoxia challenge (FiO_2=0.10; balance N_2). Normoxia was subsequently restored in each chamber to re-establish stable baseline breathing. Thereafter, a second baseline period was recorded followed by a 10 minute hypercapnia challenge ($FiCO_2$ = 0.05; balance O_2). Subsequently, a third normoxic baseline period was recorded. Rats were then exposed to a 10 minute hypoxic hypercapnic challenge (FiO_2 = 0.10; $FiCO_2$ =0.05, balance N_2).

Data analysis for whole-body plethysmography: Respiratory parameters including tidal volume (V_T), respiratory frequency (f_R), minute ventilation (V_E), expiratory time (T_e) and inspiratory time (T_i) were recorded on a breath-by-breath basis for analysis (FinePointe software Buxco Research Systems, Wilmington, NC, USA). Artefacts relating to animal movement and sniffing in respiratory flow recordings were omitted from analysis. A single baseline period during normoxia was determined by averaging the three baseline recording epochs to determine resting steady-state respiratory and metabolic parameters. Ventilatory and metabolic data were averaged and reported for the final 5 minutes of acute poikilocapnic hypoxia, hypercapnia and hypoxic hypercapnia allowing sufficient time for gas mixing in the custom plethysmograph chambers as well as steady-state assessment of metabolic and ventilatory parameters during gas challenges. Data are expressed as absolute change from baseline values. Respiratory flow recordings were assessed for the occurrence of augmented breaths (sighs) during normoxia, poikilocapnic hypoxia and hypercapnia, as well as the frequency of apnoea events (post-sigh and spontaneous apnoeas) during normoxia as previously described (Edge *et al.*, 2012). The criterion for an apnoea was a pause in breathing greater than two consecutive missed breaths. Apnoea data are expressed as apnoea index

(apnoea events per hour), combining post-sigh and spontaneous apnoeas. A sigh was defined as an augmented breath double the amplitude of the average V_T. The frequency and amplitude of sighs were determined. Poincaré plots expressing breath-to-breath (BB*n*) *versus* subsequent breath-to-breath interval (BB*n+1*) were extrapolated allowing for determination of short- (SD1) and long-term (SD2) respiratory timing variability during steady-state baseline breathing. V_T, V_E, V_T/T_i, VO_2 and VCO_2 were normalised per 100g body mass.

4.2.6 Assessment of cardiorespiratory parameters under urethane anaesthesia

Surgical protocol and cardiorespiratory measures: Following whole-body plethysmography, cardiorespiratory parameters were assessed in Sham+VEH, CIH+VEH, Sham+PREB and CIH+PREB rats (n=11-12 per group) under urethane anaesthesia (1.5 g/kg i.p.; 20% w/v) following isoflurane induction (5% by inhalation in room air). Throughout the surgical and experimental protocol, the depth of anaesthesia was carefully assessed by monitoring reflex responses to tail/paw pinch and the corneal reflex. Supplemental doses of anaesthetic were given as required. Rodents were placed in a supine position on a homeothermic blanket system (Harvard Apparatus, Holliston, MA, USA) to maintain core temperature at 37 °C, which was measured by a rectal temperature probe. A mid-cervical tracheotomy was performed, followed by intravenous (i.v.) cannulation of the right jugular vein for infusion of supplemental anaesthetic and drugs. The carotid (n=22)/femoral artery (n=1) was cannulated for the recording of arterial blood pressure and the withdrawal of blood samples for arterial blood gas, pH and electrolyte analysis (i-STAT; Abbott Laboratories Ltd). Using a foot clip, arterial oxygen saturation (SaO_2; Starr Life Sciences, PA, USA) was determined and maintained above 95% via a bias flow of supplemental O_2 passing the tracheal cannula sourced from a gas mixing system (GSM-3 Gas Mixer; CWE Inc.). A pneumotachometer (Hans Rudolf) and a CO_2 analyser (microCapStar End-Tidal CO_2 analyser; CWE Inc., USA) were connected to the tracheal cannula to measure tracheal flow and end-tidal CO_2 ($ETCO_2$), respectively. Diaphragm electromyogram (EMG) activity was continuously measured using a concentric needle electrode (26G; Natus Manufacturing Ltd., Ireland). Signals were amplified (x5,000), filtered (band pass; 500–5000 Hz) and integrated (50 ms time constant; Neurolog system, Digitimer Ltd., UK). Data were digitised via a PowerLab-LabChart v7 (ADInstruments) data acquisition system.

Experimental protocol: An arterial blood sample was obtained from each animal following a 30 minute stabilisation period, after which, a minimum 10 minute baseline recording period was observed for assessment of baseline parameters (FiO_2 = 0.25-0.40; balance N_2). The rats

were exposed to a poikilocapnic hypoxia challenge (FiO_2 = 0.12, balance N_2) for 5 minutes, followed by a recovery period. Animals were then exposed to a 5 minute hypoxic hypercapnic challenge (FiO_2 = 0.12, $FiCO_2$ = 0.05, balance N_2). Following a recovery period, sodium cyanide (NaCN; 200 µg/kg i.v.) was administered to evoke carotid body-dependent increases in ventilation. After an adequate recovery period and removal of the pneumotachometer, a second arterial blood sample was taken. Next, the serotonin type 3 (5-HT_3) receptor agonist phenylbiguanide (PBG; 25 µg/kg i.v.) was administered to stimulate pulmonary vagal afferent C-fibres (Dutta & Deshpande, 2010; Lucking *et al.*, 2018a) eliciting the classic pulmonary chemoreflex. Successively, phenylephrine (50 µg/kg i.v.), sodium nitroprusside (50 µg/kg i.v.), atenolol (2 mg/kg i.v.), propranolol (1 mg/kg i.v.) and hexamethonium (25mg/kg i.v.) were administered to assess cardiovascular responses to pharmacological manipulation with sufficient recovery periods allowed between each pharmacological challenge. Animals were euthanised by urethane (i.v) overdose. One animal (Sham+PREB, n=1) presented with uncharacteristically poor ventilatory and cardiovascular responses throughout the experimental protocol; this animal was excluded from data analysis. In all animals, blood was collected, prepared in 3% Na_2EDTA (disodium salt dehydrate) and centrifuged. Plasma was snap frozen in liquid nitrogen for subsequent analysis of corticosterone and inflammatory cytokine concentrations. Whole brains were removed, separated into pons and medulla oblongata, frozen in isopentane at −80 °C and stored at −80 °C until subsequent analysis by high-performance liquid chromatography. The lungs were removed and weighed and were allowed to air dry at 37°C for at least 48 hrs before being re-weighed to provide an index of pulmonary oedema. The caecum was removed, weighed and caecal contents were removed and snap frozen in liquid nitrogen for whole-genome shotgun sequencing. Faeces was removed from the colon for the assessment of SCFA concentrations by gas chromatography. The heart was removed, and the right ventricle was separated from the left ventricle + septum and each were weighed separately.

Data analysis of cardiorespiratory parameters in anaesthetised rats: Baseline parameters were averaged over 10 minutes of stable recording and data are presented as absolute values. For cardiorespiratory and EMG responses to poikilocapnic hypoxia and hypoxic hypercapnia the average of the last minute of recordings was determined and data were compared with the 1 minute pre-challenge baseline. Data for drug challenges were averaged into 3 or 5 second bins and the peak cardiorespiratory responses to NaCN, PBG, phenylephrine, sodium nitroprusside, atenolol, propranolol and hexamethonium administration were determined and compared to the respective 1 minute pre-challenge

baseline. Maximum apnoea and post-apnoea tachypnoea in response to PBG are expressed as the duration of the apnoea or tachypnoea period normalised in each trial to the average cycle duration determined during the 30 sec pre-challenge baseline period. All cardiorespiratory responses to chemostimulation and drug administration are expressed as percent change from the preceding baseline values.

4.2.7 Brainstem monoamine concentrations

High-performance liquid chromatography (HPLC) coupled to electrochemical detection for the measurement of brainstem monoamine concentrations: Pons (n=11-12/group) and medulla oblongata (n=11-12/group) tissues were sonicated in 1 ml of chilled mobile phase, spiked with 2ng/20µl of a N-methyl 5-HT (internal standard; Bandelin Sonolus HD 2070). Brainstem monoamine, precursor and metabolite concentrations were measured as previously described (Lucking *et al.*, 2018b; O'Connor *et al.*, 2019a). Noradrenaline (NA), dopamine (DA), serotonin (5-HT), and monoamine metabolites and precursor, 5-hydroxyindoleacetic acid (5-HIAA), homovanillic acid (HVA), 3,4-Dihydroxyphenylacetic acid (DOPAC) and $_{L}$-3,4 dihydroxyphenylalanine ($_{L}$-DOPA) were identified by their characteristic retention times. This was determined by standard injections run at regular intervals during sample analysis.

Data analysis: Class-VP5 software was used to process chromatographs. Concentrations (ng/g) of monoamines, precursors and metabolites in each sample were determined using analyte:internal standard peak response ratios.

4.2.8 Plasma and brainstem cytokine concentrations

Brainstem tissue homogenisation and protein quantification: A separate cohort of rats (Sham, n=12; CIH, n=12) were euthanised by pentobarbitone (i.v.) overdose and whole brains were removed. The pons and medulla oblongata were separated from the brain, frozen in isopentane at -80°C and stored at -80°C until subsequent determination of brainstem cytokine concentrations. Pons and medulla oblongata tissue (Sham, n=12; CIH, n=12) were weighed and sonicated (1 ml per 100 mg of tissue) in radioimmunoprecipitation assay (RIPA buffer) (10X RIPA, deionised H_20, 200Mm sodium fluoride, 100Mm, phenylmethylsulfonylfluoride (PMSF), 1X protease inhibitor cocktail and 1X phosphate inhibitor cocktail). Samples were centrifuged at 10,000 x g for 15 minutes at 4 °C, to pellet membranes and nuclei. The protein concentration of each sample was determined using a bicinchonic acid (BCA) protein quantification assay (Thermo Fisher Scientific) as per the manufacturer's instructions, at a dilution of 1:10.

Multiplex assay for measurement of plasma and brainstem cytokines: Concentrations of interleukin(IL)-1β, IL-4, IL-5, IL-10, IL-13, interferon (IFN)-γ, keratinocytechemoattractant/growth-related oncogene (KC/GRO) and tumor necrosis factor (TNF)-α were measured in plasma (all groups; n=11-12/group) as well as pons and medulla oblongata (Sham and CIH only; n=12) supernatants by sandwich immunoassay methods using commercially available detection kits (V-Plex Pro-inflammatory Panel 2 (rat) kit; Meso Scale Discovery, Gaithersburg, USA) as per manufacturer's instructions. For pons and medulla oblongata tissues 100 µg of protein sample was loaded per well as previously described (Lucking et al., 2018a). Plates were read using QuickPlex SQ 120 imager and computer (Meso Scale Discovery).

4.2.9 Plasma corticosterone

Plasma samples were thawed and concentrations of corticosterone were determined using commercially available enzyme-linked immunosorbent assay kit according to the manufacturer's instructions (ENZO Life Sciences, UK) using a spectrophotometer (SpectraMax M3, Molecular devices).

4.2.10 Microbiota composition and diversity

DNA extraction from caecal material: DNA was extracted from caecal material as previously described (Gough *et al.*, 2018).

Whole-metagenome shotgun sequencing: Whole-metagenome shotgun libraries were prepared in accordance with the Nextera XT DNA Library Preparation Guide from Illumina with the exception that the tagmentation time was increased to 7 minutes. After indexing and clean-up of the PCR products as described in the protocol, each sample was run on an Agilent bioanalyser high sensitivity chip (Agilent) to determine the size range of the fragments obtained. The concentration of the samples was also determined at this point using a Qubit High Sensitivity Assay (Life-Sciences). Samples were then pooled equimolarly and the final concentration of the pooled library was determined by quantitative PCR using the Kapa Library Quantification kit for Illumina (Roche). The pooled library was then sequenced on the Illumina NextSeq using the 2 x150 High Output kit according to standard Illumina sequencing protocols.

Metagenomic bioinformatic analysis: Shotgun metagenomic sequence files (BCL, base calls) were converted to fastq format using bcl2fastq version 2.19. Forward and reverse fastq files were processed using KneadData version 0.7.2 from the Huttenhower bioBakery suite (McIver *et al.*, 2018). A reference library was created to remove host DNA in Bowtie2 version

2.3.4 from the NCBI rat genome (*Rattus norgegicus,* GCF 000001895.5). Quality filtering was performed using the default setting (ex., phred=33) and trimming with Trimmomatic version 0.38-1. Resulting high quality paired-end reads for each sample were then concatenated in KneadData. Kraken2 version 2.0.7-beta was used for taxonomic classification with the standard database. Report files of taxonomic counts for each sample were merged into a single count file using a custom R script and ran in R version 3.5.2.

4.2.11 Faecal short-chain fatty acid concentrations

SCFA analysis and extraction were carried out by MS-Omics (Vedbaek, Denmark) as follows. Faecal water was prepared by homogenising the faecal samples (approximately 100 mg) in ultrapure water (3µl/µg). Samples were then vortexed for 2 minutes followed by centrifugation (5 minutes, 30000g, 5°C). The supernatant was transferred to a centrifuge filter and the filtered samples were used for analysis. The filtrate was acidified using hydrochloride acid, and deuterium labelled internal standards where added. All samples were analysed in a randomized order. Analysis was performed using a high polarity column (Zebron™ ZB-FFAP, GC Cap. Column 30 m x 0.25 mm x 0.25 µm) installed in a gas chromatography (GC; 7890B, Agilent) coupled with a quadropole detector (59977B, Agilent). The system was controlled by ChemStation (Agilent). Raw data was converted to netCDF format using Chemstation (Agilent), before the data was imported and processed in Matlab R2014b (Mathworks, Inc.) using the PARADISe software (Johnsen *et al.*, 2017). Data are expressed as absolute concentration in mM.

4.2.12 Statistical analysis

Data was assessed for outliers, normal distribution and equality of variances using box-plots, Shapiro-Wilk test and Levene's test, respectively. In situations of normal distribution, data were statistically compared using independent samples *t*-test and two-way ANOVA followed by Fisher's least significant test for pairwise comparisons, where appropriate. In some instances, the assumptions of no significant outliers and homogeneity of variances were violated for the two-way ANOVA. When the assumption of normal distribution was violated, data were statistically compared using non-parametric Mann-Whitney *U* test and non-parametric Kruskal-Wallis test followed by Mann-Whitney *U* test for pairwise comparisons, where appropriate. Statistical significance was assumed at $p<0.05$. Bonferroni correction was applied to adjust for multiple comparisons with the exception of microbiota composition data. Statistical significance for multiple comparisons (except microbiota composition data) was accepted at $p<0.05$ divided by the number of comparisons made. Benjamini-Hochberg

(BH) adjustment procedure was applied with the false discovery rate (FDR) set at 10% to correct for multiple testing in the relative abundance microbiota data. Microbiota data are expressed as median (IQR). All other data are expressed as mean ± SD or displayed graphically as box and whisker plots (median, IQR and minimum to maximum values). The 2D principal component analysis (PCA) was constructed using the center-log ratio transformed values (aitchison distance) computed using the ALDEx2 (Fernandes *et al.*, 2013) library in R (version 3.6.0) with Rstudio (version 1.1.453), as is appropriate for compositional data (Gloor *et al.*, 2017) using recommended parameters and 1000 permutations. For correlation analysis between bacterial species, including *Lactobacillus rhamnosus* and physiological parameters of interest, Hierarchical All-against-All association testing (HAllA) was used (version 0.8.7) with Spearman correlation as correlation metric, medoid as clustering method and $q < 0.1$ as threshold for significance. Microbiota analysis was performed in SPSS v25 and R software environment. SPSS v25 was used for all other statistical analysis. GraphPad Software v6 (GraphPad Software, San Diego, CA, USA) and R software environment were used to generate graphs. Adobe illustrator CS5 (v15) was used to edit figures.

4.3. Results

4.3.1 Body and tissue weight

CIH exposure and prebiotic administration had a significant effect on body weight (Diet*CIH, $F(1, 43) = 5.426$, $p=0.025$, $\eta^2=0.112$, Table 4.1). The combination of CIH+PREB, decreased body weight gain compared with CIH+VEH or Sham+PREB rats; Sham+PREB rats were also lighter than Sham+VEH rats. CIH exposure had no effect on caecum weight but as expected, prebiotic supplementation increased caecum weight. Differences between groups in cardiac ventricle weights relate to changes in body weight (Appendix Table C.1).

	Sham+VEH	CIH+VEH	Sham+PREB	CIH+PREB	p-value (Kruskal-Wallis)	p-value (two-way ANOVA)	Sham+VEH v CIH+VEH	CIH+VEH v CIH+PREB	Sham+PREB v CIH+PREB	Sham+VEH v Sham+PREB
Body mass (g)	368 ± 16	346 ± 21	308 ± 27	263 ± 16	N/A	Diet, **p<0.0005**; CIH, **p<0.0005**; Diet*CIH, **p=0.025**	0.057	**0.0005**	**<0.0005**	**<0.0005**
RV (mg/100g)	46 ± 7.8	50 ± 6	58 ± 9.1	61 ± 9.1	**<0.0005**	N/A	0.325	**0.004**	0.908	**0.001**
LV (mg/100g)	235 ± 24	232 ± 19	238 ± 22	236 ± 22	N/A	Diet, p=0.280; CIH, p=0.810; Diet*CIH, p=0.603	-	-	-	-
LV+RV (mg/100g)	278 ± 18	282 ± 15	299 ± 25	297 ± 29		Diet, **p=0.009**; CIH, p=0.821; Diet*CIH, p=0.569	0.578	0.139	0.806	0.023
Caecum (g/100g)	0.97 ± 0.27	0.87 ± 0.1	2.1 ± 0.46	2.3 ± 0.7	N/A	Diet, **p<0.0005**; CIH, p=0.716; Diet*CIH, p=0.345	0.709	**<0.0005**	0.293	**<0.0005**
Oedema index (% wet weight)	78 ± 1	77 ± 3	79 ± 1	76 ± 5	0.110	N/A	-	-	-	-

Table 4. 1 Body and tissue weights

BW, body weight; RV, right ventricle; LV, left ventricle; CIH, chronic intermittent hypoxia; PREB, prebiotic; VEH, vehicle. Data are shown as mean ± SD and were statistically compared using two-way ANOVA, followed by Fisher's least significant difference (LSD) post hoc where appropriate, or non-parametric Kruskal-Wallis test, followed by Mann-Whitney *U* test, where appropriate. Statistical significance for multiple comparisons was accepted at $p<0.05$ divided by the number of comparisons made, which was four i.e. $p<0.0125$. *p*-values shown in **bold** highlight significant differences.

4.3.2 Baseline ventilation and metabolism in rats during quiet rest

CIH exposure did not affect the majority of respiratory parameters during normoxia. Prebiotic fibre supplementation increased baseline V_E, V_T and V_T/T_i in Sham+PREB and CIH+PREB compared with Sham+VEH and CIH+VEH rats, respectively (Table 4.2), but the differences related to body weight (Appendix Table C.1). CIH exposure had no effect on VCO_2 production; CIH+PREB rats had significantly increased VCO_2 production compared with CIH+VEH rats, but VCO_2 production in Sham+PREB rats was not different compared with Sham+VEH (Table 4.2). CIH exposure had no effect on V_E/VCO_2 (breathing as a function of metabolism), but prebiotic administration increased V_E/VCO_2, however *post hoc* analysis revealed no difference between groups (Table 4.2). In summary, CIH exposure and prebiotic administration had modest effects on ventilation and metabolism during normoxia.

4.3.3 Respiratory timing variability, apnoeas and sighs during normoxia in rats during quiet rest

Assessments of short-term (SD1) and long-term (SD2) respiratory timing variability during normoxia did not reveal differences between groups ($p>0.05$; Fig. 4.1a-f). Apnoea index was significantly increased by CIH exposure ($X^2(3) = 9.284$, $p=0.026$, Fig. 4.1j), a consequence of alterations in spontaneous apnoea events; no statistically significant differences were evident in post-sigh apnoea events (Table 4.2). *Post hoc* analysis revealed that apnoea index was increased in CIH+PREB compared with Sham+PREB rats ($p=0.008$; Fig. 4.1j). The frequency of sighs was not affected by CIH exposure or prebiotic administration ($p>0.05$; Fig. 4.1k). Sham+PREB had elevated sigh amplitude compared with Sham+VEH rats (Table 4.2). The major finding was that CIH exposure increased apnoea index during quiet breathing at rest (normoxia) and prebiotic administration did not prevent this aberrant phenotype.

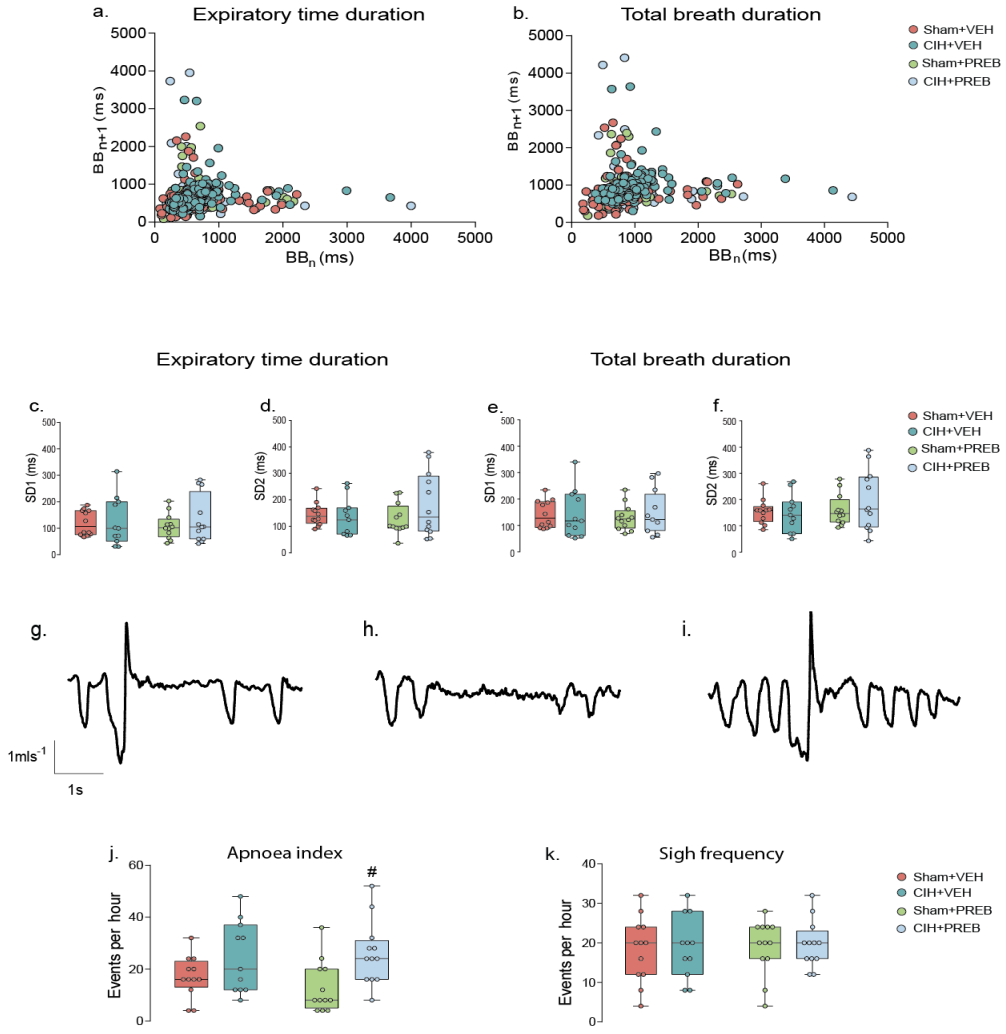


Figure 4. 1 CIH increase apnoea index

Poincaré plots of breath-to-breath (BBn) and subsequent breath-to-breath (BBn + 1) interval of expiratory duration (T_e; a) and total breath duration (T_{tot}; b) for Sham+VEH, CIH+VEH, Sham+PREB and CIH+PREB. Group data for T_e short-term variability (SD1; c) and long-term variability (SD2; d) and T_{tot} SD1 (e) and SD2 (f) in Sham+VEH, CIH+VEH, Sham+PREB and CIH+PREB rats during normoxia. Representative respiratory flow traces (downward deflections represent inspiration) illustrating a spontaneous sigh followed by an apnoea (g), a spontaneous apnoea (h) and a spontaneous sigh (i). Group data of apnoea index (j) and sigh frequency (k). CIH, chronic intermittent hypoxia; PREB, prebiotic; VEH, vehicle. Groups (c-f, j, k) are expressed as box and whisker plots (median, IQR and minimum to maximum values); n = 11-12. Groups were statistically compared using two-way ANOVA, followed by Fisher's least significant difference (LSD) *post hoc* where appropriate, or non-parametric Kruskal-Wallis test, followed by Mann-Whitney *U* test, where appropriate. Apnoea index was significantly affected by CIH exposure (p=0.026; Fig. 4.1j). Assessments of respiratory timing variability and frequency of sighs were not different between groups (p>0.05; Fig. 4.1a-f, 4.1k). # p=0.008, CIH+PREB *versus* Sham+PREB.

	Sham+VEH	CIH+VEH	Sham+PREB	CIH+PREB	p-value (Kruskal-Wallis)	p-value (two-way ANOVA)	Sham+VEH v CIH+VEH	CIH+VEH v CIH+PREB	Sham+PREB v CIH+PREB	Sham+VEH v Sham+PREB
f_R (brpm)	82 ± 8	78 ± 9	83 ± 9	81 ± 7	N/A	Diet, p=0.346; CIH, p=0.310; Diet*CIH, p=0.731	-	-	-	-
V_E (ml/min/100g)	53 ± 9	54 ± 6	63 ± 9	71 ± 6	**<0.0005**	N/A	0.498	**<0.0005**	0.038	**0.009**
V_T (ml/100g)	0.7 ± 0.1	0.7 ± 0.1	0.8 ± 0.1	0.9 ± 0.1	**<0.0005**	N/A	0.356	**0.001**	0.028	**0.009**
V_T/T_i (ml/s/100g)	2.8 ± 0.6	2.6 ± 0.4	3.1 ± 0.5	3.4 ± 0.3	N/A	Diet, **p<0.0005;** CIH, p=0.833; Diet*CIH, p=0.113	0.331	**<0.0005**	0.198	0.093
T_i (ms)	254 ± 26	277 ± 21	260 ± 28	268 ± 21	N/A	Diet, p=0.794; CIH, **p=0.032**; Diet*CIH, p=0.307	0.028	0.370	0.402	0.584
T_e (ms)	516 ± 74	520 ± 119	515 ± 71	501 ± 54	N/A	Diet, p=0.688; CIH, p=0.825; Diet*CIH, p=0.706	-	-	-	-
VO_2 (ml/min/100g)	2.7 ± 0.7	2.4 ± 0.8	3.1 ± 1.1	3.3 ± 1.1	N/A	Diet, **p=0.019**; CIH, p=0.815; Diet*CIH, p=0.420	0.467	0.028	0.681	0.251
VCO_2 (ml/min/100g)	1.9 ± 0.3	1.9 ± 0.2	2.0 ± 0.3	2.1 ± 0.3	**0.046**	N/A	0.758	**0.012**	0.525	0.166
V_E/VCO_2	28 ± 3	29 ± 4	31 ± 5	34 ± 5	N/A	Diet, **p=0.003**; CIH, p=0.107; Diet*CIH, p=0.603	0.073	0.128	0.015	0.438

Post sigh apnoea (events per hr)	12 ± 6	19 ± 13	9 ± 5	16 ± 9	0.083	N/A	-	-	-	-
Spontaneous apnoea (events per hr)	3.3 ± 5.0	5.5 ± 6.8	3.6 ± 5.2	10.0 ± 7.5	**0.044**	N/A	0.374	0.067	0.022	0.596
Sigh amplitude (ml/100g)	0.8 ± 0.2	1.2 ± 0.4	1.2 ± 0.2	1.4 ± 0.2	**<0.0005**	N/A	0.023	0.176	0.05	**<0.0005**

Table 4. 2 Baseline ventilation, apnoea, sigh and metabolism in rats during quiet rest

f_R, respiratory frequency (brpm, breaths per minute); V_E, minute ventilation; V_T, tidal volume; V_T/T_i, mean inspiratory flow; T_i, inspiratory time; T_e, expiratory time; VO_2, oxygen consumption; VCO_2, carbon dioxide production; V_E/VCO_2, ventilatory equivalent; CIH, chronic intermittent hypoxia; PREB, prebiotic; VEH, vehicle. Data are shown as mean ± SD and were statistically compared using two-way ANOVA, followed by Fisher's least significant difference (LSD) *post hoc* where appropriate, or non-parametric Kruskal-Wallis test, followed by Mann-Whitney *U* test, where appropriate. Statistical significance for multiple comparisons was accepted at $p<0.05$ divided by the number of comparisons made, which was four i.e. $p<0.0125$. *p*-values shown in **bold** highlight significant difference

4.3.4 Ventilatory and metabolic responsiveness to chemostimulation in rats during quiet rest

Ventilatory and metabolic responsiveness to hypoxic chemostimulation: No significant differences were evident in CIH+VEH compared with Sham+VEH rats. CIH+PREB rats had decreased f_R, V_E, V_T/T_i and increased T_i and T_e compared with Sham+PREB rats (Table 4.3). T_i was decreased in Sham+PREB compared with Sham+VEH rats (Table 4.3). Sigh frequency and amplitude were not different in CIH+VEH compared with Sham+VEH rats, but CIH+PREB rats had less frequent but larger sighs compared with CIH+VEH rats. Sigh frequency was reduced in CIH+PREB compared with Sham+PREB rats (Table 4.3). The major observation was that prebiotic administration reduced the frequency of sighs during hypoxia in CIH-exposed rats.

Ventilatory and metabolic responsiveness to hypercapnic chemostimulation: CIH exposure elevated sigh frequency during hypercapnia, as such CIH+VEH rats had increased generation of sigh compared with Sham+VEH rats. Other respiratory and metabolic parameters were not different in CIH+VEH compared with Sham+VEH rats in response to hypercapnia (Table 4.3). Prebiotic administration in CIH-exposed rats elevated V_T/T_i compared with CIH+VEH rats. Interestingly, Sham+PREB rats had elevated ventilation (V_E) and increased drive to breathe (V_T/T_i) in response to hypercapnia compared with Sham+VEH rats, with no change in V_E/VCO_2 (Table 4.3). Furthermore, Sham+PREB rats had augmented sigh frequency and amplitude compared with Sham+VEH rats. There was no difference between CIH+PREB and Sham+PREB rats (Table 4.3). The major finding was that prebiotic fibre supplementation increased sigh frequency and the ventilatory response to hypercapnia.

Ventilatory and metabolic responsiveness to hypoxic hypercapnia chemostimulation: No significant differences were evident in CIH+VEH compared with Sham+VEH rats. CIH+PREB rats had elevated V_E compared with CIH+VEH rats. Sham+PREB rats had an elevated ventilatory response to hypoxic hypercapnia compared with Sham+VEH rats, evident by increased V_E, V_T and V_T/T_i; V_E/VCO_2 was not different between groups (Table 4.3). Furthermore, there was no apparent difference between Sham+PREB and CIH+PREB rats. The major observation was that prebiotic administration elevated the ventilatory response to hypoxic hypercapnia.

	Sham+VEH	CIH+VEH	Sham+PREB	CIH+PREB	p-value (Kruskal-Wallis)	p-value (two-way ANOVA)	Sham+VEH v CIH+VEH	CIH+VEH v CIH+PREB	Sham+PREB v CIH+PREB	Sham+VEH v Sham+PREB
Hypoxia										
Δ f_R (brpm)	58 ± 21	46 ± 18	64 ± 12	37 ± 13	N/A	Diet, p=0.834; CIH, **p<0.0005**; Diet*CIH, p=0.125	0.082	0.221	**<0.0005**	0.338
Δ V_E (ml/min/ 100g)	46 ± 16	38 ± 10	50 ± 12	34 ± 14	N/A	Diet, p=0.935; CIH, **p=0.003**; Diet*CIH, p=0.344	0.140	0.544	**0.006**	0.462
Δ V_T (ml/100g)	0.09 ± 0.10	0.10 ± 0.08	0.03 ± 0.07	0.08 ± 0.10	N/A	Diet, p=0.093; CIH, p=0.149; Diet*CIH, p=0.584	-	-	-	-
Δ V_T/T_i (ml/s/100g)	1.6 ± 0.6	1.6 ± 0.6	2.4 ± 0.8	1.3 ± 1	N/A	Diet, p=0.244; CIH, **p=0.021**; Diet*CIH, **p=0.022**	0.993	0.406	**0.001**	0.015
Δ T_i (ms)	-79 ± 36	-81 ± 27	-108 ± 27	-65 ± 24	**0.005**	N/A	0.786	0.295	**0.001**	**0.008**
Δ T_e (ms)	-228 ± 90	-170 ± 106	-230 ± 54	-125 ± 51	N/A	Diet, p=0.365; CIH, **p=0.001**; Diet*CIH, p=0.298	0.085	0.176	**0.002**	0.921
Δ VO_2 (ml/min/ 100g)	-0.7 ± 0.7	-0.4 ± 1	-1.3 ± 1	-1.5 ± 1	N/A	Diet, **p=0.003**; CIH, p=0.858; Diet*CIH, p=0.480	0.536	**0.011**	0.705	0.095
Δ VCO_2 (ml/min/ 100g)	0.3 ± 0.2	0.3 ± 0.3	0.3 ± 0.4	0.2 ± 0.2	0.412	N/A	-	-	-	-

Δ V_E/VCO_2	19 ± 8	14 ± 7	18 ± 8	12 ± 7	N/A	Diet, p=0.487; CIH, **p=0.016**; Diet*CIH, p=0.747	0.132	0.477	0.048	0.789
Sigh frequency (events per hr)	132 ± 46	155 ± 40	145 ± 29	112 ± 19	**0.008**	N/A	0.293	**0.002**	**0.009**	0.706
Sigh amplitude (ml/ml)	1.0 ± 0.14	1.1 ± 0.2	1.2 ± 0.23	1.4 ± 0.3	**0.001**	N/A	0.538	**0.001**	0.083	0.033
Hypercapnia										
Δ *f_R (brpm)*	60 ± 21	49 ± 17	57 ± 18	50 ± 21	N/A	Diet, p=0.908; Exposure, p=0.129; Diet*Exposure, p=0.689	-	-	**-**	-
Δ V_E (ml/min/ 100g)	55 ± 18	55 ± 16	85 ± 29	73 ± 24	N/A	Diet, **p=0.001**; Exposure, p=0.385; Diet*Exposure, p=0.380	0.994	0.064	0.214	**0.002**
Δ V_T (ml/100g)	0.18 ± 0.18	0.2 ± 0.1	0.23 ± 0.1	0.3 ± 0.1	**0.019**	N/A	0.268	0.056	0.729	0.021
Δ V_T/T_i (ml/s/100g)	1.4 ± 0.7	1.6 ± 0.7	2.8 ± 1.1	2.5 ± 0.7	N/A	Diet, **p<0.0005**; Exposure, p=0.979; Diet*Exposure, p=0.327	0.480	**0.01**	0.494	**<0.0005**
Δ T_i (ms)	-53 ± 28	-59 ± 19	-72 ± 27	67 ±24	0.307	N/A	-	-	-	-
Δ T_e (ms)	-304 ± 109	-232 ± 89	-223 ± 67	-190 ± 112	0.081	N/A	-	-	-	-
Δ VCO_2 (ml/min/	0.4 ± 0.7	0.2 ± 0.6	0.7 ± 0.6	0.3 ± 0.9	0.213	N/A	-	-	-	-

100g)										
Δ V_E/VCO_2	27 ± 16	41 ± 14	28 ± 19	41 ± 33	0.150	N/A	-	-	-	-
Sigh frequency (events per hr)	10 ± 5	17 ± 6	23 ± 21	20 ± 6	**0.001**	N/A	**0.009**	0.333	0.333	**0.001**
Sigh amplitude (ml/100g)	1.1 + 0.3	1.5 + 0.3	1.6 + 0.3	1.4 + 0.2	**0.017**	N/A	0.031	0.389	0.389	**0.006**
Hypoxic hypercapnia										
Δ f_R *(brpm)*	58 ± 10	50 ± 16	65 ± 18	56 ± 11	N/A	Diet, p=0.157; Exposure, p=0.062; Diet*Exposure, p=0.790	-	-	-	-
Δ V_E (ml/min/ 100g)	76 ± 20	69 ± 15	110 ± 20	95 ± 23	N/A	Diet, **p<0.0005**; Exposure, p=0.090; Diet*Exposure, p=0.562	0.446	**0.006**	0.088	**<0.0005**
Δ V_T (ml/100g)	0.3 ± 0.2	0.3 ± 0.1	0.4 ± 0.2	0.4 ± 0.2	**0.030**	N/A	0.683	0.286	0.094	**0.010**
Δ V_T/T_i (ml/s/100g)	2.0 ± 0.9	2.0 ± 0.7	3.4 ± 0.8	2.8 ± 1.0	N/A	Diet, **p<0.0005**; Exposure, p=0.465; Diet*Exposure, p=0.204	0.713	0.070	0.135	**0.001**
Δ T_i (ms)	-57 ± 33	-73 ± 17	-76 ± 36	-74 ± 22	N/A	Diet, p=0.252; Exposure, p=0.412; Diet*Exposure, p=0.328	-	-	-	-

Δ T_e (ms)	-291 ± 194	-234 ± 112	-301 ± 96	-271 ± 54	0.450	N/A	-	-	-	-
Δ VCO_2 (ml/min/ 100g)	-0.3 ± 0.4	-0.3 ± 0.4	0.2 ± 0.4	-0.1 ± 0.6	N/A	**Diet, p=0.039**; Exposure, p=0.304; Diet*Exposure, p=0.322	0.980	0.435	0.132	0.030
Δ V_E/VCO_2	62 ± 23	55 2 ± 5	55 ± 21	53 ± 26	N/A	Diet, p=0.573; Exposure, p=0.586; Diet*Exposure, p=0.762	-	-	-	-

Table 4. 3 Ventilatory and metabolic responsiveness to chemostimulation in rats during quiet rest

f_R, respiratory frequency (brpm, breaths per minute); V_E, minute ventilation; V_T, tidal volume; V_T/T_i, mean inspiratory flow; T_i, inspiratory time; T_e, expiratory time; VO_2, oxygen consumption; VCO_2, carbon dioxide production; V_E/VCO_2, ventilatory equivalent; CIH, chronic intermittent hypoxia; PREB, prebiotic; VEH, vehicle. Data are shown as mean ± SD and were statistically compared using two-way ANOVA, followed by Fisher's least significant difference (LSD) *post hoc* where appropriate, or non-parametric Kruskal-Wallis test, followed by Mann-Whitney *U* test, where appropriate. Statistical significance for multiple comparisons was accepted at $p<0.05$ divided by the number of comparisons made, which was four i.e. $p<0.0125$. *p*-values shown in **bold** highlight significant differences.

4.3.5 Baseline cardiorespiratory and blood gas parameters in anaesthetised rats

CIH exposure had no effect on respiration in the anaesthetised rat during baseline conditions (Table 4.4). V_E and V_T were increased in CIH+PREB rats compared with CIH-exposed rats (Table 4.4). CIH exposure significantly increased diastolic blood pressure (DBP) (CIH; F (1,41) = 16.321, p<0.0005, η^2=0.285, Fig. 4.2b). As a consequence, mean arterial blood pressure (MAP) was elevated (CIH; F (1, 41) = 17.485, p<0.005, η^2=0.299). *Post hoc* analysis revealed CIH+VEH had elevated blood pressure compared with Sham+VEH rats (DBP, p=0.006, Fig. 4.2b; MAP, p=0.004, Fig. 4.2a). DBP was not restored by prebiotic administration as CIH+PREB had elevated DBP compared with CIH+VEH rats (p=0.007, Fig. 4.2b). There was no statistical difference evident in MAP between CIH+PREB compared with CIH+VEH (p>0. 05, Fig. 4.2a), and MAP was elevated in CIH+PREB compared with Sham+PREB rats (p=0.006; Fig. 4.2a). CIH exposure or prebiotic administration had no effect on systolic blood pressure or heart rate (p>0.05, Fig. 4.2c, 4.2d). CIH exposure had no effect on haematocrit and haemoglobin concentrations; Sham+PREB had reduced concentrations compared with Sham+VEH (Table 4.4).

CIH exposure increased the low-frequency band (LF) (CIH; nu, F (1, 40) = 6.170, p=0.017, η^2=0.134, Fig. 4.2 f; %, F (1, 40) = 6.723, p=0.013, η^2=0.144, Table 4.5) and decreased the high-frequency band (HF; nμ) (CIH, F (1, 40) = 1.159, p=0.014, η^2=0.142, Table 4.5) elevating the LF: HF ratio (CIH, F (1, 40) = 7.748, p=0.008, η^2=0.162, Fig. 4.2e) during steady-state baseline recordings, indicating sympathetic dominance. LF:HF was increased in CIH+VEH compared with Sham+VEH rats (p=0.059, Fig. 4.2 e). There was no difference in CIH+PREB compared with CIH+VEH rats (p>0.05), however CIH+PREB rats had elevated LF:HF ratio compared with Sham+PREB rats (p=0.053, Fig. 4.2e). After adjusting for multiple comparisons these changes were not statistically significant (Table 4.5). Other heart rate variability parameters were not different between groups (Table 4.5). The major finding was that CIH exposure caused hypertension and cardiac autonomic imbalance, which were not alleviated by prebiotic supplementation.

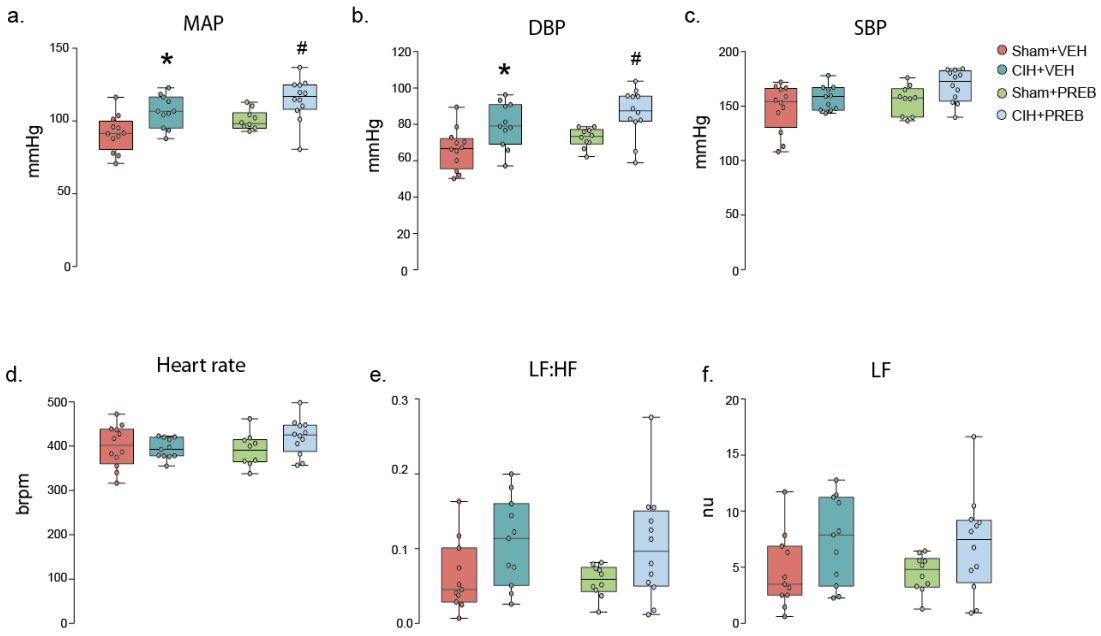


Figure 4. 2 CIH causes hypertension and cardiac autonomic imbalance

Group data for MAP (a), DBP (b), SBP (C), heart rate (D), LF: HF (e) and HF (f) for Sham+VEH, CIH+VEH, Sham+PREB and CIH+PREB. MAP, mean arterial blood pressure; DBP, diastolic blood pressure; SBP, systolic blood pressure; LF, low-frequency band; HF, high frequency band; CIH, chronic intermittent hypoxia; PREB, prebiotic; VEH, vehicle. Groups (a-f) are expressed as box and whisker plots (median, IQR and minimum to maximum values); n = 10-12 for all groups. Groups were statistically compared using two-way ANOVA, followed by Fisher's least significant difference (LSD) *post hoc* where appropriate, or non-parametric Kruskal-Wallis test, followed by Mann-Whitney *U* test, where appropriate**.** CIH significantly affected MAP, DBP, LF: HF and LF (p<0.005, p<0.0005, p=0.008 and p=0.017, respectively; Fig. 4.2a, 4.2b, 4.2e, 4.2f). There was no change in SBP or HR (p>0.05, Fig. 4.2c, 4.2d).* p=0.004, CIH+VEH *versus* Sham+VEH; # p<0.01, CIH+PREB *versus* Sham+PREB.

	Sham+VEH	CIH+VEH	Sham+PREB	CIH+PREB	p-value (Kruskal-Wallis)	p-value (two-way ANOVA)	Sham+VEH v CIH+VEH	CIH+VEH v CIH+PREB	Sham+PREB v CIH+PREB	Sham+VEH v Sham+PREB
f_R (brpm)	99 ± 11	99 ± 11	98 ± 10	93 ± 5	N/A	Diet, p=0.448; CIH, p=0.376; Diet*CIH, p=0.397	-	-	-	-
V_E (ml/ min/ 100g)	24 ± 5	21 ± 3	25 ± 3	27 ± 3	N/A	Diet, **p=0.003**; CIH, p=0.642; Diet*CIH, p=0.088	0.111	**0.001**	0.387	0.339
V_T (ml/ 100g)	0.25 ± 0.05	0.22 ± 0.03	0.26 ± 0.02	0.29 ± 0.03	N/A	Diet, **p<0.0005**; CIH, p=0.998; Diet*CIH, **p=0.019**	0.081	**<0.0005**	0.103	0.306
$ETCO_2$	5 ± 1.6	6 ± 0.5	6 ± 0.6	6 ± 0.9	N/A	Diet, p=0.274; CIH, p=0.448; Diet*CIH, p=0.316	-	-	-	-
pH	7.37 ± 0.04	7.33 ± 0.02	7.34 ± 0.02	7.34 ± 0.03	N/A	Diet, p=0.427; CIH, **p=0.049**; Diet*CIH, p=0.211	0.023	0.738	0.598	0.155
$PaCO_2$ (mmHg)	46 ± 6	51 ± 4	51 ± 4	49 ± 5	N/A	Diet, p=0.394; CIH, p=0.278; Diet*CIH, **p=0.049**	0.03	0.406	0.518	0.050
PaO_2 (mmHg)	97 ± 4	99 ± 7	97 ± 13	98 ± 6	N/A	Diet, p=0.416; CIH, p=0.863; Diet*CIH, p=0.822	-	-	-	-

Haematocrit (%)	49 ± 2	49 ± 3	45 ± 3	46 ± 4	N/A	Diet, **p<0.0005**; CIH, p=0.655; Diet*CIH, p=0.556	0.918	0.017	0.470	**0.002**
[Hb] (g/dl)	16.8 ± 0.7	16.8 ± 1.0	15.4 ± 1.0	15.7 ± 1.3	N/A	Diet, **p<0.0005**; CIH, p=0.696; Diet*CIH, p=0.580	0.907	0.013	0.510	**0.002**

Table 4. 4 Baseline ventilation, blood gases and cardiovascular parameters in anaesthetised rats

f_R, respiratory frequency (brpm, breaths per minute); V_E, minute ventilation; V_T, tidal volume; $ETCO_2$, end-tidal carbon dioxide production; Pco_2, partial pressure of arterial carbon dioxide; Pao_2, partial pressure of arterial oxygen; [Hb], haemoglobin concentration; CIH, chronic intermittent hypoxia; PREB, prebiotic; V EH, vehicle. Data are shown as mean ± SD and were statistically compared using two-way ANOVA, followed by Fisher's least significant difference (LSD) *post hoc* where appropriate, or non-parametric Kruskal-Wallis test, followed by Mann-Whitney *U* test, where appropriate. Statistical significance for multiple comparisons was accepted at $p<0.05$ divided by the number of comparisons made, which was four i.e. $p<0.0125$. *p*-values shown in **bold** highlight significant differences.

	Sham+VEH	CIH+VEH	Sham+PREB	CIH+PREB	p-value (Kruskal-Wallis)	p-value (two-way ANOVA)	Sham+VEH v CIH+VEH	CIH+VEH v CIH+PREB	Sham+PREB v CIH+PREB	Sham+VEH v Sham+PREB
Ttotal Power (ms^2)	16 ± 28	10 ± 11	4 ± 3	13 ± 15	0.653	N/A	-	-	-	-
HF (nμ)	78 ± 11	71 ± 10	84 ± 7	73 ± 10	N/A	Diet, p=0.288; CIH, **p=0.014**; Diet*CIH, p=0.662	0.138	0.648	0.039	0.301
VLF (ms^2)	0.4 ± 0.3	1.0 ± 1.7	0.4 ± 0.2	0.3 ± 0.5	0.163	N/A	-	-	-	-
LF (ms^2)	0.3 ± 0.5	0.4 ± 0.5	0.1 ± 0.1	0.5 ± 0.7	0.214	N/A	-	-	-	-
HF (ms^2)	12 ± 20	6 ± 7	3 ± 2	9 ± 12	0.590	N/A	-	-	-	-
VFL (%)	15 ± 14	24 ± 26	16 ± 11	9 ± 11	0.251	N/A	-	-	-	-
Lf (%)	4 ± 2	5 ± 3	4 ± 1	6 ± 4	N/A	Diet, p=0.658; CIH, **p=0.013**; Diet*CIH, p=0.619	0.146	0.497	0.035	0.970
HF (%)	66 ± 15	53 ± 15	70 ± 11	67 ± 11	0.109	N/A	-	-	-	-
Average RRI (ms)	153 ± 18	152 ± 9	155 ± 14	144 ± 14	N/A	Diet, p=0.445; CIH, p=0.189; Diet*CIH, p=0.238	-	-	-	-
Median RRI (ms)	153 ± 19	152 ± 10	155 ± 14	144 ± 14	N/A	Diet, p=0.460; CIH,	-	-	-	-

						p=0.199; Diet*CIH, p=0.272				
SDRR (ms)	3.3 ± 2.5	3 ± 2	2 ± 0.5	3.6 ± 2.3	0.626	N/A	-	-	-	-
CVRR	0.02 ± 0.02	0.02 ± 0.01	0.01 ± 0.003	0.03 ± 0.02	0.373	N/A	-	-	-	-
SD Rate (bpm)	8.2 ± 5.8	7.8 ± 5.2	5.2 ± 1.5	11 ± 8.4	0.380	N/A	-	-	-	-
SDSD (ms)	4.5 4.7	4.1 ± 3.8	2.6 ±1.2	5.5 ± 4.2	0.586	N/A	-	-	-	-
RMSSD (ms)	4.5 ± 4.8	4.1 ± 3.8	2.6 ± 1.2	5.5 ± 4.2	0.586	N/A	-	-	-	-
SD1 (ms)	3.2 ± 3.3	2.9 ± 2.7	1.8 ± 0.8	3.9 ± 2.9	0.586	N/A	-	-	-	-
SD2 (ms)	3.1 ± 1.9	2.8 ± 1.5	2.2 ± 0.5	3.2 ± 1.6	N/A	Diet, p=0.489; CIH, p=0.373; Diet*CIH, p=0.131	-	-	-	-

Table 4. 5 Heart rate variability in the urethane anaesthetised rats

VLF, very low frequency; LF, low frequency; HF, high frequency; RRI, R-R interval; SDRR, standard deviation of R-R interval; CVRR, coefficient of variance of R-R intervals; SD rate, standard deviation of heart rate; SDSD, standard deviation of successive R-R intervals; RMSSD, root mean square of successive R-R interval differences; SD1, short term variability; SD2, long-term variability; CIH, chronic intermittent hypoxia; PREB, prebiotic; VEH, vehicle. Data are shown as mean ± SD and were statistically compared using two-way ANOVA, followed by Fisher's least significant difference (LSD) *post hoc* where appropriate, or non-parametric Kruskal-Wallis test, followed by Mann-Whitney *U* test, where appropriate. Statistical significance for multiple comparisons was accepted at $p<0.05$ divided by the number of comparisons made, which was four i.e. $p<0.0125$. *p*-values shown in **bold** highlight significant differences.

4.3.6 Cardiorespiratory responses to 5-HT_3 receptor agonism evoking the cardiopulmonary reflex

Stimulation of 5-HT_3 receptors expressed on pulmonary vagal afferent nerve fibres, using PBG, evoked the integrated cardiopulmonary reflex. CIH exposure had no effect on hypotension, bradycardia, apnoea or post-apnoea induced tachypnoea associated with the pulmonary chemoreflex (Fig. 4.3b-e). Prebiotic supplementation altered apnoea duration (Diet, $F(1, 41) = 4.950$, $p=0.032$, $\eta^2=0.108$, Fig. 4.3b), however, *post hoc* analysis revealed no differences between groups. There was no significant difference between groups in all other parameters (Fig. 4.3c-e). The major finding was that pulmonary chemoreflex responses to vagal afferent stimulation were unaffected by CIH exposure.

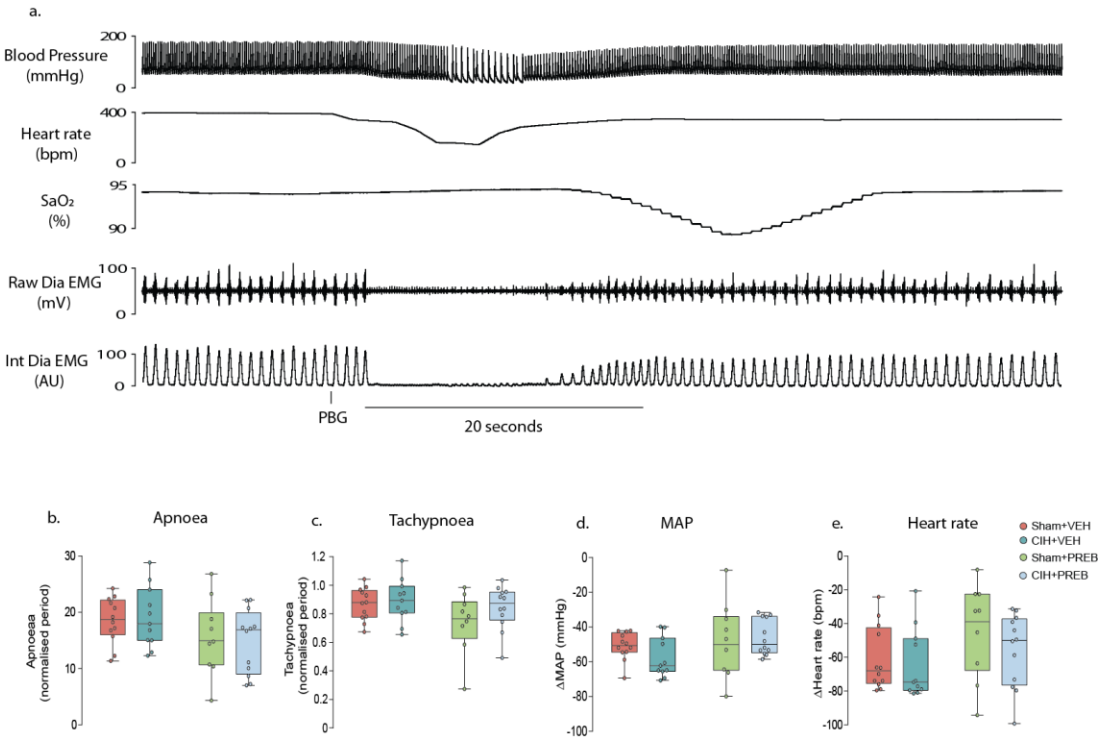


Figure 4. 3 CIH did not alter cardiorespiratory responses to pulmonary vagal afferent C-fibre stimulation

a) Representative traces of blood pressure, heart rate, arterial oxygen saturation (SpO_2) and raw and integrated diaphragm (Dia) electromyogram (EMG) activity during intravenous administration of the 5-HT_3 agonist, phenylbiguanide (25 µg.kg^{-1} i.v.). Group data for maximum apnoea duration (b) and tachypnoea (c) normalised to respective baseline respiratory period in Sham+VEH, CIH+VEH, Sham+PREB and CIH+PREB rats. Absolute change in MAP (d) and heart rate (e) in response to PBG in Sham, CIH, Sham+PREB and CIH+PREB rats. MAP, mean arterial blood pressure; CIH, chronic intermittent hypoxia; PREB, prebiotic; VEH, vehicle. Data (b-e) are expressed as box and whisker plots (median, IQR and minimum to maximum values); n= 11-12. Groups (b-e) were statistically compared using two-way ANOVA, followed by Fisher's least significant difference (LSD) *post hoc* where appropriate, or non-parametric Kruskal-Wallis test, followed by Mann-Whitney *U* test, where appropriate. CIH exposure had no effect on hypotension, bradycardia, apnoea or post-apnoea induced tachypnoea (p>0.05; Fig. 4.3b-e). Prebiotic supplementation had a significant effect on apnoea duration (p=0.032; Fig. 4.3b), with no effect on any of the other parameters (p<0.05; Fig. 4.3c-e).

4.3.7 Cardiovascular responses to pharmacological blockade of sympathetic activity in anaesthetised rats

The blood pressure response to β1 receptor antagonist administration (atenolol) was significantly increased by CIH exposure ($X^2(3) = 9.347$, $p=0.025$). CIH+VEH was not different compared with Sham+VEH rats. There was a greater depressor response in CIH+PREB compared with Sham+PREB rats; the associated bradycardia was similar between all groups (Table 4.6). Intravenous infusion of the non-selective β-adrenoceptor blocker (propranolol), and sympathetic ganglion blocker (hexamethonium) evoked similar bradycardia and hypotensive responses across all groups (Table 4.6).

	Sham+VEH	CIH+VEH	Sham+PREB	CIH+PREB	p-value (Kruskal-Wallis)	p-value (two-way ANOVA)	Sham+VEH v CIH+VEH	CIH+VEH v CIH+PREB	Sham+PREB v CIH+PREB	Sham+VEH v Sham+PREB
Propranolol (% change from baseline)										
SBP	-24 ± 9	-22 ± 6	-21 ± 6	-23 ± 5	0.906	N/A	-	-	-	-
HR	-12 ± 5	-18 ± 13	-16 ± 6	-19 ± 11	0.092	N/A	-	-	-	-
Atenolol (% change from baseline)										
SBP	8 ± 10	9 ± 5	3 ± 5	7 ± 3	**0.025**	N/A	0.268	0.538	**0.006**	0.235
HR	-27 ± 17	-28 ± 11	-28 ± 10	-30 ± 5	0.276	N/A	-	-	-	-
Hexamethonium (% change from baseline)										
SBP	-48 ± 9	-46 ± 8	-41 ± 7	-46 ± 6	N/A	Diet, p=0.205; CIH, p=0.422; Diet*CIH, p=0.184	-	-	-	-
HR	-14 ± 17	-15 ± 18	-13 ± 14	-12 ± 11	0.743	N/A	-	-	-	-

Table 4. 6 Cardiovascular responses to pharmacological blockade of sympathetic activity in urethane anaesthetised rats

SBP, systolic blood pressure; HR, heart rate; CIH, chronic intermittent hypoxia; PREB, prebiotic; VEH, vehicle. Data are shown as mean ± SD and were statistically compared using two-way ANOVA, followed by Fisher's least significant difference (LSD) *post hoc* where appropriate, or non-parametric Kruskal-Wallis test, followed by Mann-Whitney *U* test, where appropriate. Statistical significance for multiple comparisons was accepted at $p<0.05$ divided by the number of comparisons made, which was four i.e. $p<0.0125$. *p*-values shown in **bold** highlight significant differences

4.3.8 Pons and medulla oblongata neurochemistry

Comparison of $_{L}$-DOPA and DOPAC concentrations in the pons, as well as DOPAC/DA, HVA, HVA/DA, 5-HT and 5-HIAA concentrations in the medulla oblongata revealed group differences (p<0.05; Fig. 4.4a, 4.4c-f, 4.4h, 4.4i). However, *post hoc* analysis revealed that monoamine, monoamine metabolites and precursors were not different in CIH+VEH compared with Sham+VEH rats in the pons or medulla oblongata (Fig. 4.4a-j). Pontine $_{L}$-DOPA (p=0.020) and medulla oblongata 5-HIAA (p=0.008) concentrations were significantly increased, with medulla oblongata HVA (p=0.041) levels decreased in CIH+PREB compared with CIH+VEH rats. CIH+PREB rats had increased pontine $_{L}$-DOPA (p=0.038) concentrations compared with Sham+PREB rats. Sham+PREB rats had reduced pontine DOPAC (p=0.021) as well as medulla oblongata HVA (p=0.006) and HVA/DA (p=0.016) concentrations compared with Sham+VEH rats. Additionally, Sham+PREB rats had elevated pontine $_{L}$-DOPA (p=0.012) concentrations compared with Sham+VEH rats. After adjusting for multiple comparisons, differences in pontine $_{L}$-DOPA and medulla oblongata HVA concentrations in Sham+PREB compared with Sham+VEH and medulla oblongata 5-HIAA concentrations in CIH+PREB compared with Sham+PREB remained significantly different. In summary, prebiotic administration, but not CIH, altered brainstem neurochemistry.

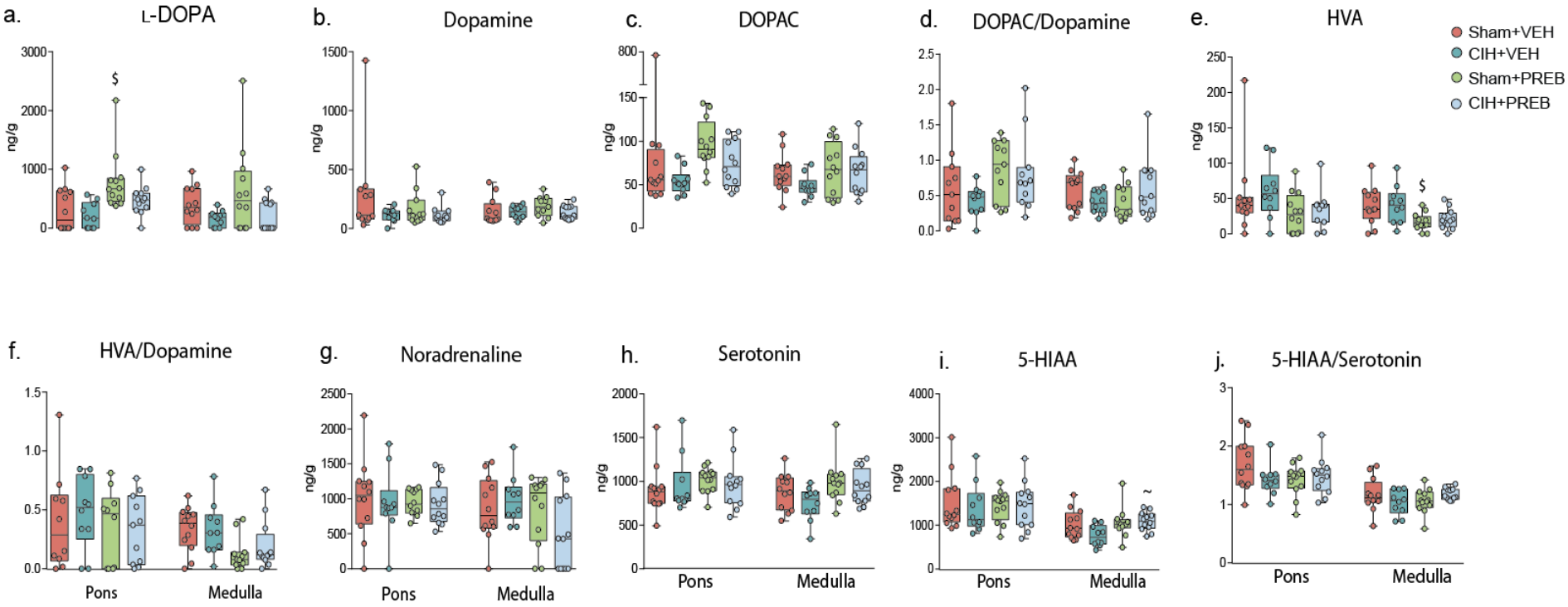


Figure 4. 4 Prebiotic administration alters brainstem neurochemistry

Group data for $_{L}$-DOPA (a), dopamine (b), DOPAC (c) DOPAC/Dopamine (d), homovanillic acid (e), homovanillic acid/dopamine ratio (f), noradrenaline (g), serotonin (h), 5-HIAA (i) and 5-HIAA/Serotonin ratio (j) in Sham+VEH, CIH+VEH, Sham+PREB and CIH+PREB. $_{L}$-DOPA, $_{L}$-3,4-dihydroxyphenylalanine; DOPAC, 3,4-dihydroxyphenylacetic acid; 5-HIAA, 5-hydroindoleacetic acid; CIH, chronic intermittent hypoxia; PREB; prebiotic; VEH, vehicle. Data (a-j) are expressed as box and whisker plots (median, IQR and minimum to maximum values); n= 10-12. Groups were statistically compared using two-way ANOVA, followed by Fisher's least significant difference (LSD) *post hoc* where appropriate, or non-parametric Kruskal-Wallis test, followed by Mann-Whitney *U* test, where

appropriate. $_{L}$-DOPA (p=0.003; Fig. 4.4a) and DOPAC (p=0.006; Fig. 4.4c) concentrations in the pontine region as well as DOPAC/DA (Diet*CIH, p=0.042; Fig. 4.4d), HVA (p=0.001; Fig. 4.4e), HVA/DA (p=0.020; Fig. 4.4f), 5-HT (Diet, p=0.043; Fig. 4.4h) and 5-HIAA (p=0.043; Fig. 4.4i) concentrations in the medulla oblongata are different. Other monoamine, metabolites and precursors were not statistically different between groups (p>0.05; Fig. 4.4b, 4.4g, 4.4h, 4.4j). ~ p=0.008, CIH+PREB *versus* CIH+VEH; $ p=0.006, Sham+PREB *versus* Sham+VEH.

4.3.9 Plasma cytokine and corticosterone concentrations

IL-4 ($X^2(3) = 8.042$, $p=0.045$, Fig. 4.5c) and TNF-α ($X^2(3) = 10.784$, $p=0.013$, Fig. 4.5h) were different between groups. *Post hoc* analysis adjusted for multiple comparisons revealed that CIH exposure had no significant effect on IL-4 or TNF-α levels. However, TNF-α and IL-4 were decreased in Sham+PREB compared with Sham+VEH rats. All other cytokines and corticosterone concentrations were not different between groups (Fig. 4.5a-b, 4.5d-g). In summary, CIH exposure had no effect on plasma cytokine or corticosterone concentrations. Prebiotic administration reduced TNF-α and IL-4 concentrations compared with VEH rats.

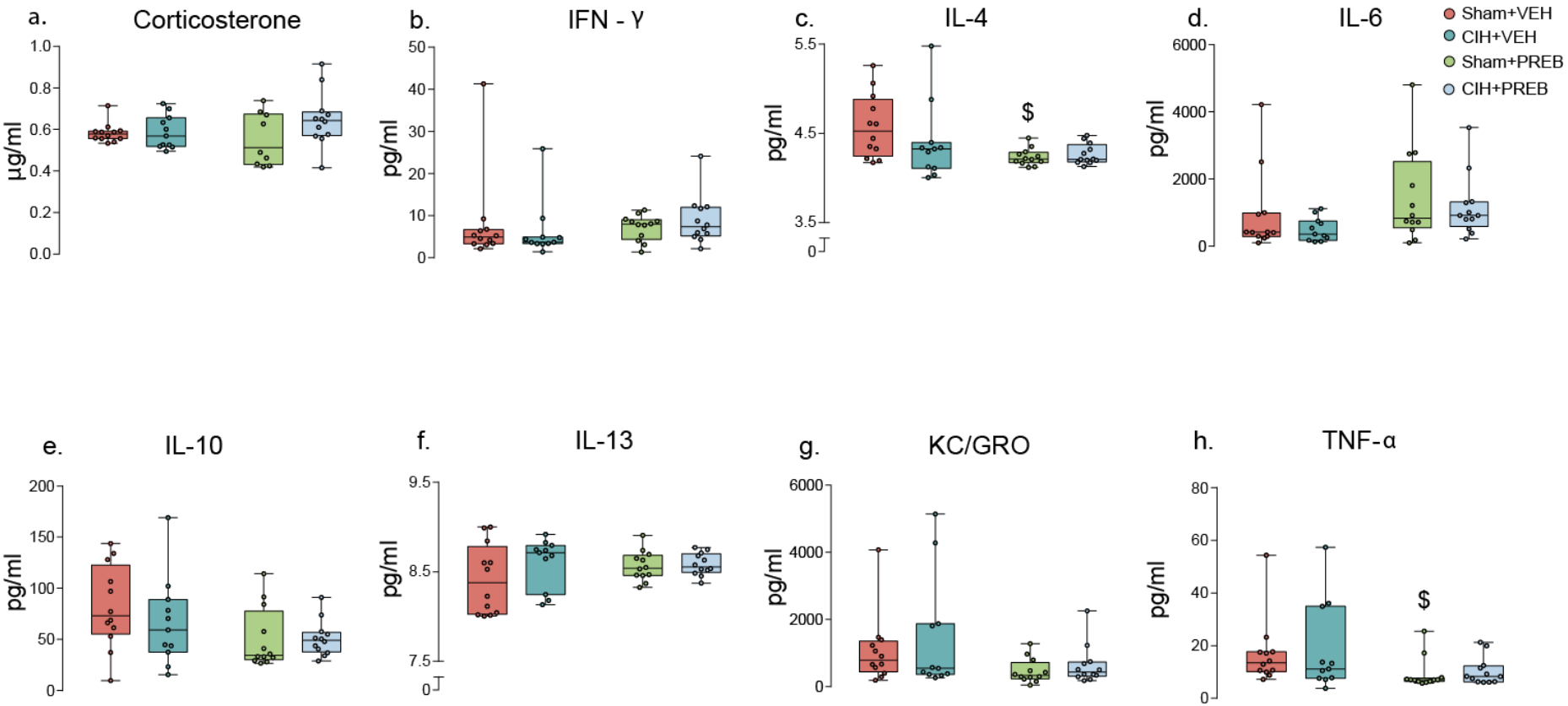


Figure 4. 5 Corticosterone and inflammatory mediators were equivalent between groups

Group data for corticosterone concentration (a), IFN-γ (b), IL-4 (c), IL-6 (d), IL-10 (e), IL-13 (f), KC/GRO (g) and TNF-α (h) in Sham+VEH, CIH+VEH, Sham+PREB and CIH+P

REB. IFN-γ, interferon-γ; IL-4, interleukin-4; IL-6, interleukin-6; IL-10, interleukin-10; IL-13, interleukin-13; TNF-α, tumor necrosis factor-α; KC/GRO, keratinocyte chemoattractant/growth-related oncogene; CIH, chronic intermittent hypoxia; PREB; prebiotic; VEH, vehicle. Data (a-h) are expressed as box and whisker plots (median, IQR and minimum to maximum values); n= 11-12. Groups (a-h) were statistically compared using two-way ANOVA, followed by Fisher's least significant difference (LSD) *post hoc* where appropriate, or non-parametric Kruskal-Wallis test, followed by Mann-Whitney *U* test, where appropriate. IL-4 (p=0.045; Fig. 4.5c) and TNF-α (p=0.013; Fig. 4.5h) were affected by prebiotic administration. $ p=0.003, Sham+PREB *versus* Sham+VEH.

4.3.10 Caecal microbiota

CIH exposure had no effect on indices of alpha diversity (Fig. 4.6b-d). Prebiotic treatment significantly reduced bacteria species evenness in all statistical comparisons, indicated by decreases in Shannon and Simpson indices of alpha diversity (Fig. 4.6c-d). However, bacterial species richness, indicated by Chao1 index was not affected by prebiotic administration (Fig. 4.6b). These findings suggest proliferation of a select number of bacterial species with no overall difference in bacterial richness. Principal component analysis revealed that CIH exposure did not affect β-diversity. Prebiotic administration shifted β-diversity in Sham+VEH and CIH+VEH compared with Sham+PREB and CIH+PREB rats, respectively (Fig. 4.6a, $p<0.001$, PERMANOVA).

Whole-metagenome shotgun sequencing identified around 3200 bacteria species of 34 phyla. The majority of bacterial species in each group are of Bacteroidetes and Firmicutes phyla (Sham+VEH, 18% and 60%; CIH+VEH, 21% and 56%; Sham+PREB, 28% and 40%; CIH+PREB, 30% and 41%, Bacteroidetes and Firmicutes, respectively). Bacteria phyla were not affected by CIH exposure; there was no statistically significant difference observed in Sham+VEH and Sham+PREB rats compared with CIH+VEH and CIH+PREB rats, respectively. Prebiotic administration significantly increased the relative abundance of the major phyla Bacteroidetes and Actinobacteria and decreased the relative abundance of Firmicutes and Proteobacteria. Minor phyla were also affected by prebiotics.

BH adjustment for multiple comparisons at bacterial species level did not reveal statistically significant differences between CIH+VEH and Sham+VEH rats given the exhaustive multiple comparisons performed. However, 222 moderate (>0.5) and 9 large effect sizes (>0.8) were evident between CIH+VEH and Sham+VEH rats; 3 species had an effect size >1. Pathogenic species, namely, *Streptomyces sp. 452* and *Raoultella planticola* were increased and *Lactobacillus rhamnosus* (>1 effect size; Fig. 4.6e), a beneficial commensal bacterial species, was decreased in CIH+VEH compared with Sham+VEH rats. Similarly, no statistically significant difference was evident between Sham+PREB and CIH+PREB rats, but moderate (>0.5) and large effect sizes (>0.8) were evident in 130 and 4 species, respectively. The pathogenic species *Helicobacter bilis* was increased whereas *Candidatus Gullanella endobia*, *Pectobacterium wasabiae* and *Corynebacterium striatum* were decreased in CIH+PREB compared with Sham+PREB rats (>0.8 effect size). A total of 420 bacterial species were statistically different in CIH+VEH rats compared with CIH+PREB rats, with 549 species different in Sham+VEH rats compared with Sham+PREB rats. The largest difference between these comparisons was due to a significant increase in the beneficial bacterial species

Bifidobacterium animalis in the prebiotic groups. Of note, some beneficial and pathogenic bacterial species, decreased and increased, respectively, in prebiotic groups but an overall augmented abundance of beneficial bacterial species and reduced abundance of pathogenic bacterial species was evident in prebiotic groups compared with Sham+VEH and CIH+VEH rats (Fig. 4.7).

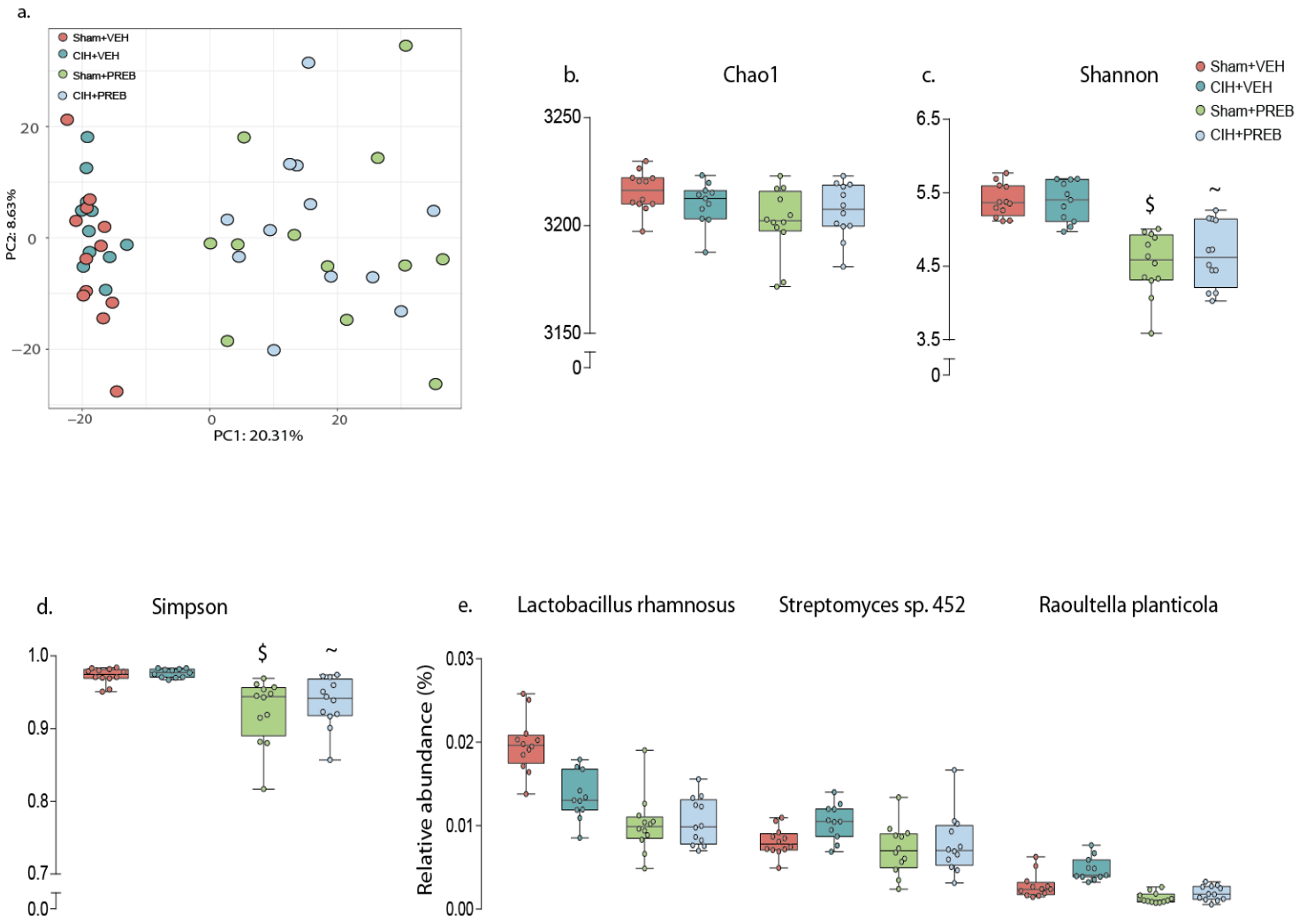


Figure 4. 6 Prebiotic administration alters rat caecal microbiota structure

Group data for principal coordinate analysis (a) in 2-dimensional representations, Chao1 (b), Shannon (c), Simpson (d) and abundance of Lactobacillus rhamnosus, Streptomyces sp. 452 and Raoultella planticola (e) in Sham+VEH, CIH+VEH, Sham+PREB and CIH+PREB. CIH, chronic intermittent hypoxia; PREB; prebiotic; VEH, vehicle. Data (a-c, e) are expressed as box and whisker plots (median, IQR and minimum to maximum values); n=11-12. Data (a-c, e) were statistically compared by non-parametric Mann-Whitney *U* test. ~ $p<0.01$, CIH+PREB versus CIH+VEH; $ $p<0.0001$, Sham+PREB versus Sham+VEH.

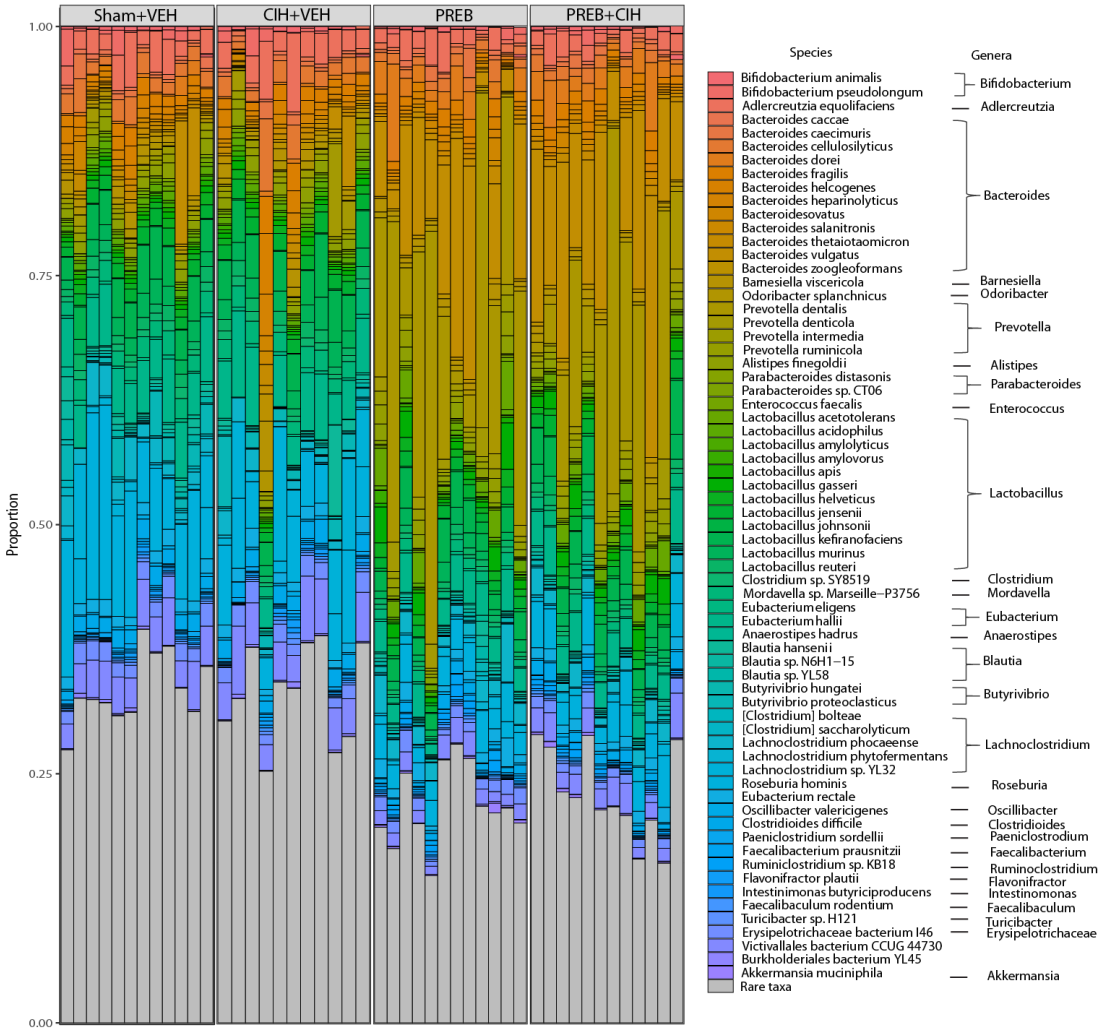


Figure 4. 7 Caecal microbiota composition.

*S*tacked barplot showing the abundance of dominant bacteria species (rare taxa cutoff of 1%) in the caecal microbiota of Sham+VEH, CIH+VEH, Sham+PREB and CIH+PREB rats. CIH, chronic intermittent hypoxia; PREB; prebiotic; VEH, vehicle. Species are ordered taxonomically.

4.3.11 Correlation analysis

Administration of *Lactobacillus rhamnosus* in rodents alters brain behaviours and function, reducing anxiety and depressive-like behaviour as well as neuromodulator receptor abundance, in particular GABA receptor expression; effects abolished in vagotomised animals (Bravo *et al.*, 2011). Considering that *Lactobacillus rhamnosus* was diminished in CIH+VEH compared with Sham+VEH rats we investigated if an association exists between *Lactobacillus rhamnosus* and physiological parameters assessed in our study. Using Hierarchical All-against-all correlation analysis the relative abundance of *Lactobacillus rhamnosus* negatively correlated with sigh frequency and amplitude during hypercapnia (Appendix Fig. C.1a-b). No significant correlations were evident between major physiological parameters, including apnoea, heart rate variability and blood pressure and *Lactobacillus rhamnosus* relative abundance. Given that hypertension is a well-established cardiovascular pathology in CIH-exposed rodents and a primary outcome measure in our study, we investigated if blood pressure parameters only (removing multiple comparison assessment of all physiological parameters) correlated with *Lactobacillus rhamnosus.* No significant correlations were evident. We assessed if other bacterial species correlated with physiological parameters. *Francisella sp. FSC1006* strongly negatively correlated with sigh frequency during hypercapnia in rats that did not receive prebiotics. No other significant correlations were evident. A total of 269, 16 and 110 bacterial species correlated with mean, diastolic and systolic blood pressure respectively, when we independently investigated if blood pressure parameters correlated with bacterial species (Appendix Tables C.9-11).

4.3.12 Faecal short-chain fatty acid concentrations

PCA analysis did not identify distinct clustering of CIH+VEH compared with Sham+VEH rats. However, separation of vehicle from prebiotic groups was evident (Fig. 4.8a). The loading plot (Fig. 4.8b) demonstrates this separation is due to higher concentrations of acetic, propanoic and hexanoic acid in prebiotic groups. Further analysis revealed that prebiotic supplementation significantly influenced faecal acetic ($X^2(3) = 22.420$, $p<0.0005$, Fig. 4.8c) and propanoic ($X^2(3) = 11.211$, $p=0.011$, Fig. 4.8d) concentrations. Prebiotic treatment significantly increased faecal acetic acid in all statistical comparisons (CIH+PREB *versus* CIH+VEH, p=0.002; Sham+PREB *versus* Sham+VEH, $p=0.001$; Fig. 4.8c), propanoic acid concentrations were increased in CIH+PREB compared with Sham+PREB rats (p=0.009; Fig. 4.8d). There was no significant difference in other SCFA concentrations (Fig. 4.8e-h). CIH exposure had no effect on SCFA, whereas prebiotic administration increased SCFA concentrations in Sham and CIH-exposed rats.

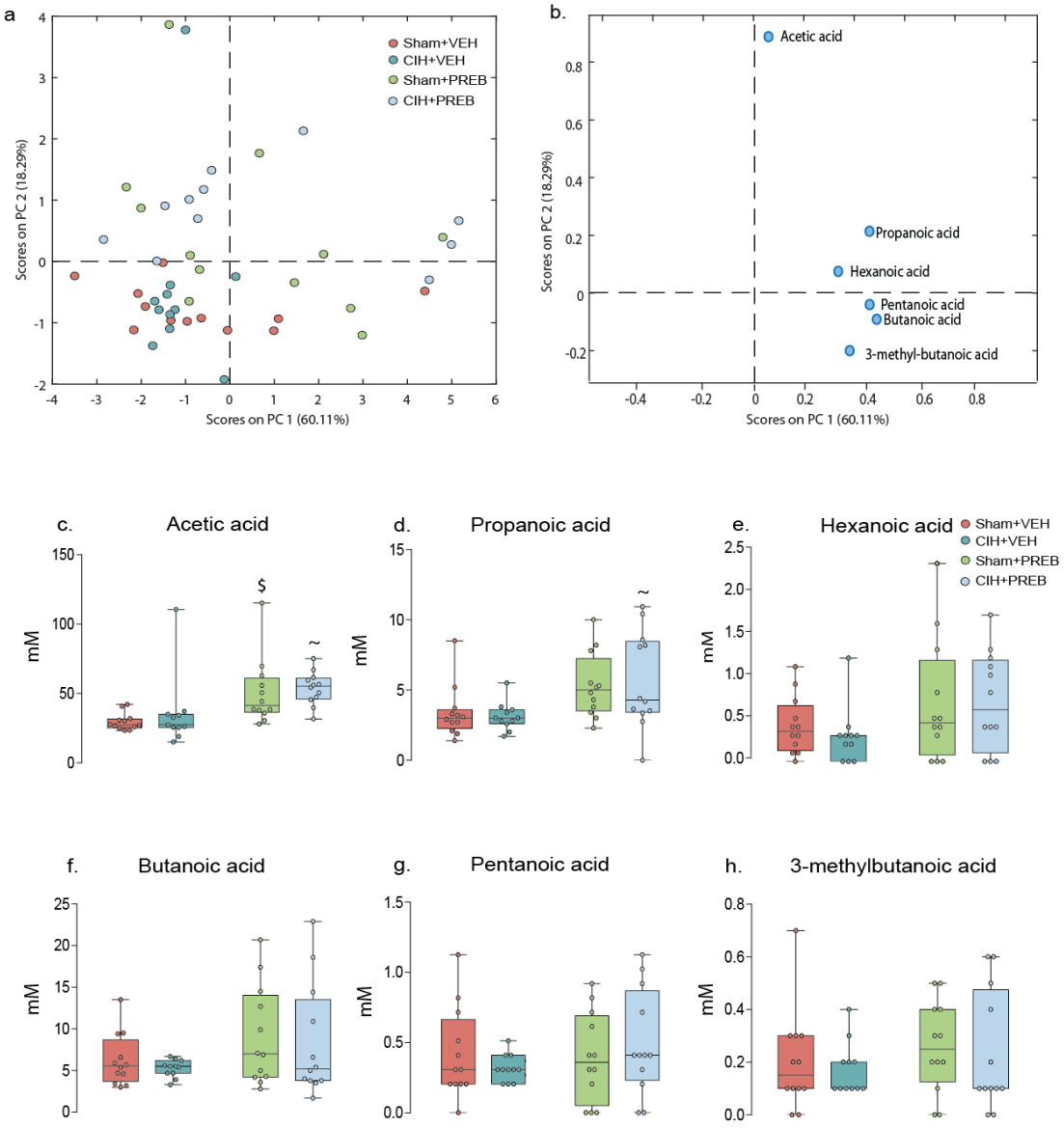


Figure 4. 8 Prebiotic administration increases faecal acetic and propanoic acid

Score plot (a) from principal component analysis (PCA) model calculated on the relative concentrations of detected SCFA and loading plot (b) from PCA model calculated on the relative concentrations showing which variables are responsible for the pattern observed in (a). Group data for acetic acid (c), propanoic acid (d), hexanoic acid (e), butanoic acid (f), pentanoic acid (g) and 3-methylbutanoic acid (h) in Sham+VEH, CIH+VEH, Sham+PREB and CIH+PREB. CIH, chronic intermittent hypoxia; PREB; prebiotic; VEH, vehicle. Data (c-h) are expressed as box and whisker plots (median, IQR and minimum to maximum values); n= 11-12. Groups (c-h) were statistically compared using two-way ANOVA, followed by Fisher's least significant difference (LSD) *post hoc* where appropriate, or non-parametric Kruskal-Wallis test, followed by Mann-Whitney *U* test, where appropriate. Acetic (p<0.0005; Fig. 4.8c) and propanoic acid (p=0.011; Fig. 4.8d) were increased as a result of prebiotic supplementation. All other SCFAs were not different (p>0.05 Fig. 4.8e-h). ~ p=0.002, CIH+VEH *versus* CIH+PREB; $ p=0.001, Sham+PREB *versus* Sham+VEH.

4.4. Discussion

There is a growing evidence-based consensus that the gut microbiota plays a modulatory role in physiological homeostasis. Recent studies posit that cardiorespiratory morbidity is linked to aberrant microbiota-gut-brain axis signalling (Ganesh *et al.*, 2018; Meng *et al.*, 2019; O'Connor *et al.*, 2019a; Toral *et al.*, 2019). Investigations in rodents reveal that exposure to CIH disturbs the gut microbiota (Moreno-Indias *et al.*, 2015; Moreno-Indias *et al.*, 2016; Lucking *et al.*, 2018b). Exposure to CIH elicits cardiorespiratory dysfunction (O'Halloran, 2016; Laouafa *et al.*, 2017; Elliot-Portal *et al.*, 2018; Laouafa *et al.*, 2019), predominantly considered to be mediated via CIH-induced carotid body sensitisation (Prabhakar *et al.*, 2007; Iturriaga *et al.*, 2009; Iturriaga *et al.*, 2017), but also suggested to relate to aberrant signalling from other sites (Docio *et al.*, 2018; Lucking *et al.*, 2018b). When viewed together, these observations encourage a new line of enquiry. Dysregulated microbiota-gut-brain axis signalling in CIH-exposed rodent models may play a modulatory role in cardiorespiratory disturbances evident in animal models of SDB. Manipulation of the gut microbiota via antibiotic administration/faecal microbiota transfer perturbs the gut microbiota and alters cardiorespiratory control (O'Connor *et al.*, 2019a). As such, prebiotic administration, promoting the expansion of beneficial microbes, could prove effective in the prevention of CIH-induced cardiorespiratory dysfunctions.

We sought to explore the interplay between cardiorespiratory physiology and the gut microbiota in a rat model of SDB, investigating if manipulation of the gut microbiota by prebiotic fibre administration could prevent or ameliorate cardiorespiratory dysfunctions evident in a CIH animal model. The principal findings of this study are: 1) CIH-exposed rats have reduced relative abundance of *Lactobacillus* species, predominantly *Lactobacillus rhamnosus*; prebiotic administration shifted the bacteria microbiota composition and diversity but did not restore *Lactobacillus rhamnosus* relative abundance; 2) CIH-exposed rats develop hypertension, which prebiotics failed to prevent; 3) CIH exposure evoked cardiac autonomic imbalance, which was not prevented by prebiotic administration; 4) CIH exposure had no effect on faecal SCFA concentrations; acetic and propanoic acid are increased in prebiotic groups; 5) CIH exposure did not affect inflammatory mediators in the periphery; prebiotic administration reduced TNF-α and IL-4 levels in Sham rats; 6) CIH exposure and prebiotic administration did not alter respiratory timing variability during normoxia; 7) CIH exposure increases the apnoea index during normoxia, which was unaffected by prebiotic administration; 8) Monoamine, monoamine precursor and

metabolite concentrations were unaffected by exposure to CIH; prebiotic administration had modest effects on brainstem neurochemistry; 9) Cardiorespiratory responsiveness to vagal afferent nerve stimulation was unaffected by CIH exposure; prebiotic administration had modest effects on apnoea duration.

In our study, both exposure to CIH and prebiotic administration had significant effects on rat body weight. Consistent with observations in previous studies, CIH exposure reduced weight gain (Zoccal *et al.*, 2008; McDonald *et al.*, 2015), likely due to a CIH-induced stress response (Hwang *et al.*, 2017). Plasma corticosterone concentrations were not different between groups determined on the day following exposure to CIH, however, corticosterone levels were not determined at early time-points during the CIH protocol, where stress-induced elevations in corticosterone may well have been evident. Remarkably, prebiotic administration prevented rodent body weight gain. In rodent and human subjects, prebiotic supplementation stimulated satiety hormone secretion (glucagon-like-peptide-1 and peptide YY) and decreased ghrelin concentrations (Parnell & Reimer, 2009, 2012). The inability of prebiotic rodent groups to gain weight may stem from modifications in hunger and satiety hormones. Differences in normalised tissue weights between groups related to differences in body weight (Appendix Table C.1). As expected, prebiotic supplemented animals had increased caecum weight, consistent with previous studies (Burokas *et al.*, 2017; Boehme *et al.*, 2019), related to augmented dietary fibre consumption.

Exposure to CIH elicited hypertension and a shift in autonomic balance towards sympathetic dominance, as evident by alterations in heart rate variability and spectral analysis parameters. However, there was no evidence of tachycardia, similar to previous findings (Zoccal *et al.*, 2007a; Yamamoto *et al.*, 2013). CIH-induced hypertension was characterised by augmented diastolic blood pressure, suggestive of elevated peripheral vascular resistance or reduced arterial compliance (Philippi *et al.*, 2010). There is considerable evidence supporting CIH-induced sensitisation of the carotid bodies, the principal peripheral oxygen sensors, with persistent elevation in chemo-afferent traffic to the NTS of the brainstem and resultant potentiation of sympathetic nervous outflow giving rise to hypertension (Fletcher *et al.*, 1992a; Kumar & Prabhakar, 2012; Iturriaga *et al.*, 2015; Del Rio *et al.*, 2016; Lucking *et al.*, 2018b). Carotid body ablation prevents CIH-induced hypertension and elevations in heart rate variability indicative of cardiac autonomic dysfunction (Iturriaga *et al.*, 2015; Del Rio *et al.*, 2016). Nevertheless, CIH-exposed guinea-pigs, with hypoxia-insensitive carotid bodies, have altered autonomic control of heart rate associated with modification in gut microbiota composition and diversity (Lucking *et al.*, 2018b). Moreover, exposure to severe CIH elicits

sympathetic over-activity and hypertension in guinea-pigs in the absence of carotid body sensitisation (Docio *et al.*, 2018), revealing sites beyond the carotid bodies that can contribute to the manifestation of CIH-induced hypertension. Numerous studies have recently linked the development of hypertension to perturbed gut microbiota and altered SCFA production, portraying that the microbiota-gut-brain axis has a regulatory role in blood pressure control (Yang *et al.*, 2015; Adnan *et al.*, 2017; Li *et al.*, 2017; Santisteban *et al.*, 2017; Yan *et al.*, 2017; Toral *et al.*, 2019).

In our study, whole-metagenome shotgun sequencing revealed novel data showing that CIH+VEH hypertensive rats have altered bacterial species compared with Sham+VEH normotensive rats. The greatest difference evident was in the relative abundance of the beneficial commensal bacterial species, *Lactobacillus rhamnosus* (>1 effect size), which was diminished in CIH+VEH compared with Sham+VEH rats. Of particular interest, *Lactobacillus rhamnosus* supplementation ameliorated CIH+HSD-induced hypertension, decreasing serum pro-inflammatory mediators and trimethylamine N-oxide (TMAO) levels in rats (Liu *et al.*, 2019). Furthermore, administration of *Lactobacillus rhamnosus* in rodents altered central GABA receptor expression; effects abolished in vagotomised animals (Bravo *et al.*, 2011). GABAergic mechanisms modulate sympathetic vasomotor outflow, arterial baroreflex activity and blood pressure (Potts *et al.*, 2003; Teixeira *et al.*, 2019). This suggests that CIH-induced reductions in the relative abundance of *Lactobacillus rhamnosus* may have contributed to the development of cardiovascular and autonomic dysfunction in our study, at least the development of hypertension. Considering that the relative abundance of *Lactobacillus rhamnosus* was reduced in CIH+VEH rats, we assessed if other species of the *Lactobacillus* genera were altered in CIH+VEH rats. Interestingly, the relative abundance of an additional 24 *Lactobacillus* species were decreased (>0.5 effect size) in CIH+VEH compared with Sham+VEH rats. These included beneficial commensal bacterial species including, *Lactobacillus johnsonii, Lactobacillus fermentum, Lactobacillus lindneri* and *Lactobacillus jensenii,* extending previous observations of reduced *Lactobacillus* abundance in CIH + high salt diet fed (CIH+HSD) and IH-exposed animal models (Moreno-Indias *et al.*, 2016; Liu *et al.*, 2019). Furthermore, the pathogenic species, *Streptomyces sp. 452* and *Raoultella planticola* were increased in CIH+VEH rats compared with Sham+VEH rats (>1 effect size).

Prebiotic treated groups had an overall increase in the abundance of beneficial species and a decrease in the abundance of pathogenic species, with reduced species evenness compared with Sham+VEH and CIH+VEH rats. The relative abundance of *Bifidobacterium* was

significantly increased by prebiotic administration consistent with previous studies (Gibson *et al.*, 1995; Boehme *et al.*, 2019). Elevated *Bifidobacterium* was predominantly related to augmented relative abundance of a recognised probiotic species, *Bifidobacterium animalis,* which has typically been associated with improvements in intestinal function (Marteau *et al.*, 2002; Guyonnet *et al.*, 2007). Increases in other *Bifidobacterium* species such as *Bifidobacterium choerinum* and *Bifidobacterium pseudolongum* were also evident in prebiotic groups.

Of interest, there were reductions in relative abundance of *Lactobacillus gasseri, Lactobacillus casei* and *Lactobacillus ruminis* (>0.5 effect size) in hypertensive CIH+PREB compared with hypertensive CIH+VEH rats, with a number of other *Lactobacillus* species increased. The relative abundance of *Lactobacillus rhamnosus* remained decreased in CIH+PREB, again drawing focus to a potential contributory role in the development of hypertension. Correlation analysis between *Lactobacillus rhamnosus* relative abundance and blood pressure revealed a correlation. However, this was an artefact of compositionality (Gloor *et al.*, 2017) as correlation analysis between *Lactobacillus rhamnosus* center-log ratio transformed values and heart rate variability and blood pressure parameters, namely mean, systolic and diastolic blood pressure did not reveal any significant correlations.

Other species of *Lactobacillus* including *Lactobacillus casei* and *Lactobacillus fermentum* (>0.8 effect size) were also decreased in Sham+PREB rats (normotensive) compared with Sham+VEH (normotensive) rats, likely as some *Lactobacillus* species cannot consume fructo- or galacto-oligossaccharides (Sims *et al.*, 2014). Of interest, there was decreased abundance of *Lactobacillus ruminis* and *Lactobacillus lindneri* and increased relative abundance of *Lactobacillus fermentum* (>0.5 effect size) in CIH+PREB compared with Sham+PREB rats. The largest difference between CIH+PREB and Sham+PREB rats was due to an increase in the relative abundance of the pathogenic species *Helicobacter bilis* in CIH+PREB rats (>0.8 effect size).

When the pattern of *Lactobacillus* species abundance between groups is considered, it is not apparent that changes in one specific species protects against or contribute to the development of hypertension. Mean arterial blood pressure significantly correlated with 269 bacterial species; 3 of these bacterial species where of *Lactobacillus*, including *Lactobacillus parabuchneri*, *Lactobacillus murinus* and *Lactobacillus casei* (Appendix Table C.9). Diastolic blood pressure correlated with 16 bacterial species, the majority of these species were pathogenic, including *Corynebacterium jeikeium* (Appendix Table C.10). It is plausible that a

complex interplay between commensal and pathogenic species creates distinct microbiota signatures that contribute to blood pressure regulation *per se* and the development of hypertension in CIH-exposed rats.

SCFAs, produced by bacterial fermentation of digestible and indigestible polysaccharides, have been associated with cardiovascular function (Pluznick, 2014). Acetate-producing bacteria taxa, such as *Holdemania* were shown to be decreased in hypertensive rodents (Yang *et al.*, 2015; Ganesh *et al.*, 2018). Intriguingly, probiotic or prebiotic administration prevented the progression of hypertension in an OSA+HFD rat model, increasing caecal acetate and various SCFA producing bacteria that are diminished in the hypertensive rats (Ganesh *et al.*, 2018). In our study, SCFA concentrations were unaffected by CIH exposure, yet, CIH-exposure caused hypertension, revealing that depletion of gut SCFAs is not obligatory for the development of CIH-induced hypertension. Prebiotic administration increased faecal acetic and propionic acid concentrations but had no beneficial effects on cardiovascular control, such that hypertension and enhanced heart rate variability were evident in CIH+PREB rats. In our study, elevations in SCFAs in prebiotic treated rodents may have had divergent effects on blood pressure regulation that offset one another given that SCFAs act via olfactory receptor 78 (Olfr78) and G-protein-coupled receptor (Gpr41) to increase and decrease blood pressure, respectively (Pluznick, 2013). Of note, elevated acetic acid has been suggested to be a crucial signalling molecule in the ability of *Bifidobacterium* to inhibit expansion of enteropathogens (Fukuda *et al.*, 2011), suggesting that in our study augmented acetic acid concentrations may have diminished the overall relative abundance of pathogenic species, such as *Helicobacter cinaedi.* Despite these beneficial changes however, prebiotic feeding did not ameliorate CIH-induced hypertension revealing that elevations in SCFA concentrations (or at least increases in acetic acid and propionic acid) do not protect against CIH-induced hypertension.

We did not examine the effects of CIH exposure on intestinal function, but of interest CIH exposure did not increase plasma (or brainstem) inflammatory cytokines in this study, although prebiotic administration decreased plasma TNF-α and IL-4 levels in Sham rats. Others have reported that CIH exposure in rodents increases plasma lipopolysaccharides (LPS), induces oxidative stress, reduces tight junction protein expression and elevates gut inflammation, contributing to intestinal barrier dysfunction (Moreno-Indias *et al.*, 2015; Wu *et al.*, 2016), a phenotype also evident in other hypertensive models (Santisteban *et al.*, 2017; Kim *et al.*, 2018). Faecal microbiota transfer from donor normotensive to hypertensive recipient rats, and prebiotic and probiotic administration each independently decrease blood

pressure, and prevent intestinal dysfunction and neuroinflammation in hypertensive models, including OSA animal models (Ganesh *et al.*, 2018; Liu *et al.*, 2019; Toral *et al.*, 2019). Furthermore, butyrate administration prevented elevated blood pressure and increased cardiac sympathetic tone in angiotensin-II-induced hypertensive mice; in tandem, butyrate treatment, increased tight junction receptor expression, reduced intestinal permeability and peripheral inflammatory markers and restored physiological oxygen status in the gut epithelia in the hypertensive mouse (Kim *et al.*, 2018).

Several research groups have identified adverse respiratory phenotypes in animal models of CIH and in persons with OSA (Edge *et al.*, 2009, 2010; Souza *et al.*, 2015a; McNicholas, 2017). Augmented normoxic ventilatory drive, increased respiratory instabilities and elevated responsiveness to hypoxic chemostimulation are common consequences of CIH exposure (Prabhakar & Peng, 2004; Edge *et al.*, 2009; Del Rio *et al.*, 2010; Souza *et al.*, 2015a); however these findings were not evident in our CIH model and are not always observed, likely due to variations in CIH paradigms (Reeves & Gozal, 2006; Zoccal *et al.*, 2008; Edge *et al.*, 2009; Edge *et al.*, 2012). There was an elevated propensity for central apnoea apparent in CIH-exposed rats, an observation commonly observed in CIH animal models (Julien *et al.*, 2008; Edge *et al.*, 2012; Donovan *et al.*, 2014; Souza *et al.*, 2015a). Prebiotic administration did not reverse CIH-induced increase in apnoea index. Increased apnoea index is proposed to manifest due to disturbances in the respiratory control network (Nsegbe *et al.*, 2004; McKay & Feldman, 2008; Ramirez, 2014; Mateika *et al.*, 2019). The pre-Bötzinger complex is the primary rhythm-generating site located within the respiratory network of the medulla oblongata of the brainstem and is implicated in apnoea generation (Lieske *et al.*, 2000; McKay & Feldman, 2008; Tan *et al.*, 2008). Carotid body plasticity and altered chemoreflex responsiveness is also suggested to be a driver of respiratory instability and apnoea (Prabhakar *et al.*, 2007; Marcus *et al.*, 2010; Julien *et al.*, 2011) and may have been a driver of apnoea in our model, although the lack of change in basal breathing and ventilatory responses to hypoxia in our study suggest a central origin.

Prebiotic administration increased chemoreflex control of breathing in response to hypercapnia and hypoxic hypercapnia. Hypercapnia is primarily sensed by central chemoreceptors residing in the brainstem. Increased ventilatory responsiveness to hypercapnia is particularly interesting given that rats exposed to pre-natal stress exhibit altered ventilatory responsiveness to hypoxic and hypercapnic chemostimulation in adulthood with evidence of altered gut microbiota (Golubeva *et al.*, 2015). Moreover, antibiotic administration and faecal microbiota transfer perturbed the gut microbiota

composition in adult rats and blunted chemoreflex control of breathing (O'Connor *et al.*, 2019a). The latter observation combined with findings from the present study suggests that microbial signatures shape central nervous system responsiveness to carbon dioxide (acidosis) with implications for a range of respiratory control disorders.

We assessed monoamines and monoamine metabolites and precursors in the pons and medulla oblongata of the brainstem that are crucial in the neuromodulation of respiratory control. No significant modifications in monoamine, metabolite and precursor concentrations were evident in the brainstem of CIH-exposed rats. Previous studies present evidence of elevated central noradrenergic terminals in brainstem sensory and motor nuclei of CIH-exposed rats (Mody *et al.*, 2011). Of note, noradrenaline has been associated with breathing irregularities in IH-exposed animals (Zanella *et al.*, 2014) and rodents with lesions of noradrenergic locus coeruleus neurones display blunted hypercapnic ventilatory responses (Gargaglioni *et al.*, 2010; de Carvalho *et al.*, 2017). Our data revealed that CIH exposure did not affect noradrenaline brainstem neurochemistry. Similarly, prebiotic administration had no effect on brainstem noradrenaline, in accordance with previous studies reporting that prebiotic supplementation did not alter noradrenaline levels in rodent brainstem, prefrontal cortex, cerebellum or frontal cortex (Kannampalli *et al.*, 2014; Burokas *et al.*, 2017). These observations indicate that noradrenaline is not likely implicated in apnoea generation in CIH-exposed rats or elevated chemoreflex control of breathing in response to hypercapnia and hypoxic hypercapnia in prebiotic treated rodents.

Transgenic mice that fail to develop dopaminergic neurones exhibit several respiratory disturbances; indeed, these mice tend to hypoventilate and have increased propensity for apnoea generation during normoxia (Nsegbe *et al.*, 2004). Furthermore, a Parkinson disease mouse model, with confirmed reduction in tyrosine hydroxylase and chemosensitive (Phox2b) neurones in the substantia nigra and retrotrapezoid nucleus respectively, displays blunted ventilatory responses to hypercapnia (Oliveira *et al.*, 2019). Notably, the modulatory role of dopamine is complex and depends on the target receptor sub-type (Beaulieu & Gainetdinov, 2011). In our study, the monoamine, metabolites and precursors of the dopaminergic pathway were not different in CIH+VEH compared with Sham+VEH rats. There was a trend for reduced dopamine turnover in the medulla oblongata of Sham+PREB rats, with elevated ventilatory responses to hypercapnia and hypoxic hypercapnia compared with Sham+VEH rats. This finding is particularly interesting given that antibiotic treated and faecal microbiota transfer rodents with perturbed gut microbiota each display blunted ventilatory responses to hypercapnia and exhibit increased brainstem dopamine turnover (O'Connor *et*

al., 2019a). Perhaps, D1 receptor activation (Lalley, 2004) underpins elevated ventilatory responses to chemostimulation in Sham+PREB rats. Previous studies demonstrate that prebiotic administration affected DOPAC concentrations in the brainstem and frontal cortex of mice (Burokas *et al.*, 2017). Yet, prebiotic administration did not alter other monoamine, metabolites and precursors of the dopaminergic pathway in animal models (Kannampalli *et al.*, 2014; Burokas *et al.*, 2017).

Infant and adult rats lacking 5-HT display unstable breathing and increased propensity for apnoea (Hodges *et al.*, 2009; Young *et al.*, 2017; Davis *et al.*, 2019; Mateika *et al.*, 2019). Furthermore, in a gestational stress model, reduced 5-HT and noradrenaline concentrations were evident in newborn rats with augmented apnoea index (Fournier *et al.*, 2013a). CIH exposure has been shown to decrease the number of serotonergic cells in the brainstem (Baum *et al.*, 2018). CIH+PREB rats revealed significantly increased 5-HIAA concentrations in the medulla oblongata compared with CIH+VEH rats. Noteworthy, lesions of raphé serotonergic neurons and transgenic rodents without 5-HT neurones display reduced respiratory response to hypercapnic chemostimulation (Dias *et al.*, 2007; Hodges *et al.*, 2008; Li & Nattie, 2008; Hodges & Richerson, 2010). However, serotonin turnover was not different in CIH+PREB rats compared with CIH+VEH. It is not likely that serotonin mediated the elevated ventilatory drive to breathe in response to hypercapnia associated with prebiotic supplementation. Altered 5-HT receptor levels and 5-HT concentrations have been observed in the rodent pre-frontal cortex after prebiotic administration (Savignac *et al.*, 2016; Burokas *et al.*, 2017). Our data suggest however that neither the serotonergic nor dopaminergic pathway are likely responsible for alterations in apnoea index. However, elevated dopamine turnover in Sham+PREB rats may be associated with increased ventilatory responses to hypercapnic chemostimulation. Based on the assessment of neuromodulators and apnoea generation in our study it may be that other neuromodulators that were not measured, such as GABA, which is altered in models of manipulated gut microbiota (Bravo *et al.*, 2011; Strandwitz *et al.*, 2019), may have influenced apnoea generation. Indeed, other mechanisms such as oxidative stress, which can be altered by the gut microbiota (Toral *et al.*, 2019), may influence central respiratory circuit function (Garcia *et al.*, 2016). No significant correlations were evident between the gut microbiota and respiratory parameters (apnoea and breathing in response to hypercapnia) in our study.

The afferent vagal pathway is a pivotal signalling pathway of the microbiota-gut-brain axis, which responds to various stimuli including cytokines, bacterial metabolites including SCFAs, gut hormones and neurotransmitters (Goehler *et al.*, 2000; Raybould *et al.*, 2003; Johnston

& Webster, 2009; Nohr *et al.*, 2015). Central integration of vagal afferent signals occurs within the NTS of the brainstem. PBG, which is a 5-HT_3 receptor agonist, activates pulmonary vagal afferent C-fibres manifesting the pulmonary chemoreflex characterised by decreased blood pressure, bradycardia, apnoea and post apnoea-induced tachypnoea. Exposure to CIH did not affect the pulmonary chemoreflex but prebiotic administration increased apnoea duration. *Post hoc* analysis determined that there were no statistically significant differences between groups suggesting that vagal influence over these critical control centres was unaltered by any potential changes in microbiota-gut-brain signalling. Of interest, cardiorespiratory responses to PBG was also unaffected in other models of disrupted gut microbiota (O'Connor *et al.*, 2019a). Thus, notwithstanding alterations to the gut microbiota in CIH+VEH rats, as well as the notable changes in the gut microbiota, SCFA concentrations and brainstem neurochemistry in prebiotic groups, no major differences in cardiorespiratory efferent responses to vagal afferent stimulation were observed revealing intact pulmonary chemoreflex circuit function in CIH-exposed and prebiotic supplemented animals. This does not preclude however, the possibility of altered vagal signalling from the gut in our models, which warrants attention in future studies.

4.4.1 Summary and conclusion

Our novel findings add to the growing body of evidence pointing to aberrant microbiota-gut-brain axis signalling in the manifestation of cardiorespiratory dysfunction in OSA animal models (Ganesh *et al.*, 2018; Liu *et al.*, 2019). Herein we confirmed that CIH exposure leads to the development of adverse cardiorespiratory and autonomic control, resulting in hypertension, cardiac autonomic imbalance and elevated propensity for apnoea. We reveal for the first time that CIH exposure decreases the relative abundance of a beneficial commensal species, *Lactobacillus rhamnosus,* and increased the abundance of several pathogenic bacterial species, with no resultant effects on SCFA concentrations, indicating that diminished SCFA concentrations are not obligatory for the manifestation of CIH-induced hypertension. Prebiotic fibre supplementation did not ameliorate cardiorespiratory malaise in CIH-exposed rats but had considerable effects on the gut microbiota, increasing the overall abundance of beneficial species including *Bifidobacterium animalis,* and decreasing the abundance of pathogenic species. However, the relative abundance of *Lactobacillus rhamnosus* remained decreased in CIH+PREB rats, suggesting a potential contributory role of *Lactobacillus rhamnosus* in the pathogenesis of hypertension. Arguing against this, however, the relative abundance of *Lactobacillus rhamnosus* was also low in Sham+PREB (normotensive rats), and there was no correlation between *Lactobacillus rhamnosus*

abundance and blood pressure measures. Correlation analysis revealed that blood pressure significantly correlated with numerous bacterial species, suggesting that a complex interplay between pathogenic and commensal species may create a distinct microbiota signature that culminates in the establishment of hypertension in CIH-exposed rats by shaping maladaptive plasticity in neural control circuitry. Of note, it is also plausible that aberrant plasticity, at least in our CIH model, occurs independently of the gut microbiota. Prebiotic administration increased acetic and propionic acid concentrations but had no beneficial effects on cardiovascular control, indicating that SCFAs (at least acetic and propionic acid) do not protect against CIH-induced hypertension in our model.

Considering our observations in tandem with the extensive literature portraying the carotid body as the dominant driver of cardiorespiratory morbidity in CIH-exposed rodents (Peng *et al.*, 2014b; Del Rio *et al.*, 2016; Iturriaga *et al.*, 2017) and the evidence that SCFA supplementation is sufficient to prevent hypertension in a rat model of OSA (Ganesh *et al.*, 2018), it is interesting to speculate that a microbiota-gut-carotid body axis may exist. G-protein coupled receptors, predominantly Olfr 78 is enriched in carotid body glomus cells playing an important role in carotid body function. Several short-chain fatty acids, including lactic, propionic and acetic acid act as potent Olfr 78 agonists (Chang *et al.*, 2015; Zhou *et al.*, 2016). Indeed, carotid body glomus cell activity is altered by metabolites of the gut microbiota (Chang *et al.*, 2015; Zhou *et al.*, 2016). However, SCFA activation of the carotid body should serve to increase sympathetic nervous outflow and raise blood pressure. This suggests that elevated plasma SCFA concentrations act at other sites to promote blood pressure homeostasis (Kimura *et al.*, 2011; Pluznick, 2013; Pluznick *et al.*, 2013; Kimura *et al.*, 2014). Remarkably, Ganesh *et al.* (2018), demonstrated that prebiotic, probiotic or acetate administration diminished hypertension in OSA+HFD fed rodents, with presumed carotid body sensitisation and sympathetic overactivity. It is also established that gut microbiota derived metabolites can exert effects on peripheral sympathetic circuits (Kimura *et al.*, 2011; Meng *et al.*, 2019). Considering these studies together, it is likely that gut microbiota metabolites have a capacity to modulate not only central integrative sites within the brainstem, but also peripheral afferent and efferent pathways contributing to blood pressure regulation and the development of CIH-induced cardiorespiratory and autonomic malaise, at least in some models. Our findings have relevance for human SDB and contribute to an emerging interest in the putative role of the gut microbiota in cardiorespiratory homeostasis and the potential application of manipulation of the gut microbiota as an adjunctive therapy for human cardiorespiratory disease.

4.5 Additional information

Competing interests: JFC is in receipt of research funding from 4D-Pharma, Mead Johnson, Nutricia, Dupont and Cremo and has been an invited speaker at meetings organised by Mead Johnson, Alkermes, Abbott Nutrition, Danone Nutricia and Janssen. All other authors report no financial, professional or personal conflicts of interest relating to this publication.

Funding: This project was funded by the Department of Physiology, and the APC Microbiome Ireland (funded by Science Foundation Ireland (SFI/ 12/RC/2273), University College Cork, Ireland. The institution had no role in the study design, data collection, data analysis, interpretation or writing of the manuscript.

Acknowledgements: The authors are grateful to staff of the Biological Services Unit, University College Cork for their support with animal housing and welfare. We thank the Healy group, Tallaght, Dublin, Ireland for supplying GOS and FOS.

4.6 References

Adnan S, Nelson JW, Ajami NJ, Venna VR, Petrosino JF, Bryan RM, Jr. & Durgan DJ. (2017). Alterations in the gut microbiota can elicit hypertension in rats. *Physiological genomics* **49,** 96-104.

Almado CE, Machado BH & Leao RM. (2012). Chronic intermittent hypoxia depresses afferent neurotransmission in NTS neurons by a reduction in the number of active synapses. *The Journal of neuroscience : the official journal of the Society for Neuroscience* **32,** 16736-16746.

AlMarabeh S, Abdulla MH & O'Halloran KD. (2019). Is Aberrant Reno-Renal Reflex Control of Blood Pressure a Contributor to Chronic Intermittent Hypoxia-Induced Hypertension? *Frontiers in physiology* **10,** 465.

Alves CC, Waitzberg DL, de Andrade LS, Dos Santos Aguiar L, Reis MB, Guanabara CC, Junior OA, Ribeiro DA & Sala P. (2017). Prebiotic and Synbiotic Modifications of Beta Oxidation and Lipogenic Gene Expression after Experimental Hypercholesterolemia in Rat Liver. *Frontiers in microbiology* **8,** 2010.

Baum DM, Saussereau M, Jeton F, Planes C, Voituron N, Cardot P, Fiamma MN & Bodineau L. (2018). Effect of Gender on Chronic Intermittent Hypoxic Fosb Expression in Cardiorespiratory-Related Brain Structures in Mice. *Front Physiol* **9,** 788.

Bavis RW, van Heerden ES, Brackett DG, Harmeling LH, Johnson SM, Blegen HJ, Logan S, Nguyen GN & Fallon SC. (2014). Postnatal development of eupneic ventilation and metabolism in rats chronically exposed to moderate hyperoxia. *Respiratory physiology & neurobiology* **198,** 1-12.

Beaulieu JM & Gainetdinov RR. (2011). The physiology, signaling, and pharmacology of dopamine receptors. *Pharmacological reviews* **63,** 182-217.

Boehme M, van de Wouw M, Bastiaanssen TFS, Olavarria-Ramirez L, Lyons K, Fouhy F, Golubeva AV, Moloney GM, Minuto C, Sandhu KV, Scott KA, Clarke G, Stanton C, Dinan TG, Schellekens H & Cryan JF. (2019). Mid-life microbiota crises: middle age is associated with pervasive neuroimmune alterations that are reversed by targeting the gut microbiome. *Molecular psychiatry*.

Bravo JA, Forsythe P, Chew MV, Escaravage E, Savignac HM, Dinan TG, Bienenstock J & Cryan JF. (2011). Ingestion of Lactobacillus strain regulates emotional behavior and central GABA receptor expression in a mouse via the vagus nerve. *Proceedings of*

the National Academy of Sciences of the United States of America **108,** 16050-16055.

Burokas A, Arboleya S, Moloney RD, Peterson VL, Murphy K, Clarke G, Stanton C, Dinan TG & Cryan JF. (2017). Targeting the Microbiota-Gut-Brain Axis: Prebiotics Have Anxiolytic and Antidepressant-like Effects and Reverse the Impact of Chronic Stress in Mice. *Biological psychiatry* **82,** 472-487.

Chang AJ, Ortega FE, Riegler J, Madison DV & Krasnow MA. (2015). Oxygen regulation of breathing through an olfactory receptor activated by lactate. *Nature* **527,** 240-244.

Davis MR, Magnusson JL & Cummings KJ. (2019). Increased central cholinergic drive contributes to the apneas of serotonin-deficient rat pups during active sleep. *J Appl Physiol (1985)* **126,** 1175-1183.

de Carvalho D, Patrone LGA, Marques DA, Vicente MC, Szawka RE, Anselmo-Franci JA, Bicego KC & Gargaglioni LH. (2017). Participation of locus coeruleus in breathing control in female rats. *Respiratory physiology & neurobiology* **245,** 29-36.

Del Rio R, Andrade DC, Lucero C, Arias P & Iturriaga R. (2016). Carotid Body Ablation Abrogates Hypertension and Autonomic Alterations Induced by Intermittent Hypoxia in Rats. *Hypertension (Dallas, Tex : 1979)* **68,** 436-445.

Del Rio R, Moya EA & Iturriaga R. (2010). Carotid body and cardiorespiratory alterations in intermittent hypoxia: the oxidative link. *The European respiratory journal* **36,** 143-150.

Dias MB, Nucci TB, Margatho LO, Antunes-Rodrigues J, Gargaglioni LH & Branco LG. (2007). Raphe magnus nucleus is involved in ventilatory but not hypothermic response to CO2. *Journal of applied physiology (Bethesda, Md : 1985)* **103,** 1780-1788.

Dinan TG & Cryan JF. (2017). The Microbiome-Gut-Brain Axis in Health and Disease. *Gastroenterology clinics of North America* **46,** 77-89.

Docio I, Olea E, Prieto LJ, Gallego-Martin T, Obeso A, Gomez-Nino A & Rocher A. (2018). Guinea Pig as a Model to Study the Carotid Body Mediated Chronic Intermittent Hypoxia Effects. *Frontiers in physiology* **9,** 694.

Donovan LM, Liu Y & Weiss JW. (2014). Effect of endothelin antagonism on apnea frequency following chronic intermittent hypoxia. *Respiratory physiology & neurobiology* **194,** 6-8.

Durgan DJ, Ganesh BP, Cope JL, Ajami NJ, Phillips SC, Petrosino JF, Hollister EB & Bryan RM, Jr. (2016). Role of the Gut Microbiome in Obstructive Sleep Apnea-Induced Hypertension. *Hypertension (Dallas, Tex : 1979)* **67,** 469-474.

Dutta A & Deshpande SB. (2010). Cardio-respiratory reflexes evoked by phenylbiguanide in rats involve vagal afferents which are not sensitive to capsaicin. *Acta physiologica (Oxford, England)* **200,** 87-95.

Edge D, Bradford A & O'Halloran KD. (2012). Chronic intermittent hypoxia increases apnoea index in sleeping rats. *Advances in experimental medicine and biology* **758,** 359-363.

Edge D & O'Halloran KD. (2015). Chronic Intermittent Hypoxia Blunts the Expression of Ventilatory Long Term Facilitation in Sleeping Rats. *Advances in experimental medicine and biology* **860,** 335-342.

Edge D, Skelly JR, Bradford A & O'Halloran KD. (2009). Ventilatory drive is enhanced in male and female rats following chronic intermittent hypoxia. *Advances in experimental medicine and biology* **648,** 337-344.

Edge D, Skelly JR, Bradford A & O'Halloran KD. (2010). Respiratory plasticity in the behaving rat following chronic intermittent hypoxia. *Advances in experimental medicine and biology* **669,** 267-270.

Elliot-Portal E, Laouafa S, Arias-Reyes C, Janes TA, Joseph V & Soliz J. (2018). Brain-derived erythropoietin protects from intermittent hypoxia-induced cardiorespiratory dysfunction and oxidative stress in mice. *Sleep* **41**.

Fernandes AD, Macklaim JM, Linn TG, Reid G & Gloor GB. (2013). ANOVA-like differential expression (ALDEx) analysis for mixed population RNA-Seq. *PloS one* **8,** e67019.

Fletcher EC, Lesske J, Behm R, Miller CC, 3rd, Stauss H & Unger T. (1992). Carotid chemoreceptors, systemic blood pressure, and chronic episodic hypoxia mimicking sleep apnea. *Journal of applied physiology (Bethesda, Md : 1985)* **72,** 1978-1984.

Fournier S, Steele S, Julien C, Fournier S, Gulemetova R, Caravagna C, Soliz J, Bairam A & Kinkead R. (2013). Gestational stress promotes pathological apneas and sex-specific disruption of respiratory control development in newborn rat. *The Journal of neuroscience : the official journal of the Society for Neuroscience* **33,** 563-573.

Fukuda S, Toh H, Hase K, Oshima K, Nakanishi Y, Yoshimura K, Tobe T, Clarke JM, Topping DL, Suzuki T, Taylor TD, Itoh K, Kikuchi J, Morita H, Hattori M & Ohno H. (2011). Bifidobacteria can protect from enteropathogenic infection through production of acetate. *Nature* **469,** 543-547.

Ganesh BP, Nelson JW, Eskew JR, Ganesan A, Ajami NJ, Petrosino JF, Bryan RM, Jr. & Durgan DJ. (2018). Prebiotics, Probiotics, and Acetate Supplementation Prevent Hypertension in a Model of Obstructive Sleep Apnea. *Hypertension (Dallas, Tex : 1979)* **72,** 1141-1150.

Garcia AJ, 3rd, Dashevskiy T, Khuu MA & Ramirez JM. (2017). Chronic Intermittent Hypoxia Differentially Impacts Different States of Inspiratory Activity at the Level of the preBotzinger Complex. *Frontiers in physiology* **8,** 571.

Garcia AJ, 3rd, Zanella S, Dashevskiy T, Khan SA, Khuu MA, Prabhakar NR & Ramirez JM. (2016). Chronic Intermittent Hypoxia Alters Local Respiratory Circuit Function at the Level of the preBotzinger Complex. *Frontiers in neuroscience* **10,** 4.

Gargaglioni LH, Hartzler LK & Putnam RW. (2010). The locus coeruleus and central chemosensitivity. *Respiratory physiology & neurobiology* **173,** 264-273.

Garvey JF, Pengo MF, Drakatos P & Kent BD. (2015). Epidemiological aspects of obstructive sleep apnea. *Journal of thoracic disease* **7,** 920-929.

Gibson GR, Beatty ER, Wang X & Cummings JH. (1995). Selective stimulation of bifidobacteria in the human colon by oligofructose and inulin. *Gastroenterology* **108,** 975-982.

Gloor GB, Macklaim JM, Pawlowsky-Glahn V & Egozcue JJ. (2017). Microbiome Datasets Are Compositional: And This Is Not Optional. *Frontiers in microbiology* **8,** 2224.

Goehler LE, Gaykema RP, Hansen MK, Anderson K, Maier SF & Watkins LR. (2000). Vagal immune-to-brain communication: a visceral chemosensory pathway. *Autonomic neuroscience : basic & clinical* **85,** 49-59.

Golubeva AV, Crampton S, Desbonnet L, Edge D, O'Sullivan O, Lomasney KW, Zhdanov AV, Crispie F, Moloney RD, Borre YE, Cotter PD, Hyland NP, O'Halloran KD, Dinan TG, O'Keeffe GW & Cryan JF. (2015). Prenatal stress-induced alterations in major physiological systems correlate with gut microbiota composition in adulthood. *Psychoneuroendocrinology* **60,** 58-74.

Gough R, Cabrera Rubio R, O'Connor PM, Crispie F, Brodkorb A, Miao S, Hill C, Ross RP, Cotter PD, Nilaweera KN & Rea MC. (2018). Oral Delivery of Nisin in Resistant Starch Based Matrices Alters the Gut Microbiota in Mice. *Frontiers in microbiology* **9,** 1186.

Guyonnet D, Chassany O, Ducrotte P, Picard C, Mouret M, Mercier CH & Matuchansky C. (2007). Effect of a fermented milk containing Bifidobacterium animalis DN-173 010 on the health-related quality of life and symptoms in irritable bowel syndrome in adults in primary care: a multicentre, randomized, double-blind, controlled trial. *Alimentary pharmacology & therapeutics* **26,** 475-486.

Haouzi P, Bell HJ, Notet V & Bihain B. (2009). Comparison of the metabolic and ventilatory response to hypoxia and H2S in unsedated mice and rats. *Respiratory physiology & neurobiology* **167,** 316-322.

Hodges MR & Richerson GB. (2010). Medullary serotonin neurons and their roles in central respiratory chemoreception. *Respiratory physiology & neurobiology* **173,** 256-263.

Hodges MR, Tattersall GJ, Harris MB, McEvoy SD, Richerson DN, Deneris ES, Johnson RL, Chen ZF & Richerson GB. (2008). Defects in breathing and thermoregulation in mice with near-complete absence of central serotonin neurons. *The Journal of neuroscience : the official journal of the Society for Neuroscience* **28,** 2495-2505.

Hodges MR, Wehner M, Aungst J, Smith JC & Richerson GB. (2009). Transgenic mice lacking serotonin neurons have severe apnea and high mortality during development. *The Journal of neuroscience : the official journal of the Society for Neuroscience* **29,** 10341-10349.

Hwang GS, Chen CC, Chou JC, Chang LL, Kan SF, Lai WH, Lieu FK, Hu S, Wang PS & Wang SW. (2017). Stimulatory Effect of Intermittent Hypoxia on the Production of Corticosterone by Zona Fasciculata-Reticularis Cells in Rats. *Scientific reports* **7,** 9035.

Iturriaga R, Andrade DC & Del Rio R. (2015). Crucial Role of the Carotid Body Chemoreceptors on the Development of High Arterial Blood Pressure During

Chronic Intermittent Hypoxia. *Advances in experimental medicine and biology* **860,** 255-260.

Iturriaga R, Moya EA & Del Rio R. (2009). Carotid body potentiation induced by intermittent hypoxia: implications for cardiorespiratory changes induced by sleep apnoea. *Clinical and experimental pharmacology & physiology* **36,** 1197-1204.

Iturriaga R, Oyarce MP & Dias ACR. (2017). Role of Carotid Body in Intermittent Hypoxia-Related Hypertension. *Current hypertension reports* **19,** 38.

Johnsen LG, Skou PB, Khakimov B & Bro R. (2017). Gas chromatography - mass spectrometry data processing made easy. *Journal of chromatography A* **1503,** 57-64.

Johnston GR & Webster NR. (2009). Cytokines and the immunomodulatory function of the vagus nerve. *British journal of anaesthesia* **102,** 453-462.

Julien C, Bairam A & Joseph V. (2008). Chronic intermittent hypoxia reduces ventilatory long-term facilitation and enhances apnea frequency in newborn rats. *American journal of physiology Regulatory, integrative and comparative physiology* **294,** R1356-1366.

Julien CA, Joseph V & Bairam A. (2011). Alteration of carotid body chemoreflexes after neonatal intermittent hypoxia and caffeine treatment in rat pups. *Respiratory physiology & neurobiology* **177,** 301-312.

Kannampalli P, Pochiraju S, Chichlowski M, Berg BM, Rudolph C, Bruckert M, Miranda A & Sengupta JN. (2014). Probiotic Lactobacillus rhamnosus GG (LGG) and prebiotic prevent neonatal inflammation-induced visceral hypersensitivity in adult rats. *Neurogastroenterology and motility : the official journal of the European Gastrointestinal Motility Society* **26,** 1694-1704.

Kelly JR, Borre Y, C OB, Patterson E, El Aidy S, Deane J, Kennedy PJ, Beers S, Scott K, Moloney G, Hoban AE, Scott L, Fitzgerald P, Ross P, Stanton C, Clarke G, Cryan JF & Dinan TG. (2016). Transferring the blues: Depression-associated gut microbiota induces neurobehavioural changes in the rat. *Journal of psychiatric research* **82,** 109-118.

Kim S, Goel R, Kumar A, Qi Y, Lobaton G, Hosaka K, Mohammed M, Handberg EM, Richards EM, Pepine CJ & Raizada MK. (2018). Imbalance of gut microbiome and intestinal

epithelial barrier dysfunction in patients with high blood pressure. *Clinical science (London, England : 1979)* **132,** 701-718.

Kimura I, Inoue D, Hirano K & Tsujimoto G. (2014). The SCFA Receptor GPR43 and Energy Metabolism. *Frontiers in endocrinology* **5,** 85.

Kimura I, Inoue D, Maeda T, Hara T, Ichimura A, Miyauchi S, Kobayashi M, Hirasawa A & Tsujimoto G. (2011). Short-chain fatty acids and ketones directly regulate sympathetic nervous system via G protein-coupled receptor 41 (GPR41). *Proceedings of the National Academy of Sciences of the United States of America* **108,** 8030-8035.

Kumar P & Prabhakar NR. (2012). Peripheral chemoreceptors: function and plasticity of the carotid body. *Comprehensive Physiology* **2,** 141-219.

Lalley PM. (2004). Dopamine1 receptor agonists reverse opioid respiratory network depression, increase CO2 reactivity. *Respiratory physiology & neurobiology* **139,** 247-262.

Laouafa S, Ribon-Demars A, Marcouiller F, Roussel D, Bairam A, Pialoux V & Joseph V. (2017). Estradiol Protects Against Cardiorespiratory Dysfunctions and Oxidative Stress in Intermittent Hypoxia. *Sleep* **40**.

Laouafa S, Roussel D, Marcouiller F, Soliz J, Gozal D, Bairam A & Joseph V. (2019). Roles of oestradiol receptor alpha and beta against hypertension and brain mitochondrial dysfunction under intermittent hypoxia in female rats. *Acta physiologica (Oxford, England)* **226,** e13255.

Li A & Nattie E. (2008). Serotonin transporter knockout mice have a reduced ventilatory response to hypercapnia (predominantly in males) but not to hypoxia. *The Journal of physiology* **586,** 2321-2329.

Li J, Zhao F, Wang Y, Chen J, Tao J, Tian G, Wu S, Liu W, Cui Q, Geng B, Zhang W, Weldon R, Auguste K, Yang L, Liu X, Chen L, Yang X, Zhu B & Cai J. (2017). Gut microbiota dysbiosis contributes to the development of hypertension. *Microbiome* **5,** 14.

Li T, Chen Y, Gua C & Wu B. (2018). Elevated Oxidative Stress and Inflammation in Hypothalamic Paraventricular Nucleus Are Associated With Sympathetic Excitation and Hypertension in Rats Exposed to Chronic Intermittent Hypoxia. *Frontiers in physiology* **9,** 840.

Lieske SP, Thoby-Brisson M, Telgkamp P & Ramirez JM. (2000). Reconfiguration of the neural network controlling multiple breathing patterns: eupnea, sighs and gasps [see comment]. *Nature neuroscience* **3,** 600-607.

Liu J, Li T, Wu H, Shi H, Bai J, Zhao W, Jiang D & Jiang X. (2019). Lactobacillus rhamnosus GG strain mitigated the development of obstructive sleep apnea-induced hypertension in a high salt diet via regulating TMAO level and CD4(+) T cell induced-type I inflammation. *Biomedicine & pharmacotherapy = Biomedecine & pharmacotherapie* **112,** 108580.

Lucking EF, Murphy KH, Burns DP, Jaisimha AV, Barry-Murphy KJ, Dhaliwal P, Boland B, Rae MG & O'Halloran KD. (2018a). No evidence in support of a prodromal respiratory control signature in the TgF344-AD rat model of Alzheimer's disease. *Respiratory physiology & neurobiology*.

Lucking EF, O'Connor KM, Strain CR, Fouhy F, Bastiaanssen TFS, Burns DP, Golubeva AV, Stanton C, Clarke G, Cryan JF & O'Halloran KD. (2018b). Chronic intermittent hypoxia disrupts cardiorespiratory homeostasis and gut microbiota composition in adult male guinea-pigs. *EBioMedicine*.

Marcus NJ, Li YL, Bird CE, Schultz HD & Morgan BJ. (2010). Chronic intermittent hypoxia augments chemoreflex control of sympathetic activity: role of the angiotensin II type 1 receptor. *Respiratory physiology & neurobiology* **171,** 36-45.

Marteau P, Cuillerier E, Meance S, Gerhardt MF, Myara A, Bouvier M, Bouley C, Tondu F, Bommelaer G & Grimaud JC. (2002). Bifidobacterium animalis strain DN-173 010 shortens the colonic transit time in healthy women: a double-blind, randomized, controlled study. *Alimentary pharmacology & therapeutics* **16,** 587-593.

Mateika JH, Komnenov D, Pop A & Kuhn DM. (2019). Genetic depletion of 5-HT increases central apnea frequency and duration and dampens arousal but does not impact the circadian modulation of these variables. *J Appl Physiol (1985)* **126,** 1-10.

McDonald FB, Williams R, Sheehan D & O'Halloran KD. (2015). Early life exposure to chronic intermittent hypoxia causes upper airway dilator muscle weakness, which persists into young adulthood. *Experimental physiology* **100,** 947-966.

McIver LJ, Abu-Ali G, Franzosa EA, Schwager R, Morgan XC, Waldron L, Segata N & Huttenhower C. (2018). bioBakery: a meta'omic analysis environment. *Bioinformatics (Oxford, England)* **34,** 1235-1237.

McKay LC & Feldman JL. (2008). Unilateral ablation of pre-Botzinger complex disrupts breathing during sleep but not wakefulness. *American journal of respiratory and critical care medicine* **178,** 89-95.

McNicholas WT. (2017). COPD-OSA Overlap Syndrome: Evolving Evidence Regarding Epidemiology, Clinical Consequences, and Management. *Chest* **152,** 1318-1326.

Meng G, Zhou X, Wang M, Zhou L, Wang Z, Wang M, Deng J, Wang Y, Zhou Z, Zhang Y, Lai Y, Zhang Q, Yang X, Yu L & Jiang H. (2019). Gut microbe-derived metabolite trimethylamine N-oxide activates the cardiac autonomic nervous system and facilitates ischemia-induced ventricular arrhythmia via two different pathways. *EBioMedicine*.

Mika A, Day HE, Martinez A, Rumian NL, Greenwood BN, Chichlowski M, Berg BM & Fleshner M. (2017). Early life diets with prebiotics and bioactive milk fractions attenuate the impact of stress on learned helplessness behaviours and alter gene expression within neural circuits important for stress resistance. *The European journal of neuroscience* **45,** 342-357.

Mody P, Rukhadze I & Kubin L. (2011). Rats subjected to chronic-intermittent hypoxia have increased density of noradrenergic terminals in the trigeminal sensory and motor nuclei. *Neuroscience letters* **505,** 176-179.

Moraes DJ, da Silva MP, Bonagamba LG, Mecawi AS, Zoccal DB, Antunes-Rodrigues J, Varanda WA & Machado BH. (2013). Electrophysiological properties of rostral ventrolateral medulla presympathetic neurons modulated by the respiratory network in rats. *The Journal of neuroscience : the official journal of the Society for Neuroscience* **33,** 19223-19237.

Moreno-Indias I, Torres M, Montserrat JM, Sanchez-Alcoholado L, Cardona F, Tinahones FJ, Gozal D, Poroyko VA, Navajas D, Queipo-Ortuno MI & Farre R. (2015). Intermittent hypoxia alters gut microbiota diversity in a mouse model of sleep apnoea. *The European respiratory journal* **45,** 1055-1065.

Moreno-Indias I, Torres M, Sanchez-Alcoholado L, Cardona F, Almendros I, Gozal D, Montserrat JM, Queipo-Ortuno MI & Farre R. (2016). Normoxic Recovery Mimicking Treatment of Sleep Apnea Does Not Reverse Intermittent Hypoxia-Induced Bacterial Dysbiosis and Low-Grade Endotoxemia in Mice. *Sleep* **39,** 1891-1897.

Nohr MK, Egerod KL, Christiansen SH, Gille A, Offermanns S, Schwartz TW & Moller M. (2015). Expression of the short chain fatty acid receptor GPR41/FFAR3 in autonomic and somatic sensory ganglia. *Neuroscience* **290,** 126-137.

Nsegbe E, Wallen-Mackenzie A, Dauger S, Roux JC, Shvarev Y, Lagercrantz H, Perlmann T & Herlenius E. (2004). Congenital hypoventilation and impaired hypoxic response in Nurr1 mutant mice. *The Journal of physiology* **556,** 43-59.

O'Connor KM, Lucking EF, Golubeva AV, Strain CR, Fouhy F, Cenit MC, Dhaliwal P, Bastiaanssen TFS, Burns DP, Stanton C, Clarke G, Cryan JF & O'Halloran KD. (2019). Manipulation of gut microbiota blunts the ventilatory response to hypercapnia in adult rats. *EBioMedicine*.

O'Halloran KD. (2016). Chronic intermittent hypoxia creates the perfect storm with calamitous consequences for respiratory control. *Respiratory physiology & neurobiology* **226,** 63-67.

O'Neill J, Jasionek G, Drummond SE, Brett O, Lucking EF, Abdulla MA & O'Halloran KD. (2019). Renal cortical oxygen tension is decreased following exposure to long-term but not short-term intermittent hypoxia in the rat. *American journal of physiology Renal physiology* **316,** F635-f645.

Oliveira LM, Oliveira MA, Moriya HT, Moreira TS & Takakura AC. (2019). Respiratory disturbances in a mouse model of Parkinson's disease. *Experimental physiology* **104,** 729-739.

Parnell JA & Reimer RA. (2009). Weight loss during oligofructose supplementation is associated with decreased ghrelin and increased peptide YY in overweight and obese adults. *The American journal of clinical nutrition* **89,** 1751-1759.

Parnell JA & Reimer RA. (2012). Prebiotic fibres dose-dependently increase satiety hormones and alter Bacteroidetes and Firmicutes in lean and obese JCR:LA-cp rats. *The British journal of nutrition* **107,** 601-613.

Peng YJ, Nanduri J, Khan SA, Yuan G, Wang N, Kinsman B, Vaddi DR, Kumar GK, Garcia JA, Semenza GL & Prabhakar NR. (2011). Hypoxia-inducible factor 2alpha (HIF-2alpha) heterozygous-null mice exhibit exaggerated carotid body sensitivity to hypoxia, breathing instability, and hypertension. *Proceedings of the National Academy of Sciences of the United States of America* **108,** 3065-3070.

Peng YJ, Yuan G, Khan S, Nanduri J, Makarenko VV, Reddy VD, Vasavda C, Kumar GK, Semenza GL & Prabhakar NR. (2014). Regulation of hypoxia-inducible factor-alpha isoforms and redox state by carotid body neural activity in rats. *The Journal of physiology* **592,** 3841-3858.

Philippi NR, Bird CE, Marcus NJ, Olson EB, Chesler NC & Morgan BJ. (2010). Time course of intermittent hypoxia-induced impairments in resistance artery structure and function. *Respiratory physiology & neurobiology* **170,** 157-163.

Pluznick J. (2014). A novel SCFA receptor, the microbiota, and blood pressure regulation. *Gut microbes* **5,** 202-207.

Pluznick JL. (2013). Renal and cardiovascular sensory receptors and blood pressure regulation. *American journal of physiology Renal physiology* **305,** F439-444.

Pluznick JL, Protzko RJ, Gevorgyan H, Peterlin Z, Sipos A, Han J, Brunet I, Wan LX, Rey F, Wang T, Firestein SJ, Yanagisawa M, Gordon JI, Eichmann A, Peti-Peterdi J & Caplan MJ. (2013). Olfactory receptor responding to gut microbiota-derived signals plays a role in renin secretion and blood pressure regulation. *Proceedings of the National Academy of Sciences of the United States of America* **110,** 4410-4415.

Potts JT, Paton JF, Mitchell JH, Garry MG, Kline G, Anguelov PT & Lee SM. (2003). Contraction-sensitive skeletal muscle afferents inhibit arterial baroreceptor signalling in the nucleus of the solitary tract: role of intrinsic GABA interneurons. *Neuroscience* **119,** 201-214.

Prabhakar NR & Peng YJ. (2004). Peripheral chemoreceptors in health and disease. *Journal of applied physiology (Bethesda, Md : 1985)* **96,** 359-366.

Prabhakar NR, Peng YJ, Kumar GK & Pawar A. (2007). Altered carotid body function by intermittent hypoxia in neonates and adults: relevance to recurrent apneas. *Respiratory physiology & neurobiology* **157,** 148-153.

Ramirez JM. (2014). The integrative role of the sigh in psychology, physiology, pathology, and neurobiology. *Progress in brain research* **209,** 91-129.

Raybould HE, Glatzle J, Robin C, Meyer JH, Phan T, Wong H & Sternini C. (2003). Expression of 5-HT3 receptors by extrinsic duodenal afferents contribute to intestinal inhibition of gastric emptying. *American journal of physiology Gastrointestinal and liver physiology* **284,** G367-372.

Reeves SR & Gozal D. (2006). Changes in ventilatory adaptations associated with long-term intermittent hypoxia across the age spectrum in the rat. *Respiratory physiology & neurobiology* **150,** 135-143.

Santisteban MM, Qi Y, Zubcevic J, Kim S, Yang T, Shenoy V, Cole-Jeffrey CT, Lobaton GO, Stewart DC, Rubiano A, Simmons CS, Garcia-Pereira F, Johnson RD, Pepine CJ & Raizada MK. (2017). Hypertension-Linked Pathophysiological Alterations in the Gut. *Circulation research* **120,** 312-323.

Savignac HM, Corona G, Mills H, Chen L, Spencer JP, Tzortzis G & Burnet PW. (2013). Prebiotic feeding elevates central brain derived neurotrophic factor, N-methyl-D-aspartate receptor subunits and D-serine. *Neurochemistry international* **63,** 756-764.

Savignac HM, Couch Y, Stratford M, Bannerman DM, Tzortzis G, Anthony DC & Burnet PWJ. (2016). Prebiotic administration normalizes lipopolysaccharide (LPS)-induced anxiety and cortical 5-HT2A receptor and IL1-beta levels in male mice. *Brain, behavior, and immunity* **52,** 120-131.

Sims IM, Ryan JL & Kim SH. (2014). In vitro fermentation of prebiotic oligosaccharides by Bifidobacterium lactis HN019 and Lactobacillus spp. *Anaerobe* **25,** 11-17.

Souza GM, Bonagamba LG, Amorim MR, Moraes DJ & Machado BH. (2015). Cardiovascular and respiratory responses to chronic intermittent hypoxia in adult female rats. *Experimental physiology* **100,** 249-258.

Strandwitz P, Kim KH, Terekhova D, Liu JK, Sharma A, Levering J, McDonald D, Dietrich D, Ramadhar TR, Lekbua A, Mroue N, Liston C, Stewart EJ, Dubin MJ, Zengler K, Knight R, Gilbert JA, Clardy J & Lewis K. (2019). GABA-modulating bacteria of the human gut microbiota. *Nature microbiology* **4,** 396-403.

Tan W, Janczewski WA, Yang P, Shao XM, Callaway EM & Feldman JL. (2008). Silencing preBotzinger complex somatostatin-expressing neurons induces persistent apnea in awake rat. *Nature neuroscience* **11,** 538-540.

Teixeira AL, Fernandes IA & Vianna LC. (2019). GABAA receptors modulate sympathetic vasomotor outflow and the pressor response to skeletal muscle metaboreflex activation in humans. *The Journal of physiology*.

Toral M, Robles-Vera I, de la Visitacion N, Romero M, Yang T, Sanchez M, Gomez-Guzman M, Jimenez R, Raizada MK & Duarte J. (2019). Critical Role of the Interaction Gut Microbiota - Sympathetic Nervous System in the Regulation of Blood Pressure. *Frontiers in physiology* **10,** 231.

Veasey SC, Zhan G, Fenik P & Pratico D. (2004). Long-term intermittent hypoxia: reduced excitatory hypoglossal nerve output. *Am J Respir Crit Care Med* **170,** 665-672.

Wu J, Sun X, Wu Q, Li H, Li L, Feng J, Zhang S, Xu L, Li K, Li X, Wang X & Chen H. (2016). Disrupted intestinal structure in a rat model of intermittent hypoxia. *Molecular medicine reports* **13,** 4407-4413.

Yamamoto K, Eubank W, Franzke M & Mifflin S. (2013). Resetting of the sympathetic baroreflex is associated with the onset of hypertension during chronic intermittent hypoxia. *Autonomic neuroscience : basic & clinical* **173,** 22-27.

Yan Q, Gu Y, Li X, Yang W, Jia L, Chen C, Han X, Huang Y, Zhao L, Li P, Fang Z, Zhou J, Guan X, Ding Y, Wang S, Khan M, Xin Y, Li S & Ma Y. (2017). Alterations of the Gut Microbiome in Hypertension. *Frontiers in cellular and infection microbiology* **7,** 381.

Yang T, Santisteban MM, Rodriguez V, Li E, Ahmari N, Carvajal JM, Zadeh M, Gong M, Qi Y, Zubcevic J, Sahay B, Pepine CJ, Raizada MK & Mohamadzadeh M. (2015). Gut dysbiosis is linked to hypertension. *Hypertension (Dallas, Tex : 1979)* **65,** 1331-1340.

Young JO, Geurts A, Hodges MR & Cummings KJ. (2017). Active sleep unmasks apnea and delayed arousal in infant rat pups lacking central serotonin. *J Appl Physiol (1985)* **123,** 825-834.

Zanella S, Doi A, Garcia AJ, 3rd, Elsen F, Kirsch S, Wei AD & Ramirez JM. (2014). When norepinephrine becomes a driver of breathing irregularities: how intermittent hypoxia fundamentally alters the modulatory response of the respiratory network. *The Journal of neuroscience : the official journal of the Society for Neuroscience* **34,** 36-50.

Zhou T, Chien MS, Kaleem S & Matsunami H. (2016). Single cell transcriptome analysis of mouse carotid body glomus cells. *The Journal of physiology* **594,** 4225-4251.

Zoccal DB, Bonagamba LG, Antunes-Rodrigues J & Machado BH. (2007). Plasma corticosterone levels is elevated in rats submitted to chronic intermittent hypoxia. *Autonomic neuroscience : basic & clinical* **134,** 115-117.

Zoccal DB, Simms AE, Bonagamba LG, Braga VA, Pickering AE, Paton JF & Machado BH. (2008). Increased sympathetic outflow in juvenile rats submitted to chronic intermittent hypoxia correlates with enhanced expiratory activity. *The Journal of physiology* **586,** 3253-3265.

Chapter 5. Discussion - The microbiota-gut-brain axis in the control of breathing and cardiovascular function

Abstract

Microbes that inhabit the gut form a diverse and complex ecosystem. Microbiota-gut-brain axis signalling has recently been linked with whole body function in both health and disease. Dysregulated microbiota-gut-brain axis communication affects an array of homeostatic functions of neurocontrol networks; consequently, myriad maladies of brain behaviours and integrative body systems manifest. Our group and others have extended this line of enquiry to investigate how microbiota-gut-brain axis signalling influences cardiorespiratory and autonomic control. We have previously described altered respiratory control and perturbed gut microbiota in rat offspring of a prenatal stress model. Furthermore, multiple studies have demonstrated that the gut microbiota impacts blood pressure control. Herein, we review recent work by our group exploring the potential for the gut microbiota to shape cardiorespiratory homeostasis. We performed a comprehensive assessment of cardiorespiratory physiology in animal models of modified gut microbiota, and sleep-disordered breathing with altered gut microbiota. We describe findings from our studies revealing that the gut microbiota contributes to the control of breathing and cardiovascular function. Our work highlights the potential relevance of the gut microbiota in human cardiorespiratory diseases such as obstructive sleep apnoea. We explore possible mechanisms of microbiota-gut-brain axis signalling that appear to play a modulatory role in cardiorespiratory control. Manipulation of the gut microbiota may be a promising approach as an adjunctive therapy in the treatment of cardiorespiratory disorders.

Keywords: Cardiorespiratory control; chronic intermittent hypoxia; microbiota manipulation; microbiota-gut-brain axis; neurochemistry; cardiorespiratory disease

Abbreviations: ABX, antibiotic administration; CIH, chronic intermittent hypoxia; FMT, faecal microbiota transfer; HFD, high-fat diet; HSD, high-salt diet; LPS, lipopolysaccharides; OSA, obstructive sleep apnoea; SCFA, short-chain fatty acids; SDB, sleep disordered breathing

5.1. Gut microbiota

Bacteria, fungi, viruses, archaea and parasites residing within the gut, form a dynamic and extensive microbial ecosystem termed the gut microbiota. Interestingly, the bacteria within the gut combine to occupy a ratio of 1:1 with host cells (Sender *et al.*, 2016). Early life factors, including delivery mode, gestational age at birth, method of feeding and early life stress have profound impact on the formation of the gut microbiome; each individual inherits a distinct gut microbiota profile (Penders *et al.*, 2006; O'Mahony *et al.*, 2009; Dunphy-Doherty *et al.*, 2018; Fouhy *et al.*, 2019). Furthermore, factors including diet, lifestyle and medication, amongst others orchestrate the continuous evolution of the gut microbiome throughout life. Broad inter-individual differences occur (Del Chierico *et al.*, 2014; Panda *et al.*, 2014; Murphy *et al.*, 2015; De Filippis *et al.*, 2016). Over the last number of years, several studies have revealed that the gut microbiota is associated with brain behaviours and whole-body homeostasis in both health and disease. The gut microbiota communicates with the brain *via* a bidirectional signalling pathway termed the microbiota-gut-brain axis. Dysregulated signalling of this multifaceted axis affects major homoeostatic neurocontrol systems promoting pathophysiological phenotypes (O'Mahony *et al.*, 2014; Desbonnet *et al.*, 2015; Hoban *et al.*, 2016; Kelly *et al.*, 2016b; Adnan *et al.*, 2017; Burokas *et al.*, 2017; Golubeva *et al.*, 2017; Li *et al.*, 2017). Studies in our laboratory and others have recently extended this research to other critically important homeostatic systems including the cardiorespiratory control network (Golubeva *et al.*, 2015; Durgan *et al.*, 2016; Santisteban *et al.*, 2017; Ganesh *et al.*, 2018; Lucking *et al.*, 2018b; O'Connor *et al.*, 2019a).

5.2. Cardiorespiratory control

The cardiorespiratory control system is composed of sensors (peripheral and central), central control regions determining rhythm and pattern and effector motor nerves and autonomic pathways. This network is an intricate homeostatic system providing regulatory mechanisms to maintain adequate blood oxygenation to meet whole-body metabolic requirements. The regulatory web of neuronal networks predominantly located in the brainstem is critical in the integration of sensory cues from the periphery as well as modulation of appropriate cardiorespiratory reflex responses. The brainstem (pons and medulla oblongata) also receives sensory traffic from the vagus nerve, a key signalling pathway of the microbiota-gut-brain axis. Notwithstanding the homeostatic capacity of the control network, adaptive and maladaptive plasticity may develop within the cardiorespiratory control circuitry, both at the central and peripheral level (Bavis, 2005; Peng *et al.*, 2009; Edge *et al.*, 2010; Joseph *et al.*, 2013; Fuller & Mitchell, 2017; Lucking *et al.*, 2018b). Maladaptive plasticity results in unfavourable outcomes for cardiorespiratory control and has adverse consequences for whole-body function, for example, breathing instability and the establishment of hypertension (Julien *et al.*, 2008; Fournier *et al.*, 2013a; Joseph *et al.*, 2013; Kinkead *et al.*, 2013; Golubeva *et al.*, 2015; Soliz *et al.*, 2016; O'Connor *et al.*, 2019a).

5.3. The gut microbiota, cardiorespiratory and autonomic control

Elaborate mechanisms of respiratory and blood pressure regulation are slowly being unravelled. Recently, investigations conducted by our group and others have proposed that the gut microbiota appears to play an important modulatory role in cardiorespiratory and autonomic control (Santisteban *et al.*, 2017; Kim *et al.*, 2018; Lucking *et al.*, 2018b; Marques *et al.*, 2018; O'Connor *et al.*, 2019a). Several studies using models that manipulate the gut microbiota, including faecal microbiota transplant strategies, antibiotic administration and probiotics, demonstrate substantial interplay between the gut microbiota and blood pressure homeostasis (Ganesh *et al.*, 2018; Lucking *et al.*, 2018b; Marques *et al.*, 2018; Toral *et al.*, 2019). Moreover, perturbed gut microbiota composition and diversity, specifically elevated Firmicutes:Bacteroidetes ratio, and decreased microbial richness and evenness has been associated with hypertension in multiple animal models (Durgan *et al.*, 2016; Adnan *et al.*, 2017; Santisteban *et al.*, 2017; Toral *et al.*, 2019). Recently, it was reported that the gut microbiota and/or gut microbiota metabolites function in autonomic control of the heart (Kim *et al.*, 2018). Additionally, our laboratory has previously described that pre-natal stress disturbs the gut microbiota composition in rat offspring with associated effects on respiratory control, resulting in elevated variability of breathing frequency during normoxia and altered ventilatory responsiveness to hypoxic and hypercapnic chemostimulation. Intriguingly, breathing frequency responsiveness to hypercapnia positively correlated with *Anaerotruncus* and *Oscillibacter* genera and enhanced variability of breathing frequency during normoxia correlated with *Mucispirillum* and *Papillibacter* (Golubeva *et al.,* 2015). Moreno-Indias *et al.*, (2015, 2016) demonstrated that respiratory dysregulation and alterations to the gut microbiota structure develop in an animal model of intermittent hypoxia. Beyond these studies, to our knowledge there are no other reports investigating the potential regulatory role of the gut microbiota on the control of breathing. We performed the first comprehensive assessment of respiratory control and cardiovascular function in animal models of manipulated gut microbiota, and sleep-disordered breathing with altered gut microbiota.

5.4. Respiratory control in animal models of manipulated gut microbiota

In O'Connor *et al.* (2019a), two methods were utilised to manipulate the gut microbiota. Adult male rats were treated with broad spectrum antibiotics (ABX) designed to deplete the gut microbiota. Additionally, rats received a faecal microbiota transfer (FMT) of pooled sham faeces in an attempt to reverse gut microbiota disruptions after antibiotic administration. However, this FMT strategy did not normalise the gut microbiota profile; instead, a second model of perturbed gut microbiota was created with a unique gut microbiota composition and increased gut microbiota diversity. Similarly, unfavourable disturbances to the gut microbiota from a FMT intervention were also evident in a clinical study wherein FMT to irritable bowel syndrome patients led to the proliferation of a distinct gut microbiota assembly with no amelioration of symptoms (Halkjaer *et al.*, 2018).

Considering that deleterious respiratory behaviours are evident in adult rats with disrupted gut microbiota following antecedent pre-natal stress (Golubeva *et al.*, 2015), and that dysregulated microbiota-gut-brain axis signalling promotes the development of aberrant brain behaviours, such as anxiety, depression and altered learning and memory (Hoban *et al.*, 2016; Burokas *et al.*, 2017; Foster *et al.*, 2017), we aimed to investigate if the gut microbiota has a modulatory role in respiratory homeostasis. Using the technique of whole-body plethysmography, allowing the assessment of respiratory control and whole-body metabolism in unrestrained unanaesthetised animals, we observed aberrant respiratory phenotypes in response to chemostimulation in ABX and FMT rats during quiet rest, with no change evident during baseline normoxic breathing. Normal ventilation during normoxia indicates a remarkably capacity for the maintenance of respiratory homeostasis within the control network. Furthermore, we presented evidence that ABX and FMT rats had depressed respiratory frequency and minute ventilation during the initial (peak) hypoxic ventilatory response (O'Connor *et al.*, 2019a), similar to the blunted hypoxic ventilatory response evident in adult rats exposed to pre-natal stress (Golubeva *et al.*, 2015). These studies suggest that refined integration of chemosensory cues from the dominant peripheral oxygen sensors, the carotid bodies, develop due to a disrupted gut microbiota signature. Although the initial hypoxic ventilatory responses were depressed in ABX and FMT rats (O'Connor *et al.*, 2019a), the phase 2 steady-state response to hypoxia remained unchanged, further displaying the ability of the network to preserve respiratory homeostasis.

The major and most intriguing finding of chapter 2 was that ABX and FMT rats have depressed ventilatory responsiveness to hypercapnia, revealing that modifications to the gut

microbiota are associated with blunted chemoreflex control of breathing in response to hypercapnia. This striking observation is physiologically significant as systemic acidosis may present during periods of elevated carbon dioxide concentrations. Hypercapnia is sensed by central chemoreceptors residing in the brainstem. Therefore, we assessed brainstem monoamine and monoamine metabolite concentrations in brainstem homogenates from ABX and FMT rats, as altered brain neurochemistry is evident in various models of disrupted gut microbiota (Clarke *et al.*, 2013; Desbonnet *et al.*, 2015; Hoban *et al.*, 2016). High-performance liquid chromatography revealed that brainstem neuromodulators specifically relating to the dopaminergic pathway were modified in ABX and FMT groups. Notably, a number of bacterial genera, predominantly from the Firmicutes phylum correlated with brainstem neurochemistry, which in turn may be responsible for the perturbed chemoreflex control of breathing evident in ABX and FMT rats. Using two different models of perturbed gut microbiota (O'Connor *et al.*, 2019a) our study suggests that dysregulated microbiota-gut-brain axis signalling culminates in deleterious outcomes for respiratory control and brainstem neurochemistry, extending previous work by our group linking the gut microbiota to respiratory control (Golubeva *et al*, 2015).

Dysregulated intestinal permeability has been associated with systemic inflammation and the transfer of bacterial metabolites such as lipopolysaccharides (LPS) into the periphery (Araujo *et al.*, 2017). Intestinal barrier dysfunction frequently occurs in models of perturbed gut microbiota, such as rodent models of maternal separation stress, hypertension and antibiotic administration (Gareau *et al.*, 2007; Tulstrup *et al.*, 2015; Ganesh *et al.*, 2018; Kim *et al.*, 2018). Consistent with these observations, ABX and FMT rats had a 'leaky' distal ileum, but not colon. It is conceivable to suggest that disrupted intestinal integrity contributed to altered brain neurochemistry and in turn the aberrant respiratory control in ABX and FMT rats. Considering the dominant role of the vagus nerve in the gut-brain axis, it presents as a potential player in the establishment and progression of cardiorespiratory disturbances evident in the ABX and FMT rats. Interestingly, no notable differences in cardiorespiratory responses to pulmonary vagal C-fibre stimulation were evident between groups, however, vagal afferent stimulation from other peripheral sites such as the gut were not examined in our study (O'Connor *et al.*, 2019a). In summary, perturbation to the gut microbiota is associated with altered respiratory control evident in response to chemosensory stimulation. Mismatches in ventilation and metabolism have consequences for acid-base balance with potential consequences for whole-body systems. Our novel findings have revealed a link

between gut microbiota and neural control of breathing with potential implications for a variety of respiratory control disorders across the lifespan.

5.5. Cardiorespiratory and autonomic control in animal models sleep-disordered breathing

In an endeavour to determine if beneficial manipulation of the gut microbiota has viable application as adjunctive therapy for human cardiorespiratory disease, studies investigating microbiota-gut-brain axis signalling in animal models are required. In CIH-exposed rodents, modelling human sleep apnoea, the influence of CIH exposure on the gut microbiota and resultant effects on cardiorespiratory physiology are complicated by CIH-induced carotid body sensitisation and resultant alterations in autonomic control. Carotid body chemoreceptors are proposed to be critical in the development of numerous CIH-induced cardiorespiratory morbidities, including hypertension and elevated hypoxic ventilatory responses (Huang *et al.*, 2009; Peng *et al.*, 2009; Del Rio *et al.*, 2016; Iturriaga *et al.*, 2017). Moreover, autonomic imbalance disrupts the gut microbiota (Kelly *et al.*, 2015; Santisteban *et al.*, 2017; Toral *et al.*, 2019), which could establish a feed-forward cycle of disability. In chapter 3, Lucking *et al*. (2018), we explored the effects of CIH exposure on gut microbiota and cardiorespiratory control in guinea-pigs, a rodent with hypoxia-insensitive carotid bodies. Using a CIH paradigm that evokes hypertension in rats, we reasoned that if cardiorespiratory impairments presented in CIH-exposed guinea-pigs in the absence of carotid body sensitisation, then peripheral structures other than the carotid bodies are potential contributors to development of CIH-induced morbidities.

CIH-exposed guinea-pigs displayed lower respiratory variability in concert with reduced frequency of sighs and central apnoeas assessed by whole body plethysmography. In the light of these adverse respiratory behaviours, we measured brainstem neuromodulators involved in the control of breathing. High-performance liquid chromatography revealed decreased concentrations of noradrenaline in the pons and medulla oblongata. Lower brainstem noradrenaline concentrations and reduced apnoea/sigh frequency are congruent observations, considering that noradrenaline promotes respiratory instabilities in mice exposed to IH (Zanella *et al.*, 2014) and elevated central noradrenergic terminals are noted in CIH-exposed rats (Mody *et al.*, 2011), that have increased propensity for generation of apnoea (Edge *et al.*, 2012). CIH exposure in guinea-pigs did not induce hypertension, but tachycardia was evident together with impaired baroreflex responsiveness. Work by another group convincingly demonstrated that exposure to an extended duration of CIH in guinea-pigs manifested in the establishment of hypertension and tachycardia, without carotid body sensitisation (Docio *et al.*, 2018). These observations illustrate that peripheral sites other than the carotid bodies contribute to cardiorespiratory and autonomic impairments

following exposure to CIH (Docio *et al.*, 2018; Lucking *et al.*, 2018b; AlMarabeh *et al.*, 2019; O'Connor *et al.*, 2019b).

16S rRNA sequencing revealed for the first time that CIH-exposed guinea-pigs exhibit altered gut microbiota composition and diversity, in the likely absence of carotid body sensitisation and elevated sympathetic nervous system activity (Lucking *et al*. 2018), consistent with observations in other CIH-exposed animal models (Moreno-Indias *et al.,* 2015; Moreno-Indias *et al.,* 2016; O'Connor *et al.,* chapter 4). It is conceivable that dysregulated microbiota-gut-brain axis signalling may have culminated in aberrant autonomic control of the heart, undesirable respiratory phenotypes and reduced noradrenaline concentrations. This is particularly intriguing in light of the evidence that ABX and FMT rats exhibit respiratory control deficits and altered brainstem neurochemistry (O'Connor *et al.*, 2019a). Butyrate, which is a metabolite of the gut microbiota, modified the gut microbiota, reduced blood pressure and normalised baroreflex activity and cardiac autonomic control in a hypertensive mouse model with perturbed gut microbiota (Kim *et al.*, 2018). Considering that dysregulated autonomic control occurs in CIH-exposed guinea-pig with altered gut microbiota (Docio *et al.*, 2018; Lucking *et al.*, 2018b) our study further supports these findings, which implicate disruption to the gut microbiota as a causal factor in the development of cardiovascular and autonomic dysfunction.

Given that manipulation of the gut microbiota *via* ABX and FMT perturbed the gut microbiota and altered respiratory behaviours and brainstem neurochemistry (O'Connor *et al.*, 2019a) and that CIH-exposed guinea-pigs, modelling human sleep apnoea, have a disturbed gut microbiota as well as perturbed respiratory and autonomic control (Lucking *et al.*, 2018b), it is reasonable to postulate that beneficial manipulation of the gut microbiota may have potential application as an adjunctive treatment in human cardiorespiratory disease. In chapter 4, we explored cardiorespiratory control and gut microbiota structure in rats exposed to CIH. We investigated if prebiotic supplementation, designed to promote the expansion of beneficial microbes, is effective in the prevention of CIH-induced cardiorespiratory dysfunctions.

Plethysmography studies revealed that CIH exposure in rats triggered an increased propensity for the generation of apnoeas during normoxia. Prebiotic administration did not prevent CIH-induced increases in apnoea index but increased chemoreflex control of breathing in response to hypercapnia and hypoxic hypercapnia. We assessed neuromodulator concentrations key in respiratory control in pontine and medulla oblongata

homogenates. High-performance liquid chromatography revealed that CIH exposure did not affect brainstem neurochemistry, whereas prebiotic administration altered monoamine precursor and metabolite concentrations in sham animals, notably $_{L}$-3,4-dihydroxyphenylalanine, homovanillic acid and 5-hydroindoleacetic acid. We confirmed also that CIH exposure did not increase pro-inflammatory brainstem cytokine concentrations, with the concentrations of IL-10 and IL-5 decreased in CIH-exposed rats. Oxidative stress and/or other brainstem neuromodulators not examined in our study (Tryba *et al.*, 2008; Garcia *et al.*, 2016), or effects at the level of the carotid body (Donovan *et al.*, 2014), could underpin aberrant CIH-related respiratory behaviours.

CIH exposure led to the development of hypertension and increased cardiac sympathetic tone in the anesthetised rat, which have previously been described (Zoccal *et al.*, 2007b; Lucking *et al.*, 2014; Peng *et al.*, 2014b; Del Rio *et al.*, 2016; Laouafa *et al.*, 2017; Laouafa *et al.*, 2019). Prebiotic administration did not prevent adverse cardiovascular and autonomic control in CIH-exposed rats (O'Connor *et al*. chapter 4). Our findings are interesting in the context of previous observations wherein prebiotic (Hylon VII) administration normalised caecal acetate concentrations, increased levels of short-chain fatty acid (SCFA) producing bacteria and prevented the development of hypertension in an obstructive sleep apnoea + high-fat diet fed (OSA+HFD) rat model. Additionally, chronic acetate administration in rat caecum during exposure to OSA+HFD restored caecal acetate concentrations and prevented hypertension (Ganesh *et al.*, 2018). Furthermore, propionate and acetate mitigated the development of hypertension in chronic angiotensin II-induced and mineralocorticoid excess-induced hypertensive rodent models (Marques *et al.*, 2017; Kim *et al.*, 2018; Bartolomaeus *et al.*, 2019). Prebiotic administration increased faecal acetic and propanoic acid concentrations in sham and CIH-exposed rats (O'Connor *et al.* chapter 4), but CIH exposure had no effect on SCFA concentrations, which clearly demonstrates that diminished SCFA concentrations are not essential to the development of cardiovascular pathologies, including hypertension in our model.

We observed for the first time, using whole-metagenome shotgun sequencing, that CIH exposure affects gut bacterial species. Specifically, the abundance of *Lactobacillus rhamnosus*, a commensal bacterial species, was diminished in CIH-exposed rats compared with sham rats. Interestingly, prebiotic administration did not restore *Lactobacillus rhamnosus* abundance in CIH-exposed rats. *Lactobacillus rhamnosus* administration prevented CIH+HSD-induced hypertension in rats (Liu *et al.*, 2019), suggesting that decreased abundance of L*actobacillus rhamnosus* evident in CIH-exposed rats may underpin the

establishment of hypertension. We advance this hypothesis with caution as *Lactobacillus rhamnosus* abundance was also decreased in sham animals treated with prebiotics, most likely because this bacterial species cannot consume galactooligossacharides and fructooligosaccharides, the prebiotic combination used in our study (Chapter 4); yet these animals were normotensive, which argues against a pivotal role for *Lactobacillus rhamnosus* in the control of blood pressure. Furthermore, there was increased abundance of a number of pathogenic species and a trend towards reduced abundance of several other *Lactobacillus* species in CIH-exposed rats. Multiple bacterial species correlated with blood pressure, suggesting that a complex interplay of changes in commensal and pathogenic species abundance may create a distinct microbiota signature that contributes to blood pressure regulation *per se* and/or drives a hypertensive phenotype following CIH exposure.

CIH exposure affects gut barrier function, resulting in gut inflammation, increased plasma oxidative stress and LPS concentrations as well as decreased tight junction receptor expression (Moreno-Indias *et al.*, 2015; Wu *et al.*, 2016), maladies which are often evident in hypertensive animal models (Santisteban *et al.*, 2017; Kim *et al.*, 2018). Although we did not examine intestinal function in our study, plasma inflammatory mediators were not affected by CIH exposure implying that gut barrier integrity was maintained. Hence, we conclude that intestinal dysfunction did not contribute to the development of CIH-induced cardiorespiratory dysfunction in our study. Notably, prebiotic administration reduced hypertension and prevented epithelial goblet cell loss and mucus barrier thinning, which were evident in OSA+HFD rats (Ganesh *et al.*, 2018). Considering the pivotal role of the vagus nerve in cardiorespiratory control and microbiota-gut-brain axis signalling we assessed cardiorespiratory responsiveness to pulmonary vagal C-fibre activation. No significant differences were evident between groups. It would be interesting to explore vagal afferent signalling from other peripheral sites, especially the gut. In summary, prebiotic fibre administration did not normalise *Lactobacillus rhamnosus* relative abundance or prevent major cardiorespiratory maladies in CIH-exposed rats. Correlation analysis revealed significant associations between blood pressure and several commensal and pathogenic bacterial species suggesting that a specific microbiota signature may at least partly contribute to the establishment of hypertension shaping maladaptive plasticity within neural control networks that underpin cardiorespiratory pathologies in CIH-exposed rats. It is interesting to speculate that a microbiota-gut-carotid body axis exists, but this warrants further investigation. Our findings add to emerging studies investigating the regulatory role of the gut microbiota in animal models of OSA.

5.6. Potential mechanisms linking cardiorespiratory and autonomic dysfunction to the gut microbiota

A number of intricate mechanisms are proposed as communication pathways of the microbiota-gut-brain axis. The vagus nerve is argued to be the primary signalling pathway. Studies in animals report that vagal afferent fibres respond to multiple stimuli within the gut, such as cytokines and gut bacterial metabolites including SCFAs (Johnston & Webster, 2009; Nohr *et al.*, 2015). Administration of probiotic species, *Lactobacillus rhamnosus* and *Bifidobacterium longum,* which reverse and ameliorate intestinal epithelial barrier dysfunction, respectively (West *et al.*, 2017; Chen *et al.*, 2019; Liu *et al.*, 2019), alter neuromodulators and neuronal activity in multiple brain regions and modify anxiety-related brain behaviours; these effects are abolished in vagotomised rodents (Bercik *et al.*, 2011b; Bravo *et al.*, 2011). Considering the governing role of the vagus nerve, it presents as a potential mechanism linking adverse cardiorespiratory and autonomic dysfunction to a disturbed gut microbiota. Vagotomy studies are required to investigate if microbiota-gut brain axis signalling *via* the vagus nerve has a modulatory role in the control of breathing and cardiovascular function.

ABX and FMT rats had disrupted gut microbiota, elevated intestinal permeability and altered respiratory control (O'Connor *et al.*, 2019a). CIH-exposed rats developed cardiorespiratory and autonomic impairments and altered gut microbiota, but did not present with systemic inflammation. Prebiotic administration did not prevent CIH-induced cardiorespiratory and autonomic dysfunction (chapter 4). The latter observation is in contrast to previous studies wherein prebiotic (Hylon VII), probiotic (*Clostridium butyricum*) and SCFA administration independently ameliorate gut barrier function and prevent/restore cardiovascular and autonomic maladies in OSA and hypertensive animal models (Ganesh *et al.*, 2018; Kim *et al.*, 2018; Liu *et al.*, 2019). Gut microbiota and metabolites are associated with gut intestinal homeostasis (Macfarlane & Macfarlane, 2012; Ganesh *et al.*, 2018; Kim *et al.*, 2018). Elevated levels of pathogenic species encourage gut barrier inflammation and intestinal damage (Riegler *et al.*, 1995; Bucker *et al.*, 2018). Beneficial bacterial species and SCFAs protect against gut dysfunction (Ganesh *et al.*, 2018; Kim *et al.*, 2018). It is plausible to suggest that increased intestinal barrier permeability by whatever means, including perturbed gut microbiota and autonomic dysfunction may compromise cardiorespiratory homoeostasis and accommodate the development of pathologies. A complex interplay of microbiota-gut-brain axis signalling mechanisms may play a regulatory role in cardiorespiratory and autonomic control (Fig. 5.1).

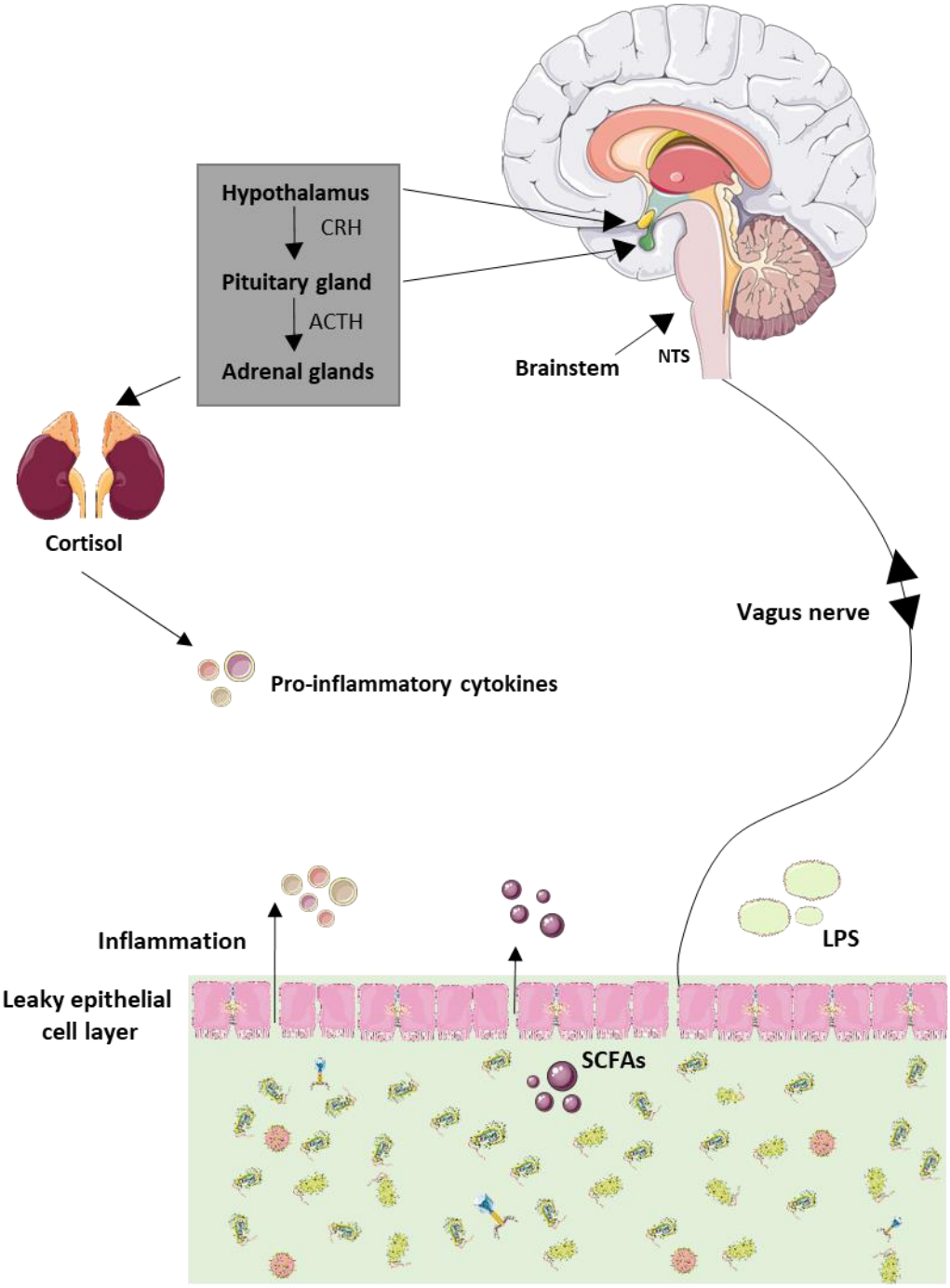


Figure 5. 1 Potential mechanisms linking aberrant cardiorespiratory and autonomic control to the gut microbiota.

Vagal signalling and intestinal epithelial barrier dysfunction are proposed communication pathways associated with develop of adverse cardiorespiratory and autonomic control. ACTH, adrenocorticotrophic hormone; CRF, corticotropin-releasing factor; HPA axis; hypothalamic pituitary adrenal axis; LPS; lipopolysaccharides; NTS, nucleus tractus solitarius; SCFA, short-chain fatty acid. Cortisol and corticosterone are released from the adrenal medulla in humans and rodents, respectively.

5.7. Future studies

Whilst we performed a comprehensive assessment of cardiorespiratory control in models of altered gut microbiota (ABX, FMT, CIH and prebiotic supplementation), many unresolved questions remain. The FMT strategy utilised in chapter 2 perturbed the gut microbiota, blunted chemoreflex control of breathing, disrupted brainstem neurochemistry and elevated intestinal permeability in vehicle- and antibiotic-treated rats. We are currently examining alternative intervention strategies (prebiotic administration, faecal microbiota transfer and natural recolonization) to establish an optimum approach that restores a control-like microbiota. We aim to determine if re-establishment of the gut microbiota reverses aberrant respiratory phenotypes in antibiotic-treated animals.

Studies should be performed in rodents exposed to more severe CIH paradigms with variations in the frequency of cycles, intensity of hypoxia and/or duration of exposure with and without the influence of a dietary intervention. These investigations would add to emerging observations in animal models of obstructive sleep apnoea using a CIH stimulus in concert with high-fat diet/high-salt diet. Considering that hypertensive CIH-exposed rats have reduced *Lactobacillus rhamnosus* abundance, which is not restored by prebiotic supplementation, studies should be performed investigating the effects of *Lactobacillus rhamnosus* administration on cardiorespiratory control in CIH-exposed rodents.

Metagenomics and metabolomics approaches to explore the gut microbiome in animal models with aberrant cardiorespiratory phenotypes would be advantageous in an attempt to determine if a distinct gut microbiota-dependent metabolic signature drives adverse cardiorespiratory control. In the event that specific microbial taxa contribute to cardiorespiratory malaise or favour homeostasis, then targeting these particular species via probiotic or narrow-spectrum antibiotic administration could function as a corrective remedy in the treatment of human disease.

Studies assessing signalling mechanisms contributing to cardiorespiratory dysregulation in animal models of altered gut microbiota including models of SDB are required. Vagal-mediated communication between the gut microbes and the brain should be examined in our models. Manipulation of the gut microbiota in vagotomised animals would enhance our understanding of the role of microbiota-gut-brain axis signalling via the vagus nerve in cardiorespiratory control. SCFAs prevented hypertension and autonomic dysfunction in animal models of SDB and hypertension, respectively (Ganesh *et al.*, 2018), but contrastingly

elevated SCFA concentration did not attenuate hypertension in our study (chapter 4). It is important to further investigate the contributory roles of SCFAs in various animal models of perturbed cardiorespiratory control. Considering that antibiotic administration and faecal microbiota transfer elevated intestinal permeability (chapter 2) and CIH-exposed animals exhibit perturbed intestinal barrier function (Wu *et al.*, 2016), investigations establishing if altered intestinal permeability contributes to modified brain neurochemistry and cardiorespiratory morbidity are necessary.

The composition of the lung and airway microbiota in animal models of cardiorespiratory disorders as well as of targeted microbiota manipulations (ABX, FMT, probiotics, prebiotics or germ free rodents) should be characterised. At present there is a dearth of studies investigating gut, lung and airway microbiota composition and diversity in patients with cardiorespiratory diseases such as obstructive sleep apnoea and chronic obstructive pulmonary disease. These studies are necessary to advance therapeutic strategies for the treatment of human cardiorespiratory disorders. It is worthy to note that beneficial modulation of the gut microbiota via prebiotics, probiotic, FMT or targeted narrow-spectrum antibiotic administration may function as adjunctive therapy for human cardiorespiratory diseases, where a perturbed gut microbiota is evident.

5.8. Conclusion

The gut microbiota signals *via* an intricate bidirectional communication pathway termed the 'microbiota-gut-brain axis'. Perturbed microbiota-gut-brain axis signalling has detrimental consequences for homeostatic regulation of neurocontrol systems; an ever-expanding array of deleterious brain behaviours and disease states manifest. To date, dysregulated communication between the gut microbes and the brain has been associated with multiple maladies including but not exclusive to stress-related pathologies such as anxiety, depression and irritable bowel syndrome and neurodevelopmental disorders such as autism. Remarkably, our findings add to the emerging field exploring microbiota-gut-brain axis signalling in homeostatic systems, extending investigations to behaviours predominantly regulated by the brainstem (pons and medulla oblongata), specifically cardiorespiratory control. Manipulation of the gut microbiota, *via* ABX, FMT and prebiotic supplementation, indicates that modification of the gut microbiota has implications for chemoreflex control of breathing especially during hypercapnia, as well as brainstem neurochemistry and intestinal permeability. These findings have relevance for whole-body health as a blunted ventilatory response to hypercapnia has detrimental consequences for acid-base balance, increasing the possibility of developing respiratory acidosis. CIH exposure, modelling human sleep apnoea, in guinea-pigs leads to the development of respiratory and autonomic dysfunction and reduced brainstem noradrenaline, suggesting that sites beyond the carotid bodies have a contributory role in the development of adverse CIH-induced cardiorespiratory phenotypes. CIH-exposed guinea-pigs have an altered gut microbiota, emerging as a potential protagonist in the manifestation of CIH-induced cardiorespiratory dysfunctions. Moreover, CIH-exposed rats have diminished relative abundance of *Lactobacillus* species, increased relative abundance of several pathogenic species, elevated apnoea index, hypertension and cardiac autonomic imbalance. Prebiotic supplementation elevated SCFA concentrations, but did not restore *Lactobacillus rhamnosus* relative abundance or cardiorespiratory pathologies in CIH-exposed rats. Our findings suggest that a complex interplay of changes in commensal and pathogenic species abundance may at least partly contribute to the development of hypertension in CIH-exposed rodents shaping aberrant plasticity in neural control networks, but it is also plausible that cardiorespiratory dysfunction in CIH-exposed rats, at least in our model, is driven independently by maladaptive plasticity with the neural circuitry controlling breathing and blood pressure. Considering that aberrant microbiota-gut-brain axis signalling extends to homeostatic neural control systems which maintain adequate oxygen and acid-base balance, vital for whole-body health, findings from our studies suggest that

dysregulated microbiota-gut-brain axis signalling has the capacity to culminate in a flood of new maladies. Given that a disturbed gut microbiota is implicated in an ever-expanding portfolio of pathologies associated with neurocontrol networks, one can conclude that there is no safe harbour from aberrant microbiota-gut-brain axis signalling. At present, there are many unresolved questions pertaining to the interplay between the gut microbiota and cardiorespiratory and autonomic control. Additional research is required to understand the elaborate signalling mechanisms of the gut-brain axis. If this can be achieved, it may shape therapeutic strategies for the treatment of human cardiorespiratory disorders.

5.9. References

Adnan S, Nelson JW, Ajami NJ, Venna VR, Petrosino JF, Bryan RM, Jr. & Durgan DJ. (2017). Alterations in the gut microbiota can elicit hypertension in rats. *Physiological genomics* **49,** 96-104.

AlMarabeh S, Abdulla MH & O'Halloran KD. (2019). Is Aberrant Reno-Renal Reflex Control of Blood Pressure a Contributor to Chronic Intermittent Hypoxia-Induced Hypertension? *Frontiers in physiology* **10,** 465.

Araujo JR, Tomas J, Brenner C & Sansonetti PJ. (2017). Impact of high-fat diet on the intestinal microbiota and small intestinal physiology before and after the onset of obesity. *Biochimie* **141,** 97-106.

Bartolomaeus H, Balogh A, Yakoub M, Homann S, Marko L, Hoges S, Tsvetkov D, Krannich A, Wundersitz S, Avery EG, Haase N, Kraker K, Hering L, Maase M, Kusche-Vihrog K, Grandoch M, Fielitz J, Kempa S, Gollasch M, Zhumadilov Z, Kozhakhmetov S, Kushugulova A, Eckardt KU, Dechend R, Rump LC, Forslund SK, Muller DN, Stegbauer J & Wilck N. (2019). Short-Chain Fatty Acid Propionate Protects From Hypertensive Cardiovascular Damage. *Circulation* **139,** 1407-1421.

Bavis RW. (2005). Developmental plasticity of the hypoxic ventilatory response after perinatal hyperoxia and hypoxia. *Respiratory physiology & neurobiology* **149,** 287-299.

Bercik P, Park AJ, Sinclair D, Khoshdel A, Lu J, Huang X, Deng Y, Blennerhassett PA, Fahnestock M, Moine D, Berger B, Huizinga JD, Kunze W, McLean PG, Bergonzelli GE, Collins SM & Verdu EF. (2011). The anxiolytic effect of Bifidobacterium longum NCC3001 involves vagal pathways for gut-brain communication. *Neurogastroenterology and motility : the official journal of the European Gastrointestinal Motility Society* **23,** 1132-1139.

Bravo JA, Forsythe P, Chew MV, Escaravage E, Savignac HM, Dinan TG, Bienenstock J & Cryan JF. (2011). Ingestion of Lactobacillus strain regulates emotional behavior and central GABA receptor expression in a mouse via the vagus nerve. *Proceedings of the National Academy of Sciences of the United States of America* **108,** 16050-16055.

Bucker R, Krug SM, Moos V, Bojarski C, Schweiger MR, Kerick M, Fromm A, Janssen S, Fromm M, Hering NA, Siegmund B, Schneider T, Barmeyer C & Schulzke JD. (2018). Campylobacter jejuni impairs sodium transport and epithelial barrier function via cytokine release in human colon. *Mucosal immunology* **11,** 474-485.

Burokas A, Arboleya S, Moloney RD, Peterson VL, Murphy K, Clarke G, Stanton C, Dinan TG & Cryan JF. (2017). Targeting the Microbiota-Gut-Brain Axis: Prebiotics Have

Anxiolytic and Antidepressant-like Effects and Reverse the Impact of Chronic Stress in Mice. *Biological psychiatry* **82,** 472-487.

Chen X, Fu Y, Wang L, Qian W, Zheng F & Hou X. (2019). Bifidobacterium longum and VSL#3((R)) amelioration of TNBS-induced colitis associated with reduced HMGB1 and epithelial barrier impairment. *Developmental and comparative immunology* **92,** 77-86.

Clarke G, Grenham S, Scully P, Fitzgerald P, Moloney RD, Shanahan F, Dinan TG & Cryan JF. (2013). The microbiome-gut-brain axis during early life regulates the hippocampal serotonergic system in a sex-dependent manner. *Molecular psychiatry* **18,** 666-673.

De Filippis F, Pellegrini N, Vannini L, Jeffery IB, La Storia A, Laghi L, Serrazanetti DI, Di Cagno R, Ferrocino I, Lazzi C, Turroni S, Cocolin L, Brigidi P, Neviani E, Gobbetti M, O'Toole PW & Ercolini D. (2016). High-level adherence to a Mediterranean diet beneficially impacts the gut microbiota and associated metabolome. *Gut* **65,** 1812-1821.

Del Chierico F, Vernocchi P, Dallapiccola B & Putignani L. (2014). Mediterranean diet and health: food effects on gut microbiota and disease control. *International journal of molecular sciences* **15,** 11678-11699.

Del Rio R, Andrade DC, Lucero C, Arias P & Iturriaga R. (2016). Carotid Body Ablation Abrogates Hypertension and Autonomic Alterations Induced by Intermittent Hypoxia in Rats. *Hypertension (Dallas, Tex : 1979)* **68,** 436-445.

Desbonnet L, Clarke G, Traplin A, O'Sullivan O, Crispie F, Moloney RD, Cotter PD, Dinan TG & Cryan JF. (2015). Gut microbiota depletion from early adolescence in mice: Implications for brain and behaviour. *Brain, behavior, and immunity* **48,** 165-173.

Docio I, Olea E, Prieto LJ, Gallego-Martin T, Obeso A, Gomez-Nino A & Rocher A. (2018). Guinea Pig as a Model to Study the Carotid Body Mediated Chronic Intermittent Hypoxia Effects. *Frontiers in physiology* **9,** 694.

Donovan LM, Liu Y & Weiss JW. (2014). Effect of endothelin antagonism on apnea frequency following chronic intermittent hypoxia. *Respiratory physiology & neurobiology* **194,** 6-8.

Dunphy-Doherty F, O'Mahony SM, Peterson VL, O'Sullivan O, Crispie F, Cotter PD, Wigmore P, King MV, Cryan JF & Fone KCF. (2018). Post-weaning social isolation of rats leads to long-term disruption of the gut microbiota-immune-brain axis. *Brain, behavior, and immunity* **68,** 261-273.

Durgan DJ, Ganesh BP, Cope JL, Ajami NJ, Phillips SC, Petrosino JF, Hollister EB & Bryan RM, Jr. (2016). Role of the Gut Microbiome in Obstructive Sleep Apnea-Induced Hypertension. *Hypertension (Dallas, Tex : 1979)* **67,** 469-474.

Edge D, Bradford A & O'Halloran KD. (2012). Chronic intermittent hypoxia increases apnoea index in sleeping rats. *Advances in experimental medicine and biology* **758,** 359-363.

Edge D, Skelly JR, Bradford A & O'Halloran KD. (2010). Respiratory plasticity in the behaving rat following chronic intermittent hypoxia. *Advances in experimental medicine and biology* **669,** 267-270.

Foster JA, Rinaman L & Cryan JF. (2017). Stress & the gut-brain axis: Regulation by the microbiome. *Neurobiology of stress* **7,** 124-136.

Fouhy F, Watkins C, Hill CJ, O'Shea CA, Nagle B, Dempsey EM, O'Toole PW, Ross RP, Ryan CA & Stanton C. (2019). Perinatal factors affect the gut microbiota up to four years after birth. *Nature communications* **10,** 1517.

Fournier S, Steele S, Julien C, Fournier S, Gulemetova R, Caravagna C, Soliz J, Bairam A & Kinkead R. (2013). Gestational stress promotes pathological apneas and sex-specific disruption of respiratory control development in newborn rat. *The Journal of neuroscience : the official journal of the Society for Neuroscience* **33,** 563-573.

Fuller DD & Mitchell GS. (2017). Respiratory neuroplasticity - Overview, significance and future directions. *Experimental neurology* **287,** 144-152.

Ganesh BP, Nelson JW, Eskew JR, Ganesan A, Ajami NJ, Petrosino JF, Bryan RM, Jr. & Durgan DJ. (2018). Prebiotics, Probiotics, and Acetate Supplementation Prevent Hypertension in a Model of Obstructive Sleep Apnea. *Hypertension (Dallas, Tex : 1979)* **72,** 1141-1150.

Garcia AJ, 3rd, Zanella S, Dashevskiy T, Khan SA, Khuu MA, Prabhakar NR & Ramirez JM. (2016). Chronic Intermittent Hypoxia Alters Local Respiratory Circuit Function at the Level of the preBotzinger Complex. *Frontiers in neuroscience* **10,** 4.

Gareau MG, Jury J, MacQueen G, Sherman PM & Perdue MH. (2007). Probiotic treatment of rat pups normalises corticosterone release and ameliorates colonic dysfunction induced by maternal separation. *Gut* **56,** 1522-1528.

Golubeva AV, Crampton S, Desbonnet L, Edge D, O'Sullivan O, Lomasney KW, Zhdanov AV, Crispie F, Moloney RD, Borre YE, Cotter PD, Hyland NP, O'Halloran KD, Dinan TG, O'Keeffe GW & Cryan JF. (2015). Prenatal stress-induced alterations in major physiological systems correlate with gut microbiota composition in adulthood. *Psychoneuroendocrinology* **60,** 58-74.

Golubeva AV, Joyce SA, Moloney G, Burokas A, Sherwin E, Arboleya S, Flynn I, Khochanskiy D, Moya-Perez A, Peterson V, Rea K, Murphy K, Makarova O, Buravkov S, Hyland NP, Stanton C, Clarke G, Gahan CGM, Dinan TG & Cryan JF. (2017). Microbiota-

related Changes in Bile Acid & Tryptophan Metabolism are Associated with Gastrointestinal Dysfunction in a Mouse Model of Autism. *EBioMedicine* **24,** 166-178.

Halkjaer SI, Christensen AH, Lo BZS, Browne PD, Gunther S, Hansen LH & Petersen AM. (2018). Faecal microbiota transplantation alters gut microbiota in patients with irritable bowel syndrome: results from a randomised, double-blind placebo-controlled study. *Gut* **67,** 2107-2115.

Hoban AE, Moloney RD, Golubeva AV, McVey Neufeld KA, O'Sullivan O, Patterson E, Stanton C, Dinan TG, Clarke G & Cryan JF. (2016). Behavioural and neurochemical consequences of chronic gut microbiota depletion during adulthood in the rat. *Neuroscience* **339,** 463-477.

Huang J, Lusina S, Xie T, Ji E, Xiang S, Liu Y & Weiss JW. (2009). Sympathetic response to chemostimulation in conscious rats exposed to chronic intermittent hypoxia. *Respiratory physiology & neurobiology* **166,** 102-106.

Iturriaga R, Oyarce MP & Dias ACR. (2017). Role of Carotid Body in Intermittent Hypoxia-Related Hypertension. *Current hypertension reports* **19,** 38.

Johnston GR & Webster NR. (2009). Cytokines and the immunomodulatory function of the vagus nerve. *British journal of anaesthesia* **102,** 453-462.

Joseph V, Behan M & Kinkead R. (2013). Sex, hormones, and stress: how they impact development and function of the carotid bodies and related reflexes. *Respiratory physiology & neurobiology* **185,** 75-86.

Julien C, Bairam A & Joseph V. (2008). Chronic intermittent hypoxia reduces ventilatory long-term facilitation and enhances apnea frequency in newborn rats. *American journal of physiology Regulatory, integrative and comparative physiology* **294,** R1356-1366.

Kelly JR, Borre Y, C OB, Patterson E, El Aidy S, Deane J, Kennedy PJ, Beers S, Scott K, Moloney G, Hoban AE, Scott L, Fitzgerald P, Ross P, Stanton C, Clarke G, Cryan JF & Dinan TG. (2016). Transferring the blues: Depression-associated gut microbiota induces neurobehavioural changes in the rat. *Journal of psychiatric research* **82,** 109-118.

Kelly JR, Kennedy PJ, Cryan JF, Dinan TG, Clarke G & Hyland NP. (2015). Breaking down the barriers: the gut microbiome, intestinal permeability and stress-related psychiatric disorders. *Frontiers in cellular neuroscience* **9,** 392.

Kim S, Goel R, Kumar A, Qi Y, Lobaton G, Hosaka K, Mohammed M, Handberg EM, Richards EM, Pepine CJ & Raizada MK. (2018). Imbalance of gut microbiome and intestinal

epithelial barrier dysfunction in patients with high blood pressure. *Clinical science (London, England : 1979)* **132,** 701-718.

Kinkead R, Guertin PA & Gulemetova R. (2013). Sex, stress and their influence on respiratory regulation. *Current pharmaceutical design* **19,** 4471-4484.

Laouafa S, Ribon-Demars A, Marcouiller F, Roussel D, Bairam A, Pialoux V & Joseph V. (2017). Estradiol Protects Against Cardiorespiratory Dysfunctions and Oxidative Stress in Intermittent Hypoxia. *Sleep* **40**.

Laouafa S, Roussel D, Marcouiller F, Soliz J, Gozal D, Bairam A & Joseph V. (2019). Roles of oestradiol receptor alpha and beta against hypertension and brain mitochondrial dysfunction under intermittent hypoxia in female rats. *Acta physiologica (Oxford, England)* **226,** e13255.

Li J, Zhao F, Wang Y, Chen J, Tao J, Tian G, Wu S, Liu W, Cui Q, Geng B, Zhang W, Weldon R, Auguste K, Yang L, Liu X, Chen L, Yang X, Zhu B & Cai J. (2017). Gut microbiota dysbiosis contributes to the development of hypertension. *Microbiome* **5,** 14.

Liu J, Li T, Wu H, Shi H, Bai J, Zhao W, Jiang D & Jiang X. (2019). Lactobacillus rhamnosus GG strain mitigated the development of obstructive sleep apnea-induced hypertension in a high salt diet via regulating TMAO level and CD4(+) T cell induced-type I inflammation. *Biomedicine & pharmacotherapy = Biomedecine & pharmacotherapie* **112,** 108580.

Lucking EF, O'Connor KM, Strain CR, Fouhy F, Bastiaanssen TFS, Burns DP, Golubeva AV, Stanton C, Clarke G, Cryan JF & O'Halloran KD. (2018). Chronic intermittent hypoxia disrupts cardiorespiratory homeostasis and gut microbiota composition in adult male guinea-pigs. *EBioMedicine*.

Lucking EF, O'Halloran KD & Jones JF. (2014). Increased cardiac output contributes to the development of chronic intermittent hypoxia-induced hypertension. *Experimental physiology* **99,** 1312-1324.

Macfarlane GT & Macfarlane S. (2012). Bacteria, colonic fermentation, and gastrointestinal health. *Journal of AOAC International* **95,** 50-60.

Marques FZ, Mackay CR & Kaye DM. (2018). Beyond gut feelings: how the gut microbiota regulates blood pressure. *Nature reviews Cardiology* **15,** 20-32.

Marques FZ, Nelson E, Chu PY, Horlock D, Fiedler A, Ziemann M, Tan JK, Kuruppu S, Rajapakse NW, El-Osta A, Mackay CR & Kaye DM. (2017). High-Fiber Diet and Acetate Supplementation Change the Gut Microbiota and Prevent the Development of Hypertension and Heart Failure in Hypertensive Mice. *Circulation* **135,** 964-977.

Mody P, Rukhadze I & Kubin L. (2011). Rats subjected to chronic-intermittent hypoxia have increased density of noradrenergic terminals in the trigeminal sensory and motor nuclei. *Neuroscience letters* **505,** 176-179.

Moreno-Indias I, Torres M, Montserrat JM, Sanchez-Alcoholado L, Cardona F, Tinahones FJ, Gozal D, Poroyko VA, Navajas D, Queipo-Ortuno MI & Farre R. (2015). Intermittent hypoxia alters gut microbiota diversity in a mouse model of sleep apnoea. *The European respiratory journal* **45,** 1055-1065.

Murphy EA, Velazquez KT & Herbert KM. (2015). Influence of high-fat diet on gut microbiota: a driving force for chronic disease risk. *Current opinion in clinical nutrition and metabolic care* **18,** 515-520.

Nohr MK, Egerod KL, Christiansen SH, Gille A, Offermanns S, Schwartz TW & Moller M. (2015). Expression of the short chain fatty acid receptor GPR41/FFAR3 in autonomic and somatic sensory ganglia. *Neuroscience* **290,** 126-137.

O'Connor KM, Lucking EF, Golubeva AV, Strain CR, Fouhy F, Cenit MC, Dhaliwal P, Bastiaanssen TFS, Burns DP, Stanton C, Clarke G, Cryan JF & O'Halloran KD. (2019a). Manipulation of gut microbiota blunts the ventilatory response to hypercapnia in adult rats. *EBioMedicine*.

O'Connor KM, Lucking EF & O'Halloran KD. (2019b). Chronic intermittent hypoxia-induced hypertension: An expired hypothesis laid to rest? *Experimental physiology*.

O'Mahony SM, Felice VD, Nally K, Savignac HM, Claesson MJ, Scully P, Woznicki J, Hyland NP, Shanahan F, Quigley EM, Marchesi JR, O'Toole PW, Dinan TG & Cryan JF. (2014). Disturbance of the gut microbiota in early-life selectively affects visceral pain in adulthood without impacting cognitive or anxiety-related behaviors in male rats. *Neuroscience* **277,** 885-901.

O'Mahony SM, Marchesi JR, Scully P, Codling C, Ceolho AM, Quigley EM, Cryan JF & Dinan TG. (2009). Early life stress alters behavior, immunity, and microbiota in rats: implications for irritable bowel syndrome and psychiatric illnesses. *Biological psychiatry* **65,** 263-267.

Panda S, El khader I, Casellas F, Lopez Vivancos J, Garcia Cors M, Santiago A, Cuenca S, Guarner F & Manichanh C. (2014). Short-term effect of antibiotics on human gut microbiota. *PloS one* **9,** e95476.

Penders J, Thijs C, Vink C, Stelma FF, Snijders B, Kummeling I, van den Brandt PA & Stobberingh EE. (2006). Factors influencing the composition of the intestinal microbiota in early infancy. *Pediatrics* **118,** 511-521.

Peng YJ, Nanduri J, Yuan G, Wang N, Deneris E, Pendyala S, Natarajan V, Kumar GK & Prabhakar NR. (2009). NADPH oxidase is required for the sensory plasticity of the carotid body by chronic intermittent hypoxia. *The Journal of neuroscience : the official journal of the Society for Neuroscience* **29,** 4903-4910.

Peng YJ, Yuan G, Khan S, Nanduri J, Makarenko VV, Reddy VD, Vasavda C, Kumar GK, Semenza GL & Prabhakar NR. (2014). Regulation of hypoxia-inducible factor-alpha isoforms and redox state by carotid body neural activity in rats. *The Journal of physiology* **592,** 3841-3858.

Riegler M, Sedivy R, Pothoulakis C, Hamilton G, Zacherl J, Bischof G, Cosentini E, Feil W, Schiessel R, LaMont JT & et al. (1995). Clostridium difficile toxin B is more potent than toxin A in damaging human colonic epithelium in vitro. *The Journal of clinical investigation* **95,** 2004-2011.

Santisteban MM, Qi Y, Zubcevic J, Kim S, Yang T, Shenoy V, Cole-Jeffrey CT, Lobaton GO, Stewart DC, Rubiano A, Simmons CS, Garcia-Pereira F, Johnson RD, Pepine CJ & Raizada MK. (2017). Hypertension-Linked Pathophysiological Alterations in the Gut. *Circulation research* **120,** 312-323.

Sender R, Fuchs S & Milo R. (2016). Are We Really Vastly Outnumbered? Revisiting the Ratio of Bacterial to Host Cells in Humans. *Cell* **164,** 337-340.

Soliz J, Tam R & Kinkead R. (2016). Neonatal Maternal Separation Augments Carotid Body Response to Hypoxia in Adult Males but Not Female Rats. *Frontiers in physiology* **7,** 432.

Toral M, Robles-Vera I, de la Visitacion N, Romero M, Yang T, Sanchez M, Gomez-Guzman M, Jimenez R, Raizada MK & Duarte J. (2019). Critical Role of the Interaction Gut Microbiota - Sympathetic Nervous System in the Regulation of Blood Pressure. *Frontiers in physiology* **10,** 231.

Tryba AK, Pena F, Lieske SP, Viemari JC, Thoby-Brisson M & Ramirez JM. (2008). Differential modulation of neural network and pacemaker activity underlying eupnea and sigh-breathing activities. *Journal of neurophysiology* **99,** 2114-2125.

Tulstrup MV, Christensen EG, Carvalho V, Linninge C, Ahrne S, Hojberg O, Licht TR & Bahl MI. (2015). Antibiotic Treatment Affects Intestinal Permeability and Gut Microbial Composition in Wistar Rats Dependent on Antibiotic Class. *PloS one* **10,** e0144854.

West C, Wu RY, Wong A, Stanisz AM, Yan R, Min KK, Pasyk M, McVey Neufeld KA, Karamat MI, Foster JA, Bienenstock J, Forsythe P & Kunze WA. (2017). Lactobacillus rhamnosus strain JB-1 reverses restraint stress-induced gut dysmotility. *Neurogastroenterology and motility : the official journal of the European Gastrointestinal Motility Society* **29**.

Wu J, Sun X, Wu Q, Li H, Li L, Feng J, Zhang S, Xu L, Li K, Li X, Wang X & Chen H. (2016). Disrupted intestinal structure in a rat model of intermittent hypoxia. *Molecular medicine reports* **13,** 4407-4413.

Zanella S, Doi A, Garcia AJ, 3rd, Elsen F, Kirsch S, Wei AD & Ramirez JM. (2014). When norepinephrine becomes a driver of breathing irregularities: how intermittent hypoxia fundamentally alters the modulatory response of the respiratory network. *The Journal of neuroscience : the official journal of the Society for Neuroscience* **34,** 36-50.

Zoccal DB, Bonagamba LG, Oliveira FR, Antunes-Rodrigues J & Machado BH. (2007). Increased sympathetic activity in rats submitted to chronic intermittent hypoxia. *Experimental physiology* **92,** 79-85.

Publications

Published articles

1. Lucking EF*, O'Connor KM*, Strain CR, Fouhy F, Bastiaanssen TFS, Burns DP, Golubeva AV, Stanton C, Clarke G, Cryan JF, O'Halloran KD ''Chronic intermittent hypoxia disrupts cardiorespiratory homeostasis and gut microbiota composition in adult male guinea-pigs''. EbioMedicine, doi: 10.1016/j.ebiom.2018.11.010.
2. O'Connor KM*, Lucking EF*, Golubeva AV, Strain CR, Fouhy F, Cenit MC, Dhaliwal P, Bastiaanssen TFS, Burns DP, Stanton C, Clarke G, Cryan JF, O'Halloran KD ''Manipulation of the gut microbiota blunts the ventilatory response to hypercapnia in adult rats''. EbioMedicine, doi: 10.1016/j.ebiom.2019.03.029.
3. O'Connor KM, Lucking EF, O'Halloran KD ''Chronic intermittent hypoxia-induced hypertension: An expired hypothesis laid to rest?''. Experimental Physiology, doi: 10.1113/EP087868, Editorial.

Manuscripts and reviews in preparation

1. O'Connor KM, Lucking EF, Bastiaanssen TFS, Peterson VL, Crispie F, Golubeva AV, Cotter PD, Clarke G, Cryan JF, O'Halloran KD ''Chronic intermittent hypoxia lowers *Lactobacillus rhamnosus* relative abundance and increases apnoea index and blood pressure: Effects of prebiotic supplementation''.
2. O'Connor KM, Lucking EF, Cryan JF, O'Halloran KD ''The microbiota-gut-brain axis in the control of breathing and cardiovascular function''. Review.
3. O'Connor KM, Bastiaanssen TFS, Crispie F, Peterson VL, Cotter PD, Clarke G, Golubeva AV, Lucking EF, Cryan JF, O'Halloran KD '' Investigation into strategies of microbiota recolonization following antibiotic treatment".

Presentations

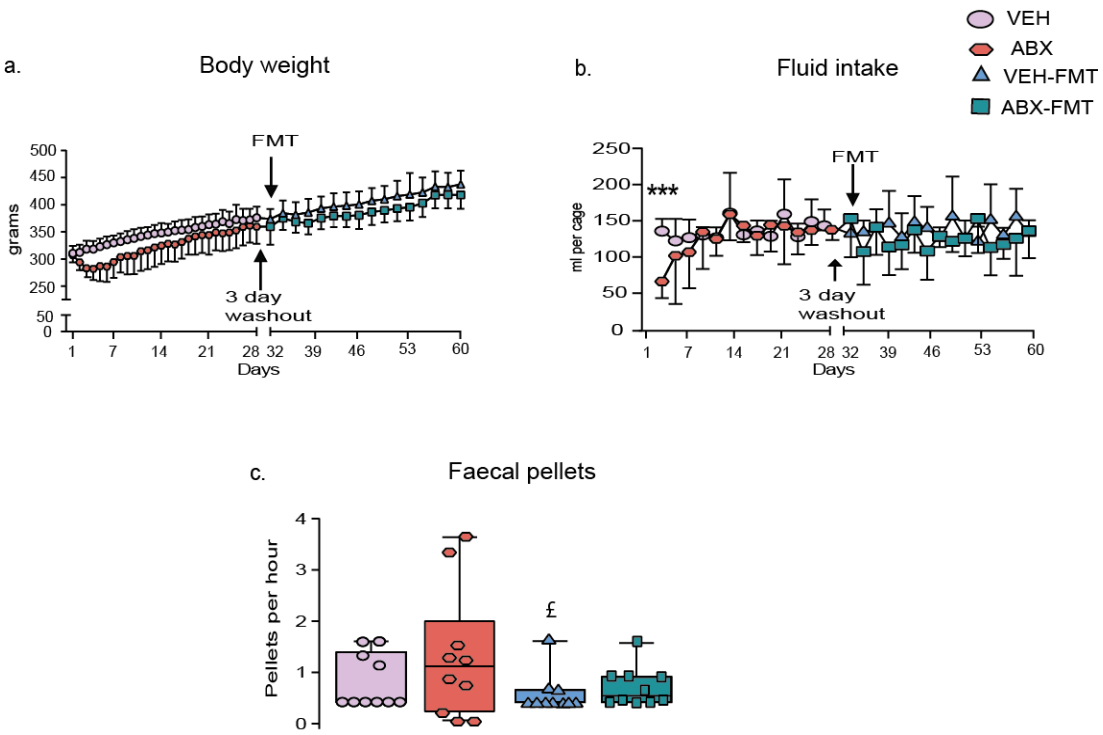
1. APC Forum 2019, University College Cork, Cork, Ireland (2019).
2. APC Forum 2018, University College Cork, Cork, Ireland (2018).
3. Research Seminar, Department of Physiology, University College Cork, Cork, Ireland (2018).
4. APC Pilot, Feasibility and Innovation Annual Seminar Platform, University College, Cork, Ireland (2017).
5. Hypoxia Research Symposium, Cork, Ireland (2016).
6. Royal Academy of Medicine in Ireland Biomedical Sciences Meeting, Cork, Ireland (2016).

Conference proceedings

1. New Horizons in Medical Research UCC (Cork, IRL). O'Connor KM, Lucking EF, Cryan JF, O'Halloran KD (2018) ''Chronic intermittent hypoxia related cardiorespiratory dysfunction in adult rats'' (Poster).
2. Experimental Biology 2018 (San Diego, USA). O'Connor KM, Lucking EF, Clarke G, Cryan JF, O'Halloran KD (2018) ''Microbiota and cardiorespiratory control: Chronic intermittent hypoxia related cardiorespiratory dysfunction in rat'' (Poster).
3. New Horizons in Medical Research UCC (Cork, IRL). Lucking EF, O'Connor KM, O'Halloran KD (2017) ''Chronic intermittent hypoxia elicits tachycardia and reduced respiratory instability in the carotid body hypoxia-insensitive guinea pig'' (Poster).
4. New Horizons in Medical Research UCC (Cork, IRL). O'Connor KM, Lucking EF, Cryan JF, O'Halloran KD (2017) ''Bugs, breathing and blood pressure: Chronic intermittent hypoxia related cardiorespiratory dysfunction in adult rats" (Poster).
5. Royal Academy of Medicine in Ireland Biomedical Sciences Meeting 2017 (Dublin, IRL). Lucking EF, O'Connor KM, Burns DP, O'Halloran KD (2017) ''Does chronic intermittent hypoxia adversely affect respiratory control in the carotid body hypoxia-insensitive guinea pig' (Poster).
6. Royal Academy of Medicine in Ireland Biomedical Sciences Meeting 2017 (Dublin, IRL). O'Connor KM, Lucking EF, Burns DP, Golubeva AV, Cryan JF, O'Halloran KD (2017) ''Bugs and Breathing: The effects of microbiota depletion and subsequent faecal matter transplant on respiratory and metabolic homeostasis" (Poster).
7. Experimental Biology 2017 (Chicago, USA). O'Connor KM, Lucking EF, Burns DP, Golubeva AV, Clarke G. Cryan JF, O'Halloran KD (2017) ''Microbiota and cardiorespiratory control: Ventilatory responsiveness to chemostimulation in adult male rats following chronic antibiotic treatment'' (Poster).
8. Experimental Biology 2017 (Chicago, USA). O'Connor KM, Lucking EF, Burns DP, Clarke G, O'Halloran KD (2017) ''Exposure to chronic intermittent hypoxia elicits aberrant respiratory plasticity in adult guinea pig'' (Poster).

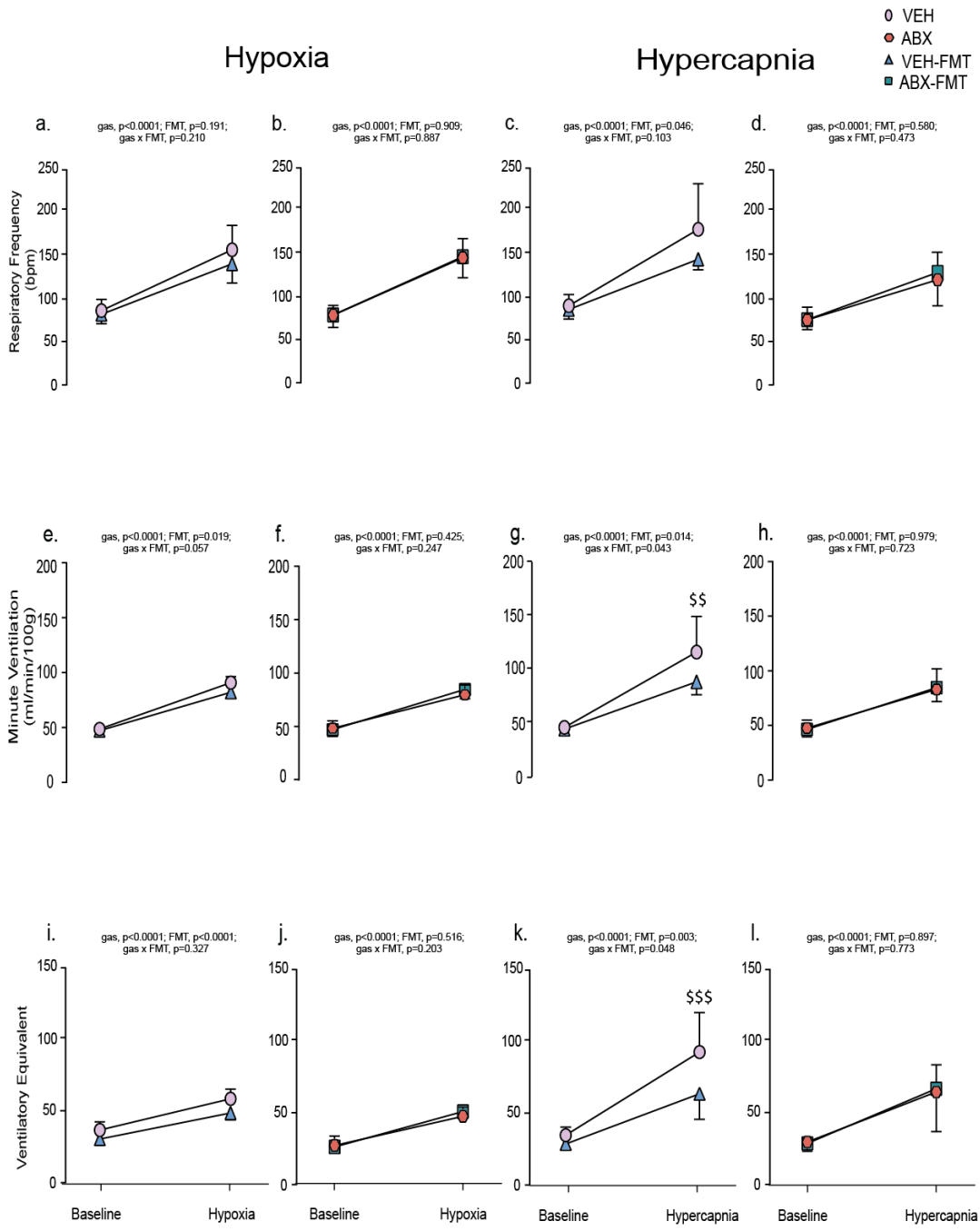
9. Oxford Control of Breathing Meeting 2017 (Oxford, UK). Lucking EF, O'Connor KM, O'Halloran KD (2017) ''Chronic intermittent hypoxia elicits tachycardia and reduced respiratory instability in the carotid body hypoxia-insensitive guinea pig'' (Poster).
10. New Horizons in Medical Research UCC (Cork, IRL). O'Connor KM, Burns DP, Lucking EF, Golubeva AV, Cryan JF, O'Halloran KD (2016) ''Microbiota and respiratory control: Blunted ventilatory responsiveness to hypercapnia in adult male rats following chronic antibiotic treatment'' (Poster).
11. Royal Academy of Medicine in Ireland Biomedical Sciences Meeting 2016 (Cork, IRL). O'Connor KM, Burns DP, Lucking EF, Golubeva AV, Cryan JF, O'Halloran KD (2016) ''Microbiota and respiratory control: Blunted ventilatory responsiveness to hypercapnia in adult male rats following chronic antibiotic treatment'' (Oral).
12. Royal Academy of Medicine in Ireland Biomedical Sciences Meeting 2016 (Cork, IRL). Lucking EF, O'Connor KM, O'Halloran KD (2016) ''Microbiota and cardiorespiratory control: Chronic antibiotic treatment alters cardiorespiratory homeostasis in urethane anesthetised rats'' (Poster).
13. APC symposium 2016 (Cork, IRL). O'Connor KM, Lucking EF, Cryan JF, O'Halloran KD (2016) ''Microbiota and respiratory control: Blunted ventilatory responsiveness to hypercapnia in adult male rats following chronic antibiotic treatment'' (Poster).
14. Physiology Society 2016 (Dublin, IRL). O'Connor KM, Lucking EF, Burns DP, Golubeva AV, Clarke G, Cryan JF, O'Halloran KD (2016) ''Microbiota and respiratory control: Blunted ventilatory responsiveness to hypercapnia in adult male rats following chronic antibiotic treatment'' (Poster).
15. Physiology Society 2016 (Dublin, IRL). Lucking EF, O'Connor KM, O'Halloran KD (2016) ''Microbiota and cardiorespiratory control: Chronic antibiotic treatment alters cardiorespiratory homeostasis in urethane anesthetised rats'' (Poster).

Appendix A. Manipulation of gut microbiota blunts the ventilatory response to hypercapnia in adult rats



Appendix Figure A.1 Body weight, fluid intake and faecal output

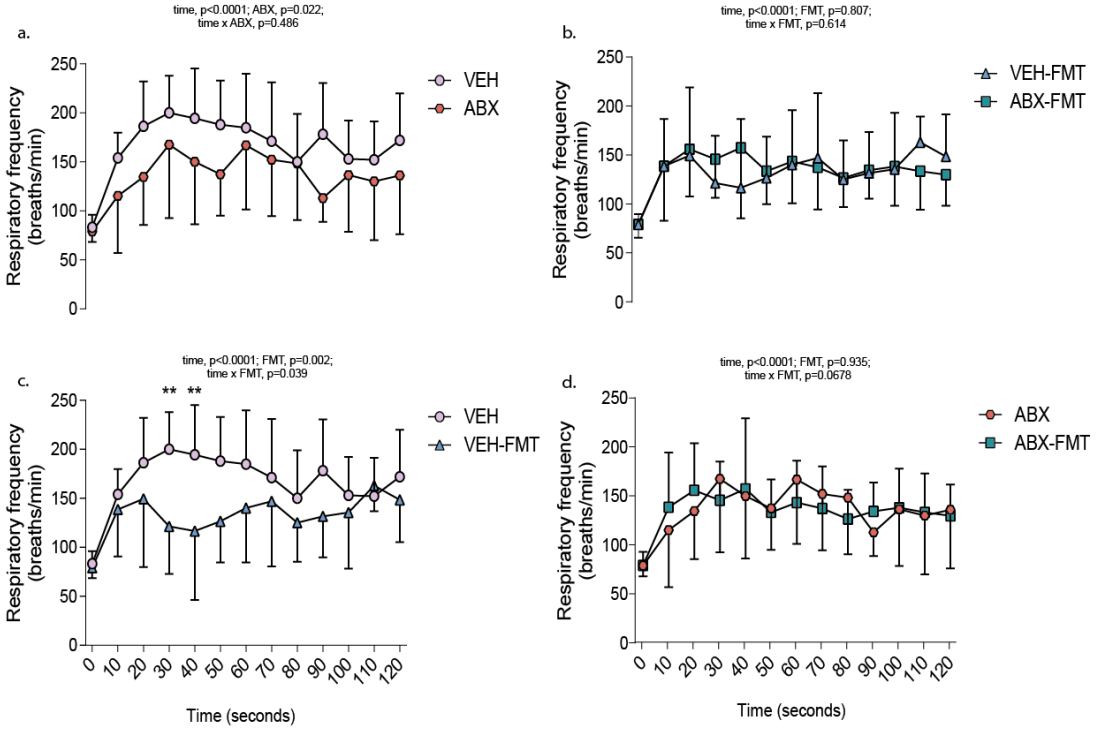
Group data for (a) animal body weights and (b) fluid intake in ml per cage (two animals per cage) over the experimental timeline. Group data (c) for excreted faecal pellets per hour; n=10 all groups. VEH, autoclaved deionised water; ABX, antibiotic-treated; VEH-FMT, VEH followed by faecal microbial transfer; ABX-FMT, antibiotic-treated followed by faecal microbial transfer. Data (a-b) are expressed as mean ± SD or (c) as box and whisker plots (median, IQR and minimum to maximum values). Data (a-b) were statistically compared by two-way ANOVA with Bonferroni post hoc test. Data (c) were statistically compared by non-parametric Kruskal-Wallis with Dunn's post hoc. *** p<0.01, ABX vs. VEH; £ p<0.005, VEH-FMT vs. ABX.



Appendix Figure A.2 Chronic antibiotic administration and faecal microbial transfer blunts hypercapnic ventilation in behaving rats during quiet rest

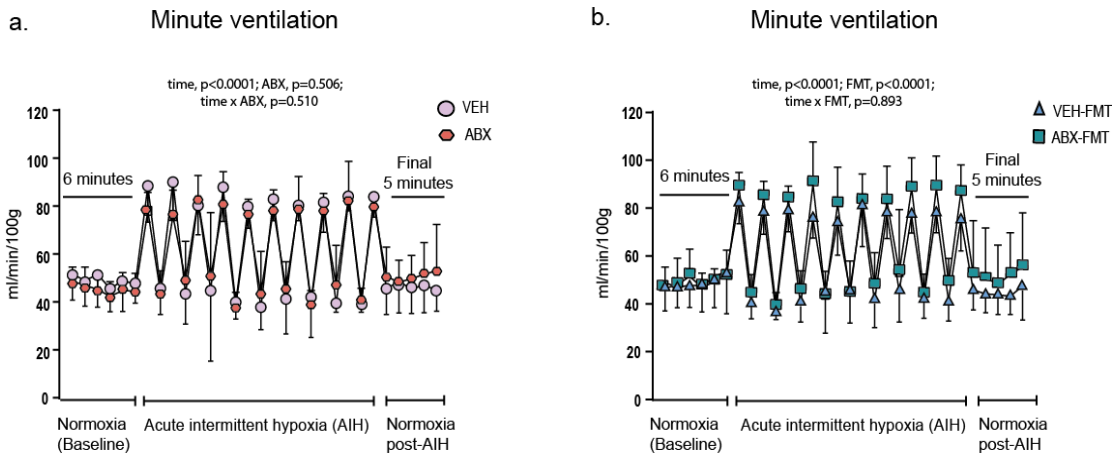
Group data for respiratory frequency (a, b, c, d), minute ventilation (e, f, g, h) and ventilatory equivalent (i, j, k, l) during normoxia and in response to hypoxia (a, b, e, f, i, j) and hypercapnia (c, d, g, h, k, l) for VEH and VEH-FMT (a, c, e, g, i, k) and ABX and ABX-FMT (b, d, f, h, j, l). VEH, autoclaved deionised water; ABX, antibiotic-treated; VEH-FMT, VEH followed by faecal microbial transfer; ABX-FMT, antibiotic-treated followed by faecal microbial transfer. Data (a-l) are expressed as mean ± SD during baseline, hypoxia and hypercapnia; n=10 for all groups. Groups were statistically compared by repeated measures two-way ANOVA with

Bonferroni post hoc where appropriate. *p*-values are shown. $$ *p*<0.01, VEH versus VEH-FMT, $$$ *p*<0.001, VEH versus VEH-FMT, Bonferroni post hoc test.



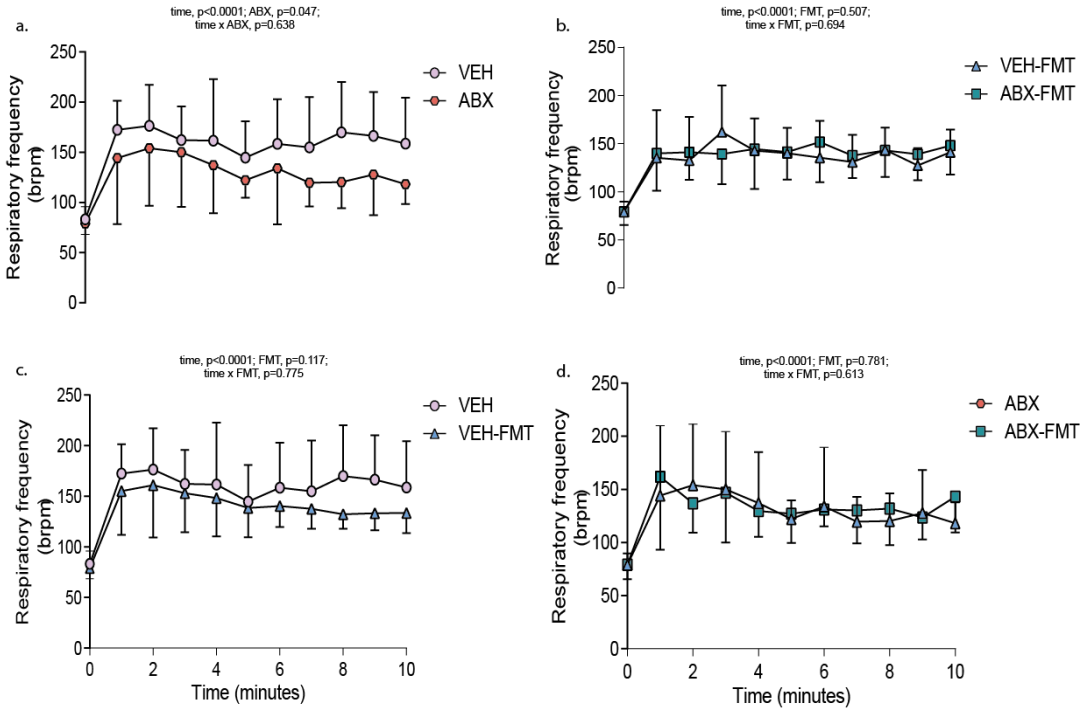
Appendix Figure A.3 Chronic antibiotic administration and faecal microbial transfer blunt the peak respiratory frequency response to hypoxia in behaving rats during quiet rest

Respiratory frequency for VEH and ABX (a), VEH-FMT and ABX-FMT (b), VEH and VEH-FMT (c), ABX and ABX-FMT (d) rats immediately before and during 120 seconds of exposure to hypoxia. VEH, autoclaved deionised water; ABX, antibiotic-treated; VEH-FMT, VEH followed by faecal microbial transfer; ABX-FMT, antibiotic-treated followed by faecal microbial transfer. Data (a-d) are expressed mean ±SD; n=10 for all groups. Data were statistically compared by repeated measures two-way ANOVA (time x ABX or time x FMT) with Bonferroni post hoc test, where appropriate. *p*-values are shown. ** $p<0.01$ compared with VEH, Bonferroni post hoc test.



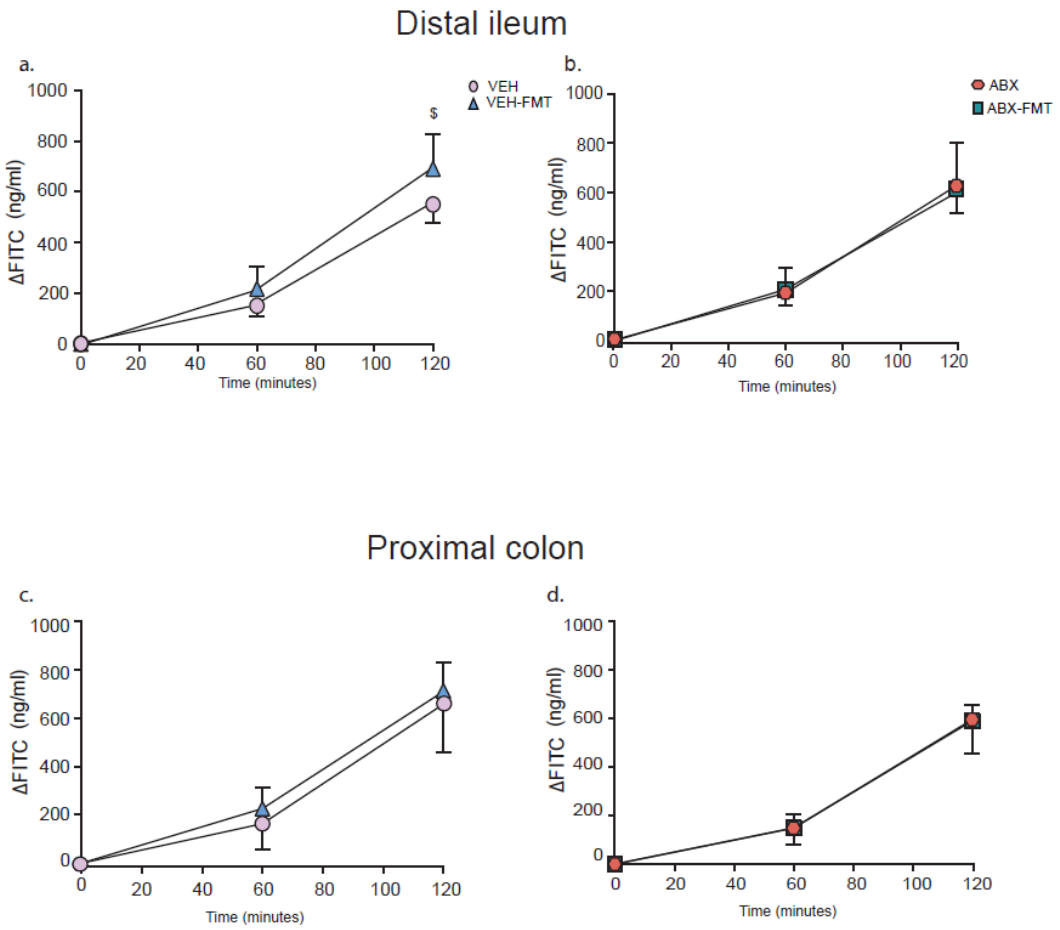
Appendix Figure A.4 Ventilatory response to acute intermittent hypoxia in behaving rats during quiet rest

Group data for minute ventilation during normoxia (6-minute baseline), acute intermittent hypoxia (AIH) and 5 minutes normoxia baseline 60 minutes following exposure to AIH for VEH and ABX (a) and VEH -FMT and ABX-FMT (b) groups. Data (a-b) are expressed as mean ± SD; n=10 for all groups. Groups were statistically compared by two-way ANOVA.



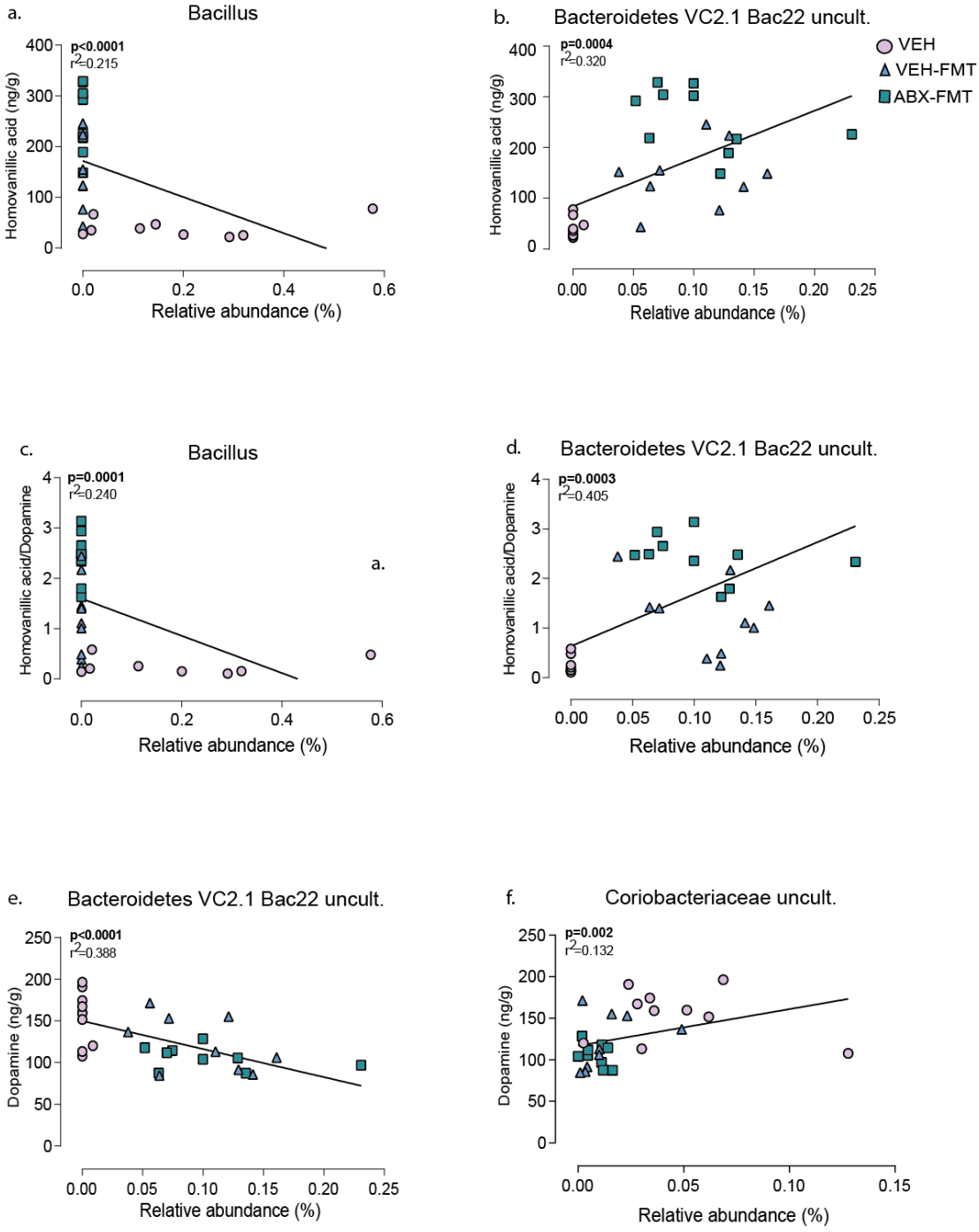
Appendix Figure A.5 Chronic antibiotic administration blunts the respiratory frequency response to hypercapnia in behaving rats during quiet rest

Respiratory frequency for VEH and ABX (a), VEH-FMT and ABX-FMT (b), VEH and VEH-FMT (c), ABX and ABX-FMT (d) rats immediately before and during10 minutes of exposure to hypercapnia. VEH, autoclaved deionised water; ABX, antibiotic-treated; VEH-FMT, VEH followed by faecal microbial transfer; ABX-FMT, antibiotic-treated followed by faecal microbial transfer. Data (a-d) are expressed mean ±SD; n=10 for all groups. Data were statistically compared by repeated measures two-way ANOVA (time x ABX or time x FMT). *p*-values are shown.



Appendix Figure A.6 Group data for FITC flux in distal ileum and proximal colon

Group data for FITC flux in distal ileum (a, b) and proximal colon (c, d) in VEH and VEH-FMT (a, c) and in ABX and ABX-FMT rats (b, d). VEH, autoclaved deionised water; ABX, antibiotic-treated; VEH-FMT, VEH followed by faecal microbiota transfer; ABX-FMT, antibiotic-treated followed by faecal microbiota transfer. Groups (a-d) showing baseline (0 min), 60 min and 120 min FITC flux for VEH (n = 4–5), ABX (n = 6), VEH-FMT (n = 5) and ABX-FMT (n = 4). Groups were statistically compared by two-way ANOVA with Bonferroni post hoc, where appropriate. $ $p < .05$, VEH-FMT versus VEH.



Appendix Figure A.7 Scatter plots for the most significant correlations between homovanillic acid, homovanillic acid/dopamine and dopamine concentrations and genus

Individual data points for correlation analysis between homovanillic acid and Bacillus (a), homovanillic acid and Bacteroidetes VC2.1 Bac22 uncult. (b) homovanillic acid/dopamine and Bacillus (c), homovanillic acid/dopamine and Bacteroidetes VC2.1 Bac22 uncult. (d), dopamine and Bacteroidetes VC2.1 Bac22 uncult. (e) and dopamine and Coriobacteriaceae uncult. (f) in VEH, VEH-FMT and ABX-FMT rats. Solid black lines represent linear regression analysis for each parameter. Spearman correlation coefficients were used to assess associations. *p*-values are shown.

% change from baseline	VEH (n=10)	ABX (n=10)	VEH-FMT (n=10)	ABX-FMT (n=10)	One-way ANOVA
f_R	75 ± 28	61 ± 18	51 ± 34	67 ± 24	0.337
V_T	24 ± 8	25 ± 8	25 ± 13	23 ± 10	0.931
V_E	110 ± 22	98 ± 19	89 ± 39	82 ± 33	0.202

Appendix Table A.1. Ventilatory response to the tenth (final) intermittent hypoxia challenge in behaving rats during quiet rest

f_R, respiratory frequency; V_T, tidal volume; V_E, minute ventilation; VEH, autoclaved deionised water; ABX, antibiotic-treated; VEH-FMT, VEH followed by faecal microbial transfer; ABX-FMT, antibiotic administration followed by faecal microbial transfer. Data are shown as mean ± SD and were statistically compared using one-way ANOVA or non-parametric Kruskal-Wallis, where appropriate.

% change from baseline	VEH (n=10)	ABX (n=10)	VEH-FMT (n=10)	ABX-FMT (n=9)	One-way ANOVA	VEH vs ABX	VEH-FMT vs ABX-FMT	VEH vs VEH-FMT	ABX vs ABX-FMT	VEH vs ABX-FMT	ABX vs VEH-FMT
f_R	0 ± 27	6 ± 13	- 6 ± 33	4 ± 14	0.692	-	-	-	-	-	-
V_T	-4 ± 13	8 ± 16	-2 ± 12	-11 ± 8	**0.029**	0.364	0.804	0.999	**0.02**	0.999	0.64
V_E	4 ± 20	16 ± 18	-6 ± 27	-7 ± 16	0.075	-	-	-	-	-	-

Appendix Table A.2 Ventilation following exposure to acute intermittent hypoxia in behaving rats during quiet rest

f_R, respiratory frequency; V_T, tidal volume; V_E, minute ventilation; VEH, autoclaved deionised water; ABX, antibiotic-treated; VEH-FMT, VEH followed by faecal microbial transfer; ABX-FMT, antibiotic treated followed by faecal microbial transfer. Data are shown as mean ± SD and were statistically compared using one-way ANOVA with Bonferroni *post hoc* where appropriate. Each p-value is adjusted to account for multiple comparisons. *p*-values highlight significant differences.

	VEH (n=10)	ABX (n=8)	VEH-FMT (n=9)	ABX-FMT (n=10)	One-way ANOVA	VEH vs ABX	VEH-FMT vs ABX-FMT	VEH vs VEH-FMT	ABX vs ABX-FMT	VEH vs ABX-FMT	ABX vs VEH-FMT
Hypoxia											
Δ f_R (brpm)	30 ± 15	34 ± 11	29 ± 21	30 ± 24	0.824	-	-	-	-	-	-
Δ V_T (ml 100g^{-1})	0.05 ± 0.06	0.06 ± 0.03	0.08 ± 0.05	0.06 ± 0.07	0.431	-	-	-	-	-	-
Δ V_E (ml min^{-1} 100g^{-1})	20 ± 10	19 ± 7	27 ± 12	20 ± 16	0.443	-	-	-	-	-	-
Δ MAP (mmHg)	-31 ± 10	-30 ± 16	-20 ± 12	-22 ± 17	0.228	-	-	-	-	-	-
Δ DBP (mmHg)	-24 ± 7	-27 ± 12	-19 ± 10	-19 ± 11	0.221	-	-	-	-	-	-
Δ SBP (mmHg)	-44 ± 17	-41 ± 16	-29 ± 18	-32 ± 24	0.299	-	-	-	-	-	-
Δ HR (bpm)	19 ± 24	21 ± 19	34 ± 16	28 ± 25	0.451	-	-	-	-	-	-
Hypoxic Hypercapnia											
Δ f_R (brpm)	31 ± 7	36 ± 12	29 ± 11	33 ± 12	0.581	-	-	-	-	-	-
Δ V_T (ml 100g^{-1})	0.17 ± 0.07	0.16 ± 0.03	0.18 ± 0.07	0.17 ± 0.05	0.84	-	-	-	-	-	-
Δ V_E (ml min^{-1} 100g^{-1})	31 ± 5	31 ± 7	38 ± 8	33 ± 8	0.14	-	-	-	-	-	-
Δ MAP (mmHg)	-20 ± 10	-18 ± 11	-2 ± 10	-10 ± 16	**0.013**	0.999	0.999	**0.017**	0.999	0.424	0.066
Δ DBP (mmHg)	-16 ± 8	-16 ± 10	-6 ± 6	-10 ± 11	0.062	-	-	-	-	-	-
Δ SBP (mmHg)	-30 ± 18	-19 ± 18	-12 ± 12	-17 ± 21	0.155	-	-	-	-	-	-
Δ HR (bpm)	15 ± 14	12 ± 15	29 ± 12	21 ± 12	0.052	-	-	-	-	-	-

Appendix Table A.3 Cardiorespiratory responsiveness to hypoxic and hypoxic hypercapnic chemostimulation in urethane anaesthetised rats

f_R, respiratory frequency (brpm, breaths per min); V_T, tidal volume; V_E, minute ventilation; MAP, mean arterial pressure; DBP, diastolic blood pressure; SBP, systolic blood pressure; HR, heart rate (bpm, beats per min); VEH, autoclaved deionised water; ABX, antibiotic-treated; VEH-FMT, VEH followed by faecal microbial transfer; ABX-FMT, antibiotic administration followed by faecal microbial transfer. Data are shown as mean ± SD and were

statistically compared using one-way ANOVA with Bonferroni *post hoc* where appropriate, or non-parametric Kruskal-Wallis test where appropriate. Data are shown as absolute change from baseline. Each *p*-value is adjusted to account for multiple comparisons. *p*-values shown in bold highlight significant differences.

	VEH (n=10)	ABX (n=8)	VEH-FMT (n=9)	ABX-FMT (n=10)	One-way ANOVA
5% Carbon Dioxide					
Δ f_R (brpm)	14 ± 14	21 ± 19	7 ± 6	10 ± 8	0.131
Δ V_T (ml 100g^{-1})	0.08 ± 0.12	0.09 ± 0.07	0.1 ± 0.05	0.11 ± 0.02	0.988
Δ V_E (ml min^{-1} 100g^{-1})	15 ± 3.9	18 ± 5.3	16 ± 6.8	15 ± 6	0.557
Δ MAP (mmHg)	10 ± 8	5 ± 5	8 ± 6	5 ± 7	0.634
Δ DBP (mmHg)	4 ± 2	4 ± 4	5 ± 3	4 ± 5	0.989
Δ SBP (mmHg)	7 ± 6	6 ± 6	7 ± 5	6 ± 9	0.98
Δ HR (bpm)	-2 ± 9	-8 ± 18	-2 ± 13	-4 ± 9	0.699
10% Carbon Dioxide					
Δ f_R (brpm)	15 ± 20	27 ± 20	6 ± 11	16 ± 12	0.079
Δ V_T (ml 100g^{-1})	0.25 ± 0.12	0.24 ± 0.08	0.26 ± 0.09	0.28 ± 0.05	0.823
Δ V_E (ml min^{-1} 100g^{-1})	32 ± 7.5	38 ± 7.2	32 ± 10.6	36 ± 10.8	0.491
Δ MAP (mmHg)	19 ± 9	14 ± 7	13 ± 7	12 ± 8	0.166
Δ DBP (mmHg)	12 ± 5	14 ± 7	10 ± 4	9 ± 6	0.163
Δ SBP (mmHg)	22 ± 10	16 ± 8	17 ± 8	14 ± 11	0.342
Δ HR (bpm)	8 ± 13	3 ± 27	6 ± 26	2 ± 11	0.917

Appendix Table A.4 Cardiorespiratory responsiveness to hypercapnic chemostimulation in urethane anaesthetised rats

f_R, respiratory frequency (brpm, breaths per min); V_T, tidal volume; V_E, minute ventilation; MAP, mean arterial pressure; DBP, diastolic blood pressure; SBP, systolic blood pressure; HR, heart rate (bpm, beats per min); VEH, autoclaved deionised water; ABX, antibiotic-treated; VEH-FMT, VEH followed by faecal microbial transfer; ABX-FMT, antibiotic administration followed by faecal microbial transfer. Data are shown as mean ± SD and were statistically compared using one-way ANOVA or non-parametric Kruskal-Wallis test, where appropriate. Data are shown as absolute change from baseline.

	VEH (n=9-10)	ABX (n=8)	VEH-FMT (n=9)	ABX-FMT (n=10)	One-way ANOVA
Baseline					
Area under the curve (mV.s)	32 ± 15	28 ± 10	32 ± 18	33 ± 14	0.904
Hypoxia					
Area under the curve (% change from baseline)	-12 ± 12	-12 ± 32	1 ± 16	-5 ± 16	0.162
5% Carbon Dioxide					
Area under the curve (% change from baseline)	6 ± 7	16 ± 14	9 ± 10	15 ± 10	0.138
10% Carbon Dioxide					
Area under the curve (% change from baseline)	29 ± 12	21 ± 12	24 ± 18	20 ± 21	0.623
Hypoxic Hypercapnia					
Area under the curve (% change from baseline)	6 ± 13	-6 ± 14	13 ± 20	9 ± 17	0.119

Appendix Table A.5 Diaphragm EMG activity during baseline and chemostimulation in urethane anaesthetised rats

VEH, autoclaved deionised water; ABX, antibiotic-treated; VEH-FMT, VEH followed by faecal microbial transfer; ABX-FMT, antibiotic administration followed by faecal microbial transfer. Data are shown as mean ± SD and were statistically compared using one-way ANOVA or non-parametric Kruskal-Wallis test, where appropriate.

	VEH (n=10)	ABX (n=7)	VEH-FMT (n=9)	ABX-FMT (n=10)	One-way ANOVA
Baseline					
Δ f_R (brpm)	-42 ± 14	-46 ± 11	-37 ± 19	-40 ± 16	0.668
Δ V_T(ml 100g^{-1})	0.17 ± 0.06	0.19 ± 0.06	0.17 ± 0.1	0.18 ± 0.09	0.917
Δ V_E (ml min^{-1} 100g^{-1})	-7 ± 4	-6 ± 3	-3 ± 7	-5 ± 9	0.730
Δ MAP (mmHg)	-1 ± 7	-6 ± 12	-1 ± 15	2 ± 9	0.561
Δ DBP (mmHg)	2 ± 7	-3 ± 11	1 ± 13	3 ± 8	0.613
Δ SBP (mmHg)	-0 ± 13	-8 ± 13	-2 ± 25	1 ± 16	0.781
Δ HR (bpm)	63 ± 26	71 ± 31	66 ± 35	57 ± 32	0.707

Appendix Table A.6 Cardiorespiratory responses to vagotomy in urethane anaesthetised rats

f_R, respiratory frequency (brpm, breaths per min); V_T, tidal volume; V_E, minute ventilation; MAP, mean arterial pressure; DBP, diastolic blood pressure; SBP, systolic blood pressure; HR, heart rate (bpm, beats per min); VEH, autoclaved deionised water; ABX, antibiotic-treated; VEH-FMT, VEH followed by faecal microbial transfer; ABX-FMT, antibiotic administration followed by faecal microbial transfer. Data are shown as mean ± SD and were statistically compared using one-way ANOVA or non-parametric Kruskal-Wallis test, where appropriate. Data are shown as absolute change from baseline.

	VEH (n=10)	ABX (n=7)	VEH-FMT (n=9)	ABX-FMT (n=10)	One-way ANOVA	VEH vs ABX	VEH-FMT vs ABX-FMT	VEH vs VEH-FMT	ABX vs ABX-FMT	VEH vs ABX-FMT	ABX vs VEH-FMT
Hypoxia											
Δ f_R (bpm)	20 ± 18	9 ± 4	19 ± 6	19 ± 11	**0.041**	0.244	0.999	0.999	**0.039**	0.999	0.129
Δ V_T (ml 100g^{-1})	0.09 ± 0.05	0.12 ± 0.04	0.14 ± 0.08	0.04 ± 0.08	**0.015**	0.999	**0.013**	0.849	0.139	0.417	0.999
Δ V_E (ml min^{-1} 100g^{-1})	16.0 ± 5.3	12.7 ± 3.8	23.0 ± 4.7	13.2 ± 10.7	**0.014**	0.999	**0.027**	0.201	0.999	0.999	**0.034**
Δ MAP (mmHg)	-23 ± 17	-18 ± 7	-27 ± 13	-29 ± 10	0.185	-	-	-	-	-	-
Δ DBP (mmHg)	-19 ± 12	-17 ± 7	-25 ± 11	-26 ± 8	0.241	-	-	-	-	-	-
Δ SBP (mmHg)	-30 ± 27	-23 ± 9	-33 ± 18	-34 ± 14	0.388	-	-	-	-	-	-
Δ HR (bpm)	21 ± 6	12 ± 14	26 ± 7	17 ± 12	**0.037**	0.391	0.243	0.999	0.999	0.999	**0.042**
Hypoxic Hypercapnia											
Δ f_R (brpm)	14 ± 12	9 ± 17	15 ± 7	20 ± 4	0.294	-	-	-	-	-	-
Δ V_T (ml 100g^{-1})	0.19 ± 0.14	0.12 ± 0.15	0.23 ± 0.07	0.18 ± 0.04	0.271	-	-	-	-	-	-
Δ V_E (ml min^{-1} 100g^{-1})	20 ± 15	14 ± 18	25 ± 5	24 ± 4	0.255	-	-	-	-	-	-
Δ MAP (mmHg)	-11 ± 20	-9 ± 22	-17 ± 15	-16 ± 11	0.729	-	-	-	-	-	-
Δ DBP (mmHg)	-9 ± 16	-8 ± 18	-19 ± 6	-15 ± 8	0.296	-	-	-	-	-	-
Δ SBP (mmHg)	-12 ± 29	-9 ± 22	-23 ± 16	-18 ± 12	0.338	-	-	-	-	-	-
Δ HR (bpm)	13 ± 8	4 ± 10	19 ± 7	14 ± 7	**0.007**	0.204	0.999	0.54	0.093	0.999	**0.004**

Appendix Table A.7 Cardiorespiratory responsiveness to hypoxic and hypoxic hypercapnic chemostimulation in urethane anaesthetised vagotomised rats

f_R respiratory frequency (bpm, breaths per min); V_T, tidal volume; V_E, minute ventilation; MAP, mean arterial pressure; DBP, diastolic blood pressure; SBP, systolic blood pressure; HR, heart rate (bpm, beats per min); VEH, autoclaved deionised water; ABX, antibiotic-treated; VEH-FMT, VEH followed by faecal microbial transfer; ABX-FMT, antibiotic administration followed by faecal microbial transfer. Data are shown as mean ± SD and were statistically compared using one-way ANOVA with Bonferroni *post hoc* where appropriate, or non-parametric Kruskal-Wallis test with Dunn's

multiple comparisons test, where appropriate. Data are shown as absolute change from baseline. Each *p*-value is adjusted to account for multiple comparisons. *p*-values shown in bold highlight significant differences.

	VEH (n=10)	ABX (n=7)	VEH-FMT (n=9)	ABX-FMT (n=10)	One-way ANOVA	VEH vs ABX	VEH-FMT vs ABX-FMT	ABX vs ABX-FMT	VEH vs VEH-FMT	VEH vs ABX-FMT	ABX vs VEH-FMT
5% Carbon Dioxide											
Δ f_R (brpm)	2.5 ± 5.4	3.3 ± 3.8	1.3 ± 5.5	4.5 ± 5.4	0.593	-	-	-	-	-	-
Δ V_T (ml 100g^{-1})	0.17 ± 0.17	0.12 ± 0.01	0.11 ± 0.04	0.12 ± 0.04	0.505	-	-	-	-	-	-
Δ V_E (ml min^{-1} 100g^{-1})	8.3 ± 4.6	9.6 ± 3.1	8.1 ± 6.1	8.4 ± 5.8	0.939	-	-	-	-	-	-
Δ MAP (mmHg)	6.8 ± 5.4	5 ± 6.1	13.9 ± 6	5.3 ± 9	0.059	-	-	-	-	-	-
Δ DBP (mmHg)	5.8 ± 2.5	5.1 ± 5.3	9 ± 3.5	5 ± 7.2	0.389	-	-	-	-	-	-
Δ SBP (mmHg)	9.1 ± 5.1	5.7 ± 8.4	15.4 ± 7.4	7.8 ± 12.5	0.147	-	-	-	-	-	-
Δ HR (bpm)	-8.6 ± 6.1	-10.2 ± 4.6	-5.2 ± 7.6	-10.1 ± 6.5	0.201	-	-	-	-	-	-
10% Carbon Dioxide											
Δ f_R (brpm)	2.1 ± 7.4	4.6 ± 3.2	2.3 ± 5.7	5.8 ± 6.6	0.502	-	-	-	-	-	-
Δ V_T (ml 100g^{-1})	0.33 ± 0.18	0.29 ± 0.04	0.26 ± 0.07	0.28 ± 0.07	0.832	-	-	-	-	-	-
Δ V_E (ml min^{-1} 100g^{-1})	16.7 ± 6.4	20.4 ± 2.8	18.0 ± 6.6	17.6 ± 9.3	0.762	-	-	-	-	-	-
Δ MAP (mmHg)	14.4 ± 8.1	11 ± 10.9	29.4 ± 10.5	18.8 ± 11.8	**0.006**	0.999	0.205	0.798	**0.022**	0.999	**0.008**
Δ DBP (mmHg)	11.4 ± 4.8	10.7 ± 10.2	21.8 ± 6.3	16.6 ± 10.1	**0.025**	0.999	0.999	0.878	0.0502	0.921	0.063
Δ SBP (mmHg)	19.6 ± 9.3	12.6 ± 14.4	37.7 ± 14.2	26.4 ± 17.5	**0.007**	0.999	0.546	0.328	0.051	0.999	**0.008**
Δ HR (bpm)	-9.7 ± 7.9	-10.2 ± 6.2	-1.7 ± 9.9	-11 ± 7.9	0.072	-	-	-	-	-	-

Appendix Table A.8 Cardiorespiratory parameter responsiveness to hypercapnic chemostimulation in urethane anaesthetised vagotomised rats

f_R, respiratory frequency (brpm, breaths per min); V_T, tidal volume; V_E, minute ventilation; MAP, mean arterial pressure; DBP, diastolic blood pressure; SBP, systolic blood pressure; HR, heart rate (bpm, beats per min); VEH, autoclaved deionised water; ABX, antibiotic-treated; VEH-FMT, VEH followed

by faecal microbial transfer; ABX-FMT, antibiotic administration followed by faecal microbial transfer. Data are shown as mean ± SD and were statistically compared using one-way ANOVA with Bonferroni *post hoc* or non-parametric Kruskal-Wallis test where appropriate. Data are shown as absolute change from baseline. Each *p*-value is adjusted to account for multiple comparisons. *p*-values shown in bold highlight significant differences.

	VEH (n=10)	ABX (n=7)	VEH-FMT (n=9)	ABX-FMT (n=10)	One-way ANOVA
% change from baseline					
Normoxia					
Area under the curve	32 ± 12	31 ± 15	28 ± 13	27 ± 10	0.788
Hypoxia					
Area under the curve	-7 ± 12	-5 ± 9	5 ± 15	-4 ± 13	0.308
5% Carbon Dioxide					
Area under the curve	1 ± 9	0 ± 7	-1 ± 5	6 ± 11	0.542
10% Carbon Dioxide					
Area under the curve	-3 ± 13	-7 ± 14	-12 ± 8	- 2 ± 8	0.176
Hypoxic Hypercapnia					
Area under the curve	-1 ± 21	-9 ± 10	0 ± 8	-8 ± 15	0.428

Appendix Table A.9 Diaphragm EMG activity and responsiveness to chemostimulation in urethane anaesthetised vagotomised rats

VEH, autoclaved deionised water; ABX, antibiotic-treated; VEH-FMT, VEH followed by faecal microbial transfer; ABX-FMT, antibiotic treated followed by faecal microbial transfer. Data are shown as mean ± SD and were statistically compared using one-way ANOVA or non-parametric Kruskal-Wallis test where appropriate. Responses are expressed as % change from preceding baseline.

	VEH (n=10)	ABX (n=8)	VEH-FMT (n=9)	ABX-FMT (n=10)	One-way ANOVA	VEH vs ABX	VEH-FMT vs ABX-FMT	VEH vs VEH-FMT	ABX vs ABX-FMT	VEH vs ABX-FMT	ABX vs VEH-FMT
L-DOPA (ng/g)	213 ± 245	2394 ± 1258	914 ± 885	1479 ± 392	**0.0001**	**0.0004**	0.618	0.366	0.999	**0.002**	0.138
DA (ng/g)	111 ± 29	103 ± 74	112 ± 29	71 ± 32	0.114	-	-	-	-	-	-
HVA (ng/g)	62 ± 48	155 ± 69	107 ± 56	143 ± 34	**0.002**	**0.007**	0.796	0.358	0.999	**0.007**	0.507
HVA/DA	0.59 ± 0.5	1.3 ± 0.4	1.0 ± 0.7	2.3 ± 1.0	**0.0001**	0.592	**0.002**	0.999	0.066	**0.0001**	0.999
NA (ng/g)	89 ± 58	222 ± 199	343 ± 124	128 ± 149	**0.002**	0.54	**0.012**	**0.004**	0.992	0.999	0.685
5-HT (ng/g)	110 ± 31	134 ± 94	121 ± 50	113 ± 60	0.857	-	-	-	-	-	-
5-HIAA (ng/g)	171 ± 30	193 ± 155	166 ± 33	146 ± 59	0.257	-	-	-	-	-	-
5-HIAA/5-HT	1.6 ± 0.3	1.7 ± 0.6	1.5 ± 0.5	1.4 ± 0.2	0.355	-	-	-	-	-	-

Appendix Table A.10 Cerebellar monoamine neurochemistry

L-DOPA, L-3,4-dihydroxyphenylalaine; DA, dopamine; HVA, homovanillic acid; NA, noradrenaline 5-HT, serotonin; 5-HIAA, 5-hydroxyindole acetic acid; VEH, autoclaved deionised water; ABX, antibiotic administration; VEH-FMT, VEH followed by faecal microbial transfer; ABX-FMT, antibiotic administration followed by faecal microbial transfer. Data are shown as mean ± SD and were statistically compared using one-way ANOVA with Bonferroni *post hoc* where appropriate, or non-parametric Kruskal-Wallis test with Dunn's multiple comparison test, where appropriate. Each *p*-value is adjusted to account for multiple comparisons. *p*-values shown in bold highlight significant differences.

Alpha diversity	VEH	VEH-FMT	p-value	(1/m)*Q
Observed species	836.5 (90.5)	891.0 (101.3)	0.035	0.013
Chao1	864.9 (84.2)	918.7 (93.3)	0.043	0.027
Shannon	6.9 (0.45)	7.1 (0.27)	0.063	0.053
Simpson	0.978 (0.01)	0.982 (0.01)	0.218	0.067
PD whole tree	43.6 (2.6)	47.0 (4.3)	0.004	0.007 $

Appendix Table A.11 Alpha diversity indices in caecal samples from VEH and VEH-FMT rats

VEH, autoclaved deionised water; VEH-FMT, VEH followed by faecal microbial transfer. Data are shown as median (IQR) and were statistically compared using unpaired non-parametric Mann-Whitney *U* test and Benjamini-Hochberg adjustment procedure with Q = 0.1 used to correct *p* values for multiple testing. $ indicates an increase in VEH-FMT.

Alpha diversity	VEH	ABX-FMT	p-value	(1/m)*Q
Observed species	836.5 (90.5)	893.0 (116.0)	0.052	0.047
Chao1	864.9 (84.2)	927.3 (114.5)	0.052	0.027
Shannon	6.9 (0.45)	7.15 (0.18)	0.043	0.02
Simpson	0.978 (0.01)	0.934 (0.01)	0.123	0.06
PD whole tree	43.6 (2.6)	45.8 (4.65)	0.052	0.04

Appendix Table A.12 Alpha diversity indices in caecal samples from VEH and ABX-FMT rats

VEH, autoclaved deionised water; ABX-FMT, antibiotic administration followed by faecal microbial transfer. Data are shown as median (IQR) and were statistically compared using unpaired non-parametric Mann-Whitney *U* test and Benjamini-Hochberg adjustment procedure with Q = 0.1 used to correct *p* values for multiple testing.

Alpha diversity	VEH-FMT	ABX-FMT	p-value	(i/m)*Q
Observed species	891.0 (101.3)	893.0 (116.0)	0.684	0.087
Chao1	918.7 (93.3)	927.3 (114.5)	0.971	0.1
Shannon	7.1 (0.27)	7.15 (0.18)	0.684	0.08
Simpson	0.982 (0.01)	0.934 (0.01)	0.739	0.093
PD whole tree	47.0 (4.3)	45.8 (4.65)	0.529	0.073

Appendix Table A.13 Alpha diversity indices in caecal samples from VEH-FMT and ABX-FMT rats

VEH-FMT, VEH followed by faecal microbiota transfer; ABX-FMT, antibiotic administration followed by faecal microbial transfer. Data are shown as median (IQR) and were statistically compared using unpaired non-parametric Mann-Whitney *U* test and Benjamini-Hochberg adjustment procedure with Q = 0.1 used to correct *p* values for multiple testing.

Phylum	VEH	VEH-FMT	p-value	(i/m)*Q
Proteobacteria	2.55 (2.426)	7.087 (1.607)	0.000	0.011 $
Bacteroidetes	29.739 (1.847)	25.166 (3.665)	0.000	0.004 $
Cyanobacteria	0.628 (0.726)	1.396 (0.731)	0.015	0.022 $
Deferribacteres	0.139 (0.301)	0.0 (0.002)	0.000	0.007 $
Verrucomicrobia	0.041 (0.149)	0.313 (1.67)	0.105	0.044
Firmicutes	65.518 (2.475)	64.799 (3.288)	0.143	0.048
Actinobacteria	0.131 (0.177)	0.136 (0.139)	0.481	0.074
Saccharibacteria	0.419 (0.49)	0.354 (0.207)	0.529	0.529
Tenericutes	0.360 (0.482)	0.363 (0.26)	0.631	0.631
No blast hit	0.085 (0.076)	0.050 (0.072)	0.684	0.100

Appendix Table A.14 Relative abundance (%) of bacterial phyla in caecal samples from VEH and VEH-FMT rats

VEH, autoclaved deionised water; VEH-FMT, VEH followed by faecal microbial transfer. Data are shown as median (IQR) and were statistically compared using unpaired non-parametric Mann-Whitney *U* test and Benjamini-Hochberg adjustment procedure with Q = 0.1 used to correct *p* values for multiple testing. $ indicates an increase or decrease in the relative abundance of bacterial taxa in VEH-FMT.

Phylum	VEH	ABX-FMT	p-value	(i/m)*Q
Proteobacteria	2.55 (2.426)	7.392 (1.628)	0.000	0.019 &
Bacteroidetes	29.739 (1.847)	27.723 (7.062)	0.023	0.03 &
Cyanobacteria	0.628 (0.726)	1.428 (1.335)	0.015	0.026 &
Deferribacteres	0.139 (0.301)	0 (0.0002)	0.000	0.015 &
Verrucomicrobia	0.041 (0.149)	0.064 (0.156)	0.71	0.17
Firmicutes	65.518 (2.475)	61.676 (8.674)	0.143	0.052
Actinobacteria	0.131 (0.177)	0.098 (0.140)	0.28	0.063
Saccharibacteria	0.419 (0.49)	0.582 (0.360)	0.315	0.067
Tenericutes	0.360 (0.482)	0.569 (1.325)	0.089	0.041
No blast hit	0.085 (0.076)	0.081 (0.066)	0.971	0.1

Appendix Table A.15 Relative abundance (%) of bacterial phyla in caecal samples from VEH and ABX-FMT rats

VEH, autoclaved deionised water; ABX-FMT, antibiotics followed by faecal microbial transfer. Data are shown as median (IQR) and were statistically compared using unpaired non-parametric Mann-Whitney *U* test and Benjamini-Hochberg adjustment procedure with Q = 0.1 used to correct *p* values for multiple testing.

Phylum	VEH-FMT	ABX-FMT	p-value	(i/m)*Q
Proteobacteria	7.087 (1.607)	7.392 (1.628)	0.912	0.1
Bacteroidetes	25.166 (3.665)	27.723 (7.062)	0.393	0.07
Cyanobacteria	1.396 (0.731)	1.428 (1.335)	0.853	0.096
Deferribacteres	0 (0.002)	0 (0.0002)	0.684	0.089
Verrucomicrobia	0.313 (1.67)	0.064 (0.156)	0.029	0.037 ¥
Firmicutes	64.799 (3.288)	61.676 (8.674)	0.218	0.056
Actinobacteria	0.136 (0.139)	0.098 (0.140)	0.684	0.085
Saccharibacteria	0.354 (0.207)	0.582 (0.360)	0.023	0.033 ¥
Tenericutes	0.363 (0.26)	0.569 (1.325)	0.218	0.059
No blast	0.050 (0.072)	0.081 (0.066)	0.634	0.1

Appendix Table A.16 Relative abundance (%) of bacterial phyla in caecal samples from VEH-FMT and ABX-FMT rats

VEH-FMT, VEH followed by faecal microbial transfer; ABX-FMT, antibiotics followed by faecal microbial transfer. Data are shown as median (IQR) and were statistically compared using unpaired non-parametric Mann-Whitney *U* test and Benjamini-Hochberg adjustment procedure with Q = 0.1 used to correct p values for multiple testing. ¥ indicates an increase or decrease in the relative abundance of bacterial taxa in VEH-FMT.

Family	VEH	VEH-FMT	p-value	(i/m) *Q
Actinobacteria				
Bifidobacteriaceae *(Bifidobacteriales)*	0.024 (0.137)	0.044 (0.584)	0.631	0.073
Nocardiaceae *(Corynebacteriales)*	0.003 (0.004)	0.0008 (0.002)	0.123	0.03
Micrococcaceae *(Micrococcales)*	0.002 (0.009)	0.007 (0.011)	0.315	0.046
Coriobacteriaceae *(Coriobacteriales)*	0.091 (0.092)	0.042 (0.099)	0.247	0.041
Bacteroidetes				
Bacteroidetes VC2.1 Bac22 *(Uncultured bacterium)*	0.0 (0.0)	0.116 (0.081)	0.000	0.001 $
Bacteroidaceae *(Bacteroidales)*	1.656 (1.139)	1.820 (0.885)	0.971	0.093
Porphyromonadaceae *(Bacteroidales)*	0.387 (0.235)	0.388 (0.327)	0.529	0.066
Prevotellaceae *(Bacteroidales)*	5.504 (3.486)	6.082 (3.709)	0.631	0.074
Rikenellaceae *(Bacteroidales)*	3.555 (3.251)	1.961 (1.097)	0.089	0.025
S24-7 *(Bacteroidales)*	17.898 (3.667)	14.416 (2.940)	0.004	0.01 $
Rat ANO60301C *(Bacteroidales)*	0.0 (0.003)	0.0 (0.0004)	0.393	0.057
Cyanobacteria				
Uncultured bacterium *(Gastranaerophilales)*	0.627 (0.724)	0.837 (0.685)	0.19	0.035
Uncultured organism *(Gastranaerophilales)*	0 (0.0006)	0.491 (0.893)	0.000	0.001 $
Deferribacteres				
Deferribacteraceae *(Deferribacterales)*	0.139 (0.301)	0 (0.002)	0.000	0.002 $
Firmicutes				
Bacillaceae *(Bacillales)*	0.13 (0.279)	0 (0.0)	0.000	0.003 $
Streptococcaceae *(Lactobacillales)*	0.004 (0.004)	0.003 (0.005)	0.912	0.091
Aerococcaceae *(Lactobacillales)*	0.006 (0.002)	0.001 (0.003)	0.529	0.067
Lactobacillaceae *(Lactobacillales)*	2.318 (3.128)	2.949 (2.691)	0.481	0.063
Caldicoprobacteraceae *(Clostridiales)*	0.015 (0.019)	0.03 (006)	0.105	0.027
Christensenellaceae *(Clostridiales)*	0.039 (0.089)	0.058 (0.039)	0.143	0.086
Clostridiaceae 1 *(Clostridiales)*	0.117 (0.371)	0.24 (0.635)	0.143	0.031
Clostridiales vadinBB60 group *(Clostridiales)*	1.746 (1.299)	3.016 (1.631)	0.001	0.008 $
Defluviitaleaceae *(Clostridiales)*	0.004 (0.008)	0.004 (0.011)	0.631	0.075
Eubacteriaceae *(Clostridiales)*	0 (0)	0 (0.001)	0.315	0.047
Family XIII *(Clostridiales)*	0.121 (0.066)	0.097 (0.028)	0.190	0.036
Lachnospiraceae *(Clostridiales)*	34.595 (7.196)	35.788 (5.362)	0.684	0.079
Peptococcaceae *(Clostridiales)*	0.431 (0.328)	0.387 (0.187)	0.579	0.07

Peptostreptococcaceae *(Clostridiales)*	0.676 (1.24)	0.950 (0.731)	0.436	0.059
Ruminococcaceae *(Clostridiales)*	21.85 (6.573)	19.23 (4.245)	0.075	0.022
Erysipelotrichaceae *(Erysipelotrichales)*	0.31 (0.23)	0.391 (0.357)	0.393	0.057
Proteobacteria				
Rhodospirillaceae *(Rhodospirillales)*	0.236 (0.38)	0.446 (0.198)	0.123	0.03
Mitochondria *(Rickettsiales)*	0 (0.001)	0 (0.0002)	0.481	0.064
Alcaligenaceae *(Burkholderiales)*	0.039 (0.094)	0.01 (0.011)	0.005	0.011 $
Burkholderiaceae *(Burkholderiales)*	0 (0)	0 (0.001)	0.393	0.058
Desulfovibrionaceae *(Desulfovibrionales)*	1.84 (2.289)	2.432 (1.405)	0.247	0.041
Helicobacteraceae *(Camplylobacterales)*	0.002 (0.003)	4.226 (1.378)	0.000	0.004 $
Enterobacteriaceae *(Enterobacteriales)*	0.004 (0.002)	0.001 (0.003)	0.007	0.012 $
Pasteurellaceae *(Pasteurellales)*	0.0008 (0.013)	0.003 (0.006)	0.971	0.093
Saccharibacteria				
Unknown family *(Unknown order)*	0.419 (0.490)	0.354 (0.207)	0.529	0.067
Tenericutes				
Anaeroplasmataceae *(Anaeroplasmatales)*	0.083 (0.277)	0.217 (0.185)	0.247	0.042
Uncultured Mollicutes bacterium *(Mollicutes)*	0 (0.001)	0 (0.002)	0.631	0.075
Uncultured bacterium *(Mollicutes RF9)*	0.062 (0.033)	0.078 (0.064)	0.529	0.068
Uncultured rumen bacteria *(Mollicutes RF9)*	0.112 (0.242)	0.073 (0.079)	0.971	0.094
Unidentified Mollicutes *(Mollicutes RF9)*	0.001 (0.003)	0.002 (0.003)	0.353	0.051
Uncultured Bacillales bacterium *(Mollicutes)*	0.012 (0.042)	0.034 (0.100)	0.218	0.04
Verrucomicrobia				
Verrucomicrobiaceae *(Verrucomicrobiales)*	0.041 (0.149)	0.313 (1.167)	0.105	0.028

Appendix Table A.17 Relative abundance (%) of bacterial families in caecal samples from VEH and VEH-FMT rats

VEH, autoclaved deionised water; VEH-FMT, VEH followed by faecal microbial transfer. Data are shown as median (IQR) and were statistically compared using unpaired non-parametric Mann-Whitney *U* test and Benjamini-Hochberg adjustment procedure with Q = 0.1 used to correct p values for multiple testing. $ indicates an increase or decrease in the relative abundance of bacterial taxa in VEH-FMT.

Family	VEH	ABX-FMT	p-value	(i/m) *Q
Actinobacteria				
Bifidobacteriaceae ***(Bifidobacteriales)***	0.024 (0.137)	0.053 (0.119)	0.28	0.044
Nocardiaceae ***(Corynebacteriales)***	0.003 (0.004)	0.003 (0.004)	0.739	0.082
Micrococcaceae ***(Micrococcales)***	0.002 (0.009)	0.001 (0.004)	0.436	0.06
Coriobacteriaceae ***(Coriobacteriales)***	0.091 (0.092)	0.036 (0.024)	0.003	0.009 &
Bacteroidetes				
Bacteroidaceae ***(Bacteroidales)***	1.656 (1.139)	2.166 (1.539)	0.315	0.048
Bacteroidetes VC2.1 Bac22 ***(Uncultured bacterium)***	0.0 (0.0)	0.1 (0.062)	0.000	0.004 &
Porphyromonadaceae ***(Bacteroidales)***	0.387 (0.235)	0.462 (0.128)	0.436	0.061
Prevotellaceae ***(Bacteroidales)***	5.504 (3.486)	3.306 (3.762)	0.075	0.022
Rikenellaceae ***(Bacteroidales)***	3.555 (3.251)	2.535 (0.804)	0.315	0.08
S24-7 ***(Bacteroidales)***	17.898 (3.667)	17.381 (3.995)	0.353	0.052
Rat ANO60301C ***(Bacteroidales)***	0.0 (0.003)	0.0009 (0.003)	0.912	0.091
Cyanobacteria				
Uncultured bacterium ***(Gastranaerophilales)***	0.627 (0.724)	1.396 (1.062)	0.035	0.029
Uncultured organism ***(Gastranaerophilales)***	0 (0.0006)	0.111 (0.442)	0.000	0.005 &
Deferribacteres				
Deferribacteraceae ***(Deferribacterales)***	0.139 (0.301)	0.0 (0.0002)	0.000	0.06 &
Firmicutes				
Bacillaceae ***(Bacillales)***	0.13 (0.279)	0.0 (0.0)	0.000	0.007 &
Streptococcaceae ***(Lactobacillales)***	0.004 (0.004)	0.001 (0.002)	0.007	0.013 &
Aerococcaceae ***(Lactobacillales)***	0.006 (0.002)	0.0 (0.002)	0.631	0.076
Lactobacillaceae ***(Lactobacillales)***	2.318 (3.128)	1.399 (1.76)	0.19	0.036
Caldicoprobacteraceae ***(Clostridiales)***	0.015 (0.019)	0.023 (0.023)	0.105	0.028
Christensenellaceae ***(Clostridiales)***	0.039 (0.892)	0.088 (0.086)	0.353	0.052
Clostridiaceae 1 ***(Clostridiales)***	0.117 (0.371)	0.14 (0.469	0.436	0.062
Clostridiales vadinBB60 group ***(Clostridiales)***	1.746 (1.299)	3.857 (3.605)	0.0009	0.014 &
Defluviitaleaceae ***(Clostridiales)***	0.004 (0.008)	0.008 (0.012)	0.579	0.07
Eubacteriaceae ***(Clostridiales)***	0 (0)	0 (0)	0.739	0.083
Family XIII ***(Clostridiales)***	0.121 (0.066)	0.115 (0.052)	0.481	0.064
Lachnospiraceae ***(Clostridiales)***	34.595 (7.196)	28.987 (10.732)	0.143	0.032
Peptococcaceae ***(Clostridiales)***	0.431 (0.328)	0.425 (0.142)	0.796	0.086
Peptostreptococcaceae ***(Clostridiales)***	0.676 (1.244)	0.351 (0.784)	0.481	0.065
Ruminococcaceae ***(Clostridiales)***	21.849 (6.573)	22.66 (4.94)	0.912	0.092
Erysipelotrichaceae ***(Erysipelotrichales)***	0.31 (0.23)	0.208 (0.238)	0.796	0.087
Proteobacteria				
Rhodospirillaceae ***(Rhodospirillales)***	0.236 (0.38)	0.36 (0.243)	0.247	0.043

Mitochondria *(Rickettsiales)*	0 (0.001)	0 (0.0004)	0.579	0.071
Alcaligenaceae *(Burkholderiales)*	0.039 (0.094)	0.048 (0.094)	0.971	0.095
Burkholderiaceae *(Burkholderiales)*	0 (0)	0.0008 (0.003)	0.052	0.021
Desulfovibrionaceae *(Desulfovibrionales)*	1.84 (2.289)	3.273 (1.256)	0.023	0.014
Helicobacteraceae *(Camplylobacterales)*	0.002 (0.003)	3.514 (1.354)	0.000	0.007 &
Enterobacteriaceae *(Enterobacteriales)*	0.004 (0.002)	0.002 (0.005)	0.19	0.037
Pasteurellaceae *(Pasteurellales)*	0.0008 (0.013)	0.002 (0.007)	1.000	0.099
Saccharibacteria				
Unknown family *(Unknown order)*	0.419 (0.490)	0.582 (0.360)	0.315	0.049
Tenericutes				
Anaeroplasmataceae *(Anaeroplasmatales)*	0.083 (0.277)	0.181 (1.059)	0.19	0.038
Uncultured Moliicutes bacterium *(Mollicutes)*	0 (0.001)	0 (0.0005)	0.85	0.089
Uncultured bacterium *(Mollicutes RF9)*	0.062 (0.033)	0.095 (0.093)	0.315	0.08
Uncultured rumen bacteria *(Mollicutes RF9)*	0.112 (0.242)	0.128 (0.321)	0.579	0.072
Unidentified Mollicutes *(Mollicutes RF9)*	0.001 (0.003)	0.002 (0.002)	0.28	0.045
Uncultured Bacillales bacterium *(Mollicutes)*	0.012 (0.042)	0.029 (0.071)	0.19	0.05
Verrucomicrobia				
Verrucomicrobiaceae *(Verrucomicrobiales)*	0.041 (0.149)	0.064 (0.156)	0.739	0.083

Appendix Table A.18 Relative abundance (%) of bacterial families in caecal samples from VEH and ABX-FMT rats

VEH, autoclaved deionised water; ABX-FMT, antibiotics followed by faecal microbial transfer. Data are shown as median (IQR) and were statistically compared using unpaired non-parametric Mann-Whitney *U* test and Benjamini-Hochberg adjustment procedure with Q = 0.1 used to correct *p* values for multiple testing. & indicates an increase or decrease in the relative abundance of bacterial taxa in VEH-FMT.

Family	VEH-FMT	ABX-FMT	p-value	(i/m)*Q
Actinobacteria				
Bifidobacteriaceae ***(Bifidobacteriales)***	0.044 (0.584)	0.053 (0.119)	0.796	0.088
Nocardiaceae ***(Corynebacteriales)***	0.0008 (0.002)	0.003 (0.004)	0.075	0.023
Micrococcaceae ***(Micrococcales)***	0.007 (0.011)	0.001(0.004)	0.035	0.019
Coriobacteriaceae ***(Coriobacteriales)***	0.042 (0.099)	0.036 (0.024)	0.315	0.051
Bacteroidetes				
Bacteroidetes VC2.1 Bac22 ***(Uncultured bacterium)***	0.116 (0.081)	0.1 (0.062)	0.853	0.09
Bacteroidaceae ***(Bacteroidales)***	1.820 (0.885)	2.166 (1.539)	0.353	0.052
Porphyromonadaceae ***(Bacteroidales)***	0.388 (0.327)	0.462 (0.128)	0.971	0.096
Prevotellaceae ***(Bacteroidales)***	6.082 (3.709)	3.306 (3.762)	0.247	0.043
Rikenellaceae ***(Bacteroidales)***	1.961 (1.097)	2.535 (0.804)	0.353	0.054
S24-7 ***(Bacteroidales)***	14.416 (2.940)	17.381 (3.995)	0.043	0.02
Rat ANO60301C ***(Bacteroidales)***	0.0 (0.0004)	0.0009 (0.003)	0.143	0.033
Cyanobacteria				
Uncultured bacterium ***(Gastranaerophilales)***	0.837 (0.685)	1.396 (1.062)	0.19	0.039
Uncultured organism ***(Gastranaerophilales)***	0.491 (0.893)	0.111 (0.442)	0.089	0.026
Deferribacteres				
Deferribacteraceae ***(Deferribacterales)***	0 (0.002)	0.0 (0.0002)	0.684	0.08
Firmicutes				
Bacillaceae ***(Bacillales)***	0 (0.0)	0.0 (0.0)	1.00	0.099
Streptococcaceae ***(Lactobacillales)***	0.003 (0.005)	0.001 (0.002)	0.003	0.009 ¥
Aerococcaceae ***(Lactobacillales)***	0.001 (0.003)	0.0 (0.002)	0.393	0.059
Lactobacillaceae ***(Lactobacillales)***	2.949 (2.691)	1.399 (1.76)	0.075	0.024
Caldicoprobacteraceae ***(Clostridiales)***	0.03 (006)	0.023 (0.023)	0.796	0.088
Christensenellaceae ***(Clostridiales)***	0.058 (0.039)	0.088 (0.086)	0.143	0.033
Clostridiaceae 1 ***(Clostridiales)***	0.240 (0.635)	0.14 (0.469)	0.353	0.055
Clostridiales vadinBB60 group ***(Clostridiales)***	3.016 (1.631)	3.857 (3.605)	0.971	0.096
Defluviitaleaceae ***(Clostridiales)***	0.00 (0.011)	0.008 (0.012)	0.971	0.097
Eubacteriaceae ***(Clostridiales)***	0 (0.001)	0 (0)	0.143	0.034
Family XIII ***(Clostridiales)***	0.097 (0.028)	0.115 (0.052)	0.28	0.046
Lachnospiraceae ***(Clostridiales)***	35.788 (5.362)	28.987 (10.732)	0.029	0.017
Peptococcaceae ***(Clostridiales)***	0.387 (0.187)	0.425 (0.142)	0.684	0.08
Peptostreptococcaceae ***(Clostridiales)***	0.95 (0.731)	0.351 (0.784)	0.023	0.015
Ruminococcaceae ***(Clostridiales)***	19.23 (4.245)	22.66 (4.94)	0.035	0.02
Erysipelotrichaceae ***(Erysipelotrichales)***	0.391 (0.357)	0.208 (0.238)	0.436	0.062
Proteobacteria				
Rhodospirillaceae ***(Rhodospirillales)***	0.446 (0.198)	0.36 (0.243)	0.631	0.077
Mitochondria ***(Rickettsiales)***	0 (0.0002)	0 (0.0004)	1.000	1.00

Alcaligenaceae *(Burkholderiales)*	0.01 (0.011)	0.048 (0.094)	0.005	0.012 ¥
Burkholderiaceae *(Burkholderiales)*	0 (0.001)	0.0008 (0.003)	0.353	0.056
Desulfovibrionaceae *(Desulfovibrionales)*	2.432 (1.405)	3.273 (1.256)	0.075	0.025
Helicobacteraceae *(Camplylobacterales)*	4.226 (1.378)	3.514 (1.354)	0.105	0.029
Enterobacteriaceae *(Enterobacteriales)*	0.001 (0.003)	0.002 (0.005)	0.631	0.078
Pasteurellaceae *(Pasteurellales)*	0.003 (0.006)	0.002 (0.007)	0.6484	0.08
Saccharibacteria				
Unknown family *(Unknown order)*	0.354 (0.207)	0.582 (0.360)	0.023	0.016
Tenericutes				
Anaeroplasmataceae *(Anaeroplasmatales)*	0.217 (0.195)	0.181 (1.059)	0.739	0.084
Uncultured Mollicutes bacterium *(Mollicutes)*	0 (0.002)	0 (0.0005)	0.529	0.069
Uncultured bacterium *(Mollicutes RF9)*	0.078 (0.064)	0.095 (0.093)	0.579	0.072
Uncultured rumen bacteria *(Mollicutes RF9)*	0.073 (0.079)	0.128 (0.321)	0.631	0.078
Unidentified Mollicutes *(Mollicutes RF9)*	0.002 (0.003)	0.002 (0.002)	0.971	0.098
Uncultured Bacillales bacterium *(Mollicutes)*	0.002 (0.003)	0.029 (0.071)	0.739	0.085
Verrucomicrobia				
Verrucomicrobiaceae *(Verrucomicrobiales)*	0.313 (1.167)	0.064 (0.156)	0.029	0.017

Appendix Table A.19 Relative abundance (%) of bacterial families in caecal samples from VEH-FMT and ABX-FMT rats

VEH-FMT, VEH followed by faecal microbial transfer; ABX-FMT, antibiotics followed by faecal microbial transfer. Data are shown as median (IQR) and were statistically compared using unpaired non-parametric Mann-Whitney *U* test and Benjamini-Hochberg adjustment procedure with Q = 0.1 used to correct p values for multiple testing. ¥ indicates an increase or decrease in the relative abundance of bacterial taxa in VEH-FMT.

Genus	VEH	VEH-FMT	p-value	(i/m)* Q
Bifidobacteriaceae (Bifidobacteriales, Actinobacteria)				
Bifidobacterium	0.024 (0.137)	0.044 (0.058)	0.631	0.07
Coriobacteriaceae (Coriobacteriales, Actinobacteria)				
Uncultured Coriobacteriaceae	0.035 (0.036)	0.007 (0.015)	0.003	0.005 $
Uncultured bacterium (Unknown order, Bacteroidetes)				
Bacteroidetes VC21 Bac22 uncultured bacterium	0 (0)	0.116 (0.081)	0.000	0.000 $
Bacteroidaceae (Bacteroidales, Bacteroidetes)				
Bacteroides	1.656 (1.138)	1.182 (0.885)	0.971	0.094
Bacteroidales S24-7 group (Bacteroidales, Bacteroidetes)				
Uncultured bacterium	17.13 (2.798)	14.372 (2.949)	0.004	0.006 $
unidentified	0.161 (0.933)	0.067 (0.059)	0.063	0.018
Porphyromonadaceae (Bacteroidales, Bacteroidetes)				
Odoribacter	0.360 (0.212)	0.296 (0.289)	0.796	0.084
Parabacteroides	0.046 (0.042)	0.099 (0.07)	0.011	0.009
Prevotellaceae (Bacteroidales, Bacteroidetes)				
Alloprevotella	1.594 (2.192)	0.748 (1.639)	0.123	0.026
Prevotellaceae NK3B31 group	1.715 (2.18)	2.017 (2.704)	0.631	0.07
Prevotellaceae UCG-001	1.743 (2.486)	2.134 (2.167)	0.393	0.051
Rikenellaceae (Bacteroidales, Bacteroidetes)				
Alistipes	3.555 (3.252)	1.961 (1.097)	0.089	0.022
Uncultured bacterium (Gastranaerophilales, Cyanobacteria)				
Uncultured bacterium	0.627 (0.725)	0.837 (0.685)	0.19	0.032
Uncultured organism	0 (0.006)	0.491 (0.893)	0.000	0.000 $
Deferribacteraceae (Deferribacterales, Deferribacteres)				
Mucispirillum	0.139 (0.301)	0 (0.002)	0.000	0.001 $
Bacillaeae (Bacillales, Firmicutes)				
Bacillus	0.13 (0.279)	0 (0)	0.000	0.001 $
Lactobacillaceae (Lactobacillales, Firmicutes)				
Lactobacillus	2.318 (3.128)	1.441 (2.691)	0.481	0.059
Caldicoprobacteraceae *(Clostridiales, Firmicutes)*				
Caldicoprobacter	0.015 (0.019)	0.0297 (0.056)	0.105	0.023
Christensenellaceae (Clostridiales, Firmicutes)				
Christensenellaceae R-7 group	0.031 (0.074)	0.046 (0.045)	0.912	0.091
Clostridiaceae 1 (Clostridiales, Firmicutes)				
Clostridium sensu stricto 1	0.116 (0.371)	0.238 (0.065)	0.143	0.028
Clostridiales vadin BB60 group (Clostridiales, Firmicutes)				
Uncultured clostridiales bacterium	0.004 (0.036)	0.045 (0.022)	0.029	0.012
Uncultured bacterium	1.317 (1.181)	2.147 (0.811)	0.002	0.004 $
Uncultured rumen bacterium	0.058 (0.096)	0.021 (0.048)	0.19	0.032

Unidentified	0.126 (0.341)	0.756 (1.352)	0.003	0.005 $
Family XIII (Clostridiales, Firmicutes)				
Anaerovorax	0.055 (0.046)	0.038 (0.013)	0.123	0.027
Lachnospiraceae (Clostridiales, Firmicutes)				
Blautia	0.07 (0.252)	0.566 (1.207)	0.052	0.016
Coprococcus 1	0.125 (0.063)	0.127 (0.06)	0.631	0.071
Coprococcus 2	0.178 (0.462)	0.011 (0.207)	0.075	0.02
Incertae Sedis	1.398 (1.351)	0.913 (0.926)	0.165	0.03
Lachnoclostridium	0.121 (0.07)	0.124 (0.040)	0.971	0.095
Lachnoclostridium 10	0.0 (0)	0.133 (0.362)	0.000	0.001 $
Lachnospiraceae NC2004 group	0.586 (1.377)	0.4 (0.391)	0.481	0.06
Lachnospiraceae NK4A136 group	22.823 (5.829)	19.789 (5.348)	0.089	0.022
Lachnospiraceae NK4B4 group	0.01 (0.116)	0.003 (0.016)	0.529	0.062
Lachnospiraceae UCG-0001	0.168 (0.195)	0.303 (0.354)	0.075	0.02
Lachnospiraceae UCG-0005	0.067 (0.088)	0.103 (0.088)	0.631	0.071
Lachnospiraceae UCG-0006	0.281 (0.218)	0.254 (0.268)	0.739	0.076
Lachnospiraceae UCG-008	0.081 (0.113)	0.009 (0.014)	0.000	0.001 $
Roseburia	0.913 (0.649)	1.798 (1.915)	0.105	0.024
Shuttleworthia	0.024 (0.036)	0.015 (0.027)	0.912	0.091
Tyzzerella	0.207 (0.19)	0.117 (0.059)	0.007	0.008 $
Lachnospiraceae [Eubacterium] oxidoreducens group	0.262 (0.278)	0.292 (0.355)	0.481	0.06
Lachnospiraceae [Eubacterium] ruminantium group	0.185 (0.276)	0.035 (0.363)	0.739	0.08
Lachnospiraceae uncultured	5.073 (4.202)	9.821 (5.779)	0.005	0.006 $
Peptococcaceae (Clostridiales, Firmicutes)				
Peptococcaceae (uncultured)	0.352 (0.312)	0.325 (0.1)	0.436	0.055
Peptococcus	0.079 (0.029)	0.085 (0.083)	0.631	0.071
Peptostreptococcaceae (Clostridiales, Firmicutes)				
Intestinibacter	0.092 (0.499)	0.046 (0.093)	0.853	0.088
Peptoclostridium	0.46 (0.906)	0.626 (0.767)	0.28	0.04
Ruminococcaceae (Clostridiales, Firmicutes)				
Anaerotruncus	0.929 (0.248)	0.764 (0.17)	0.029	0.012
Flavonifractor	0.003 (0.01)	0.065 (0.169)	0.005	0.007 $
Intestinimonas	0.064 (0.04)	0.026 (0.015)	0.011	0.009
Oscillibacter	0.908 (0.281)	0.586 (0.175)	0.019	0.01
Papillibacter	0.071 (0.188)	0.161 (0.247)	0.247	0.037

Ruminoclostridium	0.084 (0.836)	0.152 (0.094)	0.043	0.015
Ruminoclostridium 5	0.343 (0.175)	0.407 (0.27)	0.218	0.035
Ruminoclostridium 6	0.723 (0.781)	1.0 (0.9)	0.853	0.088
Ruminoclostridium 9	3.962 (1.396)	2.305 (0.576)	0.002	0.005 $
Ruminococcaceae NK4A214 group	0.239 (0.146)	0.234 (0.094)	0.971	0.095
Ruminococcaceae UCG-003	1.392 (1.069)	1.429 (0.472)	0.853	0.089
Ruminococcaceae UCG-005	0.324 (0.247)	0.417 (0.313)	0.393	0.052
Ruminococcaceae UCG-009	0.081 (0.043)	0.083 (0.029)	0.796	0.085
Ruminococcaceae UCG-010	0.282 (0.208)	0.418 (0.26)	0.143	0.029
Ruminococcaceae UCG-011	0 (0)	0.002 (0.003)	0.015	0.01
Ruminococcaceae UCG-013	0.067 (0.059)	0.204 (0.15)	0.001	0.004 $
Ruminococcaceae UCG-014	1.134 (0.706)	0.945 (0.78)	0.739	0.08
Ruminococcus 1	2.6 (1.577)	2.412 (3.09)	0.912	0.092
Ruminococcus 2	0.093 (0.114)	0.082 (0.045)	0.912	0.092
[Eubacterium] coprostanoligenes group	1.339 (1.0)	0.963 (1.529)	0.436	0.056
Ruminococcaceae uncultured	7.016 (3.051)	5.734 (2.825)	0.043	0.015
Erysipelotrichaceae (Erysipelotrichales, Firmicutes)				
Turicibacter	0.206 (0.216)	0.297 (0.295)	0.393	0.052
Erysipelotrichaceae uncultured	0.019 (0.088)	0.011 (0.017)	0.481	0.061
Rhodospirillaceae (Rhodospirillales, Proteobacteria)				
Thalassospira	0.236 (0.415)	0.361 (0.186)	0.19	0.033
Alcaligenaceae (Burkholderiales, Proteobacteria)				
Parasutterella	0.039 (0.094)	0.01 (0.011)	0.0005	0.007 $
Desulfovibrionaceae (Deltaproteobacteria, Proteobacteria)				
Bilophila	0.089 (0.327)	0.171 (0.128)	0.579	0.066
Desulfovibrio	1.753 (2.685)	2.262 (1.294)	0.353	0.048
Helicobacteraceae (Campylobacterales, Proteobacteria)				
Helicobacter	0.002 (0.003)	4.226 (1.378)	0.000	0.002 $
Enterobacteriaceae (Enterobacteriales, Proteobacteria)				
Enterobacter	0.004 (0.003)	0 (0.002)	0.004	0.006 $
Unknown Family (Unknown order, Saccharibacteria)				
Candidatus Saccharimonas	0.419 (0.49)	0.354 (0.207)	0.529	0.063
Anaeroplasmataceae (Anaeroplasmatales, Tenericutes)				
Anaeroplasma	0.083 (0.277)	0.217 (0.195)	0.247	0.037
Uncultured bacterium, (Mollicutes RF9, Tenericutes)				
Uncultured bacterium	0.062 (0.033)	0.078 (0.064)	0.529	0.064
Uncultured rumen bacterium (Mollicutes RF9, Tenericutes)				

Uncultured rumen bacterium	0.112 (0.242)	0.073 (0.079)	0.971	0.096
Uncultured Bacillales bacterium (NB1-n, Tenericutes)				
Uncultured Bacillales bacterium	0.012 (0.042)	0.034 (0.1)	0.218	0.035
Verrucomicrobiaceae (Verrucomicrobiales, Verrucomicrobia)				
Akkermansia	0.041 (0.149)	0.313 (1.167)	0.105	0.024

Appendix Table A.20 Relative abundance (%) of bacterial genera in the caecal samples from VEH and VEH-FMT rats

VEH, autoclaved deionised water; VEH-FMT, VEH followed by faecal microbial transfer. Data in these tables are the top 45% of genera plus genera with raw $p<0.05$ and present in > two animals in each group. Data are shown as median (IQR) and were statistically compared using unpaired non-parametric Mann-Whitney *U* test and Benjamini-Hochberg adjustment procedure with Q = 0.1 used to correct *p* values for multiple testing. $ indicates an increase or decrease in the relative abundance of bacterial taxa in VEH-FMT.

Genus	VEH	ABX-FMT	*p*-value	(i/m)*Q
Bifidobacteriaceae (Bifidobacteriales, Actinobacteria)				
Bifidobacterium	0.024 (0.137)	0.052 (0.119)	0.28	0.04
Coriobacteriaceae (Coriobacteriales, Actinobacteria)				
Uncultured coriobacteriaceae	0.035 (0.036)	0.008 (0.011)	0.000	0.002 &
Enterorhabdus	0.023 (0.021)	0.011 (0.01)	0.011	0.009
Uncultured bacterium (Unknown order, Bacteroidetes)				
Bacteroidetes VC21 Bac22 uncultured bacterium	0 (0)	0.1 (0.062)	0.000	0.002 &
Bacteroidaceae (Bacteroidales, Bacteroidetes)				
Bacteroides	1.656 (1.138)	2.17 (1.539)	0.315	0.045
Bacteroidales S24-7 group (Bacteroidales, Bacteroidetes)				
Uncultured bacterium	17.13 (2.798)	17.353 (3.996)	0.631	0.072
Unidentified	0.161 (0.933)	0.0429 (0.177)	0.043	0.015
Porphyromonadaceae (Bacteroidales, Bacteroidetes)				
Odoribacter	0.36 (0.212)	0.296 (0.100)	0.353	0.048
Parabacteroides	0.046 (0.042)	0.147 (0.129)	0.023	0.01
Prevotellaceae (Bacteroidales, Bacteroidetes)				
Alloprevotella	1.594 (2.192)	2.173 (2.118)	1.000	0.099
Prevotellaceae NK3B31 group	1.715 (2.18)	0.63 (2.525)	0.143	0.029
Prevotellaceae UCG-001	1.743 (2.486)	1.379 (2.066)	0.684	0.076
Rikenellaceae (Bacteroidales, Bacteroidetes)				
Alistipes	3.555 (3.252)	2.535 (0.804)	0.315	0.045
Uncultured bacterium (Gastranaerophilales, Cyanobacteria)				
Uncultured bacterium	0.627 (0.725)	1.396 (1.062)	0.035	0.012
Uncultured organism	0 (0.0006)	0.111 (0.442)	0.000	0.002 $
Deferribacteraceae (Deferribacterales, Deferribacteres)				
Mucispirillum	0.139 (0.301)	0 (0.0002)	0.000	0.003 $
Bacillaeae (Bacillales, Firmicutes)				
Bacillus	0.13 (0.279)	0 (0)	0.000	0.003 $
Lactobacillaceae (Lactobacillales, Firmicutes)				
Lactobacillus	2.318 (3.128)	1.399 (1.761)	0.190	0.033
Streptococcaceae (Lactobacillales, Firmicutes)				
Streptococcus	0.004 (0.004)	0.003 (0.005)	0.007	0.008 $
Christensenellaceae (Clostridiales, Firmicutes)				
Christensenellaceae R-7 group	0.031 (0.074)	0.081 (0.082)	0.393	0.053
Clostridiaceae 1 (Clostridiales, Firmicutes)				
Clostridium sensu stricto 1	0.116 (0.371)	0.139 (0.469)	0.436	0.056
Clostridiales vadin BB60 group (Clostridiales, Firmicutes)				
Uncultured clostridiales bacterium	0.004 (0.036)	0.031 (0.051)	0.035	0.013
Uncultured bacterium	1.317 (1.181)	2.927 (2.541)	0.011	0.01
Uncultured rumen bacterium	0.058 (0.096)	0.077 (0.099)	0.631	0.072
Unidentified	0.126 (0.341)	0.702 (0.868)	0.052	0.017
Family XIII (Clostridiales, Firmicutes)				

Anaerovorax	0.055 (0.046)	0.053 (0.033)	0.971	0.096
Lachnospiraceae (Clostridiales, Firmicutes)				
Blautia	0.07 (0.252)	0.084 (0.233)	0.796	0.085
Coprococcus 1	0.125 (0.063)	0.147 (0.138)	0.481	0.061
Coprococcus 2	0.178 (0.462)	0.155 (0.279)	0.912	0.092
Incertae Sedis	1.398 (1.351)	0.566 (0.680)	0.143	0.029
Lachnoclostridium	0.121 (0.07)	0.071 (0.164)	0.353	0.049
Lachnoclostridium 10	0 (0)	0.128 (0.16)	0.000	0.003
Lachnospiraceae NC2004 group	0.586 (1.377)	0.07 (0.223)	0.035	0.013
Lachnospiraceae NK4A136 group	22.823 (5.829)	19.099 (7.826)	0.052	0.017
Lachnospiraceae NK4B4 group	0.01 (0.116)	0.0008 (0.006)	0.247	0.037
Lachnospiraceae UCG-0001	0.168 (0.195)	0.193 (0.246)	0.739	0.081
Lachnospiraceae UCG-0005	0.067 (0.088)	0.063 (0.052)	0.436	0.056
Lachnospiraceae UCG-0006	0.281 (0.218)	0.346 (0.606)	0.684	0.076
Lachnospiraceae UCG-008	0.081 (0.113)	0.011 (0.019)	0.001	0.004 &
Roseburia	0.913 (0.649)	0.851 (1.281)	0.853	0.089
Tyzzerella	0.207 (0.19)	0.177 (0.109)	0.089	0.022
Lachnospiraceae [Eubacterium] oxidoreducens group	0.262 (0.278)	0.269 (0.465)	0.631	0.24
Lachnospiraceae [Eubacterium] ruminantium group	0.185 (0.276)	0.043 (0.155)	0.218	0.1
Lachnospiraceae uncultured	5.073 (4.202)	6.788 (4.27)	0.28	0.19
Natranaerovirga	0.005 (0.007)	0 (0.0006)	0.009	0.008
Peptococcaceae (Clostridiales, Firmicutes)				
Peptococcaceae (uncultured)	0.352 (0.312)	0.301 (0.104)	0.631	0.073
Peptococcus	0.079 (0.029)	0.09 (0.04)	0.165	0.03
Peptostreptococcaceae (Clostridiales, Firmicutes)				
Intestinibacter	0.092 (0.499)	0.016 (0.028)	0.436	0.057
Peptoclostridium	0.46 (0.906)	0.336 (0.434)	0.796	0.085
Ruminococcaceae (Clostridiales, Firmicutes)				
Anaerotruncus	0.929 (0.248)	0.82 (0.202)	0.165	0.031
Intestinimonas	0.064 (0.040)	0.031 (0.021)	0.023	0.011
Oscillibacter	0.908 (0.281)	0.701 (0.228)	0.043	0.015
Papillibacter	0.071 (0.188)	0.151 (0.169)	0.063	0.019
Ruminoclostridium	0.084 (0.836)	0.112 (0.056)	0.247	0.038
Ruminoclostridium 5	0.343 (0.175)	0.443 (0.333)	0.19	0.033
Ruminoclostridium 6	0.723 (0.781)	1.617 (1.084)	0.123	0.027
Ruminoclostridium 9	3.962 (1.396)	3.133 (2.071)	0.529	0.064
Ruminococcaceae NK4A214 group	0.239 (0.146)	0.224 (0.204)	0.436	0.057
Ruminococcaceae UCG-002	0.004 (0.006)	0.008 (0.005)	0.023	0.010
Ruminococcaceae UCG-003	1.392 (1.069)	1.089 (1.051)	0.28	0.42
Ruminococcaceae UCG-005	0.324 (0.247)	0.229 (0.172)	0.247	0.038
Ruminococcaceae UCG-009	0.081 (0.043)	0.092 (0.062)	0.28	0.42
Ruminococcaceae UCG-010	0.282 (0.208)	0.474 (0.231)	0.089	0.022
Ruminococcaceae UCG-011	0 (0)	0.001 (0.003)	0.004	0.006

Ruminococcaceae UCG-013	0.067 (0.059)	0.092 (0.158)	0.165	0.031
Ruminococcaceae UCG-014	1.134 (0.706)	1.11 (0.57)	0.912	0.093
Ruminococcus 1	2.6 (1.577)	2.239 (2.498)	0.971	0.096
Ruminococcus 2	0.093 (0.114)	0.062 (0.109)	0.579	0.067
[Eubacterium] coprostanoligenes group	1.339 (1.0)	0.841 (0.929)	0.353	0.049
Ruminococcaceae uncultured	7.016 (3.051)	8.094 (2.842)	0.436	0.057
Erysipelotrichaceae (Erysipelotrichales, Firmicutes)				
Allobaculum	0.002 (0.037)	0.037 (0.083)	0.063	0.019
Turicibacter	0.206 (0.216)	0.159 (0.229)	0.739	0.082
Erysipelotrichaceae uncultured	0.019 (0.088)	0.012 (0.006)	0.393	0.054
Rhodospirillaceae (Rhodospirillales, Proteobacteria)				
Thalassospira	0.236 (0.415)	0.281 (0.254)	0.436	0.058
Uncultured rhodospirillaceae	0 (0.0343)	0.002 (0.04)	0.436	0.058
Alcaligenaceae (Burkholderiales, Proteobacteria)				
Parasutterella	0.039 (0.094)	0.048 (0.094)	0.971	0.097
Desulfovibrionaceae (Deltaproteobacteria, Proteobacteria)				
Bilophila	0.089 (0.327)	0.124 (0.08)	0.631	0.073
Desulfovibrio	1.753 (2.685)	3.152 (1.215)	0.023	0.011
Helicobacteraceae (Campylobacterales, Proteobacteria)				
Helicobacter	0.002 (0.003)	3.515 (1.354)	0.000	0.003 &
Enterobacteriaceae (Enterobacteriales, Proteobacteria)				
Unknown Family (Unknown order, Saccharibacteria)				
Candidatus Saccharimonas	0.419 (0.49)	0.582 (0.36)	0.315	0.046
Anaeroplasmataceae (Anaeroplasmatales, Tenericutes)				
Anaeroplasma	0.083 (0.277)	0.181 (1.059)	0.19	0.034
Uncultured bacterium, (Mollicutes RF9, Tenericutes)				
Uncultured bacterium	0.062 (0.0330	0.095 (0.093)	0.315	0.046
Uncultured rumen bacterium (Mollicutes RF9, Tenericutes)				
Uncultured rumen bacterium	0.112 (0.242)	0.128 (0.321)	0.579	0.067
Uncultured Bacillales bacterium (NB1-n, Tenericutes)				
Uncultured Bacillales bacterium	0.042 (0.042)	0.029 (0.071)	0.19	0.034
Verrucomicrobiaceae (Verrucomicrobiales, Verrucomicrobia)				
Akkermansia	0.041 (0.149)	0.064 (0.156)	0.739	0.082

Appendix Table A.21 Relative abundance (%) of bacterial genera in the caecal samples from VEH and ABX-FMT rats

VEH, autoclaved deionised water; ABX-FMT, antibiotics followed by faecal microbial transfer. Data in these tables are the top 45% of genera plus genera with raw $p<0.05$ and present in > two animals in each group. Data are shown as median (IQR) and were statistically compared using unpaired non-parametric Mann-Whitney *U* test and Benjamini-Hochberg adjustment procedure with Q = 0.1 used to correct *p* values for multiple testing. & indicates an increase or decrease in the relative abundance of bacterial taxa in VEH-FMT.

Genus	VEH-FMT	ABX-FMT	p-value	(i/m)* Q
Bifidobacteriaceae (Bifidobacteriales, Actinobacteria)				
Bifidobacterium	0.044 (0.058)	0.052 (0.119)	0.796	0.086
Micrococcaceae (Micrococcales, Actinobacteria)				
Rothia	0.008 (0.011)	0.002 (0.004)	0.035	0.013
Coriobacteriaceae (Coriobacteriales, Actinobacteria)				
Gordonibacter	0.007 (0.012)	0.003 (0.003)	0.035	0.013
Uncultured bacterium (Unknown order, Bacteroidetes)				
Bacteroidetes VC21 Bac22 uncultured bacterium	0.116 (0.081)	0.1 (0.062)	0.853	0.09
Bacteroidaceae (Bacteroidales, Bacteroidetes)				
Bacteroides	1.182 (0.885)	2.17 (1.539)	0.353	0.05
Bacteroidales S24-7 group (Bacteroidales, Bacteroidetes)				
Uncultured bacterium	14.372 (2.949)	17.353 (3.996)	0.075	0.021
Unidentified	0.067 (0.059)	0.0429 (0.177)	0.353	0.05
Porphyromonadaceae (Bacteroidales, Bacteroidetes)				
Odoribacter	0.296 (0.289)	0.296 (0.100)	0.631	0.074
Parabacteroides	0.099 (0.070)	0.147 (0.129)	0.684	0.077
Prevotellaceae (Bacteroidales, Bacteroidetes)				
Alloprevotella	0.748 (1.639)	2.173 (2.118)	0.28	0.043
Prevotellaceae NK3B31 group	2.017 (2.704)	0.63 (2.525)	0.143	0.029
Prevotellaceae UCG-001	2.134 (2.167)	1.379 (2.066)	0.075	0.021
Rikenellaceae (Bacteroidales, Bacteroidetes)				
Alistipes	1.961 (1.097)	2.535 (0.804)	0.353	0.05
Uncultured bacterium (Gastranaerophilales, Cyanobacteria)				
Uncultured bacterium	0.837 (0.685)	1.396 (1.062)	0.19	0.034
Uncultured organism	0.491 (0.893)	0.111 (0.442)	0.089	0.023
Lactobacillaceae (Lactobacillales, Firmicutes)				
Lactobacillus	1.441 (2.691)	1.399 (1.761)	0.075	0.021
Streptococcaceae (Lactobacillales, Firmicutes)				
Streptococcus	0.003 (0.005)	0.001 (0.002)	0.003	0.005 ¥
Christensenellaceae (Clostridiales, Firmicutes)				
Christensenellaceae R-7 group	0.046 (0.045)	0.081 (0.082)	0.218	0.036
Clostridiaceae 1 (Clostridiales, Firmicutes)				
Clostridium sensu stricto 1	0.238 (0.005)	0.139 (0.469)	0.436	0.058
Clostridiales vadin BB60 group (Clostridiales, Firmicutes)				
Uncultured clostridiales bacterium	0.045 (0.022)	0.031 (0.051)	0.579	0.068
Uncultured bacterium	2.147 (0.811)	2.927 (2.541)	0.579	0.068
Uncultured rumen bacterium	0.021 (0.048)	0.077 (0.099)	0.105	0.025
Unidentified	0.756 (1.352)	0.702 (0.868)	0.353	0.05
Family XIII (Clostridiales, Firmicutes)				
Anaerovorax	0.038 (0.013)	0.053 (0.033)	0.052	0.017
Lachnospiraceae (Clostridiales, Firmicutes)				
Blautia	0.566 (1.207)	0.084 (0.233)	0.035	0.04

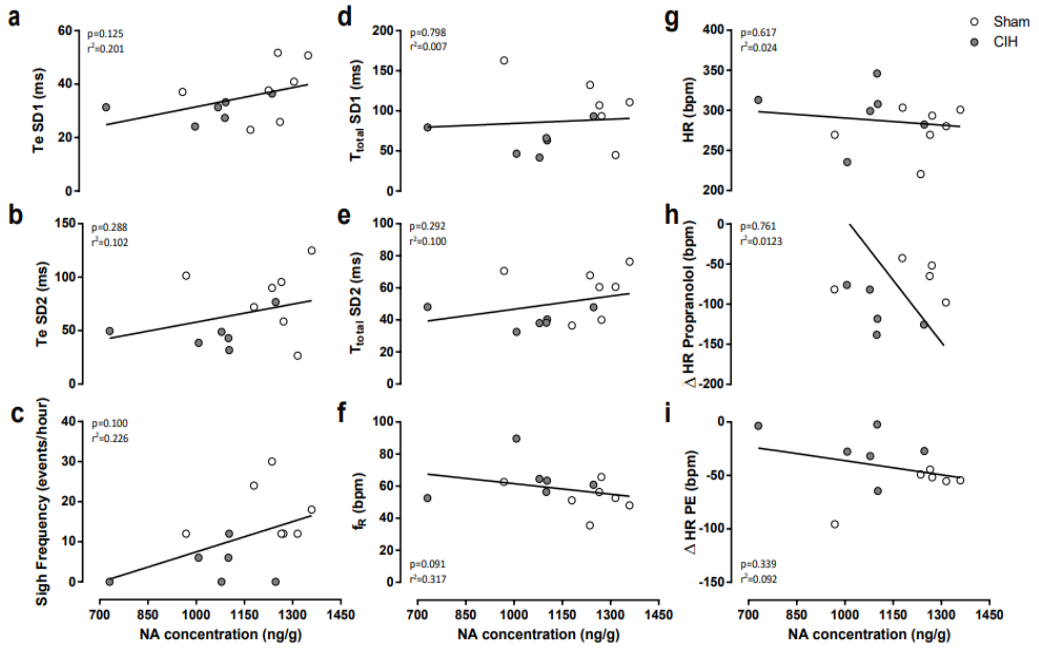
Coprococcus 1	0.127 (0.06)	0.147 (0.138)	0.28	0.043
Coprococcus 2	0.011 (0.207)	0.155 (0.279)	0.075	0.021
Incertae Sedis	0.913 (0.926)	0.566 (0.680)	0.436	0.058
Lachnoclostridium	0.124 (0.040)	0.071 (0.164)	0.218	0.036
Lachnoclostridium 10	0.313 (0.362)	0.128 (0.16)	0.853	0.09
Lachnospiraceae NC2004 group	0.4 (0.391)	0.07 (0.223)	0.052	0.018
Lachnospiraceae NK4A136 group	19.789 (5.348)	19.099 (7.826)	0.631	0.074
Lachnospiraceae UCG-0001	0.303 (0.354)	0.193 (0.246)	0.105	0.025
Lachnospiraceae UCG-0005	0.103 (0.088)	0.063 (0.052)	0.063	0.019
Lachnospiraceae UCG-0006	0.254 (0.268)	0.346 (0.606)	0.739	0.082
Roseburia	1.798 (1.915)	0.851 (1.281)	0.315	0.047
Tyzzerella	0.117 (0.059)	0.177 (0.109)	0.165	0.032
Lachnospiraceae [Eubacterium] oxidoreducens group	0.292 (0.355)	0.269 (0.465)	1.000	0.1
Lachnospiraceae [Eubacterium] ruminantium group	0.035 (0.363)	0.043 (0.155)	0.684	0.078
Lachnospiraceae [Eubacterium] ventriosum group	0.014 (0.019)	0.032 (0.046)	0.035	0.04
Lachnospiraceae uncultured	9.821 (5.779)	6.788 (4.27)	0.123	0.028
Marvinbryantia	0.002 (0.003)	0.008 (0.029)	0.043	0.016
Peptococcaceae (Clostridiales, Firmicutes)				
Peptococcaceae (uncultured)	0.325 (0.1)	0.301 (0.104)	0.739	0.083
Peptococcus	0.085 (0.083)	0.09 (0.04)	0.631	0.074
Peptostreptococcaceae (Clostridiales, Firmicutes)				
Intestinibacter	0.046 (0.093)	0.016 (0.028)	0.315	0.047
Peptoclostridium	0.626 (0.767)	0.336 (0.434)	0.007	0.008 ¥
Ruminococcaceae (Clostridiales, Firmicutes)				
Anaerotruncus	0.764 (0.170)	0.82 (0.202)	0.529	0.065
Flavonifractor	0.065 (0.169)	0.018 (0.114)	0.393	0.054
Oscillibacter	0.586 (0.175)	0.701 (0.228)	0.247	0.039
Papillibacter	0.161 (0.247)	0.151 (0.169)	0.579	0.069
Ruminoclostridium	0.152 (0.094)	0.112 (0.056)	0.105	0.025
Ruminoclostridium 5	0.407 (0.27)	0.443 (0.333)	0.912	0.094
Ruminoclostridium 6	1.0 (0.9)	1.617 (1.084)	0.89	0.023
Ruminoclostridium 9	2.305 (0.576)	3.133 (2.071)	0.035	0.04
Ruminococcaceae NK4A214 group	0.234 (0.094)	0.224 (0.204)	0.579	0.069
Ruminococcaceae UCG-003	1.429 (0.472)	1.089 (1.051)	0.579	0.07
Ruminococcaceae UCG-005	0.417 (0.313)	0.229 (0.172)	0.005	0.007 ¥
Ruminococcaceae UCG-009	0.083 (0.029)	0.092 (0.062)	0.28	0.043
Ruminococcaceae UCG-010	0.418 (0.26)	0.474 (0.231)	0.796	0.086
Ruminococcaceae UCG-013	0.204 (0.15)	0.092 (0.158)	0.043	0.04
Ruminococcaceae UCG-014	0.945 (0.78)	1.11 (0.57)	0.436	0.059
Ruminococcus 1	2.413 (3.09)	2.239 (2.498)	0.971	0.098
Ruminococcus 2	0.082 (0.045)	0.062 (0.109)	0.739	0.083
[Eubacterium] coprostanoligenes group	0.963 (1.529)	0.841 (0.929)	1.000	0.1

Ruminococcaceae uncultured	5.734 (2.825)	8.094 (2.842)	0.009	0.0087
Erysipelotrichaceae (Erysipelotrichales, Firmicutes)				
Allobaculum	0.008 (0.003)	0.037 (0.083)	0.001	0.004 ¥
Turicibacter	0.297 (0.295)	0.159 (0.229)	0.105	0.026
Rhodospirillaceae (Rhodospirillales, Proteobacteria)				
Thalassospira	0.361 (0.186)	0.281 (0.254)	0.28	0.043
Uncultured rhodospirillaceae	0.023 (0.054)	0.002 (0.04)	0.631	0.075
Alcaligenaceae (Burkholderiales, Proteobacteria)				
Parasutterella	0.01 (0.011)	0.048 (0.094)	0.005	0.007 ¥
Desulfovibrionaceae (Deltaproteobacteria, Proteobacteria)				
Bilophila	0.171 (0.128)	0.124 (0.08)	0.353	0.051
Desulfovibrio	2.262 (1.294)	3.152 (1.215)	0.035	0.014
Helicobacteraceae (Campylobacterales, Proteobacteria)				
Helicobacter	4.226 (1.378)	3.515 (1.354)	0.105	0.026
Enterobacteriaceae (Enterobacteriales, Proteobacteria)				
Enterobacter	0 (0.002)	0.002 (0.004)	0.28	0.044
Unknown Family (Unknown order, Saccharibacteria				
Candidatus Saccharimonas	0.354 (0.207)	0.582 (0.36)	0.023	0.011
Anaeroplasmataceae (Anaeroplasmatales, Tenericutes)				
Anaeroplasma	0.217 (0.195)	0.181 (1.059)	0.739	0.084
Uncultured bacterium, (Mollicutes RF9, Tenericutes)				
Uncultured bacterium	0.078 (0.064)	0.095 (0.093)	0.579	0.07
Uncultured rumen bacterium (Mollicutes RF9, Tenericutes)				
Uncultured rumen bacterium	0.073 (0.079)	0.128 (0.321)	0.631	0.075
Uncultured Bacillales bacterium (NB1-n, Tenericutes)				
Uncultured Bacillales bacterium	0.034 (0.1)	0.029 (0.071)	0.739	0.084
Verrucomicrobiaceae (Verrucomicrobiales, Verrucomicrobia)				
Akkermansia	0.313 (1.167)	0.064 (0.156)	0.029	0.012

Appendix Table A.22 Relative abundance (%) of bacterial genera in the caecal samples from VEH-FMT and ABX-FMT rats

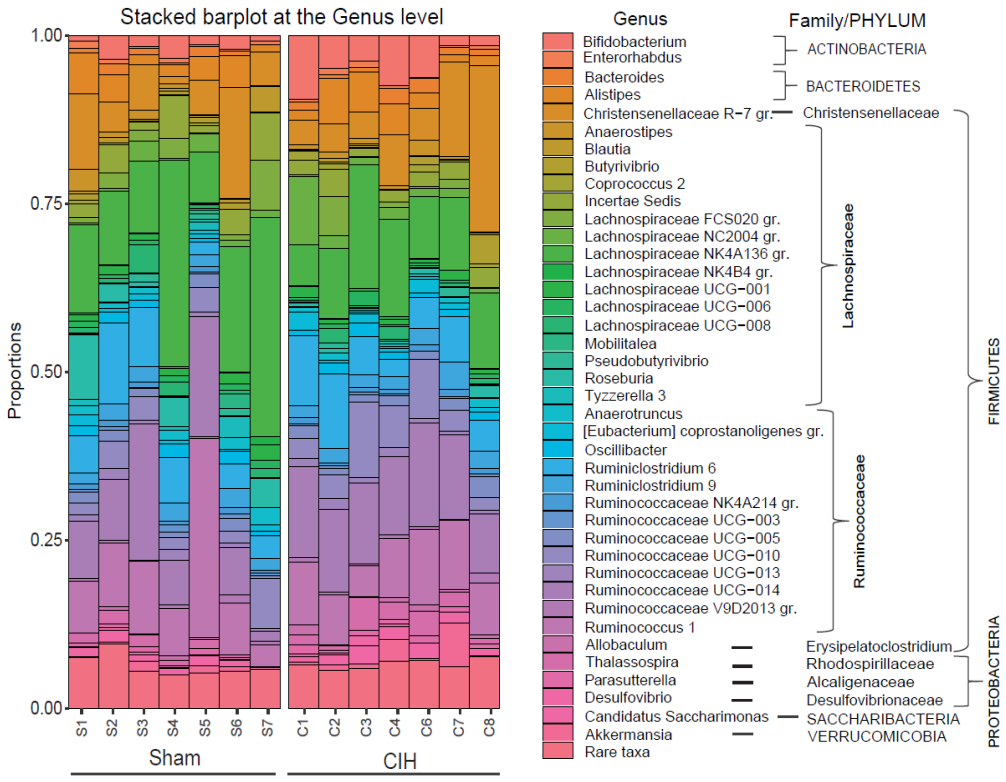
VEH-FMT, VEH followed by faecal microbial transfer; ABX-FMT, antibiotics followed by faecal microbial transfer. Data in these tables are the top 45% of genera plus genera with raw $p<0.05$ and present in > two animals in each group. Data are shown as median (IQR) and were statistically compared using unpaired non-parametric Mann-Whitney *U* test and Benjamini-Hochberg adjustment procedure with Q = 0.1 used to correct *p* values for multiple testing. ¥ indicates an increase or decrease in the relative abundance of bacterial taxa in VEH-FMT.

Appendix B. Chronic intermittent hypoxia disrupts cardiorespiratory homeostasis and gut microbiota composition in adult male guinea-pigs



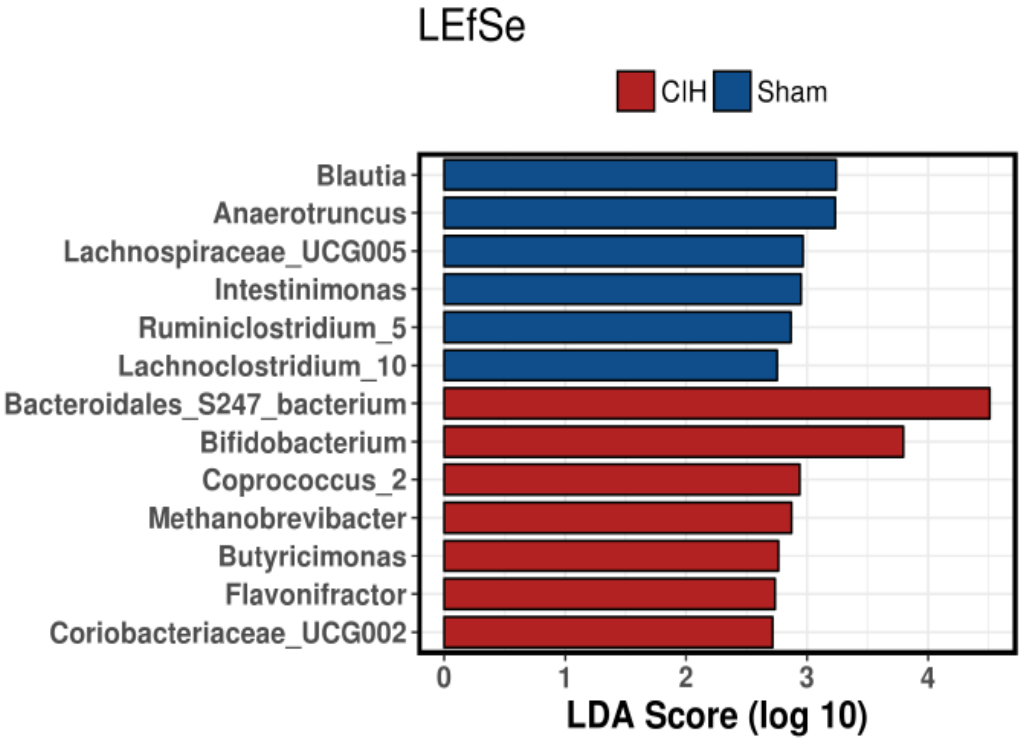
Appendix Figure B.1 No significant correlations are evident between noradrenaline concentrations of the medulla oblongata and various cardiorespiratory parameters

Individual data points for correlations between medullary noradrenaline (NA) concentrations and time to expire (Te) short-term variability (SD1; a), Te long-term variability (SD2; b), sigh frequency (c), total breath duration (Ttotal) SD1 (d), Ttotal SD2 (e) in sham and CIH-exposed awake guinea pigs, and for respiratory frequency (f_R; f), heart rate (HR; g), change in HR in response to propranolol administration (h) and change in HR in response to phenylephrine (PE) administration (i) in sham and CIH-exposed anaesthetised guinea-pigs. Solid black lines represent linear regression analysis for each parameter.



Appendix Figure B.2 Faecal microbiota composition in sham and CIH-exposed guinea-pigs

Stacked barplot showing the relative abundance of dominant bacterial genera (0.01 cut-off) in the faecal matter of sham and CIH-exposed animals. Genera are ordered taxonomically. Phyla are defined by uppercase lettering.



Appendix Figure B.3 Linear discriminant analysis effect size (LEfSe) analysis on the genus level

Histogram plots from LEfSe analysis showing significant genera associated with sham and CIH-exposed faecal microbiota, ranked based on LDA scores. Taxa with LDA scores above 2 were considered significant. Bacterial genera significantly over-represented in the sham (blue), and CIH-exposed (red) groups are shown.

	Median (IQR)			
Phylum	**Sham**	**CIH**	***p*-value**	**(i/m)*Q**
Proteobacteria	1.027 (0.885)	1.547 (2.357)	0.07	0.08
Bacteroidetes	38.072 (16.381)	45.497 (3.958)	**0.04***	**0.05**
Cyanobacteria	2.961 (2.792)	3.965 (4.492)	0.32	0.12
Verrucomicrobia	0.152 (0.497)	0.265 (1.377)	0.38	0.15
Firmicutes	53.338 (17.573)	42.92 (4.587)	**0.007***	**0.03**
Actinobacteria	1.478 (1.458)	3.14 (2.295)	0.053	0.07
Euryarchaeota	0.025 (0.072)	0.093 (0.06)	**0.007***	**0.02**
Saccharibacteria	0.518 (0.245)	0.687 (0.485)	0.21	0.1
Tenericutes	0.227 (0.528)	0.328 (0.353)	0.9	0.2
Other	0.043 (0.04)	0.058 (0.033)	0.32	0.13

Appendix Table B.1 Relative abundance (%) of bacterial phyla in the faeces of sham and CIH-exposed guinea-pigs

Data are shown as median (IQR) and were statistically compared using non-parametric Mann-Whitney *U* test and Benjamini-Hochberg adjustment procedure with the false discovery rate set at 20% to correct for multiple testing. Raw *p*-values < 0.05 are marked in bold. Significant false discovery rate adjusted p-values are in bold. CIH, chronic intermittent hypoxia. * denotes $p<0.05$ compared with Sham.

	Median (IQR)			
Family	**Sham**	**CIH**	**p-value**	**(i/m)*Q**
Methanobacteriaceae *(Methanobacteriales)*	0.025 (0.072)	0.093 (0.06)	**0.007****	0.004
Actinobacteria				
Bifidobacteriaceae *(Bifidobacteriales)*	0.682 (1.275)	2.038 (2.612)	**0.04***	0.007
Coriobacteriaceae *(Coriobacteriales)*	0.688 (0.298)	0.815 (0.513)	0.81	0.15
Corynebacteriaceae *(Corynebacteriales)*	0.003 (0.008)	0 (0.015)	0.9	0.17
Bacteroidetes				
Bacteroidaceae *(Bacteroidales)*	0.333 (0.512)	0.502 (0.713)	0.32	0.06
Porphyromonadaceae *(Bacteroidales)*	0.057 (0.033)	0.123 (0.15)	0.1	0.03
Prevotellaceae *(Bacteroidales)*	0.017 (0.037)	0.025 (0.05)	1	0.19
Rikenellaceae *(Bacteroidales)*	1.818 (1.848)	1.112 (1.745)	0.81	0.15
S24-7 *(Bacteroidales)*	34.728 (14.117)	42.193 (3.255)	0.053	0.01
Rat ANO60301C *(Bacteroidales)*	0.002 (0.005)	0.007 (0.022)	0.21	0.05
Cyanobacteria				
Uncultured bacterium *(Gastranaerophilales)*	0.973 (0.957)	1.852 (3.117)	0.17	0.04
Uncultured organism *(Gastranaerophilales)*	2.023 (1.818)	1.242 (1.572)	0.9	0.18
Uncultured rumen bacterium *(Gastranaerophilales)*	0.048 (0.092)	0.047 (0.083)	1	0.19
Firmicutes				
Streptoccaceae) *(Lactobacillales)*	0.023 (0.023)	0.018 (0.025)	0.9	0.18
Lactobacillaceae *(Lactobacillales)*	0.127 (0.112)	0.22 (0.287)	0.6	0.11
Caldicoprobacteraceae *(Clostridiales)*	0.07 (0.005)	0.01 (0.013)	0.46	0.09
Christensenellaceae *(Clostridiales)*	2.865 (2.915)	2.19 (4.57)	0.81	0.16
Clostridiaceae 1 *(Clostridiales)*	0.008 (0.005)	0.025 (0.028)	0.053	0.02
Clostridiales vadinBB60 group *(Clostridiales)*	1.418 (0.903)	1.575 (0.657)	0.81	0.16
Defluviitaleaceae *(Clostridiales)*	0.028 (0.023)	0.033 (0.015)	0.46	0.1
Eubacteriaceae *(Clostridiales)*	0.003 (0.001)	0.048 (0.123)	**0.04***	0.01
Family XIII *(Clostridiales)*	0.08 (0.04)	0.063 (0.01)	0.38	0.08
Lachnospiraceae *(Clostridiales)*	22.257 (21.812)	15.722 (3.378)	0.053	0.02
Peptococcaceae *(Clostridiales)*	0.305 (0.193)	0.19 (0.13)	0.32	0.07

Peptostreptococcaceae *(Clostridiales)*	0.015 (0.037)	0.053 (0.06)	0.053	0.03
Ruminococcaceae *(Clostridiales)*	22.68 (7.375)	21.662 (4.952)	0.62	0.12
Syntrophomonadaceae *(Clostridiales)*	0.007 (0.018)	0.002 (0.003)	0.26	0.06
Erysipelotrichaceae *(Erysipelotrichales)*	0.213 (0.238)	0.335 (0.382)	0.13	0.04
Thermoanaerobacteraceae *(Thermoanaerobacterales)*	0 (0)	0 (0.03)	0.32	0.07
Veillonellaceae *(Selenomonadales)*	0.003 (0.012)	0.002 (0.003)	0.46	0.1
Proteobacteria				
Rhodospirillaceae *(Rhodospirillales)*	0.642 (0.573)	0.942 (1.278)	0.17	0.05
Alcaligenaceae *(Burkholderiales)*	0.265 (0.23)	0.337 (0.197)	0.13	0.04
Oxalobacteraceae *(Burkholderiales)*	0.018 (0.027)	0.02 (0.022)	0.71	0.14
Desulfovibrionaceae *(Desulfovibrionales)*	0.067 (0.108)	0.095 (0.165)	0.46	0.11
Enterobacteriaceae *(Enterobacteriales)*	0.002 (0.015)	0.002 (0.012)	0.81	0.16
Saccharibacteria				
Unknown family *(Unknown order)*	0.518 (0.243)	0.683 (0.485)	0.17	0.05
CandidatusSaccharibacteriaortaxonTM7x unknown family (Unknown order)	0 (0.002)	0 (0.003)	0.81	0.17
Tenericutes				
Anaeroplasmataceae *(Anaeroplasmatales)*	0.025 (0.028)	0.007 (0.022)	0.54	0.11
Uncultured bacterium *(Mollicutes RF9)*	0.23 (0.28)	0.15 (0.388)	0.9	0.19
Uncultured rumen bacteria *(Mollicutes RF9)*	0.033 (0.07)	0.04 (0.267)	0.81	0.17
Uncultured bacterium *(Mollicutes NB1-n)*	0 (0.008)	0.005 (0.02)	0.1	0.03
Verrucomicrobia				
Verrucomicrobiaceae *(Verrucomicrobiales)*	0.152 (0.497)	0.265 (1.377)	0.38	0.09
Other	0.043 (0.04)	0.058 (0.033)	0.32	0.07

Appendix Table B.2 Relative abundance (%) of bacterial families in the faeces of Sham and CIH-exposed guinea-pigs

Data are shown as median (IQR) and were statistically compared using non-parametric Mann-Whitney *U* test and Benjamini-Hochberg adjustment procedure with the false discovery rate set at 20% to correct for multiple testing. Raw *p*-values < 0.05 are marked in bold. Significant false discovery rate adjusted p-values are in bold. CIH, chronic intermittent hypoxia. * denotes $p<0.05$ compared with Sham; ** denotes $p<0.01$ compared with Sham.

	Median (IQR)			
Genus	**Sham**	**CIH**	**p-value**	**(i/m)*Q**
Methanobacteriaceae (Methanobacteriales, Euryarchaeota)				
Methanobrevibacter	0.025 (0.072)	0.093 (0.06)	**0.007****	0.001
Bifidobacteriaceae (Bifidobacteriales, Actinobacteria)				
Bifidobacterium	0.682 (1.275)	2.034 (2.612)	**0.04***	0.008
Coriobacteriaceae (Coriobacteriales, Actinobacteria)				
Coriobacteriaceae UCG-002	0.045 (0.032)	0.103 (0.072)	0.01	0.002
Uncultured coriobacteriaceae	0.33 (0.228)	0.367 (0.11)	0.54	0.1
Enterorhabdus	0.293 (0.238)	0.187 (0.265)	0.9	0.17
Senegalimassilia	0.057 (0.037)	0.058 (0.033)	0.71	0.12
Bacteroidaceae (Bacteroidales, Bacteroidetes)				
Bacteroides	0.333 (0.512)	0.502 (0.713)	0.32	0.06
Bacteroidales S24-7 group (Bacteroidales, Bacteroidetes)				
Uncultured bacterium	34.587 (14.043)	42.002 (3.285)	0.053	0.01
Unidentified	0.082 (0.073)	0.168 (0.098)	0.053	0.01
Porphyromonadaceae (Bacteroidales, Bacteroidetes)				
Odoribacter	0.053 (0.037)	0.055 (0.125)	0.32	0.06
Prevotellaceae (Bacteroidales, Bacteroidetes)				
Prevotellaceae UCG-001	0.015 (0.042)	0.025 (0.05)	0.9	0.17
Rikenellaceae (Bacteroidales, Bacteroidetes)				
Alistipes	1.738 (1.762)	1.058 (1.74)	1	0.19
Rikenella	0.078 (0.228)	0.077 (0.047)	0.62	0.11
Uncultured bacterium (Gastranaerophilales, Cyanobacteria)				
Uncultured bacterium	0.973 (0.957)	1.852 (3.117)	0.17	0.04
Uncultured organism	2.023 (1.818)	1.242 (1.572)	0.9	0.17
Uncultured rumen bacterium	0.048 (0.092)	0.047 (0.083)	1	0.19
Lactobacillaceae (Lactobacillales, Firmicutes)				
Lactobacillus	0.127 (0.112)	0.22 (0.287)	0.62	0.11
Christensenellaceae (Clostridiales, Firmicutes)				
Christensenellaceae R-7 group	2.852 (2.885)	2.163 (4.565)	0.81	0.16
Clostridiales vadin BB60 group (Clostridiales, Firmicutes)				
Uncultured bacterium	1.392 (0.617)	1.365 (0.515)	1	0.19
Unidentified	0.02 (0.05)	0.023 (0.102)	0.71	0.13
Eubacteriaceae *(Clostridiales, Firmicutes)*				
Uncultured	0.003 (0.012)	0.048 (0.123)	**0.04**	0.009
Lachnospiraceae (Clostridiales, Firmicutes)				
Acetatifactor	0.112 (0.193)	0.085 (0.15)	0.26	0.05
Acetitomaculum	0.073 (0.29)	0.077 (0.063)	0.62	0.11

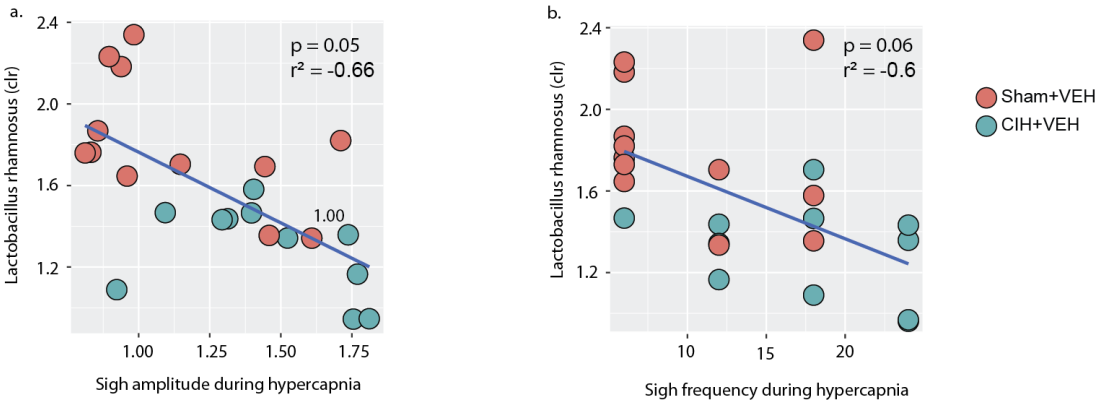
Anaerostipes	0.355 (0.537)	0.287 (0.36)	0.71	0.13
Blautia	0.245 (0.2)	0.117 (0.108)	**0.04**	0.01
Butyrivibrio	0.288 (0.383)	0.082 (0.498)	1	0.19
Cellulosillyticum	0.038 (0.05)	0.045 (0.123)	0.62	0.11
Coprococcus 2	0.063 (0.217)	0.28 (0.428)	0.053	0.02
Incertae Sedia	1.878 (3.073)	1.075 (0.605)	0.38	0.08
Lachnoclostridium	0.057 (0.06)	0.068 (0.04)	0.81	0.16
Lachnospiraceae FCS020 group	0.728 (1.333)	0.127 (0.515)	0.21	0.05
Lachnospiraceae NC2004 group	0.498 (1.135)	0.603 (0.343)	0.38	0.07
Lachnospiraceae NK4A136 group	5.945 (12.397)	4.83 (2.318)	0.26	0.05
Lachnospiraceae NK4B4 group	0.058 (0.097)	0.07 (0.055)	0.6	0.12
Lachnospiraceae UCG-0001	0.615 (0.433)	0.313 (0.418)	0.21	0.05
Lachnospiraceae UCG-0006	0.422 (0.237)	0.18 (0.167)	0.13	0.03
Lachnospiraceae UCG-008	0.358 (0.888)	0.257 (0.668)	0.46	0.09
Mobilitalea	0.073 (0.218)	0.015 (0.088)	0.32	0.06
Pseudobutyrivibrio	0.132 (0.443)	0.043 (0.332)	0.13	0.03
Roseburia	1.33 (2.263)	0.257 (0.253)	0.1	0.03
Tyzzerella 3	0.325 (0.548)	0.102 (0.147)	0.32	0.06
[Eubacterium] oxidoreducens group	0.062 (0.087)	0.043 (0.037)	1	0.2
[Eubacterium] ruminantium group	0.113 (0.24)	0.04 (0.083)	0.71	0.14
Lachnospiraceae uncultured	6.828 (5.173)	4.053 (2.198)	0.053	0.02
Lachnospiraceae uncultured bacterium	0.047 (0.818)	0.087 (0.147)	0.71	0.14
Peptococcaceae (Clostridiales, Firmicutes)				
Peptococcaceae (uncultured)	0.305 (0.192)	0.19 (0.13)	0.32	0.07
Peptostreptococcaceae (Clostridiales, Firmicutes)				
Intestinibacter	0.015 (0.036)	0.053 (0.06)	0.053	0.02
Ruminococcaceae (Clostridiales, Firmicutes)				
Anaerofilum	0.153 (0.168)	0.055 (0.065)	0.17	0.04
Anaerotruncus	0.585 (0.478)	0.335 (0.267)	**0.04***	0.01
Flavonifractor	0.107 (0.078)	0.057 (0.057)	**0.03***	0.007
Oscillibacter	0.653 (0.558)	0.477 (0.293)	0.62	0.12
Papillibacter	0.125 (0.105)	0.107 (0.073)	0.38	0.08
Ruminoclostridium	0.097 (0.13)	0.053 (0.157)	0.26	0.05
Ruminioclostridium 5	0.328 (0.172)	0.222 (0.095)	**0.04***	0.01
Ruminioclostridium 6	2.553 (2.06)	2.35 (2.52)	0.90	0.18
Ruminioclostridium 9	1.00 (0.587)	0.915 (0.408)	0.71	0.15
Ruminococcaeae NK4A214 group	0.367 (0.133)	0.41 (0.125)	0.71	0.15
Ruminococcaceae UCG-003	0.265 (0.268)	0.158 (0.077)	0.07	0.02
Ruminococcaceae UCG-004	0.188 (0.09)	0.208 (0.172)	0.81	0.17
Ruminococcaceae UCG-005	0.69 (0.46)	0.697 (0.453)	0.9	0.18
Ruminococcaceae UCG-009	0.043 (0.052)	0.053 (0.048)	0.54	0.1
Ruminococcaceae UCG-010	1.53 (1.113)	1.44 (2.658)	0.54	0.1
Ruminococcaceae UCG-011	0.008 (0.037)	0.035 (0.038)	0.07	0.03

Ruminococcaceae UCG-013	0.383 (0.517)	0.325 (0.323)	0.9	0.18
Ruminococcaceae UCG-014	3.828 (5.048)	5.265 (1.57)	0.26	0.05
Ruminococcaceae V9D2013 group	0.205 (0.195)	0.15 (0.235)	0.71	0.15
Ruminococcus 1	3.912 (1.217)	4.013 (1.507)	0.81	0.17
[Eubacterium] coprostanoligenes group	0.318 (0.22)	0.448 (0.687)	0.46	0.09
Rumiococcaceae uncultured	1.653 (1.242)	1.707 (0.555)	0.38	0.08
Erysipelotrichaceae (Erysipelotrichales, Firmicutes)				
Allobaculum	0.083 (0.21)	0.26 (0.343)	0.13	0.03
Rhodospirillaceae (Rhodospirillales, Proteobacteria)				
Thalassospira	0.642 (0.575)	0.942 (1.285)	0.21	0.05
Uncultured	0 (0.002)	0.183 (0.03)	**0.01****	0.004
Alcaligenaceae (Burkholderiales, Proteobacteria)				
Parasutterella	0.265 (0.23)	0.337 (0.197)	0.13	0.04
Desulfovibrionaceae (Deltaproteobacteria, Proteobacteria)				
Desulfovibrio	0.06 (0.103)	0.085 (0.167)	0.54	0.11
Unknown Family (Unknown order, Saccharibacteria)				
Candidatus Saccharimonas	0.518 (0.243)	0.683 (0.485)	0.17	0.04
Uncultured bacterium, (Mollicutes RF9, Tenericutes)				
Uncultured bacterium	0.23 (0.28)	0.15 (0.388)	0.9	0.18
Uncultured rumen bacterium (Mollicutes RF9, Tenericutes)				
Uncultured rumen bacterium	0.033 (0.07)	0.04 (0.267)	0.81	0.17
Verrucomicrobiaceae (Verrucomicrobiales, Verrucomicrobia)				
Akkermansia	0.152 (0.497)	0.265 (1.377)	0.38	0.08
Other				
No blast hit	0.043 (0.04)	0.058 (0.033)	0.32	0.07

Appendix Table B.3 Relative abundance (%) of bacterial* genera *in the faeces of Sham and CIH-exposed guinea-pigs.

Only genera that had a relative abundance > 0.04% in sham or CIH-exposed animals are represented in this table. Data are shown as median (IQR) and were statistically compared using non-parametric Mann-Whitney *U* test and Benjamini-Hochberg adjustment procedure with the false discovery rate set at 20% to correct for multiple testing. Raw *p*-values < 0.05 are marked in bold. Significant false discovery rate adjusted p-values are in bold. CIH, chronic intermittent hypoxia. * denotes $p<0.05$ compared with Sham; ** denotes $p<0.01$ compared with Sham.

Appendix C. Chronic intermittent hypoxia lowers *Lactobacillus rhamnosus* relative abundance and increases apnoea index and blood pressure: Effects of prebiotic supplementation



Appendix Figure C.1 Correlation analysis between the relative abundance of Lactobacillus rhamnosus and sigh events during hypercapnia.

Individual data points for correlation analysis between *Lactobacillus rhamnosus* and sigh amplitude (a) and frequency (b) during hypercapnia in sham+VEH and CIH+VEH rats. CIH, chronic intermittent hypoxia; VEH, vehicle. Solid dark blue lines represent linear regression analysis for each parameter. *p*-values are shown.

	Sham+VEH	CIH+VEH	Sham+PREB	CIH+PREB	p-value (Kruskal-Wallis)	p-value (two-way ANOVA)	Sham+VEH v CIH+VEH	CIH+VEH v CIH+PREB	Sham+PREB v CIH+PREB	Sham+VEH v Sham+PREB
RV (mg)	169 ± 31	174 ± 20	179 ± 32	161 ± 26	N/A	Diet, p=0.627; Exposure, p=0.344; Diet*Exposure, p=0.121	-	-	-	-
LV (mg)	864 ± 73	799 ± 41	730 ± 41	621 ± 72	N/A	Diet, **p<0.0005**; Exposure, **p<0.0005**; Diet*Exposure, **p=0.023**	0.207	**<0.0005**	**<0.0005**	**<0.0005**
LV+RV (mg)	1025 ± 60	997 ± 38	917 ± 61	781 ± 94	**<0.0005**	N/A	0.074	**<0.0005**	**0.001**	**0.001**
Caecum (g)	3.6 ± 1.0	3.0 ± 0.3	6.4 ± 1.2	6.0 ± 1.8	N/A	Diet, **p<0.0005**; Exposure, p=0.428; Diet*Exposure, p=0.926	0.565	**<0.0005**	0.583	**<0.0005**
Lung dry weight (mg)	316 ± 38	340 ± 13	296 ± 21	305 ± 52	**0.001**	N/A	0.052	**0.012**	0.862	**0.009**
Lung wet weight (mg)	1422 ± 146	1596 ± 182	1394 ± 112	1390 ± 244	**0.015**	N/A	0.206	0.024	0.908	0.035

Appendix Table C.1. Body and tissue weights

RV, right ventricle; LV, left ventricle; CIH, chronic intermittent hypoxia; PREB, prebiotic; VEH, vehicle. Data are shown as mean ± SD and were statistically compared using two-way ANOVA, followed by Fisher's least significant difference (LSD) *post hoc* where appropriate, or non-parametric Kruskal-Wallis test, followed by Mann-Whitney *U* test, where appropriate. Statistical significance for multiple comparisons was accepted at $p<0.05$ divided by the number of comparisons made, which was four i.e. $p<0.0125$. *p*-values shown in **bold** highlight significant differences.

	Sham+VEH	CIH+VEH	Sham+PREB	CIH+PREB	p-value (Kruskal-Wallis)	p-value (two-way ANOVA)	Sham+VEH v CIH+VEH	CIH+VEH v CIH+PREB	Sham+PREB v CIH+PREB	Sham+VEH v Sham+PREB
V_E (ml/min)	28 ± 3	29 ± 4	31 ± 5	34 ± 5	N/A	Diet, **p=0.004**; Exposure, p=0.107; Diet*Exposure, p=0.605	0.436	0.015	0.129	0.074
V_T (ml)	2.5 ± 0.3	2.5 ± 0.3	2.4 ± 0.4	2.3 ± 0.3	0.667	N/A	-	-	-	-
V_T/T_i (ml/s)	10 ± 1.9	9.2 ± 1.2	9.5 ± 1.5	8.7 ± 1.0	N/A	Diet, p=0.076; Exposure, **p=0.024**; Diet*Exposure, p=0.636	0.055	0.353	0.188	0.108
VO_2 (ml/min)	9.8 ± 2.4	8.5 ± 2.8	8.6 ± 2.8	8.6 ± 2.8	N/A	Diet, p=0.472; Exposure, p=0.385; Diet*Exposure, p=0.385	-	-	-	-
VCO_2 (ml/min)	7.0 ± 0.9	6.6 ± 0.8	5.7 ± 1.0	5.5 ± 0.8	**0.001**	N/A	0.218	**0.004**	0.795	**0.006**

Appendix Table C.2. Baseline ventilation in behaving rats during quiet rest

V_E, minute ventilation; V_T, tidal volume; V_T/T_i, mean inspiratory flow; VO_2, oxygen consumption; VCO_2, carbon dioxide production; V_E/ CIH, chronic intermittent hypoxia; PREB, prebiotic; VEH, vehicle. Data are shown as mean ± SD and were statistically compared using two-way ANOVA, followed by Fisher's least significant difference (LSD) *post hoc* where appropriate, or non-parametric Kruskal-Wallis test, followed by Mann-Whitney *U* test, where appropriate. Statistical significance for multiple comparisons was accepted at $p<0.05$ divided by the number of comparisons made, which was four i.e. $p<0.0125$. *p*-values shown in **bold** highlight significant differences.

	Sham+VEH	CIH+VEH	Sham+PREB	CIH+PREB	p-value (Kruskal-Wallis)	p-value (two-way ANOVA)	Sham+VEH v CIH+VEH	CIH+VEH v CIH+PREB	Sham+PREB v CIH+PREB	Sham+VEH v Sham+PREB
Hypoxia (% change from baseline)										
f_R	20 ± 13	23 ± 9	12 ± 17	16 ± 23	N/A	Diet, p=0.120; Exposure, p=0.697; Diet*Exposure, p=0.774	-	-	-	-
V_T	8 ± 14	15 ± 7	14 ± 10	10 ± 14	N/A	Diet, p=0.976; Exposure, p=0.687; Diet*Exposure, p=0.137	-	-	-	-
V_E	30 ± 28	42 ± 15	28 ± 25	29 ± 38	0.815	N/A	-	-	-	-
MAP	-37 ± 12	-31 ± 15	-38 ± 11	-31 ± 15	N/A	Diet, p=0.685; Exposure, p=0.398; Diet*Exposure, p=0.431	-	-	-	-
DBP	-44 ± 15	-46 ± 10	-45 ± 13	-40 ± 18	N/A	Diet, p=0.842; Exposure, p=0.682; Diet*Exposure, p=0.424	-	-	-	-
SBP	-25 ± 10	-18 ± 10	-20 ± 9.8	-14 ± 11	0.177	N/A	-	-	-	-
HR	2 ± 10	4 ± 8	4 ± 6	4 ± 13	N/A	Diet, p=0.633; Exposure, p=0.494; Diet*Exposure, p=0.990	-	-	-	-
Hypoxic hypercapnia (% change from baseline)										
f_R	38 ± 17	33 ± 13	25 ± 24	17 ± 23	**0.023**	N/A	0.944	**0.012**	0.262	0.205

V_T	67 ± 17	63 ± 17	68 ± 28	84 ± 23	0.056	N/A	-	-	-	-
V_E	128 ± 30	114 ± 23	112 ± 60	115 ± 56	N/A	Diet, p=0.644; Exposure, p=0.741; Diet*Exposure, p=0.611	-	-	-	-
MAP	-33 ± 12	-22 ± 15	-21 ± 15	-9 ± 13	N/A	Diet, **p=0.010**; Exposure, **p=0.008**; Diet*Exposure, p=0.693	0.116	0.036	0.033	0.211
DBP	-40 ± 15	-29 ± 18	-29 ± 20	-13 ± 18	N/A	Diet, **p=0.023**; Exposure, **p=0.011**; Diet*Exposure, p=0.667	0.100	0.052	0.028	0.183
SBP	-10 ± 7	-7 ± 12	-6 ± 10	-2 ± 5	0.173	N/A	-	-	-	-
HR	6 ± 4	8 ± 4	9 ± 6	8 ± 8	N/A	Diet, p=0.619; Exposure, p=0.889; Diet*Exposure, p=0.590	-	-	-	-
Sodium cyanide (% change from baseline)										
f_R	53 ± 18	51 ± 20	62 ± 21	44 ± 24	0.213	N/A	-	-	-	-
V_T	46 ± 12	45 ± 12	51 ± 15	44 ± 14	N/A	Diet, p=0.557; Exposure, p=0.311; Diet*Exposure, p=0.474	-	-	-	-
V_E	110 ± 34	112 ± 38	133 ± 41	102 ± 49	0.489	N/A	-	-	-	-
MAP	19 ± 8	18 ± 8	19 ± 8	17 ± 13	N/A	Diet, p=0.383; Exposure, p=0.728;	-	-	-	-

						Diet*Exposure, p=0.652				
DBP	22 ± 9	26 ± 23	28 ±17	28 ± 25	N/A	Diet, p=0.489; Exposure, p=0.596; Diet*Exposure, p=0.823	-	-	-	-
SBP	12 ± 8	8 ± 7	8 ± 8	8 ± 6	0.131	N/A	-	-	-	-
HR	7 ± 5	7 ± 6	8 ± 7	9 ± 9	N/A	Diet, p=0.960; Exposure, p=0.732; Diet*Exposure, p=0.994	-	-	-	-

Appendix Table C.3 Cardiorespiratory responsiveness to chemostimulation in urethane anaesthetised rats

f_R, respiratory frequency (brpm, breaths per min); V_T, tidal volume; V_E, minute ventilation; MAP, mean arterial pressure; DBP, diastolic blood pressure; SBP, systolic blood pressure; HR, heart rate (bpm, beats per min); CIH, chronic intermittent hypoxia; preb, prebiotic; VEH, vehicle. Data are shown as mean ± SD and were statistically compared using two-way ANOVA, followed by Fisher's least significant difference (LSD) *post hoc* where appropriate, or non-parametric Kruskal-Wallis test, followed by Mann-Whitney *U* test, where appropriate. Statistical significance for multiple comparisons was accepted at $p<0.05$ divided by the number of comparisons made, which was four i.e. $p<0.0125$. *p*-values shown in **bold** highlight significant differences.

	Sham+VEH	CIH+VEH	Sham+PREB	CIH+PREB	p-value (Kruskal-Wallis)	p-value (two-way ANOVA)	Sham+VEH v CIH+VEH	CIH+VEH v CIH+PREB	Sham+PREB v CIH+PREB	Sham+VEH v Sham+PREB
Phenylephrine (% change from baseline)										
SBP	43 ± 11	47 ± 16	35 ± 12	37 ± 9	**0.018**	N/A	0.999	0.015	0.667	0.049
HR	-25 ± 14	-24 ± 14	-20 ± 12	-15 ± 7	0.149	N/A	-	-	-	-
Sodium nitroprusside (% change from baseline)										
SBP	-30 ± 14	-31 ± 14	-22 ± 10	-27 ± 11	0.236	N/A	-	-	-	-
HR	13 ± 5	8 ± 3	6 ± 4	7 ± 3	N/A	Diet, **p=0.001**; Exposure, p=0.106; Diet*Exposure, p=0.053	0.013	0.245	0.842	**<0.0005**

Appendix Table C.4 Baroreflex receptor sensitivity in urethane anaesthetised rats

SBP, systolic blood pressure; HR, heart rate; CIH, chronic intermittent hypoxia; PREB, prebiotic; VEH, vehicle. Data are shown as mean ± SD and were statistically compared using two-way ANOVA, followed by Fisher's least significant difference (LSD) *post hoc* where appropriate, or non-parametric Kruskal-Wallis test, followed by Mann-Whitney *U* test, where appropriate. Statistical significance for multiple comparisons was accepted at $p<0.05$ divided by the number of comparisons made, which was four i.e. $p<0.0125$. *p*-values shown in **bold** highlight significant differences.

	Sham+VEH	CIH+VEH	Sham+PREB	CIH+PREB	p-value (Kruskal-Wallis)	p-value (two-way ANOVA)	Sham+VEH v CIH+VEH	CIH+VEH v CIH+PREB	Sham+PREB v CIH+PREB	Sham+VEH v Sham+PREB
Baseline										
Area under the curve (v.s)	0.02 ± 0.00	0.03 ± 0.01	0.03 ± 0.02	0.03 ± 0.03	0.222	N/A	-	-	-	-
Max slope (v/s)	1.0 ± 0.2	1.1 ± 0.3	1.4 ± 0.5	1.5 ± 0.7	N/A	Diet, **p=0.023**; Exposure, p=0.482; Diet*Exposure, p=0.846	0.715	0.074	0.531	0.138
Occlusion (% change from baseline)										
Area under the curve	87 ± 40	65 ± 34	96 ± 44	57 ± 41	0.073	N/A	-	-	-	-
Hypoxia (% change from baseline)										
Area under the curve	11 ± 21	6 ± 13	12 ± 11	9 ± 12	0.974	N/A	-	-	-	-
Max slope	31 ± 28	19 ± 14	22 ± 17	24 ± 19	0.511	N/A	-	-	-	-
Hypoxic hypercapnia (% change from baseline)										
Area under the curve	18 ± 15	11 ± 16	18 ± 15	26 ± 13	N/A	Diet, p=0.085; Exposure, p=0.967; Diet*Exposure, p=0.159	-	-	-	-
Max slope	47 ± 17	39 ± 21	32 ± 23	59 ± 37	N/A	Diet, p=0.216; Exposure, p=0.085; Diet*Exposure, p=0.829	-	-	-	-
Sodium cyanide (% change from baseline)										

Area under the curve	23 ± 12	30 ± 11	46 ± 25	47 ± 30	N/A	Diet, **p=0.003**; Exposure, p=0.652; Diet*Exposure, p=0.639	0.511	0.063	0.989	0.015
Max slope	70 ± 35	66 ± 17	67 ± 23	64 ± 33	N/A	Diet, p=0.829; Exposure, p=0.669; Diet*Exposure, p=0.922	-	-	-	-

Appendix Table C.5 Diaphragm EMG activity during baseline and chemostimulation in urethane anaesthetised rats

CIH, chronic intermittent hypoxia; PREB, prebiotic; VEH, vehicle. Data are shown as mean ± SD and were statistically compared using two-way ANOVA, followed by Fisher's least significant difference (LSD) *post hoc* where appropriate, or non-parametric Kruskal-Wallis test, followed by Mann-Whitney *U* test, where appropriate. Statistical significance for multiple comparisons was accepted at $p<0.05$ divided by the number of comparisons made, which was four i.e. $p<0.0125$. *p*-values shown in **bold** highlight significant differences.

	Sham+VEH	CIH+VEH	Sham+PREB	CIH+PREB	p-value (Kruskal-Wallis)	p-value (two-way ANOVA)	Sham+VEH v CIH+VEH	CIH+VEH v CIH+PREB	Sham+PREB v CIH+PREB	Sham+VEH v Sham+PREB
pH	7.37 ± 0.04	7.35 ± 0.04	7.40 ± 0.02	7.36 ± 0.04	N/A	Diet, p=0.436; Exposure, p=0.152; Diet*Exposure, p=0.301	-	-	-	-
$PaCO_2$ (mmHg)	41 ± 13	48 ± 5	50 ± 4	48 ± 6	0.140	N/A	-	-	-	-
PaO_2 (mmHg)	95 ± 6	98 ± 7	100 ± 11	106 ± 10	N/A	Diet, **p=0.033**; Exposure, p=0.100; Diet*Exposure, p=0.689	0.370	0.817	0.149	**0.002**
Haematocrit (%)	47.5 ± 2.5	46.5 ± 3.0	43.1 ± 2.8	43.9 ± 4.0	N/A	Diet, **p<0.0005**; Exposure, p=0.871; Diet*Exposure, p=0.305	0.394	0.050	0.544	**0.001**
[Hb] (g/dl)	16.2 ± 0.9	15.2 ± 1.0	14.6 ± 0.9	14.9 ± 1.3	N/A	Diet, **p<0.0005**; Exposure, p=0.943; Diet*Exposure, p=0.324	0.447	0.047	0.521	**0.002**

Appendix Table C.6 Blood gases in urethane anaesthetised rats

Pco_2, partial pressure of arterial carbon dioxide; Pao_2, partial pressure of arterial oxygen; [Hb], haemoglobin concentration; MAP, mean arterial blood pressure; SBP, systolic blood pressure; DBP, diastolic blood pressure; HR, heart rate (bpm, beat per min); CIH, chronic intermittent hypoxia; PREB, prebiotic; VEH, vehicle. Data are shown as mean ± SD and were statistically compared using two-way ANOVA, followed by Fisher's least significant difference (LSD) *post hoc* where appropriate, or non-parametric Kruskal-Wallis test, followed by Mann-Whitney *U* test, where appropriate. Statistical significance for multiple comparisons was accepted at $p<0.05$ divided by the number of comparisons made, which was four i.e. $p<0.0125$. *p*-values shown in **bold** highlight significant differences.

	Sham+VEH	CIH+VEH	p-value
Body mass (g)	353 ±19	343 ±22	0.287
RV (mg)	215 ± 17	182 ± 32	0.506
RV (mg/100g)	61 ± 6	56 ± 8	0.419
LV (mg)	803 ± 51	787 ± 71	0.844
LV (mg/100g)	228 ± 16	244 ± 21	0.311
RV+LV (mg)	1018 ± 42	2112 ± 100	0.634
RV+LV (mg/100g)	290 ± 17	300 ± 27	0.172
Caecum (g)	5.2 ± 1.0	5.0 ± 1.6	0.710
Caecum (g/100g)	1.5 ± 0.3	1.5 ± 0.5	0.496

Appendix Table C.7 Body and tissue weights in rats euthanized by pentobarbitone

BW, body weight; RV, right ventricle; LV, left ventricle; CIH, chronic intermittent hypoxia; VEH, vehicle. Data are shown as mean ± SD and were statistically compared using independent samples *t*-test or non-parametric Mann-Whitney *U* test, where appropriate.

	Sham+VEH	CIH+VEH	p-value
Pons			
IFN-γ	7.7 ± 0.6	7.8 ± 0.7	0.097
IL-1β	253 ± 26	275 ± 60	0.518
IL-4	2.2 ± 0.0008	2.2 ± 0.0008	0.131
IL-5	21 ± 0.8	20 ± 0.6	**0.044**
IL-6	38 ± 11.0	36 ± 7.1	0.756
KC/GRO	4.1 ± 0.9	4.2 ± 1.2	0.621
IL-10	4.3 ± 1.5	4.1 ± 1.8	0.902
IL-13	1.8 ± 0.04	1.8 ± 0.05	0.163
TNF-α	0.6 ± 0.04	0.6 ± 0.03	0.843
Medulla			
IFN-γ	8.1 ± 0.9	7.6 ± 1.3	0.050
IL-1β	283 ± 27	268 ± 33	0.057
IL-4	2.2 ± 0.0006	2.2 ± 0.0006	0.070
IL-5	21 ± 0.5	20 ± 0.4	**0.016**
IL-6	48 ± 18	33 ± 10	0.380
KC/GRO	4.7 ± 1.2	3.6 ± 1.4	0.052
IL-10	4.8 ± 1.8	3.0 ± 1.5	**0.035**
IL-13	1.8 ± 0.08	1.8 ± 0.06	0.906
TNF-α	0.6 ± 0.05	0.6 ± 0.04	0.373

Appendix Table C.8 Cytokine concentrations in pons and medulla oblongata

IFN-γ, interferon-γ; IL-β, interleukin-β; IL-4, interleukin-4; IL-5, interleukin-5; IL-6, interleukin-6; KC/GRO, keratinocyte chemoattractant/growth-related oncogene; IL-10, interleukin-10; IL-13, interleukin-13; TNF-α, tumour necrosis factor; CIH, chronic intermittent hypoxia; VEH, vehicle. Data are shown as mean ± SD and were statistically compared using independent samples *t*-test or non-parametric Mann-Whitney *U* test, where appropriate. *p*-values shown in **bold** highlight significant differences.

Bacterial species	p-value	Statistic	q-value
Actinobacteria			
Acidimicrobium ferrooxidans	0.000104	-0.55375	0.01888
Acidipropionibacterium sp. JS278	0.001673	-0.45942	0.04825
Actinomyces oris	0.005244	-0.41199	0.0711
Actinomyces sp. VUL4_3	0.00688	-0.39974	0.078342
Arsenicicoccus sp. oral taxon 190	0.007161	-0.39789	0.080043
Arthrobacter sp. ATCC 21022	0.005547	-0.40949	0.072506
Arthrobacter sp. PGP41	0.011805	-0.37404	0.090492
Arthrobacter sp. U41	0.000944	-0.48103	0.038102
Bifidobacterium angulatum	0.0069	-0.3996	0.078342
Bifidobacterium asteroides	0.003057	-0.43518	0.05565
Candidatus Rhodoluna planktonica	0.000625	0.495784	0.036179
Cellulomonas fimi	0.010572	-0.37945	0.089473
Cellulomonas sp. PSBB021	0.005167	-0.41265	0.0711
Coriobacterium glomerans	0.001526	-0.46298	0.047807
Corynebacterium callunae	0.008412	-0.39038	0.084904
Corynebacterium cystitidis	0.000753	-0.4892	0.037892
Corynebacterium flavescens	0.007732	-0.39433	0.082378
Corynebacterium imitans	0.012954	-0.36943	0.094512
Corynebacterium jeikeium	0.001214	-0.47167	0.041579
Corynebacterium provencense	0.010233	-0.38103	0.089069
Corynebacterium sp. ATCC 6931	0.002961	-0.4365	0.05565
Corynebacterium ulcerans	0.002466	-0.44401	0.052096
Dermacoccus nishinomiyaensis	0.008845	-0.38801	0.0871
Dietzia sp. JS16-p6b	0.010862	-0.37813	0.089611
Dietzia sp. oral taxon 368	0.014346	-0.3643	0.098887
Gordonibacter urolithinfaciens	0.012221	-0.37233	0.091368
Mycobacterium marinum	0.008272	-0.39117	0.084428
Mycolicibacterium vanbaalenii	0.010039	-0.38195	0.089069
Plantactinospora sp. KBS50	0.003655	-0.42767	0.060361
Rathayibacter toxicus	0.005213	-0.41225	0.0711
Rhodococcus jostii	0.009556	-0.38432	0.089069
Streptomyces autolyticus	0.010891	-0.378	0.089611
Streptomyces coelicolor	0.013125	-0.36877	0.095382
Streptomyces lincolnensis	3.88E-06	-0.64032	0.003521
Streptomyces noursei	0.008272	-0.39117	0.084428
Streptomyces sp. HNM0039	0.008507	-0.38986	0.085384
Streptomyces sp. SAT1	0.009195	-0.38617	0.088382
Streptomyces venezuelae	0.000904	-0.48261	0.038102
Aquificae			
Hydrogenobacter thermophilus	0.004556	-0.41818	0.066213
Persephonella marina	0.010345	-0.3805	0.089069
Bacteroidetes			

Arcticibacterium luteifluviistationis	0.008919	0.387615	0.087114
Aureitalea sp. RR4-38	0.014495	0.363768	0.098887
Chryseobacterium indologenes	0.003225	0.432938	0.056344
Croceibacter atlanticus	0.002531	0.442951	0.052249
Flavobacterium sp. HYN0056	0.000307	0.519895	0.027919
Polaribacter reichenbachii	0.011189	0.37668	0.089724
Sediminicola sp. YIK13	0.012319	0.371937	0.091721
Weeksella virosa	0.002878	0.437681	0.05565
Winogradskyella sp. PG-2	0.001007	0.478656	0.038913
Chlamydiae			
Chlamydia abortus	0.001112	0.474967	0.040408
Chloroflexi			
Caldilinea aerophila	0.00194	-0.45362	0.048422
Roseiflexus castenholzii	0.002178	-0.44901	0.049464
Roseiflexus sp. RS-1	0.005798	-0.40751	0.073656
Cyanobacteria			
Geminocystis sp. NIES-3709	0.008249	0.391304	0.084428
Gloeobacter kilaueensis	0.002999	-0.43597	0.05565
Nostoc sp. PCC 7524	0.006146	-0.40487	0.075669
Nostocales cyanobacterium HT-58-2	0.001802	0.456522	0.048422
Prochlorococcus marinus	0.003499	0.429513	0.05832
Synechococcus sp. JA-3-3Ab	4.34E-05	-0.57879	0.017794
Synechococcus sp. KORDI-49	0.006273	-0.40395	0.07569
Firmicutes			
Anaerostipes hadrus	0.007181	0.39776	0.080043
Bacillus anthracis	0.009297	-0.38564	0.088893
Bacillus clausii	0.006291	0.403821	0.07569
Bacillus cytotoxicus	0.005781	0.407642	0.073656
Bacillus kochii	0.000494	0.503953	0.031446
Bacillus pumilus	0.003781	0.426219	0.060446
Bacillus weihaiensis	0.000759	0.488933	0.037892
Blautia hansenii	0.003735	0.426746	0.060446
Blautia sp. N6H1-15	0.004882	0.415152	0.068755
Blautia sp. YL58	0.009018	0.387088	0.087614
Brevibacillus laterosporus	0.007431	0.396179	0.082054
Cellulosilyticum lentocellum	0.010177	0.381291	0.089069
Clostridium argentinense	0.004709	0.416733	0.066841
Clostridium clariflavum	0.007886	0.393412	0.083039
Clostridium cochlearium	0.014383	0.364163	0.098887
Clostridium drakei	0.003984	0.423979	0.061346
Clostridium estertheticum	0.001455	0.464822	0.047193
Clostridium sp. BNL1100	0.013229	0.368379	0.095754
Clostridium tyrobutyricum	0.014722	0.362978	0.099432
Dehalobacterium formicoaceticum	0.004542	0.418314	0.066213

Desulfosporosinus meridiei	0.008602	-0.38933	0.085867
Erysipelothrix rhusiopathiae	0.006058	0.405534	0.075669
Eubacterium eligens	0.003145	0.433992	0.05565
Eubacterium hallii	0.003155	0.43386	0.05565
Eubacterium rectale	0.002303	0.446772	0.05041
Ezakiella massiliensis	0.009795	0.383136	0.089069
Geobacillus subterraneus	0.000996	-0.47905	0.038913
Gottschalkia acidurici	0.006164	0.404743	0.075669
Lactobacillus casei	0.007754	-0.3942	0.082378
Lactobacillus murinus	0.010921	0.377866	0.089611
Lactobacillus parabuchneri	0.000853	0.484717	0.038102
Listeria welshimeri	0.000187	0.535837	0.024255
Macrococcus caseolyticus	0.010012	0.382082	0.089069
Megamonas hypermegale	0.002971	0.436364	0.05565
Oenococcus oeni	0.010345	-0.3805	0.089069
Paenibacillus beijingensis	0.01351	-0.36733	0.096252
Paenibacillus sabinae	0.006218	-0.40435	0.07569
Paenibacillus sp. FSL R5-0345	0.008869	0.387879	0.0871
Planococcus kocurii	0.007645	-0.39486	0.082182
Selenomonas sputigena	0.001511	-0.46337	0.047807
Sporosarcina ureae	0.005418	0.41054	0.072375
Staphylococcus condimenti	0.003466	0.429908	0.058312
Staphylococcus pasteuri	0.011711	0.37444	0.090492
Staphylococcus succinus	0.001148	0.473781	0.040895
Streptococcus parasanguinis	0.002087	0.450725	0.049234
Streptococcus pasteurianus	0.001914	0.45415	0.048422
Streptococcus pneumoniae	0.010261	0.380896	0.089069
Tepidanaerobacter acetatoxydans	0.000201	0.533597	0.024311
Thermincola potens	0.010572	-0.37945	0.089473
Thermoanaerobacterium thermosaccharolyticum	0.013369	0.367852	0.096252
Virgibacillus pantothenticus	0.004709	0.416733	0.066841
Bacillus xiamenensis	0.00573	0.408037	0.073656
Clostridia Thermoanaerobacterium xylanolyticum	6.74E-05	0.566403	0.017794
Fusobacteria			
Fusobacterium necrophorum	0.009582	0.38419	0.089069
Fusobacterium varium	0.011249	0.376416	0.089724
Ilyobacter polytropus	7.02E-05	0.565217	0.017794
Ignavibacteriae			
Ignavibacteria Ignavibacterium album	0.005244	0.411989	0.0711
Nitrospirae			
Thermodesulfovibrio yellowstonii	0.001927	0.453887	0.048422
Planctomycetes			
Phycisphaera mikurensis	0.014533	-0.36364	0.098887
Planctomyces sp. SH-PL62	0.00758	-0.39526	0.082182

Proteobacteria			
Xanthomonas vasicola	0.012784	0.370092	0.094277
Acetobacter aceti	0.010177	0.381291	0.089069
Acetobacter tropicalis	0.007161	-0.39789	0.080043
Acidithiobacillus ferrivorans	0.01131	-0.37615	0.089724
Acinetobacter equi	0.012818	0.36996	0.094277
Aeromonas sp. ASNIH2	0.000862	-0.48432	0.038102
Allofrancisella guangzhouensis	0.007953	0.393017	0.083039
Alteromonas addita	0.001778	0.457049	0.048422
Alteromonas sp. MB-3u-76	0.01351	0.367325	0.096252
Aminobacter aminovorans	0.002597	-0.4419	0.053015
Antarctobacter heliothermus	0.011555	-0.3751	0.090485
Arcobacter bivalviorum	0.000142	0.544269	0.021549
Arcobacter halophilus	0.014684	0.363109	0.099432
Bartonella quintana	0.003096	0.434651	0.05565
Bordetella bronchialis	0.01376	-0.3664	0.097269
Bordetella sp. H567	0.000914	-0.48221	0.038102
Bordetella sp. HZ20	0.001864	-0.4552	0.048422
Bradyrhizobium diazoefficiens	0.000813	-0.48643	0.037892
Bradyrhizobium sp. BTAi1	0.011249	-0.37642	0.089724
Burkholderia sp. JP2-270	0.010094	-0.38169	0.089069
Burkholderiales bacterium YL45	0.007645	0.394862	0.082182
Calyptogena okutanii thioautotrophic gill symbiont	0.001617	0.460738	0.048041
Campylobacter helveticus	0.004172	0.422003	0.062827
Campylobacter sp. RM16704	0.000796	0.48722	0.037892
Candidatus Blochmannia floridanus	0.006685	0.401054	0.07785
Candidatus Erwinia sp. ErCipseudotaxifoliae	0.011009	-0.37747	0.089692
Candidatus Fokinia solitaria	0.011099	-0.37708	0.089724
Candidatus Kinetoplastibacterium sorsogonicusi	0.008674	0.388933	0.086115
Celeribacter ethanolicus	0.000718	-0.49091	0.037892
Chromobacterium vaccinii	0.014495	-0.36377	0.098887
Citrobacter koseri	0.012156	-0.3726	0.091368
Corallococcus coralloides	0.010572	-0.37945	0.089473
Croceicoccus naphthovorans	0.000481	0.504875	0.031446
Cronobacter dublinensis	0.007645	-0.39486	0.082182
Cystobacter fuscus	0.00384	-0.42556	0.060514
Desulfobacterium autotrophicum	0.003689	-0.42727	0.060376
Desulfocapsa sulfexigens	0.004184	-0.42187	0.062827
Desulfohalobium retbaense	0.002403	-0.44506	0.05186
Ehrlichia sp. HF	0.002288	0.447036	0.05041
Enterobacter sp. FY-07	0.00024	-0.52793	0.025635
Enterobacter sp. ODB01	0.001223	-0.47141	0.041579
Epibacterium mobile	0.003864	-0.4253	0.060514
Erwinia billingiae	0.001236	-0.47101	0.041579

Erythrobacter seohaensis	0.003793	0.426087	0.060446
Francisella noatunensis	0.011868	0.373781	0.090594
Gammaproteobacteria bacterium DM2	0.014533	0.363636	0.098887
Gammaproteobacteria bacterium ESL0073	6.29E-05	0.568379	0.017794
Gemmobacter sp. HYN0069	0.000298	-0.52095	0.027919
Geobacter sp. M18	0.001972	-0.45296	0.048422
Geobacter uraniireducens	0.003423	-0.43043	0.058309
Gluconobacter albidus	0.000934	-0.48142	0.038102
Halocynthiibacter arcticus	0.001089	0.475758	0.040366
Halomonas sp. KO116	0.002178	-0.44901	0.049464
Halorhodospira halochloris	0.003028	0.435573	0.05565
Helicobacter cetorum	0.005482	0.410013	0.072506
Herbaspirillum frisingense	0.010289	-0.38076	0.089069
Herbaspirillum hiltneri	0.014346	-0.3643	0.098887
Kangiella koreensis	0.003067	-0.43505	0.05565
Ketogulonicigenium vulgare	0.000119	-0.5498	0.019588
Klebsiella oxytoca	0.013868	-0.36601	0.097277
Klebsiella sp. M5al	0.010687	0.37892	0.089473
Kosakonia oryzae	0.000352	0.515415	0.028363
Leisingera methylohalidivorans	0.000748	-0.48946	0.037892
Leminorella richardii	0.001054	-0.47694	0.039911
Limnobaculum parvum	0.003434	0.430303	0.058309
Luteibacter rhizovicinus	0.000381	-0.51278	0.028839
Mariprofundus aestuarium	0.008319	-0.39091	0.084428
Massilia armeniaca	0.01131	-0.37615	0.089724
Mesorhizobium japonicum	0.00537	-0.41094	0.072267
Methylobacterium phyllosphaerae	0.001742	-0.45784	0.048422
Methylobacterium sp. C1	0.007931	-0.39315	0.083039
Methylocella silvestris	0.006439	-0.40277	0.076956
Methylococcus capsulatus	0.005663	-0.40856	0.073487
Methylophilus sp. TWE2	0.009984	0.382213	0.089069
Microvirga ossetica	0.002426	0.444664	0.05186
Morganella morganii	0.01351	0.367325	0.096252
Moritella yayanosii	0.004597	0.417787	0.066285
Myxococcus hansupus	0.009768	-0.38327	0.089069
Myxococcus xanthus	0.000284	-0.52253	0.027919
Nitrosomonas sp. Is79A3	7.84E-05	0.562055	0.017794
Obesumbacterium proteus	0.000359	0.514756	0.028363
Oblitimonas alkaliphila	0.011679	-0.37457	0.090492
Octadecabacter antarcticus	0.00684	-0.4	0.078342
Oleiphilus messinensis	0.003106	0.434519	0.05565
Pandoraea pnomenusa	0.005015	-0.41397	0.070087
Pantoea sp. At-9b	0.001639	-0.46021	0.048041
Pantoea sp. PSNIH1	0.001569	-0.46192	0.048041

Paraburkholderia terrae	0.004314	0.420553	0.064239
Paraburkholderia xenovorans	0.000447	0.507378	0.031244
Paracoccus aminovorans	0.000578	-0.49855	0.034995
Paracoccus sp. CBA4604	0.006762	-0.40053	0.07825
Phaeobacter inhibens	0.006646	-0.40132	0.07785
Photobacterium damselae	0.000173	0.53834	0.024108
Porphyrobacter neustonensis	0.003936	-0.42451	0.061115
Proteus mirabilis	0.000637	0.495125	0.036179
Providencia rettgeri	0.010658	0.379051	0.089473
Pseudoalteromonas phenolica	0.000502	0.503426	0.031446
Pseudomonas alcaligenes	0.001953	-0.45336	0.048422
Pseudomonas azotoformans	0.009119	-0.38656	0.088118
Pseudomonas cichorii	0.001864	-0.4552	0.048422
Pseudomonas pseudoalcaligenes	0.013868	0.366008	0.097277
Pseudomonas sp. NC02	0.005515	-0.40975	0.072506
Pseudomonas stutzeri	0.002143	-0.44967	0.049464
Pseudomonas syringae	0.012616	-0.37075	0.093552
Pseudomonas versuta	0.011493	0.375362	0.090391
Pseudomonas viridiflava	1.01E-06	-0.67167	0.001844
Pseudoxanthomonas spadix	0.011742	-0.37431	0.090492
Psychrobacter sp. P2G3	0.001731	0.458103	0.048422
Psychromonas ingrahamii	0.011932	-0.37352	0.090697
Psychromonas sp. CNPT3	0.010862	0.378129	0.089611
Rahnella sp. Y9602	0.011805	-0.37404	0.090492
Ralstonia pickettii	0.008021	0.392622	0.083264
Rhizobacter gummiphilus	5.84E-05	-0.57049	0.017794
Rhizobium sp. 11515TR	0.002087	-0.45072	0.049234
Rhodobacter capsulatus	0.006666	0.401186	0.07785
Rhodocyclaceae bacterium	0.006093	0.40527	0.075669
Rhodomicrobium vannielii	0.01095	-0.37773	0.089611
Rhodovulum sp. MB263	0.006005	-0.40593	0.075669
Rickettsia akari	0.009426	-0.38498	0.089069
Roseomonas sp. FDAARGOS_362	0.009957	-0.38235	0.089069
Serratia ficaria	0.000802	-0.48696	0.037892
Shewanella bicestrii	0.002273	0.447299	0.05041
Shinella sp. HZN7	0.003145	-0.43399	0.05565
Sinorhizobium americanum	0.012092	-0.37286	0.091368
Sinorhizobium fredii	0.010289	-0.38076	0.089069
Sinorhizobium medicae	0.004146	-0.42227	0.062827
Sphingobium cloacae	0.001302	-0.46904	0.043017
Sphingobium indicum	0.000103	-0.55415	0.01888
Sphingobium sp. TKS	0.00022	-0.5307	0.024976
Sphingomonas sp. Cra20	0.012886	0.369697	0.094394
Sphingomonas sp. MM-1	0.013941	-0.36574	0.09741

Sulfuritalea hydrogenivorans	0.001612	-0.46087	0.048041
Thiocystis violascens	0.009876	-0.38274	0.089069
Vibrio harveyi	0.006685	-0.40105	0.07785
Vibrio rotiferianus	0.012188	0.372464	0.091368
Yersinia aleksiciae	0.000351	0.515547	0.028363
Yersinia frederiksenii	0.013581	0.367062	0.09638
Yersinia ruckeri	0.00043	-0.5087	0.031244
Spirochaetes			
Borreliella afzelii	0.011493	-0.37536	0.090391
Sphaerochaeta globosa	0.002523	-0.44308	0.052249
Treponema putidum	0.003423	0.430435	0.058309
Tenericutes			
Spiroplasma syrphidicola	0.004367	0.420026	0.064496
Tenericutes bacterium MO-XQ	0.007452	0.396047	0.082054
Thermotogae			
Defluviitoga tunisiensis	0.002726	0.439921	0.055018
Fervidobacterium nodosum	0.002066	0.45112	0.049234
Marinitoga sp. 1137	0.009688	0.383663	0.089069
Petrotoga mobilis	0.002961	0.436495	0.05565
Thermosipho melanesiensis	0.009478	-0.38472	0.089069
Verrucomicrobia			
Opitutaceae bacterium TAV5	0.010658	-0.37905	0.089473

Appendix Table C.9 Significant correlations between mean arterial blood pressure and bacterial species

Hierarchical All-against-All association testing (HAllA) was used (version 0.8.7) with Spearman correlation as correlation metric, medoid as clustering method and $q < 0.1$ as threshold for significance.

Bacterial species	p-value	statistic	q-value
Actinobacteria			
Arthrobacter sp. U41	0.000432	-0.50856	0.085106
Corynebacterium jeikeium	0.000494	-0.50395	0.085106
Streptomyces lincolnensis	5.20E-05	-0.57378	0.067098
Cyanobacteria			
Synechococcus sp. JA-3-3Ab	0.00044	-0.50791	0.085106
Proteobacteria			
Rhizobacter gummiphilus	0.000189	-0.53544	0.081474
Campylobacter sp. RM16704	0.000314	0.519236	0.085106
Gemmobacter sp. HYN0069	0.000152	-0.54216	0.078751
Halocynthiibacter arcticus	0.000126	0.54809	0.078751
Ketogulonicigenium vulgare	0.000433	-0.50843	0.085106
Luteibacter rhizovicinus	0.000449	-0.50725	0.085106
Obesumbacterium proteus	0.000422	0.509354	0.085106
Paraburkholderia xenovorans	0.000569	0.499078	0.091873
Pseudomonas viridiflava	8.09E-06	-0.62253	0.020898
Sphingobium indicum	0.00012	-0.54941	0.078751
Yersinia aleksiciae	0.000489	0.504348	0.085106
Yersinia ruckeri	0.000483	-0.50474	0.085106

Appendix Table C.10 Significant correlations between diastolic blood pressure and bacterial species

Hierarchical All-against-All association testing (HAllA) was used (version 0.8.7) with Spearman correlation as correlation metric, medoid as clustering method and $q < 0.1$ as threshold for significance.

Actinobacteria	p-value	Statistical	q-value
Candidatus Rhodoluna planktonica	0.003246	0.432675	0.083956
Corynebacterium sp. ATCC 6931	0.003466	-0.42991	0.085635
Dietzia sp. oral taxon 368	0.003067	-0.43505	0.082224
Mycobacterium ulcerans	0.000985	0.479447	0.063073
Pseudarthrobacter chlorophenolicus	0.002869	-0.43781	0.080105
Renibacterium salmoninarum	0.004433	0.419368	0.093723
Sinomonas atrocyanea	0.00377	-0.42635	0.088936
Streptomyces lincolnensis	0.002896	-0.43742	0.080105
Streptomyces xiamenensis	0.001634	-0.46034	0.069792
Bacteroidetes			
Candidatus Cardinium hertigii	0.001901	0.454414	0.070373
Chryseobacterium indologenes	0.000607	0.496838	0.063073
Sediminicola sp. YIK13	0.004288	0.420817	0.091804
Caldiserica			
Caldisericum exile	0.004262	0.42108	0.091804
Cyanobacteria			
Prochlorococcus marinus	0.002674	0.440711	0.079433
Deinococcus-Thermus			
Thermus oshimai	0.002589	-0.44203	0.077969
Firmicutes			
Aerococcus urinae	0.002333	0.446245	0.075082
Alkaliphilus metalliredigens	0.000721	0.490777	0.063073
Anaerostipes hadrus	0.000739	0.489855	0.063073
Bacillus clausii	0.002094	0.450593	0.070817
Bacillus flexus	0.00298	0.436232	0.080897
Bacillus simplex	0.00128	0.469697	0.063073
Bacillus weihaiensis	0.000109	0.552306	0.039979
Bacillus xiamenensis	0.001253	0.470487	0.063073
Blautia hansenii	0.001298	0.46917	0.063073
Blautia sp. N6H1-15	0.00071	0.491304	0.063073
Blautia sp. YL58	0.001713	0.458498	0.070373
Clostridium argentinense	0.001227	0.471278	0.063073
Clostridium cellulosi	0.003677	0.427404	0.088936
Clostridium cochlearium	0.00091	0.482345	0.063073
Clostridium drakei	0.002326	0.446377	0.075082
Clostridium estertheticum	0.001435	0.465349	0.065048
Clostridium pasteurianum	0.003924	0.424638	0.088936
Clostridium thermosuccinogenes	0.002442	0.444401	0.076707
Dehalobacterium formicoaceticum	0.00145	0.464954	0.065048
Eubacterium eligens	0.001495	0.463768	0.065748
Eubacterium hallii	0.00384	0.42556	0.088936
Eubacterium limosum	0.002752	0.439526	0.080105
Eubacterium rectale	0.001311	0.468775	0.063073

Geobacillus thermodenitrificans	0.001348	0.467721	0.063073
Gottschalkia acidurici	0.003391	0.43083	0.084734
Listeria welshimeri	0.003328	0.431621	0.084734
Macrococcus canis	0.001325	0.468379	0.063073
Mordavella sp. Marseille-P3756	0.000207	0.532675	0.050488
Natranaerobius thermophilus	0.001156	0.473518	0.063073
Paenibacillus sp. FSL R5-0345	0.001193	0.472332	0.063073
Paenibacillus sp. lzh-N1	0.004752	-0.41634	0.096739
Ruminococcus bicirculans	0.00176	0.457444	0.070373
Salimicrobium jeotgali	0.001914	0.45415	0.070373
Sporosarcina ureae	0.000598	0.497365	0.063073
Staphylococcus succinus	0.001025	0.477997	0.063073
Streptococcus agalactiae	0.001796	0.456653	0.070373
Streptococcus sp. oral taxon 431	0.002841	0.438208	0.080105
Streptococcus thermophilus	0.000454	0.506851	0.063073
Thermoanaerobacter wiegelii	0.000614	0.496443	0.063073
Thermoanaerobacterium xylanolyticum	0.003828	0.425692	0.088936
Fusobacteria			
Fusobacterium mortiferum	0.004681	0.416996	0.096185
Ilyobacter polytropus	4.98E-05	0.574967	0.036504
Sebaldella termitidis	0.000729	0.490382	0.063073
Proteobacteria			
Acetobacter aceti	0.000699	0.491831	0.063073
Agrobacterium sp. H13-3	0.002012	-0.45217	0.070817
Allofrancisella guangzhouensis	0.000399	0.511199	0.062717
Arcobacter bivalviorum	0.002589	0.442029	0.077969
Bordetella bronchialis	0.001808	-0.45639	0.070373
Calyptogena okutanii thioautotrophic gill symbiont	0.004301	0.420685	0.091804
Campylobacter hominis	0.001	0.47892	0.063073
Candidatus Carsonella ruddii	0.000841	0.485244	0.063073
Candidatus Fokinia solitaria	0.001214	-0.47167	0.063073
Candidatus Nucleicultrix amoebiphila	0.000146	0.543478	0.04336
Chromobacterium vaccinii	0.000657	-0.49407	0.063073
Citrobacter koseri	0.004009	-0.42372	0.089942
Desulfobacula toluolica	0.00208	0.450856	0.070817
Gammaproteobacteria bacterium ESL0073	3.93E-05	0.581555	0.036504
Janthinobacterium sp. 1_2014MBL_MicDiv	0.004275	-0.42095	0.091804
Klebsiella sp. M5al	0.004197	0.421739	0.091804
Lawsonia intracellularis	0.000319	0.518709	0.059562
Limnobaculum parvum	0.004941	0.414625	0.098755
Magnetospirillum gryphiswaldense	0.000258	-0.52556	0.056776
Marinobacter hydrocarbonoclasticus	0.004824	-0.41568	0.097301
Methylophilus sp. TWE2	0.001043	0.477339	0.063073
Myxococcus hansupus	0.003135	-0.43412	0.08305

Myxococcus xanthus	0.002356	-0.44585	0.075082
Nitrobacter hamburgensis	0.002136	0.449802	0.071139
Obesumbacterium proteus	0.002915	0.437154	0.080105
Paraburkholderia phymatum	0.001999	-0.45244	0.070817
Paracoccus aminovorans	0.001845	-0.4556	0.070373
Photobacterium damselae	7.67E-06	0.623847	0.016863
Pseudoalteromonas phenolica	0.00112	0.474704	0.063073
Pseudomonas stutzeri	0.003246	-0.43267	0.083956
Ralstonia pickettii	0.003912	0.424769	0.088936
Rhodospirillum rubrum	0.002506	-0.44335	0.077615
Rhodovulum sp. MB263	0.00192	-0.45402	0.070373
Rickettsia australis	0.000504	0.503294	0.063073
Shewanella bicestrii	0.000393	0.511726	0.062717
Shewanella sp. WE21	0.001152	-0.47365	0.063073
Sphingobium indicum	0.003381	-0.43096	0.084734
Sphingomonas taxi	0.000834	-0.48551	0.063073
Wolinella succinogenes	0.002787	-0.439	0.080105
Kosakonia oryzae	0.000108	0.552569	0.039979
Spirochaetes			
Borreliella afzelii	0.00091	-0.48235	0.063073
Borreliella burgdorferi	0.003852	0.425428	0.088936
Sphaerochaeta coccoides	0.003888	0.425033	0.088936
Treponema putidum	7.29E-05	0.564163	0.039979
Tenericutes			
Mycoplasma dispar	0.000927	0.481686	0.063073
Thermodesulfobacteria			
Thermodesulfobacterium commune	0.004515	0.418577	0.094532
Thermotogae			
Fervidobacterium nodosum	0.001316	0.468643	0.063073
Petrotoga mobilis	0.000158	0.541107	0.04336
Thermotoga profunda	0.001651	0.459947	0.069792
Thermotoga sp. Cell2	0.002039	-0.45165	0.070817
Thermotogae			
Opitutaceae bacterium TAV5	0.004597	-0.41779	0.095353
Tenericutes			
Tenericutes bacterium MO-XQ	0.000325	0.51805	0.059562

Appendix Table C.11 Significant correlations between systolic blood pressure and bacterial species

Hierarchical All-against-All association testing (HAllA) was used (version 0.8.7) with Spearman correlation as correlation metric, medoid as clustering method and $q < 0.1$ as threshold for significance.